



UNIVERSITY of STRATHCLYDE
**MARITIME SAFETY
RESEARCH CENTRE**

Risk-based, sensor-fused detection of flooding casualties for emergency response

© Kristian Bertheussen Karolius

Maritime Safety Research Centre (MSRC)

University of Strathclyde, Glasgow

Department of Naval architecture, Ocean & Marine engineering

A thesis presented and submitted in fulfilment of the requirements for
the degree of Doctor of Philosophy (PhD), June 2019

*This thesis is dedicated to the loving memory of Arne Mikal
Karolius - Grandfather, mentor and friend.*

Copyright statement

This thesis is the result of the author's original research. It has been composed by the author and has not been previously submitted for examination which has led to the award of a degree.

The copyright of this thesis belongs to the author under the terms of the United Kingdom Copyright Acts as qualified by University of Strathclyde Regulation 3.50. Due acknowledgement must always be made of the use of any material contained in, or derived from, this thesis.

© Kristian Bertheussen Karolius. All rights reserved.

Signed: Kristian Bertheussen Karolius

Date: 23.09.2019

Preface

This is a final dissertation for the award of Doctor of Philosophy (PhD). The research has been undertaken at the Maritime Safety Research Centre (MSRC) during the period October 2016 to June 2019. The MSRC is an industry-University partnership involving the University of Strathclyde's Department of Naval Architecture, Ocean & Marine Engineering (NAOME), cruise line operator Royal Caribbean Cruise Lines (RCCL) and the Classification Society DNV GL. The centre aims to be an international leader in marine safety research by supporting the development and nurture the implementation of Life-Cycle Risk Management, accounting rationally and formally for all cost-effective measures of risk reduction that lead to sustainable cost-effective safety-improvement for new and existing ships and offshore assets. The centre also supports the development of a modern regulatory framework to support and nurture safety culture within the marine industry.

The research culminating into this thesis has been supervised by 1st supervisor Professor Dracos Vassalos and 2nd supervisor Dr. Jakub Cichowicz. Further guidance and support have been provided from the above-mentioned industrial partners. Research output achieved during the period of study is listed as follows:

Publications directly related to the content of this PhD thesis:

Karolius K. B., Vassalos D., (2017), *“How to buy time following a flooding incident: Intelligent quantification of emergency response measures”*, Proceedings of the 16th International Ship Stability Workshop, 5-7 June, Belgrade, Serbia.

Karolius K. B., Cichowicz, J., Vassalos, D., (2018) *“Risk-based positioning of Flooding Sensors to reduce Prediction Uncertainty of Damage Survivability”*, Proceedings of the 13th International Conference on the Stability of Ships and Ocean Vehicles, 16-21 September, Kobe, Japan.

Karolius K. B., Cichowicz, J., Vassalos, D., (2019), *“Modelling of compartment connectivity and probabilistic assessment of progressive flooding stages for a damaged ship”*, Proceedings of the 17th International Ship Stability Workshop, 10-12 June, Helsinki, Finland.

Other publications produced during the period of study:

Karoliuss, K. B., Vassalos D., (2018) "*Tearing down the wall – The inclining experiment*", Ocean Engineering, 148, 15 January, 442-475.

Karoliuss, K. B., Vassalos, D., (2018) "*Weight and buoyancy is the foundation in design: Get it right*", 13th International Marine Design Conference, Helsinki, Finland, 10-14 June.

Karoliuss, K. B., Vassalos, D., (2018) "*Second generation calculation method for use in the inclining experiment*", 13th International Conference on the Stability of Ships and Ocean Vehicles, 16-21 September, Kobe, Japan.

Vassalos, D., Atzampos, G., Cichowicz, J., Paterson D., Karoliuss, K. B., Boulougouris, E., Svensen, T., Douglas, K., Luhmann, H., (2018) "*Life-Cycle Flooding Risk Management of Passenger Ships*", 13th International Conference on the Stability of Ships and Ocean Vehicles, 16-21 September, Kobe, Japan.

Vassalos, D., Atzampos, G., Paterson D., Cichowicz, J., Karoliuss, K. B., Boulougouris, E., (2019), "*Intact Stability of Passenger Ships: Safety Issue or Design Concern? Neither!*", Proceedings of the 17th International Ship Stability Workshop, 10-12 June, Helsinki, Finland.

Acknowledgements

This thesis would not have been completed, if it were not for the scientific guidance of my academic supervisors. In this respect, I would like to express my sincere gratitude to Professor Dracos Vassalos and Dr. Jakub Cichowicz for their continuous support in undertaking the PhD study and related research. They have provided me with rewarding discussions, patience and motivation, but most importantly shared their immense knowledge.

A special thanks go to my employer DNV GL, and especially my colleague and head of the Stability, Load Line & Tonnage approval section, Inge Seglem, for giving me his full support in undertaking this endeavour. From the same section, I also want to show gratitude to my colleagues Bae Jun Kwon and Nils Heimvik for their valuable help with NAPA related questions, and to my colleague from the Hydrodynamics & Stability advisory section, Odd Karsten Olufsen, for valuable feedback and support. I also want to thank my colleagues from Group Technology and Research, Ole-Christian Astrup and George Psarros for showing interest and believing in my research topic.

I would also like to thank the whole team at the MSRC for turning long working days into a social and intriguing experience. Special thanks goes to Romanas Puisa for discussions and guidance during the initial period of the PhD. I should also like to mention Professor Tor Svensen for rewarding discussions and for much sought after advice and inspiration. My sincere thanks go to my good friend and colleague Donald Paterson for fruitful discussions and sharing of ideas, and most of all true friendship.

Finally, I would like to express gratitude to my family for their support and to my wife Kathinka for sharing and supporting my life with great patience and constant encouragement. But most of all, thank you for being the perfect mother to our beautiful daughter Hedvig, for keeping me sane for the past three years and for being my best friend. I owe you everything.

Abstract

The inherent complexity of the flooding process on large passenger vessels has, in recent years, been recognised. Accounting for the fact that traditional emergency response is a highly time consuming and manual process, prone to human misjudgement or error, this might lead to severe consequences. This is also highly paradoxical given that the most important variables in an emergency are Time-to-Capsize and Time-to-Evacuate. The research culminating in this PhD dissertation has, therefore, been directed towards the development of a framework where sensor-technology and analytics are utilised to a higher degree, in an attempt to improve real-time information providing risk-informed situational awareness in flooding emergencies involving large cruise vessels, thus enabling optimised emergency response. A fully probabilistic prediction methodology has been developed and presented. The methodology takes advantage of available sensor readings as supportive evidence and utilises inference in the form of probabilistic multi-sensor data fusion techniques for manipulating conditional probability distributions. This targets the observed distribution, enabling reduction in uncertainty (probabilistic inference). The framework and its corresponding comprehensive probabilistic models are further seen to be highly suitable for implementation as a Life-Cycle flooding risk management framework. A range of probabilistic models in the form of likelihood functions have been developed for a specific sample vessel using the state-of-the-art time-domain simulation code PROTEUS3. This enables the simulation of a damaged ship in a dynamic operational climate imposed by waves. Implementation and testing of the framework on a range of realistic test scenarios reveals that the method identifies the expected damaged region for all cases despite not having an exhaustive sensor array. This clearly provides improved survival assessment to enable the crew to implement emergency response in a more timely, targeted and efficient manner in accordance with the main aim set out in the thesis. Finally, having implemented the framework on an existing cruise vessel with the as-built sensor array indicates that the methodology may be implemented on a large cruise vessel without changes to the flooding detection system, as it is seen that the as-built sensor arrays allow for accurate predictions by relying entirely on the presented methodology. This allows for reliable estimation of real-time flooding risk in passenger ships through its life-cycles and most importantly, when it really matters, namely in emergencies. This is an innovation offering unique tangible benefits.

Table of Contents

Copyright statement	3
Preface.....	4
Acknowledgements	6
Abstract	7
Table of Contents.....	8
Nomenclature.....	15
Abbreviations	16
List of Figures.....	18
List of Tables.....	26
Chapter 1 - Introduction.....	31
1.1 Overview and Background.....	31
1.1.1 An Industry in change.....	31
1.1.2 Risk-informed situational awareness	33
1.1.3 Time as a measure of risk.....	34
1.1.4 Life-Cycle risk management	35
1.1.5 Advantages in emerging technology	35
1.2 Aims and objectives	36
1.3 Outline	38
1.4 Tools for Statistical Analysis.....	39
1.5 Sample vessel.....	40
1.6 References	42
Chapter 2 - Damage Stability and Survivability of Passenger Ships.....	45
2.1 Opening remarks	45
2.2 Traditional approach to damage stability.....	45
2.3 Breach and damage extent variables.....	47
2.3.1 Damage breach	47
2.4 Vessel variables.....	49
2.4.1 Internal subdivision and openings	49
2.4.2 Striking and Stricken vessel	53
2.4.3 Loading condition.....	54
2.5 Environment variables	55
2.5.1 Wind.....	55

2.5.2 Wave	56
2.6 Variable dependencies.....	58
2.7 Time-domain flooding simulations	59
2.8 Closing remarks.....	60
2.9 References	61
Chapter 3 - Emergency Response – Traditional and Novel Approaches	66
3.1 Opening remarks	66
3.2 Traditional flooding emergency response	67
3.2.1 Damage control and mitigation.....	67
3.2.2 Rules and Regulations	68
3.2.3 Emergency Response Service	70
3.3 Innovation in flooding emergency response	71
3.3.1 Case-based reasoning decision support	72
3.3.2 Operational flooding vulnerability measure	72
3.3.3 Breach detection from floodwater inflow-rate	73
3.3.4 Virtual environment for decision support.....	74
3.4 Other uses of sensors and technology.....	75
3.4.1 Maritime industry	75
3.4.2 Other industries	76
3.5 Closing remarks.....	77
3.6 References	78
Chapter 4 - Probabilistic Inference and Multi-sensor Data Fusion.....	83
4.1 Opening remarks	83
4.2 Uncertainty	83
4.3 Probabilistic inference	86
4.4 Multi-sensor data fusion.....	86
4.4.1 Reasoning behind data fusion	87
4.4.2 Probabilistic definitions and axioms.....	88
4.4.3 Probabilistic sensor fusion	91
4.4.4 Sensor fusion example	93
4.4.5 Sequential updating	95
4.5 Closing remarks.....	98
4.6 References	98
Chapter 5 - Environment variables	101
5.1 Opening remarks	101

5.2 A priori statistics	101
5.2.1 Wave environment.....	101
5.3 Likelihood function	103
5.3.1 Motion sensors.....	103
5.4 Implementation and testing	109
5.5 Closing remarks.....	115
5.6 References	116
Chapter 6 - Damage variables.....	117
6.1 Opening remarks	117
6.2 A priori statistics	117
6.2.1 Geometrical properties of a breach	117
6.2.1.1 Longitudinal position of damage, X	119
6.2.1.2 Vertical position of damage, Z.....	121
6.2.1.3 Damage length, L.....	125
6.2.1.4 Damage height, H	129
6.2.1.5 Damage penetration, Y.....	132
6.2.2 Breach position relative to the hull.....	136
6.2.3 Initial damage extent	137
6.3 Likelihood function	139
6.3.1 Initial flooding	139
6.3.2 Progressive flooding.....	147
6.3.2.1 Progressive flooding case realisation	147
6.3.2.2 Mathematical abstraction of compartment connectivity.....	153
6.3.2.3 Real-Case example I.....	155
6.3.2.4 Progressive flooding probability.....	159
6.3.2.5 Water elevation vertical exceedance probability	162
6.3.2.6 Real-Case example II.....	165
6.3.3 Flooding sensors.....	167
6.4 Closing remarks.....	169
6.5 References	170
Chapter 7 - Vessel variables	173
7.1 Opening remarks	173
7.2 A priori statistics	173
7.2.1 Openings	173
7.2.1.1 Opening frequencies.....	173

7.2.1.2 Leak and collapse.....	175
7.2.2 Loading condition.....	177
7.2.2.1 Vessel draft, T.....	177
7.2.2.2 Vertical position of centre of gravity, KG.....	178
7.3 Likelihood functions.....	179
7.3.1 Opening status sensors.....	179
7.3.2 Draught sensors.....	181
7.3.2.1 Waterplane representation from draught sensors.....	181
7.3.2.2 Posterior update of initial damage extent from draft sensors.....	182
7.3.3 AIS “sensor” data.....	186
7.3.3.1 Posterior update of initial damage extent based on AIS.....	186
7.4 Closing remarks.....	194
7.5 References.....	195
Chapter 8 - Risk-based positioning of Flooding Sensors.....	196
8.1 Opening remarks.....	196
8.2 Criticality assessment.....	197
8.2.1 Static assessment.....	197
8.2.2 Dynamic assessment.....	198
8.3 Compartment rating.....	199
8.4 Methodology summary.....	201
8.5 Results.....	201
8.5.1 Identification of critical capsizes cases.....	201
8.5.2 Compartment rating.....	202
8.5.3 Risk-optimised flooding sensor position.....	203
8.6 Closing remarks.....	206
8.7 References.....	207
Chapter 9 - Complete multi-sensor fusion methodology.....	208
Chapter 10 - Implementation & testing.....	211
10.1 Opening remarks.....	211
10.2 Test scenarios.....	211
10.3 Presentation.....	212
10.4 Implementation and testing results.....	213
10.4.1 As built sensor array.....	213
10.4.2 Test-case 1.....	213
10.4.3 Test-case 2.....	216

10.4.4 Test-case 3.....	218
10.4.5 Test-case 4.....	222
10.4.6 Test-case 5.....	225
10.5 Closing remarks.....	229
10.6 References	230
Chapter 11 - Discussion, Recommendations and Concluding Remarks.....	231
11.1 Discussion and recommendations	231
11.2 Concluding remarks	237
Appendix I - Wave prediction method – Complete test-case results.....	241
Appendix II - GoF statistics for dam. breach dist.'s with multiple dist. candidates.....	262
Appendix III - Excerpt of (500) MC samples for initial damage extent.....	264
Appendix IV - A priori and posterior opening data	271
Appendix V - Posterior update of damage extent from sensors.....	314
V.1 A priori belief – No sensor evidence	314
V.2 Test-case 1.....	315
V.2.1 Draft and AIS sensor evidence	315
V.2.2 Flooding sensor evidence - $H_s = 0.00$ m	315
V.2.3 Flooding sensor evidence - $H_s = 5.00$ m	318
V.2.4 Flooding sensor evidence - $H_s = 10.00$ m	321
V.3 Test-case 2.....	324
V.3.1 Draft and AIS sensor evidence	324
V.3.2 Flooding sensor evidence - $H_s = 0.00$ m	325
Flooding sensor evidence - $H_s = 5.00$ m	328
V.3.3 Flooding sensor evidence - $H_s = 10.00$ m	331
V.4 Test-case 3.....	334
V.4.1 Draft and AIS sensor evidence	334
V.4.2 Flooding sensor evidence - $H_s = 0.00$ m	334
V.4.3 Flooding sensor evidence - $H_s = 5.00$ m	337
V.4.4 Flooding sensor evidence - $H_s = 10.00$ m	342
V.5 Test-case 4.....	348
V.5.1 Draft and AIS sensor evidence	348
V.5.2 Flooding sensor evidence - $H_s = 0.00$ m	348
V.5.3 Flooding sensor evidence - $H_s = 5.00$ m	351
V.5.4 Flooding sensor evidence - $H_s = 10.00$ m	354
V.6 Test-case 5.....	357

V.6.1 Draft and AIS sensor evidence	357
V.6.2 Flooding sensor evidence - $H_s = 0.00$ m	358
V.6.3 Flooding sensor evidence - $H_s = 5.00$ m	364
V.6.4 Flooding sensor evidence - $H_s = 10.00$ m	370
Appendix VI - Heat-maps for compartment flooding probability	378
VI.1 Test-case 1, $H_s = 0.00$ m.....	378
VI.2 Test-case 1, $H_s = 10.00$ m.....	379
VI.3 Test-case 2, $H_s = 0.00$ m.....	380
VI.4 Test-case 2, $H_s = 10.00$ m.....	381
VI.5 Test-case 3, $H_s = 0.00$ m.....	382
VI.6 Test-case 3, $H_s = 10.00$ m.....	383
VI.7 Test-case 4, $H_s = 0.00$ m.....	384
VI.8 Test-case 4, $H_s = 10.00$ m.....	385
VI.9 Test-case 5, $H_s = 0.00$ m.....	386
VI.10 Test-case 5, $H_s = 10.00$ m.....	387

The theory of probabilities is nothing but good sense reduced to calculation; it allows one to appreciate with exactness what accurate minds feel by a sort of instinct, without often being able to explain it. (Pierre Laplace, 1814)

Nomenclature

Symbol	Designation	Unit
Attained index of subdivision	A	[-]
Buoyancy force, or Vessel Breadth	B	[N] or [m]
Difference between TtC and TtE	Δt	[min]
Draft	T	[m]
Gross Tonnes	GT	[m ³]
Heading	ψ	[°]
Heave	z	[m]
Heel	φ	[°]
Height of damage breach	H	[m]
Length of damage breach	L	[m]
Longitudinal Centre of Gravity	LCG	[m]
Longitudinal position of damage breach (mid position)	X	[m]
Mean or expected value	μ	[-]
Metacentre height from keel	KM	[m]
Metacentre height from vertical centre of gravity	GM	[m]
Natural roll period	T_φ	[sec]
Penetration depth of damage breach	Y	[m]
Persons not evacuated before capsizing (magnitude of loss)	ΔN	[pax]
p-factor	p	[-]
Pitch	θ	[°]
Required index of subdivision	R	[-]
Righting lever arm	GZ	[m]
s-factor	s	[-]
Standard deviation	σ	[-]
Significant wave height	H_s	[m]
Subdivision length	L_s	[m]
Time to Capsize	TtC	[min]
Time to Evacuate	TtE	[min]
Transverse Centre of Gravity	TCG	[m]
Vertical Centre of Gravity	VCG or KG	[m]
Vertical position of damage breach (lower limit)	Z	[m]
Vessel depth	D	[m]
Vessel length between perpendiculars	L_{BP}	[m]
Waterplane area	WPA	[m ²]
Zero up-crossing period	T_z	[sec]

Abbreviations

Acronym	Definition
AIS	Automatic Identification System
AP, FP	Aft- and fore perpendicular
BL	Baseline
CoG	Centre of Gravity
CFD	Computational Fluid Dynamics
CAD	Computer Aided Design
CBM	Condition-Based Maintenance
CSSF	Cruise Ship Safety Forum
CDF	Cumulative probability Density Function
DCB	Damage Control Booklet
DCP	Damage Control Plan
DoF	Degrees of Freedom
DNV GL	Det Norske Veritas – Germanischer Lloyds
eSAFE	Enhanced Stability after a flooding event
PhD	Doctor of Philosophy
DBM	Dynamic Barrier Management
ERS™	Emergency Response Service ¹
EMSA	European Maritime Safety Agency
FEM	Finite Elements Method
FPSO	Floating Production, Storage and Offloading
GPS	Global Positioning System
GOALDS	Goal-Based Damage Stability for Passenger Ships
GoF	Goodness of Fit
HARDER	Harmonization of Rules and Design Rational
FLOODSTAND	Integrated Flooding Control and Standard for Stability and Crises Management
IMO	International Maritime Organization
KPI	Key Performance Indicator
MSRC	Maritime Safety Research Centre
MCMC	Markov-Chain-Monte-Carlo
MLE	Maximum Likelihood Estimation

¹ Trademark of the Classification Society DNV GL.

MS	Midship
MIT	Ministry of Infrastructure and Transport
NAOME	Naval Architecture, Ocean & Marine Engineering
NAPA	Naval Architectural PAcKage
PIT	Pressure Integration Technique
PDF	Probability Density Function
RADAR	RADio Detection And Ranging
RRDA	Rapid Response Damage Assessment
RTMM	Real Time Mission Monitor
RoRo	Roll-on Roll-off
RCCL	Royal Caribbean Cruise Lines
SRtP	Safe Return to Port
SOLAS	Safety Of Life At Sea
TtC	Time to Capsize
TtE	Time to Evacuate
WL	Waterline

List of Figures

Figure 1-1: Evolution of cruise ship size (Papanikolaou et al., 2013).	32
Figure 1-2: Interplay between TtC and TtE. Adapted from Papanikolaou et al. (2009).	34
Figure 1-3: Arrangement of flooding sensors according to IMO guideline.	41
Figure 1-4: Stability model with internal openings.	41
Figure 2-1: Damage breach geometrical properties.	47
Figure 2-2: Initial stage of damage extent and its dependency on degree of subdivision.	48
Figure 2-3: Initial and progressive stage of damage dependent on internal opening status.	49
Figure 2-4: Schematic representation of different stages of flooding.	52
Figure 2-5: Interplay between speed, displacement and heading during collision (left), and bow design geometry (right) (Lutzen, 2001).	53
Figure 2-6: Breach (hull deformation) simulated in FEM analysis (Ozguc et al, 2006).	54
Figure 2-7: Draft influence on expected breach height.	55
Figure 2-8: GZ variation with respect to time and wave position in head waves (Peşman et al., 2012).	57
Figure 2-9: High-level causal relationship between flooding variables.	58
Figure 2-10: PROTEUS3 model with internal openings.	60
Figure 4-1: Illustration of variability and uncertainty, represented with probability distributions.	84
Figure 4-2: Visualisation of trueness and precision of sensor data (DNV GL, 2018).	85
Figure 4-3: Joint, marginal and (un-normalised) conditional probability distributions.	91
Figure 4-4: Sensor fusion example.	94
Figure 4-5: Illustration of sequential or recursive updating using recursive Bayes theorem.	97
Figure 5-1: Status of Global drifter array (PhOD, 2019).	102
Figure 5-2: Distribution for the significant wave height H_s	103
Figure 5-3: Distribution for the zero up-crossing period T_z conditional on $H_s = 5.0$ m.	103
Figure 5-4: Time-series for roll motion with amplitude filter.	104
Figure 5-5: Average highest one-third roll data-points from 20 min simulations.	106
Figure 5-6: Average highest one-third pitch data-points from 20 min simulations.	106
Figure 5-7: Average highest one-third heave data-points from 20 min simulations.	106
Figure 5-8: Numerical and analytical representation of likelihood function $PDF(\text{Roll} H_s)$	108
Figure 5-9: Numerical and analytical representation of likelihood function $PDF(\text{Pitch} H_s)$	108
Figure 5-10: Numerical and analytical representation of likelihood function $PDF(\text{Heave} H_s)$	108
Figure 5-11: A priori, and likelihood functions (World-wide).	110
Figure 5-12: A priori and posterior including actual and expected value (World-wide).	110
Figure 5-13: Cumulative a priori and posterior including actual and expected value (World-wide).	110
Figure 5-14: A priori, and likelihood functions (North-Atlantic).	111

Figure 5-15: A priori and posterior including actual and expected value (North-Atlantic).	111
Figure 5-16: Cumulative a priori and posterior including actual and expected value (North-Atlantic).	111
Figure 5-17: A priori, and likelihood functions (Caribbean).	112
Figure 5-18: A priori and posterior including actual and expected value (Caribbean).	112
Figure 5-19: Cumulative a priori and posterior including actual and expected value (Caribbean).	112
Figure 5-20: A priori, and likelihood functions (Extreme wave).	113
Figure 5-21: A priori and posterior including actual and expected value (Extreme wave).	113
Figure 5-22: Cumulative a priori and posterior including actual and expected value (Extreme wave).	113
Figure 5-23: Recursive update for increasing wave height in time.	114
Figure 5-24: Non-recursive update for increasing wave height in time.	115
Figure 6-1: Proportions of ship size (represented by length LBP) in GOALDS database.	118
Figure 6-2: Subdivision length of sample vessel.	120
Figure 6-3: Numerical PDF and CDF for scaled longitudinal damage position, X.	120
Figure 6-4: Analytical PDF and CDF for longitudinal damage position, X.	121
Figure 6-5: Distribution for Z as a function of T.	122
Figure 6-6: Numerical PDF and CDF for vertical damage position, Z.	123
Figure 6-7: Cullen & Frey graph for vertical damage position, Z.	123
Figure 6-8: Analytical PDF and CDF for vertical damage position, Z.	124
Figure 6-9: PDF and CDF density function for Z conditional on T.	125
Figure 6-10: Numerical PDF and CDF for damage length, L.	126
Figure 6-11: Cullen & Frey graph for damage length, L.	126
Figure 6-12: Analytical PDF and CDF for damage length, L.	127
Figure 6-13: L maximum boundary curve.	128
Figure 6-14: Sampled damage lengths, L, plotted on given X location.	129
Figure 6-15: Dependency between Z and H.	130
Figure 6-16: Numerical PDF and CDF for damage height, H.	130
Figure 6-17: Cullen & Frey graph for damage height, H.	131
Figure 6-18: Joint PDF of H and Z represented as copula.	132
Figure 6-19: Dependency between L and Y.	133
Figure 6-20: Numerical PDF and CDF for damage penetration, Y.	134
Figure 6-21: Cullen & Frey graph for damage penetration, Y.	134
Figure 6-22: Analytical PDF and CDF for damage penetration, Y.	135
Figure 6-23: Joint PDF of Y and L represented as copula.	135
Figure 6-24: Breach longitudinal position, length and height in relation with hull.	136
Figure 6-25: Hull-waterline intersection curve for transverse penetration reference.	136
Figure 6-26: Breach-Compartment overlap check for 300 samples.	138
Figure 6-27: Influence on flooding from variables T, Z and Hs (static consideration).	139

Figure 6-28: Height from calm-waterplane, ΔZ , of initial flooding as a function of wave height, H_s	141
Figure 6-29: Numerical and analytical distributions for flooding height from WL.	142
Figure 6-30: Exceedance probability of flooding height from WL, dZ	143
Figure 6-31: Example distribution for two initial damage extents.....	144
Figure 6-32: Upper example compartment (located above calm waterline).	145
Figure 6-33: Event (probability) tree of damage extents.....	148
Figure 6-34: Example compartmentation with doors and possible flooding realisations	149
Figure 6-35: Compartments mathematical abstraction as graph.....	153
Figure 6-36: Sampled edge existence in example compartmentation represented as uncertain graph	154
Figure 6-37: Initial damage extent of the case study.	156
Figure 6-38: Progressive flooding realization 1, $P = 0.233$	158
Figure 6-39: Progressive flooding realization 2, $P = 0.206$	158
Figure 6-40: Progressive flooding realization 3, $P = 0.115$	159
Figure 6-41: Progressive flooding realization 36, $P = 0.001$	159
Figure 6-42: Event (probability) tree of progressive flooding realisations.	160
Figure 6-43: ΔZ , between internal and external water elevation, as a function of wave height, H_s	163
Figure 6-44: Numerical and analytical distribution for internal flooding height from WL.....	164
Figure 6-45: Numerical exceedance probability for internal flooding height from WL.	164
Figure 6-46: Reference system for openings position in relation with the residual waterplane	165
Figure 6-47: Event (probability) tree of flooding sensor status realisations.	168
Figure 7-1: Proximate inverse cumulative density function for sampling of opening frequencies.....	174
Figure 7-2: Door leak and collapse pressure heights modelled with probability distributions.....	175
Figure 7-3: Numerical and analytical dimensionalised draft distribution.	177
Figure 7-4: Operating loading conditions.	178
Figure 7-5: Bi-variate distribution for KG and T developed from operating loading conditions.	179
Figure 7-6: Mathematical representation of waterplane using draft sensor measurements.....	182
Figure 7-7: Interval of possible Z values for a given initial damage extent.....	183
Figure 7-8: Probability distribution for Z conditional on T	184
Figure 7-9: Ship section with upper and lower compartment and their vertical limits.	185
Figure 7-10: Vertical position of Breach as a function of Striking vessel length.....	187
Figure 7-11: Length of Breach as a function of Striking vessel length.....	187
Figure 7-12: Height of Breach as a function of Striking vessel length.	187
Figure 7-13: Breach penetration as a function of Striking vessel length.....	188
Figure 7-14: Likelihood function for Z (left), and samples compared with data-points (right).....	189
Figure 7-15: Likelihood function for L (left), and samples compared with data-points (right).....	189
Figure 7-16: Likelihood function for H (left), and samples compared with data-points (right).....	190
Figure 7-17: Likelihood function for Y (left), and samples compared with data-points (right).	190

Figure 7-18: Example of integrand intervals (bounds) for the respective breach variables for specific initial damage extents	191
Figure 7-19: Minor damage extent example	192
Figure 7-20: Major damage extent example.....	192
Figure 7-21: Likelihood functions, and corresponding likelihood for specific striking vessel length.....	193
Figure 8-1: Initial categorisation of static damage cases, (1-s) diagram.....	197
Figure 8-2: Illustration of limit between critical loss - and survival scenarios.	198
Figure 8-3: Actual damage length as a result of zonal representation.....	199
Figure 8-4: Reduction in damage length to damp the effects of transient flooding.....	199
Figure 8-5: P1S diagram illustrating damage cases in terms of risk along ship length.....	200
Figure 8-6: Identified capsizes cases in the uncertain region of the (1-P) diagram.	202
Figure 8-7: Compartment risk rating: All stages.....	204
Figure 8-8: Compartment risk rating: Initial stages.	204
Figure 8-9: Compartment risk rating: Progressive stages.	204
Figure 8-10: Graphical representation of the compartment risk rating: Initial stage.	205
Figure 8-11: Graphical representation of the compartment risk rating: Progressive stage.....	205
Figure 9-1: Schematic layout of the multi-sensor data fusion methodology.....	209
Figure 10-1: Test-case 1, Striking vessel length: 50.0 m, $H_s = 0.0$ m.....	214
Figure 10-2: Test-case 2, Striking vessel length: 100.0 m, $H_s = 0.0$ m.....	216
Figure 10-3: Additional progressive flooding extent for Test-case 2, Striking vessel length: 100 m, $H_s = 5.0$ m and $H_s = 10.0$	218
Figure 10-4: Test-case 3, Striking vessel length: 150.0 m, $H_s = 0.0$ m.....	219
Figure 10-5: Compartments part of the 99% CI for the calm-water case, time step $t = 5.0$ min.....	220
Figure 10-6: Heat map for calm-water case, time step $t=5.0$ min representing the probability that a compartment is flooded.....	221
Figure 10-7: Test-case 4 (major), Striking vessel length: 200.0 m, $H_s = 0.0$ m.....	222
Figure 10-8: Heat map for calm-water case, time step $t = 5.0$ min representing the probability that a compartment is flooded.....	224
Figure 10-9: Heat map for wave-case, $H_s = 10.0$ m, time step $t = 30.0$ min representing the probability that a compartment is flooded.....	225
Figure 10-10: Test-case 5, Striking vessel length: 250.0 m, $H_s = 0.0$ m	226
Figure 10-11: Test-case 5, Striking vessel length: 250 m, $H_s = 10.0$ m, $t = 30$ min	228
Figure 10-12: Heat map for wave-case, $H_s = 10.0$ m, time step $t = 30.0$ min representing the probability that a compartment is flooded.....	229
Figure I-1: A priori, and likelihood functions (C1-World-wide).....	242
Figure I-2: A priori and posterior including actual and expected value (C1-World-wide).	242
Figure I-3: Cumulative a priori and posterior including actual and expected value (C1-World-wide).	242

Figure I-4: A priori, and likelihood functions (C2-World-wide).....	243
Figure I-5: A priori and posterior including actual and expected value (C2-World-wide).	243
Figure I-6: Cumulative a priori and posterior including actual and expected value (C2-World-wide).	243
Figure I-7: A priori, and likelihood functions (C3-World-wide).....	244
Figure I-8: A priori and posterior including actual and expected value (C3-World-wide).	244
Figure I-9: Cumulative a priori and posterior including actual and expected value (C3-World-wide).	244
Figure I-10: A priori, and likelihood functions (C4-World-wide).....	245
Figure I-11: A priori and posterior including actual and expected value (C4-World-wide).....	245
Figure I-12: Cumulative a priori and posterior including actual and expected value (C4-World-wide).....	245
Figure I-13: A priori, and likelihood functions (C5-World-wide).....	246
Figure I-14: A priori and posterior including actual and expected value (C5-World-wide).....	246
Figure I-15: Cumulative a priori and posterior including actual and expected value (C5-World-wide).....	246
Figure I-16: A priori, and likelihood functions (C1- North-Atlantic).....	247
Figure I-17: A priori and posterior including actual and expected value (C1- North-Atlantic).	247
Figure I-18: Cum. a priori and posterior including actual and expected value (C1-North-Atlantic).....	247
Figure I-19: A priori, and likelihood functions (C2-North-Atlantic).....	248
Figure I-20: A priori and posterior including actual and expected value (C2-North-Atlantic).....	248
Figure I-21: Cum. a priori and posterior including actual and expected value (C2-North-Atlantic).....	248
Figure I-22: A priori, and likelihood functions (C3-North-Atlantic).....	249
Figure I-23: A priori and posterior including actual and expected value (C3-North-Atlantic).....	249
Figure I-24: Cum. a priori and posterior including actual and expected value (C3-North-Atlantic).....	249
Figure I-25: A priori, and likelihood functions (C4-North-Atlantic).....	250
Figure I-26: A priori and posterior including actual and expected value (C4-North-Atlantic).....	250
Figure I-27: Cum. a priori and posterior including actual and expected value (C4-North-Atlantic).....	250
Figure I-28: A priori, and likelihood functions (C5-North-Atlantic).....	251
Figure I-29: A priori and posterior including actual and expected value (C5-North-Atlantic).....	251
Figure I-30: Cum. a priori and posterior including actual and expected value (C5-North-Atlantic).....	251
Figure I-31: A priori, and likelihood functions (C1-Caribbean).....	252
Figure I-32: A priori and posterior including actual and expected value (C1-Caribbean).	252
Figure I-33: Cum. a priori and posterior including actual and expected value (C1-Caribbean).	252
Figure I-34: A priori, and likelihood functions (C2-Caribbean).....	253
Figure I-35: A priori and posterior including actual and expected value (C2-Caribbean).	253
Figure I-36: Cum. a priori and posterior including actual and expected value (C2-Caribbean).	253
Figure I-37: A priori, and likelihood functions (C3-Caribbean).....	254
Figure I-38: A priori and posterior including actual and expected value (C3-Caribbean).	254
Figure I-39: Cum. a priori and posterior including actual and expected value (C3-Caribbean).	254
Figure I-40: A priori, and likelihood functions (C4-Caribbean).....	255

Figure I-41: A priori and posterior including actual and expected value (C4-Caribbean).	255
Figure I-42: Cum. a priori and posterior including actual and expected value (C4-Caribbean).	255
Figure I-43: A priori, and likelihood functions (C5-Caribbean).....	256
Figure I-44: A priori and posterior including actual and expected value (C5-Caribbean).	256
Figure I-45: Cum. a priori and posterior including actual and expected value (C5-Caribbean).	256
Figure I-46: A priori, and likelihood functions (C1-Extreme wave).	257
Figure I-47: A priori and posterior including actual and expected value (C1-Extreme wave).	257
Figure I-48: Cum. a priori and posterior including actual and expected value (C1-Extreme wave).	257
Figure I-49: A priori, and likelihood functions (C2-Extreme wave).	258
Figure I-50: A priori and posterior including actual and expected value (C2-Extreme wave).	258
Figure I-51: Cum. a priori and posterior including actual and expected value (C2-Extreme wave).	258
Figure I-52: A priori, and likelihood functions (C3-Extreme wave).	259
Figure I-53: A priori and posterior including actual and expected value (C3-Extreme wave).	259
Figure I-54: Cum. a priori and posterior including actual and expected value (C3-Extreme wave).	259
Figure I-55: A priori, and likelihood functions (C4-Extreme wave).	260
Figure I-56: A priori and posterior including actual and expected value (C4-Extreme wave).	260
Figure I-57: Cum. a priori and posterior including actual and expected value (C4-Extreme wave).	260
Figure I-58: A priori, and likelihood functions (C5- Extreme wave).	261
Figure I-59: A priori and posterior including actual and expected value (C5-Extreme wave).	261
Figure I-60: Cum. a priori and posterior including actual and expected value (C5-Extreme wave).	261
Figure II-1: GoF statistics for damage length L.	262
Figure II-2: GoF statistics for vertical damage location Z.....	262
Figure II-3: GoF statistics for damage penetration Y.....	263
Figure VI-1: TC-1, $H_s = 0$ m, Time-step, $t = 5$ min	378
Figure VI-2: TC-1, $H_s = 0$ m, Time-step, $t = 10$ min	378
Figure VI-3: TC-1, $H_s = 0$ m, Time-step, $t = 15$ min	378
Figure VI-4: TC-1, $H_s = 0$ m, Time-step, $t = 20$ min	378
Figure VI-5: TC-1, $H_s = 0$ m, Time-step, $t = 25$ min	378
Figure VI-6: TC-1, $H_s = 0$ m, Time-step, $t = 30$ min	378
Figure VI-7: TC-1, $H_s = 10$ m, Time-step, $t = 5$ min	379
Figure VI-8: TC-1, $H_s = 10$ m, Time-step, $t = 10$ min.....	379
Figure VI-9: TC-1, $H_s = 10$ m, Time-step, $t = 15$ min.....	379
Figure VI-10: TC-1, $H_s = 10$ m, Time-step, $t = 20$ min.....	379
Figure VI-11: TC-1, $H_s = 10$ m, Time-step, $t = 25$ min.....	379
Figure VI-12: TC-1, $H_s = 10$ m, Time-step, $t = 30$ min.....	379
Figure VI-13: TC-2, $H_s = 0$ m, Time-step, $t = 5$ min	380
Figure VI-14: TC-2, $H_s = 0$ m, Time-step, $t = 10$ min.....	380

Figure VI-15: TC-2, $H_S = 0$ m, Time-step, $t = 15$ min.....	380
Figure VI-16: TC-2, $H_S = 0$ m, Time-step, $t = 20$ min.....	380
Figure VI-17: TC-2, $H_S = 0$ m, Time-step, $t = 25$ min.....	380
Figure VI-18: TC-2, $H_S = 0$ m, Time-step, $t = 30$ min.....	380
Figure VI-19: TC-2, $H_S = 10$ m, Time-step, $t = 5$ min.....	381
Figure VI-20: TC-2, $H_S = 10$ m, Time-step, $t = 10$ min.....	381
Figure VI-21: TC-2, $H_S = 10$ m, Time-step, $t = 15$ min.....	381
Figure VI-22: TC-2, $H_S = 10$ m, Time-step, $t = 20$ min.....	381
Figure VI-23: TC-2, $H_S = 10$ m, Time-step, $t = 25$ min.....	381
Figure VI-24: TC-2, $H_S = 10$ m, Time-step, $t = 30$ min.....	381
Figure VI-25: TC-3, $H_S = 0$ m, Time-step, $t = 5$ min.....	382
Figure VI-26: TC-3, $H_S = 0$ m, Time-step, $t = 10$ min.....	382
Figure VI-27: TC-3, $H_S = 0$ m, Time-step, $t = 15$ min.....	382
Figure VI-28: TC-3, $H_S = 0$ m, Time-step, $t = 20$ min.....	382
Figure VI-29: TC-3, $H_S = 0$ m, Time-step, $t = 25$ min.....	382
Figure VI-30: TC-3, $H_S = 0$ m, Time-step, $t = 30$ min.....	382
Figure VI-31: TC-3, $H_S = 10$ m, Time-step, $t = 5$ min.....	383
Figure VI-32: TC-3, $H_S = 10$ m, Time-step, $t = 10$ min.....	383
Figure VI-33: TC-3, $H_S = 10$ m, Time-step, $t = 15$ min.....	383
Figure VI-34: TC-3, $H_S = 10$ m, Time-step, $t = 20$ min.....	383
Figure VI-35: TC-3, $H_S = 10$ m, Time-step, $t = 25$ min.....	383
Figure VI-36: TC-3, $H_S = 10$ m, Time-step, $t = 30$ min.....	383
Figure VI-37: TC-4, $H_S = 0$ m, Time-step, $t = 5$ min.....	384
Figure VI-38: TC-4, $H_S = 0$ m, Time-step, $t = 10$ min.....	384
Figure VI-39: TC-4, $H_S = 0$ m, Time-step, $t = 15$ min.....	384
Figure VI-40: TC-4, $H_S = 0$ m, Time-step, $t = 20$ min.....	384
Figure VI-41: TC-4, $H_S = 0$ m, Time-step, $t = 25$ min.....	384
Figure VI-42: TC-4, $H_S = 0$ m, Time-step, $t = 30$ min.....	384
Figure VI-43: TC-4, $H_S = 10$ m, Time-step, $t = 5$ min.....	385
Figure VI-44: TC-4, $H_S = 10$ m, Time-step, $t = 10$ min.....	385
Figure VI-45: TC-4, $H_S = 10$ m, Time-step, $t = 15$ min.....	385
Figure VI-46: TC-4, $H_S = 10$ m, Time-step, $t = 20$ min.....	385
Figure VI-47: TC-4, $H_S = 10$ m, Time-step, $t = 25$ min.....	385
Figure VI-48: TC-4, $H_S = 10$ m, Time-step, $t = 30$ min.....	385
Figure VI-49: TC-5, $H_S = 0$ m, Time-step, $t = 5$ min.....	386
Figure VI-50: TC-5, $H_S = 0$ m, Time-step, $t = 10$ min.....	386
Figure VI-51: TC-5, $H_S = 0$ m, Time-step, $t = 15$ min.....	386

Figure VI-52: TC-5, $H_S = 0$ m, Time-step, $t = 20$ min.....	386
Figure VI-53: TC-5, $H_S = 0$ m, Time-step, $t = 25$ min.....	386
Figure VI-54: TC-5, $H_S = 0$ m, Time-step, $t = 30$ min.....	386
Figure VI-55: TC-5, $H_S = 10$ m, Time-step, $t = 5$ min.....	387
Figure VI-56: TC-5, $H_S = 10$ m, Time-step, $t = 10$ min.....	387
Figure VI-57: TC-5, $H_S = 10$ m, Time-step, $t = 15$ min.....	387
Figure VI-58: TC-5, $H_S = 10$ m, Time-step, $t = 20$ min.....	387
Figure VI-59: TC-5, $H_S = 10$ m, Time-step, $t = 25$ min.....	387
Figure VI-60: TC-5, $H_S = 10$ m, Time-step, $t = 30$ min.....	387

List of Tables

Table 1-1: Sample vessel particulars.	41
Table 1-2: Internal openings of sample vessel.....	42
Table 2-1: Opening allowance categories for watertight doors.....	50
Table 2-2: Door combinatorics.....	51
Table 5-1: Excerpt of sampled variables for time-series.....	105
Table 5-2: Sensor readings and statistical prediction data.....	109
Table 6-1: Overview of data samples from GOALDS, and HARDER databases.....	118
Table 6-2: Statistical variables related to collision damage.....	119
Table 6-3: Goodness of fit (GoF) statistics and criteria for MLE of distribution for Z.....	124
Table 6-4: Goodness of fit (GoF) statistics and criteria for MLE of distribution for L.....	127
Table 6-5: Goodness of Fit (GoF) statistics and criteria for MLE distribution for L.....	134
Table 6-6: Summary of example conditions.....	145
Table 6-7: Posterior update of flooding prob. of example extent (Upper) implementing initial flooding likelihood for increasing wave heights.....	146
Table 6-8: Opening frequencies for example compartmentation.....	149
Table 6-9: Summary of case realisations for example compartmentation.....	152
Table 6-10: Prog. flooding case (realisation) prob. from manual calculation and sampling scheme.....	155
Table 6-11: Prog. flooding case (realisation) prob. from manual calculation and sampling scheme.....	156
Table 6-12: CI and corresponding number of related progressive extents for 1,000 samples.....	157
Table 6-13: Progressive extents representing a 90% CI, including initial extent.....	157
Table 6-14: Floating position in intact and damaged case.....	166
Table 6-15: Ten most likely progressive extents representing calm-water cases.....	166
Table 6-16: Ten most likely progressive extents representing calm-water cases.....	167
Table 7-1: Assumed (expected) opening frequency for sample vessel opening categories.....	174
Table 7-2: Opening leak and collapse heads, including probabilistic models and parameters.....	176
Table 7-3: Sensor likelihood, including sensor reliability (false positives/negatives).....	180
Table 7-4: Simple example of posterior update of door status probability using sensor status.....	181
Table 7-5: Posterior update of initial damage extent probability.....	185
Table 7-6: Marginal distributions for damage breach variables related to collision energy.....	186
Table 7-7: Example initial damage extents (minor and major).....	192
Table 7-8: Posterior update of initial damage extent probability from AIS data.....	193
Table 8-1: Colour coding for compartment criticality.....	203
Table 10-1: Summary of test-scenarios: Striking-vessel length (top two rows), stricken vessel loading condition, resulting breach and wave environment.....	212

Table I-1: Sensor readings and statistical prediction data for all test-cases.....	241
Table III-1: Excerpt of 500 samples from the Monte Carlo sampling for initial damage extent.	264
Table IV-1: A priori and posterior opening data.	271
Table IV-2: A priori and posterior opening data.	292
Table V-1: A priori belief - Ten most likely cases based on no sensor evidence.	314
Table V-2: TC-1 - Ten most likely cases inferred from draft and AIS sensor.	315
Table V-3: TC-1 - Ten most likely cases inferred from flooding sensors, $H_S = 0.0$ m, time = 5 min.	315
Table V-4: TC-1 - Ten most likely cases inferred from flooding sensors, $H_S = 0.0$ m, time = 10 min.	316
Table V-5: TC-1 - Ten most likely cases inferred from flooding sensors, $H_S = 0.0$ m, time = 15 min.	316
Table V-6: TC-1 - Ten most likely cases inferred from flooding sensors, $H_S = 0.0$ m, time = 20 min.	317
Table V-7: TC-1 - Ten most likely cases inferred from flooding sensors, $H_S = 0.0$ m, time = 25 min.	317
Table V-8: TC-1 - Ten most likely cases inferred from flooding sensors, $H_S = 0.0$ m, time = 30 min.	318
Table V-9: TC-1 - Ten most likely cases inferred from flooding sensors, $H_S = 5.0$ m, time = 5 min.	318
Table V-10: TC-1 - Ten most likely cases inferred from flooding sensors, $H_S = 5.0$ m, time = 10 min.	319
Table V-11: TC-1 - Ten most likely cases inferred from flooding sensors, $H_S = 5.0$ m, time = 15 min.	319
Table V-12: TC-1 - Ten most likely cases inferred from flooding sensors, $H_S = 5.0$ m, time = 20 min.	320
Table V-13: TC-1 - Ten most likely cases inferred from flooding sensors, $H_S = 5.0$ m, time = 25 min.	320
Table V-14: TC-1 - Ten most likely cases inferred from flooding sensors, $H_S = 5.0$ m, time = 30 min.	321
Table V-15: TC-1 - Ten most likely cases inferred from flooding sensors, $H_S = 10.0$ m, time = 5 min.	321
Table V-16: TC-1 - Ten most likely cases inferred from flooding sensors, $H_S = 10.0$ m, time = 10 min.	322
Table V-17: TC-1 - Ten most likely cases inferred from flooding sensors, $H_S = 10.0$ m, time = 15 min.	322
Table V-18: TC-1 - Ten most likely cases inferred from flooding sensors, $H_S = 10.0$ m, time = 20 min.	323
Table V-19: TC-1 - Ten most likely cases inferred from flooding sensors, $H_S = 10.0$ m, time = 25 min.	323
Table V-20: TC-1 - Ten most likely cases inferred from flooding sensors, $H_S = 10.0$ m, time = 30 min.	324
Table V-21: TC-2- Ten most likely cases inferred from draft and AIS sensor.	324
Table V-22: TC-2- Ten most likely cases inferred from flooding sensors, $H_S = 0.0$ m, time = 5 min.	325
Table V-23: TC-2- Ten most likely cases inferred from flooding sensors, $H_S = 0.0$ m, time = 10 min.	325
Table V-24: TC-2- Ten most likely cases inferred from flooding sensors, $H_S = 0.0$ m, time = 15 min.	326
Table V-25: TC-2- Ten most likely cases inferred from flooding sensors, $H_S = 0.0$ m, time = 20 min.	326
Table V-26: TC-2- Ten most likely cases inferred from flooding sensors, $H_S = 0.0$ m, time = 25 min.	327
Table V-27: TC-2- Ten most likely cases inferred from flooding sensors, $H_S = 0.0$ m, time = 30 min.	327
Table V-28: TC-2- Ten most likely cases inferred from flooding sensors, $H_S = 5.0$ m, time = 5 min.	328
Table V-29: TC-2- Ten most likely cases inferred from flooding sensors, $H_S = 5.0$ m, time = 10 min.	328
Table V-30: TC-2- Ten most likely cases inferred from flooding sensors, $H_S = 5.0$ m, time = 15 min.	329
Table V-31: TC-2- Ten most likely cases inferred from flooding sensors, $H_S = 5.0$ m, time = 20 min.	329
Table V-32: TC-2- Ten most likely cases inferred from flooding sensors, $H_S = 5.0$ m, time = 25 min.	330
Table V-33: TC-2- Ten most likely cases inferred from flooding sensors, $H_S = 5.0$ m, time = 30 min.	330

Table V-34: TC-2- Ten most likely cases inferred from flooding sensors, $H_S = 10.0$ m, time = 5 min.	331
Table V-35: TC-2- Ten most likely cases inferred from flooding sensors, $H_S = 10.0$ m, time = 10 min.	331
Table V-36: TC-2- Ten most likely cases inferred from flooding sensors, $H_S = 10.0$ m, time = 15 min.	332
Table V-37: TC-2- Ten most likely cases inferred from flooding sensors, $H_S = 10.0$ m, time = 20 min.	332
Table V-38: TC-2- Ten most likely cases inferred from flooding sensors, $H_S = 10.0$ m, time = 25 min.	333
Table V-39: TC-2- Ten most likely cases inferred from flooding sensors, $H_S = 10.0$ m, time = 30 min.	333
Table V-40: TC-3- Ten most likely cases inferred from draft and AIS sensor.	334
Table V-41: TC-3 - Ten most likely cases inferred from flooding sensors, $H_S = 0.0$ m, time = 5 min.	334
Table V-42: TC-3 - Ten most likely cases inferred from flooding sensors, $H_S = 0.0$ m, time = 10 min.	335
Table V-43: TC-3 - Ten most likely cases inferred from flooding sensors, $H_S = 0.0$ m, time = 15 min.	335
Table V-44: TC-3 - Ten most likely cases inferred from flooding sensors, $H_S = 0.0$ m, time = 20 min.	336
Table V-45: TC-3 - Ten most likely cases inferred from flooding sensors, $H_S = 0.0$ m, time = 25 min.	336
Table V-46: TC-3 - Ten most likely cases inferred from flooding sensors, $H_S = 0.0$ m, time = 30 min.	337
Table V-47: TC-3 - Ten most likely cases inferred from flooding sensors, $H_S = 5.0$ m, time = 5 min.	337
Table V-48: TC-3 - Ten most likely cases inferred from flooding sensors, $H_S = 5.0$ m, time = 10 min.	338
Table V-49: TC-3 - Ten most likely cases inferred from flooding sensors, $H_S = 5.0$ m, time = 15 min.	338
Table V-50: TC-3 - Ten most likely cases inferred from flooding sensors, $H_S = 5.0$ m, time = 20 min.	339
Table V-51: TC-3 - Ten most likely cases inferred from flooding sensors, $H_S = 5.0$ m, time = 25 min.	340
Table V-52: TC-3 - Ten most likely cases inferred from flooding sensors, $H_S = 5.0$ m, time = 30 min.	341
Table V-53: TC-3 - Ten most likely cases inferred from flooding sensors, $H_S = 10.0$ m, time = 5 min.	342
Table V-54: TC-3 - Ten most likely cases inferred from flooding sensors, $H_S = 10.0$ m, time = 10 min.	343
Table V-55: TC-3 - Ten most likely cases inferred from flooding sensors, $H_S = 10.0$ m, time = 15 min.	344
Table V-56: TC-3 - Ten most likely cases inferred from flooding sensors, $H_S = 10.0$ m, time = 20 min.	345
Table V-57: TC-3 - Ten most likely cases inferred from flooding sensors, $H_S = 10.0$ m, time = 25 min.	346
Table V-58: TC-3 - Ten most likely cases inferred from flooding sensors, $H_S = 10.0$ m, time = 30 min.	347
Table V-59: TC-4 - Ten most likely cases inferred from draft and AIS sensor.	348
Table V-60: TC-4 - Ten most likely cases inferred from flooding sensors, $H_S = 0.0$ m, time = 5 min.	348
Table V-61: TC-4 - Ten most likely cases inferred from flooding sensors, $H_S = 0.0$ m, time = 10 min.	349
Table V-62: TC-4 - Ten most likely cases inferred from flooding sensors, $H_S = 0.0$ m, time = 15 min.	349
Table V-63: TC-4 - Ten most likely cases inferred from flooding sensors, $H_S = 0.0$ m, time = 20 min.	350
Table V-64: TC-4 - Ten most likely cases inferred from flooding sensors, $H_S = 0.0$ m, time = 25 min.	350
Table V-65: TC-4 - Ten most likely cases inferred from flooding sensors, $H_S = 0.0$ m, time = 30 min.	351
Table V-66: TC-4 - Ten most likely cases inferred from flooding sensors, $H_S = 5.0$ m, time = 5 min.	351
Table V-67: TC-4 - Ten most likely cases inferred from flooding sensors, $H_S = 5.0$ m, time = 10 min.	352
Table V-68: TC-4 - Ten most likely cases inferred from flooding sensors, $H_S = 5.0$ m, time = 15 min.	352
Table V-69: TC-4 - Ten most likely cases inferred from flooding sensors, $H_S = 5.0$ m, time = 20 min.	353
Table V-70: TC-4 - Ten most likely cases inferred from flooding sensors, $H_S = 5.0$ m, time = 25 min.	353

Table V-71: TC-4 - Ten most likely cases inferred from flooding sensors, $H_S = 5.0$ m, time = 30 min.	354
Table V-72: TC-4 - Ten most likely cases inferred from flooding sensors, $H_S = 10.0$ m, time = 5 min.	354
Table V-73: TC-4 - Ten most likely cases inferred from flooding sensors, $H_S = 10.0$ m, time = 10 min.	355
Table V-74: TC-4 - Ten most likely cases inferred from flooding sensors, $H_S = 10.0$ m, time = 15 min.	355
Table V-75: TC-4 - Ten most likely cases inferred from flooding sensors, $H_S = 10.0$ m, time = 20 min.	356
Table V-76: TC-4 - Ten most likely cases inferred from flooding sensors, $H_S = 10.0$ m, time = 25 min.	356
Table V-77: TC-4 - Ten most likely cases inferred from flooding sensors, $H_S = 10.0$ m, time = 30 min.	357
Table V-78: TC-5 - Ten most likely cases inferred from draft and AIS sensor.	357
Table V-79: TC-5 - Ten most likely cases inferred from flooding sensors, $H_S = 0.0$ m, time = 5 min.	358
Table V-80: TC-5 - Ten most likely cases inferred from flooding sensors, $H_S = 0.0$ m, time = 10 min.	359
Table V-81: TC-5 - Ten most likely cases inferred from flooding sensors, $H_S = 0.0$ m, time = 15 min.	360
Table V-82: TC-5 - Ten most likely cases inferred from flooding sensors, $H_S = 0.0$ m, time = 20 min.	361
Table V-83: TC-5 - Ten most likely cases inferred from flooding sensors, $H_S = 0.0$ m, time = 25 min.	362
Table V-84: TC-5 - Ten most likely cases inferred from flooding sensors, $H_S = 0.0$ m, time = 30 min.	363
Table V-85: TC-5 - Ten most likely cases inferred from flooding sensors, $H_S = 5.0$ m, time = 5 min.	364
Table V-86: TC-5 - Ten most likely cases inferred from flooding sensors, $H_S = 5.0$ m, time = 10 min.	365
Table V-87: TC-5 - Ten most likely cases inferred from flooding sensors, $H_S = 5.0$ m, time = 15 min.	366
Table V-88: TC-5 - Ten most likely cases inferred from flooding sensors, $H_S = 5.0$ m, time = 20 min.	367
Table V-89: TC-5 - Ten most likely cases inferred from flooding sensors, $H_S = 5.0$ m, time = 25 min.	368
Table V-90: TC-5 - Ten most likely cases inferred from flooding sensors, $H_S = 5.0$ m, time = 30 min.	369
Table V-91: TC-5 - Ten most likely cases inferred from flooding sensors, $H_S = 10.0$ m, time = 5 min.	370
Table V-92: TC-5 - Ten most likely cases inferred from flooding sensors, $H_S = 10.0$ m, time = 10 min.	371
Table V-93: TC-5 - Ten most likely cases inferred from flooding sensors, $H_S = 10.0$ m, time = 15 min.	372
Table V-94: TC-5 - Ten most likely cases inferred from flooding sensors, $H_S = 10.0$ m, time = 20 min.	373
Table V-95: TC-5 - Ten most likely cases inferred from flooding sensors, $H_S = 10.0$ m, time = 25 min.	375
Table V-96: TC-5 - Ten most likely cases inferred from flooding sensors, $H_S = 10.0$ m, time = 30 min.	376

*When a coincidence seems amazing, that's because the human mind isn't wired to naturally comprehend probability & statistics.
(Neil de Grasse Tyson, 2014)*

Chapter 1 - Introduction

1.1 Overview and Background²

1.1.1 An Industry in change

Responsible for carrying 90% of the world's trade, the maritime industry is the backbone of the global economy, which has continuously surged over the last half century. This growth has been largely driven by globalisation and the consequent increase in trade. The world is changing fast, and so is the maritime industry. New megaships continue to outsize older designs driven by economies of scale, which offer a competitive edge to ship-owners and operators in an ever-burgeoning market. This inconceivable growth of international trade and the introduction of new technologies mean that the maritime industry risks are evolving. The new giants of the sea and the increasing complexity of on-board systems, advanced technology and their interactions are posing challenges to the maritime industry in terms of new, potentially hidden, risks. We continue to strive towards a safer industry, but is the current, largely rule based regime capable of keeping up with today's immense pace of change? Safety of passenger ships has traditionally attracted considerable attention because of their ever-increasing size, complex subdivision and large number of passengers carried, as is highlighted in Figure 1-1. The relevance of this perspective has lately been strengthened due to the cruise segments constant upsurge since the 2008 recession. To this end, an intensive search for better and more optimal design solutions has emerged in the last few decades, especially following the introduction of risk-based ship design methods (Papanikolaou et al., 2009) and the introduction of safety equivalence and risk-based standards, such as the probabilistic damage stability regulations, outlined in Reg. I/5 and Reg. II-1/6 to 8 of SOLAS, respectively (IMO, 2006). Utilising these methods of risk reduction, numerous means for reaching more optimal and cost-effective designs have been developed through the introduction of risk control options, or safety barriers aimed at either accident prevention, or post-accident mitigation and control.

² Larger parts of this chapter have been published in Karolius K. B., Vassalos D., (2017), "*How to buy time following a flooding incident – intelligent quantification of emergency response measures*", Proceedings of the 16th International Ship Stability Workshop, 5-7 June, Belgrade, Serbia.

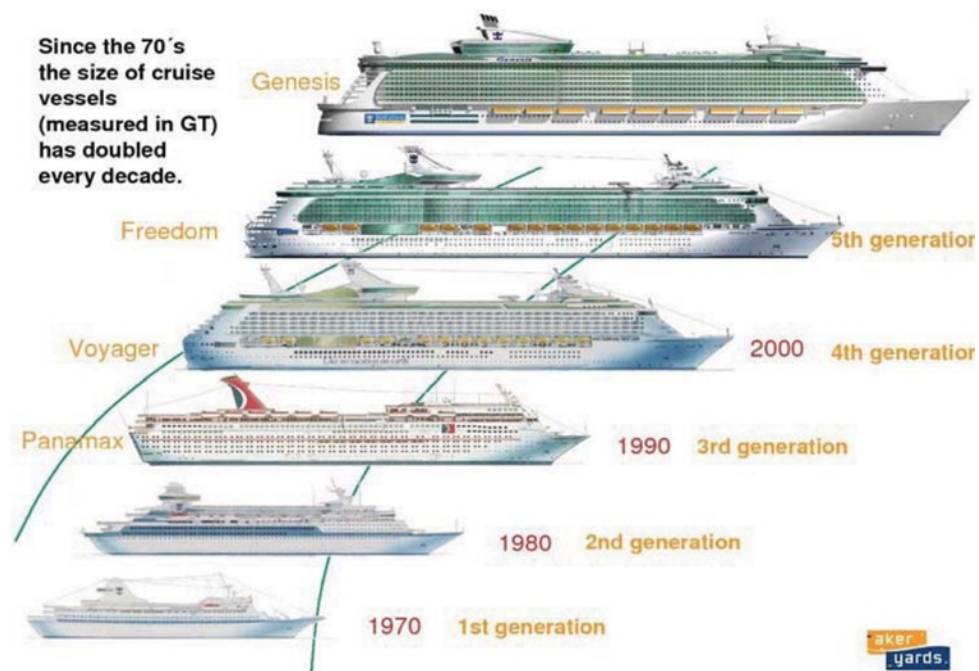


Figure 1-1: Evolution of cruise ship size (Papanikolaou et al., 2013).

Considering hull breach and flooding incidents, development of such measures has primarily focused on survivability and mitigation, rather than prevention. It seems now, however, that the attention has shifted towards research and development of preventative measures, utilising technological advances to a higher extent, as for example in advanced collision avoidance systems, aiming at preventing hull damages altogether (Statheros et al., 2008), (Johansen et al., 2016). This change in focus seems to be driven by emerging trends such as vessel surveillance, connectivity and automation, but also the fact that human cognitive responses in a complex navigational climate is recognised as the *Achilles heel* and primary source of error (Allianz, 2017). Despite this latter shift in focus from mitigation towards prevention, it is the author's belief that there is still a lot of room for improvement in vessel survivability through modernisation and optimisation of the traditional concept of emergency response and damage control by taking full advantage of advances in science and technology. One would assume that the recognised human cognitive shortcomings under normal operational conditions would be even more relevant during complex, high stress emergency incidents, something that previous accidents have confirmed far too often (MIT, 2013).

1.1.2 Risk-informed situational awareness

Safety barriers implemented to reduce flooding risk can roughly be classified as passive means built-in (inherent) to the design such as watertight bulkheads, hull-shape, etc., or as active means, which may relate to processes, people, technology, etc. The latter involves actions undertaken to control a flooding incident, namely emergency response and damage control. Furthermore, some of the built-in barriers need physical activation, e.g., sliding watertight doors, pumps/valves, cross/down-flooding arrangements, etc. and are therefore highly dependent on active means and may require human intervention (e.g. actuation). The interface between the decision-maker and the actual situation is critical: if the decision-maker does not know the full extent or severity of the emergency, the mitigation strategy chosen to manage the response will be inadequate, or ineffective at best. Ultimately, effectiveness of corrective actions depends on the decision-makers real-time information for risk-informed situational awareness and their ability for optimal use of their available knowledge to make timely decisions and implement the right corrective actions.

Numerous studies indicate that a significant proportion of maritime accidents are caused by human error. In flooding incidents, it is difficult for the human mind to comprehend the immensity of the situation, encompassing numerous possible damage states, their water propagation and progressive flooding through pipes, doors and other internal openings and the effects of multiple free surface and motions induced by external forces. A reliable overview of the situation requires considering and determining the state of multiple variables and their interactions, e.g., damage extent, flooding rate, environmental conditions, availability of safety barriers and supporting systems. Due to inherent dynamics of the emergency, the situation may become unmanageable long before the crew will be able to collect all this information, assess the situation and respond to the threat. Even when information is available, it is often scattered, fragmented and highly uncertain, and the ability to take the correct and optimal decisions is limited at best. Most importantly, time is of the essence in emergencies, hence, advanced and robust tools for providing accurate and real-time information for optimal and risk-informed situational awareness on the flooding emergency to support decisions are invaluable.

1.1.3 Time as a measure of risk

Two of the most important variables in flooding incidents involving passenger ships are the *Time to Capsize* (TtC) and the *Time to Evacuate* (TtE) (Vassalos et al., 1998). These concepts are illustrated by the graph shown in Figure 1-2: if the time it takes to evacuate the vessel exceeds the time it takes for the vessel to capsize and sink, loss of human life becomes inevitable. The magnitude of loss (ΔN), proportional to risk, will be closely related to the difference between these times (Δt), but most importantly it can be targeted as a measure of potential improvement.

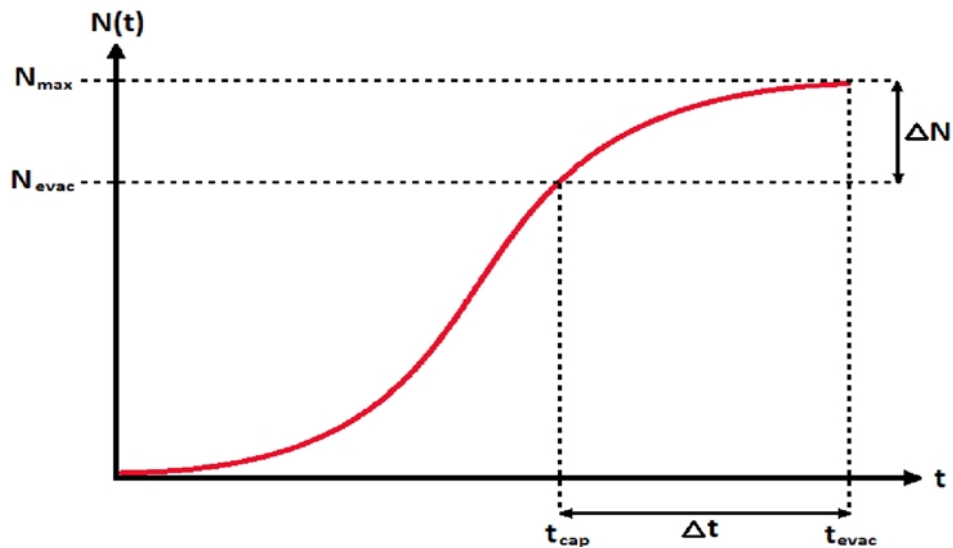


Figure 1-2: Interplay between TtC and TtE. Adapted from Papanikolaou et al. (2009).

Providing better and more accurate information to the crew facilitates decision-making to decrease Δt , so that more lives can be saved in an emergency. In an ideal design, the time to capsize should be long enough in all damage scenarios, and the below inequality should be dogmatic.

$$t_{evacuate} < t_{capsize} \quad \text{Eq. 1-1}$$

But the perfect design, alas, is neither realistic nor economically feasible. We do, however, have a range of resources at our disposal, and providing better tools to improve real-time information in decision making, would make implementation of mitigating actions more timely and targeted, consequently saving more lives.

1.1.4 Life-Cycle risk management

Risk management is a life-cycle process and should entail quantifying the life-cycle risk of a vessel from risk-reduction in design, through managing residual risks in normal operations and finally to crisis-risk-management and emergency response in emergency situations. A generic framework for addressing life-cycle risk systematically are lacking in the maritime industry, stemming from a history of being largely rule-based relying on minimum (often deterministic) standards of safety, thus failing to nurture a more comprehensive risk management framework. For life-cycle flooding risk management, the above-mentioned accident prevention, or post-accident mitigation and control safety measures must be monitored and assessed during all vessel life-cycles ensuring optimal performance in accordance with a minimum acceptable safety-baseline. The risk must be continuously monitored and reviewed against identified Key Performance Indicators (KPI's) to ensure changes in design or operation resulting in deviations from the baseline are adhered to and properly managed, and in the case of a flooding emergency, the various safety barriers are available and working optimally as intended. More comprehensive monitoring would further provide extensive data for feedback and continuous improvement of management and operations and even for future vessel designs.

1.1.5 Advantages in emerging technology

The inherent complexity of the flooding process and the lack of a more comprehensive life-cycle (flooding) risk management framework on large passenger vessels has in recent years been recognised. The availability of more advanced tools has continuously nurtured and supported the idea of a Risk-Based design framework for improved functionality, performance, and novelties in the design stage and throughout operation, while at the same time being risk-informed and therefore improving the safety culture. Similar advancements have also been seen for the emergency phase. The perception of the vessel itself being the best lifeboat has for instance been agreed upon by industry and resulted in attempts to provide new regulatory solutions. In particular, the most recent developments resulted in significant changes in the approach to damage stability and flooding response. Among the pivotal advancements are the IMO's regulations for Safe Return to Port (SRtP) (IMO, 2006). Although the regulations mainly focus on redundancy of on-board systems, they also provide guidance for what should be available for decision making post damage, based on flooding

extent and residual stability. Specifically, SOLAS Reg. II-1/8-1.3 (IMO, 2006) requires that on-board stability loading computers must be capable of providing operational information to the Master for safe return to port after a flooding incident. Moreover, SOLAS Reg. II-1/22-1 (IMO, 2006) requires installation of flooding sensors in watertight spaces below the bulkhead deck. However, a major shortcoming of the IMO requirements is that the SRtP flooding scenarios are deterministic and limited to single watertight compartments. In realistic scenarios and real flooding emergencies, it is essential to determine the actual damage extent and produce a reliable estimate of the time available for safe evacuation and abandonment. Hence, the decision-support tools for emergency flooding management systems must be far more robust than those required by the regulations, and as history has shown, might even be better off if increasingly automated? The research culminating in this PhD dissertation has been directed at the development of a framework where sensor-technology and analytics are utilised to a higher degree, in an attempt to improve risk information and, hence, provide a means for a more comprehensive life-cycle flooding risk management framework for large cruise vessels. The main application presented in this thesis will be within the emergency phase for improved and risk-informed situational awareness in flooding emergencies. Such improvement would result in more optimised, targeted and timely activation of active mitigation barriers prolonging the time available for safe and ordered evacuation and abandonment or even enabling safe return to port. Indeed, staying upright and afloat.

1.2 Aims and objectives

The main aim of the presented research has been to develop and test a framework/methodology for improved real-time information providing risk-informed situational awareness to the vessel crew in flooding emergencies, in particular damage extent and location, following hull breach in a collision incident with reduction of uncertainty stemming from merging probabilistic methods with sensor technology and analytics. Such a framework, utilising probabilistic supportive evidence for quantified decision making, should provide improved survival assessment and enable the crew to implement emergency responses in a timely, targeted and efficient manner. The development will further act as a more comprehensive life-cycle flooding risk management framework for continuous risk monitoring and management to bridge the remaining life-

cycles (design and operation). To achieve this aim, the following objectives have been identified:

1. Present a critical review of relevant topics and literature, identifying how traditional emergency response is executed in a flooding incident and what novel approaches have been proposed for improvement. Finally, the review is intended to identify gaps in the subject matter, which may be addressed by the research output of this PhD study.
2. Utilise sensors and analytics (technology) to reduce uncertainty on collision damage extent, location and related parameters in flooding emergencies. The methodology, based on *Bayesian inference*, will use available statistics as a priori information and sensor data as continuously updated evidence (i.e. sequential updating utilising multi-sensory data fusion techniques). This also entails analysis of the flooding process and damage stability characteristics for identification of the most relevant variables and to develop a priori distributions and corresponding probabilistic likelihood functions applicable to the multi-sensor framework combining state-of-the-art time-domain simulation software tools and available statistics.
3. Test this methodology with the use of currently available sensors onboard ships (sensor layout as built) within flooding emergency response scenarios. To enable testing, the methodology will be coded within a demonstration platform, reading emulated sensor data, and providing sequentially updated information. For testing purposes, time-series from time-domain simulations will be interpreted as actual sensor readings imposed by realistic environmental influences and dynamic responses of a damaged ship.
4. Reduce uncertainty of the prediction of high-risk damage cases. The confidence in prediction can be improved by development of a method for risk-based positioning of flooding sensors (in an attempt to ensure that the remaining uncertainty is transferred away from high-risk cases). The method would help identify critical areas in the design stage, and areas of importance for monitoring during operation and in emergencies.
5. Offer conclusions and recommendations highlighting key findings from the research on application of the probabilistic inference framework for ship survivability in flooding emergencies. Finally, discuss the feasibility for practical implementation of such a framework as a life-cycle flooding risk management framework.

1.3 Outline

The thesis is structured in 11 chapters, and 6 appendices. Each chapter starts with opening remarks aiming to provide some background information on the subject matter. Similarly, closing remarks have been included for summarising the main findings derived in each chapter. For a more orderly presentation, the list of relevant references is included at the end of each chapter in the order they are presented in the text. A number of appendices with supplementary figures and data follows the main body of the thesis. References to relevant appendices are provided throughout the text. The two following sections start by introducing the main statistical tools, which have been utilised in the development and the description of the sample vessel used for implementation and testing. Chapter 2 starts by introducing the most important variables affecting the outcome of a flooding incident with emphasis on collision damage with the intention to provide some context to the problem at hand. The main aim of the chapter is to formulate the problem and to identify the key variables influencing the outcome, for use within this development.

Chapter 3 examines how traditional emergency response is executed in a flooding incident, and what alternative approaches/techniques have been proposed for improvement. Its aim is to identify gaps in the current framework, which may be bridged by the developed framework presented herein. The chapter further includes sections on other uses of sensors and technology in both the maritime industry and other industries comprising concepts and notions for life-cycle risk management using new technology and increased utilisation of sensors. Chapter 4 aims to give a general introduction to uncertainty and probabilistic inference, including a more detailed review of a specific inference technique for uncertainty reduction, namely *Multi-sensor Data Fusion*. The chapter will focus on basic theory, definitions and application. It will also provide an example to illustrate the concept. Chapter 5 through Chapter 7 will each address the variables identified in Chapter 2; relevant to environment, damage extent and the ship response. As the multi-sensor data fusion relies heavily on a priori statistics and likelihood functions, all these chapters will share the same structure consisting of sections presenting the development of a priori probability distributions, derivation of likelihood functions for each relevant variable and presentation of results and examples from implementation as well as testing.

Chapter 8 presents the methodology developed for risk-based positioning of flooding sensors, in an attempt to ensure a reduction of uncertainties by focusing on high-risk damage cases. In Chapter 9, the developed methodology is presented using a schematic diagram, summarising all its components, and making reference to the respective chapters they were introduced in the thesis. The result for the complete implementation of the framework, covering all the variables will be presented in Chapter 10, where results are presented from applying the developed methodology to the range of test damage cases with the existing sensor layout (as built) of the sample vessel. Discussions and recommendations as well as concluding remarks are included in Chapter 11. This final chapter discusses the impact of the probabilistic inference framework on damage survivability of ships and the feasibility of practical implementation for use as a life-cycle flooding risk management framework.

1.4 Tools for Statistical Analysis

A range of statistical tools and methods have been employed to develop the various probabilistic models during the research and they will be covered briefly in the following. Other, generic and engineering, software tools are referenced throughout the text. Most a priori probability distributions and likelihood functions are derived by processing the corresponding datasets in the statistical software *R* (R Core team, 2013), supported by a range of libraries. In addition to the already built-in base functions of *R*, the most significant packages used are the *fitdistrplus*, *copula* and *vinecopula*. The *fitdistrplus* package of *R* is a general package for fitting univariate parametric distributions to continuous censored or non-censored data and discrete data. The package provides means for a variety of estimation methods, such as *maximum likelihood*, *moment matching*, *quantile matching* and *maximum goodness-of-fit* estimation. For the purpose of identifying and fitting distributions in this development, the Maximum Likelihood Estimation (MLE) method has been utilised. A skewness and kurtosis plot such as the one proposed by Cullen & Frey (1999) is provided by the *fitdistrplus* package. The plot displays skewness and kurtosis values for common distributions in order to help the choice of distributions to fit the data. For some distributions (normal, uniform, logistic, exponential), there is only one possible value for skewness and kurtosis. Thus, the distribution is represented by a single point in the plot.

For other distributions, areas of possible values are represented as lines (as for the gamma and lognormal distributions) or areas (as for the beta distribution). More information about the `fitdistrplus` package may be found in Delignette-Muller et al. (2015). The `copula` and `vinecopula` packages provide tools for the statistical analysis of copula models for capturing conditional dependencies between variables (more specifically copula models represent the mathematical relationship between the marginals of a bivariate distribution). Both packages include tools for parameter estimation, model selection, simulation, goodness-of-fit tests and visualisation of copula models. More specific details on the relevant copulas are given in Chapter 6. More theory and general information on copulas may be found in Aas et al. (2009) while the R packages `copula` and `vinecopula` are detailed in Hofert et al. (2017) and Schepsmeier et al. (2018), respectively. The presented methodology entails dynamic real-time update of probabilistic models, coded as a fully working damage stability platform. For the purpose of implementation, the scripting language Python (Python Core team, 2015) has been utilised with a range of libraries, most notably NumPy (Travis, 2006) and SciPy (Jones et al., 2001). Most of the plots and figures presented in the thesis were created with use of Python's library Matplotlib (Hunter et al., 2007).

1.5 Sample vessel

The high-fidelity ship model chosen for the development and testing of the framework is based on a large modern cruise vessel of 100,000 *GT*, currently in operation. The vessel's main particulars are presented in Table 1-1 while the watertight arrangement and current flooding sensor layout in accordance to MSC.1/Circ.1291 (IMO, 2008) is presented in Figure 1-3. In total, the vessel has 52 pneumatic level sensors fitted in dry spaces and a further 94 of the same type located in tanks. The vessel is equipped with four pneumatic draft sensors (one fore, one aft, and two amidships, located at either side). The vessel's internal compartment connectivity comprises a total of 910 openings, covering doors, hatches, etc., as summarised in Table 1-2. The openings are assigned to a range of categories based on their watertightness in accordance with Ruponen & Routi (2011). Furthermore, opening allowance category is specified in accordance with MSC.1/Circ. 1380 (IMO, 2010). The openings are shown in Figure 1-4.

Table 1-1: Sample vessel particulars.

Parameter	Symbol	Value	Designation
Length between perpendiculars	L_{BP}	273.00	m
Breadth	B	36.00	m
Depth	D	21.00	m
Gross tonnage	GT	100,000	m ³
Number of passengers	-	2,800	persons
Number of crew	-	1,050	persons

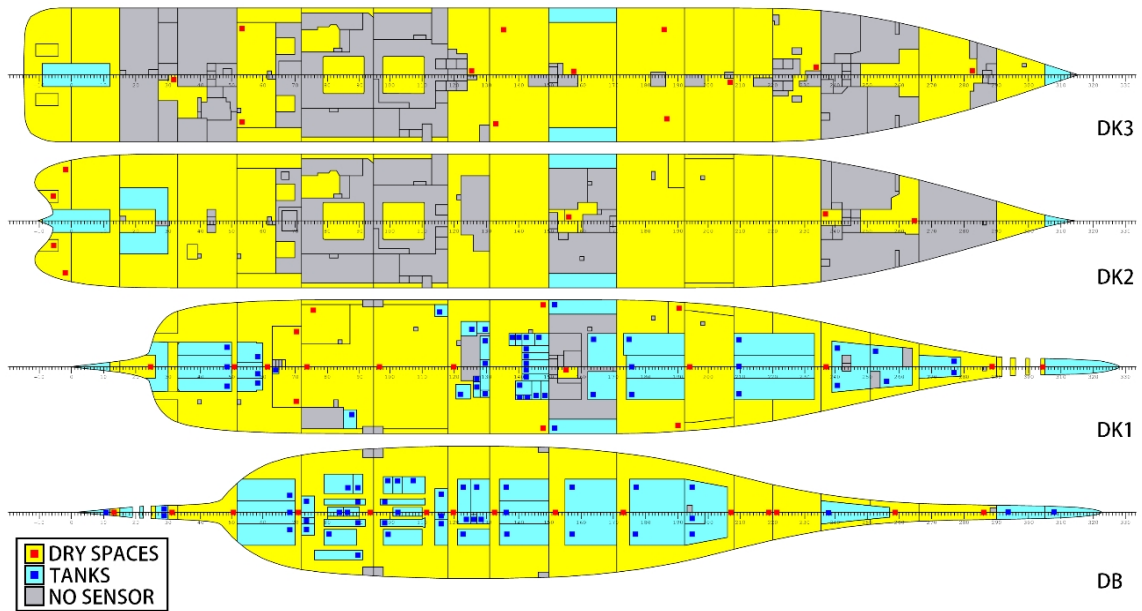


Figure 1-3: Arrangement of flooding sensors according to IMO guideline.

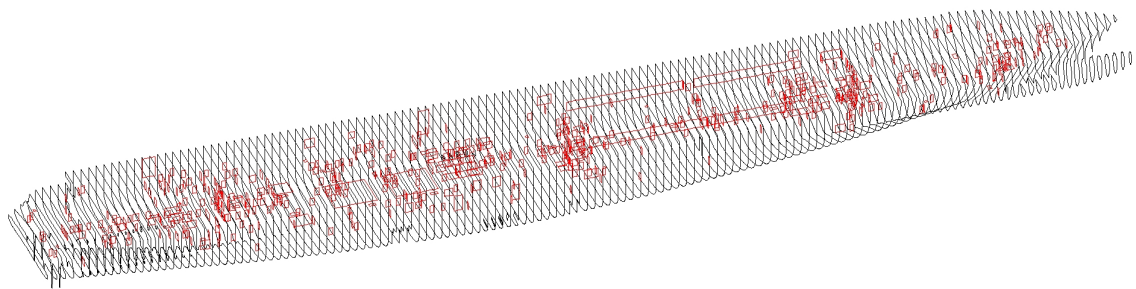


Figure 1-4: Stability model with internal openings.

Table 1-2: Internal openings of sample vessel.

Description	WT category	Ope. Allow. category	No. of Ope.
Sliding watertight door	A1	C	15
Watertight hatch	A1	C	1
Hinged cold room door	A2	NA	9
Hinged provisions room door	A2	NA	18
Sliding cold room doors	A2	NA	3
Sliding light-watertight door	A2	C	4
Sliding provisions room door	A2	NA	9
Sliding semi-watertight door	A2	B	15
Escape hatch	B1	A	15
Hinged weathertight door	B1	A	12
Sliding weathertight door	B1	A	2
Hinged double fire door	B2	NA	49
B-class structure	B3	NA	5
Hinged escape door	B3	NA	54
Hinged non-watertight door	B3	NA	86
Sliding fire door	B3	NA	23
Hinged fire door	B4	NA	286
Sliding lift door	B4	NA	67
Hinged lift door	B4	NA	1
Unprotected doorway or connection	C	NA	236
Sum	-	-	910

1.6 References

Papanikolaou A., Vassalos D., Skjong R., Skovbakke J. J., Jensen J., McGeorge D., (2009), *“Risk-Based Ship Design”*, Springer, Berlin.

International Maritime Organization, (2006), Reg. I/5 and II-1/6 to 8 of *“SOLAS Consolidated Edition 2009”*, as adopted in IMO Res. MSC 216(82)).

Papanikolaou, A., Hamann, R., Lee, B-S., Mains, C., Olufsen, O., Vassalos, D., Zaraphonitis, G., (2013), *“GOALDS - Goal Based Damage Stability for Passenger Ships”*, Conference proceedings of Transactions of the Society of Naval Architects and Marine Engineers (SNAME), January.

Statheros, T., Howells, G., Maier, K., (2008), *“Autonomous Ship Collision Avoidance Navigation Concepts”*, Technologies and Techniques. Journal of Navigation”, 61(1), 129-142.

Johansen A. T., Cristofaro A., Perez T., (2016), "*Ship Collision Avoidance Using Scenario-Based Model Predictive Control*", IFAC - Papers on-line, Volume 49, Issue 23, 2016, Pages 14-21.

Allianz Global Corporate & Speciality (AGCS), (2017), "*Safety and Shipping Review 2017*", Annual review of trends and developments in shipping losses and safety.

Ministry of Infrastructure and Transports (MIT), Marine Casualties Investigative Body, (2012), "*Cruise Ship Costa Concordia, Marine Casualty on January 13, 2012, Report on the Safety Technical Investigation*", Public investigation report.

Vassalos D., Jasionowski A., Dodworth K., Allan T., Matthewson B., & Paloyannidis P., (1998), "*Time-Based Survival Criteria for Ro-Ro Vessels*", RINA Spring Meetings, London.

International Maritime Organization, (2006), Reg. II-1/8-1 of "*SOLAS Consolidated Edition 2009*", as adopted in IMO Res. MSC 216(82)).

International Maritime Organization, (2006), Reg. II-1/8-1.3 of "*SOLAS Consolidated Edition 2009*", as adopted in IMO Res. MSC 216(82)).

International Maritime Organization, (2006), Reg. II-1/22-1 of "*SOLAS Consolidated Edition 2009*", as adopted in IMO Res. MSC 216(82)).

R Core Team, (2014), "*R: A language and environment for statistical computing*", R Foundation for Statistical Computing, Vienna, Austria, Online access: <http://www.R-project.org/>.

Cullen A. C., Frey H. C., (1999), "*Probabilistic Techniques in Exposure Assessment*" 1st edition, Plenum Publishing Co.

Delignette-Muller, M. L., and Dutang C., (2015), "*fitdistrplus: An R Package for Fitting Distributions*", Journal of Statistical Software, February, Volume 64, Issue 4.

Aas, K., Czado, C., Frigessi, A., Bakken, H., (2009), "*Pair-copula construction of multiple dependence*", Insurance: Mathematics and Economics 44(2):182–198.

Hofert M., (2017), "*Package copula*", Online access: <https://cran.r-project.org/web/packages/copula/copula.pdf>.

Schepsmeier, U., Stoeber, J., Brechmann, E. C., Graeler, B., Nagler, T., Erhardt, T., Almeida, C., Min, A., Czado, C. and Hofmann, M., (2018), "*Package VineCopula*", Online access: <https://cran.r-project.org/web/packages/VineCopula/VineCopula.pdf>.

Python Core Team, (2015), "*Python: A dynamic, open source programming language*", Online access: Python Software Foundation. URL <https://www.python.org/>.

Travis E, Oliphant, (2006), "*A guide to NumPy*", USA: Trelgol Publishing, (2006).

Jones E., Oliphant E., Peterson P., et al., (2001), "*SciPy: Open Source Scientific Tools for Python*", Online access: <http://www.scipy.org/>.

Hunter, J. D., (2007), "*Matplotlib: A 2D graphics environment*", Computing In Science & Engineering Vol. 9, No. 3, pages 90-95.

International Maritime Organisation (IMO), (2008), "*Guidelines for flooding detection systems on passenger ships*", MSC.1/Circ.1291, ref. T1/2.04, 9 December.

Ruoponen, P., Routi, A-L., (2011), "*Guidelines and criteria on leakage occurrence modelling*", deliverable D2.2b from work package WP2, from the Integrated Flooding Control and Standard for Stability and Crises Management (Floodstand) research project, funded by the European commission, FP7-RTD- 218532.

International Maritime Organisation (IMO), (2010), "*Guidelines watertight doors on passenger ships which may be opened during navigation*", MSC.1/Circ.1380, ref. T4/3.01, 10 December.

Chapter 2 - Damage Stability and Survivability of Passenger Ships

2.1 Opening remarks

As the presented framework deals with flooding and damage stability, it would be beneficial to provide some context to the problem before delving into more details of the research. To that end, this chapter introduces the variables governing the flooding process and determining the outcome of a flooding incident. Furthermore, although the emphasis is on collision damages, as this has been the focus of this research, the concepts presented and discussed in the following can be readily generalised to any scenario following hull breach and subsequent flooding. The chapter will cover the traditional (i.e. static) approach to damage stability and will present the main physical variables governing vessel stability to which traditional regulations and rule requirements apply. The issue, however, lies in the fact that these variables provide a very limited representation of vessel survivability, particularly if taken in isolation from their main influencing variables. For this purpose, these variables may be divided into main groups according to what part of the problem they are mostly affiliated with. Here, the variables are divided between *Breach- and damage* related variables, *Vessel* variables, and finally *environmental* variables, as detailed in the following sections.

2.2 Traditional approach to damage stability

In the realm of hydrostatics, a vessel's stability is directly related to two main factors, namely its ability to stay afloat, and its ability to return to operational equilibrium position when acted upon by an excitation force. The former is governed by the well-known *Archimedes Principle*, namely the underwater volume and resulting hydrostatic pressure giving rise to the vessels buoyancy, B , while the latter is directly related to the vessel waterplane area, WPA , which decides its metacentric height, KM , and the interplay with the position of the vertical centre of gravity, KG , namely the vessels GM . This is especially true for small heel angles, but for larger heel angles, vessel stability is normally measured using

the well-known GZ curve (righting-lever curve) as the waterplane area tends to change with increased angles of heel. Both GM and the GZ curve play important roles also in dynamic stability. Specifically, the former will determine relative motions between ship and waves and the area under the latter corresponds to the change of potential energy of the ship in response to the excitation. Both GM and the GZ curve have been, and still are, the main parameters being regulated in the intact stability regulations such as the 2008 IS Code (IMO, 2008a). The parameters are easily enhanced in the design phase when, considering that for an intact vessel, they are closely related to vessel beam and vertical centre of gravity, KG . However, when the hull is breached, and part of the internal volume flooded, the ship will sink, heel and trim until a new condition of equilibrium is reached in which reserve buoyancy (i.e. buoyancy above the initial waterline) has been brought into effect to replace the lost buoyancy. Whether or not the reserve buoyancy will compensate for the loss due to flooding depends highly on the vessel internal subdivision and the ability to prevent water propagation from the damaged compartments to other internal compartments (progressive flooding).

The latter is based on the assumption that the ship will survive the initial stages of flooding (transient phase), which is not the case for a large proportion of damage cases in most of the existing ships as well as a significant part of damages even in current newbuildings. This presents a limitation in the current approach as the focus for transient flooding must be on passive protection. If there is sufficient reserve-buoyancy to replace the lost-buoyancy, static equilibrium will be reached with a new heel angle resulting in a change in freeboard, GM and GZ curve characteristics. If the reserve buoyancy is insufficient to compensate for the lost buoyancy the ship will sink, and if GM becomes negative with the vessel upright and with no remaining area under the residual GZ curve when heeled (i.e. GZ curve post damage) the ship will capsize. These facts have led the regulatory framework for damage stability, such as SOLAS Reg. II-1/6 to 8 (IMO, 2006) to continue using such traditional variables, by imposing requirements on the residual GZ curves in a static manner; similarly to intact stability, but post damage (range, max value, etc). However, it will be demonstrated in the following that the processes governing the stability of damaged ships are complex and influenced by a broad range of variables and such complexity cannot be accurately captured by static consideration of simple characteristic parameters such as GM or GZ .

2.3 Breach and damage extent variables

2.3.1 Damage breach

The damage breach represents the geometrical properties of the damage opening connecting the vessel internal space to the sea, resulting from the collision (or grounding/contact) impact. The damage breach is often also termed damage extent. However, in the following a clear distinction will be made between these notions and it will be shown that the damage breach is one of the direct variables influencing the damage extent. The governing variables for the breach size are the geometrical properties as illustrated in Figure 2-1. Such definitions were initially introduced by Lützen (2001, 2002), and have further been developed by Bulian (2011, 2017). Similar definitions for grounding damage have also been introduced by Zaraphonitis et al. (2015). The geometrical properties of the breach comprise size governing variables, namely length, height and penetration depth (designated by L , H and Y respectively) and position governing variables corresponding to longitudinal and vertical position (designated by X and Z respectively) of its origin. Obviously, a real breach is unlikely to be completely regular in shape due to the structural dynamics and mechanics involved in the collision, but these simplifications are necessary to enable the development of related statistics describing the breach geometry as initially introduced by Lützen (2001) and further developed in Chapter 6 of this thesis.

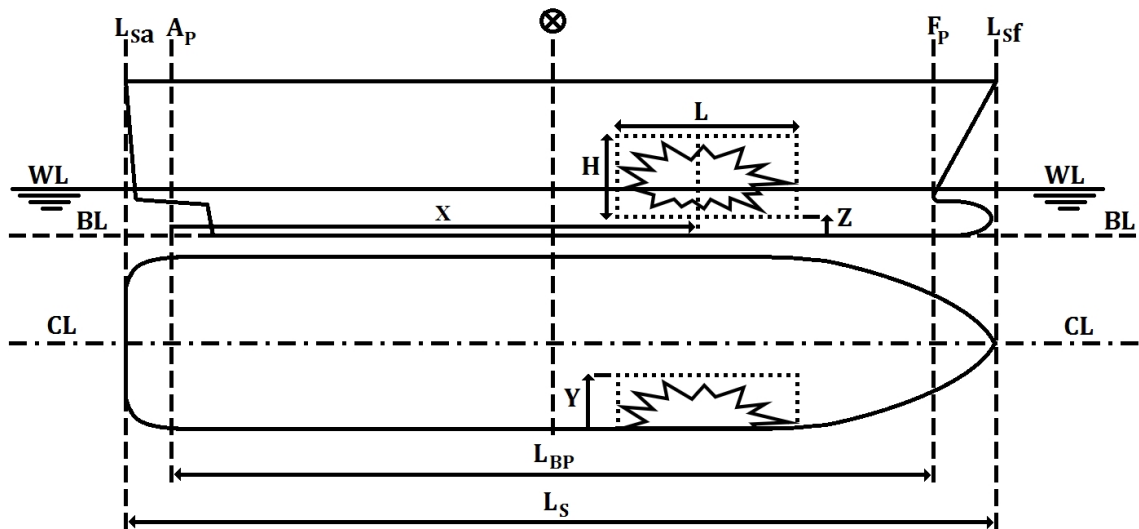


Figure 2-1: Damage breach geometrical properties.

It is clear that the size of the damage breach is among the main variables that will determine the rate of floodwater ingress. Other variables affecting the floodwater ingress rate involve such parameters as draft, wave height etc., as will be discussed in more detail in the following sections. Ingress rate in the first few seconds of flooding is further closely related to the phenomenon of *transient flooding*, which entails excessive heel angle due to the abrupt inflow of large mass of floodwater. Transient flooding have not been included in the present development, simply because if the vessel would capsize in the first few minutes following the breach, use of any operational emergency-response prediction tools would be inconsequential. The breach will further govern which compartments are open to sea and the group of compartments with direct connection to the damage breach is defined as the *initial damage extent*. The compartments forming the damage extent are considered as lost buoyancy even if they are not flooded. The actual boundaries of the initial damage extent are dependent on the vessel's internal subdivision, as a low degree of subdivision will enable smaller breaches to cause large initial damage extent, and subsequent large loss of buoyancy, while high degree of subdivision, will prevent smaller breaches to cause major loss of buoyancy, as illustrated in Figure 2-2. However, exploring singularly this route leads to complex internal subdivision with impact on weight, ergonomony and functionality. Presence of internal openings within the boundaries of the initial extent may lead to the *progressive damage extent*. Initial and progressive damage extents are also termed initial- and progressive-stages of damage in relation with the flooding sequence, where the initial stage would become an origin or source of flooding for the progressive stages. The progressive extent will be discussed in more detail together with the subdivision in the next section.

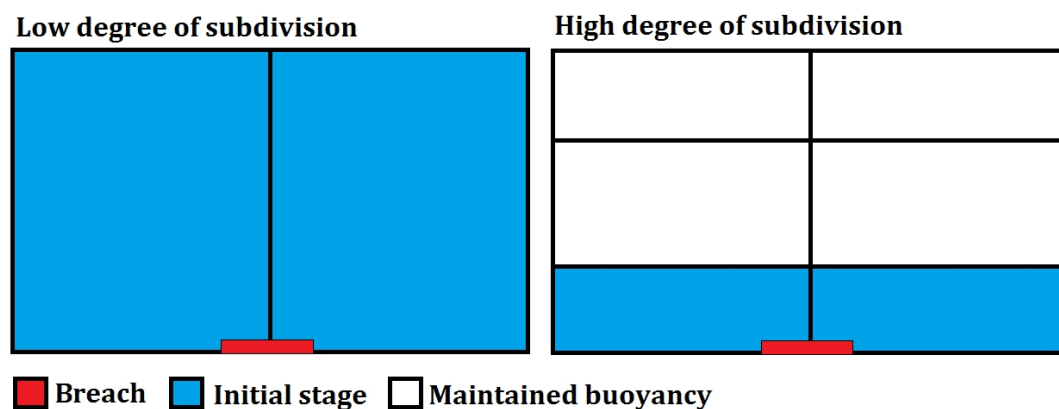


Figure 2-2: Initial stage of damage extent and its dependency on degree of subdivision.

2.4 Vessel variables

2.4.1 Internal subdivision and openings

As discussed in the previous section, the internal subdivision of a vessel will determine how a breach opening will translate into the initial damage extent in terms of lost buoyancy. The internal arrangement comprises a range of internal openings such as ducting, piping, doors, hatches, windows, shafts, etc., connecting compartments between the horizontal and vertical watertight subdivision, which will further influence the flooding progression. This is closely related to opening types and watertight integrity (Watertight, Weathertight, Unprotected), their status (Open, Closed) and their position. This connectivity of compartments is, therefore, highly dynamic, as openings such as doors and hatches may be opened and closed during the operation of the vessel for specific periods of time (opening frequency) or leak or collapse under the floodwater pressure. The possible progression of floodwater through the internal openings gives rise to the progressive damage extent (or stage) as illustrated in Figure 2-3. The progressive extent is often divided in several subsequent stages depending on the sequence of openings being submerged and adjacent compartments progressively flooded.

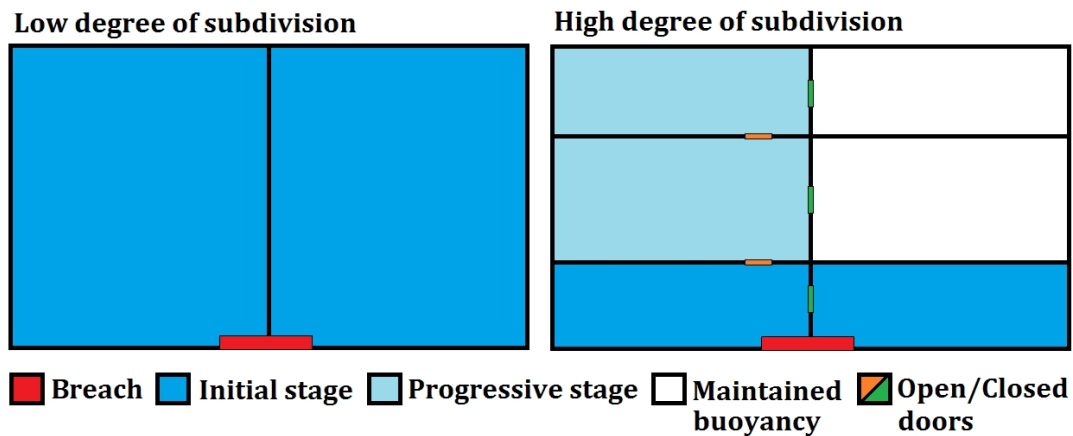


Figure 2-3: Initial and progressive stage of damage dependent on internal opening status.

Requirements for flooding sensors as set forth by SOLAS Reg. II-1/22-1 (IMO, 2006), aim at providing an estimated overview over the damage extent in terms of what compartments are imposed by floodwater, but provide only a limited view as sensors are only required in a limited number of compartments. There is also requirement for sensors on power-

operated sliding watertight doors located in main watertight bulkheads, as set forth by SOLAS Reg. II-1/13-6 (IMO, 2006). However, door status would not necessarily ensure that flooding status is known, as its relative position with respect to the floodwater level within the compartment is generally unknown and compartments without flooding sensors would require inspection by crew. Non-watertight doors (e.g. fire doors) without status sensors could also affect the flooding outcome. They can withstand flooding to a certain degree when closed, but they will be prone to leakage and may eventually collapse due to the build-up of hydrostatic pressure. Opening vulnerability to leakage and collapse is related to the type of closing appliance (opening type) and is governed by the category of watertight integrity. Categorisation of openings and their vulnerability to leakage and collapse has been investigated in the project FLOODSTAND (Ruponen & Routi, 2011), where several full-scale model tests were performed, identifying leak and collapse pressure heads for a range of opening categories. One of the findings of the project (Jalonen et al., 2017) is that the non-watertight doors may withstand pressure heads up to 3.5 m before they collapse. Another issue with the closing appliances on internal openings (particularly doors) stems from the combinatorial element related to their open/closed status as was highlighted in the European project EMSA III (Jasionowski et al., 2015). Assessment of the impact of a single open watertight door on stability led to the observation that, while varying from door to door, the impact was small in comparison with the impact of combinations of multiple open doors. Furthermore, it was recognised that the impact on stability was insensitive to opening allowance category of doors comprising that particular combination. More specifically, an opened door of category C would degrade stability, on average, to similar extent as opening the door of category A. The various opening allowance categorisations as defined in MSC.1/Circ. 1380 (IMO, 2010) are summarised in Table 2-1.

Table 2-1: Opening allowance categories for watertight doors.

Categories	Opening allowance
Category A doors	Permitted to remain open during navigation by the Administration according to SOLAS regulation II-1/22.4 (category removed from MSC.1/Circ.1564).
Category B doors	May be opened during navigation to permit the passage of passengers or crew, according to SOLAS regulation II-1/22.3.
Category C doors	Shall be closed before the voyage commences and shall be kept closed during navigation according to SOLAS regulation II-1/22.1 and II-1/22.6.
Category D doors	Shall be closed before the voyage commences and shall be kept closed during navigation according to SOLAS regulation II-1/22.1.

The combinatorial character of the door status problem results in the immense number of possible combinations, N , increasing exponentially with the number of n doors available, governed by Eq. 2-1 and illustrated in Table 2-2.

$$N = 2^n \qquad \text{Eq. 2-1}$$

From Table 2-2, it is clear that the stability assessment involving all possible combinations of doors is infeasible, thus resulting in the necessity for developing more simplified models, such as the one presented in the EMSA III project (Jasionowski et al., 2015). However, there are a discrete number of possible initial damage extents, and for every one of these, there are also a discrete number of directly connected compartments. This entails that we need to consider only status of doors directly within the boundary of a specific initial damage extent (and all subsequent flooding stages thereafter). This view will help limit the problem as will be demonstrated in Chapter 6.

Table 2-2: Door combinatorics.

Number of doors, n	Number of combinations, N
1	2
2	4
3	8
⋮	⋮
50	1125899906842624
⋮	⋮
98	316912650057057350374175801344
99	633825300114114700748351602688
100	1267650600228229401496703205376

Large cruise vessels have an internal subdivision and compartment connectivity of unparalleled complexity when considering internal floodwater propagation. The heeling moment from floodwater weight requires down- and cross- flooding arrangements in an attempt to lower the damaged vessels KG (increase GM) or to reduce the heeling angle respectively. The complex subdivision also leads to the problem of multiple free surface effects. As the hull is breached, water will rush through various compartments at different levels, and could significantly reduce stability even when the floodwater amount is relatively small.

In principle, the complete flooding process (or evolution) can be divided into these successive stages: *transient*, *progressive* and *stationary* stage. Transient stage, which entails the first seconds following the floodwater ingress through the breach opening may result in large heel angle to the damaged side, particularly when the opening is large, located below the waterline and the inflow area unobstructed. This is followed by the progressive flooding stage, where floodwater progresses from the initial damage extent through various internal openings: unprotected, open or not-closed-in-time or as a result of hydrostatic pressure difference leading to leakage or structural collapse.

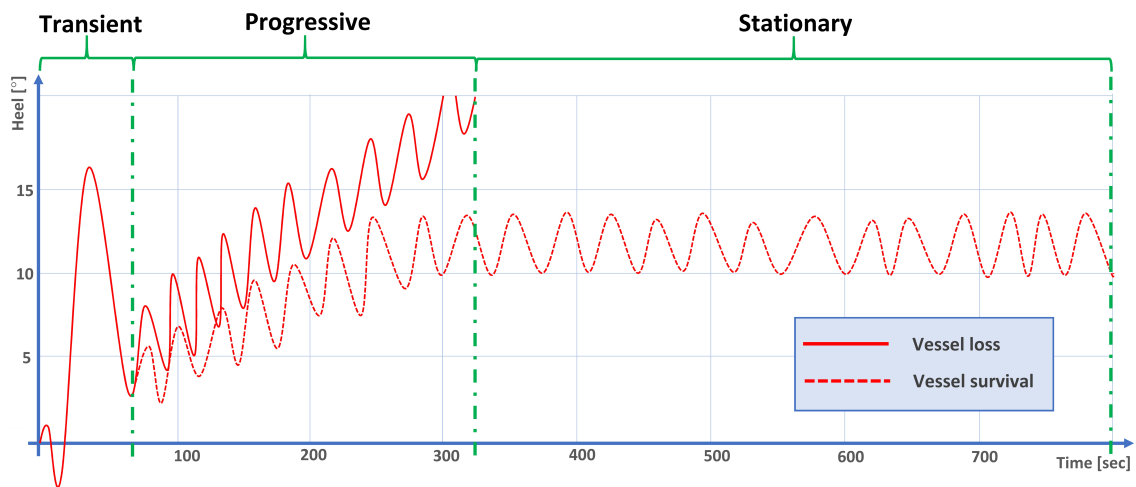


Figure 2-4: Schematic representation of different stages of flooding.

The progressive flooding may be seen as sequence of subsequent flooding stages (or phases) when new openings are being submerged as the vessel heels or sinks due to continuously increasing floodwater mass. This escalation of flooding will continue as long as new openings continue to be submerged and leak or collapse. The vessel will eventually sink or capsize, unless she reaches a new equilibrium without further openings being submerged (or failing) and where the flooding process is contained within the final watertight boundaries. Provided that there is sufficient residual stability and positive buoyancy to withstand the dynamic impact of environmental excitations in the latter case the ship will have reached a stationary state. The various flooding stages are illustrated in Figure 2-4.

2.4.2 Striking and Stricken vessel

A collision is a two-ship incident involving striking and stricken vessels (Lützen, 2001). We must assume that any vessel may take on the role of either striking or stricken and that both may incur hull breach and subsequent flooding. The interplay between the vessels involved will impose the highest influence on the damage breach, and the main influencing variables are those related to the available energy: the direction and magnitude of the related force during impact (energy transfer). Such variables comprise the involved vessel speed, mass and heading as well as structural crashworthiness and specific geometric features, related in particular to the striking vessel bow shape and height. Speed, mass and heading interplay, including bow design geometry is illustrated in Figure 2-5. Substantial work has been done in the area of modelling vessel variable dependency regarding collision damage, such as Pedersen (1999 & 2010), Lutzen (2001), and on vessel crashworthiness, such as Törnqvist (2003) and Paik & Sea (2007). Assessment of vessel crashworthiness often employs advanced Finite Elements Method (FEM) simulations such as Ozguc et al. (2006), Paik (2007a-b), and Prabowo et al. (2017), as illustrated in Figure 2-6.

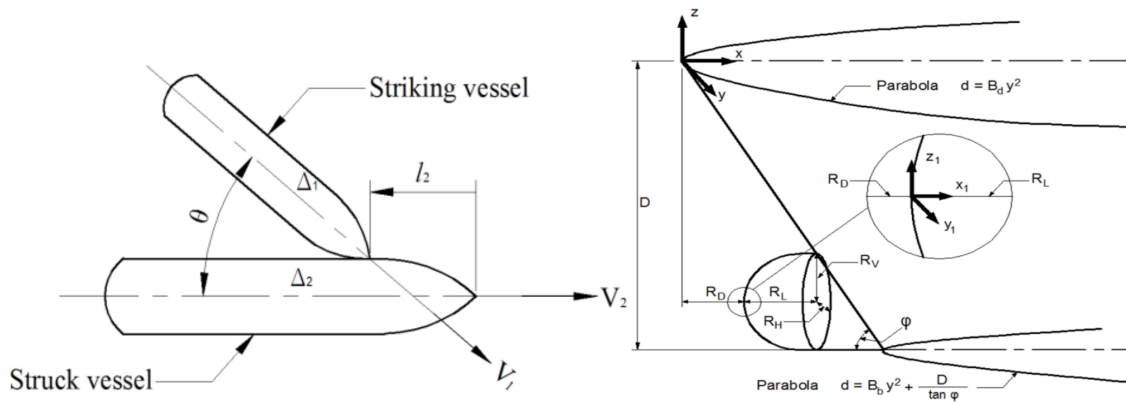


Figure 2-5: Interplay between speed, displacement and heading during collision (left), and bow design geometry (right) (Lutzen, 2001).

Vessel geometry and structural crashworthiness are both design variables, hence in an emergency they are set (invariant) and outside of the operator's control. However, knowing the details of the other ship involved in a collision scenario, namely its displacement, speed, heading, and bow geometry (bow height) would provide a useful indication in the assessment of the size (i.e. extent) of the breach. In most of the cases such information can

be retrieved (at least partly) from Automatic Identification System (AIS) required by SOLAS Reg. V/19 (IMO, 2006), and it would be available to the operators assessing post-collision impact. The AIS information can be incorporated as evidence into the framework of probabilistic sensor fusion to support inference on the damage extent. This approach is discussed in detail in Section 7.3.3 of this thesis.

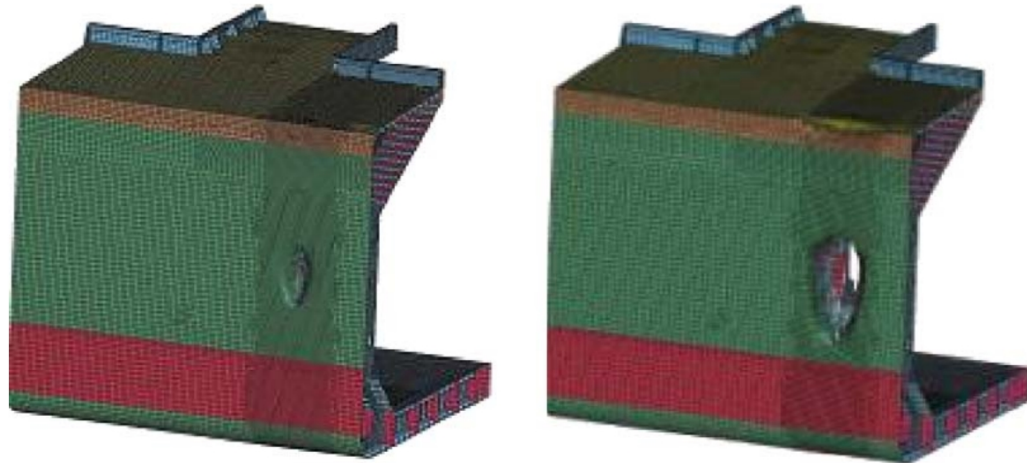


Figure 2-6: Breach (hull deformation) simulated in FEM analysis (Ozguc et al, 2006).

2.4.3 Loading condition

A range of parameters associated with the vessel's loading condition (lightship weight, cargo and tank content) will determine its centre of gravity, CoG (represented by TCG, VCG, LCG), which in combination with the hull-shape will govern the floating position, righting moment and dynamic responses in waves. The floating position in terms of draft, heel and trim will govern the vertical position of the breach opening in relation to the baseline. Considering a collision scenario and the draft alone, the vertical position of the damaged breach would differ between a scenario where the striking vessel were operating in ballast-condition, compared to operating in full-load condition. This is illustrated in Figure 2-7.

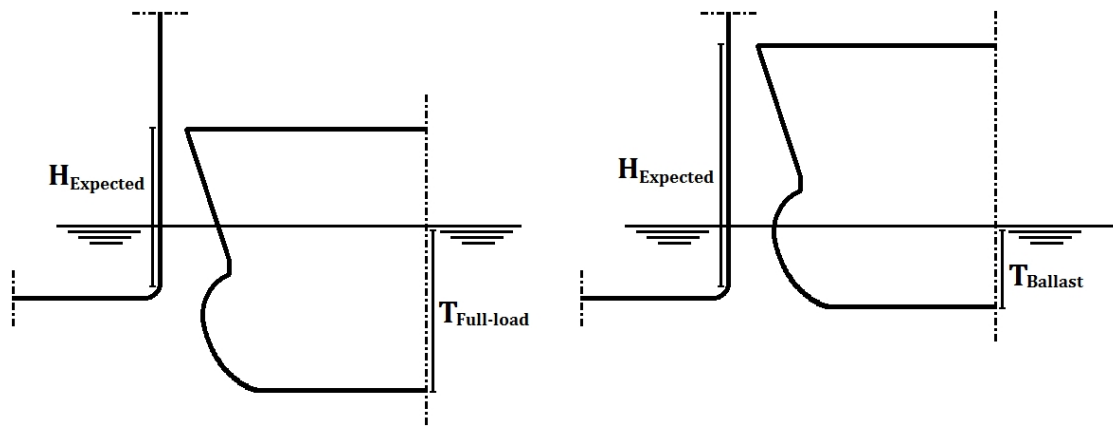


Figure 2-7: Draft influence on expected breach height.

Similarly, this would also apply to the stricken vessel's operating condition. Shallow-draught stricken ships (e.g. cruise ships) are expected to suffer collision damages extending to much lower compartments than the deep-draught ships (e.g. laden tankers). However, cargo ships may not have as many decks below the bulkhead deck. Regardless, knowledge on vessel draft would provide additional supportive information in assessing the vertical damage extent. A vessel's loading condition is known by the operators from the onboard loading computer as required by SOLAS Reg. II-1/8-1.3 (IMO, 2006). Many new designs, such as the sample vessel utilised in this thesis, also have pneumatic draft sensor, which will provide a continuous measure on the vessels draft, heel and trim. The information on vessel draft can, similar to the AIS data, be incorporated into the probabilistic fusion framework to support inference on the vertical damage extent and this is discussed in more detail in section 7.3.3 of this thesis.

2.5 Environment variables

2.5.1 Wind

Wind forces produce drifting motions and induce additional heeling moment. This is especially important for large cruise vessels with large superstructures and a significant wind profile. Wind gust may also, in addition to waves, result in roll angles that may submerge openings located above the calm waterplane. This has been partly accounted for by the IMO weather criterion incorporated in the 2008 IS Code (IMO, 2008b) but remains mandatory only for assessment of intact vessels. The probabilistic damage stability

regulations of SOLAS 2009 Reg. II-1/7-2 (IMO, 2006) only account for the additional wind heeling moment in a static consideration by imposing a wind heeling arm. Although wind forces create considerable heeling moments, they have traditionally not been systematically accounted for when considering a damaged ship. The main reason for this is that in most situations waves and wind are colinear. Hence, in real beam-seas situation (considered to be most severe in waves) the wind force would help resist capsize rather than strengthen the action of waves (Papanikolaou, 2007). Regardless of this intuitive expectation the regulatory framework for damage stability assumes the adverse effect of wind on survivability. Wind sensors (anemometers) are today fitted on all operating vessels, in line with SOLAS Reg. V/5 (IMO, 2006) and provide speed and direction of the wind acting on the vessel. Pneumatic draft sensors would, in providing dynamic floating position (heel and trim), indirectly provide information on the induced wind-moment from its manifestation on the vessel floating position and will be utilised in the presented development.

2.5.2 Wave

Waves, particularly in high sea states, induce complicated, highly non-linear, dynamic responses on a vessel. In damaged condition, they create coupled, complex, dynamic interactions between the waves themselves, floodwater and the damaged ship, affecting vessel survivability. The coupled dynamic interactions with the floodwater will in many cases result in subdued vessel motions due to its added damping and added inertia effects (as in the case of anti-rolling tanks) but may in some scenarios critically impair vessel survivability. The waves will also affect the vessel stability in terms of its righting lever-arm, GZ . As the waves pass the vessel, there will be a dynamically changing underwater volume (and waterplane area), which result in a dynamically changing GZ and subsequently in stability performance. This is illustrated in Figure 2-8 for an intact vessel, nevertheless, highlighting the influence on stability performance from waves. The wave action further increases floodwater ingress by gradually pumping water into damaged spaces and into low-freeboard decks that would not be flooded in calm water, causing multiple free-surface effects and progressive flooding through non-watertight openings, further adding to the complexity of the coupled dynamic interactions.

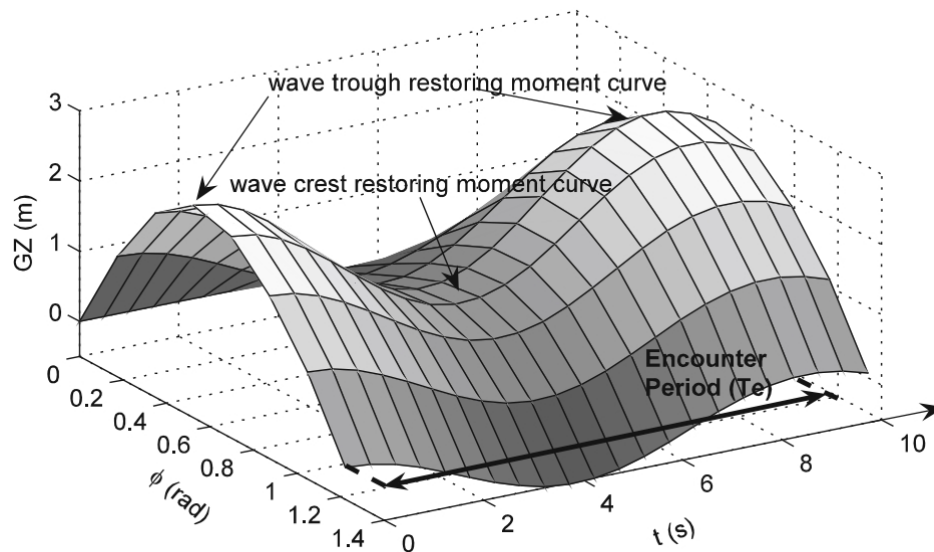


Figure 2-8: GZ variation with respect to time and wave position in head waves (Peşman et al., 2012).

Surface waves are generated by wind and do, in large-scale, depend on it. It is therefore tempting to use wind sensors to gain additional information on the wave environment. The correlation between wind and waves does not necessarily mean that wind measured at the vessel location provide additional information on the observed wave environment. Naturally there are some local dependencies, indicating that measuring strong winds would imply large waves. Observing waves does not thereby mean that there are strong winds in the area, simply because waves may travel thousands of miles and waves observed at the vessel location have been developed by a wind climate or environment some distance from the current vessel location. Local, small-scale, correlations between wind and waves are more difficult to capture than global effects, indicating that wind sensors would not be optimal for making inference about the wave environment. There are other alternatives, such as wave-radars but these are not found on most vessels today. Motion sensors, however, are presently found onboard most vessels and may be utilised, as waves are the main contributor to vessel motions. The sensor observations may be used to support inference about the wave environment as will be discussed in more detail in Chapter 5.

2.6 Variable dependencies

In Figure 2-9, the above introduced variables and their casual dependencies are illustrated in a highly simplified but orderly manner.

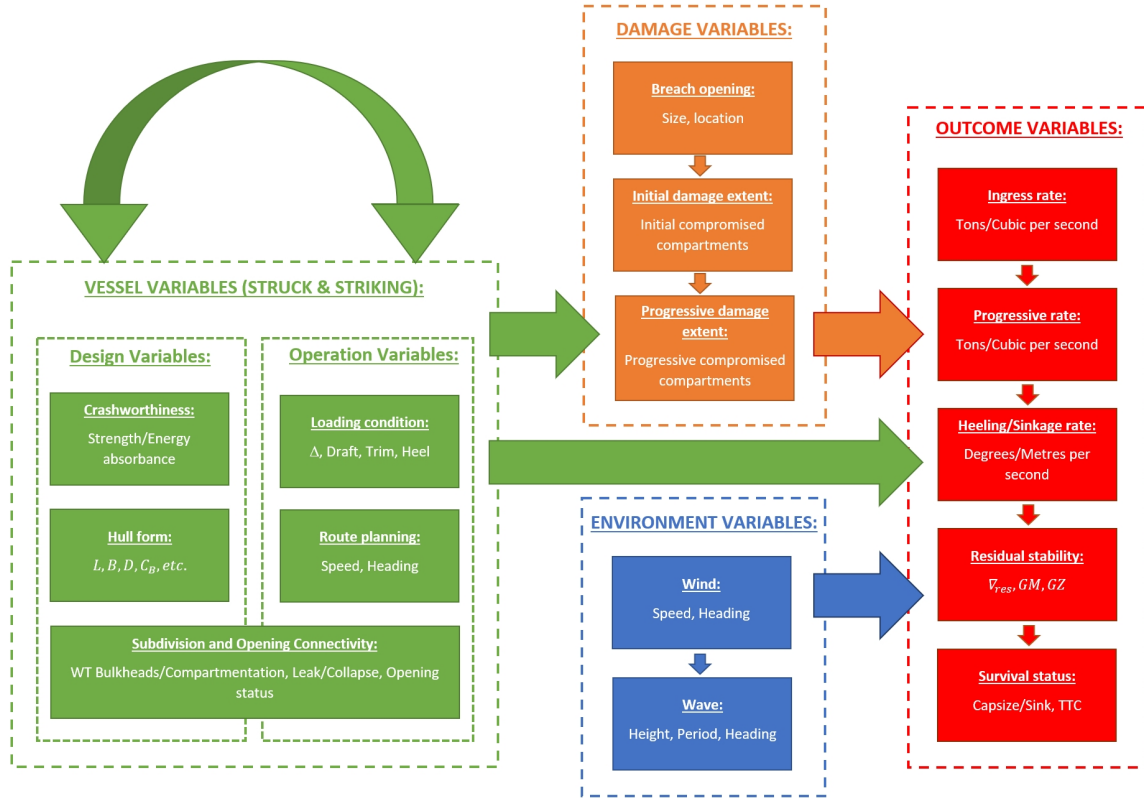


Figure 2-9: High-level causal relationship between flooding variables.

The Damage variables are shown in orange, covering the Breach-opening and the related damage extents (initial and progressive). The environmental variables have been illustrated in blue, covering both Wind and Waves. The response variables are illustrated in red, covering the respective deterioration rates, stability parameters and survival status. The vessel-related variables are illustrated in green and have been divided between Design- and Operation-variables, where the Internal Subdivision and Opening Connectivity are related to both categories, because they are fixed during the design phase, but dynamically change status during the operational phase related to their opening frequencies.

2.7 Time-domain flooding simulations

Traditionally, the consideration of a vessel's damage stability performance has been largely reduced to static assessment of GM , and calm-water GZ for fast and computationally efficient calculations. However, these simplified considerations inevitably fail to cater for all relevant aspects, and critically may undermine safety. Supported by an enhanced understanding of the governing phenomena involved in damage stability and flooding in waves resulting from vast experience following accidents and model-testing, has enabled us to assess the flooding evolution in time-domain capturing also dynamical aspects in greater detail. Time-domain simulations have been used for decades, since the invention of the computer, enabling implementation and solutions to complex problems originating from pioneering work by Newton, Euler, Froude, Stokes, Green, Rayleigh. The benefits have in recent years been augmented due to greater availability and affordability of computational power and efficient algorithms enabling us to solve ever-more complex problems. A range of advanced time-domain simulating computer code that enables the estimation of outcomes post damage have in recent years been developed, such as CAPSIM (Spanos & Papanikolaou, 2001), (Spanos, 2002), IST (Santos, 2003), and FREDYN (Van't Veer & De Kat, 2000), (De Kat & Paulling, 2001).

In the presented development, time-domain simulations of a damaged ship are utilised in order to produce relevant statistics for implementation within the framework. Probabilistic multi-sensor data fusion relies heavily on probability distributions in the form of a priori belief and likelihood functions representing a mapping between the observations made from sensors, and possible states of reality. In this context, time-domain simulations become highly beneficial because it is impossible to collect the required data sets from full-scale flooding tests as this would entail hull breach and possible vessel loss. Furthermore, this would have to be performed for thousands of scenarios in order to generate data-sets suitable for reducing uncertainty as will be discussed in more detail in Chapter 4. The large volumes of data needed also render physical model tests and the more advanced Computational Fluid Dynamics (CFD) infeasible due to high cost and prohibitive computational time. In the development of this framework, the time-domain simulation code PROTEUS3 has been utilised. The details of the underlying physics of the software will not be discussed in this thesis, but for information general evolution of the software can be

found in Turan (1993), Vassalos (1995), Letizia et al. (1995), Letizia (1996), and Jasionowski (2001). The PROTEUS3 model of the sample ship is illustrated in Figure 2-10.

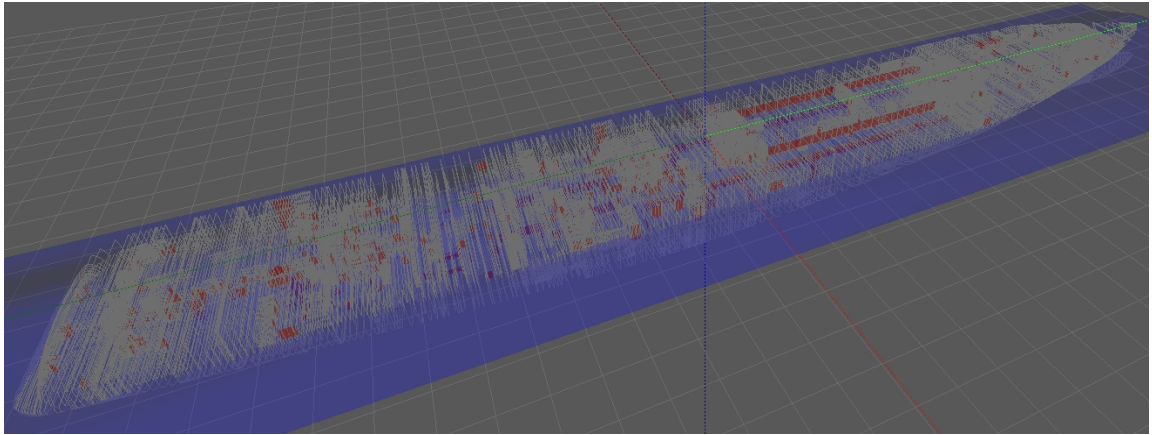


Figure 2-10: PROTEUS3 model with internal openings.

2.8 Closing remarks

In the foregoing sections of this chapter, a comprehensive review of relevant variables involved in a flooding incident has been presented. The emphasis has been on collision damage on large cruise ships, but the presented concepts can readily be generalised into any scenario following hull breach and subsequent flooding on any ship type. It is clear that the problems encountered by the operators in flooding emergencies are not easily comprehensible and supportive tools would be highly beneficial. The reviewed variables have been divided into Breach- and Damage-related variables, Vessel variables, and Environmental variables, a categorisation that will be maintained in the remainder of the thesis. The various variables from each of the categories that have been implemented in the methodology is summarised as follows. For the Breach- and Damage-related variables the breach geometrical properties and available statistics will be assessed, including how the breach translates to the initial extent of damage. The dependency with the vessel variables, in terms of floating position (specifically draft) will be assessed and implemented. It has also been established that the damage extent is traditionally separated between initial and progressive extent (or stages). Such a separation will be maintained in the following development.

Implemented vessel specific variables are for the stricken vessel; internal openings encompassing their status, their leak and collapse pressure heads governing the progressive extent of damage, as well as the vessel loading condition and subsequent floating position. Trim has been disregarded, as large cruise vessels operate on a very narrow trim range but could be readily refined and implemented for future developments. For the striking vessel, an attempt to account for known energy available, governed by the striking vessel's main particulars, provided by AIS data will be presented, utilising available damage statistics. Other design- related variables, such as crashworthiness and internal subdivision in excess of openings has been disregarded simply because they are invariant during operation. For the environment variables, the influence from waves will be the main focus, because the pneumatic draft sensor would, in providing dynamic floating position (heel and trim), indirectly provide information on the induced wind-moment from its manifestation on the vessel floating position.

2.9 References

International Maritime Organization (IMO), (2008a), "*Part A of the International Code on Intact Stability 2008*", as adopted in IMO Res. MSC.267(85).

International Maritime Organization (IMO), (2006), "*Reg. II-1/6 to 8 of SOLAS Consolidated Edition 2009*", as adopted in IMO Res. MSC 216(82)).

Lutzen, M., (2001), "*Ship Collision Damage*", PhD thesis, Technical University of Denmark, Department of Mechanical Engineering.

Lutzen, M., (2002), "*Damage Distributions*", Report No. 2-22-D-2001-01-4 of work package WP2, deliverable D2.2 from the Harmonization of Rules and Design Rational (HARDER) research project, funded by the European Commission, DG XII-BRITE.

Bulian, G., (2011), "*Report detailing derivation of updated probability distributions of collision damage characteristics for passenger ships*", Report No. GOALDS-D-3.1-GL- Collision Damage Characteristics – rev1 of work package WP3, deliverable D3.1 from the GOAL based Damage Stability (GOALDS) research project, funded by the European Commission, FP7-DG.

Bulian, G., (2017), "*Description of geometrical and probabilistic model for collision damage*", report No. eSAFE-WP2D2.1.1, Rev. 1 of work package WP2, deliverable D2.1.1 from the

Enhanced Stability after a flooding event (eSAFE) research project (Joint industry project on Damage Stability for cruise ships).

Zaraphonitis, G., Bulian, G., Lindroth, D., Hamann, R., Luhmann, H., Cardinale, M., Routi A-L., Bertin, R., Harper, G., (2015), *“Evaluation of risk from raking damages due to grounding, Final report”*, report No. 2015-0168, Rev. 2 from the EMSA III research project, funded by the European Maritime Safety Agency, EMSA/OP/10/2013.

Zaraphonitis, G., Bulian, G., Hamann, R., Eliopoulou, E., Cardinale, M., Luhmann, H., (2017), eSAFE-D2.2.1 - *“Description of methodology. Joint Industry Project “eSAFE - enhanced Stability After a Flooding Event” – A joint industry project on Damage Stability for Cruise Ships”*, 29 March (Rev.2).

Kehren, F.-I., Krüger S., (2007), *“Development of a Probabilistic Methodology for Damage Stability regarding Bottom Damages”*, Proceedings of the 10th International Symposium on Practical Design of Ships and Other Floating Structures (PRADS2007), Houston, Texas, USA.

Krüger, S., Dankowski, H., (2009), *“On the Evaluation of the Safety level of the Stockholm Agreement”*, Proceedings of the 10th International Marine Design Conference (IMDC2009), Trondheim, Norway, 26 - 29 May.

International Maritime Organization (IMO), (2006), *“Reg. II-1/22-1 of SOLAS Consolidated Edition 2009”*, as adopted in IMO Res. MSC 216(82)).

International Maritime Organization (IMO), (2006), *“Reg. II-1/13-6 of SOLAS Consolidated Edition 2009”*, as adopted in IMO Res. MSC 216(82)).

Ruponen, P., Routi, A-L., (2011), *“Guidelines and criteria on leakage occurrence modelling”*, deliverable D2.2b from work package WP2, from the Integrated Flooding Control and Standard for Stability and Crises Management (Floodstand) research project, funded by the European commission, FP7-RTD- 218532.

Jalonen R., Ruponen P., Weryk M., Naar H., Vaher S., (2017), *“A study on leakage and collapse of non-watertight ship doors under floodwater pressure”*, Marine Structures 51.

Jasionowski, A., Luhman, H., Bertin, R., Routi, A-L., Cardinale, M., Harper, G., (2015), *“Evaluation of risk from watertight doors”*, report No. 2015-0167 Rev 7 from the EMSA III research project, funded by the European Maritime Safety Agency, EMSA/OP/10/2013.

International Maritime Organisation (IMO), (2010), MSC.1/Circ. 1380, *“Guidance for watertight doors on passenger ships which may be opened during navigation”* Ref. T4/3.01.

Pedersen, P. T., Zhang, S., (1999), *“Collision Analysis for MS DEXTRA”*, Paper number (2) SAFER EURORO Spring meeting, NANTES 28 April.

Pedersen, P., (2010), *“Review and application of ship collision and grounding analysis procedures”*, Marine Structures 23, 241–262.

Törnqvist, R., (2003), *“Design of Crashworthy Ship Structures”*, PhD thesis, Technical University of Denmark, Department of Mechanical Engineering.

Paik, J. K., Sea, J. K., (2007), *“A method for progressive structural crashworthiness analysis under collisions and grounding”*, Thin-Walled Structures 45, 15–23.

Ozguç, O., Das, K. P., Barltrop, N., (2006), *“A comparative study on the structural integrity of single and double side skin bulk carriers under collision damage”*, Marine Structures 18.

Paik, J. K., (2007a), *“Practical techniques for finite element modelling to simulate structural crashworthiness in ship collision and grounding (Part I: Theory)”*, Ships and Offshore Structures, 2(1) 69-80.

Paik, J. K., (2007b), *“Practical techniques for finite element modelling to simulate structural crashworthiness in ship collision and grounding (Part I: Verification)”*, Ships and Offshore Structures, 2(1) 81-85.

Prabowo, A. R., Bahatmaka, A., Cho, J. H., Sohn, J. M., Bae, D., M., Samuel, S. Cao, B., (2017), *“Analysis of structural crashworthiness on a non-ice class tanker during stranding accounting for the sailing routes”*, International Congress of the Maritime Association of the Mediterranean - IMAM 2017, Lisbon, Portugal.

International Maritime Organization, (2006), *“Reg. V/19 of SOLAS Consolidated Edition 2009”*, as adopted in IMO Res. MSC 216(82)).

International Maritime Organization, (2006), "*Reg. II-1/8-1.3 of SOLAS Consolidated Edition 2009*", as adopted in IMO Res. MSC 216(82)).

International Maritime Organization (IMO), (2006), "*Reg. II-1/7-2 of SOLAS Consolidated Edition 2009*", as adopted in IMO Res. MSC 216(82)).

International Maritime Organization (IMO), (2008b), "*Part A Ch.2.3 of the International Code on Intact Stability 2008*", as adopted in IMO Res. MSC.267(85).

Papanikolau, P. A., (2007), "*Review of Damage Stability of Ships Recent Developments and Trends*", Proceedings 10th Int. Symposium on Practical Design of Ships and Other Floating Structures (PRADS) 2007 Houston, October.

International Maritime Organization, (2006), "*Reg. V/5 of SOLAS Consolidated Edition 2009*", as adopted in IMO Res. MSC 216(82)).

Peşman, E., Taylan, M., (2012), "*Influence of varying restoring moment curve on parametric roll motion of ships in regular longitudinal waves*", Journal of Marine Science and Technology 17: 511–522.

Spanos, D. and Papanikolaou, A., (2001), "*On the Stability of Fishing Vessels with Trapped Water on Deck*", Journal Ship Technology Research-Schiffstechnik, Vol. 48, September.

Spanos, D., (2002), "*Numerical Simulation of Flooded Ship Motions in Seaways and Investigation of the Behaviour of Passenger/RoRo Ferries*", PhD Thesis, National Technical University of Athens, School of Naval Architecture and Marine Engineering.

Santos, T.A., Soares, G.C., (2003), "*Investigation into the Effects of Shallow Water on Deck Ship Motions*", Proceedings of the 8th International Conference on Stability of Ships and Ocean Vehicles, Madrid, Spain.

Van 't Veer R. and DeKat J.O., (2000), "*Experimental and Numerical Investigation on Progressive Flooding and Sloshing in Complex Compartment Geometries*", Proceedings of the 7th International Conference on Stability for Ships and Ocean Vehicles, STAB 2000, Vol. A, Launceston, Tasmania, February, pp. 305-321.

DeKat J.O., Paulling J.R., (2001), "*Prediction of extreme motions and capsizing of ships and offshore vehicles*", Proceedings of the 20th International Conference on Mechanics and Arctic Engineering, Rio de Janeiro, Brazil, June.

Turan, O., (1993), "*Dynamic Stability Assessment of Damaged Passenger Ships using a Time Simulation approach*", PhD Thesis, Strathclyde University, NAOME, Glasgow, UK.

Vassalos, D., (1995), "*Capsize Resistance Prediction of a Damaged Ship in a random Sea*", Transactions RINA, Vol. 137.

Letizia L., Vassalos D., (1995), "*Formulation of a Non-Linear Mathematical Model for a Damaged Ship with Progressive Flooding*", International Symposium on Ship Safety in a Seaway, Kalingrad, Russia, May.

Letizia L., (1996), "*Damage Survivability of Passenger Ro-Ro Vessels Subjected to Progressive Flooding in a Random Sea*", PhD Thesis, Strathclyde University, NAOME, Glasgow, UK.

Jasionowski, (2001), "*An Integrated Approach to Damage Ship Survivability Assessment*", PhD Thesis, Strathclyde University, NAOME, Glasgow, UK.

Chapter 3 - Emergency Response – Traditional and Novel Approaches

3.1 Opening remarks

As the main application of the developed framework has been on emergency response, the following chapter presents a critical review of the literature and topics addressing the main challenges outlined in the introduction on real-time information for situational awareness and outcome prediction in flooding emergencies. The chapter is divided into three sections, starting with the traditional way the emergency response is executed on board of a cruise ship. This includes techniques such as damage control and mitigation, review of the relevant rules and regulations as well as emergency response services provided by class or other third-party organisations. The ensuing section discusses innovations in emergency response. In particular it addresses case-based reasoning for decision support, measuring and monitoring ship's vulnerability to flooding and breach detection. The section concludes with the review of the virtual environment for decision support. The last section is presenting the review of use of sensors and sensor-based technologies in other industries comprising concepts and notions for life-cycle risk management. The review is based on the premise that emergency response may be defined as an implemented approach, effort or action intended to mitigate the impact of a hazardous incident on the public and the environment. For example, the UK government have included the following general definition of emergency response in their non-statutory guidance document accompanying the Civil Contingencies Act of 2004, Emergency Response and Recovery (UK Gov, 2013):

“Emergency Response encompasses the decisions and actions taken to deal with the immediate effects of an emergency. It is the decisions and actions taken in accordance with the strategic, tactical and operational objectives defined by emergency responders....”

The implemented approach or efforts can be taken by various stakeholders or emergency responders at various points in time, e.g. within seconds by the vessels crew, within minutes by rescue service agencies, or even hours and days by other governmental agencies,

insurance companies and the ship-owner organisation. The former is more hands-on mitigation actions for reducing the severity of the outcome, while the latter can be more in the form of plans made and actions taken for reconstruction and rehabilitation of involved parties following an emergency as well as mitigation of media coverage and public outcry. In this thesis, the application of the framework is on the immediate actions by the crew following a damage and subsequent flooding incident, and on the support providing the information necessary for timely and correct decisions and actions.

3.2 Traditional flooding emergency response

3.2.1 Damage control and mitigation

Emergency response in ship flooding incidents have traditionally been focused on damage control actions, which are, according to the Oxford dictionary, defined as an:

“Action taken to limit the damaging effects of an accident or error”.

In a flooding scenario, these comprise containing or controlling the flooding process to limit or mitigate the severity of the outcome by either, enabling the ship to survive and return safely to port, or in detaining the flooding progression to allow for safe and orderly evacuation. This involves implementation and activation of the various built-in safety barriers and, therefore, is highly dependent on active means and responses ensuring integrity of the watertight subdivision, i.e. watertight compartmentation and boundary management. According to a range of onboard damage control plans for large cruise vessels investigated during the research, including recommendations developed by the Cruise-Chip-Safety-Forum (2016), normal procedures would involve closing immediately all watertight, light- and semi-watertight doors and hatches and emergency closing valves. Propulsion should be stopped, but only after giving considerations to navigational circumstances such as positioning of the vessel in relation to wave/wind heading. Assessment of availability of critical systems, such as electrical generation, propulsion, steering and thrusters, navigational equipment and all safety systems are crucial. Responding personnel, or damage control teams, should be mustered to inspect the damaged area to assess the situation in terms of number of compartments compromised, flooding rates and possible escalation of the emergency. However, before any personnel can enter the suspected compromised area, the power supply to the area in question needs to be shut down.

Continuous sounding of tank levels (manual sounding for cross reference with sensors) and updating the stability calculations by the onboard stability software is important to assess criticality of intermediate progressive flooding stages and to predict the stationary state equilibrium in the final stage of flooding. Once the situation is evaluated with a reasonable confidence, active mitigation procedures may be implemented, such as activating of drop-down hatches for down-flooding of floodwater for increasing damaged GM , and opening cross flooding valves for reducing induced heeling moments. Bilge pumps should be started for discharging floodwater overboard and ballast system used for transferring liquids in order to improve residual stability (counter ballasting), keeping in mind possible implications on hull strength. To improve residual stability and reduce impact of free surfaces cruise vessels are also recommended to drain all swimming pools. The stability assessment should be a continuous process following implementation of new mitigating measures, but a final survivability assessment and decision for possible evacuation (or even vessel beaching) needs to be eventually taken, as evacuation and abandonment of thousands of persons takes time. It is evident that the flooding emergency response, as traditionally implemented onboard a vessel, is a labour intensive and largely manual process, easily permitting human misjudgement or error that might have severe consequences. High-level situation assessment is often based on subjective interpretation of the available fragmented information, thus cringing to a checklist mentality where detailed situation-specific consideration is essential might worsen the situation and it is important to understand that any corrective action could aggravate the situation if implemented based on wrongful assumptions.

3.2.2 Rules and Regulations

Legislation regulating flooding emergency response mostly impose documentation requirements. Damage control often refers to the Damage Control Plans (DCP) and Damage Control Booklets (DCB) required to be onboard vessels by Reg. II-1/19 of SOLAS (IMO, 2006). These documents intend to provide the crew with information on the vessel watertight compartmentation and the equipment maintaining watertight boundaries in the event of hull breach and flooding. This information enables the crew to prevent further deterioration of the situation and to take effective action to mitigate and, where possible, recover loss of buoyancy and stability. The content of DCP/DCB is specified in the appendix

to the explanatory notes of SOLAS (resolution MSC.429(98)) (IMO, 2017). The DCP should be permanently exhibited or readily available on the navigation bridge, in the control station and, in case of cargo ships, in the cargo control room, the ship office or other suitable location. In addition to damage control plans, the damage control booklet containing relevant information, should be made available to ship officers. Both documents should be provided in the working language of the ship and official language of the SOLAS Convention if this is different from the working language on board. As both documents are ship-specific they must be approved by the administration or the classification society acting on its behalf. The content of such onboard documentation is detailed in IMO MSC/Circ. 919 *Guidelines for Damage Control Plans* (IMO, 1999) for vessels constructed before 2009-01-01, and IMO MSC.1/Circ. 1245 *Guidelines for Damage Control Plans and Information to the Master* (IMO, 2007) for vessels constructed on or after 2009-01-01.

Passenger ships over 120 m in length (or having three or more main vertical zones) and constructed on or after 2010-07-01 have to demonstrate compliance with the IMO regulations adopted by MSC.216(82) and referred to as *Safe Return to Port* (SRtP) (IMO, 2006). The SRtP regulations set the functional requirement for safety-critical systems, following flooding or fire casualties. Flooding detection systems with flooding sensors in watertight spaces below the bulkhead deck are required by SOLAS Reg. II-1/22-1 (IMO, 2006) and they can be used to estimate the damage extent. However, the sensor layout requirements by the current IMO regulations as set out in guidance note MSC.1/Circ.1291 (IMO, 2008), apply to compartments above a certain size, i.e. those that either have a volume in cubic metres larger than the vessel moulded displacement per centimetre immersion (at deepest subdivision draught), or have a volume in excess of 30 cubic metres. Arguably, the geometrical properties of the compartments alone form insufficient criteria for the positioning of the flooding sensors for the accurate monitoring of flooding process and estimating survivability during flooding casualties and Chapter 8 will demonstrate that criticality of a compartment cannot be captured by size alone. In addition to the requirements for documentation, software and flooding sensor positioning, there are further regulations detailing drills for damage control teams, as specified by SOLAS Reg. II-1/19-1 (IMO, 2017), aiming at essential training of vessel crew.

3.2.3 Emergency Response Service

It has become more customary for the major classification societies (and other third parties) to offer so-called emergency response expert services. Such services provide the ship -owner and operator with technical support in the critical period after a vessel has been involved in an incident that may affect its stability or structural strength. The services enable access to technical and analytical resources of in-house experts and tools. Their assistance normally covers calculation of damage stability and structural strength and may also include routing to nearest repair facilities. The Emergency Response Service started in the early 90's, following the adoption of MARPOL 73/78 Annex I, which requires, in accordance with Resolution MEPC.117 (52), Regulation 37.4 (IMO, 2017), that all oil tankers of 5,000 tons deadweight or more shall have prompt access to computerised, shore-based, damage stability and structural strength calculation tools. The U.S. Coast Guard OPA 90 in 33 CFR 155.240 for oil tankers and offshore oil barges (U.S. Gov., 1990) have an identical requirement in force since 21 January 1995 for vessels operating in U.S. waters. The requirement entails that access to the shore-based calculations program must be available 24 hours a day. Furthermore, the ISM Code, Section 8, (IMO, 2018) requires the company to establish procedures (including the use of drills and exercises) to respond to potential emergency shipboard situations.

Emergency Response Services provided by class can be a valuable resource in augmenting emergency preparedness programmes as required by the ISM Code. Although enrolling the vessel to a damage response service is compulsory for tanker operators, owners of other vessel types have realised the benefits from such services. For example, the classification society DNV GL offers such a service (ERSTM)³, which they started operating in 1992 with initial focus on oil tankers. Since then, the number of vessels and offshore units registered has been growing continuously and now it exceeds 4,000 vessels. The majority, about 60%, of the enrolled ships are tankers and container ships, however, the remaining 40% of enrolled vessels are evenly split amongst other ship types, i.e. bulk carriers, gas carriers, cruise and RoRo ships as well as offshore drilling units and FPSO's.

³ Similar services offered by ABS is called Rapid Response Damage Assessment (RRDA).

Most of the services follow similar process, namely during the response, the ship computer model is updated according to actual load distribution while draft and damage information are reported by the operators via phone or radio communication to the shore station. This enables in-house experts to assess the situation and provide recommendations with regard to the course of actions. The involvement of the shore-based experts not affected directly by the stressful situation at hand brings obvious benefits and increases chances of taking the correct decision. Furthermore, the stability and strength computer models available at the ERS can often be more detailed than their on-board counterparts. The ERS may also have at their disposal design plans and drawings of the vessel which are more extensive than the documents available onboard the vessel, which may provide additional support in the decision making. There are, however, obvious drawbacks to this approach. Despite the service providing a 24- hour watch all year round, there will be a minimum response time. Contact must be established, then information on the situation would need to be communicated, and consequently the shore-based support may be provided too late in an extremely time-critical situation. Furthermore, an overview of the situation based on second-hand information from the remote source may be fragmented, inaccurate and somewhat biased (subjective). For this reason, emergency response service is intended solely to support the decision-making process whereas ultimate responsibility for the decisions taken resides with the vessel operators.

3.3 Innovation in flooding emergency response

Recent years have seen significant developments in computational tools for use in onboard emergency response, especially following the introduction of loading computer software tools such as NAPA (NAPA, 2019) and ShipLoad (Kongsberg Maritime, 2019). There have also been developed more advanced time-domain simulation computer codes enabling estimation of outcomes post damage, as mentioned in Chapter 2. However, these are not yet fully commercialised and used as onboard emergency response assessment tools to the same extent as the static loading computer software. This is mainly because they may require considerable computational effort (and hence time), which may be unavailable in already time-critical situations. The computational overheads can be reduced by introducing various simplifications, but these will increase uncertainty in the outcome estimates. To be able to predict the future, we need to know the present, and to be able to estimate the

flooding evolution with the required degree of confidence we rely on accurate prediction of the initial damage. The importance of this fact is well recognised across the industry and resulted in a range of developments that will be reviewed in the following.

3.3.1 Case-based reasoning decision support

Ölcer and Majunder (2006) have suggested a case-based reasoning decision support method using pre-calculated damage cases. Each of these damage cases has corresponding counter-flooding advice for maximising the residual freeboard and stability. The method comprises searching the database for finding the overall closest match (identified with use of closeness function) to the real damage case and providing decision support based on the case that is the closest match. The variables used in the closeness function include damage location, floating position and survivability index. It is, however, not specified how these variables can be estimated by the crew for an actual flooding scenario. The method reflects door status (open/closed) in the pre-calculated cases but does not account for all their combinations of open/closed, rather either open, closed or intermediate status. The method is highly dependent on the pre-calculated cases, and their sampling density as identifying the closest case necessarily do not mean the actual case. The method is also deterministic and does not reflect variability nor uncertainties, and no dynamic influences, such as from wind and waves has been accounted for.

3.3.2 Operational flooding vulnerability measure

Jasionowski (2010, 2011) proposes a method presenting to the crew an overall measure of vulnerability to flooding. The author's reasoning is that knowledge of real-time risk is vital within the first minutes following the loss of watertight integrity but can be even more effective before the actual crisis occurrence, as to allow the crew to act ahead of the anticipated casualty. The method, therefore, aims at informing the crew in real-time on the current vulnerability state of the vessel during normal operation aiming at increasing their vigilance in specific operations, taking into consideration actual loading conditions, environment and the actual watertight integrity conditions, i.e. watertight door status. Vulnerability is measured as the probability that a vessel might capsize within a given time when subject to any feasible flooding scenario. The method is not case specific since the vulnerability is related to the expected outcome from all possible damage cases. It does,

however, provide a visual guidance highlighting the potentially critical cases enabling the crew to act (e.g. close the highlighted door) or monitor closely specific locations within the vessel and to improve their day-to-day management and operation to reduce vessel vulnerability to flooding.

3.3.3 Breach detection from floodwater inflow-rate

Napa Ltd initially presented an approach for estimation of damage size and location using floodwater ingress-rate readings from flooding sensors (Penttilä et al., 2010). The method presented utilises a quasi-static approach, attempting to determine the breach by matching progressive flooding simulation parameters to the measured result from flooding sensors. The method, described in more detail in (Ruponen, 2007) is based on the conservation of mass and Bernoulli's equation with semi-empirical discharge coefficients assigned for each opening. The results of breach detection demonstrate good match with the actual breach but are limited to small, single compartment damages only. It is also shown that the accuracy of such approximations depends strongly on sensors' density and arrangement and the authors recommend optimisation of sensors' layout for improved precision. Furthermore, the study does not include large hull breaches, and are limited to $0.01 - 2.0 \text{ m}^2$.

An improved approach for flooding prediction on-board a damaged ship is presented in Ruponen et al. (2012, 2015 & 2017). Similar to the earlier method, it utilises, level sensors and quasi-static simulations, but it also accounts for status of watertight doors and ship floating position to better capture progressive flooding. The breach detection method is simplified to be less time-consuming, modelling each measured flooding as a separate breach to sea, assuming each breach extends from deck-to-deck. The validation studies include one full-scale trial showing that the method captures accurately floating position during the progressive flooding and in final equilibrium, but it overestimates the time-to-flood compared with the real cases. Furthermore, it excludes the possibility of undetected flooding and impact of waves. In the more recent incarnation of the tool, Ruponen et al. (2015) introduce a colour coding for use in the user interface for simple pictorial way of presenting the situation and its severity to the crew. The graphical reporting method is backed by interviews with ship officers of large cruise vessels, and the applied colour coding is in line with the proposed method for assessing and communicating the safety status of vessels in maritime distress situations, namely Vessel TRIAGE (Nordström et al. 2016).

Deterministic nature and sole reliance on flooding sensors means that the estimation method is limited to breaches located below waterline. This implies that the compartments lying above the flooded waterplane which could form part of the initial damage extent (breach), would not be considered as a part of the damage until the upper part of the breach is submerged. This, obviously, also depends on whether there are flooding sensors fitted in the upper deck rooms. The authors further consider positioning of the sensors and influence on breach detection and clearly highlight the need for use of level sensors rather than limit switches for accurate breach estimation. They also emphasise the importance of sufficient sensor density for accurate and fast survivability assessment within their framework. It is noteworthy that their (i.e. Napa) involvement in the EU project FLOODSTAND (Jalonen et al., 2012) a few years earlier resulted in improved recommendations for positioning of flooding sensors (IMO, 2014). In short, these guidelines recommend two flooding sensors in each watertight compartment, one on each side of the ship to ensure fast detection.

3.3.4 Virtual environment for decision support

Varela et al. (2004, 2007, 2011, 2014 & 2015) present a virtual environment for improved decision support, focusing on interactive virtual three-dimensional (3D) presentation to the operators for simulating and visualising flooding or fire emergencies. The model is intended to assist the operator in emergencies to coordinate damage control teams by displaying the 3D visualisation of internal subdivision for an intuitive and clear representation. The method considers progressive flooding by implementing the algorithm based on the quasi-static Pressure Integration Technique (PIT) for the calculations (Santos et al. 2001, 2002), similar to that of NAPA. The authors reason that the interaction and close-to real behaviour of the virtual objects in the modelling framework has a major advantage over the drawings, or even to 3D Computer Aided Design (CAD) models for reviewing state of the emergency and ship condition in real-time emergencies. However, for a large cruise vessel this may prove difficult due to the size and complexity, given that the necessary computational capability of the system was demonstrated on medium-sized naval vessels. Furthermore, the demonstrator does not account for sensor type nor positioning, and requires a manually reported breach size from the operators, relying heavily on their subjective assessment of the damage extent. The implementation is a visualisation platform rather than flooding prediction tool and seems, therefore, more suitable for emergency response training.

3.4 Other uses of sensors and technology

3.4.1 Maritime industry

Advancements in digitalisation of the industry offer unprecedented opportunities for use of (big) data from sensors. In addition to more traditional systems (Radar, AIS, GPS, Autopilot) for computer aided and automated navigation, there are, more recently introduced, digital platforms for performance monitoring, remote diagnostics and maintenance, predictive analytics, automation and autonomy. Performance monitoring may comprise a range of monitoring regimes, such as general voyage monitoring of the vessel's operational modes, and exposed weather conditions. More detailed monitoring may involve engine and on-board systems performance monitoring covering diagnostics (pressures, temperatures, frequencies, etc.), fuel consumption and emissions. The two latter also relate to hull and propeller performance monitoring (e.g. fouling). Detailed monitoring of systems performance is essential for Condition-Based Maintenance (CBM), where Key Performance Indicators (KPI's) based on the monitoring of actual condition of components are used to plan for (preventive) maintenance of critical systems as opposed to the maintenance based on periodic inspections (Lazakis et al., 2016).

One of the fields developing particularly fast relates to the operation of autonomous and remotely controlled ships and there have been several industrial projects seeking to pilot the implementation of such technologies, e.g. DNV GL (2018). In spite of the fast development, autonomous-, and especially unmanned- vessels, is still an immature field where new ideas and technical solutions still are being introduced and tested to meet the societal expectations, particularly with regard to safety. Moreover, the progressing digitalisation and implementation of new emerging technologies mean that the ships become increasingly connected not only internally but also externally to the outside environment through ship-to-shore connections. This increasing connectivity raises the question of ship cyber security (Direnzo et al., 2015), a problem never before seen in the maritime industry. Another concept emerging is the digital-twin, which takes the technological advances and data harvesting techniques to the next level, by creating a high-fidelity digital model of a vessel in an attempt to manage the assets risk through its life-cycle.

The historical data and continuous sensor updates are employed to mirror the operational life of the actual ship by its digital twin (Ludvigsen et al., 2016). The digital twin concept incorporates many of the techniques discussed above. Another application where the sensors play important role is associated with the concept of safety barriers. It was already discussed in the foregoing chapters that in complex designs various safety barriers are introduced to monitor and efficiently manage risk. However, in order to ensure the efficiency of barrier elements their condition has to be supervised throughout the life-cycle of a vessel. The suitable, and relatively new (for the maritime industry), process set up to undertake the task is known as Dynamic Barrier Management (DBM). Similar to the concept of CBM, DBM aims at continuous monitoring and management of safety critical barriers by utilising sensor measurements and analytics to assess and detect degradation and deviation from required (and accepted) safety-baseline (Astrup et al., 2015). It will be evident throughout this thesis that the developed framework herein is highly commensurate with the philosophy behind DBM utilising sensor technology to monitor safety barriers and related variables, focusing on active and passive flooding barriers, and would therefore be appropriate for use as a life-cycle flooding risk management framework.

3.4.2 Other industries

Other industries have longer and more extensive history of utilising sensor technology for real-time information as well as reducing and managing risk in a more comprehensive manner, e.g. NASA's Real Time Mission Monitor (RTMM) (Blakeslee et al., 2007). Another good example is the use of safety systems in cars, where system surveillance and autonomy have become a standard (Eskandarian, 2012). The car industry has also adopted the digital-twin, for example Siemens utilised its lifecycle management software to create digital-twins for Maserati (Austin-Morgan, 2017). According to Siemens, utilising data from both the real and digital vehicles to optimise the development processes, resulted in drastic reductions in production cost and time for Maserati. In Germany, the digital twin is actually required by the regulators of wind-farm turbines (FGW, 2016a-b) and a manufacturer must provide a validated simulation model in the form of a digital-twin before the delivery of a turbine. The U.S. Air Force is currently piloting the use of a digital-twin in its acquisition process (Warwick, 2015).

They intend to maintain development of a digital-twin during the design and construction stage so the fully developed digital-twin is delivered together with the physical product. The main aim is to enable to use sensor data from the physical asset, imposed on the digital-twin model, to evaluate risk throughout its life-cycle. In spite of the fact that the offshore oil and gas industry is closely related to the maritime industry it has been managing its assets and risks very differently. While traditionally the maritime industry preferred the passive (built-in) safety measures, the oil and gas industry has been more inclined to follow more pro-active approaches (PSA, 2018). A great example is the concept of Dynamic Barrier Management, which originated from the offshore oil and gas industry and was later recognised and adopted in the maritime industry as being suitable for life-cycle risk management.

3.5 Closing remarks

The above review demonstrates that the traditional emergency response is a labour intensive and largely manual process, prone to human misjudgement or error that might lead to severe consequences. The tools supporting the emergency response focus mainly on controlling and containing the flooding process. However, in the lack of proper situational assessment the process under control is rather hypothetical and may be significantly different from the actual one. This may result in implementing suboptimal (in the best case) or even utterly wrong mitigation measures. In the latter case the action intended to improve the situation may in fact worsen it. The legislative framework regulating the emergency response specifies mostly the documentation requirements rather than the responses themselves. Third party emergency response services can certainly provide second opinion free from the bias caused by the stress of the situation at hand. However, obvious drawbacks to this approach comprise its minimum response time and reliance on second-hand information and would clearly benefit from having direct access to relevant sensor measurements rather than relying singlehandedly on the operators (biased) perception.

A range of more innovative approaches has been reviewed, aiming for improved flooding emergency response. It is identified, however, that those are either too generic in providing an overall risk vulnerability covering all possible cases rather than the actual case being realised (limited to the operational phase, e.g. Jasionowski (2010, 2011)), or completely

deterministic not catering for any of the natural variability of such a stochastic problem (limited to emergency phase, e.g. Ruponen et al. (2012, 2015 & 2017)). Finally, we have covered how technology has been emerging and utilised in the maritime industry on a range of areas, and how other industries have been doing so for some time. Using lessons learned from other industries and taking advantage of the growing ranges of methods in utilising the rapidly increasing amount of data generated on vessels provide great opportunities for more cost-effective and safe operations, and the means to develop and adopt a more comprehensive life-cycle risk management framework also in the maritime industry. The challenges ahead lie in persuading the maritime industry to abandon their current trend in keeping data in proprietary silos, and rather move towards data-sharing and data-transparency, benefitting the industry as a whole.

3.6 References

UK Gov, (2013), *“Emergency Response and Recovery”*, Non-statutory guidance document accompanying the Civil Contingencies Act of 2004, Revised version October.

Cruise Ship Safety Forum (CSSF), (2016), *“Damage Stability and Survivability: Operational measures to enhance survivability in case of flooding”*, CSSF Recommendation 311/2016.

International Maritime Organization (IMO), (2006), *“Reg. II-1/19 of SOLAS Consolidated Edition 2009”*, as adopted in IMO Res. MSC 216(82)).

International Maritime Organisation (IMO), (2017), *“Revised Explanatory Notes to the SOLAS Chapter II-1 Subdivision and Damage Stability Regulations”*, as adopted by Res. MSC.429(98).

International Maritime Organisation (IMO), (1999), *“Guidelines for Damage Control Plans”*, MSC/Circ.919 15 June, Ref. T1/3.02.

International Maritime Organisation (IMO), (2007), *“Guidelines for Damage Control Plans and Information to the Master”*, MSC.1/Circ.1245 29 October, Ref. T1/2.04.

International Maritime Organisation (IMO), (2006), *“Amendments to the International Convention for the Safety of Life at Sea”*, Resolution MSC.216(82) adopted 8 December.

International Maritime Organization (IMO), (2006), *“Reg. II-1/22-1 of SOLAS Consolidated Edition 2009”*, as adopted in IMO Res. MSC 216(82)).

International Maritime Organisation (IMO), (2008), *“Guidelines for Flooding Detection Systems on Passenger Ships”*, MSC.1/Circ.1291 9 December, Ref. T1/2.04.

International Maritime Organization (IMO), (2017), *“Reg. II-1/19-1 of SOLAS Consolidated Edition 2009”*, as adopted in IMO Res. MSC 421(98)).

International Maritime Organisation (IMO), (2017), *“Reg. Annex I/5/37.4 of MARPOL Consolidated Edition 2017”*, as adopted by res. MEPC.117(52), 2004.

U.S. Government, (1990), *“The Oil Pollution Act of 1990 (OPA)”*, (101 H.R.1465, P.L. 101-380), Code of Federal Regulations (annual edition), Title 33 – Navigation and Navigable Waters, Part 155 – Oil or Hazardous Material Pollution Prevention Regulations for Vessels, Section 155.240 – Damage Stability Information for Oil Tankers and Offshore Oil Barges, adopted 1. July 2006.

International Maritime Organisation (IMO), (2018), *“Reg. A/8 of ISM Code Consolidated Edition 2018”*, as adopted by res. A.741(18), 1993.

Napa Ltd, (2019), *“NAPA Loading Computer Software”*, <https://www.napa.fi/software-and-services/ship-operations/napa-loading-computer/> (accessed 14-04-2019).

Kongsberg Maritime, (2019), *“ShipLoad Loading Computer Software”*, <https://www.kongsberg.com/maritime/products/tank-gauging-and-measurment-systems/loading-and-stability-systems/shipload-loading-computer/> (accessed 14-04-2019).

Ölçer, A.I., Majumder, J., (2006), *“A Case-based Decision Support System for Flooding Crises Onboard Ships”*, Quality and Reliability Engineering 22(1): 59 – 78, February.

Jasionowski, A., (2010), *“Decision Support for Crisis Management and Emergency Response”*, Proceedings of the 11th International Ship Stability Workshop, Wageningen Netherlands.

Jasionowski, A., (2011), *“Decision support for ship flooding crisis management”*, Ocean Engineering 38, 1568–1581.

Penttilä P., Ruponen, P., (2010), *“Use of Level Sensors in Breach Estimation for a Damaged Ship”*, 5th International Conference on Collision and Grounding of Ships, Espoo, Finland.

Ruponen, P., (2007), *“Progressive Flooding of a Damaged Passenger Ship”*, PhD thesis, Helsinki University of Technology, Department of Mechanical Engineering, Ship Laboratory, Espoo.

Ruponen, P., Larmela, M., Pennanen, P., (2012), *“Flooding Prediction Onboard a Damaged Ship”*, Proceedings of the 11th International Conference on the Stability of Ships and Ocean Vehicles 23-28 September, Athens, Greece.

Ruponen, P., Lindroth, D., Pennanen, P., (2015), *“Prediction of Survivability for Decision Support in Ship Flooding Emergency”*, Proceedings of the 12th International Conference on the Stability of Ships and Ocean Vehicles 14-19 June, Glasgow, UK.

Ruponen, P., Pulkkinen, A., Laaksonen, J., (2017), *“A Method for Breach Assessment Onboard a Damaged Passenger Ship”*, Applied Ocean Research 64, 236-248.

Nordström, J., Goerlandt, F., Sarsama, J., Leppänen, P., Nissilä, M., Ruponen, P., Lübcke, T., Sonninen, S., (2016), *“Vessel TRIAGE: A Method for Assessing and Communicating the Safety Status of Vessels in Maritime Distress Situations”*, Safety Sciences 85, 117-129.

Jalonen R., Ruponen P., Jasionowski A., Maurier P., Kajosaari M., Papanikolaou A., (2012), *“FLOODSTAND - Overview of Achievements”*, Proceedings of the 11th International Conference on Stability of Ships and Ocean Vehicles, STAB2012, Athens, Greece, pp. 819–829.

International Maritime Organization (IMO), (2014), *“Guidelines for Flood Sensor Placement and Technical Requirements”*, SDC2/INF.6, submitted by Finland.

Varela, J. M., Santos, T. A., Guedes Soares, C., 2004, *“Visualization and Control of a Flooding Simulation Onboard Using a 3D Virtual Environment”*, Proceedings of the Congress on Computational Methods in Engineering (CMCE 2004), 31 May - 2 June, Lisbon, Portugal.

Varela, J. M., Guedes Soares C., (2007), *“A virtual Environment for Decision Support in Ship Damage Control”*, IEEE Computer Graphics and Applications, 27(4): 58-67.

Varela, J. M., Cacho, A. J., Guedes Soares C., (2011), *“Virtual Environment for Simulation and Study of Maritime Scenarios”*, In book: Marine Technology and Engineering (Vol. 1) Publisher: Taylor & Francis Group Editors: C. Guedes Soares, Y. Gorbato, N. Fonseca, A.P. Teixeira.

Varela J. M., Rodrigues J. M., Guedes Soares C., (2014), "*On-board Decision Support System for Ship Flooding Emergency Response*", ICCS 2014, the 14th International Conference on Computational Science, Vol. 29, 1688-1700.

Varela J. M., Rodrigues J. M., Guedes Soares C., (2015), "*3D simulation of ship motions to support the planning of rescue operations on damaged ships*", ICCS 2015, the 15th International Conference on Computational Science, Vol. 51, 2397-2405.

Santos, T. A. and Guedes Soares, C., (2001), "*Ro-Ro Ship Damage Stability Calculations Using the Pressure Integration Technique*", International Shipbuilding Progress, 48(2): 169-188.

Santos, T. A., Winkle, I. E. and Guedes Soares, C., (2002), "*Time Domain Modelling of the Transient Asymmetric Flooding of Ro-Ro Ships*", Ocean Engineering, 29: 667-688.

Lazakis, I., Dikis, K., Michaels, A. L., Theotokatos, G., (2016), "*Advanced Ship Systems Condition Monitoring for Enhanced Inspection, Maintenance and Decision Making in Ship Operations*", Transportation Research Procedia, Vol. 14, 1679-1688.

DNV GL, (2018), "*The ReVolt: A new inspirational ship concept*", Online article: <https://www.dnvgl.com/technology-innovation/revolt/> (accessed 12-02-2019).

Direnzo, J., Goward, D. A., Roberts, F. S., (2015), "*The Little-Known Challenges of Maritime Cyber Security*", Proceedings of the 6th International Conference on Information, Intelligence, Systems and Applications (IISA).

Ludvigsen, K. B., Jamt, K. L., Husteli, N., Smogeli, Ø., (2016), "*Digital Twins for Design, Testing and Verification throughout a Vessel's Life-Cycle*", Conference: COMPITAt: Lecce, Italy, May.

Astrup O. C., Wahlstrøm, A., King, T., (2015), "*A framework Addressing Major Accident Risk in the Maritime Industry*", Proceedings of the World Maritime Technology Conference, U.S. – SNAME.

Blakeslee, R., Hall, J., Goodman, M., Parker, P., Freudinger, L., He, M., "*The Real Time Mission Monitor - A Situational Awareness Tool for Managing Experiment Assets*", NASA Science Technology Conference (NSTC2007), June 19-21.

Eskandarian, A., (2012), "*Handbook of Intelligent Vehicles*", Book: Springer-Verlag London Ltd., ISBN: 978-0-85729-084-7.

Austin-Morgan, T., (2017), "*Maserati has fused cutting-edge digitalisation methods with Italian passion to meet customer demand*", EurekaMagazine, October 2, Online article: <http://www.eurekamagazine.co.uk/design-engineering-features/interviews/maserati-has-fused-cutting-edge-digitalisation-methods-with-italian-passion-to-meet-customer-demand/161332/> (accesses 01-01-2019).

Fördergesellschaft Windenergie und andere Erneuerbare Energien (FGW), (2016), "*Technical Guidelines for Power Generating Units and Systems – Demands on Modelling and Validating Simulation Models of the Electrical Characteristics of Power Generating Units and Systems*", Part 4 (TG 4).

Fördergesellschaft Windenergie und andere Erneuerbare Energien (FGW), (2016), "*Technical Guidelines for Power Generating Units and Systems – Certification of the Electrical Characteristics of Power Generating Units and Systems in Low-, Medium-, High and Extra-High Voltage Grids*", Part 8 (TG 8).

Warwick, G., (2015), "*USAF Selects Lead Programs For 'Digital Twin' Initiative*", Aviation Week & Space Technology, Januar 26, Online article: <https://aviationweek.com/technology/usaf-selects-lead-programs-digital-twin-initiative> (accesses 01-01-2019).

Norwegian Petroleum Safety Authority (PSA), (2018), "*Integrated and Unified Risk Management in the Petroleum Industry*", Risk Management Memorandum.

Chapter 4 - Probabilistic Inference and Multi-sensor Data Fusion

4.1 Opening remarks

Use of probabilistic methods for managing and reducing uncertainty is an important part of the framework presented in this thesis. The notion of uncertainty, its main types and relevant definitions will be introduced in the first section 4.2. Although, any detailed coverage of general probabilistic methods is outside the scope of the thesis, probabilistic inference will be briefly introduced in the second section 4.3 in order to provide some context and background. For more detailed information on probabilistic methods, reference is made to literature such as Chung (2000), DeGroot & Schervish (2019) and Feller (1968). A third section 4.4 covers basic theory, definitions and application of multi-sensor data fusion techniques, including relevant probabilistic definitions and axioms. For this purpose, main definitions have been adopted from Durant-Whyte & Henderson (2016). The development of a priori distributions and likelihood functions (sensor models) for each of the variables covered in Chapter 2 are detailed in Chapter 5 through Chapter 7.

4.2 Uncertainty

Traditional approaches recognise two main categories of uncertainty, namely *aleatoric*, and *epistemic* uncertainty (Schweder & Hjort, 2016). The terms aleatoric-variability and epistemic-uncertainty, or simply *variability* and *uncertainty*, are also used for the respective categories (Bitner-Gregersen et al., 2012) and will be adopted in the following due to their more intuitive and descriptive character. The variability (aleatoric – alea – Latin – the game of dice) concerns the inherent randomness of the variables describing a stochastic process. This is a natural property of the population or system that we are modelling due to the systems stochastic nature, and it is simply an effect of chance, e.g. the variability of wave loads on a vessel and subsequent vessel movements over time. It is not possible to reduce variability through further data collection because it is a natural property of the variable in question and is always there. The uncertainty (epistemic – Greek – knowledge) can be

reduced by further data collection and represents our level of knowledge about the system being modelled. Typically, we may be uncertain about parameters being used in a model (probability distribution) of the system. Uncertainty may have a range of sources, such as measurement or precision uncertainty (measurement error) or data uncertainty (number of samples or lack thereof). DNV GL has in their *Guideline for Offshore Structural Reliability Analysis* (Skjong et al., 1995) classified the epistemic uncertainty as follows:

- Measurement Uncertainty: *Uncertainty due to imperfection of an instrument used to register a quantity.*
- Statistical Uncertainty: *Uncertainty due to limited information such as a limited number of observations of a quantity.*
- Model Uncertainty: *Uncertainty due to imperfections and idealisations made in physical model formulations as well as in choices of probability distribution types for representation of uncertainties.*

Combination of variability and uncertainty is known as the total uncertainty where some proportion stem from the range of uncertainties and some from the natural variability of the system. Since variability and uncertainty are very different, they ought to be modelled separately, e.g. knowing the extent to which an estimate is uncertain can help identify gaps in information and target future data collection. Both categories can, however, be described by probability distributions as is illustrated in Figure 4-1.

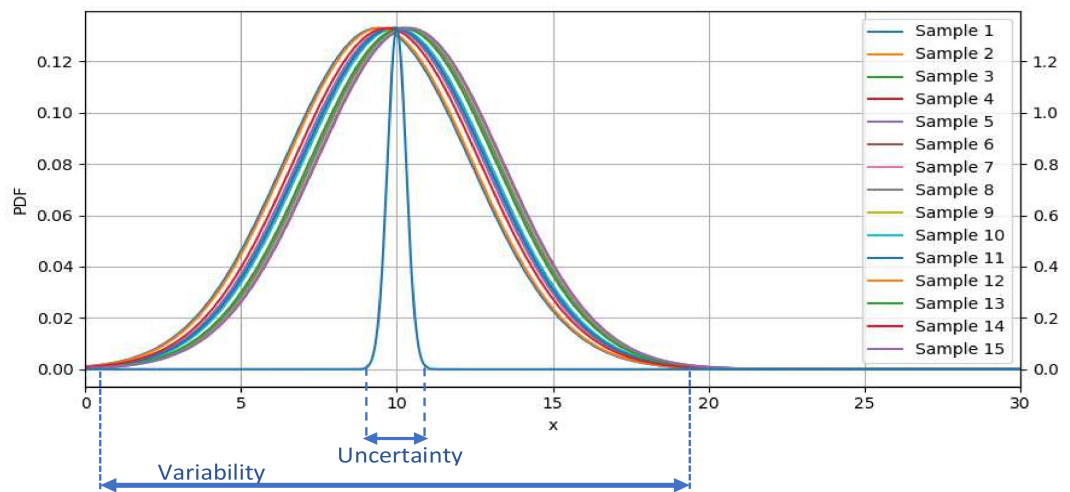


Figure 4-1: Illustration of variability and uncertainty, represented with probability distributions (The variability is fixed, while its mean is uncertain and modelled with a normal distribution).

The measurement uncertainty is highly related to sensors and sensor reliability: their ability to sense and return accurate measurements of the measured process of interest. A sensor-based measurement accuracy is in accordance with ISO 5725-1 (ISO, 1994) divided in two categories, namely *Trueness* and *Precision*, where Trueness refers to the closeness of agreement between the arithmetic mean of a large number of test results and the true or accepted reference value, while Precision refers to the closeness of agreement between test results, as is illustrated in Figure 4-2.

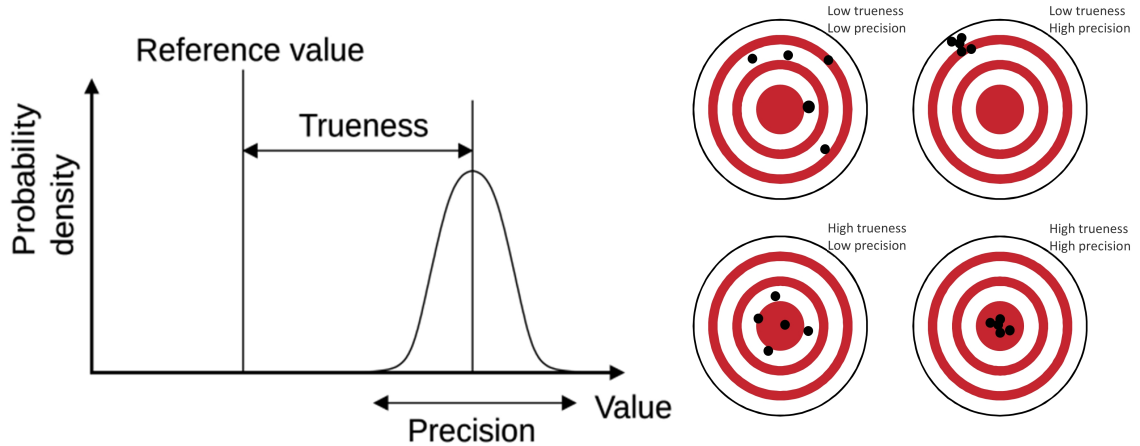


Figure 4-2: Visualisation of trueness and precision of sensor data (DNV GL, 2018).

The various epistemic uncertainty sources have not been the main focus of this research, simply because there are well-known techniques available for their assessment and consideration through the use of traditional statistical methods, e.g. Sensitivity analysis (Saltelli, 2002), Taylor-Series Approximation (Ang et al., 1975) and Monte-Carlo Simulation (Vose, 2008). Nonetheless, measurement uncertainty related to sensors may be implemented in sensor likelihood functions (sensor models) and have been implemented accordingly for our binary sensor types (door sensor, flooding sensor) in Chapter 5 through Chapter 7 with focus on false-negative and -positive readings. The main focus of the presented research will be the variability naturally inherent in damage stability and flooding in a dynamic environment, and despite the fact that it is irreducible, there are ways in which conditional probability distributions may be manipulated in combination with sensor evidence to obtain a strengthened belief on the potential variability of a process, using Bayesian Inference and multi-sensor data fusion techniques as will be introduced in the following sections.

4.3 Probabilistic inference

The Oxford dictionary defines inference as:

“A conclusion reached on the basis of evidence and reasoning”.

Inference based on information recorded by our senses is one of the key cognitive functions performed by the human brain. Introducing probability into inference, enables us to attach numbers to our beliefs and related uncertainty, and thereby provides a basis from which to argue the inferred conclusions quantitatively rather than relying solely on intuition. There are two primary schools of thought on probabilistic inference, namely traditional statistical inference, often termed frequentist inference, and Bayesian inference (Western & Jackman, 1994). Classical statistical inference uses a conventional type of statistics, covering well known topics such as estimation, regression, hypothesis testing, confidence intervals, etc. In contrast, Bayesian inference is fundamentally all about modifying conditional probabilities. At the heart of Bayesian inference lies Bayes theorem (Bayes, 1763). It uses a priori probability distributions for unknown quantities, which are updated once new evidence emerges to posterior probability distributions with the help of likelihood functions and the laws of probability. Knowledge is always uncertain to some degree, but we may alter our beliefs based on the strength of the available evidence, which is exactly what Bayes theorem represents. The framework presented in this thesis will adopt and utilise the latter inference approach because the idea of likelihood functions pairs perfectly with a system relying on sensor information as will be seen in the following chapter.

4.4 Multi-sensor data fusion

“Data fusion is the process of combining information from a number of different sources to provide a robust and complete description of an environment or process of interest” (Durant-Whyte & Henderson, 2016)

The process of fusing, or aggregating, scattered information from a range of independent sensors (thereof multi-sensor) is important for applications where large amount of data must be combined, to obtain information of adequate quality for supporting decision-making. Data fusion is applied in a wide range of industries, such as military systems,

surveillance and monitoring systems, process control systems, and in information systems. It also plays central role in autonomous systems and robotics because it allows essential measurements and information to be combined to generate knowledge with high level of confidence (or lack of uncertainty), to enable decisions to be executed autonomously. Due to the complex and multivariate nature of the problem multi-sensor data fusion process is highly relevant for decision making in flooding emergencies. The following chapter introduces the concept of multi-sensor data fusion, with particular focus on probabilistic data fusion methods as well as key aspects of modelling, estimation and fusion techniques.

4.4.1 Reasoning behind data fusion

In all data fusion problems, there exist some process or quantity whose actual state or value cannot be known exactly with the use of a single and direct source of information. Information is, therefore, obtained indirectly from various related sources (or variables), and the actual state is inferred, i.e. predicted under uncertainty. To use the problem of damage stability as an example, an estimate of lost buoyancy or flooded compartments following a collision incident cannot be obtained from a single measurement or direct source and must be deduced from a range of flooding sensors from various compartments. Furthermore, the damage extent also depends on the status of internal openings such as watertight doors, hence additional sensor observations may be used in order to increase the confidence in the prediction. To enable utilisation of multi-sensor fusion techniques, the problem needs to be defined explicitly, or more specifically, the relationship between the observations and the actual state of the process or quantity of interest must be identified. Formally, this can be expressed by means of the following definitions adopted from Durant-Whyte & Henderson (2016).

- The quantity, or process of interest can be represented by variable, X . Variable X may assume any value from the set x of possible states; $X \in x$, where $x = [x_1, x_2, \dots, x_n]$. The current state of X can be simply denoted as: $X = x_i$.
- Sensor observations are made to gain more knowledge of the state of X . Such sensor observations can be represented by Z , which is contained in the set z of possible observations, i.e. $Z \in z$, where $z = [z_1, z_2, \dots, z_n]$. An observation made of Z corresponds to a single value of the set z , i.e. $Z = z_i$.

- For an observation Z to be of any value, its relation to the quantity or process of interest is needed. That is, for every specific quantity or process, $X = x_i$, an observation model exists that describes possible observations in $Z \in z$. More specifically, for each specific X there exist a set of observations Z .
- Given an observation $Z = z_i$ from a sensor, the main goal is, therefore, to infer the actual state of the quantity or process of interest, X . For this purpose, a mapping model or function is needed that maps observations to states of the quantity or process of interest, i.e. $f(Z = z_i) \rightarrow X \in x$. This mapping is performed by the likelihood functions (also termed sensor model), which in the following will be denoted by $\Lambda(x)$.

4.4.2 Probabilistic definitions and axioms

For understanding the main reasoning behind sensor fusion, some probability definitions and axioms need to be revisited. A probability density function (PDF) for a random variable X , denoted $P(X = x)$ or $PDF(X = x)$, may take a scalar or vector form and may either be discrete or continuous variables. The PDF is considered a probabilistic model of the random variable X , as it is a representation of the probability for the random variable to take on a given state (or value) $X = x$. In the following, the PDF will be denoted simply as $P(x)$. For a PDF to be considered valid, the following must be true:

- It should always be positive, i.e., $P(x) > 0$ for any value of x .
- It should integrate (sum) to a total probability of 1, i.e.:

$$\int_x P(x) dx = 1 \quad \text{Eq. 4-1}$$

A joint PDF for two (or more) random variables is denoted as $P(x,y)$. In the case of multivariate PDFs, integrating over each of the variables x and y yields the respective marginal probability density functions given by Eq. 4-2 and Eq. 4-3. The integral over all variables would result in a total probability of 1 as given by Eq. 4-4.

$$P(y) = \int_x P(x,y) dx \quad \text{Eq. 4-2}$$

$$P(x) = \int_y P(x,y) dy \quad \text{Eq. 4-3}$$

$$\int_x \int_y P(x,y) dy dx = 1 \quad \text{Eq. 4-4}$$

A conditional PDF, e.g., probability density function for x , conditioned on that variable y assumes a specific value, is denoted by $P(x|y)$ and defined by the ratio of joint PDF to the marginal PDF as given by Eq. 4-5. A similar definition can be given for y conditioned on x as given by Eq. 4-6. As the initial variable is conditioned by the second, the conditioning provides additional information for the initial variable, and they are considered dependent.

$$P(x|y) = \frac{P(x,y)}{P(y)} \quad \text{Eq. 4-5}$$

$$P(y|x) = \frac{P(x,y)}{P(x)} \quad \text{Eq. 4-6}$$

Eq. 4-5 or Eq. 4-6 can be used to derive the *Chain rule* of conditional probability, as given by Eq. 4-7, which is used to represent a joint PDF in terms of its conditional and marginal distributions. The Chan rule may further be extended to any number of n random variables as in Eq. 4-8.

$$P(x,y) = P(x|y)P(y) \quad \text{Eq. 4-7}$$

$$P(x_1, x_2, \dots, x_n) = P(x_1 | x_2, \dots, x_n) P(x_2 | x_3, \dots, x_n) \dots P(x_{n-1} | x_n) P(x_n) \quad \text{Eq. 4-8}$$

Rearranging and substituting Eq. 4-7 into Eq. 4-3, results in the *total probability theorem*, as given by Eq. 4-9. The theorem is basically an expression for the marginal distribution of one variable in terms of the marginal distribution of another variable, and states that the PDF of a state x can be obtained by considering all the ways in which x can occur given that the state y takes a specific value.

$$P(x) = \int_y P(x|y)P(y)dy \quad \text{Eq. 4-9}$$

If the knowledge that variable y takes a specific value does not provide any additional information about the value of variable x , they are considered independent, as given by Eq. 4-10. Hence, by substituting Eq. 4-10 into Eq. 4-7, we obtain Eq. 4-11.

$$P(x|y) = P(x) \quad \text{Eq. 4-10}$$

$$P(x,y) = P(x)P(y) \quad \text{Eq. 4-11}$$

Another form of independence can be obtained through conditional independence. Using three random variables x , y and z , the conditional probability of the variable x , given both

variables y and z can be defined and denoted by $P(x | y, z)$. There may, however, be situations where knowledge of the value of variable z makes the value of variable x independent of the value of variable y . This is represented by Eq. 4-12. This conditional independence may further be utilised by applying the *Chain rule* to the joint density function for the three random variables x , y and z , represented by Eq. 4-13, and if this is combined with Eq. 4-12, we obtain Eq. 4-14.

$$P(x|y,z) = P(x|z) \tag{Eq. 4-12}$$

$$P(x,y,z) = P(x,y|z)P(z) = P(x|y,z)P(y|z)P(z) \tag{Eq. 4-13}$$

$$P(x,y|z) = P(x|z)P(y|z) \tag{Eq. 4-14}$$

Since x is independent of y , given knowledge of z , represented by Eq. 4-14, the joint PDF of variables x and y conditioned on z is simply the product of the marginal distributions of x and y , each conditioned on variable z , which is corresponding to Eq. 4-11. The concept of conditional independence is important, and it plays a significant role in constructing the fusion algorithms for the framework. In order to illustrate this, we may consider a state of a system x . If two observations are made of the state of x , namely z_1 and z_2 , it is obvious that the two observations are not independent as they both depend on the common state of x . This is given by Eq. 4-15.

$$P(z_1, z_2) \neq P(z_1)P(z_2) \tag{Eq. 4-15}$$

However, it is reasonable to assume that the observations are independent if the true state of x is known, i.e. the observations z_1 and z_2 are conditionally independent given the state of x , which is represented by Eq. 4-16.

$$P(z_1, z_2 | x) = P(z_1 | x)P(z_2 | x) \tag{Eq. 4-16}$$

For the purpose of data fusion, this would not be a bad definition of the true state of x ; simply what the two observations z_1 and z_2 have in common. This important definition is advantageous to the sensor fusion framework and will be elaborated in more detail in the next section.

4.4.3 Probabilistic sensor fusion

It has been stated in section 4.3 that Bayes theorem is at the heart of probabilistic sensor fusion and is all about modifying conditional probabilities. Bayes theorem encodes variables x and z as a joint probability distribution $P(x,z)$, as illustrated in Figure 4-3. Applying the chain rule of conditional probability with respect to both variables separately, results in Eq. 4-17 and Eq. 4-18. Combining these two expressions and rearranging leads to the well-known Bayes theorem; Eq. 4-19. The power of Bayes theorem lies in its ability to provide the conditional probability of x from known evidence, z .

$$P(x,z) = P(x|z)P(z) \quad \text{Eq. 4-17}$$

$$P(x,z) = P(z|x)P(x) \quad \text{Eq. 4-18}$$

$$P(x|z) = \frac{P(z|x)P(x)}{P(z)} \quad \text{Eq. 4-19}$$

In direct translation to sensor fusion the belief about a state of a quantity, or process of interest, x , may be inferred from sensor observations, z . Bayes theorem is consisting of four components, which will be covered in the following with focus on what role they play in sensor fusion. The theorem has been reintroduced on the next page, however, now represented with three conceptual components as seen in Eq. 4-20.

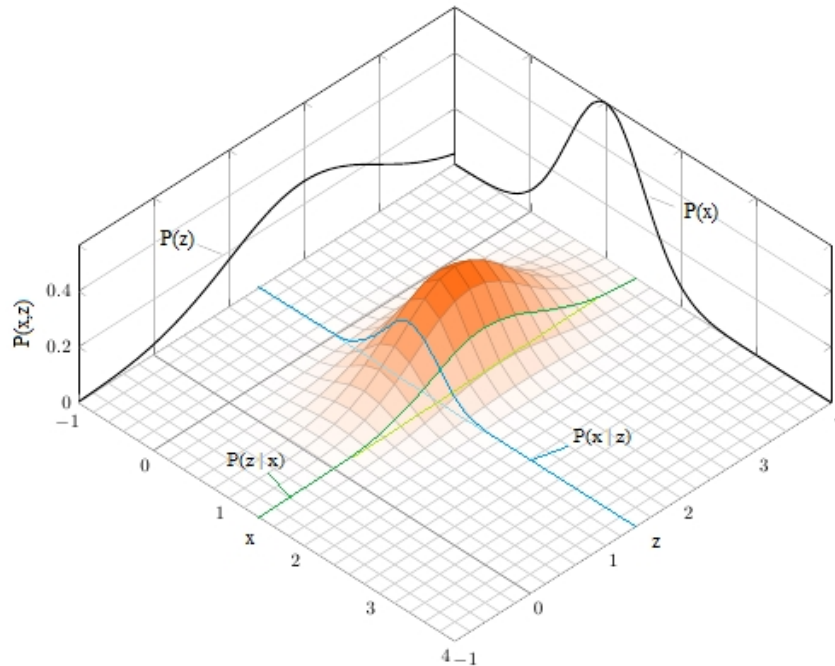


Figure 4-3: Joint, marginal and (un-normalised) conditional probability distributions.

$$P(x|z) = \frac{P(z|x)}{P(z)} \cdot P(x) \quad \text{Eq. 4-20}$$

2
3
1

The first component is known as the a priori distribution and represents the belief about the state of the process or quantity in question x , before any additional information is available (e.g. in terms of sensor observation z). The a priori is often derived from historical statistics, or operational measurements. Without any further information available (e.g. coming from sensors), this would be the only basis for making any conclusions about the state of x . Graphically, (as in Figure 4-3), the state of x could take any value along the x -axis according to the marginal distribution $P(x)$. However, receiving an observation (or new evidence) results in the second component, namely the posterior updated belief. In simple terms, the observation directs to the specific location on the x -axis and determine what conditional distribution is being observed. The third component is slightly more unintuitive. Its numerator contains the so-called likelihood function. This is, similar to the posterior, a conditional distribution, but rather than being an informed update of the state of x , it determines the likelihood of getting a specific sensor reading, z , conditioned on the fact that the state of x has taken a particular value. In the following when developing the likelihood functions, we denote them with $\Lambda(x)$.

In the denominator, we have uninformed evidence, covering the entire z -axis interval in Figure 4-3, and represented by the marginal probability distribution $P(z)$. This component can be seen as a measure of *informativeness* of our new information about x . This is simply because this factor represents the ratio between added information in terms of informed evidence (conditional distribution) to the total uninformed evidence (marginal). It can, therefore, be seen as the gain in information (entropy) from taking a sensor observation (Cover & Thomas, 1991). In practical application, however, the likelihood function alone serves the role of a sensor model mapping between the observations and the actual state of the process or quantity in question, x , whilst marginal evidence is only acting as a normalising constant. On this basis, the theorem could be rewritten as in Eq. 4-21, where C represents the normalising constant, which is obtained by utilising the fact that the total probability should sum to one.

$$P(x|z) = C P(z|x) P(x) = C \Lambda(x) P(x) \quad \text{Eq. 4-21}$$

The above clearly illustrates the advantage Bayes theorem has in a sensor fusion framework, as it provides a direct means of combining observed information with a priori belief about the state of the process or quantity of interest. The observed information in this case is fragmented, collected from various sensor arrays, and then fused into a new, more complete, belief of the state of x . For multiple sensor observations from an array of sensors as represented by Eq. 4-22, the conditional independence discussed above may be utilised. The likelihood function for the sensor observations is represented by Eq. 4-23 and by employing Bayes theorem given by Eq. 4-21 directly, we obtain Eq. 4-24.

$$Z = [z_1, z_2, \dots, z_n] \quad \text{Eq. 4-22}$$

$$P(Z | x) = P(z_1, z_2, \dots, z_n | x) \quad \text{Eq. 4-23}$$

$$P(x | Z) = C P(z_1, z_2, \dots, z_n | x) P(x) \quad \text{Eq. 4-24}$$

In practice, it would be difficult to do this directly because it would require the knowledge of the joint distribution $P(z_1, z_2, \dots, z_n | x)$. This entails knowing the joint distribution of all possible combinations of observations conditioned on the underlying state. However, it is usually quite reasonable to assume that given the true state of x , the information obtained from one information source is conditionally independent of the information obtained from other sources, conditioned on the true state of x . This allows using Eq. 4-14 and in the case of two sensors results in Eq. 4-25 from information from sensors z_1 and z_2 . This could be further generalised for a range or array of n sensors, as in Eq. 4-26.

$$P(x | z_1, z_2) = C P(z_1 | x) P(z_2 | x) P(x) \quad \text{Eq. 4-25}$$

$$P(x | Z) = C \prod_{i=1}^n P(z_i | x) P(x) = C \prod_{i=1}^n \Lambda_i(x) P(x) \quad \text{Eq. 4-26}$$

4.4.4 Sensor fusion example

Let us consider an arbitrary variable of interest, x . Our initial belief about the variable x is governed by its a priori distribution $P(x)$ represented, in this specific case, by a normal probability distribution Eq. 4-27.

$$P(x) \sim N(\mu = 13, \sigma = 5) \quad \text{Eq. 4-27}$$

The a priori distribution is represented by the red curve in Figure 4-4. It is clear that the a priori belief about variable x has large uncertainty due to the large standard deviation $\sigma = 5$. There are two sensor observations (readings) available, namely z_1 and z_2 , showing single value readings $z_1 = 12$ and $z_2 = 14$.

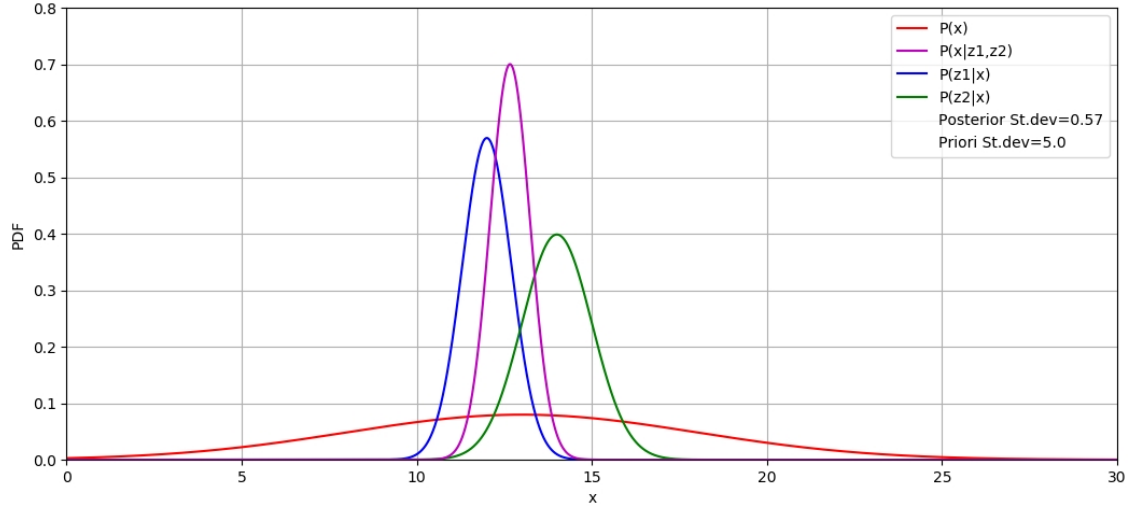


Figure 4-4: Sensor fusion example.

The uncertainty related to the sensor readings is represented by their trueness and precision, as introduced in section 4.2. In simple terms, the trueness and precision represent the sensors' ability to sense the actual value of the variable x . In this particular example the sensor trueness is perfect, and the sensor precision is high, but not optimal. For simplicity, the likelihood functions for the sensors are also represented by normal distributions Eq. 4-28 and Eq. 4-29.

$$\Lambda_1(x) = P(z_1|x) \sim N(\mu = 12, \sigma = 0.7) \quad \text{Eq. 4-28}$$

$$\Lambda_2(x) = P(z_2|x) \sim N(\mu = 14, \sigma = 1.0) \quad \text{Eq. 4-29}$$

The sensors perfect trueness is represented by mean sensor readings corresponding to the distributions mean value μ , and the precision is governed by the variability of the distribution represented by the standard deviation σ . It is also clear that sensor one provides more precise readings seen from its lower standard deviation. Having established all the necessary distributions, Eq. 4-26 may be applied directly and following normalisation results in Eq. 4-30. It is clear that the product of two Normal (Gaussian) distributions still

forms a Normal (Gaussian) distribution. This relates to the notion of conjugate priors, which is an important concept in Bayesian Inference (Raiffa & Schlaifer, 1961).

$$\begin{aligned}
 P(x | z_1, z_2) &= C P \Lambda_1(x) \Lambda_2(x) P(x) && \text{Eq. 4-30} \\
 &= C N(\mu = 12, \sigma = 0.7) N(\mu = 14, \sigma = 1) N(\mu = 13, \sigma = 5) \\
 &= N(\mu = 12.662, \sigma = 0.569)
 \end{aligned}$$

The updated posterior belief has significantly reduced uncertainty compared with any of the single observation sources and a priori belief especially. This is mathematically represented by Eq. 4-31. In this specific example the actual reduction of standard deviation between the a priori and the posterior beliefs, is almost nine-fold, as shown by Eq. 4-32. The example clearly illustrates the impact of probabilistic multi-sensor data fusion on confidence in variable prediction.

$$\sigma_{P(x|Z)} < \sigma_{P(Z|x)} \ll \sigma_{P(x)} \quad \text{Eq. 4-31}$$

$$\sigma_{Reduction} = \frac{\sigma_{P(x)}}{\sigma_{P(x|Z)}} = \frac{5}{0.569} = 8.776 \quad \text{Eq. 4-32}$$

4.4.5 Sequential updating

The above example is a fusion process relying on a single source of information, and a subsequent posterior update. Data obtained from actual sensor readings is different as it arrives continuously in real-time. From this data stream, we want to update the posterior belief of our unknown state of interest, x , in real-time as new information is made available at each time-step k . The previous time steps, $k - 1$, and the current time-step, k , may be represented by Eq. 4-33, where the last component in curly brackets is representing a decomposition between sensor information, z_k , received in the current time-step, and all information, Z^{k-1} , from the past.

$$Z^k = [z_{t=1}, z_{t=2}, \dots, z_{t=k-1}, \dots, z_{t=k}] = \{z_k, Z^{k-1}\} \quad \text{Eq. 4-33}$$

Direct application of Eq. 4-26 would require storing of all past sensor data Z^{k-1} , and implementing all this previous data in the posterior update. However, we may translate Eq. 4-26 to its recursive form and to take advantage of the fact that all previous data is already indirectly stored in the previously updated posterior distribution from the past time-step.

The posterior update in time can be interpreted as a recursive state transition of a *Markovian process* (Gagniuc, 2017) in which the next state x_k depends solely on the immediately preceding state x_{k-1} . This may be proven by firstly representing the joint distribution of the state x and the total sensor information from all time-steps, Z^k , using the *Chain rule* of conditional probability from Eq. 4-7, now represented by Eq. 4-34. The second term in Eq. 4-34 may be translated using Bayes theorem, which result in Eq. 4-35. The total sensor information Z^k may be decomposed in the current information z_k and all past information Z^{k-1} , represented by Eq. 4-33, which results in Eq. 4-36. Conditional independence between past and current sensor information, represented by Eq. 4-16 results in Eq. 4-37. Applying Bayes theorem to the two last terms of Eq. 4-37, results in Eq. 4-38. By using the *Chain rule* of conditional probability from Eq. 4-7 on the first term of Eq. 4-38, rearranging and again decomposing the numerator using Eq. 4-33 results in Eq. 4-39. Finally, by again using the *Chain rule* of conditional probability from Eq. 4-7 on the numerator of Eq. 4-39, results in the recursive form of Bayes formula represented by Eq. 4-40.

$$P(x, Z^k) = P(x | Z^k) P(Z^k) \quad \text{Eq. 4-34}$$

$$P(x, Z^k) = \frac{P(Z^k | x) P(x)}{P(Z^k)} P(Z^k) = P(Z^k | x) P(x) \quad \text{Eq. 4-35}$$

$$P(x, Z^k) = P(z_k, Z^{k-1} | x) P(x) \quad \text{Eq. 4-36}$$

$$P(x, Z^k) = P(z_k | x) P(Z^{k-1} | x) P(x) \quad \text{Eq. 4-37}$$

$$P(x, Z^k) = P(z_k | x) P(x | Z^{k-1}) P(Z^{k-1}) \quad \text{Eq. 4-38}$$

$$P(x | Z^k) = \frac{P(z_k | x) P(x | Z^{k-1}) P(Z^{k-1})}{P(z_k, Z^{k-1})} \quad \text{Eq. 4-39}$$

$$P(x | Z^k) = \frac{P(z_k | x) P(x | Z^{k-1})}{P(z_k | Z^{k-1})} = \frac{A_k(x) P(x | Z^{k-1})}{P(z_k | Z^{k-1})} \quad \text{Eq. 4-40}$$

In this recursive representation, we notice that at time k we only need to keep a representation of the current state and may otherwise ignore the past. The advantage of Eq. 4-40 is therefore that we only need to compute and store the posterior likelihood $P(x | Z^{k-1})$ which contains a complete representation of the past information. When new information is made available in the form of $P(z_k | x)$, the previous posterior takes the role of the current

prior and the normalised product of the two becomes the new posterior $P(x|Z^k)$. Therefore, Eq. 4-40 represents a significant improvement in computational and memory requirements over Eq. 4-26. The recursive process of sequential update in time is illustrated in Figure 4-5.

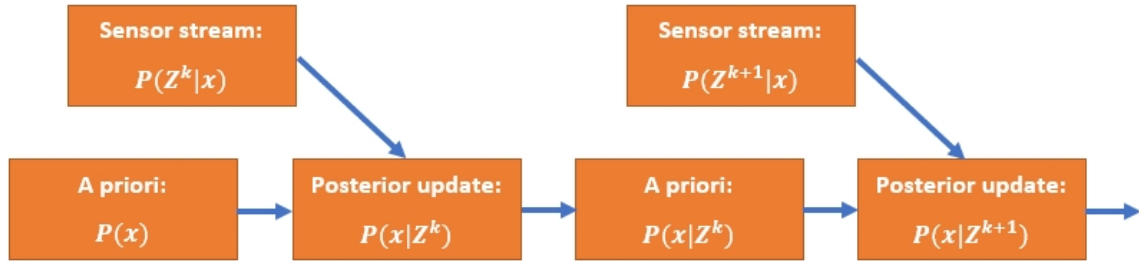


Figure 4-5: Illustration of sequential or recursive updating using recursive Bayes theorem.

The tasks associated with making inference about a time-evolving state x are known as filtering, and in relation with Bayesian inference, Eq. 4-40 is often termed *Bayes filter*. It is noteworthy that filtering, or estimation of a time-varying system, that in addition to the above mentioned observation model in the form of the likelihood function, the Markovian property needs to be included with a state transition model that describes the probability of a specific state, or location x_k dependent on the previous state or location x_{k-1} , described by $P(x_k | x_{k-1})$ or $P(x_k | u_k, x_{k-1})$ if an known control input, u , is provided to the system. The former is needed in dynamic tracking prediction (radar, imaging) and the latter inclusion of control inputs are important in robotics where known actuators implement control inputs and will influence the robots' position in time. Practical implementation of recursive or sequential filtering of time-evolving systems involves well-known techniques such as Kalman filtering, particle-filtering and Markov-Chain-Monte-Carlo (MCMC). For more detail information on the mentioned filtering techniques, reference is made to more extensive literature such as Candy (2016), Särkkä (2013) and Haug (2012). Given the nature of the problem at hand, the normal and recursive form of Bayes formula represented by Eq. 4-26 and Eq. 4-40, respectively, proved to be sufficient for all sensor fusion algorithms developed and applied within this thesis.

4.5 Closing remarks

In the above chapter, we have initially reviewed the two traditional concepts of uncertainty, namely Aleatoric, and Epistemic, referred to simply as Variability and Uncertainty. The former category will be the focus within this thesis, but sensor uncertainty will be attempted implemented in the developed likelihood functions in the form of false-positives and -negatives. The review visited also the two primary schools of thought on probabilistic inference, namely traditional statistical inference and Bayesian inference. The latter approach has been adopted and utilised in the framework reported within this thesis, because the idea of likelihood functions translates perfectly with a system relying on sensor information. The concept of multi-sensor data fusion have been introduced, with the main focus on probabilistic data fusion methods and provided a simple intuitive example. Finally, sequential updating has been reviewed and illustrated as a memory efficient way of using the previous posterior as the current a priori belief.

4.6 References

Chung, K. L., (2000), "*A Course in Probability Theory, 3rd Edition*", Book: Published by Academic Press, 2000, ISBN 9780121741518.

DeGroot, M. H., Schervish, J. M., (2019), "*Probability & Statistics, 5th Edition*", Book: Published by Pearson, ISBN 0134687000.

Feller, W., (1968), "*An Introduction to Probability Theory and Its Applications, Vol. 1, 3rd Edition*", Book: Published by Wiley, ISBN 0471257087.

Durrant-Whyte H., Henderson T .C. (2016) "*Chapter: Multisensor Data Fusion*", In: Siciliano B., Khatib O. (eds), Springer Handbook of Robotics, Springer, Cham.

Schweder, T., Hjort, N. L., (2016), "*Confidence, Likelihood, Probability – Statistical Inference with Confidence Distributions*", Book: Published by Cambridge University press, ISBN 978-0-521-86160-1.

Bitner-Gregersen, E. M., Eide, L. I., Hørte, T., Skjong, R., (2012), "*Ship and Offshore Structure Design in Climate Change Perspective*", Published with open access at SpringerLink.com, ISBN 978-3-642-34137-3.

Skjong, R., Bitner-Gregersen, E. M., Cramer, E., Croker, A., Hagen, Ø., Korneliussen, G., Lacasse, S., Lotsberg, I., Nadim, F., Ronold, K. O., (1995), "*Guidelines for offshore structural reliability analysis*", DNV report no 95-2018.

International Organization for Standardization (ISO), (1994), "*Accuracy (trueness and precision) of measurement methods and results – Part 1: General principles and definitions*", ISO standard No. ISO 5725-1:1994(E).

DNV GL, (2018), "*Guidance on definition of requirements for sensor system reliability*", Internal report No. 2018-0732, rev. 0.

Saltelli, A. (2002). "*Sensitivity Analysis for Importance Assessment*". Risk Analysis Vol. 22 (3): 1-12.

Ang, A. H-S. and Tang, W. H. (1975), "*Probability Concepts in Engineering Planning and Design, Volume 1*", Book: Published by John Wiley & Sons, ISBN 978-0471032007.

Vose, D., (2008), "*Risk Analysis: A Quantitative Guide*", Book: Published by John Wiley & Sons, ISBN 978-0-470-51284-5.

Western B., Jackam, S., (1994), "*Bayesian Inference for Comparative Research*", American Political Science Review Vol. 88, No. 2, June.

Rev. Thomas Bayes, (1763), "*Essay Towards Solving a Problem in the Doctrine of Chances*", published posthumously in the Philosophical Transactions of the Royal Society.

Cover, T. M., Thomas, J. A., (1991), "*Elements of Information Theory*", Book: Published by John Wiley & Sons, ISBN 0-471-20061-1.

Raiffa, H., & Schlaifer, R., (1961), "*Applied Statistical Decision Theory*", Book: Published by Harvards University's Graduate School of Business Administration - Division of Research, ISBN: ISBN 0-87584-017-5

Gagniuc, P.A., (2017), "*Markov Chains: From Theory to Implementation and Experimentation*", Book: Published by John Wiley & Sons, ISBN: 978-1-119-38755-8.

Candy J.V., (2016), "*Bayesian Signal Processing: Classical, Modern, and Particle Filtering Methods (Adaptive and Cognitive Dynamic Systems: Signal Processing, Learning,*

Communications and Control”, Book: Published by Wiley-IEEE Press; 2 edition, July 12, ISBN: 978-1119125457.

Särkkä S., (2013), “*Bayesian Filtering and Smoothing (Institute of Mathematical Statistics Textbooks)*”, Book: Published by Cambridge University Press, 5 Sept., ISBN: 978-1107030657.

Haug A. J., (2012), “*Bayesian Estimation and Tracking: A Practical Guide*”, Book: Published by John Wiley & Sons, ISBN: 978-0-470-62170-7.

Chapter 5 - Environment variables

5.1 Opening remarks

As highlighted in Chapter 2, vessels operate in a highly dynamic environment, subjected to wind and waves, which in case of a flooding casualty will affect the flooding evolution and subsequent outcome. The main framework developed herein, intends to capture the influence of the environment to improve accuracy of the prediction. This chapter will focus on the impact from waves and more specifically, on the significant wave height and how multi-sensor data fusion could be used to provide a probabilistic real-time estimate on the actual significant wave height based on vessel motions. The chapter will not address the impact of wind as it will be indirectly accounted for in Chapter 6, where draft sensors will be utilised for estimating the vessels actual (real-time) floating position.

5.2 A priori statistics

5.2.1 Wave environment

The wave height is known a priori from wave statistics. Historically, the information about the sea conditions has been derived from visual observations by ships operating in the limited regions of the world's oceans. Today, however, these observations are based on more sophisticated techniques such as moored or drifting wave/weather buoy arrays and orbiting satellites. Weather buoys are equipped with accelerometers measuring the heave acceleration and inclinometers measuring the angular rate of change of the buoy caused by waves passing during a specified time-period. An onboard computer uses statistical wave models to process these measurements and to generate data that are transmitted to shore stations. These data often include significant wave height, H_s , and mean zero up-crossing period, T_z , during a minimum of 20-minute sampling intervals. The positions of the global drifter buoy array as on December 2018 are presented in Figure 5-1. The data from such measurements are used as basis for modelling long-term variation of the wave environment in the form of joint probability distributions of wave height and period. The models may either be global, derived for world-wide operation or local, derived for specific operational areas.

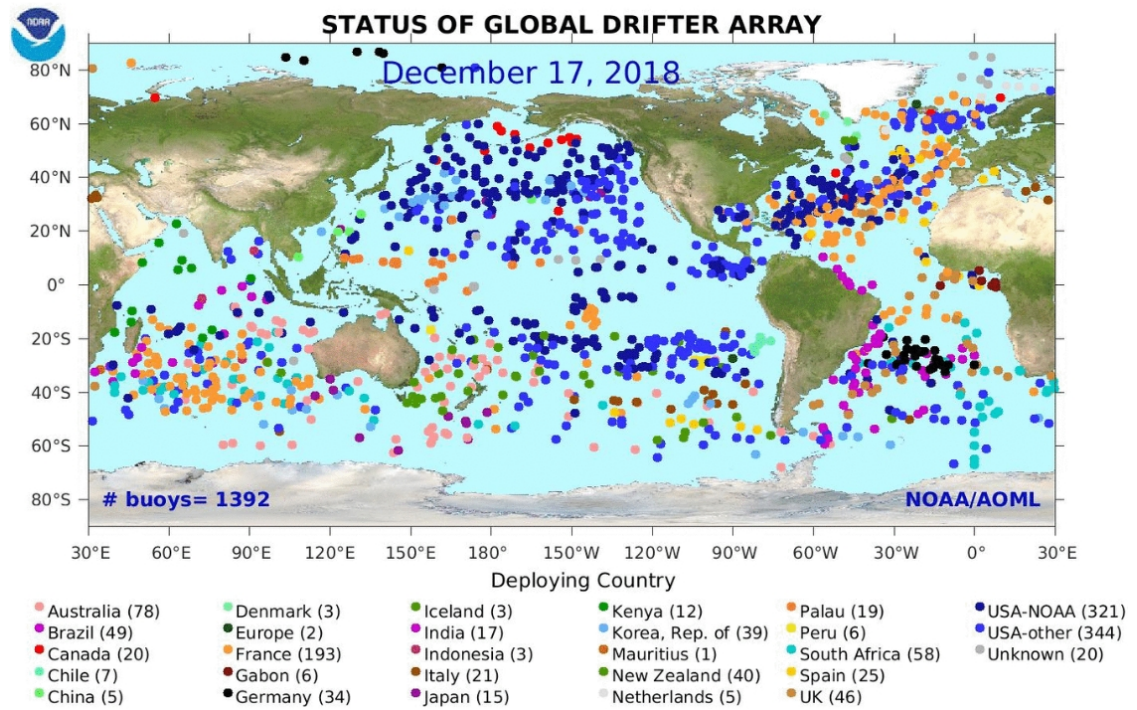


Figure 5-1: Status of Global drifter array (PhOD, 2019).

The probability distribution for the significant wave height is modelled by a 3-parameter Weibull distribution given by Eq. 5-1 and illustrated in Figure 5-2 for world-wide operation, North Atlantic and the Caribbean. The zero-up crossing period, T_z , conditional on significant wave height, H_s , is modelled by a lognormal distribution given by Eq. 5-2 to Eq. 5-4 and illustrated in Figure 5-3 for a specific significant wave height of 5 m for the same operational areas. Wave scatter diagrams for the North Atlantic and word-wide operation, a map of other operational sea areas and related distribution coefficients, may be found in Appendix C of DNVGL-RP-C205 (DNV GL, 2017).

$$PDF(H_s) = \frac{\beta_{H_s}}{\alpha_{H_s}} \left(\frac{H_s - \gamma_{H_s}}{\alpha_{H_s}} \right)^{\beta_{H_s} - 1} \exp \left(- \left(\frac{H_s - \gamma_{H_s}}{\alpha_{H_s}} \right)^{\beta_{H_s}} \right) \quad Eq. 5-1$$

$$PDF(T_z | H_s) = \frac{1}{\sigma t \sqrt{2\pi}} \exp \left(- \frac{(\ln t - \mu)^2}{2\sigma^2} \right) \quad Eq. 5-2$$

$$\mu(H_s) = a_0 + a_1 H_s^{a_2} \quad Eq. 5-3$$

$$\sigma(H_s) = b_0 + b_1 e^{b_2 H_s} \quad Eq. 5-4$$

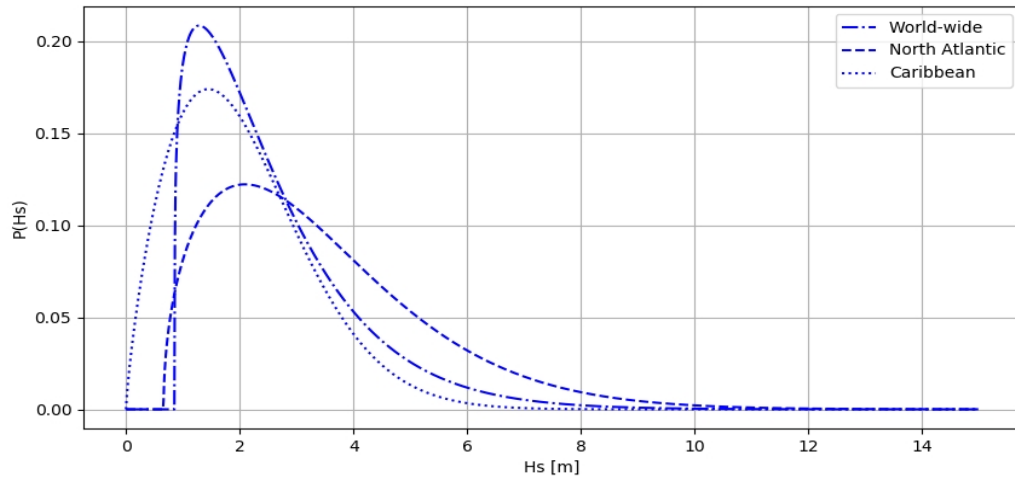


Figure 5-2: Distribution for the significant wave height H_s .

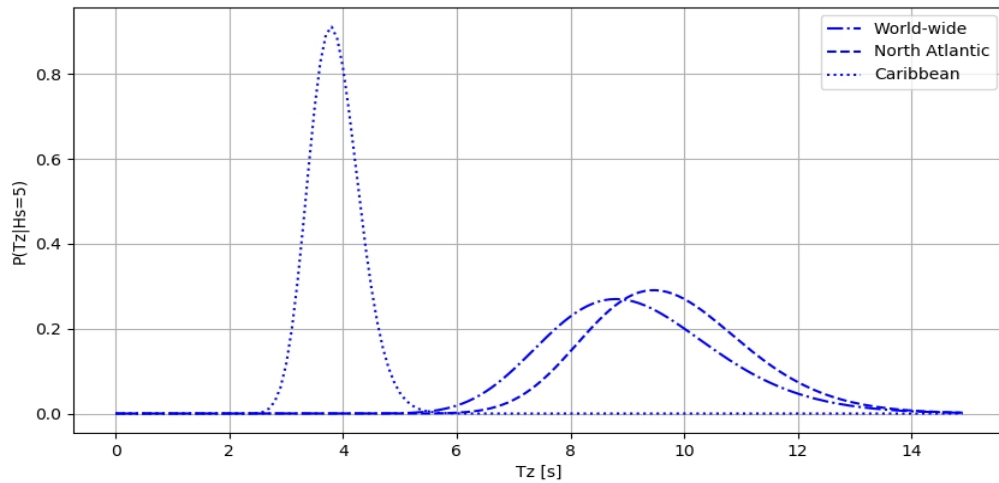


Figure 5-3: Distribution for the zero up-crossing period T_z conditional on $H_s = 5.0$ m.

5.3 Likelihood function

5.3.1 Motion sensors

The sensors that can be used for the significant wave height prediction method are roll, φ , pitch, θ , and heave, Z , sensors. They are available on many modern ships for providing compensation data to echo-sounders, fishing sonars and shipboard cranes, etc. Other important parameters affecting ship motions are heading, ψ , the vertical centre of gravity, KG , and draught, T . Heading affects roll and pitch responses whereas KG (or GM) and draught affect the vessel's natural roll period, T_φ . The latter two variables may be known from

onboard sensors, hence it would be possible to develop conditional probability distributions incorporating also this information in the fusion process for better accuracy. However, for simplicity and to enable the development of intuitive understandable likelihood functions (of smaller number of dimensions), they have been disregarded at this point. Instead, available marginal a priori knowledge of draft, T , and vertical centre of gravity, KG , has been used as basis.

The development of the likelihood function (sensor model) entailed a range of time-domain simulations in waves. The simulations were performed with 4 Degrees of Freedom (DoF) (sway, heave, roll, pitch) at zero forward speed (dead-ship condition). The H_s , being the variable of interest, was sampled uniformly from the interval $[1, 15 \text{ m}]$ (uniform sampling ensured even coverage of the whole interval of wave heights in consideration). Draft, T , and the vertical centre of gravity, KG , were randomly sampled from the a priori distributions as discussed more in detail in section 7.2.2. Heading was sampled uniformly on the interval $[0, 360^\circ)$. Finally, the waves zero-up crossing period, T_z , was randomly sampled from the conditional (on wave height) probability distribution given in the foregoing by Eq. 5-2 for world-wide operation. Given the stochastic nature of sea waves, roll, pitch and heave are also expressed as significant values φ_s , θ_s and Z_s respectively, with the definition consistent with that of significant wave height, H_s (i.e. the average of one-third of the highest values).

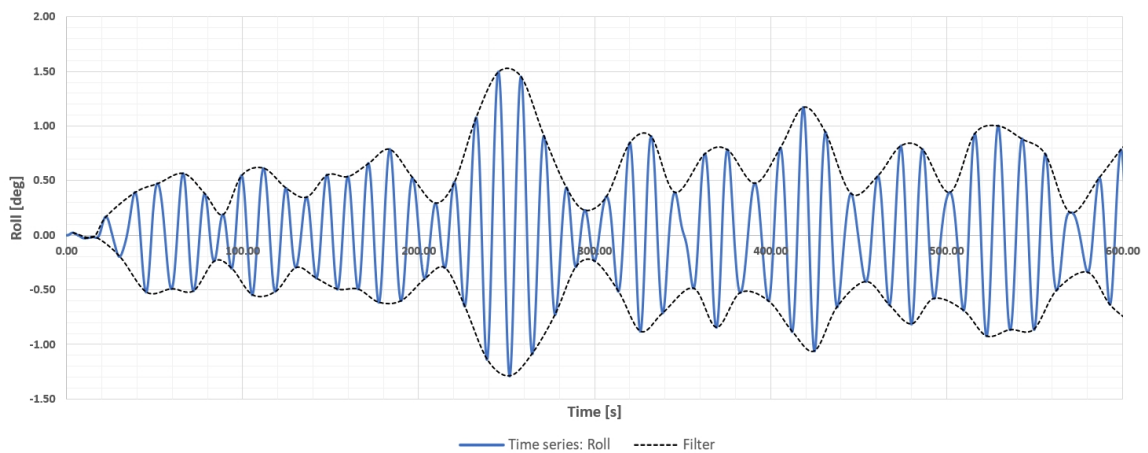


Figure 5-4: Time-series for roll motion with amplitude filter.

In order to calculate the significant values, motion amplitudes have been extracted by applying a simple filter as is illustrated in Figure 5-4, and the average of the highest one-third of the amplitudes have been calculated for a 20-minute time-window for positive values of both port-, and starboard side. The 20 minutes sliding time-window relates to the minimum time-period used for measurements of significant wave height from weather buoys. For the time-domain simulations, 10,000 samples were therefore simulated for a period of 20 minutes. An excerpt of 10 samples is shown in Table 5-1, and the data points resulting from the simulations representing the highest one-third of the amplitude for the variables are presented in Figure 5-5 to Figure 5-7 respectively as a function of H_s .

Table 5-1: Excerpt of sampled variables for time-series.

H_s [m]	T_z [s]	H_g [°]	T [m]	Δ [t]	KG [m]
14.471	9.669	339.310	7.966	50164.80	16.854
9.728	7.699	0.601	8.273	52783.84	16.593
13.804	15.726	182.441	8.150	51728.07	16.551
5.589	10.924	151.384	8.196	52118.65	16.551
6.329	8.515	57.209	7.752	48360.59	17.388
4.948	9.435	138.551	7.863	49295.62	16.844
0.569	4.299	89.829	7.923	49799.00	16.932
6.374	9.155	27.350	7.986	50333.13	16.842
5.233	10.309	17.365	8.126	51526.17	16.712
3.301	9.567	28.133	7.677	47730.88	17.699

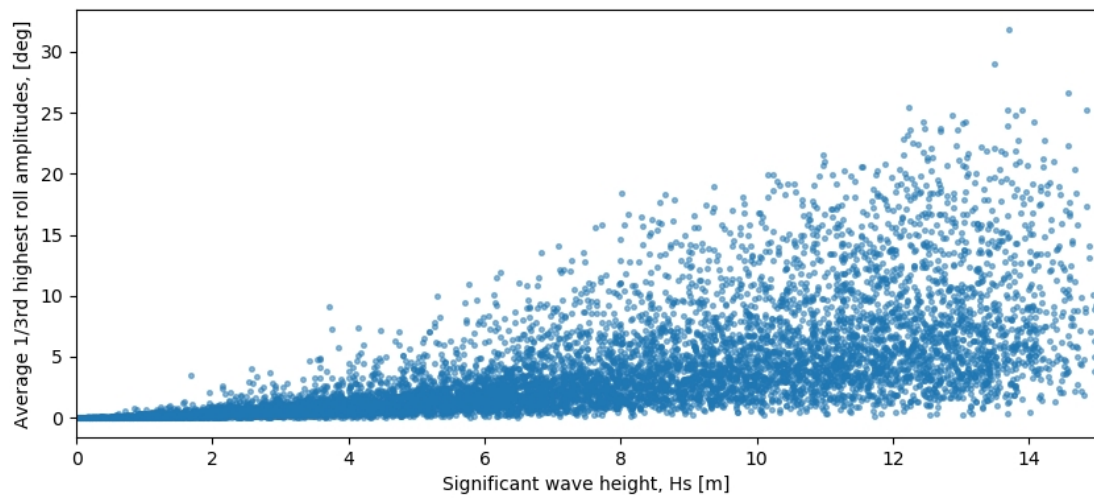


Figure 5-5: Average highest one-third roll data-points from 20 min simulations.

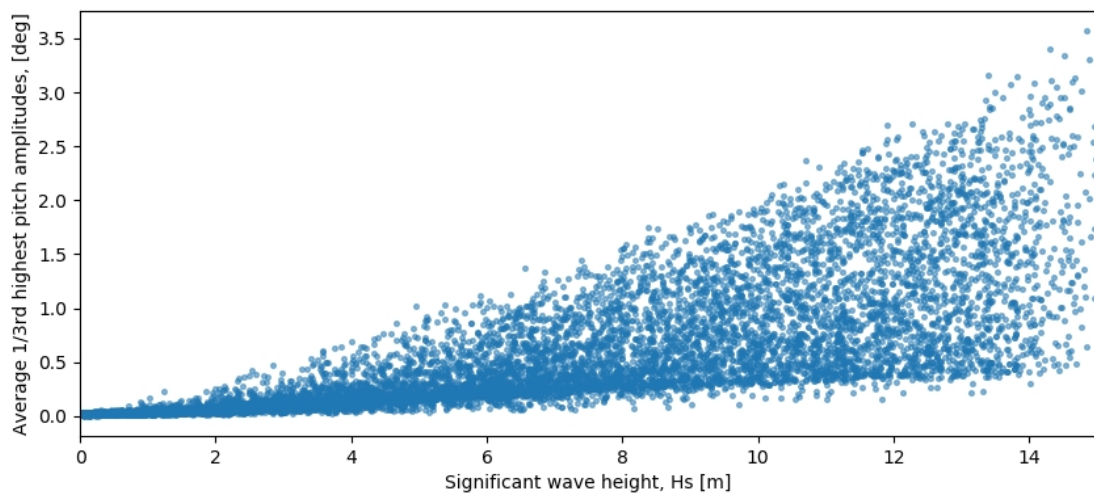


Figure 5-6: Average highest one-third pitch data-points from 20 min simulations.

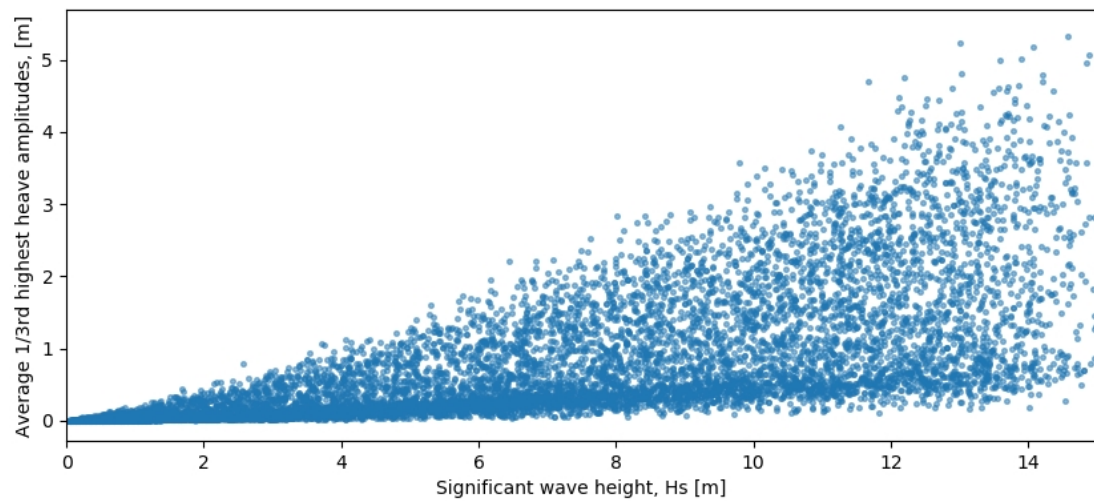


Figure 5-7: Average highest one-third heave data-points from 20 min simulations.

For developing likelihood functions, bivariate distributions have been fitted to the data points by using the maximum likelihood estimation (MLE) method. In the approach followed herein, the probability distribution functions for the motion variables (along y-axis) are parametrised as a function of H_s , resulting in a bivariate distribution also covering the full H_s interval (x-axis) with the regression coefficients identified by the MLE method. The specific roll amplitude $[\varphi_s]$ is represented by a Burr type XII distribution whilst, specific heave $[Z_s]$ and pitch $[\theta_s]$ amplitudes are represented by a log-normal distribution. Distributions and relevant parameter functions for roll are represented by Eq. 5-5 to Eq. 5-8, pitch by Eq. 5-9 to Eq. 5-11 and heave by Eq. 5-12 to Eq. 5-14. Numerical and analytical representations of the distributions are illustrated in Figure 5-8, Figure 5-9 and Figure 5-10 for roll, pitch and heave respectively.

$$\Lambda_{\varphi_s}(H_s) = PDF(\varphi_s | H_s) = \frac{\alpha\beta}{\lambda} \left(\frac{\varphi_s}{\lambda}\right)^{\alpha-1} \left[1 + \left(\frac{\varphi_s}{\lambda}\right)^{\alpha}\right]^{-\beta-1} \quad \text{Eq. 5-5}$$

$$\alpha(H_s) = a + be^{cH_s}, a = 2.129, b = -1.302, c = -0.287 \quad \text{Eq. 5-6}$$

$$\beta(H_s) = a + be^{cH_s}, a = 1.717, b = 6.030, c = -0.560 \quad \text{Eq. 5-7}$$

$$\lambda(H_s) = a + be^{cH_s}, a = -3.105, b = 3.105, c = 0.111 \quad \text{Eq. 5-8}$$

$$\Lambda_{\theta_s}(H_s) = PDF(\theta_s | H_s) = \frac{1}{\theta_s \sigma \sqrt{2\pi}} e^{-\frac{(\ln \theta_s - \mu)^2}{2\sigma^2}} \quad \text{Eq. 5-9}$$

$$\mu(H_s) = a + be^{cH_s}, a = 0.676, b = -4.783, c = -0.164 \quad \text{Eq. 5-10}$$

$$\sigma(H_s) = a + be^{cH_s}, a = 0.578, b = 0.00, c = -9.156 \quad \text{Eq. 5-11}$$

$$\Lambda_{Z_s}(H_s) = PDF(Z_s | H_s) = \frac{1}{Z_s \sigma \sqrt{2\pi}} e^{-\frac{(\ln Z_s - \mu)^2}{2\sigma^2}} \quad \text{Eq. 5-12}$$

$$\mu(H_s) = a + be^{cH_s}, a = 0.601, b = -5.408, c = -0.217 \quad \text{Eq. 5-13}$$

$$\sigma(H_s) = a + be^{cH_s}, a = 0.764, b = 1.130, c = -0.625 \quad \text{Eq. 5-14}$$

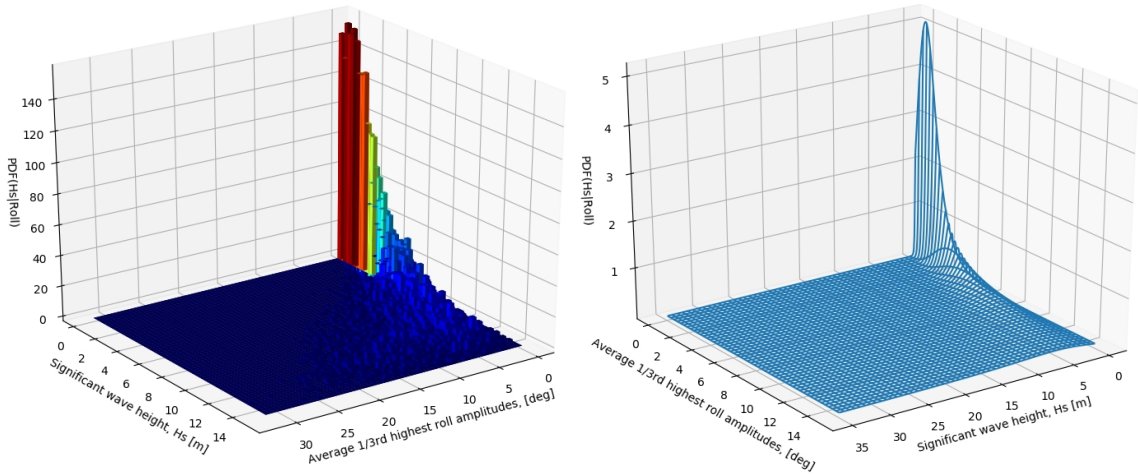


Figure 5-8: Numerical and analytical representation of likelihood function $PDF(Roll | H_s)$.

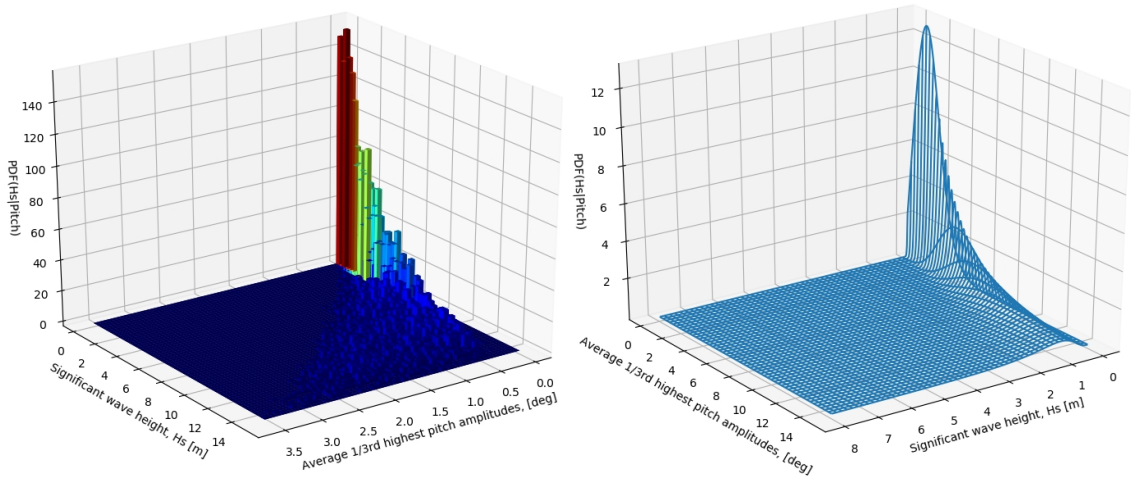


Figure 5-9: Numerical and analytical representation of likelihood function $PDF(Pitch | H_s)$.

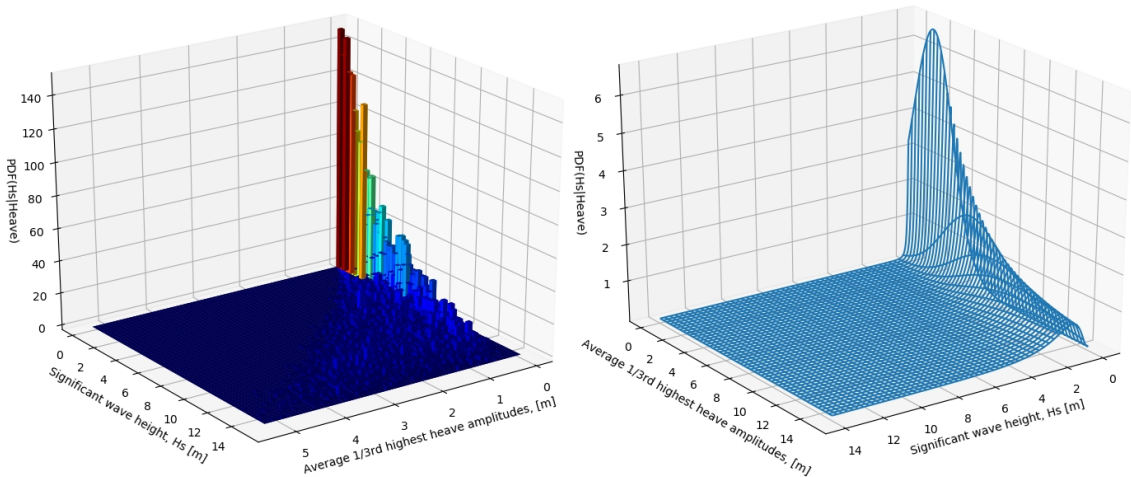


Figure 5-10: Numerical and analytical representation of likelihood function $PDF(Heave | H_s)$.

5.4 Implementation and testing

For developing test-cases, five wave environments have been randomly sampled from each of the distributions for the specified operational areas as introduced above, resulting in a total of 15 test-cases (wave environments). Each of the sampled wave environments has been used for simulating the test-vessel in time-domain for the specified time interval of 20 minutes. The output from the simulations mimics the actual sensor readings, enabling testing the accuracy of the presented prediction method. Only one sample from each operational area has been presented in the following, while complete results are presented in Appendix I. The resulting predictions for each of the operational areas are presented in Figure 5-11 to Figure 5-13 for world-wide, Figure 5-14 to Figure 5-16 for the North-Atlantic and Figure 5-17 to Figure 5-19 for the Caribbean. The figures show that the unbiased sample sea states have H_s lower than 4.0 m and within that range the prediction method yields satisfactory results. However, to verify that the method works with more extreme sea states another, biased sample was made, with the H_s higher than 10.0 m. For this sample, the North-Atlantic has been used as a priori distribution. The complete results for these samples are also presented in Appendix I while a single case of $H_s = 10.0$ m is presented in Figure 5-20 to Figure 5-22. Average one-third highest amplitude (i.e. significant) readings from sensors for each operational area, including extreme operation and corresponding statistical prediction data are presented in Table 5-2.

Table 5-2: Sensor readings and statistical prediction data.

Variables	Operational Area			
	World-wide	North-Atlantic	Caribbean	Extreme wave
Roll φ_s [°]	7.333	0.094	0.580	10.933
Pitch θ_s [°]	0.119	0.037	0.072	0.818
Heave Z_s [m]	0.294	0.093	0.054	2.564
Actual H_s [m]	2.893	1.692	1.781	10.312
Expected $\overline{H_s}$ [m]	3.429	1.815	2.458	9.762
Difference ΔH_s [m]	-0.536	-0.123	-0.677	0.549
Priori σ [-]	2.189	3.333	2.366	3.333
Posterior σ [-]	0.849	0.580	0.670	1.760
Difference $\Delta\sigma$ [-]	-1.340	-2.753	-1.696	1.573

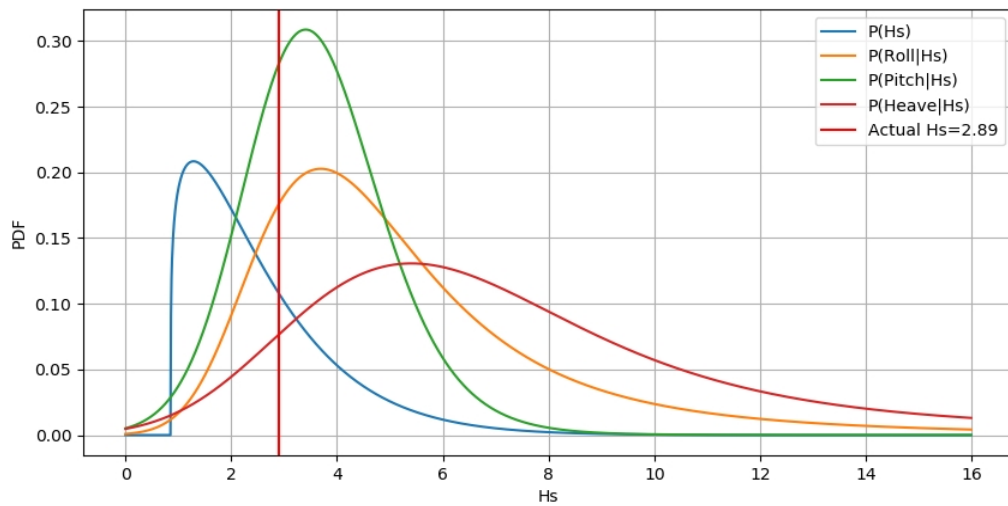


Figure 5-11: A priori, and likelihood functions (World-wide).

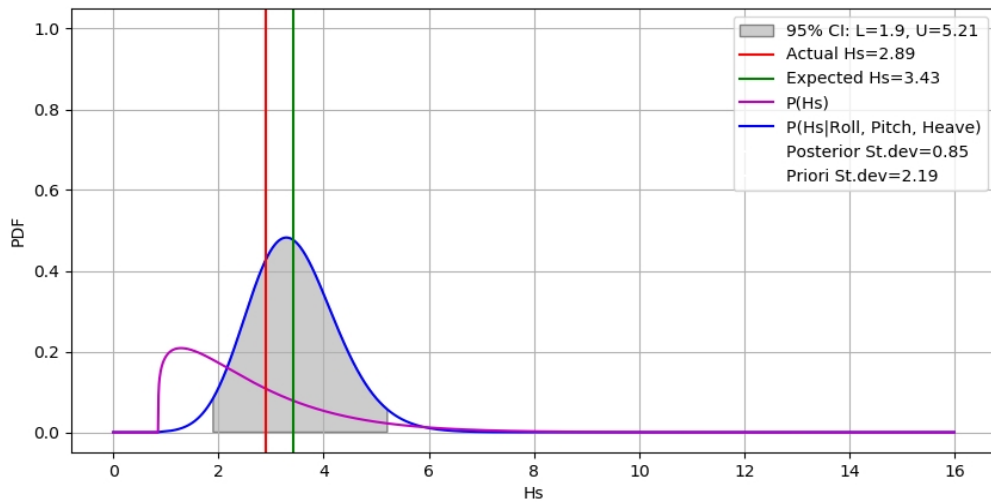


Figure 5-12: A priori and posterior including actual and expected value (World-wide).

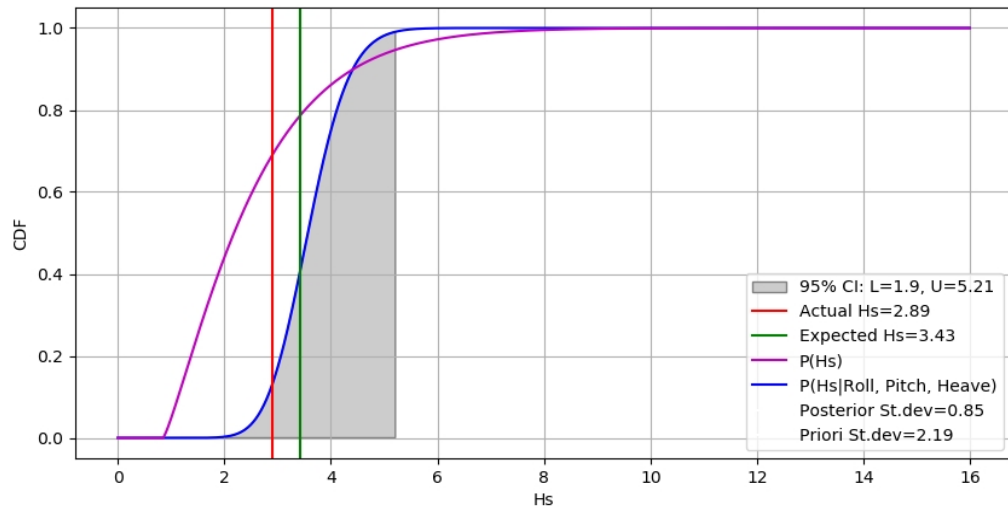


Figure 5-13: Cumulative a priori and posterior including actual and expected value (World-wide).

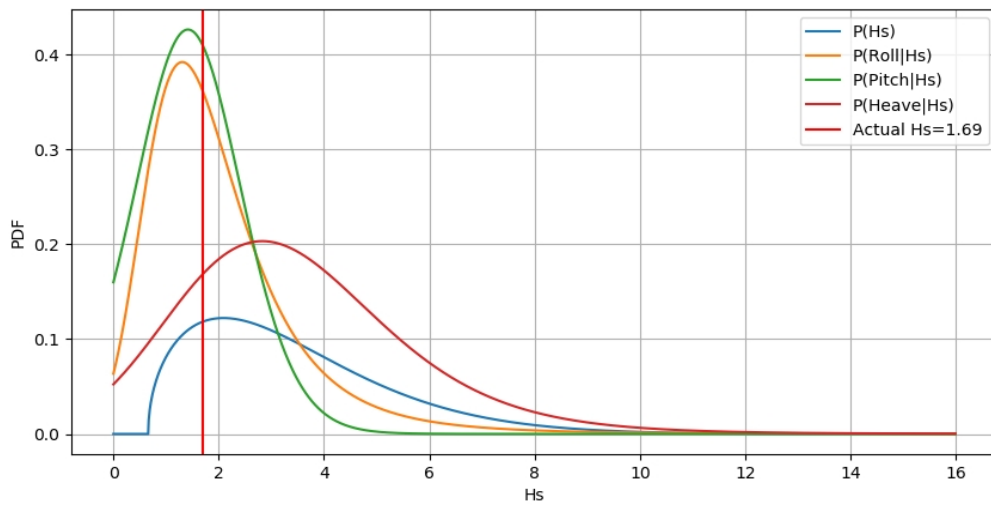


Figure 5-14: A priori, and likelihood functions (North-Atlantic).

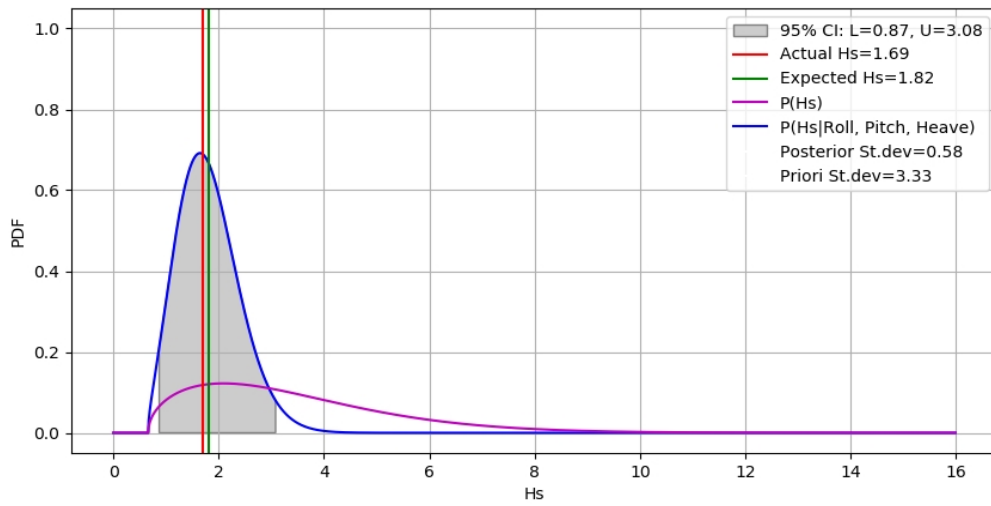


Figure 5-15: A priori and posterior including actual and expected value (North-Atlantic).

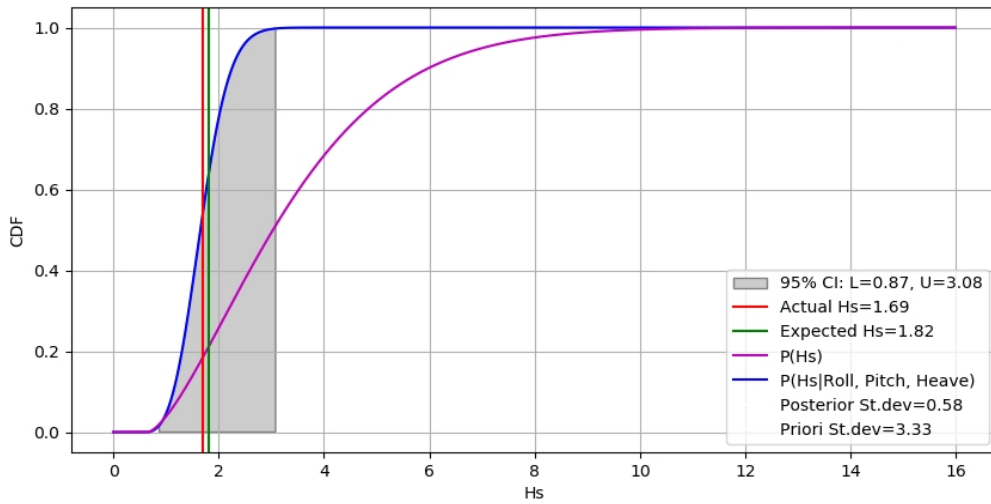


Figure 5-16: Cumulative a priori and posterior including actual and expected value (North-Atlantic).

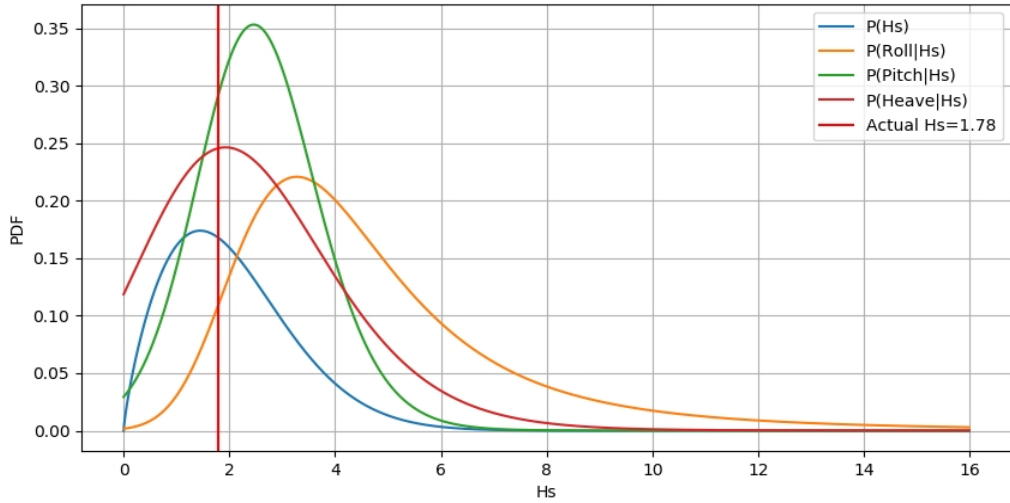


Figure 5-17: A priori, and likelihood functions (Caribbean).

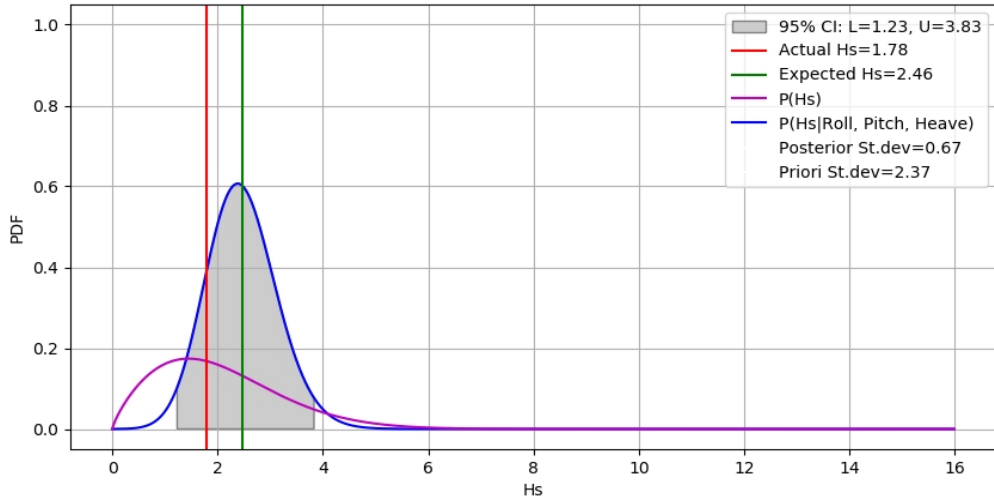


Figure 5-18: A priori and posterior including actual and expected value (Caribbean).

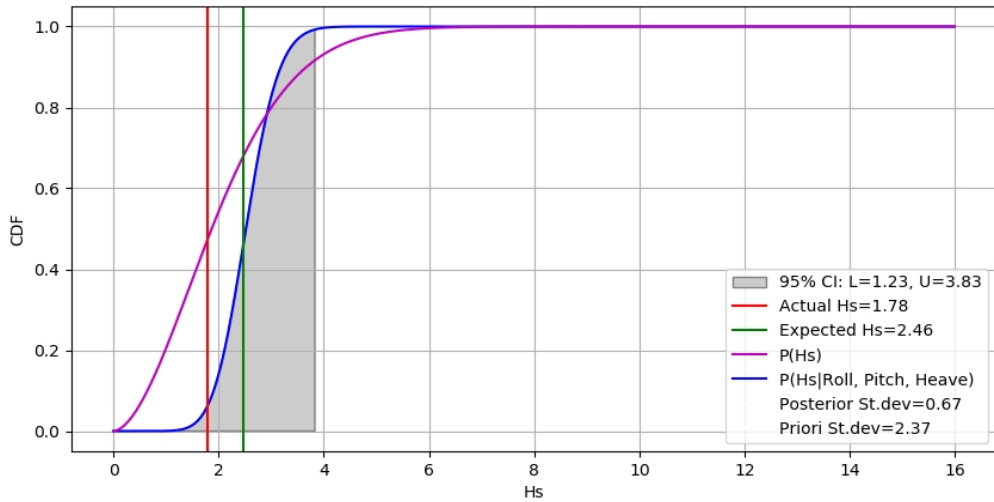


Figure 5-19: Cumulative a priori and posterior including actual and expected value (Caribbean).

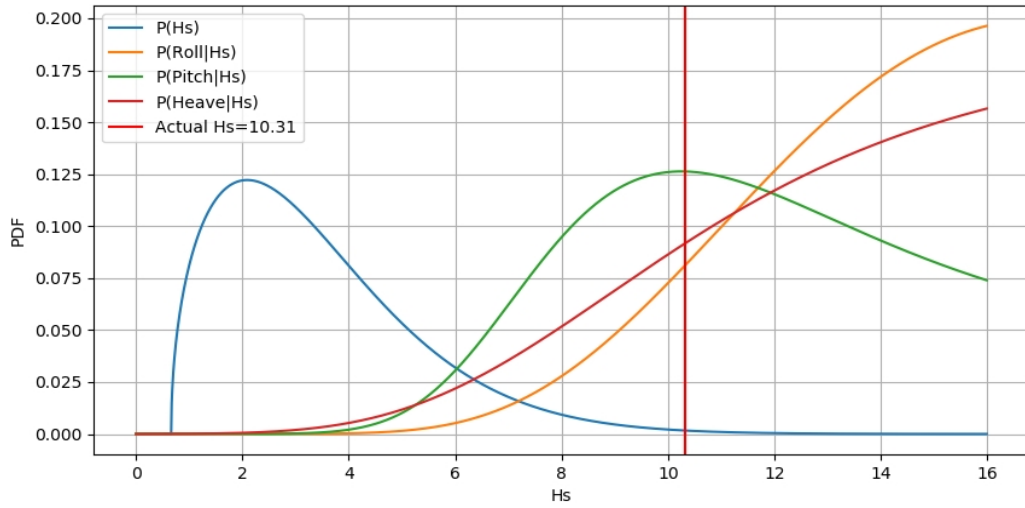


Figure 5-20: A priori, and likelihood functions (Extreme wave).

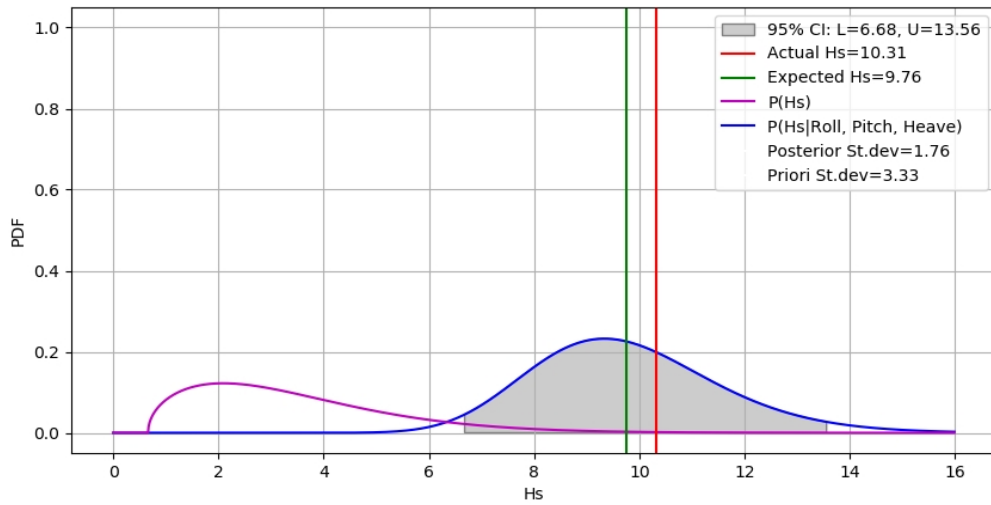


Figure 5-21: A priori and posterior including actual and expected value (Extreme wave).

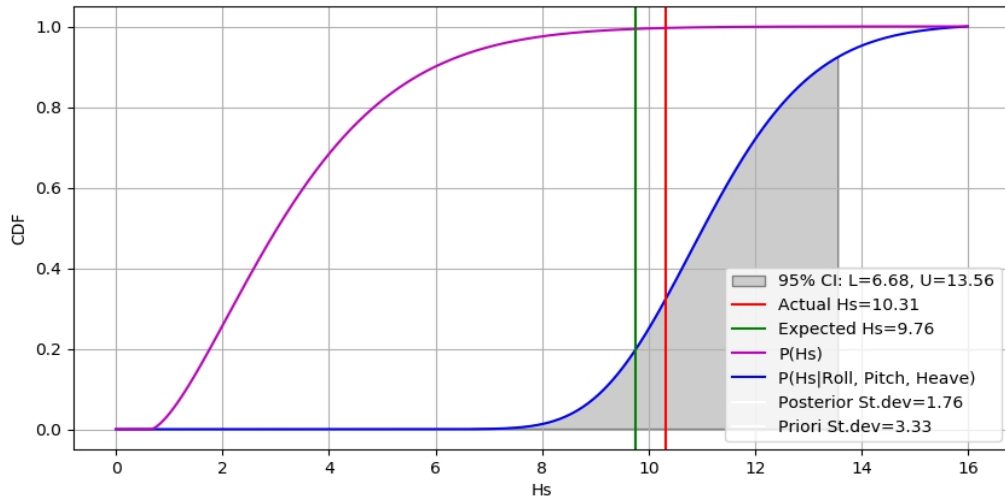


Figure 5-22: Cumulative a priori and posterior including actual and expected value (Extreme wave).

It is noteworthy that the extreme predictions underestimate the actual H_s and that the relative standard deviation for the estimate of the expected sea state is larger (measured in relation to the standard deviation based on the a priori distribution) than in the case of the unbiased sample. Nevertheless, the resultant standard deviation is still significantly lower than the standard deviation obtained based on the priori belief. The underestimation may be a result of using incorrect a priori distribution for such extreme waves, as waves exceeding 10.0 m are a seldom occurrence even in the North Atlantic, clearly supported by its a priori distribution. There are two alternative implementation methods for the wave-height prediction entailing fixed or recursively updated a priori belief. The former was implemented in the above and is given by the non-recursive Bayesian formula given by Eq. 4-26 whilst the latter utilises the recursive form of the model given by Eq. 4-40. In order to demonstrate the differences in results obtained by these two approaches several time-domain simulations performed with distinct wave characteristics (increasing wave height with time) were combined into a single time history. For both methods, a priori distribution was the world-wide operation. The prediction utilising recursive update is presented in Figure 5-23, which shows clearly that the confidence band around the estimate of H_s contracts rapidly. However, the recursive update method is insensitive to rapid increase in wave height. The reason for this is that, as was highlighted in Chapter 4, a prediction for dynamical system requires a Markovian transition model which was not implemented for the wave prediction method.

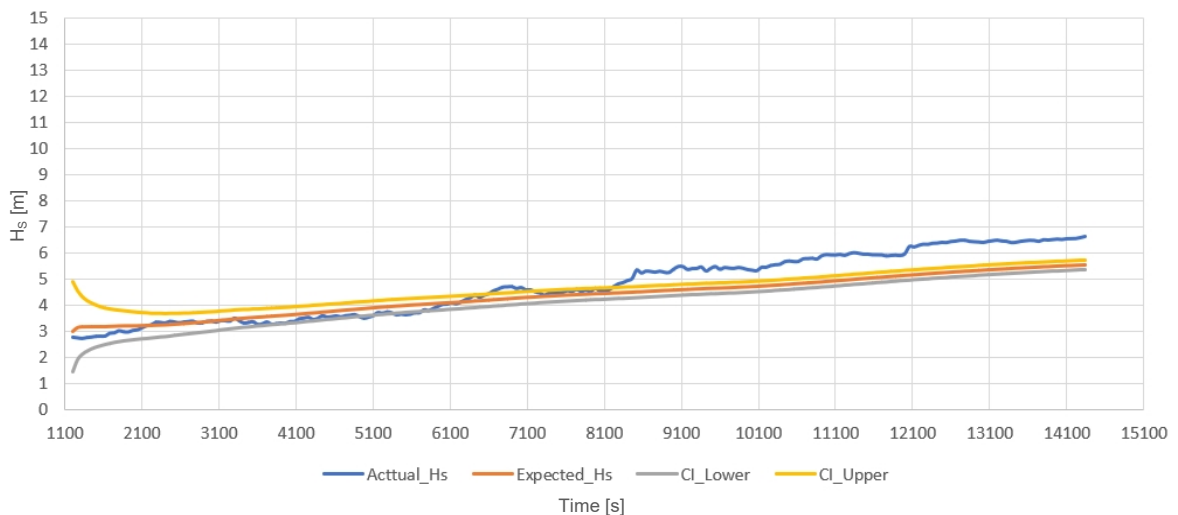


Figure 5-23: Recursive update for increasing wave height in time.

The results of analysis of the same time series by the non-recursive model is presented in Figure 5-24. In this case, the variant of Bayes formula given by Eq. 4-26 maintains in every time-step the same initial a priori belief represented by Eq. 5-1. The prediction now seems to follow the actual wave height better but with a much wider confidence band (although significantly narrower than the confidence band based on a priori belief alone).

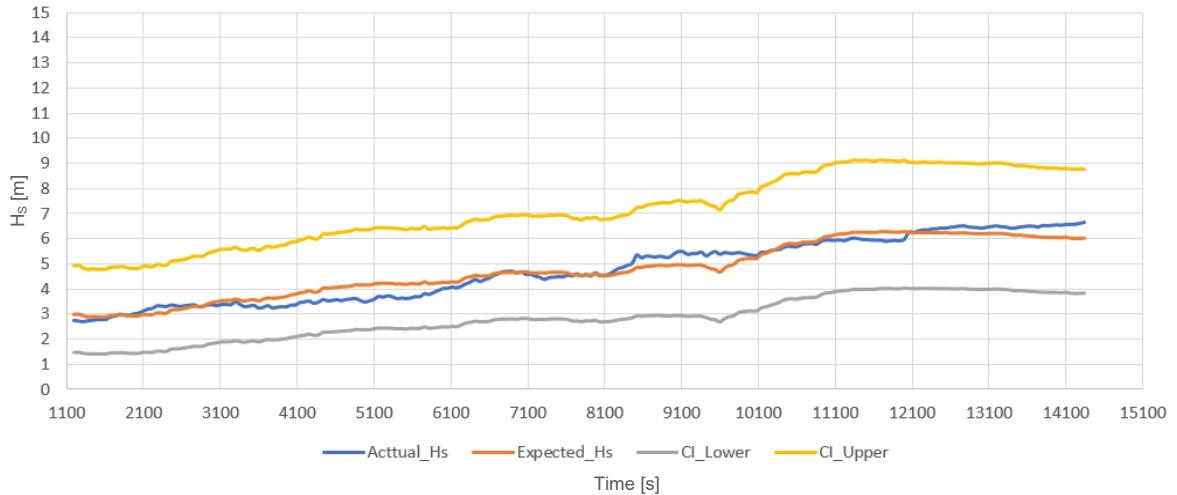


Figure 5-24: Non-recursive update for increasing wave height in time.

5.5 Closing remarks

The method presented in this chapter utilises motion sensors for predicting significant wave height, H_s . Its main objective is to reduce the uncertainty in wave height prediction *at the instant* of collision, based on the past sensor readings, however, knowledge on the actual wave environment during operation would provide additional evidence towards providing an operational risk measure (or vulnerability). It is noteworthy that although the motion sensors data is likely to be available *post collision* as well as the statistics for flooded ship responses, they can be considered unknown as their generation would require a prohibitive number of time-domain simulations of the damaged ship. This would be a drawback in case of fast-changing wave conditions *post collision*. However, knowing the significant wave height in one-time instance, may provide an exceedance probability for future instances. There are available alternative options for further decrease in uncertainty and easy extrapolation of the method to the case of damaged ship. One alternative is to use a wave radar (Grønlie, 2004) which would provide an estimate of wave height and period from

direct measurements. Another alternative would entail a direct link to data stream from the closest weather buoys in the vicinity of the vessels operational area. Finally, wave height estimation data based on satellite imaging could be further explored. Overall, the method provides an intuitive illustration on how probabilistic sensor fusion works and how it may be applied to continuous distributions. In Chapter 6, we will see how this translates to the discrete domain for assessing specific damage extents.

5.6 References

The Physical Oceanography Division (PhOD), (2019), Website: <http://www.aoml.noaa.gov/phod/gdp/index.php> (accessed 16-02-2019).

DNV GL, (2017), "*Environmental conditions and environmental loads*", Recommended practice DNVGL-RP-C205, August.

Grønlie, Ø. (2004). "*Wave Radars – A comparison of different concepts and techniques*", Hydro International, volume 8, number 5, June.

Chapter 6 - Damage variables

6.1 Opening remarks

As already discussed in Chapter 2, the damage extent is traditionally split into initial and progressive extent (or stages) and such a separation will be maintained in the following. We will start with the initial damage extent by developing probability distributions for geometrical variables of the breach as introduced in Chapter 2. These are regarded as a priori statistics of the breach, but they may also be translated into specific discrete a priori beliefs of the initial damage extent in terms of damaged compartments (lost buoyancy) and corresponding probabilities. The progressive extent is directly related to the vessel's internal arrangement and, in particular, the states of internal openings determining the possible routes for the progression of floodwater. The a priori distributions for opening frequencies as well as doors leaking and collapse will be covered in detail in section 7.2.1.

In this chapter, however, they will be discussed in relation to the progressive extent. The last section within this chapter will cover the flooding sensors likelihood function. In fact, it will entail implementation of many of the probabilistic models that will be reviewed in the next Chapter 7 to account for dependency of the damage extents on the variables discussed in Chapter 2 and illustrated by Figure 2-9. As an example, the possible progression stages are important when developing the likelihood functions for the flooding sensors as they should encode the probability of a particular flooding sensor indicating flooding, given a particular damage extent, comprising both initial and progressive stage. As such, the probability is obviously dependent on opening states and subdivision connectivity, determining, in the first place, whether the floodwater is present in specific sensor location.

6.2 A priori statistics

6.2.1 Geometrical properties of a breach

The development of the probability distributions for the a priori information regarding the geometrical properties of a breach utilises as a basis the project GOALDS database of ship casualty data (Bulian, 2011). The GOALDS database is an update of the HARDER

database (Lützen, 2002), which is the underlying basis for the probabilistic damage stability framework of SOLAS (IMO, 2006) mentioned in the introduction. The GOALDS accidents database consists of 1,016 collisions, 472 groundings and 39 contacts as summarised in Table 6-1 (Papanikolaou et al., 2013). The distributions derived from these research projects, are the backbone of the SOLAS probabilistic framework. However, there are some limitations in utilising the SOLAS distributions as a priori distributions within a sensor fusion framework. Firstly, the distributions were simplified to enable harmonisation for all ship types and may therefore lack some important ship-type dependent properties. This involves covering the conditional dependencies of certain variables as will be seen in the next section. Further simplifications are imposed to facilitate the use of the data for the regulatory framework. More details on such limitations are discussed in the following section.

Table 6-1: Overview of data samples from GOALDS, and HARDER databases.

Database	Collision	Grounding	Contact
HARDER	832	312	35
Additions	184	160	4
GOALDS	1016	472	39

At this stage the development of a priori distributions is based on the dataset for collision damages only. However, the same methodology as presented could be easily adopted and implemented for grounding damages as well. Furthermore, the variables have not been non-dimensionalised to prevent overestimation of the variables when scaled up to large cruise vessels (the data comes from a larger proportion of smaller vessels, as illustrated in Figure 6-1). The database can, however, be regarded as a measure of available energy, and damage penetration sources in international trading routes and should be used with given dimensions if correct assumptions are applied as was mentioned in Chapter 2 and described in more detail in the following section.

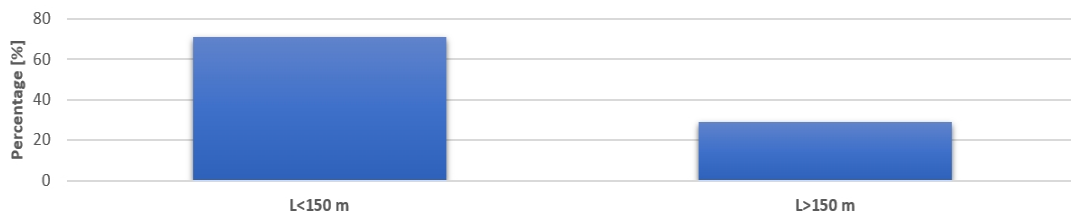


Figure 6-1: Proportions of ship size (represented by length LBP) in GOALDS database.

The longitudinal damage position, X , has, however, been scaled to correspond to a given ship subdivision length, ensuring that the breaches sampled from the developed distributions are manifested on the striking vessel hull. The main statistical variables related to collision damages are summarised in Table 6-2.

Table 6-2: Statistical variables related to collision damage.

Variable	Description
X [m]	Longitudinal position of midpoint of damage from AP
Z [m]	Vertical position of lower damage limit from BL
L [m]	Length of damage in longitudinal direction
H [m]	Height of damage in vertical direction
Y [m]	Depth of damage penetration in transverse direction

6.2.1.1 Longitudinal position of damage, X

Longitudinal position of damage, X , is associated with the centre of the damage and depends on the vessel's subdivision length, L_S , i.e.; $P(X | L_S)$. This means that the centre of the damage must be located within the interval $[L_{S_{aft}}, L_{S_{fwd}}]$. The dataset for variable, X , is normalised so that the resulting distribution ranges from 0 to 1, where 0 corresponds to $L_{S_{aft}}$ and 1 corresponds to $L_{S_{fwd}}$ as is illustrated in Figure 6-2. SOLAS 2009 (IMO, 2006) and other developments such as the eSAFE project (Bulian, 2017) have adopted a uniform probability density function, i.e. any damage position alongside the hull is equally likely. The statistics from the GOALDS database, however, indicate a larger concentration of damages in the fore region. This is because a damage breach can result from three different collision scenarios as listed below:

- The vessel may be the striking ship with the majority of the damages affecting forward half of the ship.
- The vessel may be the stricken ship, being struck by another ship's bow, with damages distributed uniformly along the side (including side damage in the fore region).
- Ship-to-ship collision, where both vessels will suffer higher amount of damage in the fore-region.

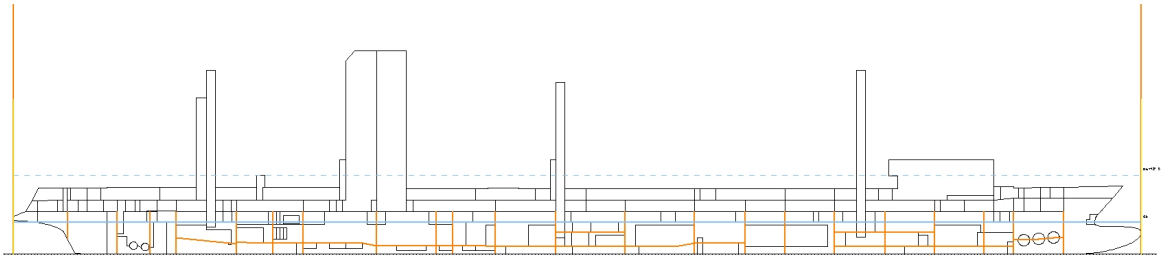


Figure 6-2: Subdivision length of sample vessel.

Given that the data covers all three cases above, it clearly explains the bias towards forward damages. In SOLAS the bias is addressed by the requirements for collision bulkheads to account for bow damages as required by SOLAS Reg. II-1/12.1 (IMO, 2006). However, from the complete risk perspective of a collision damage the distribution of the damage location needs to consider that a vessel could take any of the above-mentioned roles. A numerical PDF and CDF from all sample cases for the variable, X , from the database is presented in Figure 6-3.

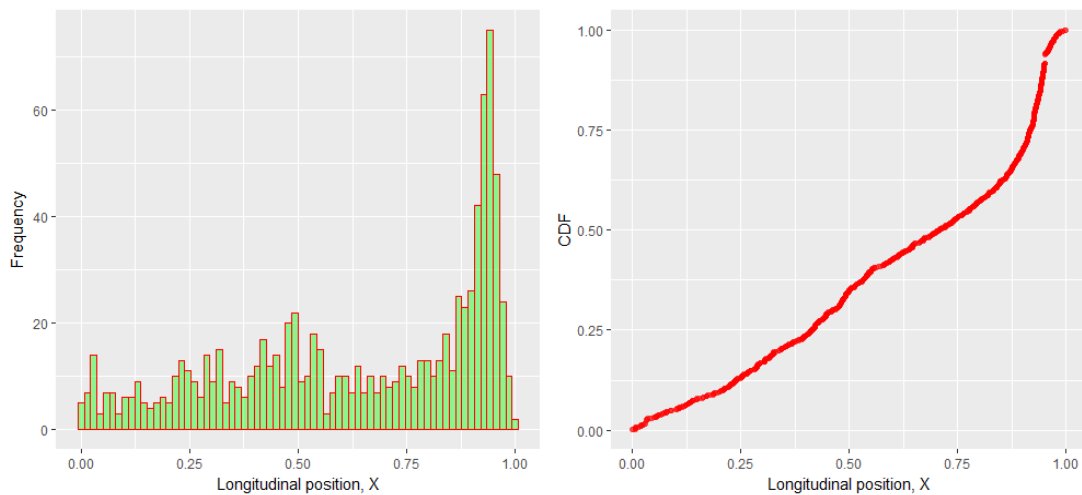


Figure 6-3: Numerical PDF and CDF for scaled longitudinal damage position, X .

From the numerical distributions, only the data between 0 and 0.8 may suggest to be uniformly distributed. It might even indicate a slight linear increase, while between 0.8 and 1, there is a traditional bell-shape distribution. There is no pre-defined suitable distribution available in R for this particular distribution shape. However, an analytical probability distribution can be constructed by combining a linear function with a bell-shaped function

and is given by Eq. 6-1 and Eq. 6-2 for the PDF and CDF respectively, where $x \in [0, 1]$, and Eq. 6-3 is used to calculate the absolute location of the damage.

$$PDF(X) = -\frac{A(X-B)}{c^2} e^{-\frac{D(x-B)^2}{2c^2}} + AEX + F \quad \text{Eq. 6-1}$$

$$CDF(X) = \frac{A}{D} e^{-\frac{D(B-X)^2}{2c^2}} + \frac{AEX^2}{2} + FX \quad \text{Eq. 6-2}$$

$$X_{L_S} = X \cdot L_S + L_{S_{aft}} \quad \text{Eq. 6-3}$$

The distribution coefficients obtained with maximum likelihood estimation (MLE) technique are as follows: $A = 0.2956$, $B = 0.9944$, $C = 0.0580$, $D = 1.3124$, $E = 1.6525$ and $F = 0.5310$. The fitted distributions (PDF & CDF) are illustrated in Figure 6-4.

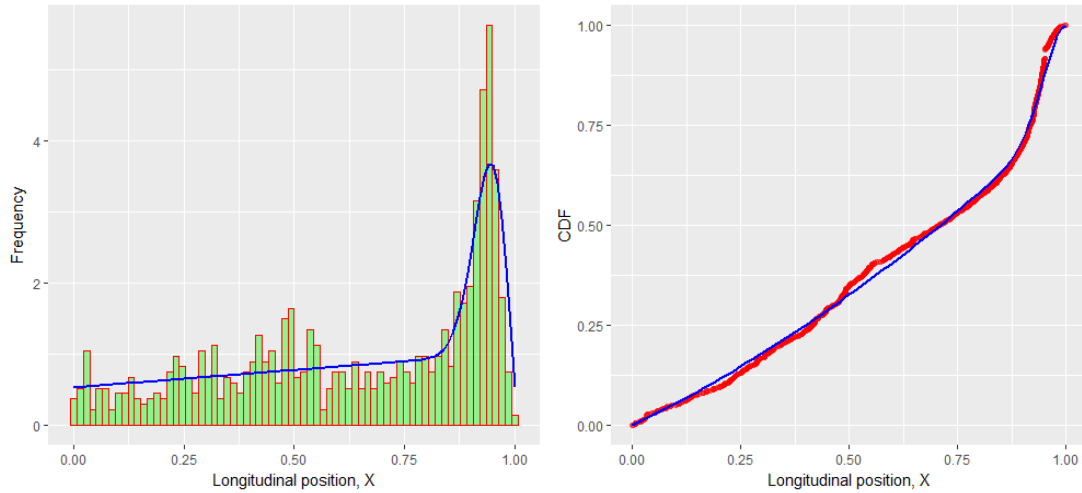


Figure 6-4: Analytical PDF and CDF for longitudinal damage position, X .

6.2.1.2 Vertical position of damage, Z

The GOALDS database provides the lower vertical position of damage, Z , from the vessel baseline, BL . However, it was already discussed in Chapter 2 that the distribution of the vertical position could be considered conditional on the vessel's draught, T . It can be argued that probability of damaging lower compartments when operating on a maximum summer load-line is different from probability of damaging the same group of compartments while operating at shallow draught in ballast condition, particularly when the draught range is

broad. Even in the case of vessels operating within the narrow band of draughts (such as passenger ships) utilising the waterline as a reference point (governed by the vessel draught) would provide a more realistic representation. Furthermore, linking the distribution of vertical position to the vessel's draught would enable taking advantage of draught sensors for uncertainty reduction as will be shown in section 7.3.3. The variation in probability depending on draught is illustrated in Figure 6-5, for three different cases.

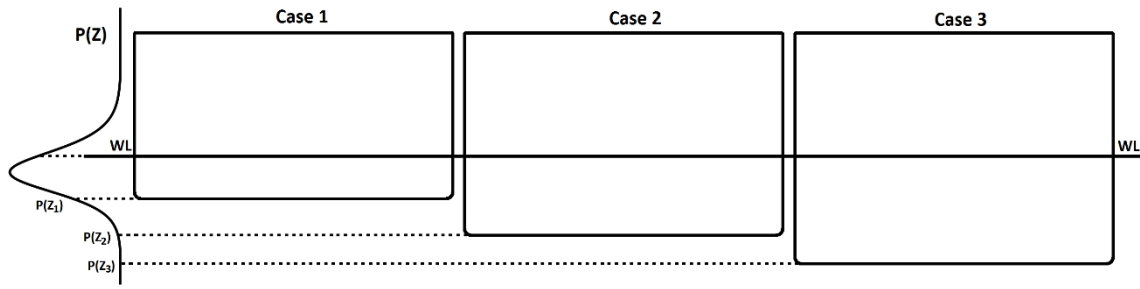


Figure 6-5: Distribution for Z as a function of T .

- Case 1: Small T , and subsequent large probability of having a lower Z value extending to, and below BL .
- Case 2: Medium T , and lower probability of having a lower Z value extending to, and below BL .
- Case 3: Large T , and very low probability of having a lower Z value extending to, and below BL .

Converting the reference from BL to the vessel draught, T , or more specifically, the waterline, WL , results in the numerical distribution illustrated in Figure 6-6. The PDF is clearly a bell-shaped curve, which is distributed around the waterline, represented at reference point $Z = 0$. It can be noticed that the mean value of the distribution is located slightly below the waterline. Changing the vessel draught will obviously alter the expected Z value accordingly, and the distribution for Z conditional on the vessel draught, i.e., $P(Z|T)$, may be given as a function of draught. A suitable model of the distribution can be determined with the help of a *Cullen & Frey* graph shown Figure 6-7.

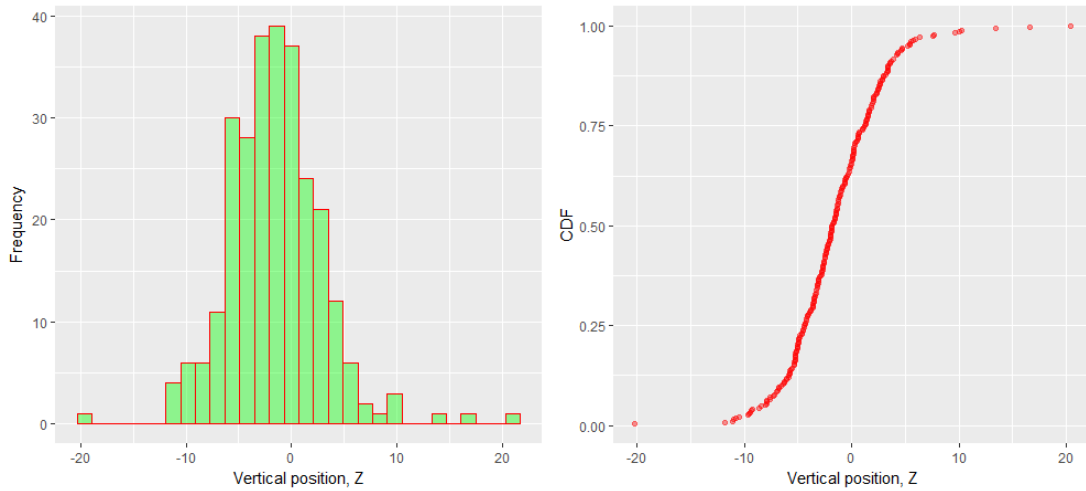


Figure 6-6: Numerical PDF and CDF for vertical damage position, Z .

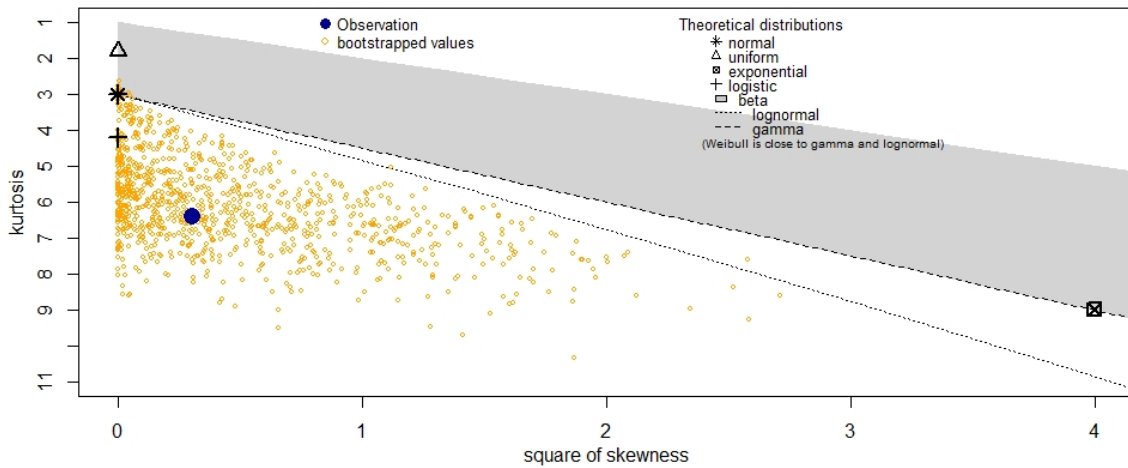


Figure 6-7: Cullen & Frey graph for vertical damage position, Z .

The Cullen & Frey graph indicates that the distribution may be represented by a logistic function (closest match). A normal distribution may also be a possible candidate, but seem less so, as the observed values lie further away on the graph. Having several candidates, we may produce goodness of fit (GoF) statistics for deciding the optimal distribution. In simple terms, the GoF statistics describes how well the model fits into a set of observations or data; the smaller the statistic, the better the fit. By performing MLE, we obtain the GoF statistics and criteria as is seen in Table 6-3. The GoF statistics suggest that the logistic function is the optimal fit, which is supported by the Q-Q and P-P plots presented in Appendix II.

Table 6-3: Goodness of fit (GoF) statistics and criteria for MLE of distribution for Z.

GoF Statistic/Criteria	Logistic distribution	Normal distribution
Kolmogorov-Smirnov Statistic	0.03125606	0.0533253
Cramer-von Mises Statistic	0.03168159	0.1891007
Anderson-Darling Statistic	0.30001377	1.3917191
Akaike's Information Criterion	1572.217	1595.649
Bayesian Information Criterion	1579.428	1602.861

The analytical distribution is plotted in Figure 6-8 together with the numerical data. The logistic probability distributions are given by Eq. 6-4 and Eq. 6-5, and corresponding coefficients location, m , and scale, s , obtained from the MLE are; $m = -1.6218$, and $s = 2.4004$.

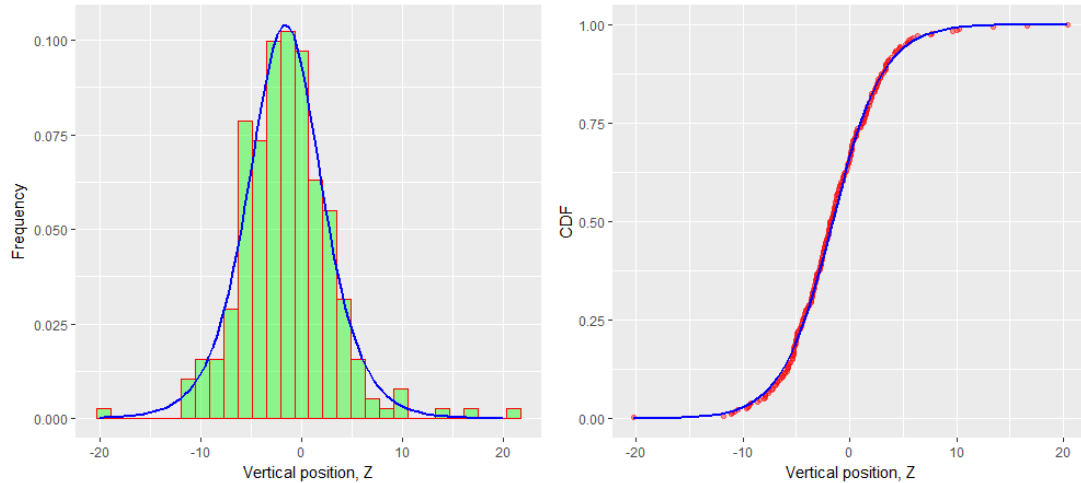


Figure 6-8: Analytical PDF and CDF for vertical damage position, Z.

The expected (mean) value of the distribution is represented by the location parameter, m . Correcting the expected value for vessel draft using Eq. 6-6 produces the conditional PDF and CDF represented by Eq. 6-7 and Eq. 6-8, respectively. The conditional distributions are now given as a function of vessel draft (waterplane) as is seen in Figure 6-9.

$$PDF(Z) = \frac{e^{-\frac{m-Z}{s}}}{s(1 + e^{-\frac{m-Z}{s}})^2} \quad \text{Eq. 6-4}$$

$$CDF(Z) = \frac{1}{(1 + e^{-\frac{m-Z}{s}})} \quad \text{Eq. 6-5}$$

$$\bar{E}(T) = T + m \quad \text{Eq. 6-6}$$

$$PDF(Z|T) = \frac{e^{-\frac{T+m-Z}{s}}}{s(1 + e^{-\frac{T+m-Z}{s}})^2} \quad \text{Eq. 6-7}$$

$$CDF(Z|T) = \frac{1}{(1 + e^{-\frac{T+m-Z}{s}})} \quad \text{Eq. 6-8}$$

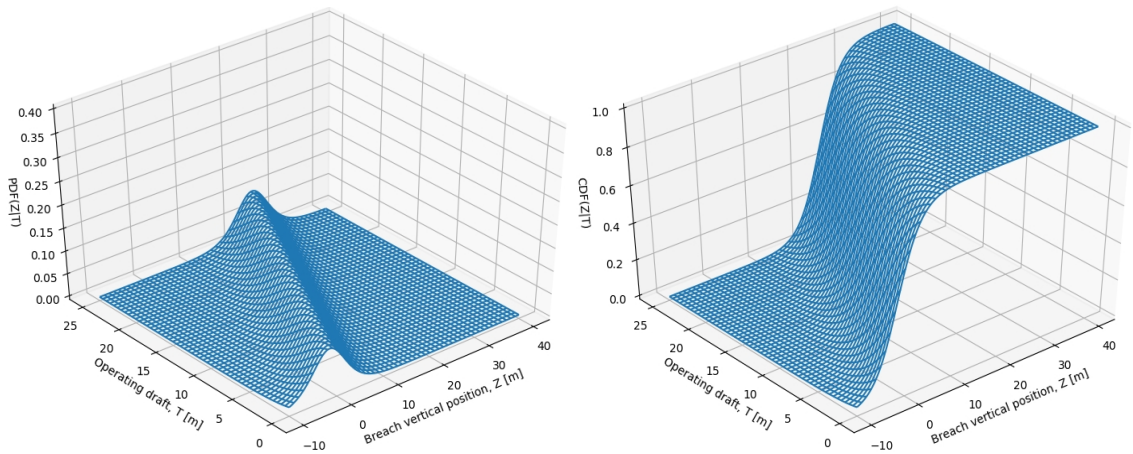


Figure 6-9: PDF and CDF density function for Z conditional on T.

6.2.1.3 Damage length, L

The empirical PDF and CDF for the damage length, L , are presented in Figure 6-10. In order to aid selection of the suitable model distribution, a Cullen & Frey graph is again produced as shown in Figure 6-11. The graph indicates that the empirical model corresponds well to Gamma or the Weibull distribution. Another distribution of the same family, namely the Burr distribution, may also be checked for correspondence, despite not being included in the Cullen & Frey graph.

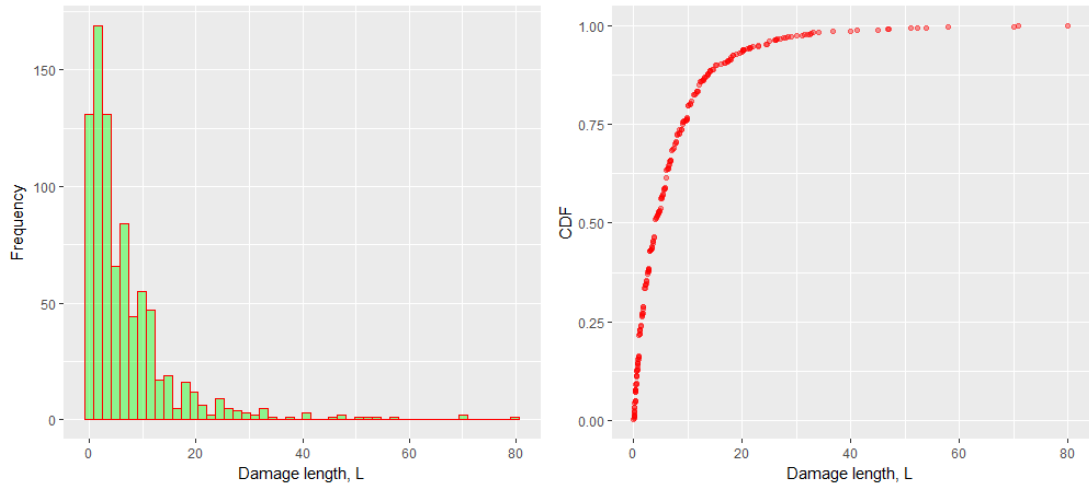


Figure 6-10: Numerical PDF and CDF for damage length, L .

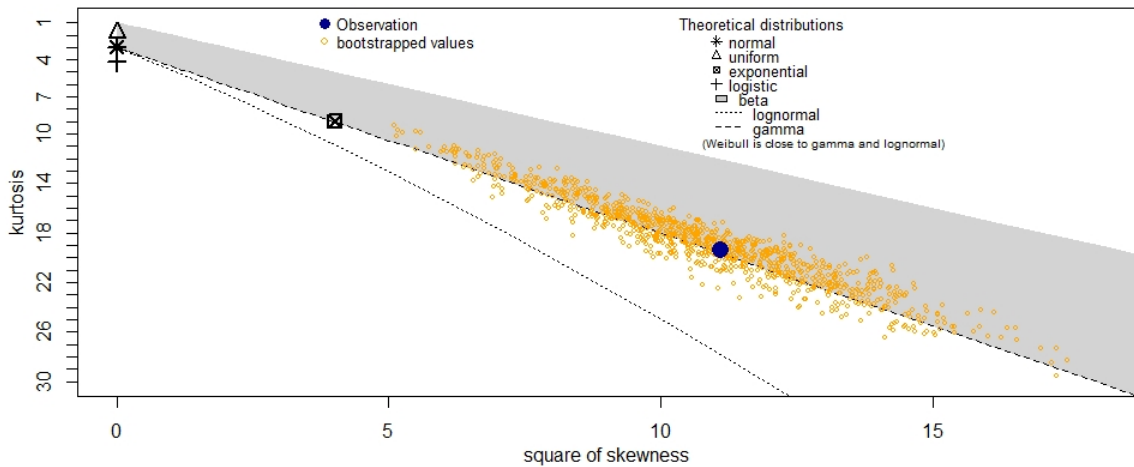


Figure 6-11: Cullen & Frey graph for damage length, L .

Having multiple candidates, Goodness of Fit statistics and criteria associated with MLE are produced and is presented in Table 6-4. The GoF statistics show similar values for all distributions, not providing any obvious best fit. The Q-Q and P-P plot (Appendix II) also confirms that all the distributions are good approximations for the data. However, looking more closely on the Q-Q plot, it indicates that the Burr distribution represents the tails of the distribution slightly better than the remaining two distributions and would be the better analytical representation for the data. The analytical distribution is plotted in Figure 6-12.

The Burr probability distributions are given by Eq. 6-9 and Eq. 6-10, and corresponding shape coefficients a and b , and rate coefficient, r , obtained from the MLE are $a = 5.9883$, $b = 0.9576$ and $r = 0.0276$.

Table 6-4: Goodness of fit (GoF) statistics and criteria for MLE of distribution for L .

GoF Statistic/Criteria	Logistic distribution	Normal distribution
Kolmogorov-Smirnov Statistic	0.03438846	0.04017173
Cramer-von Mises Statistic	0.12081172	0.23706216
Anderson-Darling Statistic	1.00649641	1.69926542
Akaike's Information Criterion	4943.266	4953.525
Bayesian Information Criterion	4952.749	4963.008

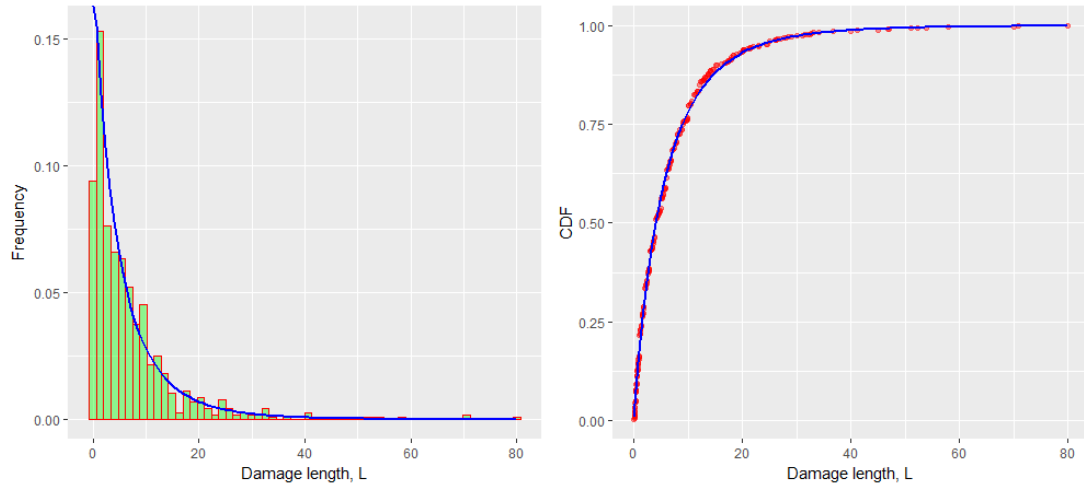


Figure 6-12: Analytical PDF and CDF for damage length, L .

$$PDF(L) = \frac{ab(Lr)^b}{L(1 + (Lr)^b)^{(a+1)}} \quad Eq. 6-9$$

$$CDF(L) = 1 - \frac{1}{(1 + (Lr)^b)^{(a+1)}} \quad Eq. 6-10$$

Direct sampling from the above distribution may result in damages extending beyond the longitudinal limits $L_{s_{fwd}}$ and $L_{s_{aft}}$, respectively. This would not represent realistic damages, nor represent the database, since only damages being manifested on the vessel are included. The damage length may, therefore, be considered conditional on the longitudinal position,

X . For example, if the X location of the damage is 20 m forward of $L_{s_{aft}}$, the damage length cannot be longer than 40 meters. Further, even if the damage is located at midship, maximum damage length cannot be longer than the vessels subdivision length, L_s . In mathematical terms, the damage length is limited by the L boundary curve given by Eq. 6-11. The boundary curve is shown graphically in Figure 6-13. To avoid representing the boundary as piece-wise linear using two functions, an alternative boundary can be represented by Eq. 6-12.

$$L_{boundary}(X) = \begin{cases} 2L_s X & \text{for } X \in [0, 0.5] \\ 2L_s(1 - X) & \text{for } X \in [0.5, 1] \end{cases} \quad \text{Eq. 6-11}$$

$$L_{boundary}(X) = 2L_s X(X^3 - 2X^2 + 1) \quad \text{Eq. 6-12}$$

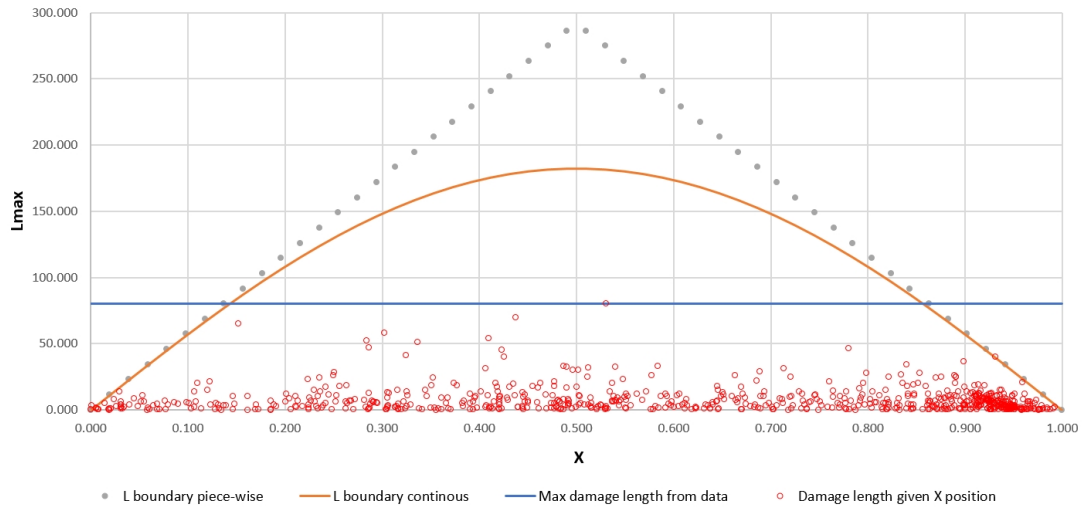


Figure 6-13: L maximum boundary curve.

This curve will produce damages with smaller length than that of the full vessel length. However, as the database does not contain any damages longer than 80 m (represented by the horizontal blue line in Figure 6-13,) use of the quadratic model is justifiable. Furthermore, by checking the non-dimensionalised damage lengths from the GOALDS database, it is confirmed that the maximum damage length is approximately $0.5L_s$. The updated boundary curve given by Eq. 6-12 ensures that the maximum damage length is $0.625L_s$ (found by setting $X = 0.5$ in the equation). This is slightly more conservative than the data indicate but is still a reasonable assumption. The boundary curve does not need to

be implemented in the distribution and, for simplicity, the sampled damage length may be limited by the boundary curve in a separate step using rejection sampling. To illustrate the validity of this approach, 10,000 sampled damage lengths are presented in Figure 6-14. The data points limited by the boundary curve is seen to correspond with the data points from the database as is illustrated in Figure 6-13. The notation of Eq. 6-9 and Eq. 6-10 can be changed to $PDF(L | X)$ and $CDF(L | X)$ respectively as long as the boundary curve is enforced during the sampling process.

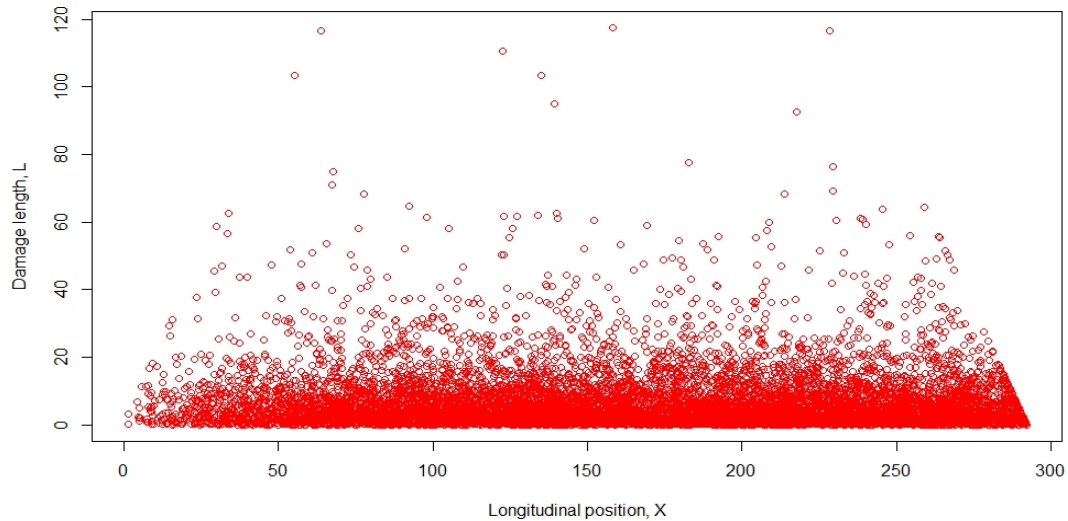


Figure 6-14: Sampled damage lengths, L , plotted on given X location.

6.2.1.4 Damage height, H

The available data indicate that the damage height, H , can be considered conditional on the vertical position of the lower damage limit, Z . The dependency is illustrated by the graph in Figure 6-15, where the marginals for both Z and H are presented together with their numerical PDF's. The probability of the damage height, H , conditional on lower position of damage, Z , is denoted by $P(H | Z)$. Having already established an appropriate marginal distribution for the vertical position of damage, Z , in the above section 6.2.1.2, we will initially focus on identifying a marginal distribution for the damage height, H . The numerical distribution's PDF and CDF for the damage height, H , are presented in Figure 6-16. A Cullen & Frey graph as shown in Figure 6-17 is used to identify the best model for the distribution. From the graph, the data seems to lie on the area indicating a Beta distribution. The Beta distribution is, however, limited to the interval $x \in [0,1]$, so a Generalised Beta Prime distribution would be more appropriate.

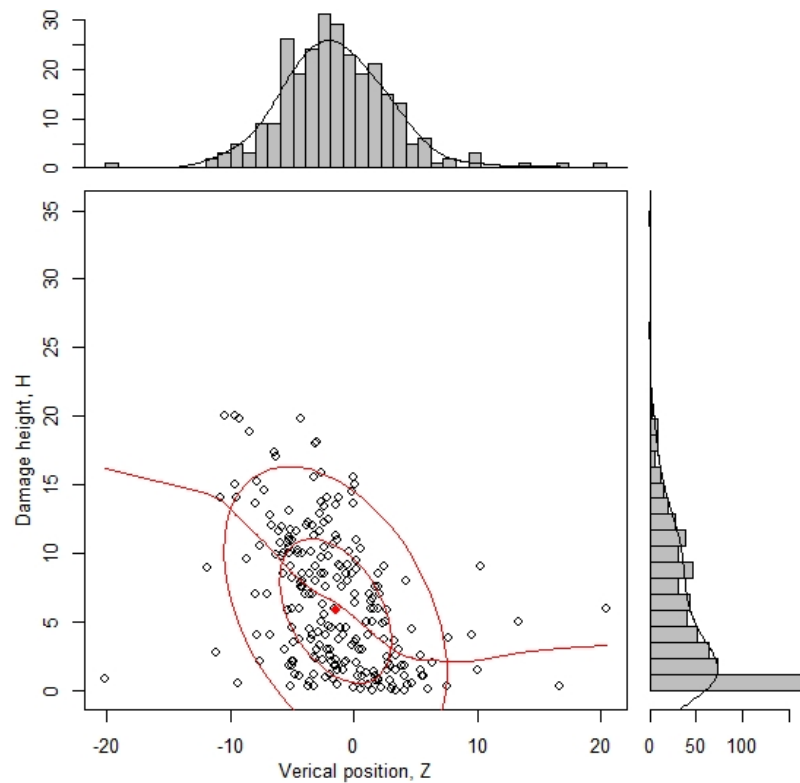


Figure 6-15: Dependency between Z and H .

By performing MLE, we obtain the shape coefficients $a = 6.8089$, $p = 0.0838$ and $q = 1.1089$ and scale coefficient $b = 15.7057$. The marginal analytical PDF and CDF for damage height, H , are shown in Figure 6-18. The CDF is given by Eq. 6-13, where $B(p,q)$ is the Beta function. There is no closed form solution for the CDF.

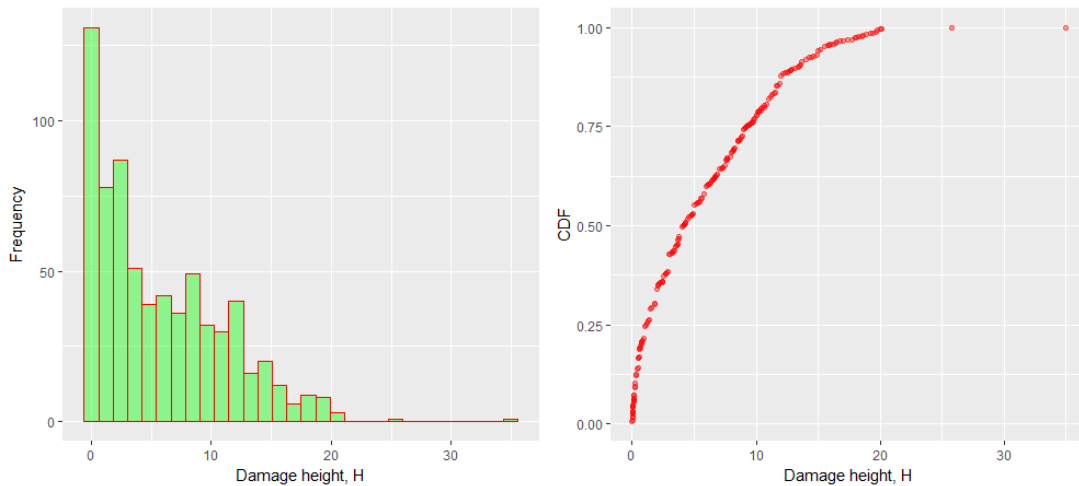


Figure 6-16: Numerical PDF and CDF for damage height, H .

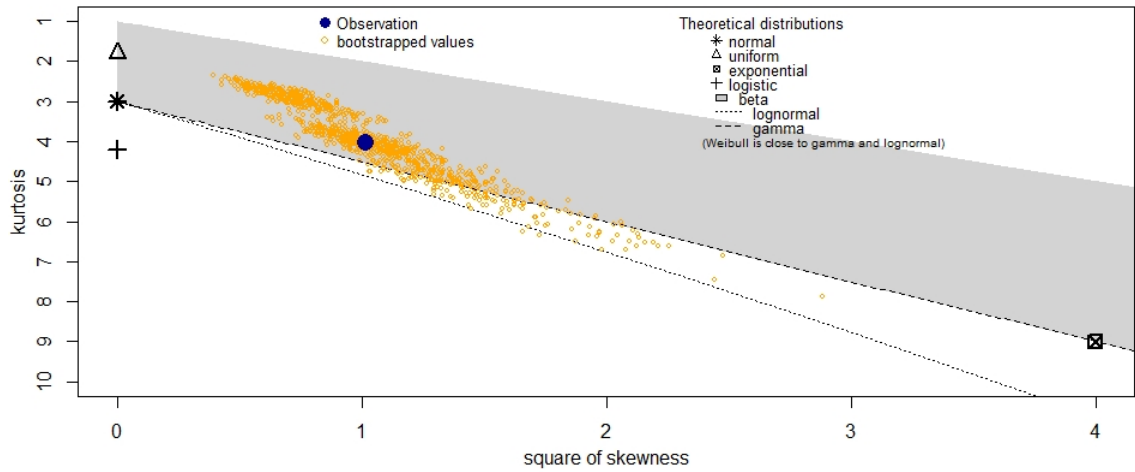


Figure 6-17: Cullen & Frey graph for damage height, H .

$$PDF(H) = \frac{a\left(\frac{H}{b}\right)^{(ap-1)}}{bB(p,q)\left(1 + \left(\frac{H}{b}\right)^a\right)^{(p+q)}} \quad Eq. 6-13$$

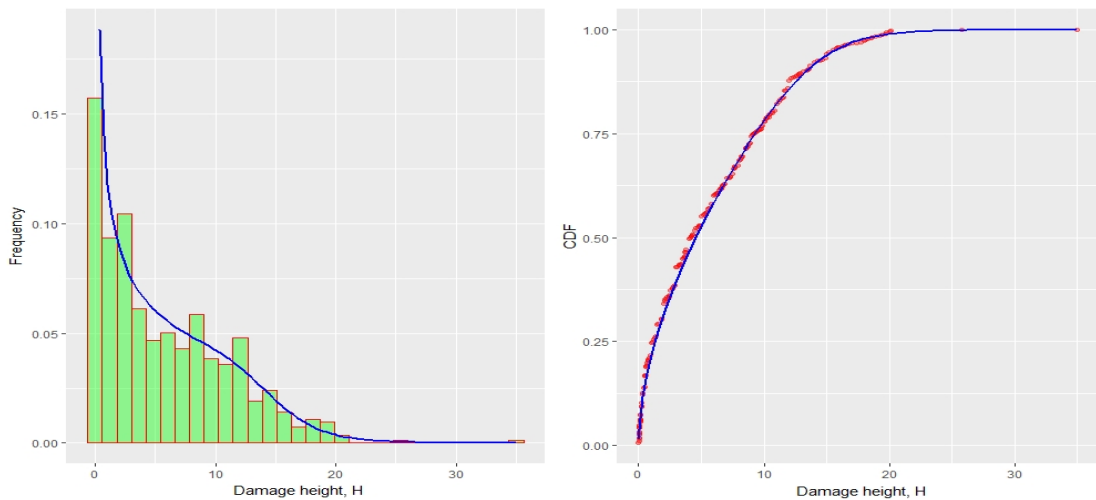


Figure 6-18: Analytical PDF and CDF for damage height, H .

Having established analytical distributions for both marginals, H and Z , they may be combined utilising copula theory. Details on copula theory is outside the scope of this thesis, but in summary copulas are a well-known technique for modelling conditional or multivariate probability distributions. Sklar's theorem (Sklar, 1959) states that any multivariate joint distribution can be written in terms of univariate marginal distribution functions and a copula, which describes (or couples) the dependence structure between the

variables on a unit square. For the purpose of identifying an optimal copula, a specific library has been used in the statistical software R, namely the *Vinecopula* library, which enables to identify the best copula from a range of copula-families. Applying the provided fitting function, the *Rotated Tawn type 2* (90 degrees rotation) copula, with parameters $\text{par} = -1.74$, $\text{par}2 = 0.53$, is identified as being the optimal fit from the range of available copulas in the package. The PDF for H conditional on Z represented by the chosen copula is illustrated in Figure 6-19. The figure also suggests that the copula is a good representation of the data points seen in Figure 6-15. For more information on this specific copula, see Tawn (1988).

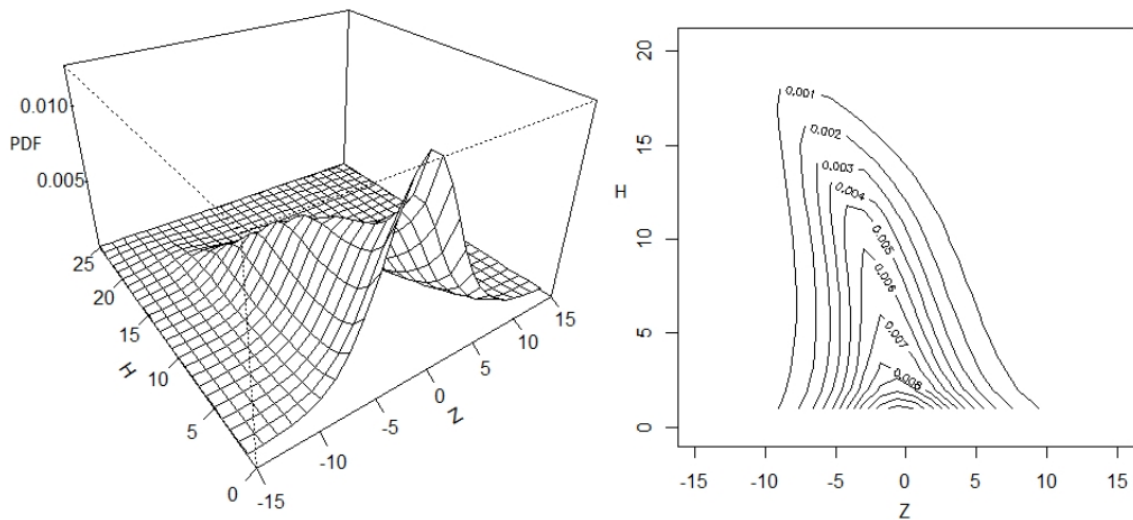


Figure 6-19: Joint PDF of H and Z represented as copula.

6.2.1.5 Damage penetration, Y

The last parameter for a damage extent is the transverse penetration, Y . The database suggests that the penetration is dependent on the damage length, L . This is illustrated by the graph in Figure 6-20, where the marginals for both Y and L are presented together with their numerical PDF's. From the graph, a clear increase in damage penetration is seen with increasing damage length. This is, however, only seen in the interval $L \in [0, 30 \text{ m}]$ and relates to head-on high energy collisions, which is directly dependent on the striking vessel breadth. For larger damage lengths, outside the range of normal ship breadths, the statistics in the database suggests that the penetration is decreasing with damage length.

This is because extreme damage lengths would be a result of collision damages with high angle of attack, producing long damage length and shallower penetrations (similar to grounding side raking damages). The numerical distribution's PDF and CDF for the damage penetration, Y , are presented in Figure 6-21. A Cullen & Frey graph presented in Figure 6-22 shows that the data seems to correspond very well with that of an Exponential or a Gamma distribution. Producing GoF statistics as seen in Table 6-5, there is a slightly better fit seen for the Exponential distribution. Q-Q and P-P plot are found in Appendix II. The MLE results in the rate-coefficient, $\lambda = 0.2968$ for the Exponential distribution. The marginal analytical PDF and CDF for damage penetration, Y , are shown in Figure 6-23. The PDF and CDF is given by Eq. 6-14 and Eq. 6-15, respectively.

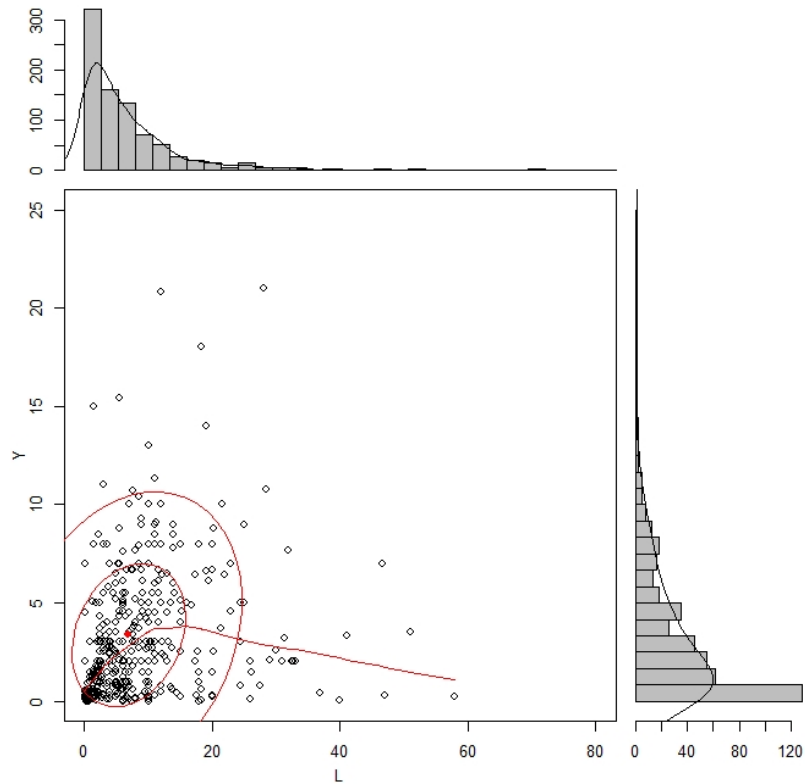


Figure 6-20: Dependency between L and Y .

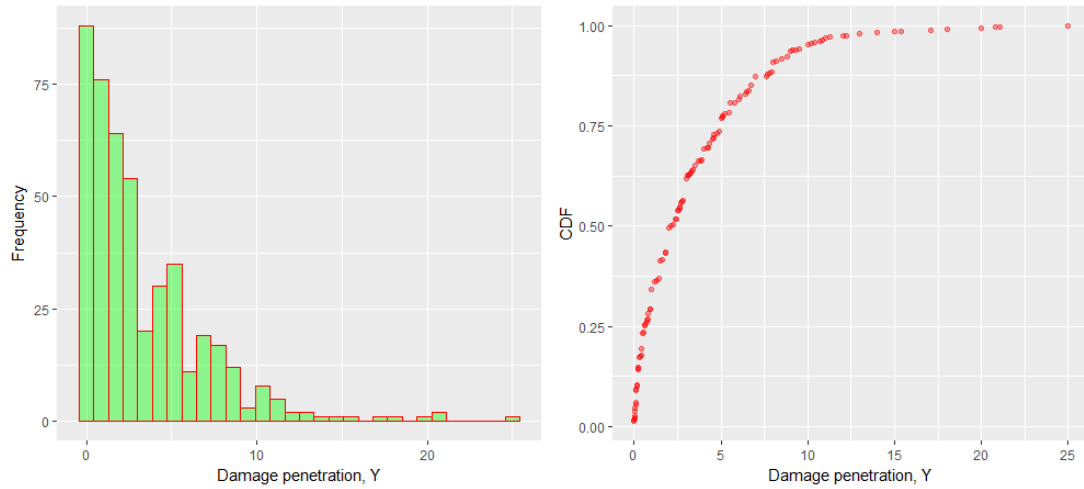


Figure 6-21: Numerical PDF and CDF for damage penetration, Y.

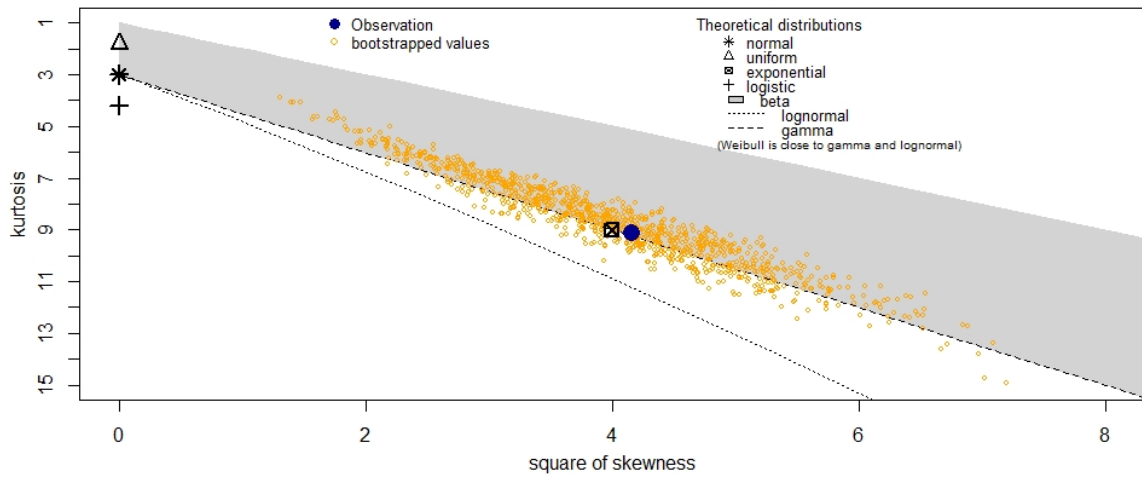


Figure 6-22: Cullen & Frey graph for damage penetration, Y.

Table 6-5: Goodness of Fit (GoF) statistics and criteria for MLE distribution for L.

GoF Statistic/Criteria:	Exponential	Gamma
Kolmogorov-Smirnov Statistic	0.09504132	0.09504132
Cramer-von Mises Statistic	0.72445322	0.72445323
Akaike's Information Criterion	2017.289	2019.289
Bayesian Information Criterion	2021.410	2027.530

$$PDF(Y) = \lambda e^{-\lambda Y} \quad \text{Eq. 6-14}$$

$$CDF(Y) = 1 - e^{-\lambda Y} \quad \text{Eq. 6-15}$$

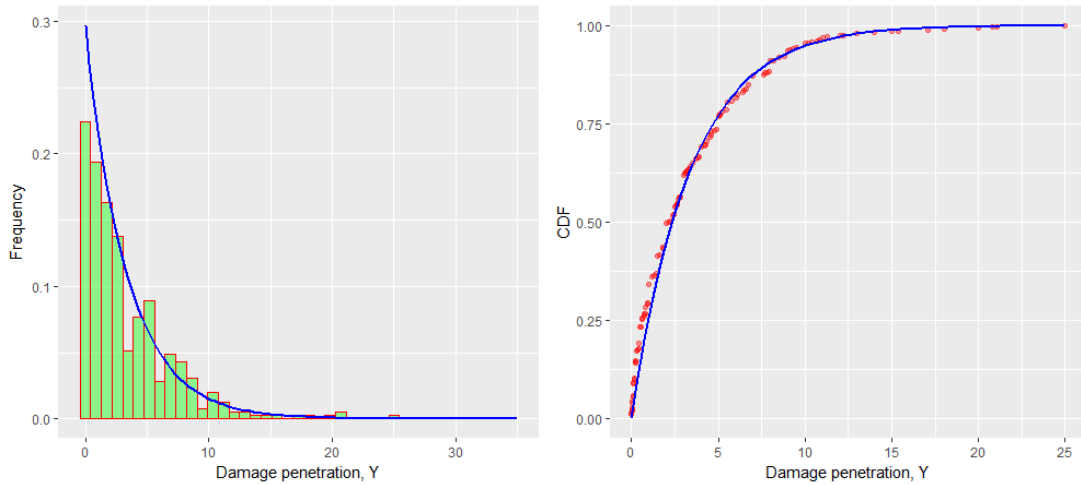


Figure 6-23: Analytical PDF and CDF for damage penetration, Y .

Having established analytical distributions for both marginals, Y and L , an appropriate copula may be identified using the *Vinecopula* library in R. Applying the provided fitting function, the *survival BB8 copula*, with parameters $\text{par} = 2.32$, $\text{par2} = 0.87$, is identified as being the optimal fit. PDF for Y conditional on L represented as copula is illustrated in Figure 6-24. The figure also suggests that the copula is a good representation of the data points seen in Figure 6-20. For more information on this particular copula, see Joe (1997).

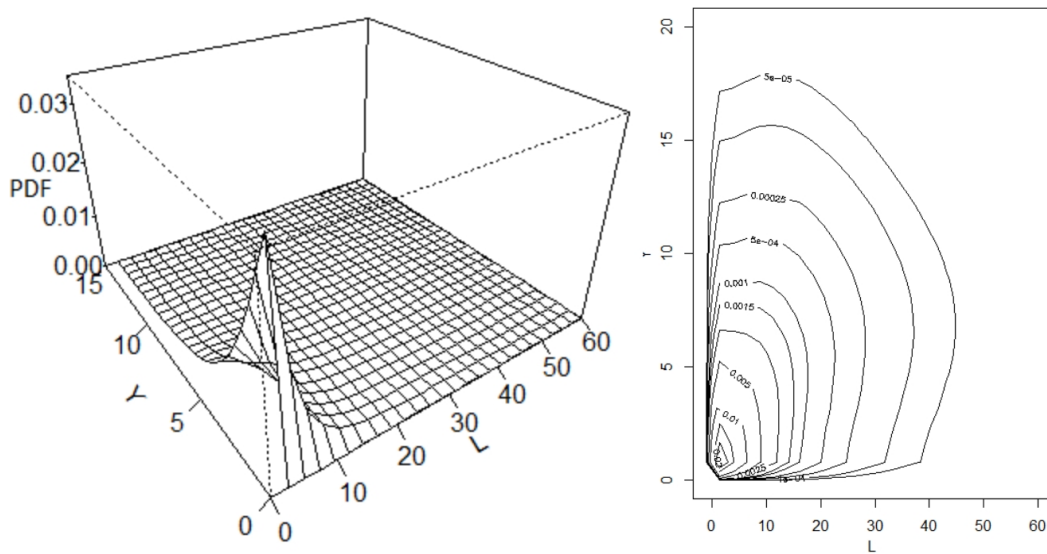


Figure 6-24: Joint PDF of Y and L represented as copula.

6.2.2 Breach position relative to the hull

Figure 6-25 shows an example of a breach sampled from the above developed distributions. The breach is positioned based on vertical (from baseline, BL) and longitudinal (from aft perpendicular, AP) reference. The damage penetration, however, is not as straightforward due to the side shell curvatures.

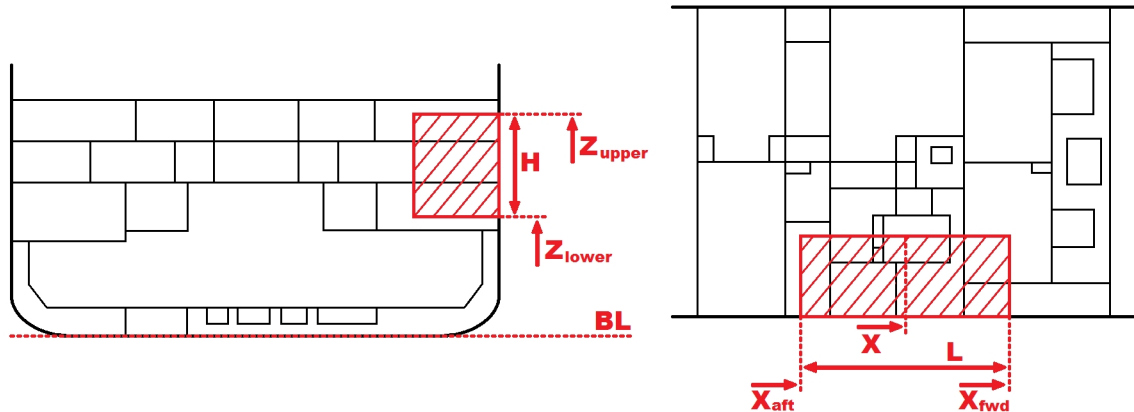


Figure 6-25: Breach longitudinal position, length and height in relation with hull.

The penetration depths are known, but the reference starting point of the penetration is varying with height from baseline and ship length. To avoid breaches outside the hull, the breaches are positioned using the hull-waterplane intersection as transverse reference. This is in line with the alternative sampling scheme as suggested by Bulian (2017). The hull-waterline intersection may be presented by three piecewise least-square fitted curves as is seen in Figure 6-26.

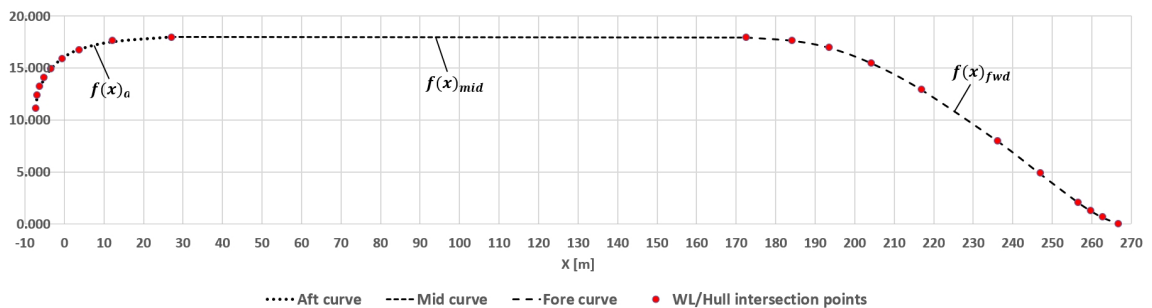


Figure 6-26: Hull-waterline intersection curve for transverse penetration reference.

6.2.3 Initial damage extent

The distributions derived in the previous sections can be combined into a joint distribution for a specific breach or damage characteristic, as represented by Eq. 6-16.

$$f(\text{breach}) = f(X,Z,T,L,H,Y) \quad \text{Eq. 6-16}$$

Since the breach extent is defined in the continuous space, a range of damage breaches would result in the same initial damage extent and subsequent compartments being damaged. It would therefore be beneficial to express the breach in terms of a specific initial damage extent (i.e., damaged rooms and lost buoyancy). This can be achieved by translating the expression for breach extent into the discrete space for specific damaged compartments. For a specific initial damage extent represented as damaged compartments, the above continuous variables are bounded by upper and lower limits. These boundaries are intervals in the planes x , y and z for the respective variables. For example, for a breach to result in a specific initial damage extent x , the damage length, L , can take any value within the specific interval $L \in [l_1, l_2]$. If the variable takes on a value outside this interval, a different extent would be realised. Other variables have their own respective intervals for a specific initial damage extent, x , which together forms the complete integration domain σ . Since the damage case has intervals or boundaries of possible solutions representing the domain, each variable must be integrated over its specific boundary as illustrated in Eq. 6-17.

$$f(x) = \int_{\sigma(\text{initial damage})} f(X,Z,T,L,H,Y) dXdZdTdLdHdY \quad \text{Eq. 6-17}$$

The above approach is similar to that adopted by the probabilistic damage stability requirements of SOLAS (2009). However, the approach used in SOLAS is largely simplified - relying on a zonal subdivision of the vessel arrangement and simplified integration techniques. The analytical formulae for p-factor, r-factor and v-factor in SOLAS (2009) are based on the mathematical processing of the distributions of damage characteristics and the use of the *Wendel* diagram. Relevant details of this approach for the case of collision damages can be found in Lützen (2001) and Pawłowski (2004). The simplifications are justifiable as compartments may comprise complex shapes and the interval for the variables become difficult to identify.

Solving the above integral also becomes an issue without using numerical methods. Because of these challenges, an alternative method will be adopted in the following, namely Monte-Carlo (MC) sampling. This is an approach commensurate with the *non-zonal* approach utilised in the EMSA III and eSAFE projects (Zaraphonitis et al., 2015 & 2017). Similar MC sampling approaches has been used by Kehren & Krüger (2007) and Krüger & Dankowski (2009). By sampling from the above defined distributions, it is possible to identify for each sampled breach, what compartments are compromised. Sufficient sample size ensures that all possible initial damage extents are accounted for. Specific cases will be sampled numerous times, which will account for their respective probability (p-factors). For simplicity, only the starboard side has been used for sampling in the presented development for testing and implementation. Sampling from the distributions has been done in the statistical software R, where a large sample size of 1,000,000 were used to ensure convergence and coverage of all possible initial damage extents. Damages not accounted for by the sampling, since we used such a large sample size, are assumed to have a negligible probability. The sampled breaches have been translated into volumes in the stability software *NAPA* and checked against every compartment in the vessel arrangement to see if there are any overlaps in geometrical properties between compartments and the breach. Overlap would mean that the compartment is damaged and part of the initial damage extent. An excerpt of 500 samples is shown in Appendix III. Only a smaller selection is shown due to the large number of samples. Finally, an illustration of 300 samples is presented in Figure 6-27. The sample of 1,000,000 starboard breaches resulted in 19,225 unique initial damage extents and the frequencies of occurrence are taken as estimates of the probability. This represents the a priori list of possible initial damage extents, which will be used in the development.

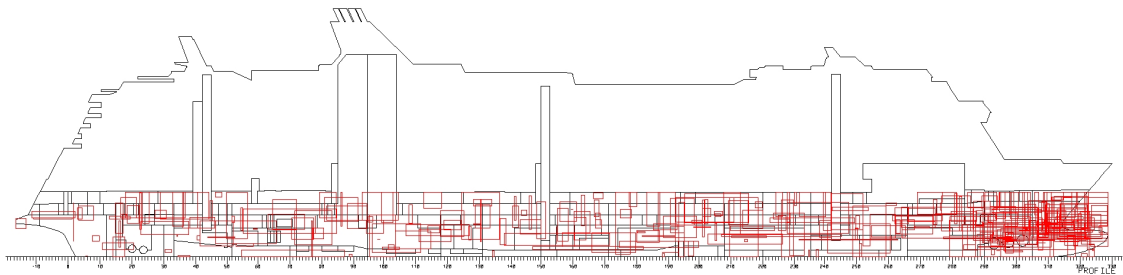


Figure 6-27: Breach-Compartment overlap check for 300 samples.

6.3 Likelihood function

6.3.1 Initial flooding

The identified initial damage extents introduced in the previous section are only covering whether or not compartments are affected by the breach and in that respect may be considered compromised. However, this does not necessarily entail that they will be flooded when for example the breach (entire or in part) may be located above the waterline. Therefore, the probability that an initial damage extent will result in loss of buoyancy and if the flooding sensors will indicate flooding depends on whether there is floodwater ingress through the damage breach. As some initial damage extents will have much higher probability of flooding due to their location with respect to the waterline, this relationship should be captured by the likelihood function for the flooding sensors. The probability of flooding is determined by three variables and their interplay, namely; the lower limit of the vertical position of damage breach, Z , the draft of the intact vessel, T , and the significant wave height, H_s . Figure 6-28 may illustrate the relationship between the variables.

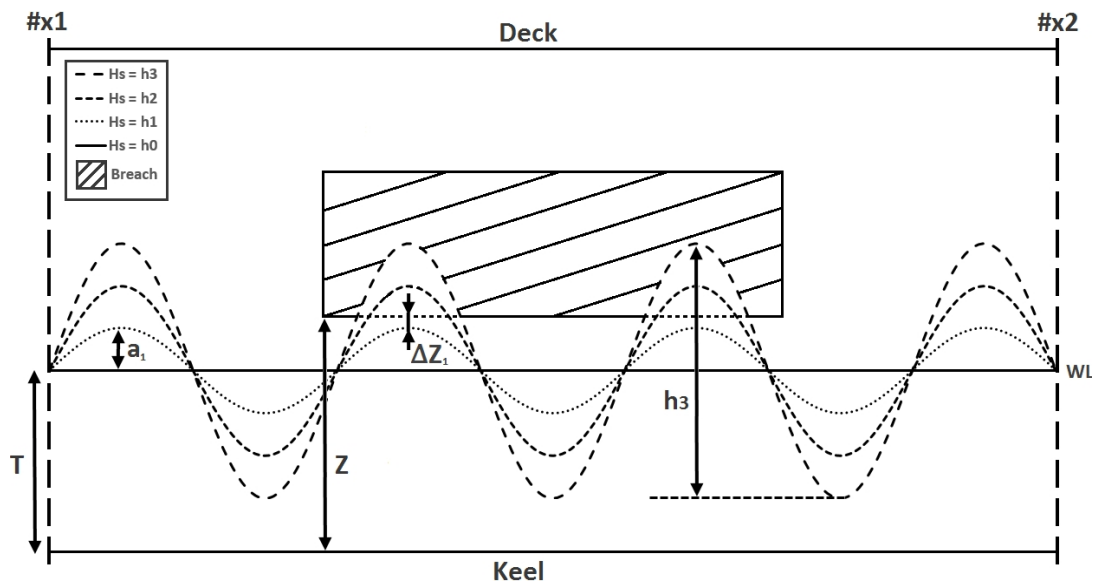


Figure 6-28: Influence on flooding from variables T , Z and H_s (static consideration).

The figure illustrates a ship section (#x1 - #x2) with even keel trim that has a breach opening located slightly above the calm waterline. The calm waterline is represented by $H_s = h_0 = 0$. There are three additional waterlines representing three different regular

sinusoidal waves with heights $H_s = \{h_1, h_2, h_3\}$, for which the following is true; $h_3 > h_2 > h_1 > 0$. It is clear from the figure that neither the calm water condition h_0 nor the lowest wave condition h_1 would result in flooding through the damage breach. These cases can be considered to have a positive flooding margin given by Eq. 6-18, were a is the wave amplitude for a specific wave height H_s . However, the remaining wave conditions h_2 and h_3 , result in negative flooding margin ΔZ and will consequently lead to flooding through the damage breach.

$$\Delta Z = Z - (T + a) \quad \text{Eq. 6-18}$$

A draft increase $\Delta T = \Delta Z_0$ may now be considered, which will remove the positive flooding margin for wave condition h_1 , enable flooding, and further result in a zero margin ($\Delta Z_0 = 0$) for the still-water case, h_0 . The particular case of $T = Z$ could, therefore, be considered a limit condition and will be important in defining the likelihood function. Furthermore, relative (with respect to water surface) motions of the ship and the stochastic nature of a waves need to be accounted for. That is, flooding occurs when $W_E > Z_E$, where W_E and Z_E are the elevation of the water surface and the lower limit of the breach (both measured from the same vertical reference), respectively. The probability of flooding may therefore be denoted by Eq. 6-19, where W_M and V_M are motions of the water surface, and the vessel respectively. However, as the vessel motion is governed by the wave motion, represented by the significant wave height, this notation may be simplified to Eq. 6-20.

$$P(F | Z, T, W_M, V_M) = P(W_E > Z_E | Z, T, W_M, V_M) \quad \text{Eq. 6-19}$$

$$P(F | Z, T, W_M, V_M) = P(W_E > Z_E | Z, T, H_s) \quad \text{Eq. 6-20}$$

For the purpose of implementing wave-dynamics, the time-domain simulation tool PROTEUS3 has been utilised, with the aim at developing a probability density function for initial flooding through the damage breach, conditional on the relevant variables; Z , T , and H_s , as represented by Eq. 6-20. The results will be employed to derive a sensor model, representing the probability of particular values of T , and H_s , given a particular initial damage extent (represented by Z) imposed by flooding. For illustrating purposes, an initial damage extent located highly above the waterline imposed by flooding may be considered.

The model should return a low likelihood for smaller values of H_s and draft T , simply because to realise flooding for higher extents, this has to be a result of larger wave heights and/or deeper drafts. The vessels KG (or GM) and wave encounter heading would in fact also affect the initial flooding probability, but similarly to what was done in Chapter 5, these have been covered by their marginal a priori distributions.

In order to derive the distribution, 10,000 simulations have been performed, with the significant wave height sampled from the interval [1-15 m], heading from the interval [0,360°) while draught, T , and KG were sampled from their respective marginal distributions as discussed more in detail in section 7.2.2. The waves zero up-crossing period, T_z , conditional on the wave height have been sampled from the probability distribution given by Eq. 5-2 for world-wide operation. Following simulation in time-domain for 30 minutes for each sample, the maximum water elevation at random longitudinal positions along the vessel side-shell was identified, as water ingress may be assumed through any breach opening located at (or below) this water elevation. The water elevation is represented as the difference in height from the calm-waterplane and is given by Eq. 6-21. The values of ΔZ at which flooding occurs are presented in Figure 6-29, indicating that the values of ΔZ are scattered and growing with increasing wave height.

$$\Delta Z = Z - T$$

Eq. 6-21

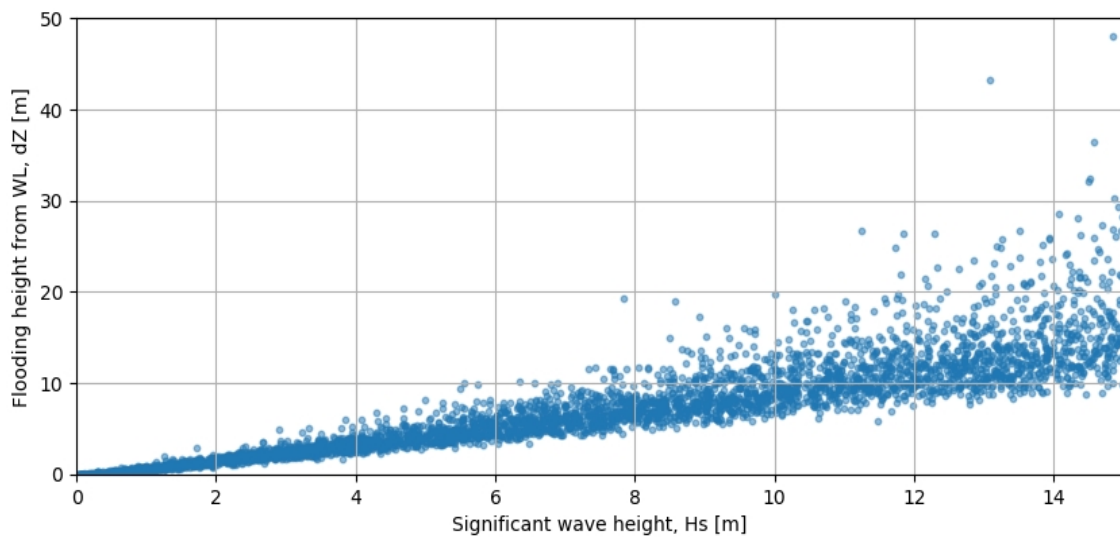


Figure 6-29: Height from calm-waterplane, ΔZ , of initial flooding as a function of wave height, H_s .

The limiting condition for which $T = Z$, discussed earlier in this chapter, is clearly noticeable in the figure for wave height $H_s = 0$. The data points are represented well by a *Burr* distribution, as given by Eq. 6-22. The corresponding coefficients have been obtained by MLE and represented as a function of H_s as given by Eq. 6-23 to Eq. 6-25. The zero reference of the y-axis is represented by the waterline rather than the vessel baseline. Histogram and analytical distributions are shown in Figure 6-30.

$$PDF(\Delta Z|H_s) = \frac{\alpha\beta}{\lambda} \left(\frac{\Delta Z}{\lambda}\right)^{\alpha-1} \left[1 + \left(\frac{\Delta Z}{\lambda}\right)^{\alpha}\right]^{-\beta-1} \quad \text{Eq. 6-22}$$

$$\alpha(H_s) = a + be^{cH_s}, a = 141.311, b = -141.309, c = -0.012 \quad \text{Eq. 6-23}$$

$$\beta(H_s) = a + be^{cH_s}, a = 0.148, b = 8.515, c = -0.422 \quad \text{Eq. 6-24}$$

$$\lambda(H_s) = a + be^{cH_s}, a = -28.634, b = 29.753, c = 0.020 \quad \text{Eq. 6-25}$$

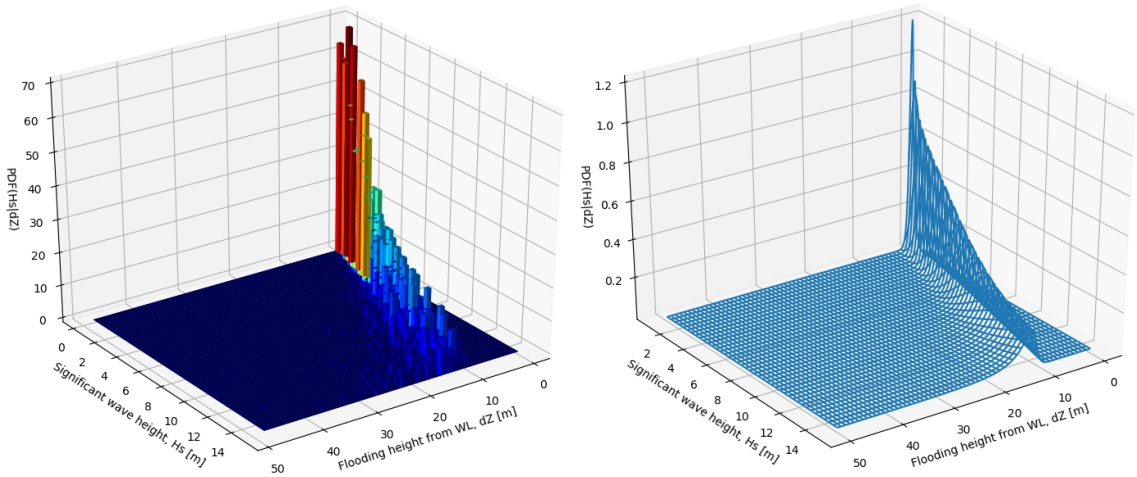


Figure 6-30: Numerical and analytical distributions for flooding height from WL.

From Figure 6-30, it is easy to see that the closer to the waterline a lower limit of a breach is located (the shorter its distance from WL), the more likely is it to be flooded. Similarly, the probability will increase with increasing wave height but so will the uncertainty around the mean. It is noteworthy that the distribution given by Eq. 6-22 represents the probability of obtaining a specific ΔZ value for which flooding occur, conditional on H_s . Flooding would, however, occur for all ΔZ values below this specific value, and the probability of flooding would be given by the exceedance probability denoted $P(\Delta Z \geq z|H_s)$. This is represented by

the cumulative probability distribution function of Eq. 6-22, obtained by integration and denoted by Eq. 6-26. The resulting Eq. 6-27 is valid on the interval $\Delta Z \in [0, \infty]$, otherwise Eq. 6-28 is governing as is shown in Figure 6-31.

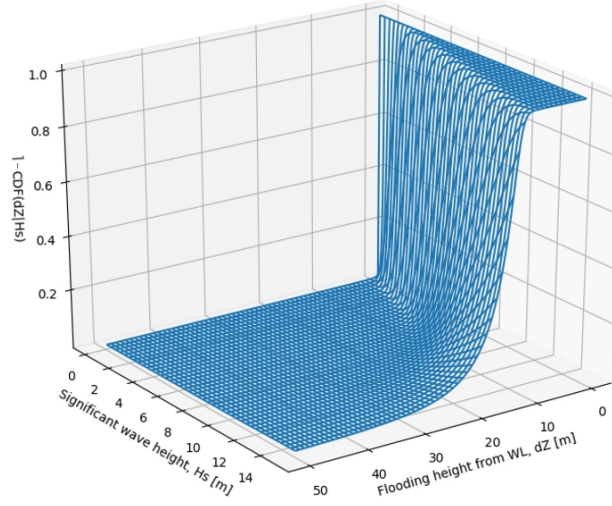


Figure 6-31: Exceedance probability of flooding height from WL, ΔZ .

$$P(\Delta Z \geq z | H_s) = \int_{\infty}^{\Delta Z} \frac{\alpha \beta}{\lambda} \left(\frac{\Delta Z}{\lambda}\right)^{\alpha-1} \left[1 + \left(\frac{\Delta Z}{\lambda}\right)^{\alpha}\right]^{-\beta-1} dZ \quad \text{Eq. 6-26}$$

$$P(\Delta Z \geq z | H_s) = \left[1 + \left(\frac{\Delta Z}{\lambda}\right)^{\alpha}\right]^{-\beta}, \quad \Delta Z \in [0, \infty] \quad \text{Eq. 6-27}$$

$$P(\Delta Z \geq z | H_s) = 1, \quad \Delta Z \in [-\infty, 0] \quad \text{Eq. 6-28}$$

From the figure it is clear that the limit condition at $H_s = 0$ is represented by a step function. As the damage extent is known, and not the actual ΔZ value of the breach, it must be assumed that the probability of flooding (conditioned on the initial damage extent) may come from any of the ΔZ values within the interval $\Delta Z \in [\Delta Z_1, \Delta Z_2]$. This can be accounted for by integrating Eq. 6-27 and Eq. 6-28 over the specific interval as given by Eq. 6-29. The integration results in the likelihood functions given by Eq. 6-30 to Eq. 6-33. As we are developing a likelihood function, the distribution is now represented as H_s conditioned on $\Delta Z_1, \Delta Z_2$, and denoted using $\Lambda(\Delta Z_1, \Delta Z_2)$.

$$\Lambda(\Delta Z_1, \Delta Z_2) = P(H_s | \Delta Z_1, \Delta Z_2) = \int_{\Delta Z_1}^{\Delta Z_2} \left[1 + \left(\frac{\Delta Z}{\lambda}\right)^{\alpha}\right]^{-\beta} dZ \quad \text{Eq. 6-29}$$

$$\Lambda(\Delta Z_1, \Delta Z_2) = P(H_s | \Delta Z_1, \Delta Z_2) = C \left(\Delta Z_{22} F_1 \left(\frac{1}{\alpha'} \beta; 1 + \frac{1}{\alpha'} - \left(\frac{\Delta Z_2}{\lambda} \right)^\alpha \right) + \dots \right. \quad \text{Eq. 6-30}$$

$$\left. \dots - \Delta Z_{12} F_1 \left(\frac{1}{\alpha'} \beta; 1 + \frac{1}{\alpha'} - \left(\frac{\Delta Z_1}{\lambda} \right)^\alpha \right) \right), \quad \text{if } \Delta Z_1 > 0 \text{ and } \Delta Z_2 > 0 \quad \text{Eq. 6-31}$$

$$\Lambda(\Delta Z_1, \Delta Z_2) = P(H_s | \Delta Z_1, \Delta Z_2) = C \left(\Delta Z_{22} F_1 \left(\frac{1}{\alpha'} \beta; 1 + \frac{1}{\alpha'} - \left(\frac{\Delta Z_2}{\lambda} \right)^\alpha \right) - \Delta Z_1 \right), \quad \text{if } \Delta Z_1 < 0 \quad \text{Eq. 6-32}$$

$$\Lambda(\Delta Z_1, \Delta Z_2) = P(H_s | \Delta Z_1, \Delta Z_2) = C(\Delta Z_2 - \Delta Z_1), \quad \text{if } \Delta Z_1 < 0 \text{ and } \Delta Z_2 < 0 \quad \text{Eq. 6-33}$$

$$C = \frac{1}{\Delta Z_2 - \Delta Z_1} \quad \text{Eq. 6-34}$$

Figure 6-32 shows sample distributions for two initial damage extents. Case 1 with vertical integrand interval $Z_{1,1} = 1 \text{ m}$, $Z_{2,1} = 4 \text{ m}$, significant wave height $H_{s,1} = 5 \text{ m}$ and draft $T_1 = 7.5 \text{ m}$. Case 2 with vertical integrand interval $Z_{1,2} = 9.0 \text{ m}$, $Z_{2,2} = 12.0 \text{ m}$, significant wave height $H_{s,2} = 3 \text{ m}$ and draft $T_1 = 8 \text{ m}$.

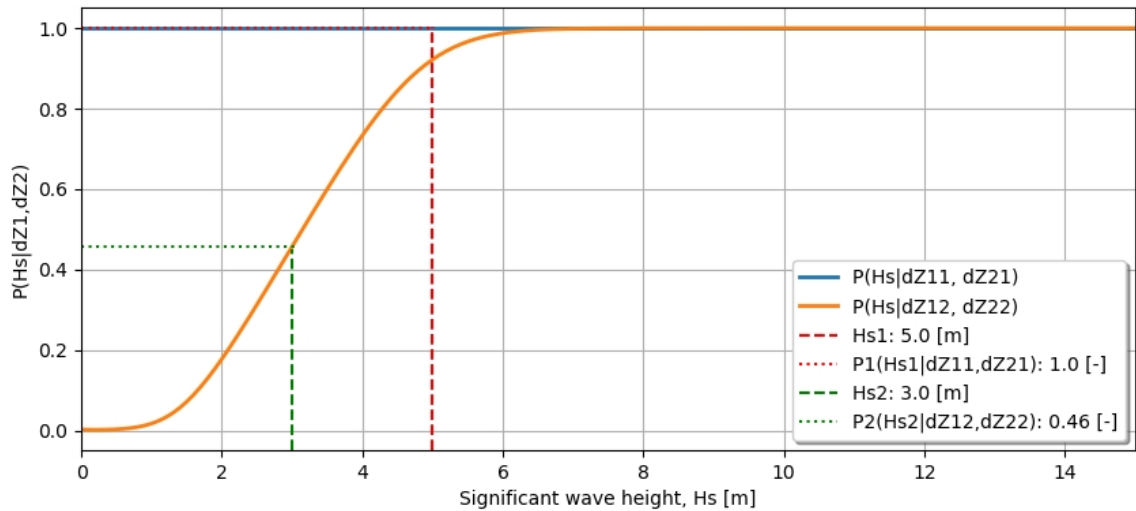


Figure 6-32: Example distribution for two initial damage extents.

As shown in the figure, Case 1 will flood regardless of the significant wave height due to both integrands (vertical limits) being located below the calm waterline. Case 2, however, will not flood for calm water conditions as both integrands are located above the waterline and the probability of flooding is increasing with wave height. Another example shows a complete posterior update of the a priori probability for all the initial damage cases (as

derived in the previous section) using known draught, T , and range of wave heights, H_s as sensor evidence. For illustrating the change in flooding probability with increasing wave height, a specific damage extent with high vertical location has been chosen and imposed by four different wave heights, namely calm-sea, one moderate and two more extreme wave heights. The draft has in this example been kept constant. The four example cases are summarised in Table 6-6 and the example damage extent comprising a single compartment is illustrated in Figure 6-33.

Table 6-6: Summary of example conditions.

Case	Draft, T [m]	Wave height, H_s [m]	Integrand interval: Z_1, Z_2 [m] (from BL)
Case 1	8.20	0.00	10.80, 14.20
Case 2	8.20	2.00	10.80, 14.20
Case 3	8.20	6.00	10.80, 14.20
Case 4	8.20	12.00	10.80, 14.20

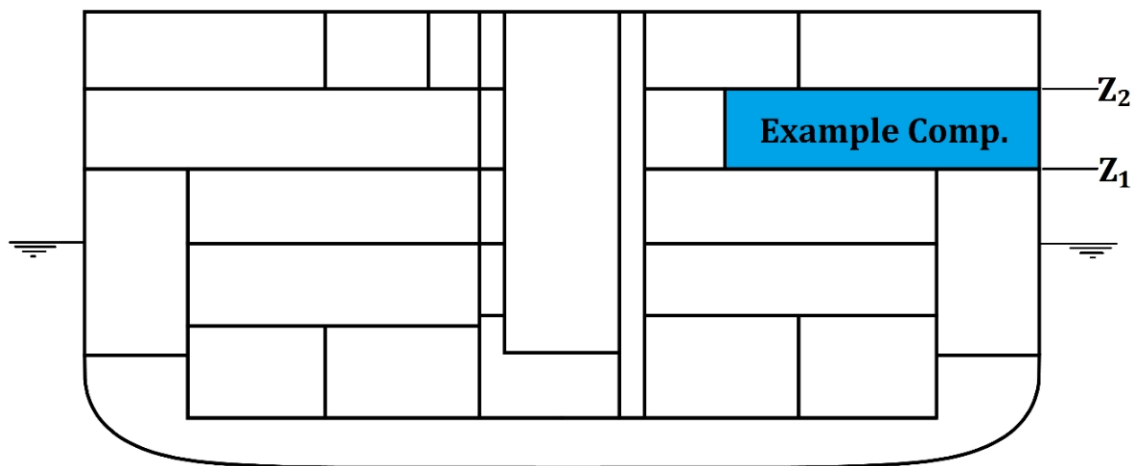


Figure 6-33: Upper example compartment (located above calm waterline).

The result following the posterior update for the respective (increasing) wave heights are presented in Table 6-7. The posterior update has been executed with use of Eq. 4-26 from Chapter 4, and by calculating the posterior update for all initial damage extents, as was identified in the previous section for correct normalisation. However, only the upper example compartment has been included in the table for illustration. The damage extent has been denoted as x in the table rather than using the integrands.

Table 6-7: Posterior update of flooding probability of example extent (Upper) implementing initial flooding likelihood for increasing wave heights.

Wave height $H_s[m]$	Draft $T [m]$	A priori $P(x)$	Likelihood $P(H_s x)$	Posterior $P(x H_s)$
0.000	8.200	4.477e-4	0.000	0.000
2.000	8.200	4.477e-4	1.285e-3	7.469e-7
6.000	8.200	4.477e-4	0.707	3.361e-4
12.000	8.200	4.477e-4	0.999	4.477e-4

The calculated posterior presented in the table for the respective wave heights represents the initial flooding likelihood, but does also take into consideration the a priori belief, and is therefore slightly biased. The posterior flooding probability, in our specific example, is low for all the wave heights simply because the a priori is considerable low (4.477e-4). For this reason, when discussing the initial flooding probability in the following, it is the flooding likelihood that has been considered. It follows from above that the initial flooding probability is zero in calm water condition simply because the water elevation would never exceed the lower Z -position of the damage extent. Increasing the wave height to two metres results in marginal change of the initial flooding probability with flooding to occur approximately once in every thousand runs.

Running the case in sea state of $H_s = 6.0 m$ boosts the initial flooding probability considerably, and flooding will occur in approximately seven out of ten runs. Finally, the extreme case of $H_s = 12.0 m$ results in an initial flooding probability of close to one. Flooding is actually almost certain for most of the initial damage extents due to the extreme wave height. Since flooding is certain for all cases, the only governing factor remaining is in fact the a priori probability (deciding which extent is realised), as is illustrated by the posterior being identical to the a priori. We may now take a closer look at how the probabilities have shifted between all the initial damage extents following the posterior update (translating the probability from breach probability to flooding probability) for the respective wave heights, and how this affects uncertainty. The reduction in uncertainty can be illustrated by using traditional statistical methods such as confidence intervals (CI). In the following, a 95% CI has been used. From the a priori list of damage extents, we find that the number of cases (highest proportion) that results in 95% of the probability is 3,024 cases out of the total 19,225 cases identified in section 6.2.2.

This is because the available probability is largely spread between all cases. Checking the calm-water case, the 95% *CI* comprises only 1,763 cases out of the total 19,225 cases, and it is clear that due to the available evidence of a particular wave height, we have had a reduction in uncertainty (reduction of 1,261 cases), and a boost in confidence for the remaining cases resulting in the *CI*. The main reason is simply that the probability that was assigned to the upper extents, when we considered the breach probability alone, has been transferred to the lower extents, and in fact only to those with their lower *Z* positioned below the calm-waterline (being a step function for $H_s = 0$). For the cases with increasing wave heights, the *CI* will be reduced for every increase, until the most extreme case actually returns the *CI* to its original value of 3,024 cases because the wave height is sufficiently high to flood all the initial extents regardless of their vertical position, and the governing factor remaining is the a priori as was mentioned above.

6.3.2 Progressive flooding⁴

6.3.2.1 Progressive flooding case realisation

The flooding probability introduced in the previous chapter encodes the probability of floodwater ingress to the initial extent (or stage) of damage. In this chapter we will develop a probabilistic model for the progressive flooding extent, which encodes the probability of the realisation of a particular progressive flooding extent originating from a known initial damage extent. A simple event (probability) tree, as shown in Figure 6-34, can illustrate the various realisations of initial and corresponding progressive extents. The top event represents any breach resulting from a collision damage (or contact/grounding), which branches out to all the possible initial damage extents (as was identified in section 6.2.3). A range of respective progressive damage extents may originate from each of these initial extents depending on the openings open/closed state, leak/collapse resistance and the openings position in relation to the floodwater elevation during the flooding evolution. All branches of progressive extents stemming from each of the initial extents, should sum to the initial extent probability according the total probability theorem, as given by Eq. 6-35, where $x = \textit{initial}$, $y = \textit{progressive}$.

⁴ Larger parts of this chapter have been presented in Karolius K. B., Cichowicz, J. and Vassalos, D., (2018), "Modelling of compartment connectivity and probabilistic assessment of progressive flooding stages for a damaged ship", Proceedings of the 17th International Ship Stability Workshop, 10-12 June 2019, Helsinki, Finland

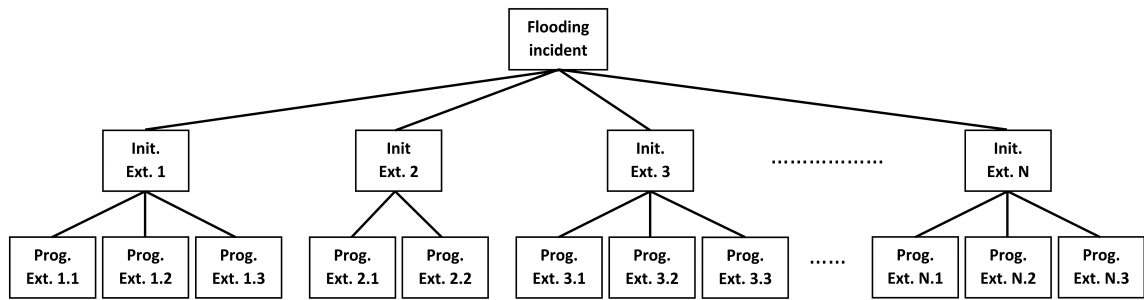


Figure 6-34: Event (probability) tree of damage extents (First row: breach resulting from collision damage or contact/grounding, second row: possible initial extents of damage, third row: possible progressive extents of damage).

$$P(x) = \int_y P(x|y)P(y)dy \quad \text{Eq. 6-35}$$

For example, the progressive extents in the leftmost branch are representing all possible progressive extents originating from initial damage extent number one (if there is no progressive extent the initial extent remains unchanged and considered as total extent, which would still be represented with a separate branch in the tree). The actual number of possible realisations of progressive extents will be governed by the number of connections in direct contact with the initial damage extent, and subsequent connections thereafter. An initial damage extent comprising a single compartment with just a couple of connections would therefore be expected to have a smaller number of possible progressive extents than an initial damage extent comprising several compartments and multiple connections. This being said, it would not necessarily be so as the probability of progressive flooding will be governing, e.g. if all the doors leading from the extent with several compartments connected had a progressive flooding probability of one, the progressive extent where all connected compartments were progressively flooded would in fact be the only realisation possible. The various realisations are highly related to the combinatorics problem as was discussed in Chapter 2. To illustrate the combinatorial problem with multiple permutations, we may consider an example compartmentation shown in Figure 6-35. The compartmentation comprises six rooms (compartments): *A*, *B*, *C*, *D*, *E* and *F*, and six watertight doors: *a*, *b*, *c*, *d*, *e* and *f*. Compartment *F*, marked in yellow, is breached and considered as the initial damage extent.

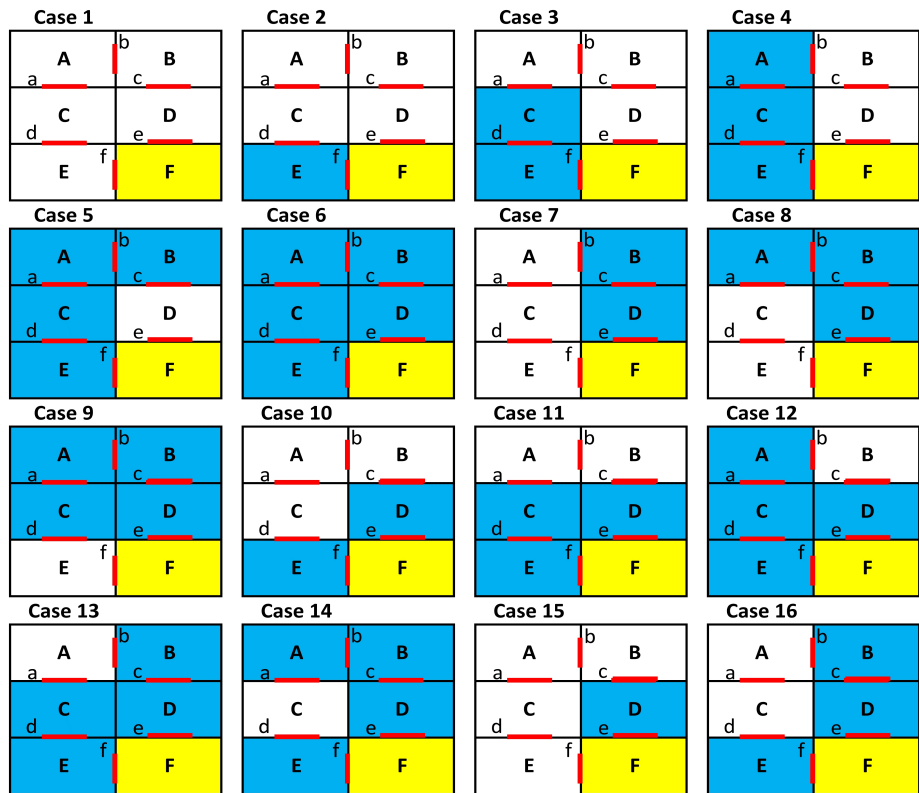


Figure 6-35: Example compartmentation with doors and possible flooding realisations (Doors are marked in red, initial flooding is marked in yellow, and progressively flooded compartments are marked in blue).

For simplicity, we assume that the probability of progressive flooding is solely governed by the door opening status (frequency), disregarding other variables as was mentioned in the previous section. A door's opening status may be modelled by a Bernoulli process with the opening frequency represented by the parameter λ , as shown by Eq. 6-36. The assumed opening frequency for the example compartmentation is summarised in Table 6-8.

$$P(\text{open}) = \lambda, P(\text{closed}) = 1 - \lambda$$

Eq. 6-36

Table 6-8: Opening frequencies for example compartmentation.

Door, n	Opening frequency, λ
a	0.90
b	0.95
c	0.10
d	0.30
e	0.05
f	0.70

To calculate the realisation probability of Case 1, all the various door status combinations that are possible needs to be considered. In total, there are $2^6 = 64$ possible permutations (combinations) of door statuses in this specific case. Out of these, 16 permutations result in Case 1 being realised (i.e. there are 16 door combinations without progressive flooding, and where the flooding is limited to room F). The probability of Case 1 may therefore be calculated by summing all these combinations as shown by Eq. 6-37, where n is the number of combinations resulting in a specific initial damage extent x .

$$P(X = x) = \sum_{i=1}^n P_{x_i} \quad \text{Eq. 6-37}$$

It may be shown that this results in a probability of: $P(X = \text{Case 1}) = 0.285$. Another way to calculate the realisation probability may be illustrated as in the following. For Case 1 to be realised, doors e and f have to be closed ($open = 1, closed = 0$) whilst the status of the remaining doors status is not affecting the outcome. Hence, the probability of this particular case is simply the joint probability of the two relevant doors being closed (using the probability rule of conditionality governed by Eq. 6-38 and calculated in Eq. 6-39).

$$P(X = x) = P(e, f) = P(e)P(f) \quad \text{Eq. 6-38}$$

$$\begin{aligned} P(X = \text{Case 1}) &= P(e = 0, f = 0) && \text{Eq. 6-39} \\ &= (1 - \lambda_e)(1 - \lambda_f) \\ &= (1 - 0.05)(1 - 0.70) \\ &= 0.285 \end{aligned}$$

The second case, Case 2 may be calculated by the same method (it is only governed by doors d, e and f). For the case to be realised, doors d and e have to be closed and door f has to be open whilst the status of the remaining doors does not affect the realisation. The probability of Case 2 may again simply be calculated as the joint status probability of the three relevant doors denoted by Eq. 6-40.

$$\begin{aligned} P(X = \text{Case 2}) &= P(d = 0, e = 0, f = 1) && \text{Eq. 6-40} \\ &= (1 - \lambda_d)(1 - \lambda_e)\lambda_f \\ &= (1 - 0.30)(1 - 0.05)0.70 \\ &= 0.4655 \end{aligned}$$

The process can be repeated for all 16 flooding cases from Figure 6-35, but we will consider Case 6, with all doors part of the progressive boundary, as a final example. This case may result from flooding progression by two routes with multiple door realisations leading to the same case. In fact, seven realisations will result in Case 6, summarised below by Eq. 6-41 to Eq. 6-47 with the total probability as given by Eq. 6-48.

$$\begin{aligned}
 P_1(X_1 = \text{Case 6}) &= P(a = b = c = d = e = f = 1) = \dots && \text{Eq. 6-41} \\
 &= \lambda_a \lambda_b \lambda_c \lambda_d \lambda_e \lambda_f = \dots \\
 &= 0.90 \cdot 0.95 \cdot 0.10 \cdot 0.30 \cdot 0.05 \cdot 0.70 = 0.0009
 \end{aligned}$$

$$\begin{aligned}
 P_2(X_2 = \text{Case 6}) &= P(a = b = c = d = e = 1, f = 0) = \dots && \text{Eq. 6-42} \\
 &= \lambda_a \lambda_b \lambda_c \lambda_d \lambda_e (1 - \lambda_f) = \dots \\
 &= 0.90 \cdot 0.95 \cdot 0.10 \cdot 0.30 \cdot 0.05 \cdot (1 - 0.70) = 0.0004
 \end{aligned}$$

$$\begin{aligned}
 P_3(X_3 = \text{Case 6}) &= P(a = b = c = d = f = 1, e = 0) = \dots && \text{Eq. 6-43} \\
 &= \lambda_a \lambda_b \lambda_c \lambda_d (1 - \lambda_e) \lambda_f = \dots \\
 &= 0.90 \cdot 0.95 \cdot 0.10 \cdot 0.30 \cdot (1 - 0.05) \cdot 0.70 = 0.0171
 \end{aligned}$$

$$\begin{aligned}
 P_4(X_4 = \text{Case 6}) &= P(a = b = c = e = f = 1, d = 0) = \dots && \text{Eq. 6-44} \\
 &= \lambda_a \lambda_b \lambda_c (1 - \lambda_d) \lambda_e \lambda_f = \dots \\
 &= 0.90 \cdot 0.95 \cdot 0.10 \cdot (1 - 0.30) \cdot 0.05 \cdot 0.70 = 0.0021
 \end{aligned}$$

$$\begin{aligned}
 P_5(X_5 = \text{Case 6}) &= P(a = b = d = e = f = 1, c = 0) = \dots && \text{Eq. 6-45} \\
 &= \lambda_a \lambda_b (1 - \lambda_c) \lambda_d \lambda_e \lambda_f = \dots \\
 &= 0.90 \cdot 0.95 \cdot (1 - 0.10) \cdot 0.30 \cdot 0.05 \cdot 0.70 = 0.0081
 \end{aligned}$$

$$\begin{aligned}
 P_6(X_6 = \text{Case 6}) &= P(a = c = d = e = f = 1, b = 0) = \dots && \text{Eq. 6-46} \\
 &= \lambda_a (1 - \lambda_b) \lambda_c \lambda_d \lambda_e \lambda_f = \dots \\
 &= 0.90 \cdot (1 - 0.95) \cdot 0.10 \cdot 0.30 \cdot 0.05 \cdot 0.70 = 0.0001
 \end{aligned}$$

$$\begin{aligned}
 P_7(X_7 = \text{Case 6}) &= P(b = c = d = e = f = 1, a = 0) = \dots && \text{Eq. 6-47} \\
 &= (1 - \lambda_a) \lambda_b \lambda_c \lambda_d \lambda_e \lambda_f = \dots \\
 &= (1 - 0.90) \cdot 0.95 \cdot 0.10 \cdot 0.30 \cdot 0.05 \cdot 0.70 = 0.0001
 \end{aligned}$$

$$P(X = \text{Case 6}) = \sum_{i=1}^{n=7} P_{X_i} = P_1 + P_2 + P_3 + P_4 + P_5 + P_6 + P_7 = \dots \quad \text{Eq. 6-48}$$

$$\dots = 0.0009 + 0.0004 + 0.0171 + 0.0021 + 0.0081 + 0.0001 + 0.0001 = 0.0287$$

Table 6-9 summarises the probability calculations for all the example flooding cases. The second calculation methodology comprises less combinations of doors, as only the doors located within the flooding boundary is of interest. However, Case 1 and 2 are the simplest of the example cases, and it is relatively easy to calculate their realisation probability by first principles calculations, being governed by a few doors. If more doors are governing, such as in Case 6, increasing various realisations of doors may result in the same progressive damage extent, which will complicate the problem. Nevertheless, the manual calculations method cannot be applied to a realistic case of a large cruise vessel with thousands of possible initial damage extents and numerous connections, hence an alternative approach is essential.

Table 6-9: Summary of case realisations for example compartmentation.

Case, i	Calculation formulae	Result
$P_{\text{Case 1}} =$	$(1.00 - 0.05) \cdot (1.00 - 0.70)$	$= 0.2850$
$P_{\text{Case 2}} =$	$(1.00 - 0.30) \cdot (1.00 - 0.05) \cdot 0.70$	$= 0.4655$
$P_{\text{Case 3}} =$	$(1.00 - 0.90) \cdot (1.00 - 0.05) \cdot 0.30 \cdot 0.70$	$= 0.0200$
$P_{\text{Case 4}} =$	$(1.00 - 0.95) \cdot (1.00 - 0.05) \cdot 0.90 \cdot 0.30 \cdot 0.70$	$= 0.0090$
$P_{\text{Case 5}} =$	$(1.00 - 0.10) \cdot (1.00 - 0.05) \cdot 0.90 \cdot 0.95 \cdot 0.30 \cdot 0.70$	$= 0.1535$
$P_{\text{Case 6}} =$	$0.0009 + 0.0004 + 0.0171 + 0.0021 + 0.0081 + 0.0001 + 0.0001$	$= 0.0287$
$P_{\text{Case 7}} =$	$(1.00 - 0.70) \cdot (1.00 - 0.95) \cdot 0.10 \cdot 0.05$	$= 0.0001$
$P_{\text{Case 8}} =$	$(1.00 - 0.70) \cdot (1.00 - 0.90) \cdot 0.95 \cdot 0.10 \cdot 0.05$	$= 0.0001$
$P_{\text{Case 9}} =$	$(1.00 - 0.30) \cdot (1.00 - 0.70) \cdot 0.05 \cdot 0.10 \cdot 0.95 \cdot 0.90$	$= 0.0009$
$P_{\text{Case 10}} =$	$(1.00 - 0.30) \cdot (1.00 - 0.10) \cdot 0.05 \cdot 0.70$	$= 0.0220$
$P_{\text{Case 11}} =$	$(1.00 - 0.90) \cdot (1.00 - 0.10) \cdot 0.30 \cdot 0.05 \cdot 0.70$	$= 0.0009$
$P_{\text{Case 12}} =$	$(1.00 - 0.95) \cdot (1.00 - 0.10) \cdot 0.90 \cdot 0.30 \cdot 0.70 \cdot 0.05$	$= 0.0004$
$P_{\text{Case 13}} =$	$(1.00 - 0.90) \cdot (1.00 - 0.95) \cdot 0.30 \cdot 0.70 \cdot 0.05 \cdot 0.10$	$= 0.0000$
$P_{\text{Case 14}} =$	$(1.00 - 0.30) \cdot (1.00 - 0.90) \cdot 0.70 \cdot 0.05 \cdot 0.10 \cdot 0.95$	$= 0.0002$
$P_{\text{Case 15}} =$	$(1.00 - 0.70) \cdot (1.00 - 0.10) \cdot 0.05$	$= 0.0135$
$P_{\text{Case 16}} =$	$(1.00 - 0.30) \cdot (1.00 - 0.95) \cdot 0.70 \cdot 0.05 \cdot 0.10$	$= 0.0001$
$Sum =$	$\sum_{i=1}^n P_{\text{Case } i}$	$= 1.0000$

6.3.2.2 Mathematical abstraction of compartment connectivity

The problem of opening permutations can be addressed more efficiently than the direct calculations with the help of *Graph Theory*. Graph Theory is a well-known mathematical modelling technique for representing pairwise connections between objects (nodes) with the relationship maintained by edges (lines). The application of graphs ranges from the evacuation modelling software *Evi* (Vassalos et al., 2001) through social networks (Zweig & Abufouda, 2016) to navigational- and road-networks (Thomson & Richardson, 1995). Any exhaustive review of theory and applications of graph theory is outside the scope of this thesis, but reference is made to introductory texts such as Bondy & Murty (1976). In modelling of compartment connectivity as a graph, the compartments are simply represented by the nodes (points) and openings are represented by edges (lines). For example Dankowski & Krüger (2013) represented compartment connectivity by deterministic directed graphs (i.e. without the ability to account for probabilities). A graph model of the example compartmentation from Figure 6-35 is presented in Figure 6-36. For the purpose of compartment connectivity, we are not interested in distances between locations (as is often used for road networks); instead the weights may represent the probability of progressive flooding between compartments, or opening frequencies, depending on how we define the problem.

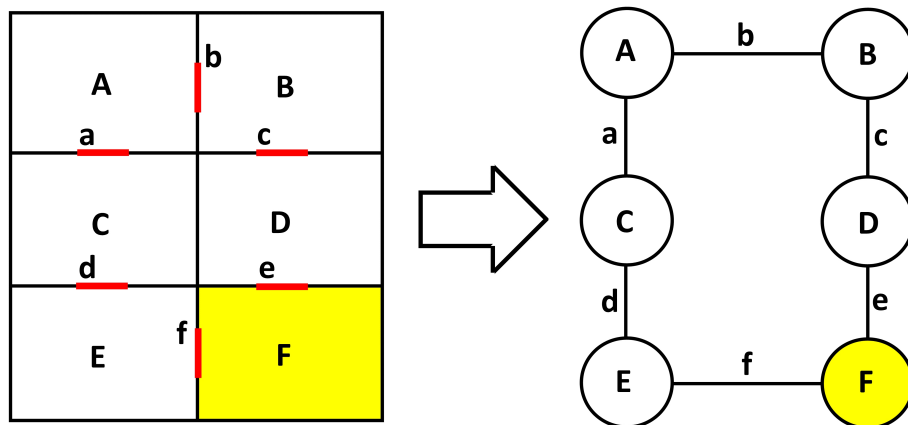


Figure 6-36: Compartments mathematical abstraction as graph (compartment or node marked in yellow is initial damage extent, or source node).

Representing the edges by probabilities turns the graph into an *uncertain graph*, a well-known technique utilised for example in network reliability (Khan et al., 2018). In the compartment connectivity example, existence of the edge implies possible progressive

flooding between the nodes (compartments). However, progressive flooding only occurs if at least one of the edges is connected to the initial damage extent (the source node). This conditionality can be accounted for readily by implementing search algorithms for traversing the graph structure. Such algorithms comprise Breadth-First-Search (BFS) (Moore, 1959), and Depth-First Search (DFS) (Trémaux, 1859–1882). In the example compartmentation, the opening frequencies can be used to sample (create) the connections (edges) between the compartments (nodes) for multiple instances (samples). An example of such sampled realisations is shown in Figure 6-37, where dashed lines represent non-existing edges and continuous lines represent existing edges.

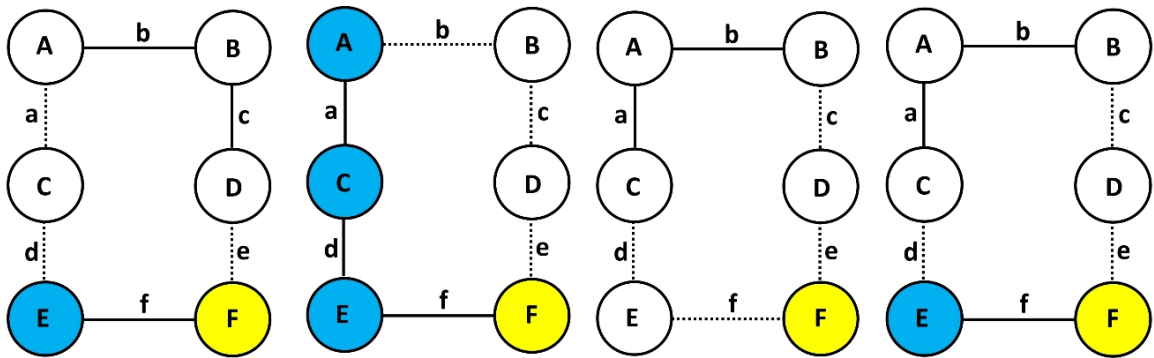


Figure 6-37: Sampled edge existence in example compartmentation represented as uncertain graph (Dashed lines represent non-existing edges or no progressive flooding realization, and continuous lines represent existing edges or progressive flooding realization. Initial flooding is marked in yellow, and progressively flooded compartments are marked in blue).

The nodes (compartments), having existing edges and a valid connection to the source node (initial extent) are part of the progressive extent (blue nodes in the figure). The sampling process, if done sufficient number of times, should result in accurate approximation of the realisation probability of the openings, while search algorithms account for the conditionality of the connections (i.e. they return only the relevant progressive stages with connection to the source node, representing the initial extent of damage). The sum of each flooding realisation (initial and progressive combined), divided by the number of samples, represents the estimate of the respective case-realisation probabilities. In order to verify the approach, the example flooding cases are sampled with $N = 10,000$ samples. The results shown in Table 6-10 demonstrate good agreement with the calculated probabilities.

Table 6-10: Progressive flooding case (realisation) probability from manual calculation and sampling scheme.

Case, i	P, calculation	P, sampling
$P_{\text{Case 1}} =$	0.2850	0.2847
$P_{\text{Case 2}} =$	0.4655	0.4650
$P_{\text{Case 3}} =$	0.0200	0.0201
$P_{\text{Case 4}} =$	0.0090	0.0091
$P_{\text{Case 5}} =$	0.1535	0.1542
$P_{\text{Case 6}} =$	0.0287	0.0287
$P_{\text{Case 7}} =$	0.0001	0.0001
$P_{\text{Case 8}} =$	0.0001	0.0001
$P_{\text{Case 9}} =$	0.0009	0.0009
$P_{\text{Case 10}} =$	0.0220	0.0220
$P_{\text{Case 11}} =$	0.0009	0.0010
$P_{\text{Case 12}} =$	0.0004	0.0004
$P_{\text{Case 13}} =$	0.0000	0.0000
$P_{\text{Case 14}} =$	0.0002	0.0002
$P_{\text{Case 15}} =$	0.0135	0.0135
$P_{\text{Case 16}} =$	0.0001	0.0001
Sum =	1.0000	1.0000

6.3.2.3 Real-Case example I

Due to lack of actual data, the opening frequencies for the example case are based on their opening allowance category (supported by data adopted from the EMSA III project (Jasionowski et al., 2015), which has been derived from onboard records of various vessel types). The opening frequencies are discussed more in detail in the next Chapter 7. Protected, non-watertight openings not imposed by any category, has been given an assumed opening frequency of 0.5 for the purpose of illustration. The assumed frequencies are summarised in Table 6-11 for the various opening categories. In reality, such values would vary with specific doors depending on compartment type and crew/passenger traffic. The probability of doors being closed in time by crew is represented by a correction factor. In the EMSA project, such a correction has been modelled as a function of time, however, for illustration purposes, this has been taken as constant 90% success rate (only for watertight doors). In this specific example the correction factor accounts also for reliability of the doors. To limit the result, a single initial damage extent has been chosen to be implemented with the sampling methodology, to produce progressive extent realisations.

Table 6-11: Progressive flooding case (realisation) probability from manual calculation and sampling scheme.

Opening Allowance category	Opening Frequency	Corrected Frequency
A	0.850	0.085
B	0.600	0.060
C	0.100	0.010
Protected non-WT	0.500	0.500
Unprotected non-WT	1.000	1.000

Furthermore, for the purpose of illustration, we have at this point considered the opening frequencies alone disregarding other variables such as leak/collapse heads and position of openings in relation with the floodwater elevation (this will obviously result in compartments being marked as part of the progressive extent (lost buoyancy), but not necessarily flooded). Other variables such as leak/collapse heads and position of openings in relation with the floodwater elevation will be discussed in more detail in the next section. The initial damage case selected for illustration is a 2-zone damage, comprising 2 compartments and is illustrated in Figure 6-38. For implementation of the sampling methodology, we generated $N = 1,000$ samples using the Bernoulli process, resulting in a corresponding number of graphs representing the state-space. The traversing search algorithm (BFS in this specific example), identified 86 unique progressive extents originating from specific initial extent, stemming from 6 openings with direct connection to the initial extent's boundary.

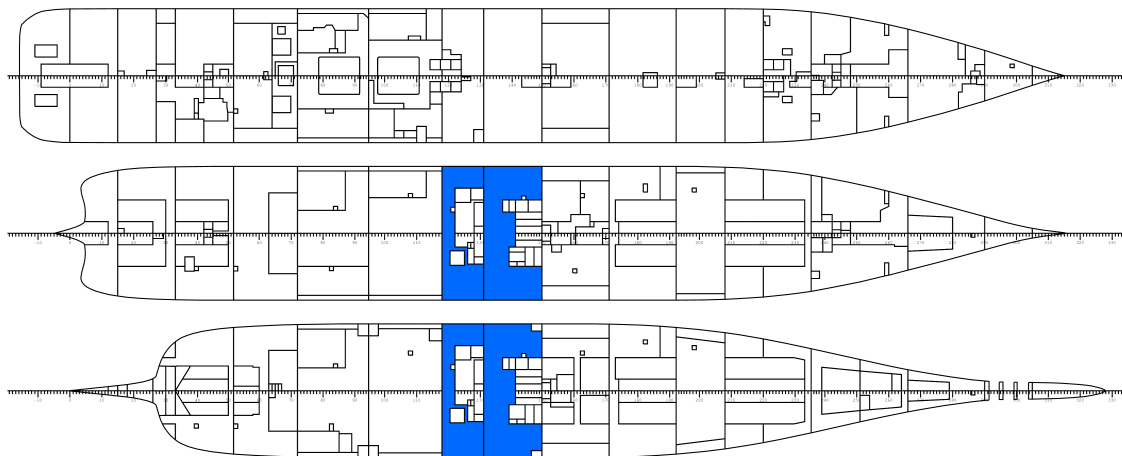


Figure 6-38: Initial damage extent of the case study.

In order to rank the cases, we again make use of confidence intervals (CI). The summary results of CI-based ranking are shown in Table 6-12. For example, the 90% CI simply indicate that there is a 90% probability that following a damage breach comprising the initial extent, the progressive extent would result in one out of nine cases as is seen in Table 6-13. Case No. 3 is seen to represent the initial stage alone, where no additional compartments are progressively flooded.

Table 6-12: Confidence Intervals (CI) and corresponding number of related progressive extents for 1,000 samples.

Confidence Interval, CI [%]	Number of progressive extents
50	3
80	6
90	9
95	36
99	76
100	86

Table 6-13: Progressive extents representing a 90% Confidence Interval (CI), including initial extent (two leftmost compartments).

Case No.	Probability	Compartments (lost buoyancy)
1	0.233	R070101 R080116 EX070101 R070102
2	0.206	R070101 R080116 EX070101 EX080101 R070102
3	0.115	R070101 R080116
4	0.112	R070101 R080116 EX080101
5	0.072	R070101 R080116 R070102
6	0.055	R070101 R080116 EX080101 R070102
7	0.052	R070101 R080116 EX070101
8	0.046	R070101 R080116 EX070101 EX080101
9	0.005	R070101 R080116 EX070101 EX080101 R070102 R080201
SUM	0.896 (≈ 0.9)	

For the purpose of illustration, only the cases representing the 50% CI has been included, as seen in Figure 6-39 to Figure 6-41. Realisation No. 36, corresponding to the transition to the 95% CI have also been included as seen in Figure 6-42, for illustrating a less probable, but larger progressive extent. From the various progressive extent realisations presented in Table 6-13, it is seen that the 90% CI are mostly comprising smaller A-class boundary

compartments within the watertight boundaries as would be expected, simply due to the assignment of a 50% opening rate. More substantial progressive extents with compromised watertight boundaries are only seen above the 90% CI, as is represented by case realisation No. 36 in Figure 6-42.



Figure 6-39: Progressive flooding realization 1, $P = 0.233$.



Figure 6-40: Progressive flooding realization 2, $P = 0.206$.



Figure 6-41: Progressive flooding realization 3, $P = 0.115$.

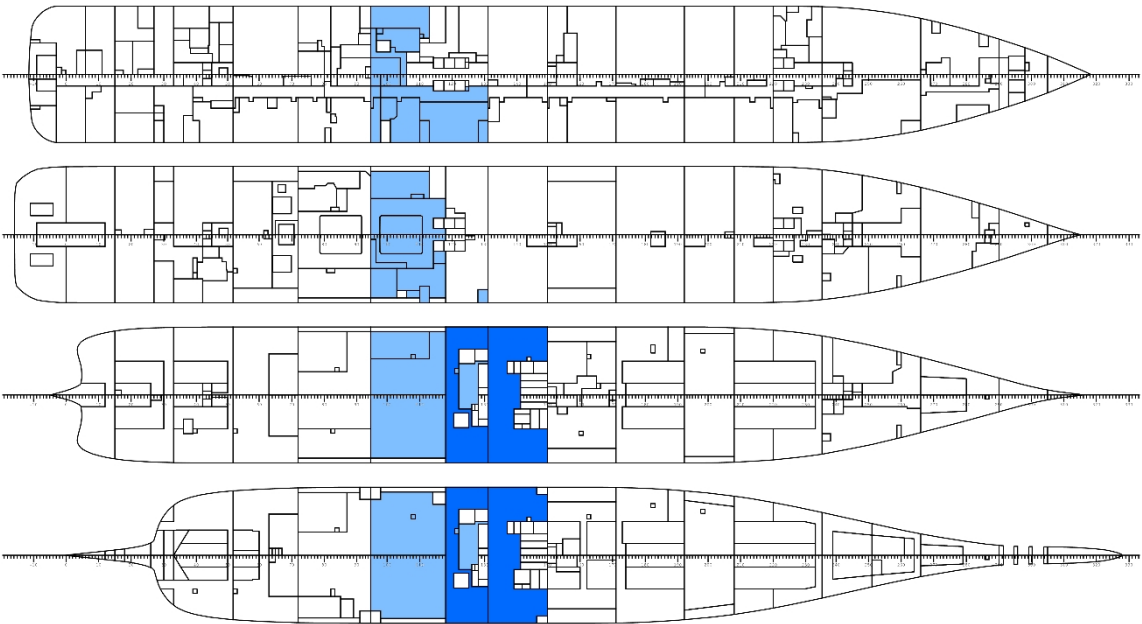


Figure 6-42: Progressive flooding realization 36, $P = 0.001$

6.3.2.4 Progressive flooding probability

In the above examples, we have assumed that the opening status probability has been the sole contributor to the progressive flooding probability. This, as already indicated, is not the case as openings, even when closed, are prone to leak and collapse. The openings position in relation to the waterplane is obviously also a determinant as openings located above the floodwater elevation at the time in question would not progressively flood even if open.

Similarly, leaking or collapsing require build-up of the hydrostatic pressure head. In the following, a representation of the progressive flooding probability will be introduced for application within the above sampling scheme, considering all the governing factors. In this respect, we may summarise the various conditions that will result in progressive flooding as follows:

1. Opening has status *open*, has connection to initial damage extent, and floodwater surface elevation, W_e exceeds openings lower vertical position, Z , or;
2. Opening has status *closed*, has connection to initial damage extent, leak head is smaller than collapse head producing substantial leak before collapse, and floodwater surface elevation, W_e exceeds openings leak pressure height, H_{leak} or;
3. Opening has status *closed*, has connection to initial damage extent, there is no substantial leak before collapse, and floodwater surface elevation, W_e exceeds openings collapse pressure height, H_{col} .

The above progressive flooding conditions, and their corresponding non-flooding conditions may be illustrated in an event tree as shown in Figure 6-43. The condition that the respective openings must be connected to the flooding source is covered by the search algorithm separately and has not been represented in the event tree.

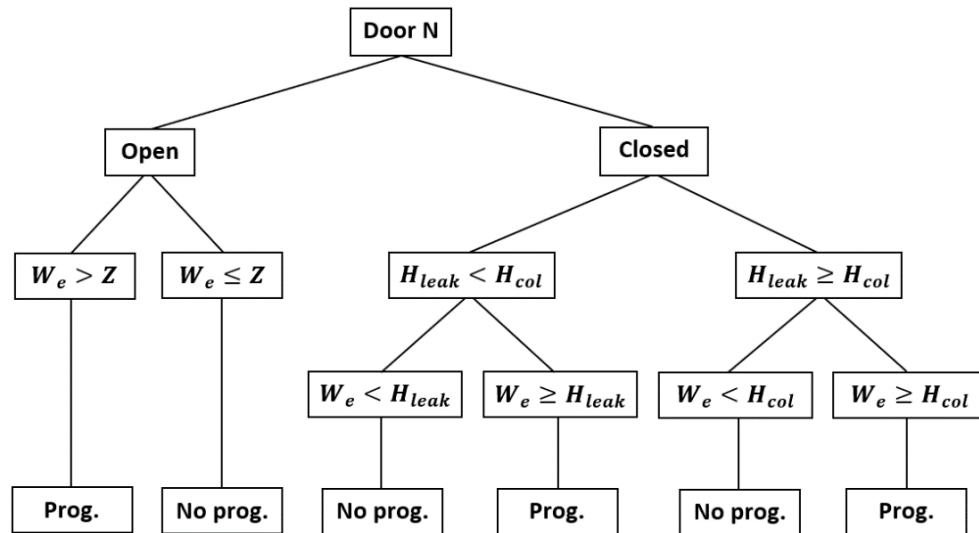


Figure 6-43: Event (probability) tree of progressive flooding realisations.

In the event tree, the closed status has two branches or sub-sets corresponding to the leak and collapse heads giving the least resistance towards progressive flooding. Most openings will have a period of leakage before sufficient head has been built-up resulting in structural collapse (left branch of the closed status). The right branch show leakage head higher than the collapse head which is slightly misleading as this would never be the case. It may, however, be that an opening will go straight into structural collapse without having a period of substantial leakage and is what this sub-set really represents. The condition of connection to the initial damage extent has been omitted as this will be accounted for in the search algorithms as illustrated in the foregoing. The event tree can be used to derive a generic formula representing the progressive flooding probability. The opening condition is characterised by one of two mutually exclusive statuses, i.e. either $N = 1$ (open) or $N = 0$ (closed), as given by Eq. 6-49. Using complementary events, this is translated to Eq. 6-50.

$$P(N = 1 \cup N = 0) = P(N = 1) + P(N = 0) \quad \text{Eq. 6-49}$$

$$P(N = 1 \cup N = 0) = P(N = 1) + (1 - P(N = 1)) \quad \text{Eq. 6-50}$$

For each of the two events (or opening statuses), there are subsets that will result in progressive flooding. The *open* realisation has one subset, while the *closed* realisation has two subsets, clearly seen in the event tree. The respective events (opening statuses) have been represented by Eq. 6-51 and Eq. 6-52, where $PF = 1$ represents progressive flooding.

$$P(N = 1 \cap PF = 1) = P(N = 1)P(W_e > Z) \quad \text{Eq. 6-51}$$

$$P(N = 0 \cap PF = 1) = (1 - P(N = 1)) \cdot \dots \quad \text{Eq. 6-52}$$

$$\dots \cdot [P(H_{leak} < H_{col})P(W_e \geq H_{leak}) + P(H_{leak} \geq H_{col})P(W_e \geq H_{col})]$$

The respective equations represent all the events that result in progressive flooding, and the total progressive flooding probability would simply be the sum of all the subsets, which is represented by Eq. 6-53.

$$P(PF = 1) = P(N = 1 \cap PF = 1) + P(N = 0 \cap PF = 1) \quad \text{Eq. 6-53}$$

$$= P(N = 1)P(W_e > Z) + (1 - P(N = 1))[P(W_e \geq H_{leak})], \text{ where } H_{leak} < H_{col}$$

$$= P(N = 1)P(W_e > Z) + (1 - P(N = 1))[P(W_e \geq H_{col})], \text{ where } H_{leak} \geq H_{col}$$

It can be recalled from the previous section that the probability of particular opening status depends on its opening frequency, λ , and can be modelled by a Bernoulli process. The Bernoulli process may therefore be used for representing the door status probability terms of Eq. 6-53. The opening frequencies, their a priori distributions and corresponding likelihood functions will be discussed in more detail in Chapter 7 covering the vessel variables. The remaining terms in Eq. 6-53 are all related to the floodwater elevation, or more specifically, vertical positions and their distances to the floodwater elevation, either in the form of openings lower limits or pressure heights. Regardless of the vertical positions type, they are all depending on the probability of the water-elevation exceeding a certain vertical threshold and would therefore be well represented by the same probabilistic model.

6.3.2.5 Water elevation vertical exceedance probability

For developing a probabilistic model for the exceedance probability of the floodwater elevation, a similar approach to the one presented for the initial flooding probability in section 6.3.1 (initial flooding) have been followed. Now, however, the vessel is no longer in intact condition, and the water surface elevation of interest is that of the internal floodwater surface. The sampling approach is identical to the one presented in section 6.3.1 but to account for damaged ship conditions 10,000 damage breaches have been sampled from the distributions derived in section 6.2.1.

Sampling of the vessel's loading condition and wave related variables mirrored the process followed in section 6.3.1, while door status, and leak and collapse heads have been randomly sampled from distributions that are introduced in section 7.2.1. Following simulation in time-domain for 30 minutes, the maximum surface elevation within the flooded compartments were identified, providing the floodwater elevation from the external waterplane, ΔZ . This, combined with the corresponding significant wave heights, enabled the development of a probability distribution for floodwater exceedance at any compartment within the flooding extent, conditional on the significant wave height, H_s . The identified values of ΔZ at which floodwater elevation exceedance occurs are plotted against the corresponding wave height, H_s , in Figure 6-44.

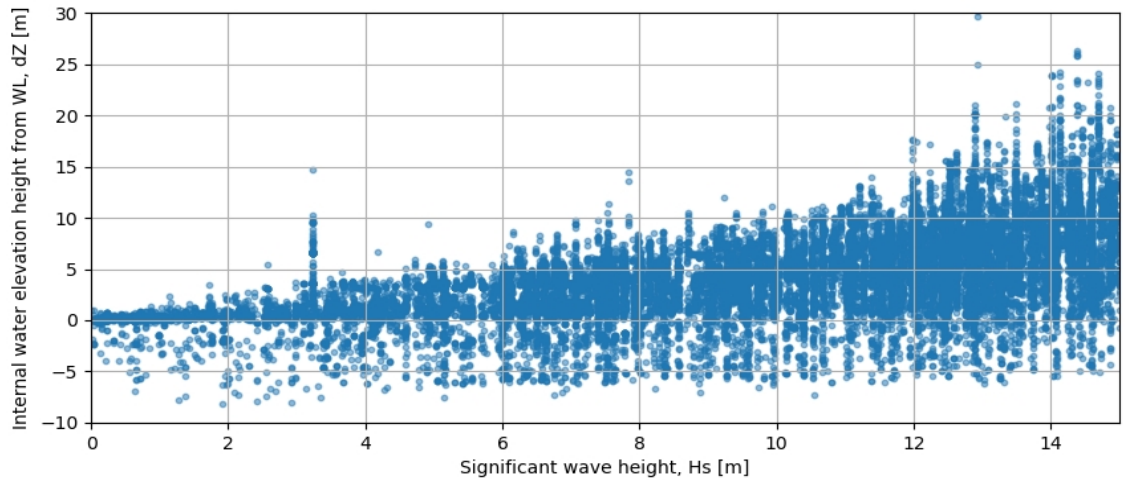


Figure 6-44: ΔZ , between internal and external water elevation, as a function of wave height, H_s .

Similarly to what was seen for the initial flooding probability, the variability (scatter) is increasing with growing wave height. Some points, however have negative values of ΔZ indicating that for some cases the internal floodwater height is located below the external waterplane. This is a result of slow progressive flooding and the floodwater levels failing to reach the external waterplane within the duration of simulations. Some outliers are also seen (e.g. for wave height just above $H_s = 3.0$ m). The outliers at a specific wave height are all originating from the same simulation case, as all the flooded compartments within a single simulation run represents independent data points. After further investigation, the reason for the extreme water-elevation (for the case at $H_s = 3.0$ m) is identified to be a result of capsize after 90 seconds.

The data points presented in Figure 6-44 are well represented by a Generalised-Logistic probability distribution, as given by Eq. 6-54. The corresponding coefficients obtained by MLE techniques and represented as a function of H_s as given by Eq. 6-56 to Eq. 6-58. Analytical and numerical distributions are shown in Figure 6-45. The probability of exceedance is obtained from the cumulative distribution as is represented by Eq. 6-55 and illustrated in Figure 6-46. As we are only interested in an actual ΔZ position, and not an interval as for the damage extents, Eq. 6-55 may be used directly without the need for integration. The final probabilistic model for progressive flooding is obtained by substituting Eq. 6-55 into Eq. 6-53 for the respective probability of exceedance terms. The door status probability is further substituted by the Bernoulli process, which result in Eq. 6-59.

$$P(\Delta Z|H_s, W_e) = -\left(\frac{\gamma}{\beta}\right)\left(e^{\left(\frac{\alpha-\Delta Z}{\beta}\right)}\right)\left(1 + e^{\left(\frac{\alpha-\Delta Z}{\beta}\right)}\right)^{-\gamma-1} \quad \text{Eq. 6-54}$$

$$P(W_e \geq \Delta Z|H_s, W_e) = \left(1 + e^{\left(\frac{\alpha-\Delta Z}{\beta}\right)}\right)^{-\gamma} \quad \text{Eq. 6-55}$$

$$\alpha(H_s) = a + be^{cH_s}, a = -4.853, b = 5.316, c = 0.059 \quad \text{Eq. 6-56}$$

$$\beta(H_s) = a + be^{cH_s}, a = -26.546, b = 26.138, c = -0.005 \quad \text{Eq. 6-57}$$

$$\gamma(H_s) = a + be^{cH_s}, a = 0.096, b = 0.382, c = 0.065 \quad \text{Eq. 6-58}$$

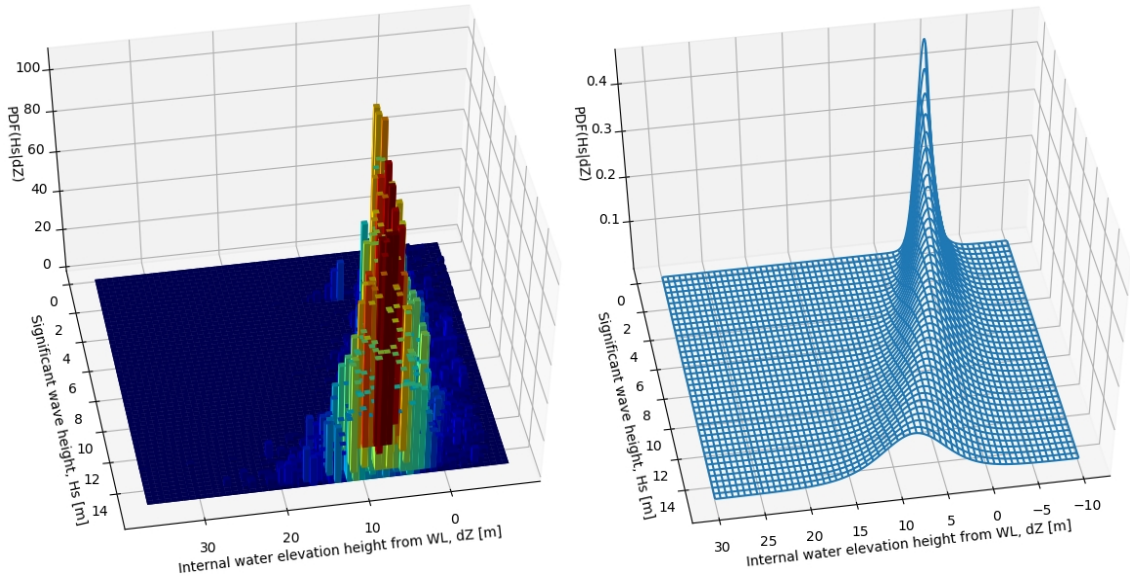


Figure 6-45: Numerical and analytical distribution for internal flooding height from WL.

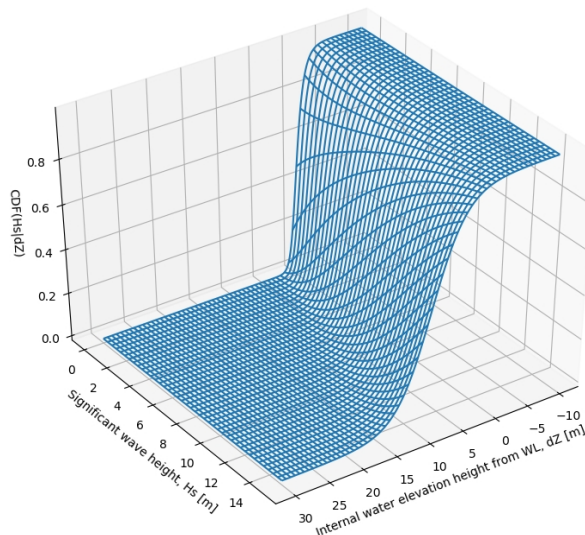


Figure 6-46: Numerical exceedance probability for internal flooding height from WL.

The ΔZ is now represented as the height from the external residual waterplane, denoted W_e . More details on how the relative heights are obtained, representing the residual waterplane in mathematical terms utilising the pneumatic drafts sensors are included in section 7.3.2. The representation of ΔZ for unprotected openings, and leak and collapse pressure heads for protected openings corrected for residual heel, φ , and trim, θ , are given by Eq. 6-60 and Eq. 6-61 supported by Figure 6-47.

$$P(PF = 1) = \lambda \left(1 + e^{\left(\frac{\alpha - \Delta Z}{\beta} \right)} \right)^{-\gamma} + (1 - \lambda) \left(1 + e^{\left(\frac{\alpha - \min(\Delta Z_{leak}, \Delta Z_{col})}{\beta} \right)} \right)^{-\gamma} \quad \text{Eq. 6-59}$$

$$\Delta Z = (Z - W_e) \cos(\varphi) \cos(\theta) \quad \text{Eq. 6-60}$$

$$\Delta Z_{col/leak} = (Z - W_e) \cos(\varphi) \cos(\theta) + H_{col/leak} \quad \text{Eq. 6-61}$$

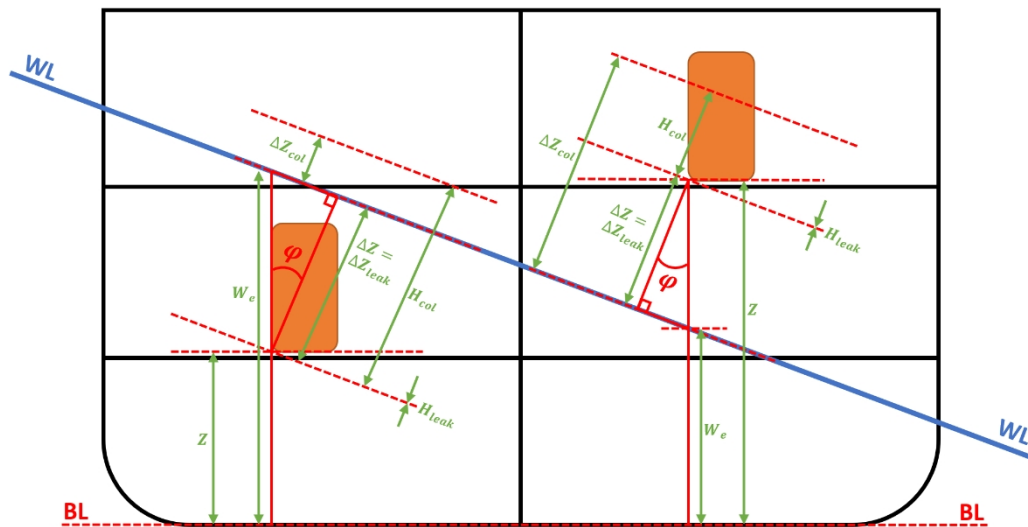


Figure 6-47: Reference system for openings position in relation with the residual waterplane (leftmost door: $H_{leak} = 0$, $H_{col} = h_1$, rightmost door: $H_{leak} = 0$, $H_{col} = h_2$, where $h_1 > h_2$.)

6.3.2.6 Real-Case example II

Application of the probabilistic model for progressive flooding is illustrated in the following by a real-case example. The same initial damage extent as was used in the previous real-case example has been revisited to highlight the impact of implementing the progressive flooding model, in comparison to relying on opening frequencies alone. The initial damage extent is illustrated in Figure 6-38 of section 6.3.2.3. The floating positions of intact and damaged ship are shown in Table 6-14. The residual floating position and the

known distance, ΔZ , from each opening to the waterplane can be used to calculate the progressive flooding probability for the respective openings using Eq. 6-59 to Eq. 6-61. The *Uncertain Graph Sampling* (UGS) method presented in section 6.3.2.2 have been performed for two wave environments, namely: calm-water and wave height of $2.0 \text{ m } H_s$.

Table 6-14: Floating position in intact and damaged case.

Parameter	Intact	Residual
Draft, T [m]	8.00	8.453
Trim, Tr [m]	0.00	-0.03
Heel, φ [°]	0.00	0.60

Table 6-15: Ten most likely progressive extents representing calm-water cases.

Cases	Prob.	Comp. (lost buoyancy)
1	0.254	EX070101, R080116, R070101, R070102, EX080101
2	0.184	EX080101, R070102, R070101, R080116, EX070101, R080202, R080201
3	0.065	R070201, EX080101, R070102, R070101, R080116, EX070101
4	0.065	EX080101, R070102, R070101, R080116, EX070101, R080201
5	0.062	R070201, R070203, EX080101, R070102, R070101, R080116, EX070101
6	0.046	R070201, R070203, EX080101, R070102, R070101, R080116, EX070101, R080202, R080201
7	0.045	R070201, EX080101, R070102, R070101, R080116, EX070101, R080202, R080201
8	0.035	R070201, R070202, R070205, EX080101, R070102, R070101, R080116, EX070101
9	0.033	R070201, R070202, R070203, R070205, EX080101, R070102, R070101, R080116, EX070101
10	0.030	R070201, R070205, EX080101, R070102, R070101, R080116, EX070101

Applying 1,000 samples to the UGS method results in a total of 21 possible calm-water progressive extents and 55 possible progressive extents in waves. In comparison, the previous example, produced 86 possible cases, many of them unrealistic such as Case No. 36 seen in Figure 6-42. As expected, the calm-water case identifies only extents with openings located below the waterplane while the in-waves case includes also extents with openings located slightly above the waterplane. The ten most likely extents are for calm-water cases presented in Table 6-15 and in-waves cases are shown in Table 6-16.

Table 6-16: Ten most likely progressive extents representing calm-water cases.

Cases	Prob.	Comp. (lost buoyancy)
1	0.187	EX080101, R070102, R070101, R080116, EX070101, R080202, R080201
2	0.156	EX070101, R080116, R070101, R070102, EX080101
3	0.068	R070201, R070202, R070203, R070205, EX080101, R070102, R070101, R080116, EX070101, R080202, R080201
4	0.066	R070201, R070203, EX080101, R070102, R070101, R080116, EX070101, R080202, R080201
5	0.054	R070201, R070202, R070203, R070205, EX080101, R070102, R070101, R080116, EX070101
6	0.050	R070201, R070203, EX080101, R070102, R070101, R080116, EX070101
7	0.042	R070201, EX080101, R070102, R070101, R080116, EX070101, R080202, R080201
8	0.041	R070201, R070202, R070205, EX080101, R070102, R070101, R080116, EX070101, R080202, R080201
9	0.038	R070201, R070203, R070205, EX080101, R070102, R070101, R080116, EX070101, R080202, R080201
10	0.036	EX080101, R070102, R070101, R080116, EX070101, R080201

6.3.3 Flooding sensors

The likelihood function for the flooding sensors should encapsulate the relationship between combined initial and progressive damage extent (as sensors may be positioned in either) and the related observation states, such as wave height and floating position, and the probability of a specific sensor to indicate flooding. The probability that specific flooding sensor, z_F will indicate flooding (i.e. $z_F = 1$) given the particular (combined) damage extent, $x_D = x_i$, wave height, H_s and damaged floating position, W_e , is denoted as $P(z_F = 1|x_D, H_s, W_e)$. In the previous section we have seen how the possible progressive extent realisations are identified and how each initial damage extent evolves into a range of combined damage extents by appending the initial extents with the possible progressive flooding scenarios. Similarly to the openings, flooding sensors will indicate flooding only if they are located within the boundary of damage extent boundary and are below the floodwater surface. This enables us to adapt the probabilistic model developed for the internal openings as a likelihood function for the flooding sensors. The only difference is that a sensor model needs to account for the possibility of false-negative and false-positive readings as briefly discussed in Chapter 4. We may again represent the model as an event tree as shown in Figure 6-48. The error state represents the proportion of time the sensor is not operational, given by its rate of error, λ_e . From the figure it is clear that two sub-sets result in sensor

status showing flooding, $z_F = 1$, while two sub-sets result in sensor status showing no-flooding, $z_F = 0$. The likelihood function for the flooding sensors is simply the summation of both sub-sets resulting in flooding status as is represented by Eq. 6-62, where E_s and W_s represents the error- and working-states respectively. Substituting for the error rate, λ_e , and the exceedance probability we obtain Eq. 6-63. Finally, by multiplying with the initial flooding likelihood developed in section 6.3.1, we obtain Eq. 6-64, which is the complete likelihood function for the flooding sensors for respective damage extents, where $x_D = [\Delta Z_1, \Delta Z_2]$.

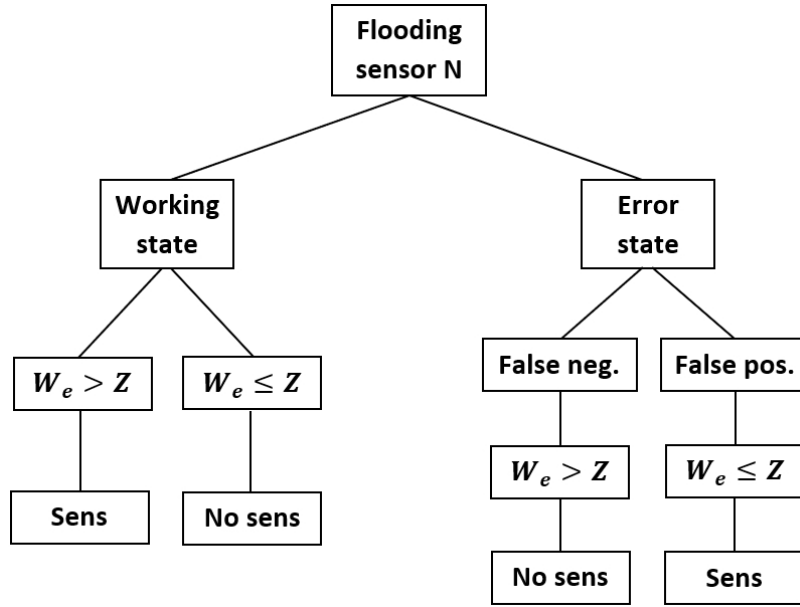


Figure 6-48: Event (probability) tree of flooding sensor status realisations.

$$\begin{aligned}
 P(z_F = 1 \mid x_D, H_s, W_e) &= P(W_s)P(W_e > Z) + P(E_s)P(W_e \leq Z) && \text{Eq. 6-62} \\
 &= (1 - \lambda_e) \left(1 + e^{\left(\frac{\alpha - \Delta Z}{\beta}\right)}\right)^{-\gamma} + \lambda_e \left(1 - \left(1 + e^{\left(\frac{\alpha - \Delta Z}{\beta}\right)}\right)^{-\gamma}\right)
 \end{aligned}$$

$$P(z_F = 1 \mid x_D, H_s, W_e) = (1 - 2\lambda_e) \left(1 + e^{\left(\frac{\alpha - \Delta Z}{\beta}\right)}\right)^{-\gamma} + \lambda_e \quad \text{Eq. 6-63}$$

$$\Lambda(\Delta Z_1, \Delta Z_2) = P(H_s \mid \Delta Z_1, \Delta Z_2) \left[(1 - 2\lambda_e) \left(1 + e^{\left(\frac{\alpha - \Delta Z}{\beta}\right)}\right)^{-\gamma} + \lambda_e \right] \quad \text{Eq. 6-64}$$

6.4 Closing remarks

The above chapter discussed in detail damage related variables. The a priori distributions developed from available damage statistics with the use of MLE techniques utilise advanced modelling approaches such as copulas for capturing conditional dependencies between variables. The distributions have been used to identify possible ship-specific initial damage extents, in terms of compromised compartments open to sea, with corresponding discrete a priori probabilities, using Monte Carlo sampling techniques. We have further developed a probabilistic model encoding the initial flooding probability in terms of water elevation exceedance of the respective extent's vertical position. The model is conditional on vessel draft and significant wave height, governing stochastic vessel movements, and was achieved by time-domain simulations for an intact vessel in waves. The model is one of two acting as the likelihood function for the flooding sensors (detection likelihood). A simple example was presented to illustrate the impact of draught and wave height on the probability of flooding compartments depending on their location with respect to the waterplane. The method for calculating probability of progressive flooding uses graph theory for modelling pairwise connections between compartments. This enables the use of an Uncertain Graph Sampling (UGS) method for capturing probabilities and application of state-of-the-art search algorithms to ensure conditionality of connection to source node (initial extent).

A simple example demonstrated that the sampling methodology converges to actual probabilities calculated from first principles whereas another, more realistic, example, illustrated the process of inferring of the likely progressive extents for a specific initial damage extent. It is noteworthy, however, that the latter example is still simplified as it did not account for variables such as leak/collapse heads and position of openings in relation with the floodwater. The leak/collapse heads and position of openings relative to the floodwater level was accounted for by a probabilistic model developed on a basis of time-domain simulations in waves. This model was further adapted to represent the likelihood function for the flooding sensor (together with the initial flooding probability) by introducing the reliability rate accommodating false readings. The model was tested with the real-case example in both, calm-water and in-waves condition with wave height of 2.0 meters H_s . The complete model including doors and flooding sensors significantly improved the accuracy of the flooding prediction compared with the simpler model.

6.5 References

Bulian, G., (2011), "*Report detailing derivation of updated probability distributions of collision damage characteristics for passenger ships*", Report No. GOALDS-D-3.1-GL- Collision Damage Characteristics – rev1 of work package WP3, deliverable D3.1 from the GOAL based Damage Stability (GOALDS) research project, funded by the European Commission, FP7-DG.

Lützen, M., (2002), "*Damage Distributions*", Report No. 2-22-D-2001-01-4 of work package WP2, deliverable D2.2 from the Harmonization of Rules and Design Rational (HARDER) research project, funded by the European Commission, DG XII-BRITE.

International Maritime Organization, (2006), "*Reg. II-1/6 to 8 of SOLAS Consolidated Edition 2009*", as adopted in IMO Res. MSC 216(82)).

Papanikolaou, P., Rainer, H., Lee B. S., Christian M., Olufsen O., Vassalos D., Zaraphonitis G., (2013), "*GOALDS - Goal Based Damage Ship Stability and safety standards*", Accident Analysis and Prevention 60, 353–365.

Bulian, G., (2017), "*Description of geometrical and probabilistic model for collision damage*", report No. eSAFE-WP2D2.1.1, Rev. 1 of work package WP2, deliverable D2.1.1 from the Enhanced Stability after a flooding event (eSAFE) research project (Joint industry project on Damage Stability for cruise ships).

International Maritime Organization, (2006), "*Reg. II-1/12.1 of SOLAS Consolidated Edition 2009*", as adopted in IMO Res. MSC 216(82)).

Sklar, A. (1959), "*Fonctions de Répartition à n Dimensions et Leurs Marges*", Publications de l'Institut Statistique de l'Université de Paris, 8, 229-231.

Tawn, J. A. (1988), "*Bivariate extreme value theory: models and estimation*" Biometrika, 397–415.

Joe, H., (1997). "*Multivariate Models and Dependence Concepts*", Monographs on Statistics and Applied Probability 73, London: Chapman and Hall.

Lutzen, M., (2001), "*Ship Collision Damage*", PhD thesis, Technical University of Denmark, Department of Mechanical Engineering.

Pawłowski, M., (2004), "*Subdivision and Damage Stability*", Euro-MTEC series book: Published by: Fundacja Promocji Przemysłu Okrętowego i Gospodarki Morskiej, Gdańsk.

Zaraphonitis, G., Bulian, G., Lindroth, D., Hamann, R., Luhmann, H., Cardinale, M., Routi A-L., Bertin, R., Harper, G., (2015), "*Evaluation of risk from raking damages due to grounding, Final report*", report No. 2015-0168, Rev. 2 from the EMSA III research project, funded by the European Maritime Safety Agency, EMSA/OP/10/2013.

Zaraphonitis, G., Bulian, G., Hamann, R., Eliopoulou, E., Cardinale, M., Luhmann, H., (2017), "Description of methodology", report No. eSAFE-WP2D2.2.1, Rev. 2 of work package WP2, deliverable D2.1.1 from the Enhanced Stability after a flooding event (eSAFE) research project (Joint industry project on Damage Stability for cruise ships).

Kehren, F.-I., Krüger S., (2007), "*Development of a Probabilistic Methodology for Damage Stability regarding Bottom Damages*", Proceedings of the 10th International Symposium on Practical Design of Ships and Other Floating Structures (PRADS2007), Houston, Texas, USA.

Krüger, S., Dankowski, H., (2009) "*On the Evaluation of the Safety level of the Stockholm Agreement*", Proceedings of the 10th International Marine Design Conference (IMDC2009), Trondheim, Norway, 26 - 29 May.

Vassalos, D., Kim, H., Christiansen, G., Majumder, J., (2001), "*A Mesoscopic Model for Passenger Evacuation in a Virtual Ship-Sea Environment and Performance-Based Evaluation*", Pedestrian and Evacuation Dynamics – April 4-6, Duisburg.

Zweig, K. A., Abufouda, M., (2016) "*A theoretical model for understanding the dynamics of online social networks decay*", arXiv preprint arXiv:1610.01538.

Thompson, R. C., Richardson, D. E., (1995), "*A Graph Theory approach to road network generalization*", Proceedings of the 16th International Cartographic Conference, Barcelona, Spain, 3-9 September, pp. 1871-1880.

Bondy, J. A. and Murty, U. S. R. (1976), "*Graph Theory with Applications*", Elsevier Science Publishing Co., Inc..

Dankowski, H., Krüger, S., (2013), "*Progressive Flooding Assessment of the Intermediate Damage Cases as an Extension of a Monte-Carlo based Damage Stability Method*", Proceedings of the PRADS201320-25, CECO, Changwon City, Korea

Khan, A., Bonchi, F., Gullo, F., Nufer, A., (2018), "*Conditional Reliability in Uncertain Graphs*", IEEE Transactions on Knowledge and Data Engineering, Volume: 30 , Issue: 11, November 1st, pp. 2078 – 2092.

Moore, E. F., (1959), "*The shortest path through a maze*", Proceedings of the International Symposium on the Theory of Switching. Harvard University Press. pp. 285–292. As cited by Cormen, Leiserson, Rivest, and Stein, (2001), "*Introduction to Algorithms*", Book published by: MIT press, ISBN: 0-262-03293-7.

Trémaux, C. P., 1859–1882, École polytechnique of Paris (X:1876), French engineer of the telegraph in Public conference, December 2, 2010 – by professor Jean Pelletier-Thibert in Académie de Macon (Burgundy – France) – (Abstract published in the Annals academic, March 2011).

Jasionowski, A., Luhman, H., Bertin, R., Routi, A-L., Cardinale, M., Harper, G., (2015), "*Evaluation of risk from watertight doors*", report No. 2015-0167 Rev 7 from the EMSA III research project, funded by the European Maritime Safety Agency, EMSA/OP/10/2013.

Chapter 7 - Vessel variables

7.1 Opening remarks

As discussed in Chapter 2, main vessel-specific variables considered herein relate to the stricken vessel. These include attributes of internal openings (status, leakage and collapse pressure heads) as well as vessel's loading condition and floating position. Trim has been disregarded, as large cruise vessels operate within a very narrow trim range but would be easily refined and implemented for future developments. The chapter will also present an attempt to account for impact energy related to the striking vessel's main particulars based on AIS data and available damage statistics (design related variables discussed in Chapter 2, such as crashworthiness and internal subdivision apart from openings has been disregarded). The following will initially present available a priori statistics for the relevant variables, followed by developed likelihood functions. The a priori belief of striking vessel size is indirectly covered by damage extent a priori presented in the previous Chapter 6 and will therefore not be repeated within this chapter.

7.2 A priori statistics

7.2.1 Openings

7.2.1.1 Opening frequencies

Statistics for door open/closed frequencies are available for main watertight doors from status sensors required by SOLAS Reg. II-1/13 (IMO, 2006). Non-watertight doors are normally not fitted with such status sensors. However, since they are more prone to leak or collapse than the watertight doors (e.g. power operated sliding watertight doors) such statistics are of secondary importance (in the cases the time-element of flooding progression can be disregarded). Nevertheless, if required, the opening frequencies for non-watertight doors may be obtained either by fitting status sensors or they can be estimated on a basis of crew/passenger traffic data. As introduced in Chapter 6, door opening status may be modelled by a Bernoulli process (Eq. 6-36) where specific door opening frequency, λ , describes its averaged proportion of open to closed in a given time interval. Herein, due to

lack of detailed data for actual opening frequencies for the sample vessel, the opening frequencies of individual doors are based on their opening allowance category as derived in the EMSA III project (Jasionowski, 2015) from onboard records of various vessels. The records don't provide one-set of frequencies per category but permit the creation of proximate distributions for random sampling as is illustrated in Figure 7-1.

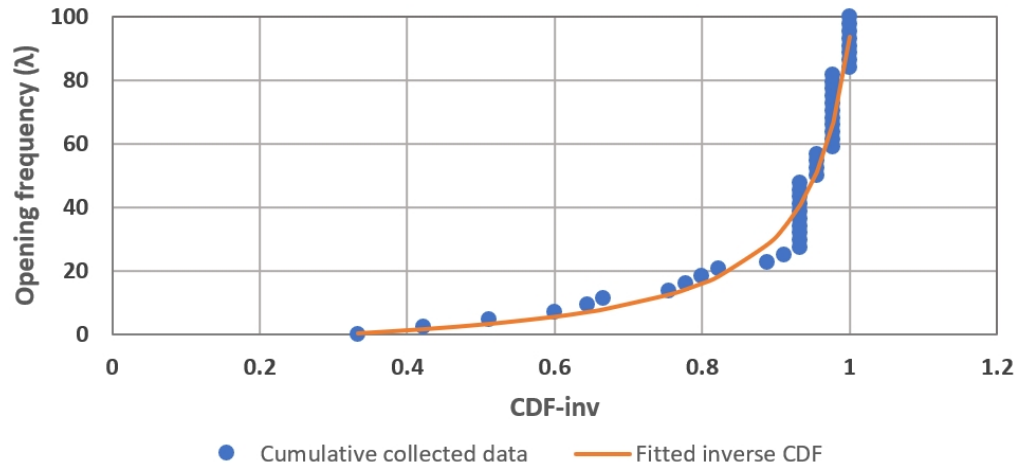


Figure 7-1: Proximate inverse cumulative density function for sampling of opening frequencies (category C-doors).

Table 7-1: Assumed (expected) opening frequency for sample vessel opening categories.

Description	Opening allowance category	Opening frequency, λ
Sliding watertight door	C	0.095
Watertight hatch	C	0.169
Hinged cold room door	NA	0.044
Hinged provisions room door	NA	0.057
Sliding cold room doors	NA	0.057
Sliding light-watertight door	C	0.075
Sliding provisions room door	NA	0.055
Sliding semi-watertight door	B	0.584
Escape hatch	A	0.522
Hinged weathertight door	A	0.032
Sliding weathertight door	A	0.417
Hinged double fire door	NA	0.690
B-class structure	NA	0.000
Hinged escape door	NA	0.564
Hinged non-watertight door	NA	0.649
Sliding fire door	NA	0.620
Hinged fire door	NA	0.444
Sliding lift door	NA	0.134
Hinged lift door	NA	0.095
Unprotected doorway or connection	NA	1.000

Specific doors in the sample vessel have been given a randomly sampled opening frequency from the available data from the EMSA project, in line with its respective opening allowance category using the proximate distributions. This results in different opening frequencies for all doors despite being of the same category for a realistic assessment. A detailed overview of the sampled opening frequency for all openings in the sample vessel is presented in Appendix IV, while the expected frequency (averaged) per door category is presented in Table 7-1.

7.2.1.2 Leak and collapse

Data regarding the resistance to leaking and collapse for a specific door may be available from the door manufacturers. However, only minimum requirements for pressure testing of watertight doors is specified in SOLAS Reg. II-1/16.2 (IMO, 2006), which would not provide a detailed measure of the actual collapse pressure. Various opening categories and their vulnerability to leakage and collapse has been investigated in the project Floodstand (Ruponen & Routi, 2011), as was mentioned in the introduction, where several full-scale model tests were performed, identifying leak and collapse pressure heads for a range of opening categories. However, there would be some uncertainty related to such estimated values as these numbers are based on tests performed on a small sample of doors only. Even if we were to test a specific door design several times for the respective pressures, they would be seen to vary around some mean due to small variations in structural soundness. The variations (uncertainties) in collapse and leak pressure heights should therefore be accounted for in a probabilistic framework, as illustrated in Figure 7-2.

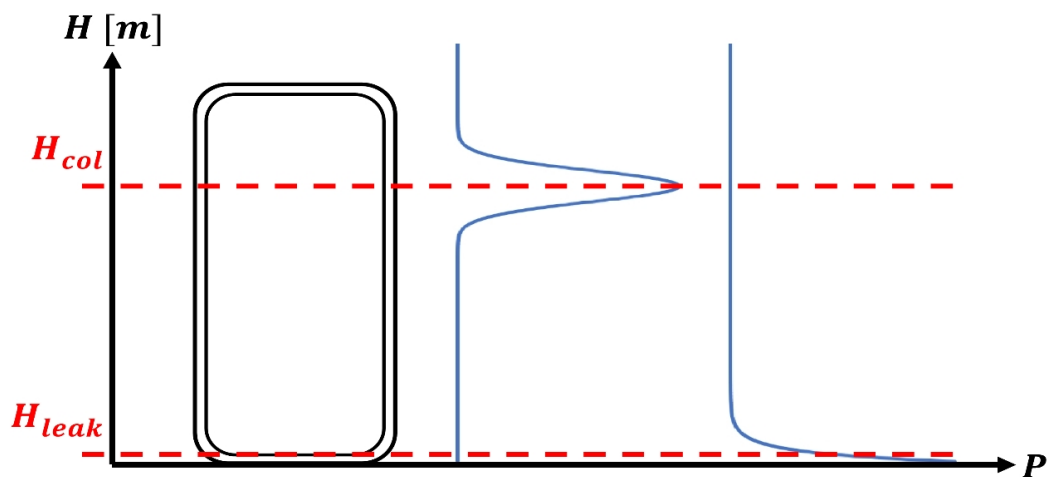


Figure 7-2: Door leak and collapse pressure heights modelled with probability distributions.

Table 7-2: Opening leak and collapse heads, including probabilistic models and parameters ($E(\lambda)$ and $N(\mu,\sigma)$ represent Exponential and Normal distribution respectively).

Description	Leak H	Dist.	Col. H	Dist.	Bottom gap
	[m]	$E(\lambda)/N(\mu,\sigma)$	[m]	$N(\mu,\sigma)$	[-]
Sliding watertight door	NA	NA	20.0	$N(H_{col}, 0.1)$	NA
Watertight hatch	NA	NA	15.0	$N(H_{col}, 0.1)$	NA
Hinged cold room door	0	$E(100/3)$	3.50	$N(H_{col}, 0.1)$	No
Hinged provisions room door	0	$E(100/3)$	3.50	$N(H_{col}, 0.1)$	No
Sliding cold room doors	0	$E(100/3)$	3.50	$N(H_{col}, 0.1)$	No
Sliding light-watertight door	2.5	$N(H_{leak}, 0.1)$	8.00	$N(H_{col}, 0.1)$	No
Sliding provisions room door	0	$E(100/3)$	3.50	$N(H_{col}, 0.1)$	No
Sliding semi-watertight door	2.5	$N(H_{leak}, 0.1)$	8.00	$N(H_{col}, 0.1)$	No
Escape hatch	0	$E(100/3)$	2.50	$N(H_{col}, 0.1)$	No
Hinged weathertight door	0	$E(100/3)$	2.50	$N(H_{col}, 0.1)$	No
Sliding weathertight door	0	$E(100/3)$	1.00	$N(H_{col}, 0.1)$	No
Hinged double fire door	0	$E(100/3)$	2.00	$N(H_{col}, 0.1)$	Yes
B-class structure	0	$E(100/3)$	1.50	$N(H_{col}, 0.1)$	No
Hinged escape door	0	$E(100/3)$	2.50	$N(H_{col}, 0.1)$	Yes
Hinged non-watertight door	0	$E(100/3)$	1.50	$N(H_{col}, 0.1)$	No
Sliding fire door	0	$E(100/3)$	1.00	$N(H_{col}, 0.1)$	Yes
Hinged fire door	0	$E(100/3)$	2.50	$N(H_{col}, 0.1)$	Yes
Sliding lift door	0	$E(100/3)$	1.50	$N(H_{col}, 0.1)$	No
Hinged lift door	0	$E(100/3)$	1.50	$N(H_{col}, 0.1)$	No
Unprotected doorway or conn.	NA	NA	NA	NA	NA

In the figure, the collapse head is normally distributed around the specified mean collapse pressure, while the leak head is modelled by exponential distribution. Doors with higher leak resistance could also be modelled by a normal distribution as is seen two examples of in Table 7-2. Leakage through a gap at the bottom of doors (if present) is defined as a deterministic process governed solely on the position of the gap in relation with the floodwater level and modelled independently from the opening itself. Although doors (particularly hinged) may be characterised by different leakage/collapse heads depending on the direction of the pressure gradient (e.g. pushing towards or away from the door frame) in this development, for simplicity, the pressure is assumed identical for both directions. The details of doors' models are shown in Table 7-2 above. Modelling of the leak- and collapse pressure heads as probability distributions must account for the fact that the actual heads are given as distributions. This needs to be considered when implementing the probability of exceedance from section 6.3.2.4 (Eq. 6-59) as shown Eq. 7-1.

$$P(PF = 1) = \lambda \left(1 + e^{\left(\frac{\alpha - \Delta Z}{\beta} \right)} \right)^{-\gamma} + \dots \quad \text{Eq. 7-1}$$

$$\dots + (1 - \lambda) \iint_{Z_{leak}, Z_{col}} \left(1 + e^{\left(\frac{\alpha - \min(Z_{leak}, Z_{col})}{\beta} \right)} \right)^{-\gamma} pdf(Z_{leak}, Z_{col}) dZ_{leak} dZ_{col}$$

where, $pdf(Z_{leak}, Z_{col}) = pdf(Z_{leak})pdf(Z_{col})$, assuming independence.

7.2.2 Loading condition

7.2.2.1 Vessel draft, T

The a priori statistics for the sample vessels' draft might be available from its operational data. In the absence of actual operational data (as in the case of the sample vessel) the distributions can be derived from statistical data. Discrete draft distributions have for this purpose been adopted from the research project eSAFE (Paterson & Atzampos, 2017), and rescaled to our sample vessels' operating range. The discrete draft distribution is shown in Figure 7-3. The data have further been fitted to a continuous distribution in the form of a bounded Beta distribution, governed by Eq. 7-3. The continuous distribution is also illustrated in the figure. Coefficients for the draft distribution are $\alpha = 5.2$, $\beta = 1.8$, and bounds are $a = 7.1$, $b = 8.25$, and $B(\alpha, \beta)$ is the Beta function.

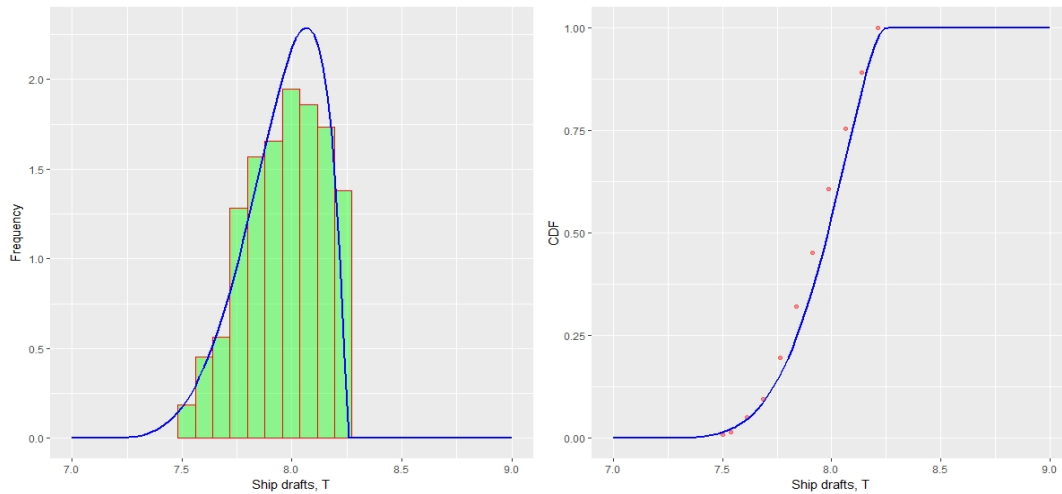


Figure 7-3: Numerical and analytical dimensionalised draft distribution.

$$P(T) = \frac{(x - a)^{\alpha - 1} (b - x)^{\beta - 1}}{B(\alpha, \beta) (b - a)^{\alpha + \beta - 1}} \quad \text{Eq. 7-2}$$

7.2.2.2 Vertical position of centre of gravity, KG

In absence of the actual operational data the a priori statistics for vertical centre of gravity, KG , are based on the stability booklet, although in reality the data would be available from the on-board loading computer. Nevertheless, the standard loading conditions from the stability booklet should reflect actual operating conditions of the vessel and has been illustrated in Figure 7-4. The damage stability limit curve, as required by SOLAS Reg. II-1/5-1 (IMO, 2006) has been included for illustration. Herein, it is assumed that the loading conditions are normally distributed around the mean value represented in the figure by the dotted regression line. The orange lines correspond to 99% confidence bounds while the distribution is given by Eq. 7-3 to Eq. 7-5.

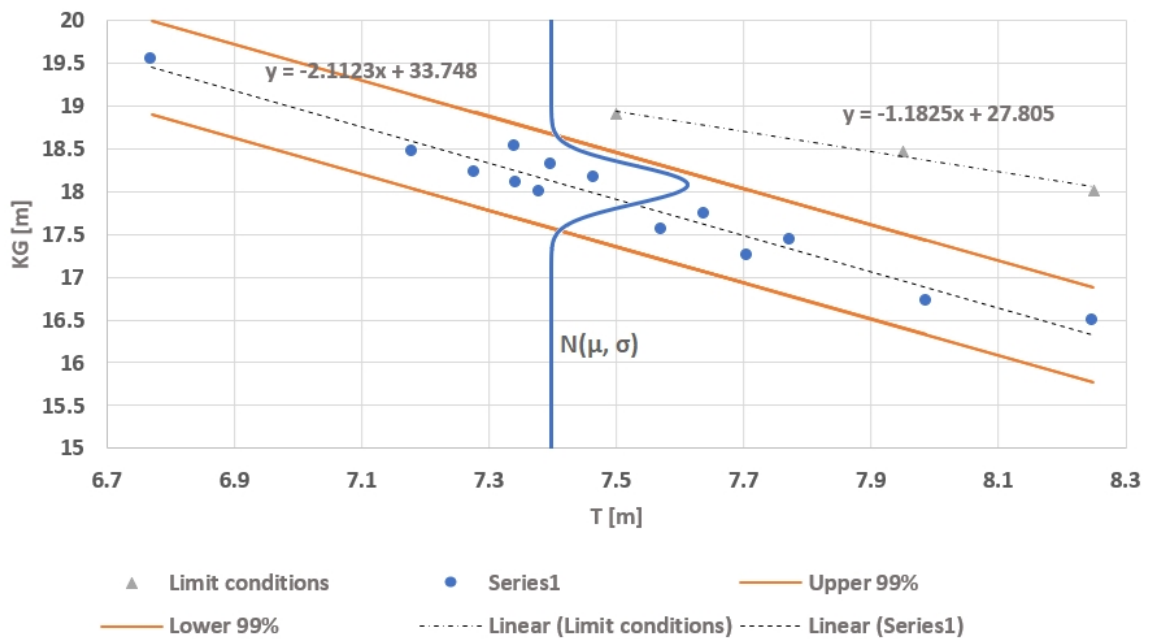


Figure 7-4: Operating loading conditions.

$$P(KG|T) = \frac{1}{\sqrt{2\pi\sigma^2}} e^{-\frac{(KG-\mu)^2}{2\sigma^2}} \quad \text{Eq. 7-3}$$

$$\mu(T) = -2.112T + 33.748 \quad \text{Eq. 7-4}$$

$$\sigma = \sqrt{\frac{\sum|x-\mu|^2}{N}} = 0.1778 \quad \text{Eq. 7-5}$$

As the mean value in Eq. 7-3 is represented by a linear function of the draught, T , given by Eq. 7-4, the distribution of KG is conditional on draught T , which can be denoted as $P(KG | T)$. The joint, bi-variate, probability distribution $P(KG, T)$ can be derived with the help of the chain rule as given by Eq. 4-7. A sample of 1,000 loading conditions drawn from the distribution is shown in Figure 7-5. The figure shows clearly that the vessel is operating in a narrow draught range biased towards the area of the summer load-line draught, as is expected. The leftmost standard loading condition is the lightship condition, and obviously not an area where you would expect actual operating conditions.

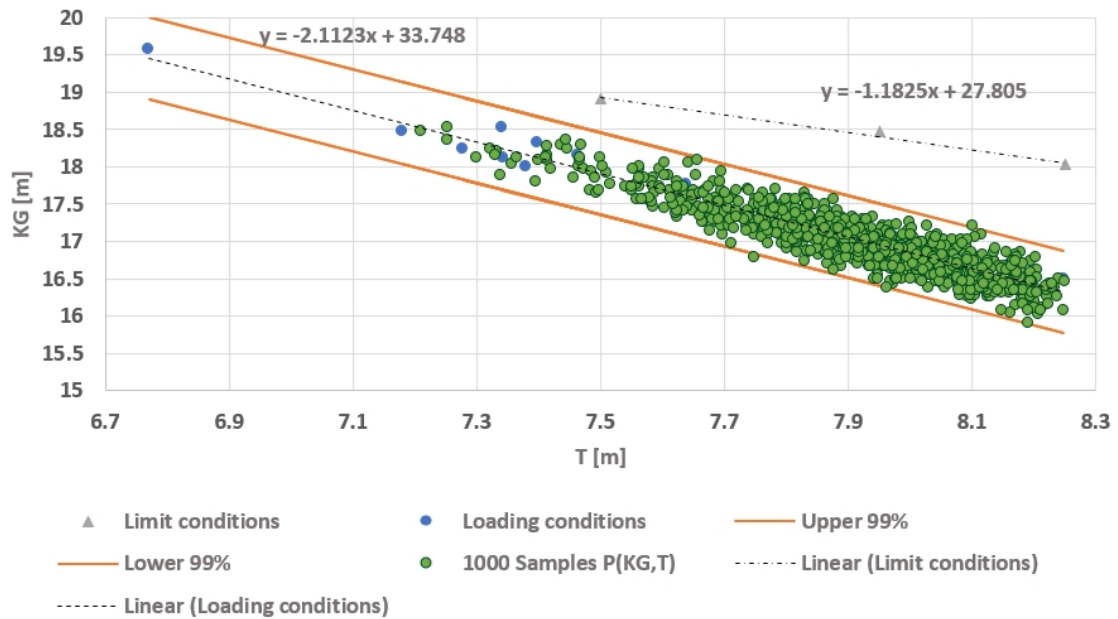


Figure 7-5: Bi-variate distribution for KG and T developed from operating loading conditions.

7.3 Likelihood functions

7.3.1 Opening status sensors

The sample vessel has status sensors with indication to the operators fitted for all watertight, semi-watertight and light-watertight sliding doors. These doors also have remote closing from the bridge. The likelihood function for the status sensor for doors should encode the probability of receiving a specific (either *open* = 1 or *closed* = 0) status from the sensor, z , conditional on actual door status, x . The likelihood function should therefore allow for four possible permutations of a sensor and door statuses:

1. Sensor showing door open, provided that the door is open; $P(z = 1 | x = 1)$
2. Sensor showing door closed, provided that the door is closed; $P(z = 0 | x = 0)$
3. Sensor showing door open, provided that the door is closed; $P(z = 1 | x = 0)$
4. Sensor showing door closed, provided that the door is open; $P(z = 0 | x = 1)$

The two initial combinations obviously correspond to the intended function of the sensors. The remaining two represent sensor errors in the form of false negatives and positive readings as already discussed in Chapter 4. Some sensor types have built in error indication for this purpose, and may be logged, providing an error-, or reliability-rate for a specific sensor. Alternatively, sensor error- or reliability rates may be provided by the manufacturer. In this development, assumed sensor success rate for providing both open and closed indication is 99%, which results in the probabilities (or likelihoods) presented in Table 7-3.

Table 7-3: Sensor likelihood, including sensor reliability (false positives/negatives).

Sensor status, z	Actual door status, x	
	$x = 1$ (open)	$x = 0$ (closed)
$z = 1$	0.99	0.01
$z = 0$	0.01	0.99

The above success rates assume that the sensors are operational (i.e. not part of the damage breach). This relates directly to systems availability post damage (case specific and highly dependent on the actual damage breach (initial extent) as discussed in Chapter 6) and should be accounted for either by sensor reliability figure or by the direct update of the likelihood function. Sensor availability has not been implemented in the framework at this stage. As the above likelihoods encodes discrete cases, the simplified version of Bayes theorem given by Eq. 4-26 cannot be applied directly. Instead, marginal probability distribution, $P(z)$ needs to be considered explicitly as given in Eq. 7-6, where status x' is the complement or opposite of status x .

$$P(x | z) = \frac{P(z|x)P(x)}{P(z)} = \frac{P(z|x)P(x)}{P(z|x)P(x) + P(z|x')P(x')} \quad \text{Eq. 7-6}$$

The posterior update is illustrated by a simple example considering five doors with known a priori (opening frequencies) and specific sensor readings, z . Use of the likelihood

functions derived above results in posterior probability updates as summarised in Table 7-4, clearly indicating the increased confidence from the available sensor evidence.

Table 7-4: Simple example of posterior update of door status probability using sensor status.

Door No.	$P(x = 1)$	z	$P(Z = z X = 1)$	$P(X = 1 Z = z)$
Door 1	0.50	0	0.01	0.010
Door 2	0.10	0	0.01	0.001
Door 3	0.05	1	0.99	0.839
Door 4	0.95	1	0.99	0.999
Door 5	0.20	0	0.01	0.003

7.3.2 Draught sensors

7.3.2.1 Waterplane representation from draught sensors

The sample vessel is fitted with four pneumatic draft sensors located on both sides at forward and aft ends of the hull. The draught sensors readings enable continuous assessment of the floating position (expressed in terms of draught, heel and trim). The draught sensors are also used to construct a plane corresponding to the instantaneous waterplane of the ship. Mathematically, a plane is uniquely described by any three non-colinear points in space is required as shown given by Eq. 7-7.

$$a(x - x_0) + b(y - y_0) + c(z - z_0) = 0 \quad \text{Eq. 7-7}$$

In the equation a, b and c are components of a vector $[a, b, c]^T$ normal to the plane while (x_0, y_0, z_0) is an arbitrary point in the plane. The x and y are coordinates of the draught sensor in the body-fixed coordinate system and the z -coordinate the height of the water column at sensor's location (Figure 7-6). A correction should be applied for the actual heel and trim, otherwise the values obtained from the plane are only appropriate for smaller heel and trim values. As four sensors are available, redundancy is provided, in addition to better accuracy as several planes may be produced, and the waterplane height may be represented as their mean. The significance of the mathematical representation of the real-time waterplane is that it provides a reference point to any arbitrary points within the vessel (e.g. external or internal openings). This is crucial in predicting of the flooding progression and forms the basis for the probabilistic modelling of flooding sensors as discussed in Chapter 6.

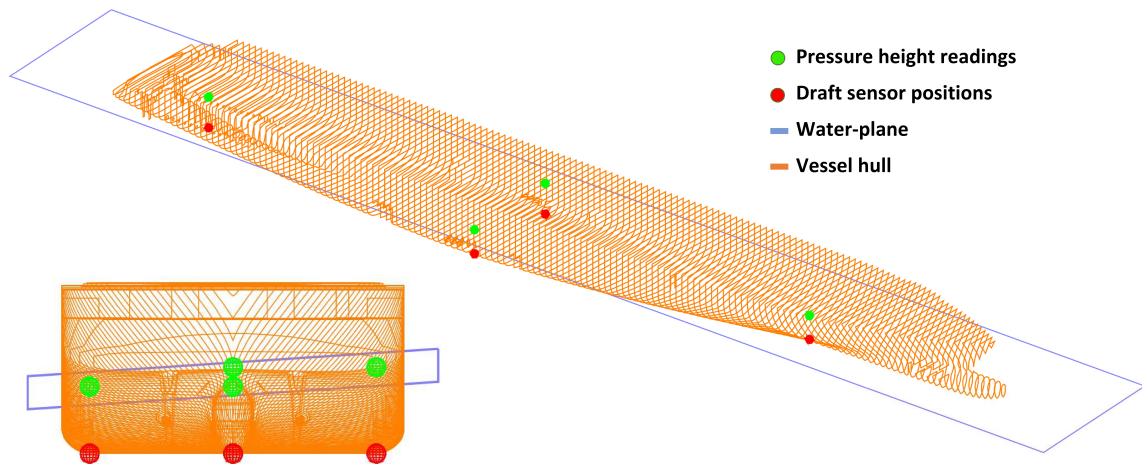


Figure 7-6: Mathematical representation of waterplane using draft sensor measurements.

7.3.2.2 Posterior update of initial damage extent from draft sensors

As established in Chapter 2, the vessels draught influences the vertical extent of the breach and this knowledge can be utilised for an updated belief of initial damage extent conditional on vessel draft. The draught sensor model (likelihood function) for this purpose should therefore encapsulate the probability of a particular draught observation by draught sensor given the particular initial damage extent (a set of compromised rooms). The specific initial damage extent has a range of possible lower vertical breach boundaries, Z , governed by the lower and upper limit of the lower-most compartment within the damage extent directly related to the integration intervals as was discussed in Chapter 6.

This has been illustrated with an example in Figure 7-7, denoting the lower and upper limit as Z_1 and Z_2 respectively, for an initial damage extent example comprising three compartments (1, 2 and 3). It is evident that a Z value slightly above Z_2 would exclude compartment three from the damage and the extent would take the form as a completely different damage extent. Similarly, using a Z value slightly below Z_1 would include additional lower compartments, and again become a different damage extent. The specific damage extent (uniquely represented by compartments 1, 2, and 3) will therefore only be realised if the lower position of the breach take on a value within the specific interval (considering the Z variable alone).

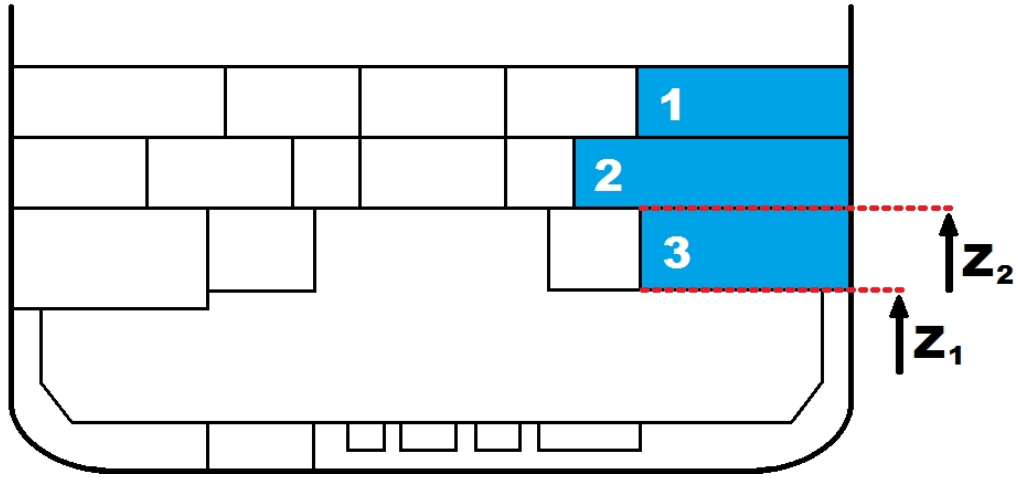


Figure 7-7: Interval of possible Z values for a given initial damage extent.

In summary, it is clear that the lower damage extent, Z_1 , cannot be lower than the lower limit of the lower-most compartment, and likewise, the upper damage extent, Z_2 , cannot be any higher than the upper limit of the lower-most compartment for this particular initial damage extent. As the damage extent is given, and not the actual Z value of the breach and knowing that a range of breaches may result in the same damage extent, it must be assumed that the probability of a particular draft (conditioned on the damage case) may come from any of the Z values within the interval $Z \in [Z_1, Z_2]$. An analytical representation of the conditional probability of Z , given draft T have already been developed in Chapter 6, and is reintroduced in Eq. 7-8 and illustrated in Figure 7-8.

$$PDF(Z|T) = \frac{e^{\frac{T+m-Z}{s}}}{s \left(1 + e^{\frac{T+m-Z}{s}}\right)^2} \quad \text{Eq. 7-8}$$

The distribution may be translated to the necessary likelihood function, $\Lambda(Z_1, Z_2)$, directly by interchanging the conditionality between the variables to $P(T|Z)$, and further by representing the Z variable as its respective interval, i.e. $\Lambda(Z_1, Z_2) = P(T|Z) = P(T | Z_1, Z_2)$. The vertical interval has to be accounted for by integration, given by Eq. 7-9, which results in the draft sensor likelihood function given by Eq. 7-10. Taking advantage of hyperbolic functions, an alternative form of the model is given by Eq. 7-11.

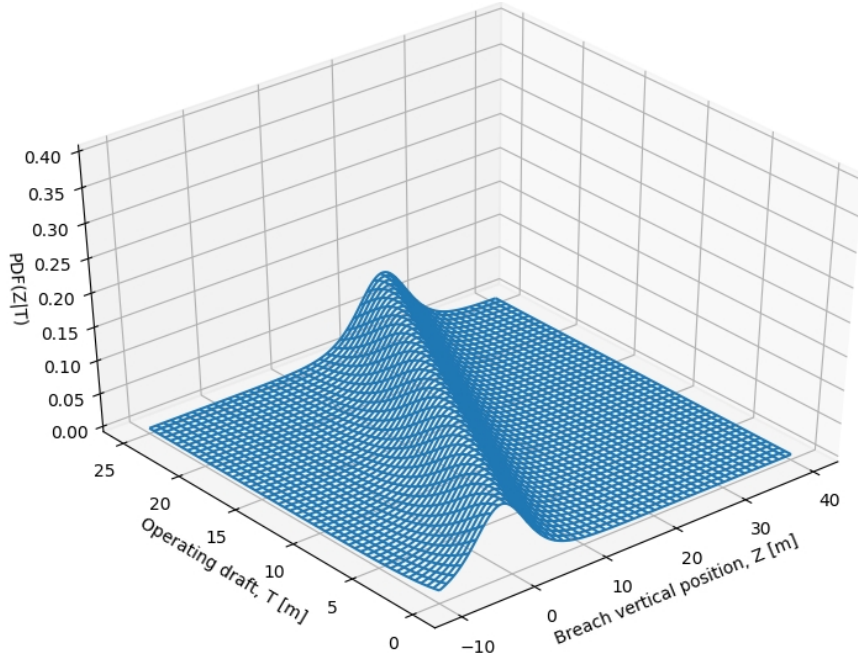


Figure 7-8: Probability distribution for Z conditional on T.

$$PDF(Z_1, Z_2 | T) = \int_{Z_1}^{Z_2} PDF(Z|T) dz \quad Eq. 7-9$$

$$PDF(Z_1, Z_2 | T) = \frac{1}{e^{\frac{m+T-Z_2}{s}} + 1} - \frac{1}{e^{\frac{m+T-Z_1}{s}} + 1} \quad Eq. 7-10$$

$$\Lambda(Z_1, Z_2) = PDF(T | Z_1, Z_2) = C \sinh\left(\frac{Z_1 - Z_2}{2s}\right) \operatorname{sech}\left(\frac{m+T-Z_1}{2s}\right) \operatorname{sech}\left(\frac{m+T-Z_2}{2s}\right) \quad Eq. 7-11$$

$$C = \frac{1}{2(Z_1 - Z_2)} \quad Eq. 7-12$$

A simple example illustrating how the probabilities of damage extents are updated based on known operating drafts is presented in the following. Two operating drafts are considered in the example, namely maximum summer load line draft, $T_s = 8.25 \text{ m}$, and the lightship draft, $T_l = 6.75 \text{ m}$ (selected purely for illustration purposes as not being an actual operating condition). For simplicity, the focus is on a small section of the sample vessel with a single lower compartment and an upper compartment considered as two separate initial damage extents (shown together in Figure 7-9). The two respective initial damage extents a priori probability has been obtained in Chapter 6 from the Monte Carlo sampling.

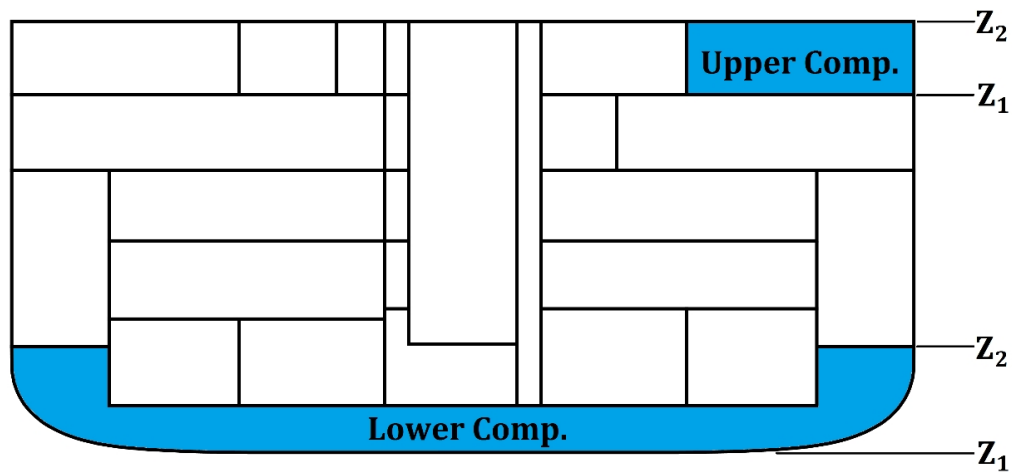


Figure 7-9: Ship section with upper and lower compartment and their vertical limits.

The updated posterior belief for the respective initial extents based on two draughts under considerations (considered as evidence) and incorporating likelihood function given by Eq. 7-11 is shown in Table 7-5, where specific initial damage extents are denoted by x ($x = Z_1, Z_2$).

Table 7-5: Posterior update of initial damage extent probability.

Damage extent	A priori	Draft, T	Likelihood	Posterior
	P(x)	[m]	P(T x)	P(x T)
Lower comp. damage extent	0.002032	6.75	0.0707	0.00216
		8.25	0.0488	0.00149
Upper comp. damage extent	0.000215	6.75	0.0054	0.00017
		8.25	0.0098	0.00032

The results show clearly that the probability of damaging lower compartments is reduced for deeper draughts and increased for shallower draughts governed by their relative vertical distance from the expected damage region. Similarly, upper compartments are assigned higher probability of damage for deeper draughts and lower probability of damage for shallower draughts. This is as expected, and in line with our argument made in the introductions. A much higher difference would be expected for other vessel types with a larger operational draft range.

7.3.3 AIS “sensor” data

7.3.3.1 Posterior update of initial damage extent based on AIS

An argument presented in Chapter 2 implied that the breach size and the subsequent initial damage extent depend on the energy exchanged between the ships involved in collision incident. The energy in turn is related to (among the other) the size, speed and heading of the ships. In the following, an attempt is made to assess such relationships and utilise it for the development of likelihood functions (the a priori belief, as already mentioned, have been covered by the a priori damage distributions developed in Chapter 6). It is noteworthy that the available damage statistics have a very few data-points that include speed and heading of the striking vessels. This also applies to the size variables with the length of the striking vessel recorded most often. For this reason the length is a parameter of choice for representing the size of the striking vessels. The breach variables influenced by the available energy are: vertical position, Z , length, L , height, H , and transverse penetration, Y . The longitudinal position, X , relates to the heading at the instant of collisions and is assumed unconditional on the striking vessels size.

The likelihood function for AIS data should represent the probability of receiving a specific vessel length from the AIS, conditional on the respective damage variables. This is the conditional distribution of (or relationship between) the vessel length, and the respective damage variables. Relevant distributions are already identified and assessed from available accident statistics in detail in Chapter 6, and summarised in Table 7-6. These distributions are marginal, assuming to cover all vessel sizes. However, since the actual size could be known from AIS data the distributions can instead be given as conditional with the relevant parameters represented as a function of vessel length, hence capturing the conditionality, as shown in figures Figure 7-10 to Figure 7-13.

Table 7-6: Marginal distributions for damage breach variables related to collision energy.

Variable	Distribution	Parameters
Z	Logistic	$m = -1.6218, s = 2.4004$
L	Burr	$a = 5.9883, b = 0.9576, r = 0.0276$
H	GBP2	$a = 6.8089, b = 15.7057, p = 0.0838, q = 1.1089$
Y	Exponential	$\lambda = 0.2968$

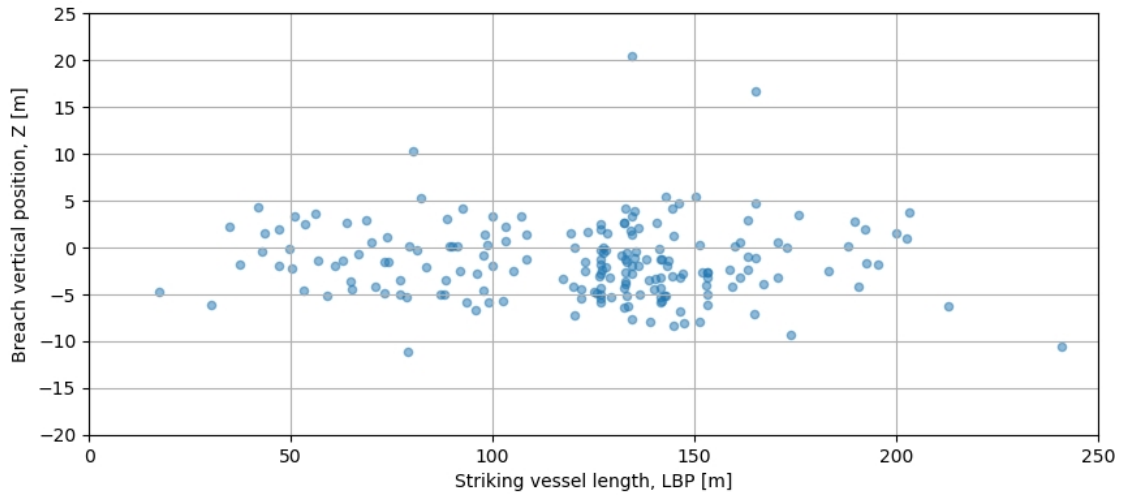


Figure 7-10: Vertical position of Breach as a function of Striking vessel length.

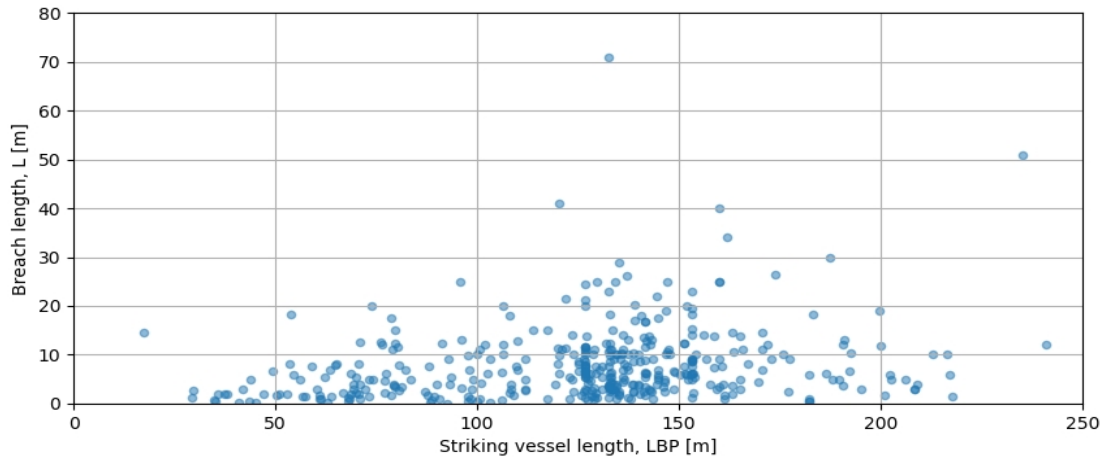


Figure 7-11: Length of Breach as a function of Striking vessel length.

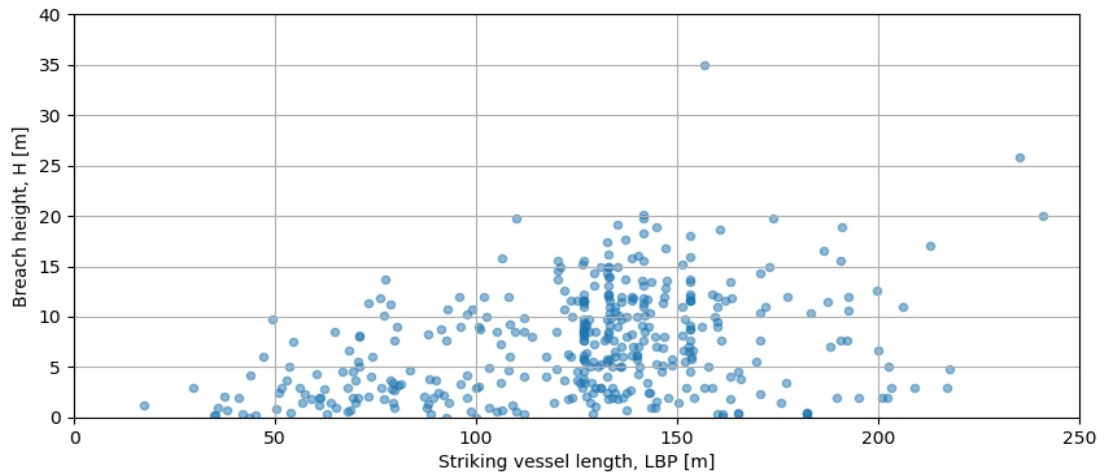


Figure 7-12: Height of Breach as a function of Striking vessel length.

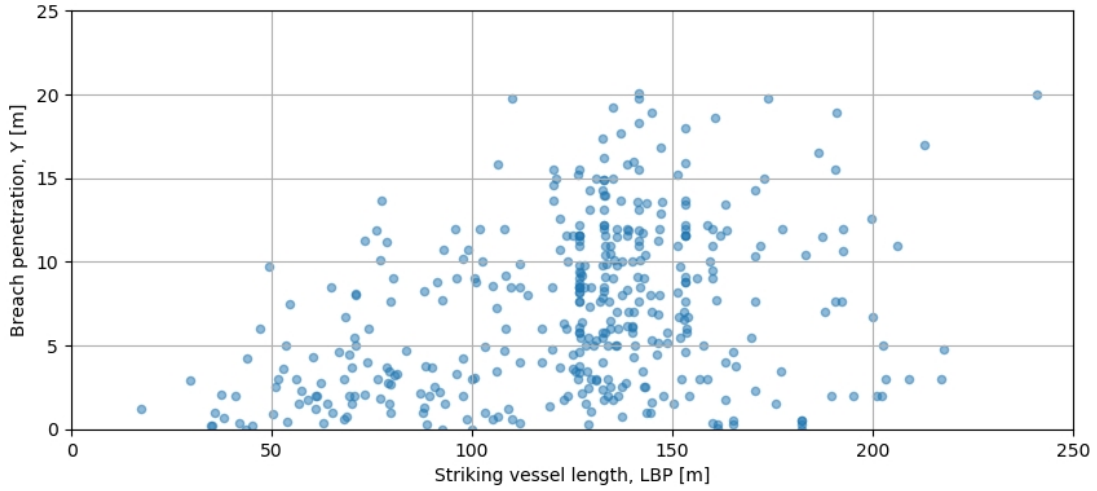


Figure 7-13: Breach penetration as a function of Striking vessel length.

From the above scatter-plots, it is evident that the breach variables are mainly located in the lower regions for smaller striking vessel lengths. As the striking vessel length increases, the valid range of breach variables are expanding to also include the upper region. This suggests that smaller breach sizes are also viable for larger striking vessel lengths and is presumably a consequence of not accounting for the speed nor heading. Nonetheless, it is clearly indicating that more extreme breach sizes are highly unlikely for minor striking vessel lengths, due to the lack of available energy as was expected. By utilising the observation of growing spread (or standard deviation), we may construct the conditional distributions by representing their respective distribution coefficients as functions of the striking vessel length with new fitting coefficients. By applying maximum likelihood estimation the analytical distributions and respective fitting coefficients has been obtained as presented in Eq. 7-13 to Eq. 7-21. Corresponding graphs are presented in Figure 7-14 to Figure 7-17, including 200 samples from the distributions plotted together with the actual data-points for comparison. Figures are plotted on the interval $L_{BP} = [50, 250 \text{ m}]$ as the probability are exponentially increasing for lower values of L_{BP} , defeating the figures illustrative purpose.

$$PDF(Z - T|L_{BP}) = \frac{e^{-\frac{T+m-Z}{s}}}{s(1 + e^{-\frac{T+m-Z}{s}})^2} \quad \text{Eq. 7-13}$$

$$s(L_{BP}) = aL_{BP} + b, \quad a = 0.0209, \quad b = 0.0030 \quad \text{Eq. 7-14}$$

$$m(L_{BP}) = aL_{BP} + b, \quad a = -0.0035, \quad b = -1.2329 \quad \text{Eq. 7-15}$$

$$PDF(L|L_{BP}) = \frac{ab(Lr)^b}{L(1+(Lr)^b)^{(a+1)}, \quad a = 5.9883, b = 0.9576 \quad \text{Eq. 7-16}$$

$$r(L_{BP}) = a + be^{cL_{BP}}, \quad a = 0.0185, b = 0.3015, c = -0.0420 \quad \text{Eq. 7-17}$$

$$r(L_{BP}) = a + be^{cL_{BP}}, \quad a = 0.0185, b = 0.3015, c = -0.0420 \quad \text{Eq. 7-18}$$

$$b(L_{BP}) = a + be^{cL_{BP}}, \quad a = -121.9882, b = 122.0882, c = 0.0010 \quad \text{Eq. 7-19}$$

$$PDF(Y|L_{BP}) = \lambda e^{-\lambda Y} \quad \text{Eq. 7-20}$$

$$\lambda(L_{BP}) = a + be^{cL_{BP}}, \quad a = 0.2524, b = 29.7476, c = -0.0883 \quad \text{Eq. 7-21}$$

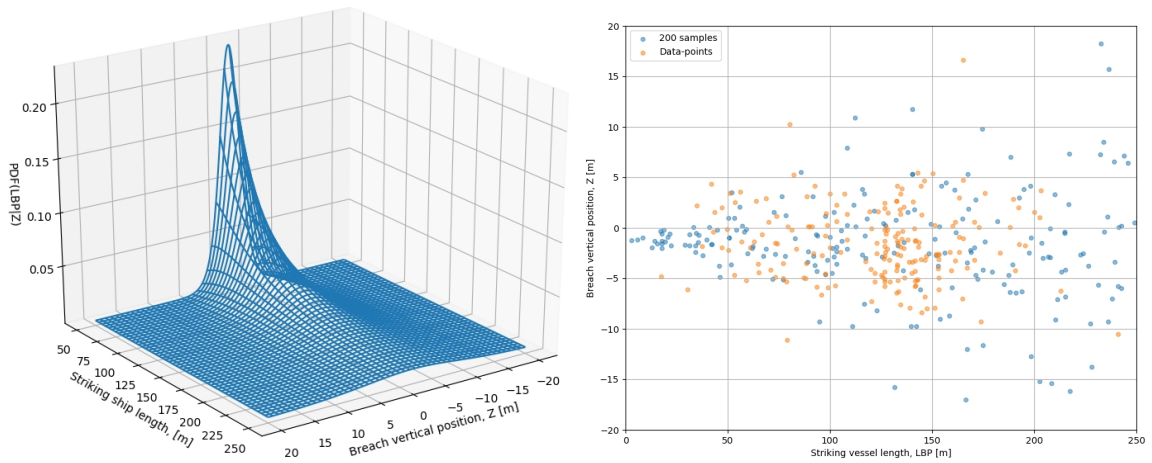


Figure 7-14: Likelihood function for Z (left), and samples compared with data-points (right).

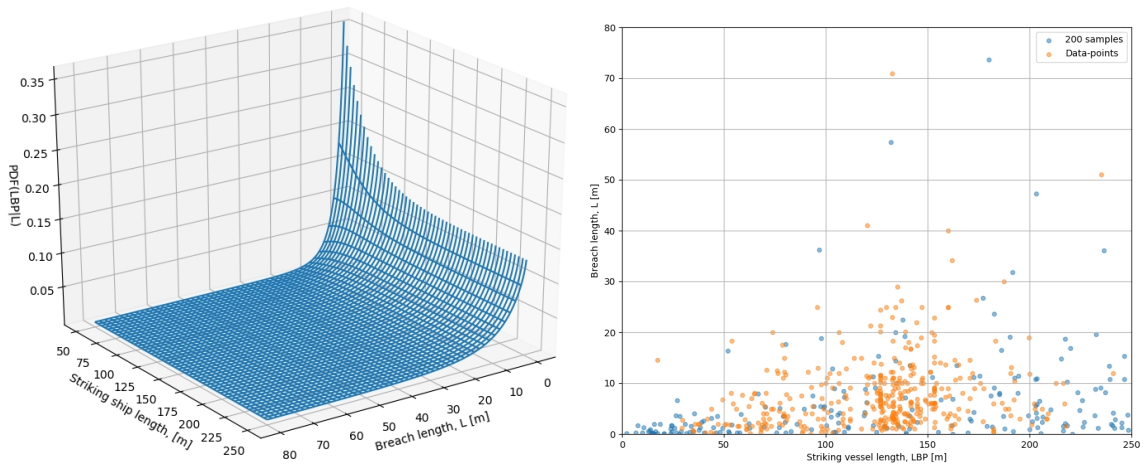


Figure 7-15: Likelihood function for L (left), and samples compared with data-points (right).

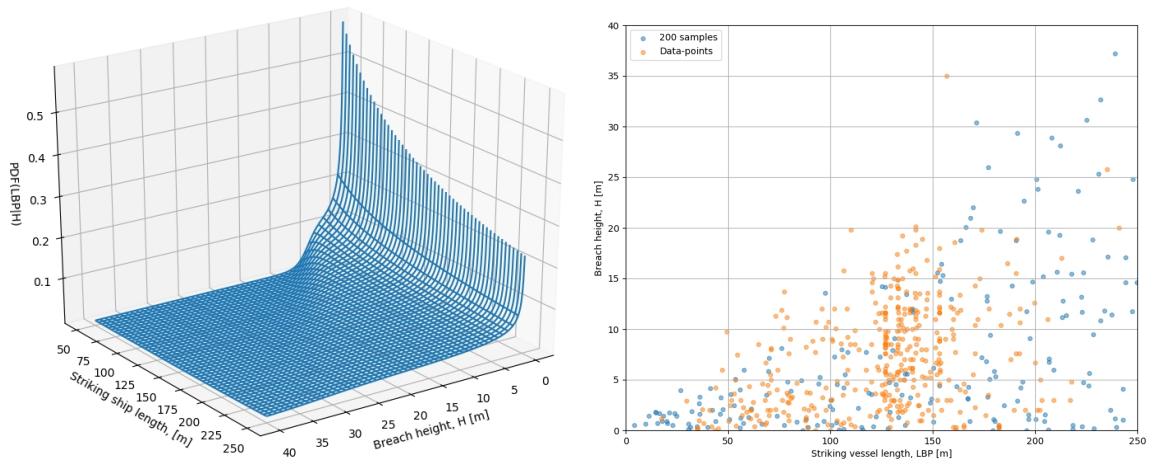


Figure 7-16: Likelihood function for H (left), and samples compared with data-points (right)

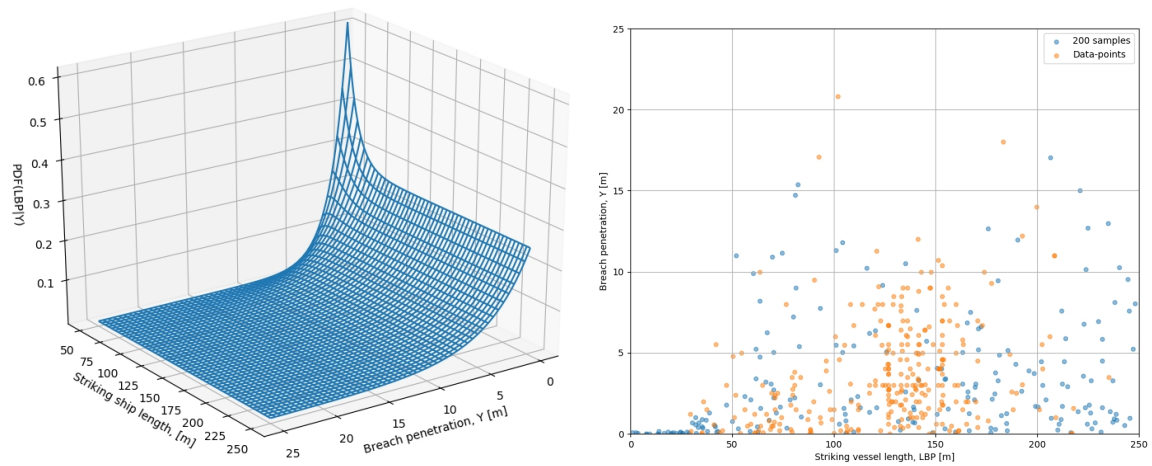


Figure 7-17: Likelihood function for Y (left), and samples compared with data-points (right).

As for the likelihood function for the draught sensor already introduced (Eq. 7-11), the discrete initial damage extents are of interest rather than continuous breach variables, and the distributions need to be integrated over the relevant intervals related to specific initial damage extents (or damage cases) comprising the integration domain. For highly complex subdivisions, identifying the relevant intervals for the integration domain (i.e. the upper and lower bounds) may prove difficult and time consuming. An alternative method involves identifying the domain by random sampling. In this approach the bounds are associated with extreme coordinates of the sample point lying within the specific extent. The method is also time-consuming but much simpler than identification by the compartment extents. Furthermore, the time overheads are not of prime importance as the process is executed only once. Example of the integration domain is illustrated in Figure 7-18 for the respective

variables while the resulting likelihood functions after integration are given by Eq. 7-22 to Eq. 7-25 (considering the distribution parameters from above valid). The function ${}_2F_1(a,b;c;z)$ in Eq. 7-24 is the *Hypergeometric* function.

$$\Lambda(Z_1, Z_2) = PDF(L_{BP} | Z_1, Z_1) = \frac{1}{2(Z_1 - Z_2)} \sinh\left(\frac{Z_1 - Z_2}{2s}\right) \operatorname{sech}\left(\frac{m+T-Z_1}{2s}\right) \operatorname{sech}\left(\frac{m+T-Z_2}{2s}\right) \quad \text{Eq. 7-22}$$

$$\Lambda(L_1, L_2) = PDF(L_{BP} | L_1, L_1) = \frac{1}{L_2 - L_1} \left((1 + (rL_1)^b)^{-a} - (1 + (rL_2)^b)^{-a} \right) \quad \text{Eq. 7-23}$$

$$\Lambda(H, H_2) = PDF(L_{BP} | H_1, H_1) = \frac{\left(\frac{H_2}{b}\right)^{ap} {}_2F_1\left(p, p+q; p+1; -\left(\frac{H_2}{b}\right)^a\right) - \left(\frac{H_1}{b}\right)^{ap} {}_2F_1\left(p, p+q; p+1; -\left(\frac{H_1}{b}\right)^a\right)}{(H_2 - H_1)pB(p, q)} \quad \text{Eq. 7-24}$$

$$\Lambda(Y, Y_2) = PDF(L_{BP} | Y_1, Y_1) = \frac{1}{Y_2 - Y_1} (e^{-\lambda Y_1} - e^{-\lambda Y_2}) \quad \text{Eq. 7-25}$$

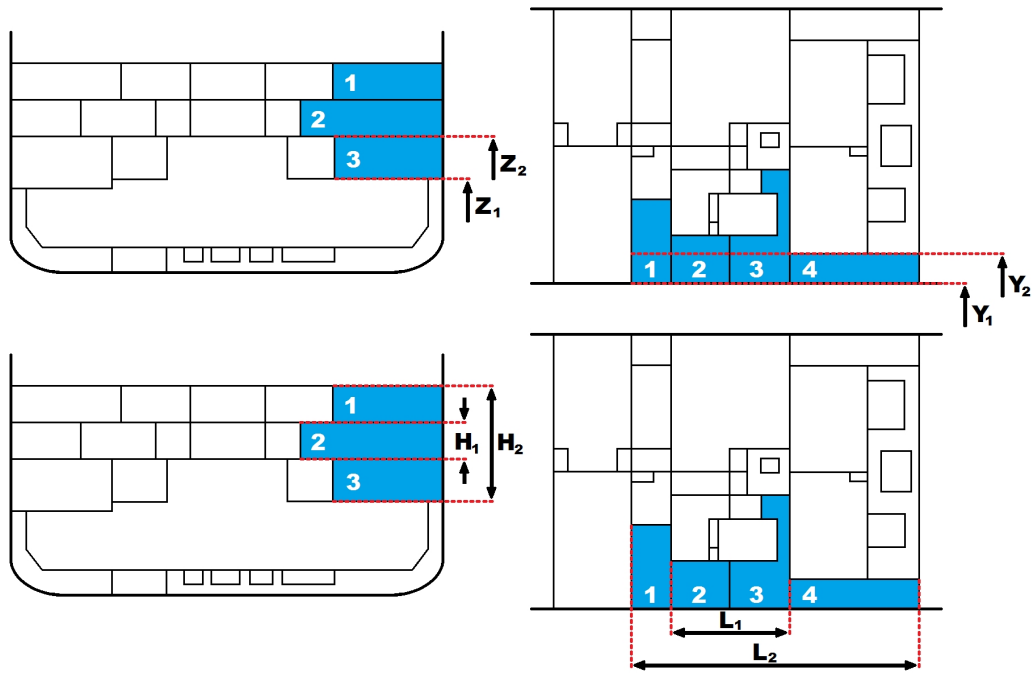


Figure 7-18: Example of integrand intervals (bounds) for the respective breach variables for specific initial damage extents (right case with three damage comp. differ from the left case with four damaged comp).

A simple example may illustrate the use of likelihood functions developed above for the posterior update from known AIS data of the striking vessel length. For this purpose, a small striking vessel length of 35.0 m has been implemented, and it is assumed that the length information is received through the AIS receiver and implemented in the update. The example utilise a priori belief of the initial damage extents developed and presented in the

previous Chapter 6. To keep the example simple and yet illustrative only likelihood function representing breach lengths has been implemented (as given by Eq. 7-23). The example uses a small striking vessel length to illustrate that larger extent damages would, in the posterior update, be assigned a reduced probability, simply because the limited collision energy would render larger extents less likely. The posterior update is demonstrated for two damage cases; minor, 1-zone, and major, 4-zones, extents summarised in Table 7-7 and shown in Figure 7-19 and Figure 7-20.

Table 7-7: Example initial damage extents (minor and major).

Extent	L-interval [m]	H- interval [m]	Y- interval [m]	Z- interval [m]	Comp.	Zones
Minor	0.00-16.00	0.00-11.20	0.00-12.70	0.00-8.40	2	1
Major	42.00-104.00	0.00-5.50	0.00-5.50	0.00-5.50	10	4

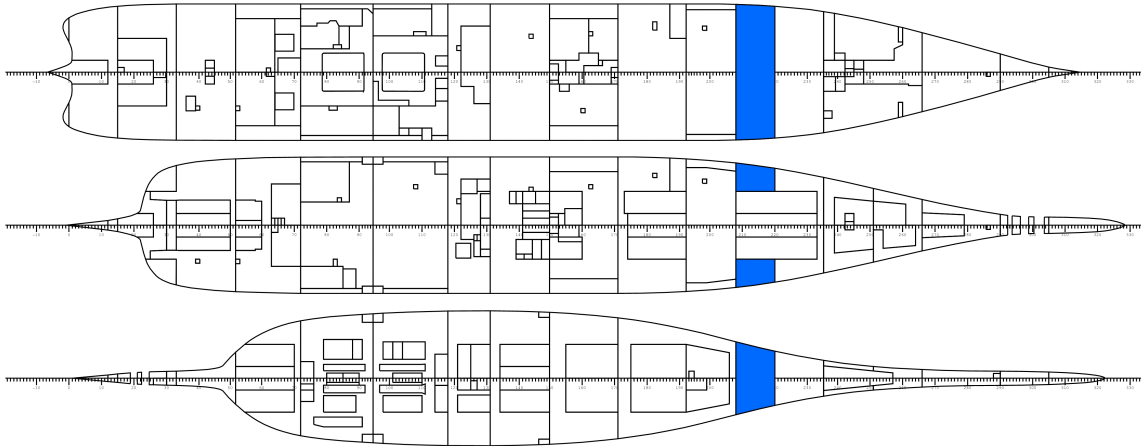


Figure 7-19: Minor damage extent example.

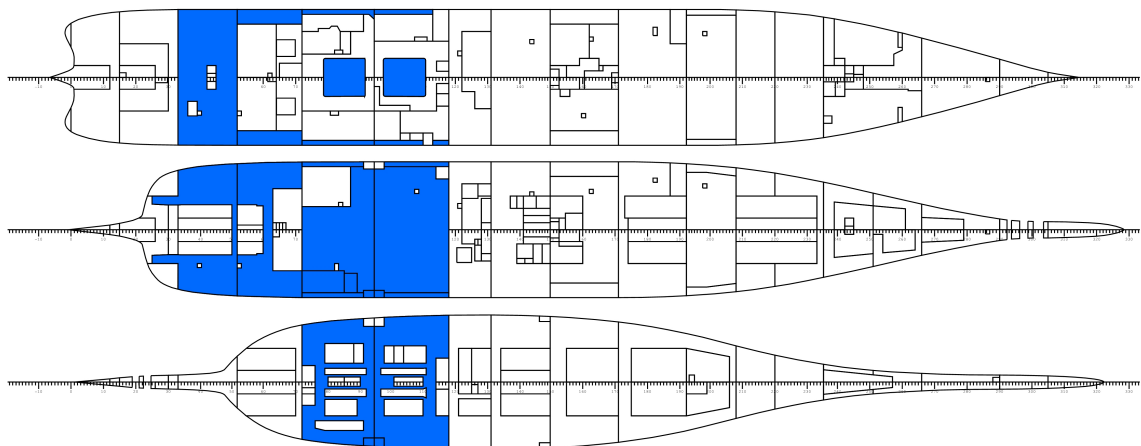


Figure 7-20: Major damage extent example.

The updated belief of longitudinal extent following the posterior update and normalisation (by means of Eq. 4-26 introduced in Chapter 4) is presented in Table 7-8. Normalisation is obtained by utilising the fact that the sum of the probability of all the damage cases should be one. The likelihood functions for specific integration interval $L \in [L_1, L_2]$, and the vessel's length, L_{BP} are illustrated in Figure 7-21 for both minor and major damage extents. The graphs clearly show that the developed likelihood functions assigns an increase in probability to the minor damage extent, while a decrease in probability to the major damage extent, when supported by the knowledge of a minor striking vessel length, as was expected.

Table 7-8: Posterior update of initial damage extent probability from AIS data.

Extent	A priori	Draft, T	Likelihood	Posterior
	$P(x)$	[m]	$P(L_{BP} x)$	$P(x L_{BP})$
Minor	0.0026	8.20	0.0616	0.0029
Major	1.24e-05	8.20	1.91e-06	4.28e-10

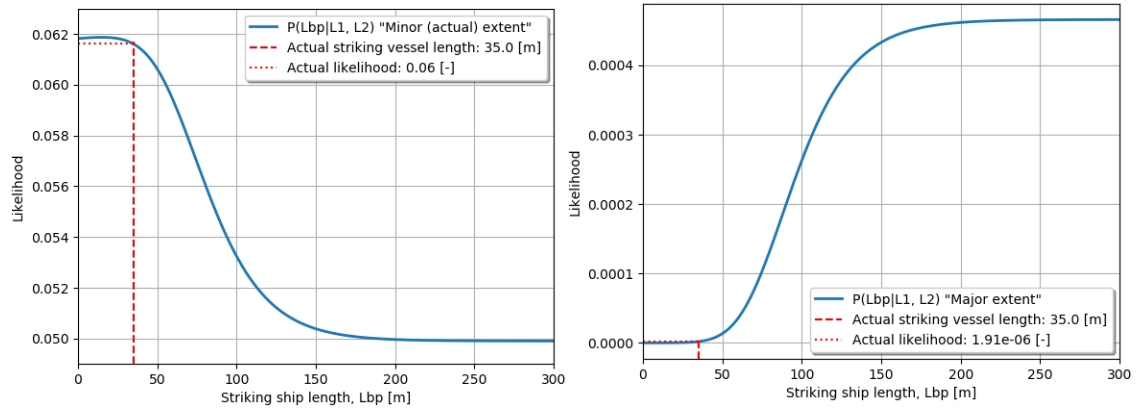


Figure 7-21: Likelihood functions, and corresponding likelihood for specific striking vessel length of 35.0 m (Minor damage extent: Left and Major damage extent: Right).

The posterior update has also a significant impact on uncertainty of prediction of the initial extent. Considering for example the 95% confidence interval (CI), the a priori list of damage extents consist of 3,024 cases out of the total 19,225 cases. Following the posterior update, the number of cases with 95% confidence reduces to just 1,323 cases, simply by shifting attention from the unlikely major extent cases the more likely minor extents in line with the available evidence. The above posterior update considers only the likelihood function representing the breach length. Considering the remaining likelihood functions in

the posterior update (simply the product of all likelihoods) the number of cases contributing to the 95% *CI* would be reduced to 311. The above examples show clearly that the posterior update with AIS data as evidence can provide a way to effectively prioritise cases based on the size of the striking ship. Notably, the same “boosting” effect may not be observed when the striking ship is large, i.e. large size of the striking ship does not necessarily imply large damage breach. This is because speed of the striking ship and heading are not explicitly accounted for by the likelihood functions (i.e. they are marginalised from the underlying probability distribution).

7.4 Closing remarks

In the above the vessel related variables has been reviewed, and appropriate a priori-, and likelihood distributions has been developed and presented. Due to lack of available data from the sample vessel, a priori probabilities for the openings have been assumed based on door category based on the data presented in the EMSA III project (Jasionowski et al., 2015). Hydrostatic pressure heads for door leakage and collapse have been based on recommendations of the *Floodstand* project (Ruponen & Routi, 2011). In addition, the relevant pressure heads were modelled as distributions around the Floodstand values to account for uncertainties. Loading condition specific variables has also been covered, such as draft T and KG . The draft a priori has been assumed using a discrete distribution adopted from the *eSAFE* project (Paterson & Atzampos, 2017), but scaled to our sample vessel, and fitted with an analytical distribution in the form of a *Beta* distribution. The KG a priori has been developed based on a range of standard loading conditions obtained from the vessel’s stability booklet, which have been assumed normally distributed around a function of the vessels drafts, accounting for the conditionality between the two variables.

Likelihood function developed for the door status sensor utilise a discrete version of Bayes formula and account for possible sensor accuracy in terms of sensor false negative and positive readings. Implementation of door status sensor has been illustrated by a simple example. We have further presented how the draft sensors are utilised to model the instantaneous waterplane and use it as a reference for internal openings and sensor locations. The likelihood function for updating the posterior probability for the initial damage extent based on actual operating draft has been developed and presented, including

a simple example illustrating an upper- and a lower single compartment initial damage extent. The examples indicate that the developed likelihood functions work well, and in line with our initial statements from Chapter 2. Finally, a likelihood function for accounting AIS data has been developed and presented. Due to insufficient number of sample points with defined speed and heading the model only considers size of the striking ship (represented solely by length), but from the example provided, seems to provide large reduction in uncertainty by updating the posterior belief based on actual knowledge on the size of the striking vessel, especially so for smaller vessel lengths. The update will be further supported by implementing information received from the flooding sensors as was discussed in section 6.3.3, providing a more targeted prediction as will be seen in Chapter 10.

7.5 References

International Maritime Organization (IMO), (2006), “*Reg. II-1/13 of SOLAS Consolidated Edition 2009*”, as adopted in IMO Res. MSC 216(82)).

Jasionowski, A., Luhman, H., Bertin, R., Routi, A-L., Cardinale, M., Harper, G., (2015), “*Evaluation of risk from watertight doors*”, report No. 2015-0167 Rev 7 from the EMSA III research project, funded by the European Maritime Safety Agency, EMSA/OP/10/2013.

International Maritime Organization (IMO), (2006), “*Reg. II-1/16.2 of SOLAS Consolidated Edition 2009*”, as adopted in IMO Res. MSC 216(82)).

Ruponen, P., Routi, A-L., (2011), “*Guidelines and criteria on leakage occurrence modelling*”, deliverable D2.2b from work package WP2, from the Integrated Flooding Control and Standard for Stability and Crises Management (Floodstand) research project, funded by the European commission, FP7-RTD- 218532.

Paterson, D., Atzamos, G., (2017), “*Analysis of onboard data with regards to probabilities of initial draughts*”, report No. eSAFE- D1.2.1, Rev. 5.0 of work package WP1, deliverable D1.2.1 from the Enhanced Stability after a flooding event (eSAFE) research project (Joint industry project on Damage Stability for cruise ships).

International Maritime Organization (IMO), (2006), “*Reg. II-1/5-1 of SOLAS Consolidated Edition 2009*”, as adopted in IMO Res. MSC 216(82)).

Chapter 8 - Risk-based positioning of Flooding Sensors⁵

8.1 Opening remarks

As already discussed in Chapter 3, recent research shows that predicting the evolution of the flooding process for progressive flooding scenarios, purely based on flooding sensors is possible, but is highly dependent on sensor type, position and density (Ruponen et al. 2010 & 2017). A high-density array of flooding sensors has proven to increase the accuracy of flooding assessment and compartment coverage, but such dense network of sensors may be impractical or even not feasible at all. On the other hand, the result of standard damage stability assessment demonstrates that only certain combinations of damaged compartments will result in critical high-risk cases leading to vessel loss. This knowledge may be utilised to identify locations for flooding sensors accounting for such high-risk cases, subsequently enabling optimal positioning of the sensors and facilitating rapid and accurate survivability assessment. It is the aim of this chapter to present the methodology for assessing the position of sensors by determining optimal locations based on the identification of critical damage cases and associated floodwater propagation paths. The evaluation is carried out in two steps. Firstly, the initial assessment is performed to identify critical damages by utilising (static) probabilistic damage stability calculations in accordance with SOLAS Reg. II-1/6 to 8 (IMO, 2009) and the well-known p- and s-factors. The assessment considers progressive flooding through openings, resulting in a stepped GZ curve, an approach more realistic than is currently mandated by the regulations. As a second assessment, the identified critical damage cases are investigated in time-domain simulations to assess the impact of dynamic factors, such as waves, on the flooding process and to identify a limit (threshold) for the onset of high-risk cases and floodwater propagation paths, which may be used for optimal risk-based positioning of sensors.

⁵ Main content of this chapter has been published in Karolius K. B., Cichowicz, J. and Vassalos, D., (2018) "*Risk-based positioning of Flooding Sensors to reduce Prediction Uncertainty of Damage Survivability*", 13th International Conference on the Stability of Ships and Ocean Vehicles, Japan, 16-21 Sept. 2018

8.2 Criticality assessment

8.2.1 Static assessment

Initially, a static assessment has been performed in the stability software NAPA using the probabilistic approach of SOLAS (2009) Reg. II-1/6 to 8. The SOLAS damages were generated up to 7-zones and, in order to produce detailed arrangement model, all internal openings have been represented as geometric objects rather than points. The latter enabled the use of WEPROGR2 (NAPA, 2018) calculation method for modelling of progressive flooding through the openings submerged in the final stage. In the method, each damage was represented with an initial stage, i.e. initial damage extent, and a progressive stage, involving compartments progressively flooded as a result of submerged openings. After reaching equilibrium at each stage, new openings are checked and additional rooms added to the progressive flooding sequence. The approach accounts for all types of doors and unprotected internal openings. As all non-watertight openings were considered as progressive flooding points with relevant connections, weathertight points were added to the lifeboat deck for assessment of the range criteria of the regulations. The model and internal openings have already been illustrated in Figure 1-4 in Chapter 1. Evacuation arrangements and control stations were excluded from the assessment. Following probabilistic damage assessment, the s-factor is used for grouping the damage cases into 3 categories as is illustrated in Figure 8-1.

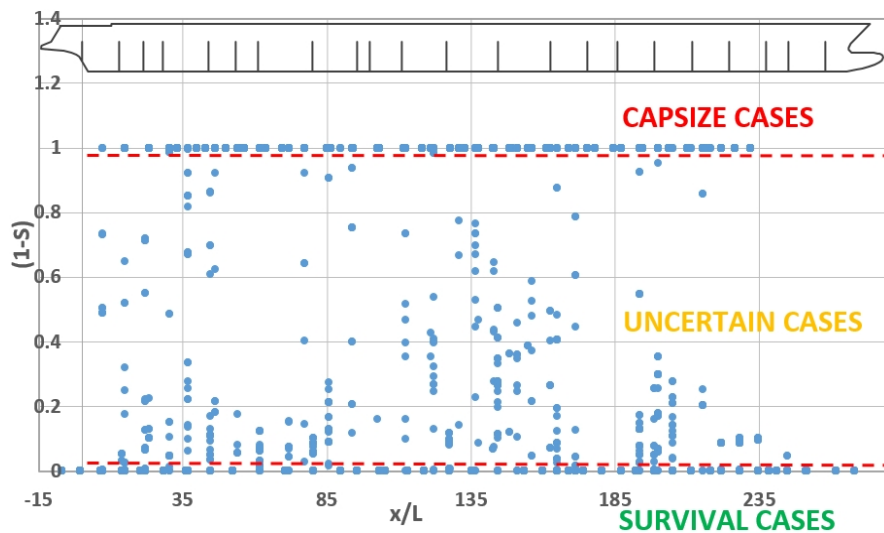


Figure 8-1: Initial categorisation of static damage cases, (1-s) diagram.

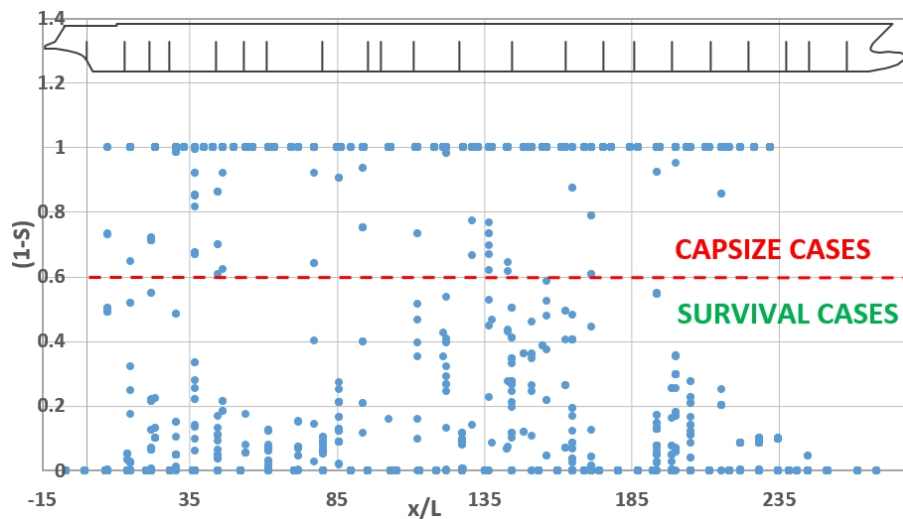


Figure 8-2: Illustration of limit between critical loss - and survival scenarios.

Cases with $s = 0$ were considered as capsize cases (irrespective of the actual mode of loss, e.g. floatability failure or insufficient residual stability margin for survival in waves). Cases with $s = 1$ were considered survival cases with sufficient residual stability margin for surviving in waves. The remaining cases with $0 < s < 1$, uncertain in terms of survival in waves, were all checked in the dynamic damage assessment to identify a limit for critical cases as is illustrated in Figure 8-2.

8.2.2 Dynamic assessment

As a vessel operates in a highly dynamic environment, this needs to be accounted for when assessing its survival resistance to flooding incidents. For the purpose of this study, all the time-domain simulations in waves were carried out with use of the time-domain simulation code PROTEUS3. The time-domain simulations were performed in a very conservative, dead-ship conditions with irregular beams seas of 7 metres H_s . All the internal openings were assigned relevant leakage and collapse pressure heads. The capsize criteria are based on the ITTC guidelines (ITTC, 2011) with a run resulting in capsize if instantaneous roll angle exceeds 30 degrees, or the 3-minute average heel exceeds 20 degrees. SOLAS damages in the stability software NAPA are generated using a zonal approach by applying a series of subdivision boundaries. Replication of the NAPA damages for the numerical simulations would involve generating large shell openings in the affected

area, leading to transient capsizing in many cases. To overcome this, and to dampen the transient effect, only one-third of the aft- and fore-most zones were included in the damage. The compartments missing out due to this reduction were added to the damage definition manually with the help of a compartment-connection table. An example of such approach is given in Figure 8-3 and Figure 8-4 for a 4-zone damage case.

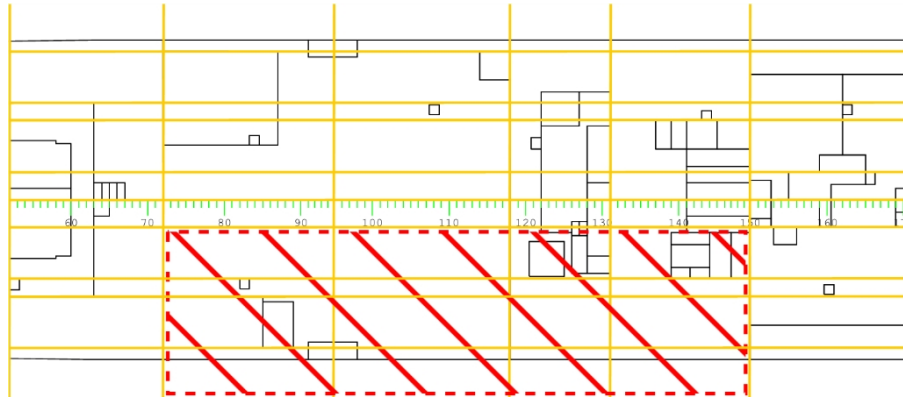


Figure 8-3: Actual damage length as a result of zonal representation.

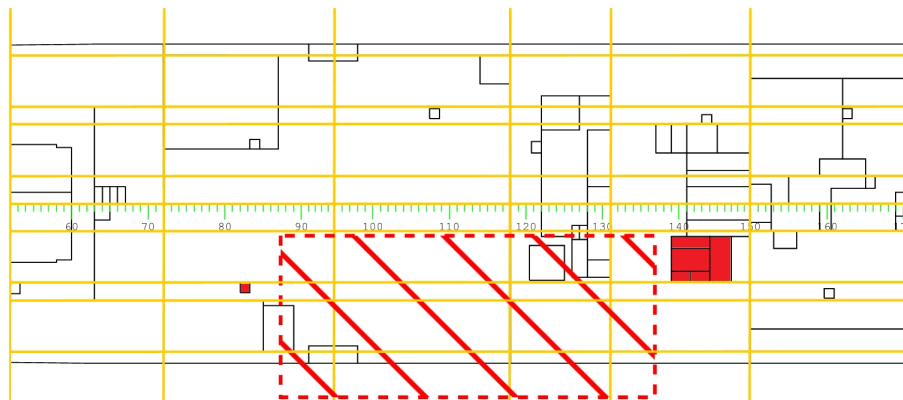


Figure 8-4: Reduction in damage length to damp the effects of transient flooding.

8.3 Compartment rating

An initial approach was to use the well-known $p(1 - s)$ diagram as seen in Figure 8-5 to identify critical cases and areas within the ship. This proved not to be detailed enough for the purpose of this study as the diagram may provide false criticality for certain cases comprising high number of zones. It is noteworthy that as each damage case is graphically represented using the mid position of the damage length, hence the marker position does

not necessarily match the location of the critical compartments. This can be illustrated with the help of a 4-zone damage centred at midship. This damage may be shown to be highly critical due to its inclusion of the engine room. The engine room, however, is located further aft than the x-coordinate from the $p(1-s)$ diagram, and as such, the criticality position is deceptively presented at midship, while in reality, the critical compartment (the engine room) lies further aft. For a more detailed representation of critical areas, each compartment has been assigned a criticality metric as described in the following. Firstly, it is recognised that all the capsized cases have a survival index $s = 0$. This enables representing the risk from flooding by the p-factor alone, as in Eq. 8-1.

$$Risk = p(1 - s) \rightarrow Risk = p \quad \text{Eq. 8-1}$$

Individual compartments can be given a risk rating based on all critical damage cases it is taking part in, by summing up relevant p-factors as in Eq. 8-2.

$$Risk_{Comp_k} = \sum_i^n p_{dam_i} \quad \text{Eq. 8-2}$$

Were, $n =$ number of i damage cases, resulting in flooding compartment k .

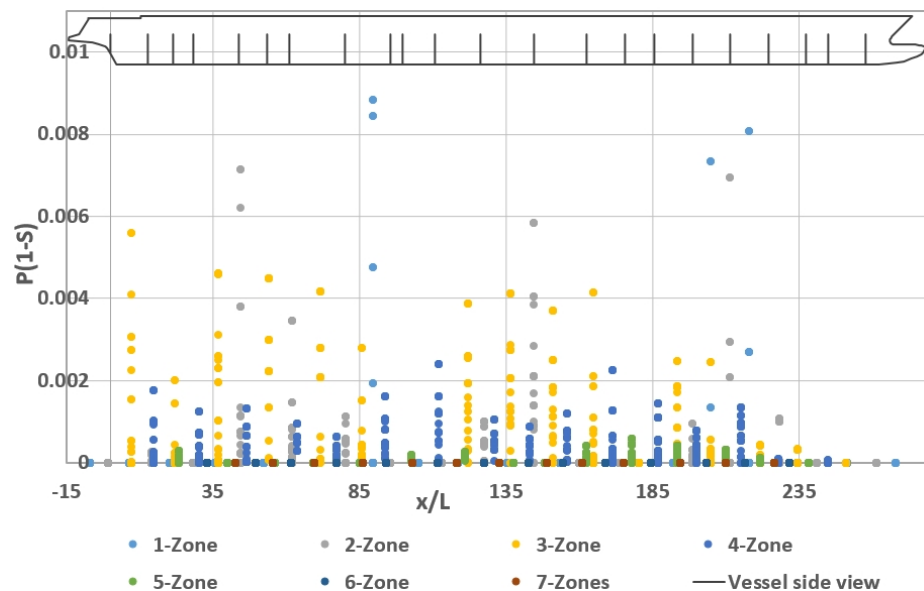


Figure 8-5: PIS diagram illustrating damage cases in terms of risk along ship length.

8.4 Methodology summary

The following summarises the methodology applied for identification of critical cases, and subsequent compartment rating.

- 1) Assessment of static cases from static stability software (NAPA or similar):
 - a) Remove all cases with $s = 1$ (these cases have sufficient residual stability margin to survive in waves).
 - b) Disregard all cases $s = 0$ (many of these cases capsize or sink in still water, and the remaining are assumed to capsize in waves due to insufficient residual stability margin).
- 2) For all cases with $0 < s < 1$, use time-domain simulations (PROTEUS3 or similar) to assess survivability in waves. This will identify a limit for critical dynamic capsize cases.
- 3) Compartment criticality rating:
 - a) Calculate the criticality rating for individual rooms (by summing p-factors of the relevant damage cases) and rank the rooms accordingly.
 - b) Screen all capsize cases and identify critical flood pathways. Identify common or partly-common flood pathways.
 - c) Recommend sensor positioning.

8.5 Results

8.5.1 Identification of critical capsize cases

The static calculations up to 7-zone damages resulted in a total of 5,564 different damage cases. The assessment was carried out at a single loading condition (the summer load-line, d_s). This loading condition is recognised as the worst damage stability loading condition of SOLAS. It is also shown that passenger ships normally operate around this condition most of the time (Paterson & Atzamos, 2017). Of all the damage cases, a total of 1,568 cases resulted in $s = 1$, indicating survival, and 3,450 cases resulted in $s = 0$, indicating capsize. This left 546 cases with marginal survival factor, i.e. $0 < s < 1$. (Figure 8-1). The simulations in

waves showed that there is no clear limit as presented in Figure 8-2. Instead, there is a transition area within which neither capsizes nor survival is definitive. This transition area as shown in Figure 8-6, may be due to the stochastic nature of the flooding process in waves.

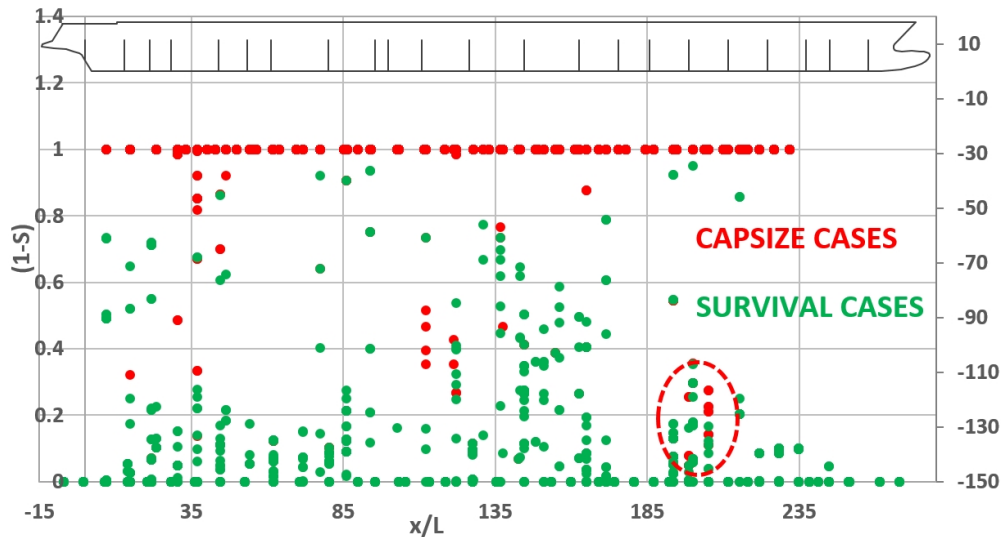


Figure 8-6: Identified capsizes cases in the uncertain region of the $(1-P)$ diagram.





In particular, it can relate to the so-called capsizes band (Vassalos et al. 1998), where the same flooding case may result in either capsizes or survival depending on particular wave realisation during the time-domain simulations. Furthermore, several of the capsizes cases, marked in red in the lower right corner of Figure 8-6, are attributed to transient capsizes in response to sudden ingress of floodwater. In total, following the dynamic assessment 108 of the 546 cases with $0 < s < 1$, 108 have been identified as capsizes. In total, there were 3,558 capsizes cases which can be used in the compartment risk rating (including the initial $s = 0$ cases). It is noteworthy that the large number of capsizes cases is mainly due to the excessive damage extents considered in the calculations (up to 7-zones). Of the total amount of capsizes cases, 1,690 are located on port side, while 1,868 are located on starboard side, due to asymmetries in the vessel internal subdivision and openings arrangement.

8.5.2 Compartment rating

Rating of the compartments (by means of Eq. 8-2) is presented in the bar chart in Figure 8-7 (due to the high number of compartments, the compartment names are not presented in the figures). The rating can be separated between initial and progressive stages as shown

in Figure 8-8 and Figure 8-9, respectively. The compartments have been represented graphically with colour coding corresponding to criticality (Table 8-1). Figure 8-10 and Figure 8-11 show the results for initial and progressive flooding stages plotted on the deck layout. The figures show a clear distinction between compartment criticality in the two flooding stages. In the initial stage, many of the critical compartments lie in the mid region of the vessel around the waterline. They also tend to be larger compartments in line with the IMO guidelines for sensor positioning. In case of progressive stages of flooding (Figure 8-11), there are several smaller compartments (specifically stairwells, elevator shafts, and vertical escape shafts) that are given the highest risk rating. Interestingly, the large, upper, compartments are shown to be of secondary criticality despite being a direct cause (due to their size) of capsizing when flooded. This is because the larger compartment in the upper decks are flooded in the progressive stages through the smaller compartments, acting as flood-water pathways. The smaller compartments are therefore involved in a higher number of critical cases.

Table 8-1: Colour coding for compartment criticality (Risk is normalised according to maximum risk considering all compartments).

Risk/Criticality	Range	Colour	
Very high	75% < Risk < 100%	Red	
High	50% < Risk < 75%	Orange	
Low	25% < Risk < 50%	Yellow	
Very low	0% < Risk < 25%	Green	

8.5.3 Risk-optimised flooding sensor position

The results of compartment rating show clearly that the criticality information can be utilised in risk-optimised positioning of the flooding sensors. In the case of compartments for which IMO requires installation of sensors, their number and location can be analysed in detail in order to increase accuracy of flooding detection. Furthermore, additional sensors could be installed inside the compartments not covered by the requirements but scoring high in the criticality rating. This should enable controlling of critical spaces and flooding pathways not only for flooding detection but also for monitoring of the flooding progress during actual casualties. Finally, openings belonging to the critical flooding pathways should also be monitored in order to allow for better assessment of the extent of the progressive flooding.

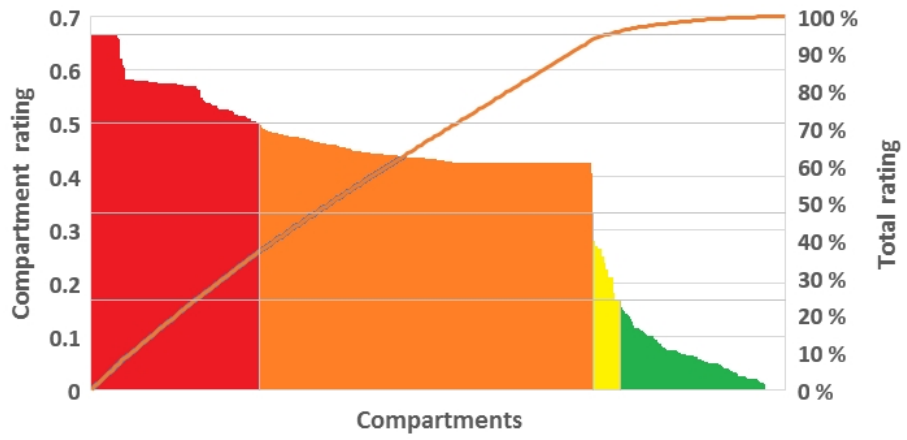


Figure 8-7: Compartment risk rating: All stages.

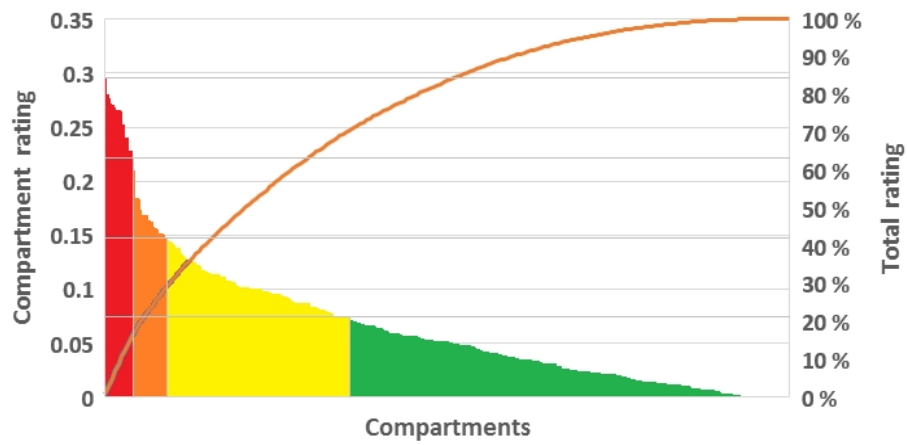


Figure 8-8: Compartment risk rating: Initial stages.

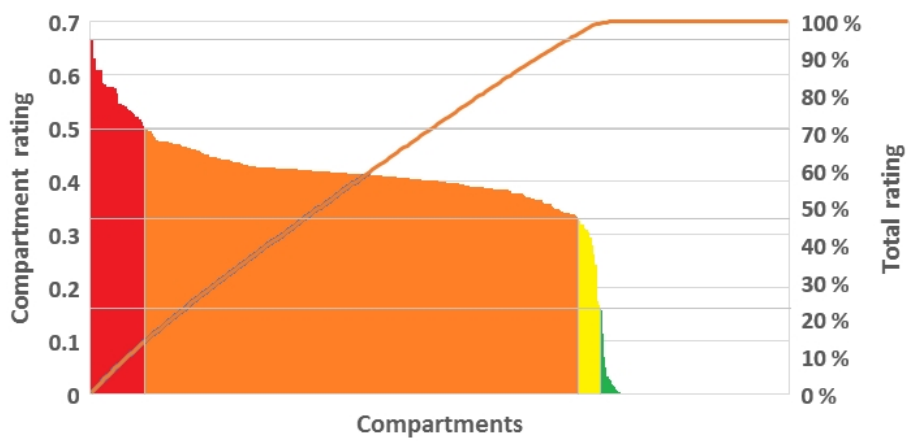


Figure 8-9: Compartment risk rating: Progressive stages.

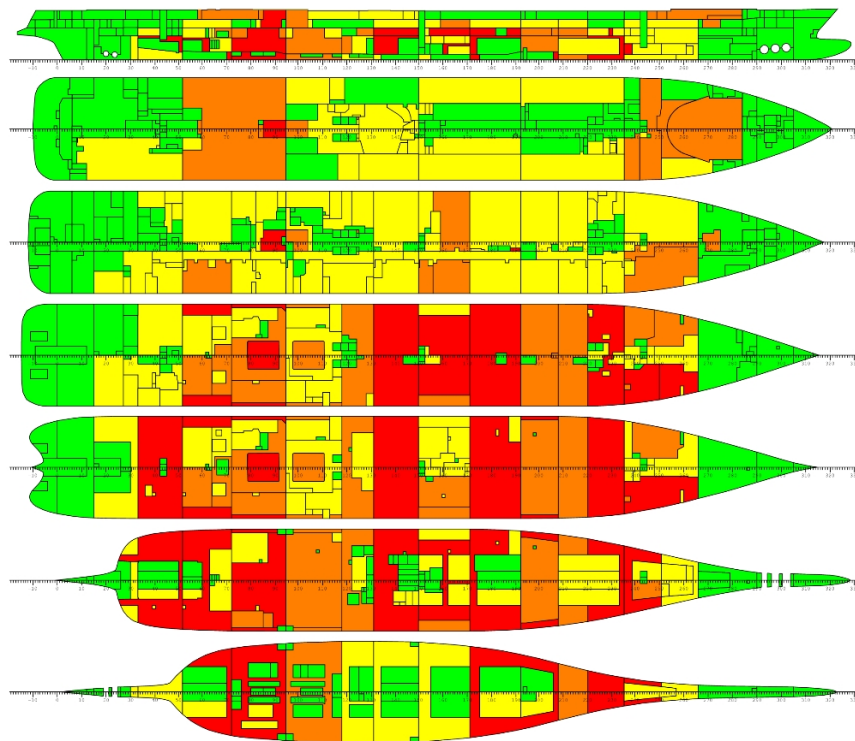


Figure 8-10: Graphical representation of the compartment risk rating: Initial stage.

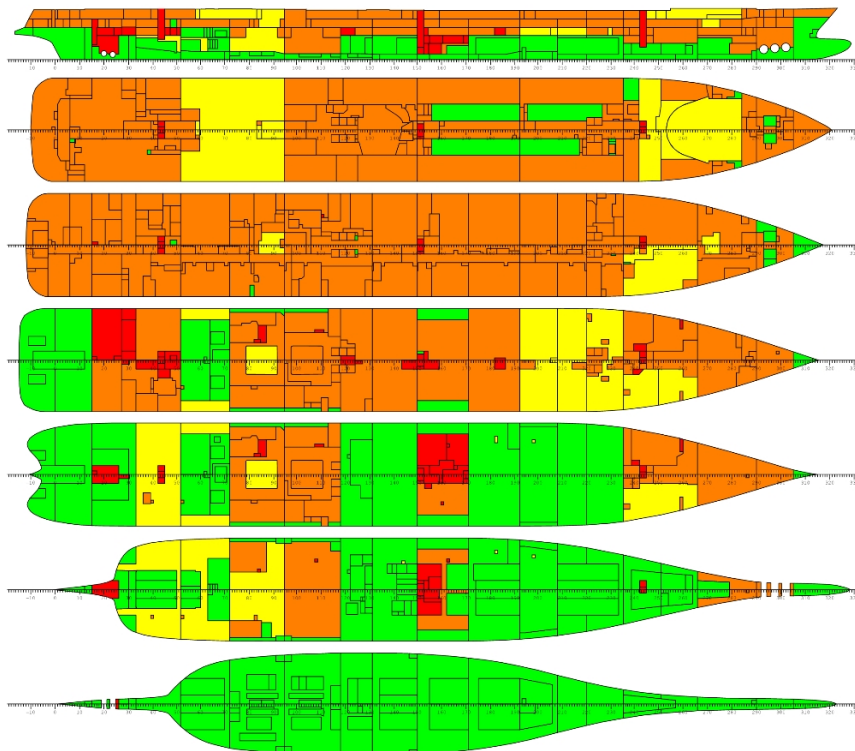


Figure 8-11: Graphical representation of the compartment risk rating: Progressive stage.

8.6 Closing remarks

This chapter outlines the methodology for risk-based positioning of flooding sensors aiming at reducing uncertainty in the assessment of survivability of damaged ships. The results confirm that the extent of a damage case or geometrical properties of the compartments alone are insufficient criteria for the positioning of the flooding sensors for the accurate estimate of survivability during flooding casualties. The regulatory requirements should be also complemented by the systematic, risk-based rating to determine critical spaces and flooding pathways. This should lead to targeted and efficient sensor positioning. The results also show that the same compartment may have different criticality rating in the initial and progressive stages of flooding. For this reason, these stages should be ranked separately. Smaller compartments may form critical flooding paths to larger rooms (through up- and cross-flooding) and should also be fitted with sensors for early warning of capsizing. Separating the initial and progressive stages may also help to identify the optimal sensor type and position. Specifically, the following can be taken into account:

- Initially damaged compartments below waterline: Flooding sensors for initial estimate of the damage extent, i.e. breach detection.
- Initially damaged compartments above waterline: Alternative sensor types for vertical breach detection (CCTV, Conductive wire loop on vessel skin, etc.).
- Progressively flooded compartments: Pathway monitoring for assessing survivability and watertight integrity.
- Openings: Status of the openings forming the critical flooding pathways should be closely monitored (e.g. open/close status, leaking, hydrostatic head build-up).

Finally, considering the presented methodology as part of a life-cycle framework, in addition to identify sensor locations, applying the method in the design stage would enable to assess and possibly reduce critical flooding paths, and to help decide on category (watertightness) of doors to install in the identified flooding pathways.

8.7 References

Penttilä P., Ruponen P., 2010, “*Use of Level Sensors in Breach Estimation for a Damaged Ship*”, 5th International Conference on Collision and Grounding of Ships, 2010, pp. 80-86.

Takkinen E., Ruponen P., Pennanen P., 2017, “*Required Flooding Sensor Arrangement for Reliable Automatic Damage Detection*”, Smart Ship Technology, 24-25 January 2017, London, UK.

Ruponen, P., Pulkkinen, A., and Laaksonen, J., 2017, “*A method for breach assessment onboard a damaged passenger ship*”, Applied Ocean Research 64 (2017), pp. 236-248.

International Maritime Organization (IMO), 2009, “*Safety of Life at Sea*” (SOLAS) Reg. II-1/6 to 8, explanatory notes in MSC.281(85).

NAPA Ltd., 2018 “*NAPA for Design Manuals*”.

The International Towing Tank Conference (ITTC), Recommended Procedures and Guidelines, 2011, “*Numerical Simulation of Capsize Behaviour of Damaged Ships in Irregular Beam Seas*”, Doc. No. 7.5-02 -07-04.4, Rev. 00.

Paterson, D., Atzampos, G., (2017), “*Analysis of onboard data with regards to probabilities of initial draughts*”, report No. eSAFE- D1.2.1, Rev. 5.0 of work package WP1, deliverable D1.2.1 from the Enhanced Stability after a flooding event (eSAFE) research project (Joint industry project on Damage Stability for cruise ships).

Vassalos, D., Jasionowski, A., Dodworth, K., Allan, T, Matthewson, B and Paloyannidis, P, (1998), “*Time-based Survival Criteria for Ro-Ro Vessels*”, RINA Spring Meeting.

Chapter 9 - Complete multi-sensor fusion methodology

In the foregoing chapters, comprehensive probabilistic models have been developed for use within a multi-sensor fusion methodology. In the following, their combined implementation as a complete methodology or framework will briefly be discussed and reviewed. The review will be supported by the schematic layout of the methodology illustrated in Figure 9-1. The main variable of interest, X , is the damage extent and location. This is represented by a set of compartments within the damage breach (initial extent, i), which may be connected to additional compartments through the internal subdivision boundaries (progressive extent, j). The complete set of compartments therefore comprises two disjoint subsets, x_i, x_j , as represented by Eq. 9-1 to Eq. 9-3.

$$X(x_i, x_j) = [x_i, x_j] \quad \text{Eq. 9-1}$$

$$x_i = [comp_{i,1}, comp_{i,2}, \dots, comp_{i,N_i}] \quad \text{Eq. 9-2}$$

$$x_j = [comp_{j,1}, comp_{j,2}, \dots, comp_{j,N_j}] \quad \text{Eq. 9-3}$$

Initial screening by the fusion process is based on the evidence from draught sensors and AIS. This is done only once and at the time instant time t_0 immediately before the collision as is seen at the bottom of Figure 9-1. Since this initial update is non-recursive, Eq. 4-26 may be used directly, combining the a priori list of initial damage extents, as obtained in Section 6.2.3, (subset x_i) with the AIS likelihood functions; Eq. 7-22 to Eq. 7-25. The next fusion process is done recursively for each time, $t_k = t_{k-1} + \Delta t$, at fixed time-steps, Δt . Initially, the posterior update of the opening probabilities combines the a priori opening frequencies with the sensor readings for opening status using Eq. 7-6. This must be part of the recursive process, as doors may change status. The updated posterior opening probabilities are then merged with the a priori leak- and collapse model (from Section 7.2.1.2), and in combination with the currently observed wave height and floating position (from Section 7.2.2.1), it forms the progressive flooding probabilities for the respective openings, using Eq. 6-59.

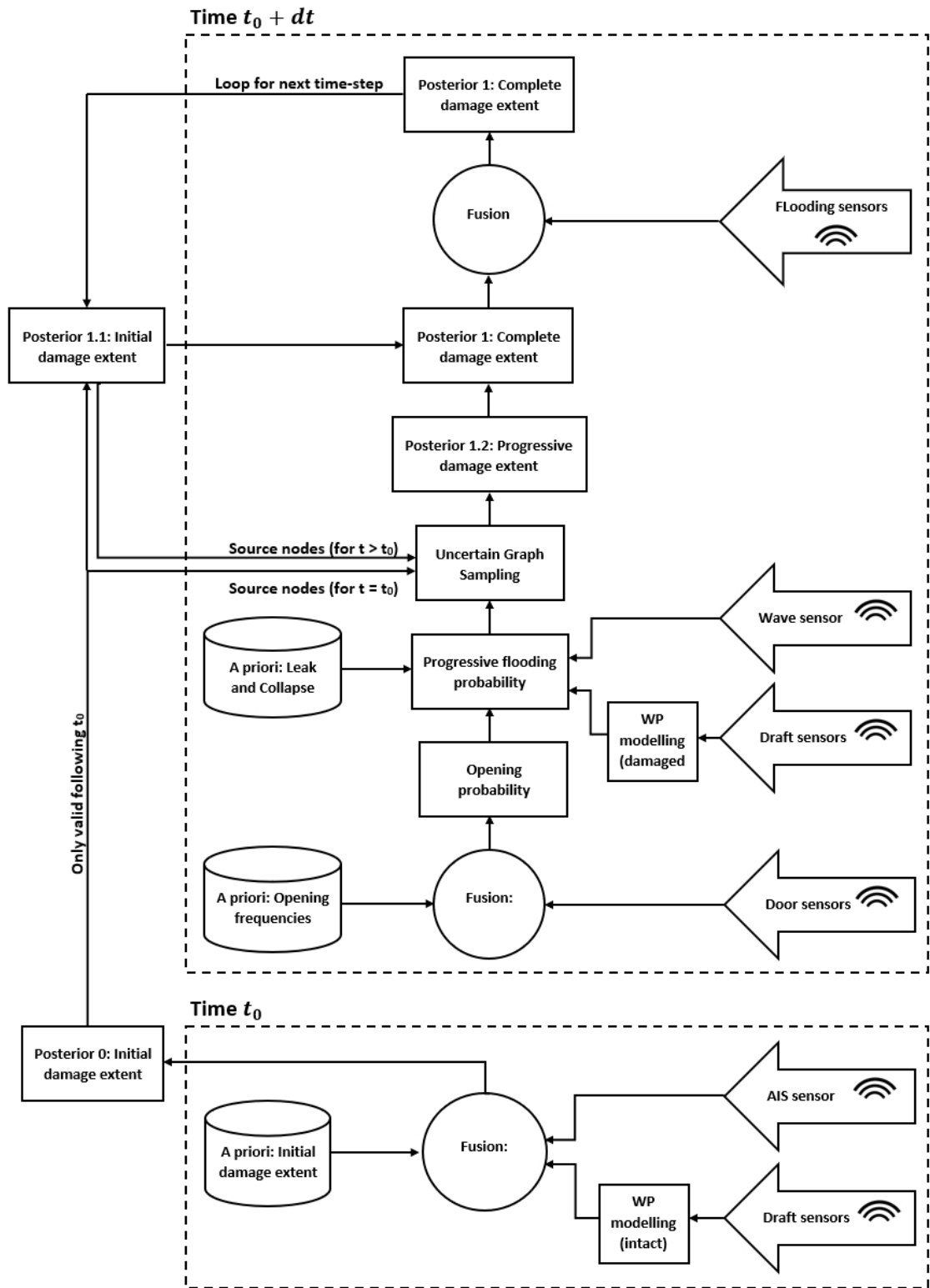


Figure 9-1: Schematic layout of the multi-sensor data fusion methodology.

Possible realisations of progressive extents (subset x_j), are sampled with the help of the Uncertain Graph Sampling (UGS) method (presented in Section 6.3.2), for each of the initial damage extents. The combined sets (i and j), represent the complete samples space of possible flooding realisations, $X(x_i, x_j)$, with each of the samples assigned a new posterior probability of occurrence. Once all the flooding realisations are established the flooding sensor readings can be utilised to provide the final update at this time-step. This is done using Eq. 4-40 in combination with the damage extent probabilities and Eq. 6-64. The final posterior probability acts as the a priori for the next time step. As the UGS method is applied for every time-step, the various sampled progressive extents may differ between the time-steps simply because new evidence might be made available (e.g. change in residual draft). The a priori for the next time-step should therefore be in the form of the initial extents alone (subset i). This is obtained from the summation of all the n progressive subsets j originating from i , represented by Eq. 9-4.

$$P_i = \sum_{j=1}^n p_j \tag{Eq. 9-4}$$

This posterior belief of the complete damage extent is looped back as source nodes for the UGS method, acting as a priori for the next time steps as is shown in the upper left corner of Figure 9-1.

Chapter 10 - Implementation & testing

10.1 Opening remarks

In the following chapter, all the probabilistic models developed above will be combined and implemented (coded) as a demonstration platform for application within flooding emergency scenarios. The platform will read emulated sensor data and provide sequential updates based on the methodology described in the previous chapters. Time series from PROTEUS3 have been interpreted as actual sensor readings. The test scenarios are presented in section 10.2 while section 10.3 discusses in detail how the result will be presented throughout this chapter. The main results are presented in section 10.4 where the as-built vessel and corresponding sensors layout is used as basis. The results follow the successive updates triggered by new sensor evidence to improve the accuracy of flooding prediction, and to highlight the ensuing reduction in uncertainty for each implemented update.

10.2 Test scenarios

Five striking vessels have been chosen with size represented by their length of 50, 100, 150, 200 and 250 meters, respectively. The damage breaches have been sampled from the distributions developed in section 7.3.3, conditioned on the striking vessel's length. The dependencies between the individual dimensions of the breach are given by the distributions developed in Chapter 6. The longitudinal position of damage, X , is unconditional on the striking vessel's length. Finally, three different significant wave heights have been chosen and applied to all test-cases: calm-water, medium wave height ($5.0 m H_s$), and extreme wave height ($10.0 m H_s$). For every test-case the stricken vessel loading condition, represented by the draft, T , and the vertical centre of gravity, KG , has been sampled from the distributions developed in section 7.2.2. All the loading conditions assume that the vessel operates at even keel $Tr = 0$. The vessel's heading has been sampled uniformly on the interval $[0, 360^\circ)$, and the openings' status, and leak- and collapse heads

have been sampled from the distributions developed in section 7.2.1.2. The sampled values for leak- and collapse heads, and statuses of internal openings are presented in Appendix IV. The test-scenarios and corresponding variables are summarised in Table 10-1. The results for individual breaches, in combination with the respective wave environments, will be presented in designated sub-sections within section 10.4.

Table 10-1: Summary of test-scenarios: Striking-vessel length (top two rows), stricken vessel loading condition, resulting breach and wave environment.

Striking vessel	V1	V2	V3	V4	V5
Length, L_{BP} [m]	50.00	100.00	150.00	200.00	250.00
Stricken vessel	L1	L2	L3	L4	L5
Draft, T [m]	7.89	7.72	7.93	8.21	8.13
Vertical centre of gravity, KG [m]	17.13	17.51	17.21	16.55	16.71
Trim, Tr [m]	0.00	0.00	0.00	0.00	0.00
Breach boundary	B1	B2	B3	B4	B5
Longitudinal pos., X [m]	165.7	103.1	239.6	257.6	145.3
Vertical pos., Z [m]	6.72	6.23	7.23	6.41	2.40
Length, L [m]	1.23	1.73	4.89	17.85	53.49
Height, H [m]	0.74	1.89	1.23	4.12	5.16
Penetration, Y [m]	0.21	0.64	1.54	1.84	1.20
Number of zones (initial)	1	1	1	2	4
Number of compartments (initial)	1	1	3	3	6
Wave environment	W1	W2	W3	W4	W5
Heading, H_g [°]	12.45	94.23	69.78	268.12	349.99
Wave height, H_s [m]	0, 5, 10	0, 5, 10	0, 5, 10	0, 5, 10	0, 5, 10

10.3 Presentation

The ten most likely initial damage extents based on no sensor evidence is presented in Table V-1 (section V.1 of Appendix V). From the table it is evident that the 100% CI corresponds to all the a priori cases as was identified in Chapter 6 following the Monte Carlo (MC) sampling. Furthermore, the distribution of damage cases is biased towards single compartment damages located in the fore region of the vessel in line with the distributions developed in Chapter 6. Due to large volume of data the posterior update from door status sensors are not discussed in detail within this chapter but the comprehensive summary is given in Appendix IV. The remaining updates, unique for each test-case, are summarised and discussed in the following sections. The sensor evidence from draft and AIS sensors for each test-case, accounted for by Eq. 4-26, is implemented only once. It is based on the last observable draft reading and AIS data received from the striking vessel just before the

collision incident. The posterior updates from the flooding sensors (Eq. 4-40) are executed every 5 minutes. Given the 30 minutes duration of the PROTEUS3 simulations, this entails six successive updates at 5, 10, 15, 20, 25 and 30 minutes. For presenting the results, tables representing posterior updates for each time-step will be included for each test-case comprising the ten-most likely damage cases (to limit the amount of data). Due to the large number of tables, the detailed result tables are found in Appendix V, while the main findings are summarised and discussed in the following. In the figures illustrating the actual damage extent, the dark blue colour represents the initial extent, while the successive progressive extents are shown in a lighter shade of blue. The locations of flooding sensors relevant to the test-cases are shown as green markers.

10.4 Implementation and testing results

10.4.1 As built sensor array

The sample vessel as-built sensor array was illustrated in the introduction (Figure 1-3) and comprises a total of 52 pneumatic and 94 level sensors fitted in dry spaces and tanks, respectively. The sensor arrangement is in agreement with the IMO regulations as set out in guidance note MSC.1/Circ.1291 (IMO, 2008), which focuses on compartments above a certain size limit (i.e. those that either have a volume in cubic metres larger than the vessel moulded displacement per centimetre immersion at deepest subdivision draught or have a volume in excess of 30 cubic metres). The vessel has in addition four draft sensors fitted, one fore, one aft, and two at midship, located at either side. Door status sensors are fitted on all doors classified as watertight (power operated-, semi-, and light-watertight doors).

10.4.2 Test-case 1

Test-case 1, executed in calm water ($H_s = 0.0\text{ m}$), is presented in Figure 10-1. It comprises a single initially breached compartment (R100009) and no progressively flooded compartments. The case remains a single-compartment flooding case throughout the duration of the simulations as there are no openings located within the compartment boundary enabling progressive flooding. The breach is caused by a collision with the smallest striking vessel (50 meters length). Detailed results for the test-case are presented in section V.2 of Appendix V.

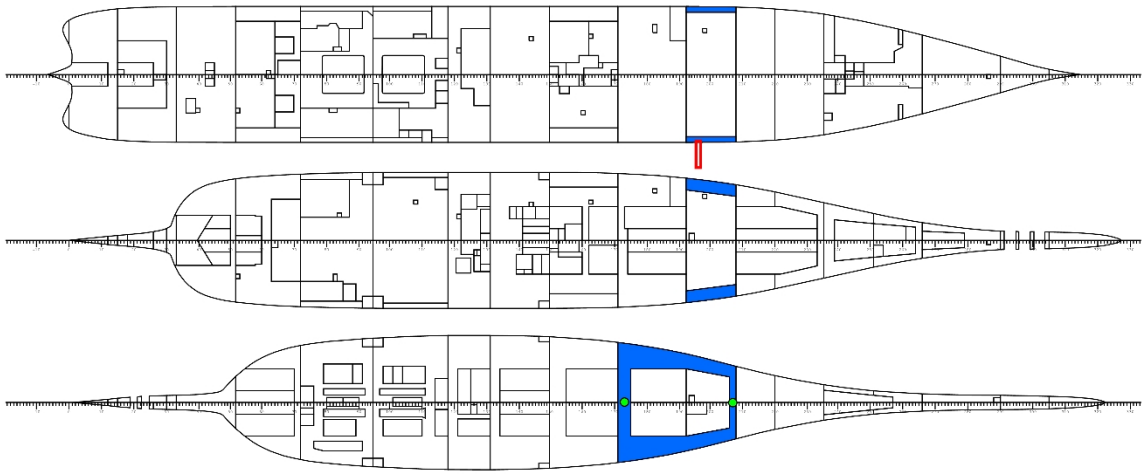


Figure 10-1: Test-case 1, Striking vessel length: 50.0 m, $H_s = 0.0$ m (Breach shown as red square, Initial flooding shown in dark blue (no progressive flooding) and flooding sensors shown in green).

The initial update incorporating sensor evidence from draft and AIS sensors are shown in section V.2.1, Table V-2. This specific case benefits from the combined effect of the a priori statistics biased towards single-compartment damages and initial posterior update shifting the focus from larger damages to the smaller extent due to the available evidence of small size of the striking ship. The initial posterior update reduces the number of possible initial extents contributing to 99% CI from 10,915 to 1,106 cases (nearly a tenfold reduction). Detailed results incorporated with evidence from flooding sensors are shown in Table V-3 to Table V-8 in section V.2.2 for the calm water case. Table V-3 shows the update at time step $t = 5.0$ min, indicating that the prediction is increasingly closing in towards the actual damaged region. There are two flooding sensors showing positive reading, both located in the actually damaged compartment (R100009) and the ten most likely cases are some combination involving the actually flooded compartment. Following the initial time-step update the actual case (DAM16 with no progressive extent) is ranked on a third place, with probability of 0.14. Two higher ranked cases are both progressive extent realisations of the case DAM199 with probabilities of 0.15 and 0.20, respectively. With the exception of R110203 the additional compartments included within these two progressive variants of DAM199 are not fitted with flooding sensors. The flooding sensor in R110203, however, would not indicate flooding even if DAM199 was the actual case as it is not yet submerged (still located 0.1 m above the external waterplane). In combination with the calm water condition, the case is still highly ranked by the likelihood function.

The first time-step update reduces the number of cases contributing to 99% CI from the previous 1,106 cases (draft and AIS update) to only 23 cases. At the next time step, $t = 10.0 \text{ min}$ shown in Table V-4, the sensor in compartment R110203 is located slightly below the calm-waterplane. This in turn results in the likelihood function to assign a reduced probability for DAM199, because if this was the actual case, it is more likely that the sensor indicates flooding than not. Some probability is, however, still assigned to DAM199 as the methodology accounts for slow ingress/leakage (internal waterplane not yet equilibrated with the external waterplane). The results in Table V-4 show the actual case (DAM16) ranked first with a probability of 0.32 whereas the two realisations of DAM199 are ranked second and third on the list with probabilities 0.17 and 0.14, respectively. The number of cases representing the 99% CI is reduced to 19 cases from the previous 23. The same trend is maintained in the following time steps seen in Table V-5 to Table V-8. We may also note the increased number of cases corresponding to the 100% CI in comparison to Table V-2 considering initial extents alone. This is due to the sampled progressive extent realisations from the Uncertain *Graph Sampling* (UGS) approach as was presented in section 6.3.2. The 100% CI is now representing all possible unique combinations of initial- and progressive extents represented by the last row of the event tree shown in figure 6.34.

At the final time-step, $t = 30.0 \text{ min}$ seen in Table V-8, the actual case has probability of 0.97 and the 99% CI is represented by six cases. In contrast, the two realisations of DAM199 are still ranked second and third but have reduced probabilities of 0.008 and 0.006, respectively. Results with a significant wave height of $H_s = 5.0 \text{ m}$ are shown in Table V-9 to Table V-14 in section V.2.3. There are no openings connected to the actual initial extent, hence the case is a single compartment flooding throughout irrespective of an increase in wave height. Reference is again made to Figure 10-1. Nonetheless, increase in wave height has an impact on the accuracy of the prediction. At the first time-step, $t = 5 \text{ min}$ (Table V-9) it is clear that the actual case is ranked first with a probability of 0.41, which indicates that the increase in wave height provides additional evidence enabling the prediction to converge towards the actual case faster than in the calm-water cases. It is also seen at the remaining time-steps that the case is gaining probability at a higher rate in comparison to the calm-water case above, e.g. the actual case is the sole contributor to the 99% CI at time-step, $t = 20 \text{ min}$ (Table V-12) whereas the calm-water case involves 14 cases to represent the same CI for the respective time-step.

The same trend is also seen in extreme wave case ($H_s = 10.0\text{ m}$) presented in Table V-15 to Table V-20 in section V.2.4, where the actual case is assigned a probability of 0.91 already at the first time-step, $t = 5\text{ min}$. The 99% CI is represented by 24 cases and it becomes the sole case contributing to the 99% CI at $t = 10\text{ minutes}$ (Table V-16). The main reason for the increase in confidence when implementing the evidence on increased wave height is the nature of the likelihood function. The likelihood function assigns probability to the respective damage cases (combined extents) by asking: “*what is the probability of a distinct sensor to indicate a particular status, given that the damage extent under consideration is the actual one?*”. Large wave heights increase the probability of a sensor to indicate flooding (even with higher vertical position) if it is located in the actual damage case. Thus, when no indication is given by sensors in a specific damage extent, the probability of that extent being the actual case is subsequently reduced.

10.4.3 Test-case 2

Test-case 2, involving striking ship of 100 m length, is illustrated in Figure 10-2, showing one initially breached compartment (R070101) and three progressively flooded compartments (R070201, EX070101, R070102). Similarly to Test-case 1 there are no additional openings within the damage extent which could enable further escalation of flooding.

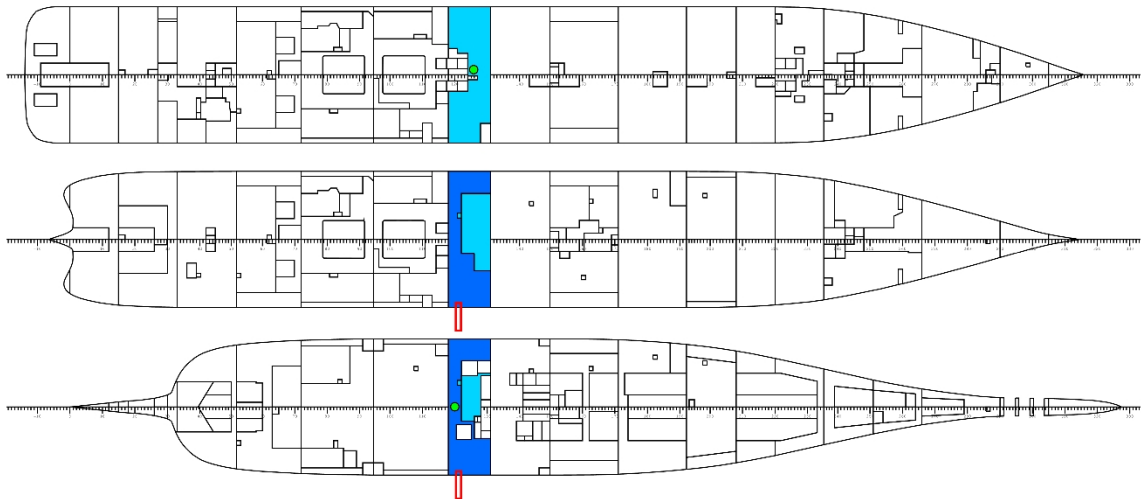


Figure 10-2: Test-case 2, Striking vessel length: 100.0 m, $H_s = 0.0\text{ m}$ (Breach shown as red square, Initial flooding shown in dark blue, progressive flooding shown in light blue and flooding sensors shown in green).

Detailed result for the second test case is presented in section V.3 of Appendix V. The posterior update from AIS and draft sensors presented in Table V-21, show the actual case DAM421 ranked 8th. The update sees a reduction in number of cases representing 99% CI from 10,915 cases to 3,062 cases. The smaller reduction than seen for Test-case 1 is primarily due to the larger size of the striking vessel (i.e. damages of larger extents are included in the 99% CI). Detailed calm-water results are shown in Table V-22 to Table V-27 in section V.3.2. The initial Table V-22 shows the update for initial time step $t = 5.0 \text{ min}$, indicating that various progressive extent realisations of the actual damage DAM421 are dominating the ten most likely cases with the actual case ranked fourth on the list with a probability of 0.05. Top-ranked (with probability 0.4) is a realisation of the actual case but without compartment R070201 included in the progressive extent. Compartment R070201 has a flooding sensor fitted but it does not indicate flooding because flooding to compartment R070201 is slow, due to leakage through an escape hatch, thus the floodwater level has not reached the sensor. In fact it will not reach the sensor in any time-steps because the internal floodwater will not reach the level of waterplane within the 30-minute simulation time. As a result, the likelihood function assigns lower probability to the actual case than to the realisations without R070201.

At the last time step, $t = 30 \text{ min}$ (Table V-27) the actual case has a probability of 0.07 and ranks 4th while the top-ranked case (without R070201) has a probability of 0.56. The 99% CI comprises 19 cases, down from 81 cases at the initial time-step. Results in waves are shown in Table V-28 to Table V-33 for 5 meters H_s and Table V-34 to Table V-39 for 10 meters H_s . Like the calm-water case, the sensor in R070201 is not indicating flooding but now only in the first two time-steps. As the wave-induced motions enhance the leakage through the opening, the internal waterplane exceeds the sensor height resulting in flooding indication at an earlier stage in the flooding evolution. This is shown in Table V-29 for $H_s = 5.0 \text{ m}$ and Table V-36 for $H_s = 10.0 \text{ m}$, where it is also evident that this has resulted in a boost in confidence for the actual case, now having a probability of 0.07 and 0.13 for the respective wave cases and time-steps. In the successive time-steps for the wave case, $H_s = 5.0 \text{ m}$, the actual case is top-ranked with a final probability of 0.17 at the last time step (Table V-33). The wave case, $H_s = 10.0 \text{ m}$, also show the same boost for the actual case just following the flooding indication in R070201 but in the last few time steps there are

progressive extent realisations with even more compartments that are assigned a larger proportion of the probability. In both the wave cases there are additional, compared to the calm-water case. The additional spaces, small A-class compartments: R070205, R070203 and R070202, are located around midship within the same watertight zone as the initial flooding as shown in Figure 10-3 at the final time-step.



Figure 10-3: Additional progressive flooding extent for Test-case 2, Striking vessel length: 100 m, $H_s = 5.0$ m and $H_s = 10.0$ (Breach shown as red square, Initial flooding shown in dark blue, initial progressive flooding shown in light blue, additional progressive flooding shown in lighter blue and flooding sensors shown in green).

10.4.4 Test-case 3

Test-case 3 in calm-water is illustrated in Figure 10-4, showing three initially breached compartments (R160111, R160201, R160204) and five progressively flooded compartments (R160202, R160205, EX160101, R160103, R160206). Similar to the previous cases there are no internal openings enabling further progressive flooding. Detailed result for this test-case are presented in section V.4 of Appendix V. The posterior update from AIS and draft sensors have been presented in Table V-40, where we again see that the 99% CI is represented by 3,416 compared with the 10,915 a priori. The result with evidence from flooding sensors are for the calm-water case shown in Table V-41 to Table V-46 for the respective time-steps. The initial time-step update at, $t = 5.0$ min, presented in Table V-41 show that the actual case DAM49 is not included within the ten most likely cases in spite of the positive readings from two flooding sensors located within the flooding boundary.

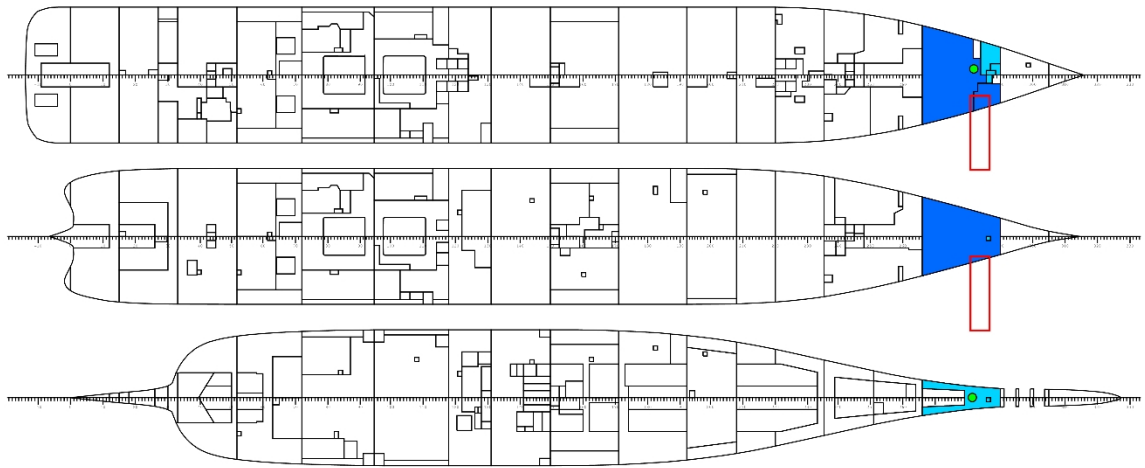


Figure 10-4: Test-case 3, Striking vessel length: 150.0 m, $H_s = 0.0$ m (Breach shown as red square, Initial flooding shown in blue, progressive flooding shown in light-blue and flooding sensors shown in green).

The actual case ranks 46 following the initial flooding sensor update. The cases representing the ten most likely cases are all some combination of the compartments showing positive flooding readings with a range of compartments not fitted with flooding sensors. This indicates that the prediction is in fact targeting the actual damaged region, just not the actual case (unique combination of initial and progressive extent). This is illustrated in Figure 10-5, where all compartments contributing to the 99% CI for time step, $t = 5.0$ min are marked red. It is noteworthy that there are only 38 compartments within the 99% CI although corresponds to 2,741 possible flooding cases (combinations of the 38 compartments). The progressive flooding realisation of DAM359, ranked second on the list, is in fact identical to the actual case (with the difference stemming from the distinct initial extents). Since only two out of the 38 compartments representing the 99% CI, have flooding sensors, it is impossible to distinguish between the cases resulting in many possible flooding combinations. The first posterior update offering only a minor reduction is also highlighted by the 99% CI, reduced to 2,741 from the previous 3,416. For the successive time-steps, the same trend is maintained, where various progressive realisations of DAM359, DAM120, DAM18, DAM1992 and DAM134 are representing the ten most likely cases. The two realisations of DAM359, including the one identical to the actual case, are ranked first and second. The actual case rank is varying around 46-138 for the successive time-steps. Results with wave heights of $H_s = 5.0$ m and $H_s = 10.0$ m are shown in Table V-47 to Table V-52 and Table V-53 to Table V-58 respectively.

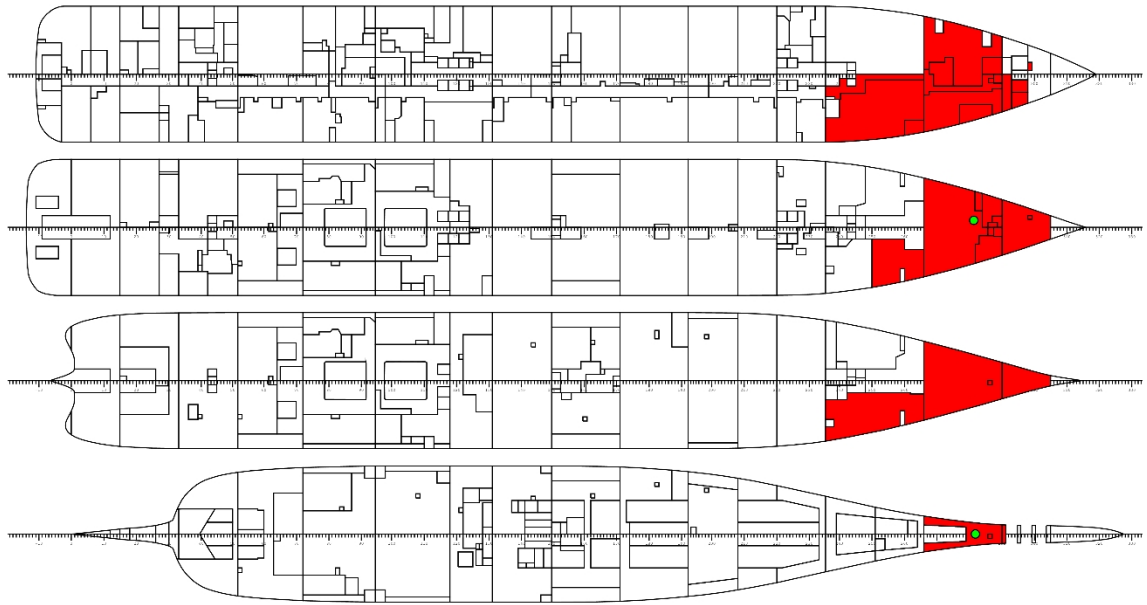


Figure 10-5: Compartments part of the 99% CI for the calm-water case, time step $t = 5.0$ min (Compartments are shown in red and available (two) sensors is shown in green).

There are no openings connected to the actual initial extent preventing escalation of flooding and making Figure 10-4 still valid. The results still follow the same trend as was seen above, with the same cases representing various combinations of the compartments with positive sensor reading and surrounding compartments without flooding sensors. It is also seen that the progressive stages are increasing in number of realised compartments similar to what was observed in the former test-cases above. The demonstration platform has been implemented to maintain the differentiation between initial and progressive extent. It provides an additional information to the vessel operators but at the same time it makes the accurate predictions more difficult than looking at the flooding extent alone. In fact, many combinations of the compromised rooms in the top-ranking scenarios are identical to the actual case. It would therefore be beneficial to unquify these combinations (sum their probabilities) rather than maintaining a reference to the actual damage names and separated initial- and progressive flooding extents. Applying this approach to test-case 3 for the calm-water case, the actual damage case would be ranked second on the list with a probability around 0.08 for all time-steps, outranked only by an almost identical case with one additional compartment. This is a considerable increase in prediction performance compared with the alternative presentation method, observing an increase in rank from 138 to 2, and a reduction in the 99% CI from 1,510 to 785 cases.

Another way of presenting the results would be to provide flooding probability per compartment by adding contributions of probabilities from damage cases involving the compartment in question. This would enable presenting the most likely compartments being flooded independently and utilise colour coding, or heat maps similar to that in Chapter 8. Such approach has been implemented for test-case 3 for the calm-water case at time-step, $t = 5.0 \text{ min}$, and is presented in Figure 10-6. The colours are representing the probability, where red correspond to a probability of one, yellow to a probability of 0.01 and green to a probability of zero (the probability is linearly mapped to an RGB colour profile). Heat maps for all test-cases for the calm-water case and the extreme wave height of $H_s = 10.00 \text{ m}$, for all time-steps are in presented Appendix VI. The intermediate wave height has been disregarded to limit the number of figures. Nonetheless, the way the predictions are presented depended on the application, and in some cases, it may be beneficial to maintain a clear differentiation between initial and progressive extents, e.g. to predict breach size and subsequent time-to-capsize or to provide support in deciding on actions for flooding containment.

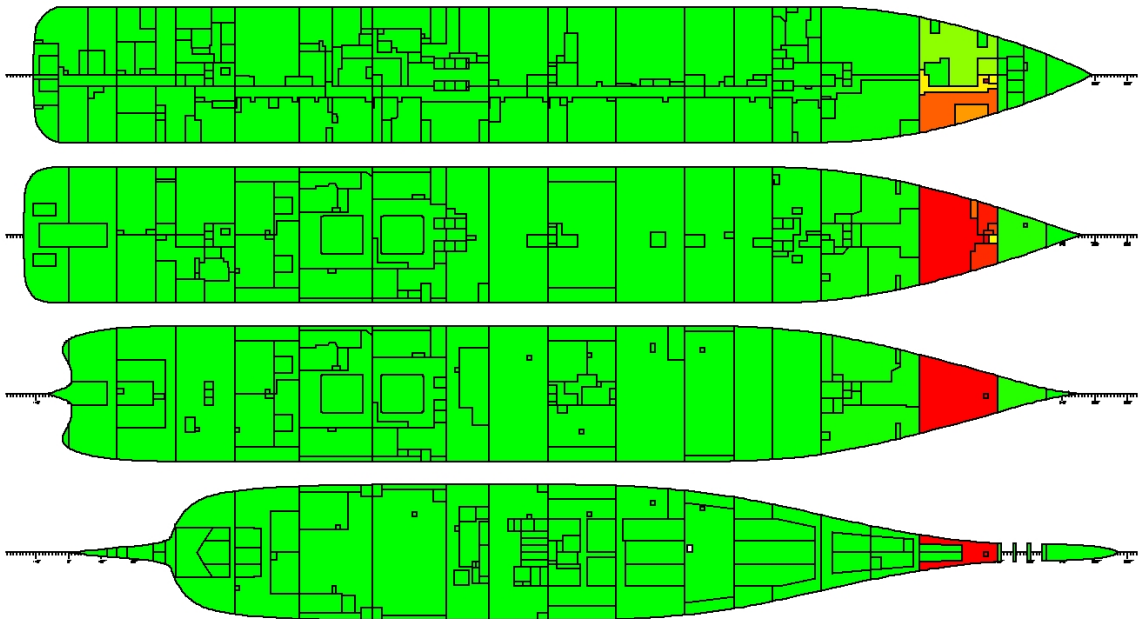


Figure 10-6: Heat map for calm-water case, time step $t=5.0 \text{ min}$ representing the probability that a compartment is flooded (Red represents a probability of 1.00, yellow a probability of 0.01 and green a probability of 0.00, governed by the mapping $(R, G, B) = P: (1, 0, 0) = 1, (1, 1, 0) = 0.01, (0, 1, 0) = 0$).

10.4.5 Test-case 4

Test-case 4 is illustrated in Figure 10-7, showing three initially breached compartments (R180001, R170101, R180002) and one progressively flooded compartment (EX170201). The case is again maintained as such throughout the whole flooding evolution as there is no progressive flooding. This also applies for the wave cases, and the figure is applicable to those as well. It is further seen in the figure that the sensor might be located within the breach. This is, however, not the case as the sensor is located below the breach extent. Cable routing have not been considered at this stage, and we cannot say for certain whether or not this is within the damage extent and compromised, but we assume that the sensor is fully functional. Detailed result is presented in section V.5 of Appendix V.

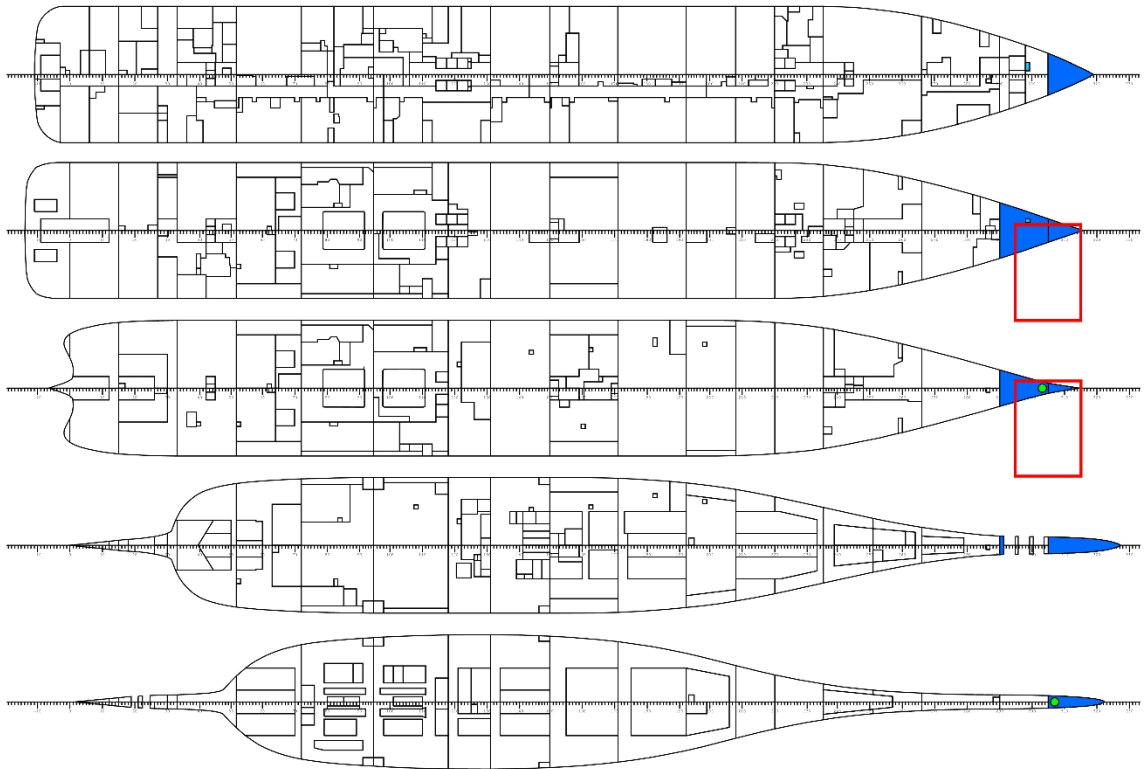


Figure 10-7: Test-case 4 (major), Striking vessel length: 200.0 m, $H_s = 0.0$ m (Breach shown as red square, Initial flooding shown in dark-blue, progressive flooding shown in light-blue and flooding sensors shown in green).

The initial update incorporating sensor evidence from draft and AIS sensors are shown in Table V-59 of section V.5.1, and further inclusion of cases to the 99% CI is seen due to the further increase in striking vessel length (200.0 m). The increase is however less than before, seen in rate of change per meter ship length, but is as expected seen in relation with the distributions developed in section 7.3.3 (reduced from 10,915 to 3,459 while we saw a reduction from 10,915 to 1,106 for ship length of 50.0 m). Detailed result incorporated with evidence from flooding sensors are shown in Table V-60 to Table V-65 in Section V.5.2 for the calm water case. The initial Table V-60 shows the update for initial time step $t = 5.0 \text{ min}$, showing the actual case DAM342 part of the ten most likely cases, at rank 8, with a probability of 0.02. The remaining cases are again seen to be various combinations of the compartments indicating flooding, combined with a range of other compartments without flooding sensors. The top ranked case is a progressive flooding realisation of DAM29 and almost identical to the actual case, except it is missing compartment R180002. From the previous posterior update from draft and AIS sensors, it is clear that this case was initially more likely, and therefore still ranked higher than the actual case simply because there is not enough evidence to distinguish them, resulting in the likelihood function to assign probability to both. Following normalisation, the actual case will still be ranked lower.

The uncertainty represented by the 99% CI has been reduced from the previous 3,459 cases to 120 cases. We may again utilise the heat-map approach as to illustrate how the actual damaged region is localised following the flooding sensor update for time-step, $t = 5.0 \text{ min}$. The heat map is shown in Figure 10-8, and it clearly showing the expected damage region. As time progresses, the actual case is de-ranked, and is seen on a rank 27 at time-step, $t = 30.0 \text{ min}$, while progressive flooding realisations of cases DAM29, DAM352 and DAM7528 are governing the top rows in the table, which indicates less accurate predictions if the prediction entails predicting the actual damage case maintaining a distinction between initial – and progressive extent. However, as we mentioned above, the prediction accuracy is depending on the application (what we want to predict), and if it is the most likely flooding extent for decision support, acting on DAM29 would not really be any different that acting on the actual case just because of a small difference represented by R180002 (miniscule compartment located within R180001).

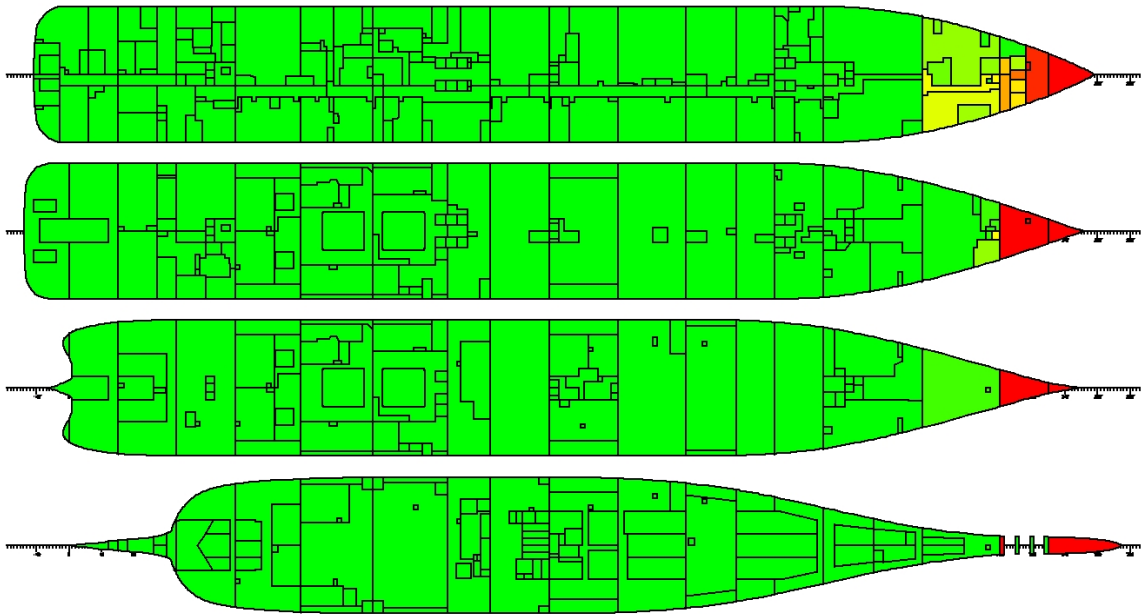


Figure 10-8: Heat map for calm-water case, time step $t = 5.0$ min representing the probability that a compartment is flooded (Red represents a probability of 1.00, yellow a probability of 0.01 and green a probability of 0.00, governed by the mapping $(R, G, B) = P: (1, 0, 0) = 1, (1, 1, 0) = 0.01, (0, 1, 0) = 0$).

The graphical representation would provide significant supportive information to the crew, regardless of the actual case not being ranked on top. It is also important to highlight that the actual case is still within the 99% CI. Results incorporated with more extreme significant wave heights of $H_s = 5.0$ m and $H_s = 10.0$ m are shown in Table V-66 to Table V-71 and Table V-72 to Table V-77 respectively. The same trend is seen as for the calm-water case, but due to waves, the prediction seems to be slightly improved (similar to what was seen for test-cases 1-2). The actual case is not ranked on top but is for the last time-step seen on a rank 10 with probability 0.024 for $H_s = 5.0$ m, and a rank 11 with probability of 0.015 for $H_s = 10.0$ m. DAM29 almost identical to the actual case, but excluding R180002, is ranked on top for all wave-cases and their respective time-steps. The uncertainty represented by the 99% CI has, however, grown for the wave cases compared with the calm-water cases due to the additional realisations of progressive flooding stages, and their inclusion in the 99% CI due to few sensors (similar to test-case 3). This being said, the graphical representation in the form of the heat map for wave case, $H_s = 10.0$ m, have for the last time-step been included in Figure 10-9 and is almost identical to that of the calm-water case.

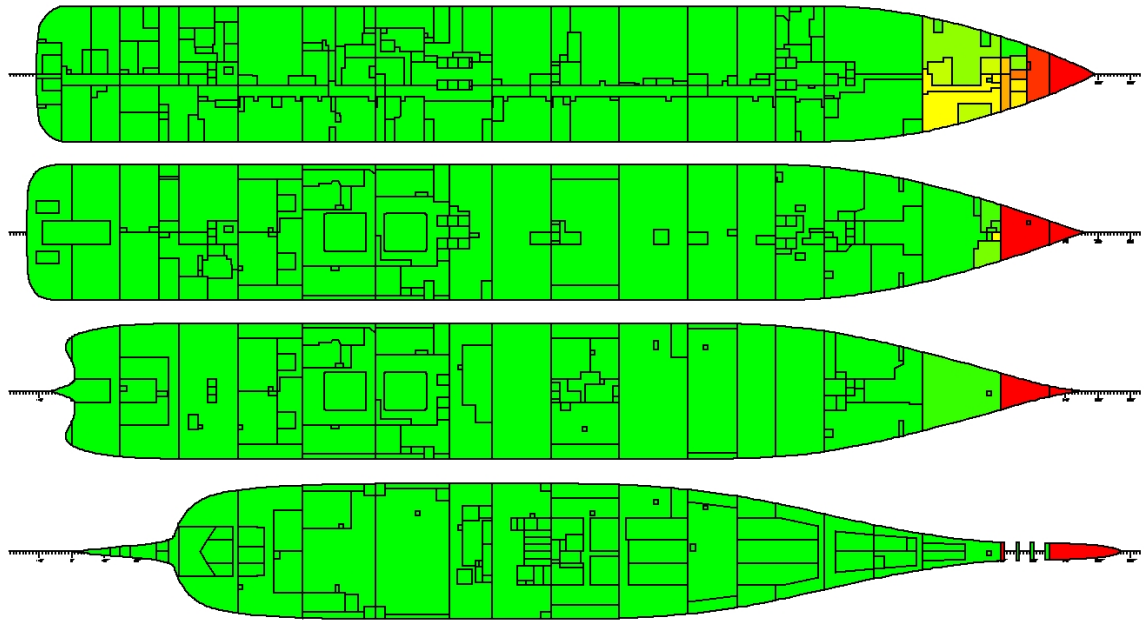


Figure 10-9: Heat map for wave-case, $H_s = 10.0$ m, time step $t = 30.0$ min representing the probability that a compartment is flooded (Red represents a probability of 1.00, yellow a probability of 0.01 and green a probability of 0.00, governed by the mapping $(R, G, B) = P: (1, 0, 0) = 1, (1, 1, 0) = 0.01, (0, 1, 0) = 0$).

This indicates that regardless of the increase in confidence intervals for the list of cases distinguishing between flooding stages, the independent compartment probability is essentially unchanged. Even when additional cases are assigned to the CI's, the additional cases are still some combination of the compartments within the expected damage region, and the independent compartment probabilities would therefore only see a minor adjustment.

10.4.6 Test-case 5

The final test-case 5 is illustrated in Figure 10-10, for a significant wave height $H_s = 0.0$ m. The case comprises five initially breached compartments (R100009, R090009, R080116, R100108, R090113) and four progressively flooded compartment (R080201, EX080101, EX100101, R100107). The same extent is maintained throughout the whole flooding evolution as there is no progressive flooding in any of the time-steps. Test-case 5 has the largest initial damage extent of all the cases, comprising 4 watertight zones as is seen in the figure. From the figure, it is also seen that three sensors are close to the breach boundary.

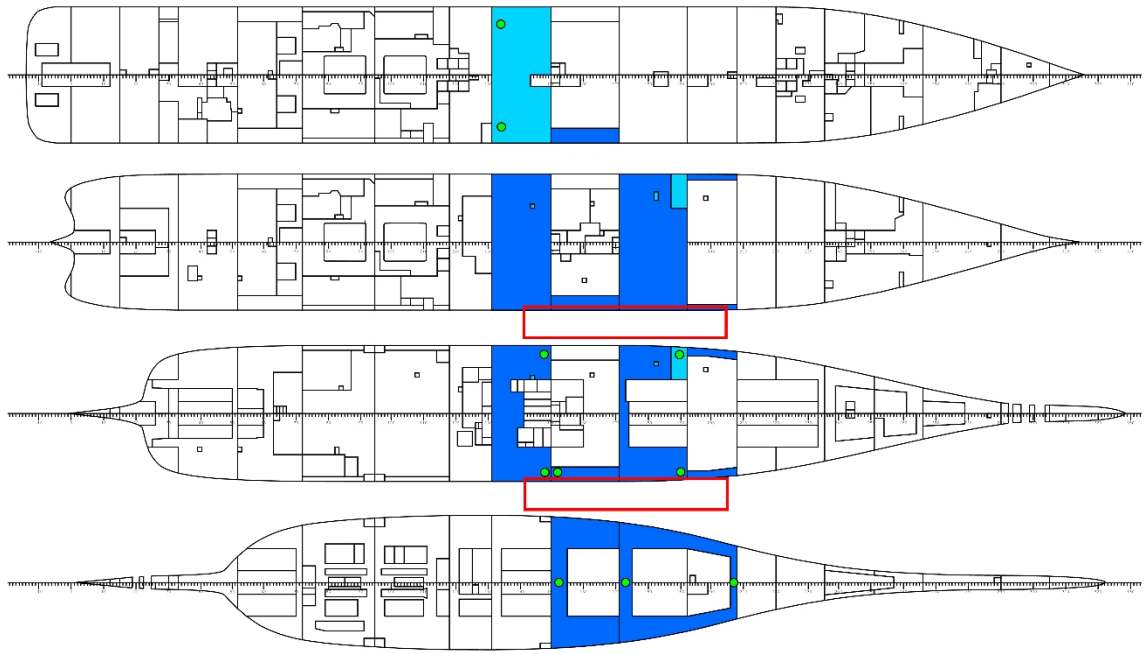


Figure 10-10: Test-case 5, Striking vessel length: 250.0 m, $H_s = 0.0$ m (Breach shown as red square, Initial flooding shown in dark-blue, progressive flooding shown in light-blue and flooding sensors shown in green).

Further investigation reveals, however that the aft- and foremost sensors both are located below the breach extent ($z_{sens} = 1.85$ m, whereas the lower position of the breach is $z_{breach} = 2.4$ m), while the mid sensor are located 0.70 m inward of the breach ($y_{sens} = 16.0$ m from midship, whereas the breach penetration only extends to $y_{breach} = 16.7$). As was highlighted for the previous test-case, cable routing may still be a problem, but has not been considered at this point. Another point to make, is that sensors may be fitted with indication if the signal is lost (which would be the case if the sensor or cabling is damaged), and this could be considered evidence in itself and implemented to the likelihood function, indicating that the compartment is part of the initial damage extent. In the following example, we assume that the sensors all are operational and provide proper indication. Detailed result for the final test-case is presented in section V.6 of Appendix V. The initial update incorporating sensor evidence from draft and AIS sensors are shown in Table V-78 of section V.6.1. Yet again the same trend is seen with further increase in the 99% CI, but less than the increase seen in the initial test-cases corresponding to smaller striking vessels.

This indicates that the information related to knowledge on the vessel size in the smaller regions of striking vessel is more sensitive than it is in the upper region, e.g. incorrect evidence in the smaller vessel regions would be increasingly reflected as an incorrect CI. The 99% CI is now reduced from 10,915 to 3,461 cases. For the previous case (striking ship length of 200.0 m), there was a reduction from 10,915 to 3,459, while a reduction from 10,915 to 1,106 and from 10,915 to 3,062 was seen for ship length of 50.0 m and 100.0 m respectively. This is a result of the decreasing rate of change of the standard deviation in the distributions developed in section 7.3.3, if assessed along the x-axis (ship-length). Detailed result incorporated with evidence from flooding sensors are shown in Table V-79 to Table V-84 in section V.6.2 for the calm water case. The initial Table V-79 shows the update for initial time step $t = 5.0 \text{ min}$, showing the actual case DAM7043 part of the ten most likely cases, at rank 8, with a probability of 0.005. It is further seen that all the ten most likely cases are some realisation of the actual initial case, and the case ranked on top with probability of as much as 0.82 only differs from the actual case by one compartment (R080201 not included).

This compartment has a flooding sensor which is located below the waterplane but does not yet show indication (similar to test-case 2 above) and is the reason for its high rank. The progressive flooding rate for the calm-water case is not sufficient for equilibrating the external and internal waterplanes, and the sensor would not be submerging within the 30-min simulation time. The 99% CI has from the previous posterior update been reduced from 3,461 to 8 cases. The list is maintained more or less the same for the remaining time-steps due to the negative flooding indication in R080201, only seeing a slight increase of the actual case to rank 3, and 99% CI represented by 5 cases in the final time-step. Results incorporated with more extreme significant wave heights of $H_s = 5.0 \text{ m}$ and $H_s = 10.0 \text{ m}$ are shown in Table V-85 to Table V-90 and Table V-91 to Table V-96 respectively. For a wave height of $H_s = 5.0 \text{ m}$, the actual case is ranked 14th while the same cases from before is ranked first. The actual case is maintaining a rank around 11-14 for the successively time-steps, but due to the increased wave height, the flooding sensor in R080201 is indicating flooding in the fifth time-step, $t = 25 \text{ min}$ (Table V-89), resulting in the actual case to be increased to 3rd rank for the last two time-steps with a probability of 0.053-0.065.

There are two other realisations of DAM7043 ranked first and second with probability of 0.47 and 0.15 respectively, both with additional compartments without flooding sensors included (R080202 & R080304) (Table V-90). Based on the available evidence, these cases are more likely. For the significant wave-height of $H_s = 10.0\text{ m}$, the progressive flooding rate is further increased, and the sensor in R080201 is indicating flooding already in the third time-step, $t = 15\text{ min}$ (Table V-93). In the following time-step an additional compartment progressively floods, namely R080202, the one indicated in the previous case ($H_s = 5.0\text{ m}$) to be more likely. The actual case is now ranked first on the list with a probability of 0.53, and the 99% CI is represented by 45 cases (Table V-94). For the successively time-steps the actual case is increased to a top rank with probability of 0.55 seen in the last time-step (Table V-96). The final extent included with the additional compartment R080202 (minor A-class compartment) is illustrated in Figure 10-11, and a heat-map representing the extreme wave case at the last time-step is illustrated in Figure 10-12, clearly replicating the actual damaged region from Figure 10-11 in red (yellow region is due to extreme H_s representing $P \approx 0.01$).

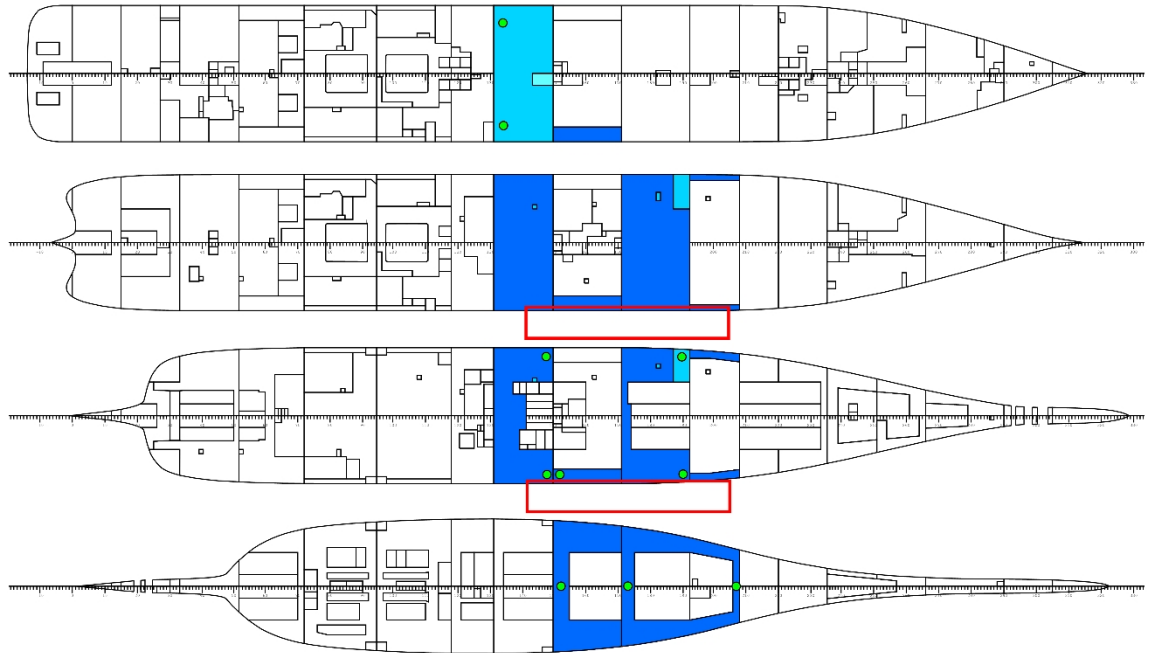


Figure 10-11: Test-case 5, Striking vessel length: 250 m, $H_s = 10.0\text{ m}$, $t = 30\text{ min}$ (Breach shown as red square, Initial flooding shown in dark-blue, progressive flooding shown in light-blue and flooding sensors shown in green).

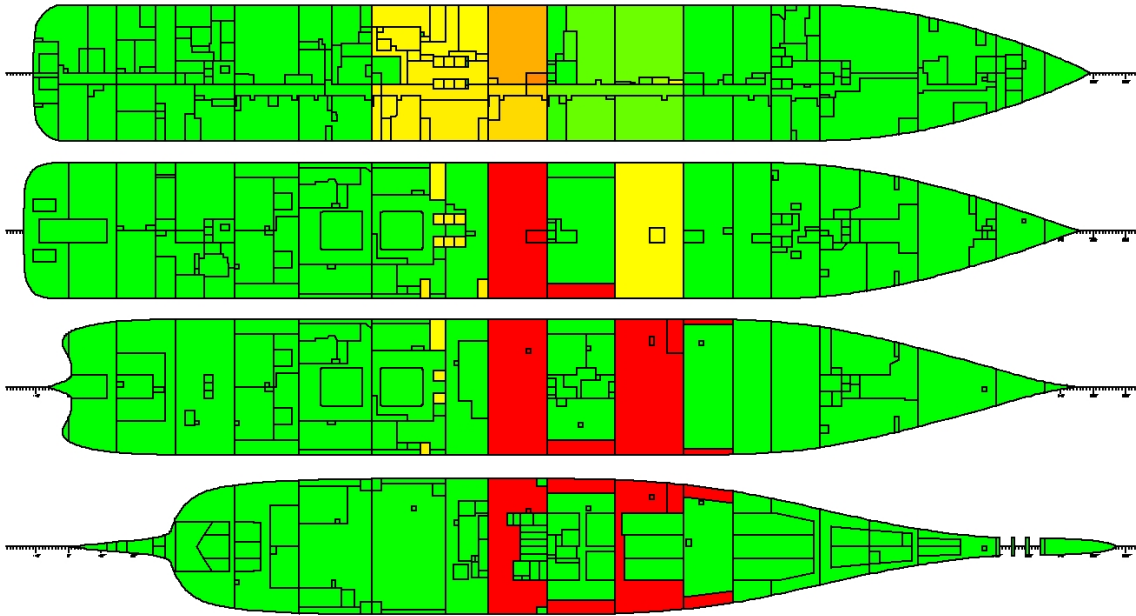


Figure 10-12: Heat map for wave-case, $H_s = 10.0$ m, time step, $t = 30$ min, representing the probability that a compartment is flooded (Red represents a probability of 1.00, yellow a probability of 0.01 and green a probability of 0.00, governed by the mapping $(R, G, B) = P: (1, 0, 0)=1, (1, 1, 0)=0.01, (0, 1, 0)=0$).

10.5 Closing remarks

In this chapter all the probabilistic models (likelihood functions) developed in the previous chapters have been implemented within a demonstration platform for application within the (flooding) emergency phase. The demonstration platform has been applied to five test-cases reading emulated sensor data obtained from time domain simulations. The sequential updates executed every 5 minutes allowed to identify the flooding extent with increasing confidence. The accuracy of prediction varied between the cases mainly because the differentiating between initial and progressive damage extents (requiring a unique combination of flooded compartments in the respective stages). However, considering the total flooding extent allows identifying of the actual flooding case with high confidence even if not all the compromised compartments are fitted with flooding sensors. More detailed discussion of the findings are included in the next chapter where main conclusions and recommendations are presented.

10.6 References

International Maritime Organisation (IMO), (2008), "*Guidelines for flooding detection systems on passenger ships*", MSC.1/Circ.1291, ref. T1/2.04, 9 December.

Chapter 11 - Discussion, Recommendations and Concluding Remarks

11.1 Discussion and recommendations

The main aim of the research undertaken has been to develop and test a framework for providing real-time information to the crew for improved and risk-informed situational awareness in flooding emergencies resulting from ship-to-ship collision, specifically with respect to damage extent and location. The application of the developed framework during the emergency phase, leading to valuable risk-informed information and decision making, demonstrates clearly that the main aim of the research has been fulfilled. The methodology adopted lead to identifying the targeted damaged region with high confidence in all five test-cases in spite of sparse sensor coverage. The results were presented as unique combination of flooded compartments (i.e. exact damage case) or in the form of heat-maps with individual locations ranked according to the probability of being flooded. The sequential updates increase the accuracy of the prediction (represented by number of cases within the confidence interval) providing quantitative evidence to support decision-making.

The fundamental ambition of providing supportive information was to provide improved risk-informed situational awareness to support survival assessment and to facilitate timely, targeted and efficient emergency response. The heat-maps presented in the results demonstrate that the predictions are converging to the region of the actual damage within the first time-steps in all test-cases. Rapid prediction of the compromised area enables fast and targeted deployment of the damage control teams, while the active mitigation measures may be implemented at an earlier stage based on the probabilistic evidence for the most likely flooding extent. The evidence allows effective monitoring and management of the openings within the flooding boundary as well as optimised use of other resources such as bilge or ballast systems as well as cross- and down flooding arrangements.

Furthermore, it increases flexibility for use of openings in the areas not affected by the casualty, thus allowing more flexibility in managing traffic and, if necessary, facilitating evacuation. Considering the strategy for presenting the prediction, it is noteworthy that maintaining the distinction between the flooding stages may lead to the situation where the actual case may not be among the top-ranked extents. This is a consequence of the absence of flooding sensors in minor A-class compartments. As a matter of fact, the use of clearly defined stages is important for deterministic predictions such as breach estimation based on floodwater inflow rate (NAPA, as discussed in Chapter 3). However, making such distinction is not essential within the probabilistic framework. On the contrary, the result of the test-cases show unambiguously that the top-ranked cases form various combinations of the actual damage extent supplemented by smaller A-class compartments. Hence, the prediction is easily verifiable and relevant for the survivability assessment. The developed method does not rely on a complete flooding sensor array (i.e. coverage) to produce estimates, as the likelihood functions allow for combining the sensor information with other sources such as probabilistic models considering water elevation exceedance, wave responses, etc. In a way, the likelihood functions act as filters in a process of *case filtering*. The fact that the framework generates accurate predictions even with the as-built sensor array demonstrates that the methodology may be implemented on a large cruise vessel without changes to the flooding detection system.

On the other hand, this entails that existing sensor arrays may be optimised for faster and more accurate predictions. This could either be in the form of the above-mentioned risk-based optimisation method, or simply to optimise in terms of general prediction accuracy in the form of uncertainty (CI). Due to insufficient time, the risk-based approach for sensor positioning developed in the course of this research (Chapter 8) (or any other means of sensor optimisation) were not implemented within the framework. Hence the method (or rather extension to the present method) could not be tested and the improvement measured. In this respect, additional research is needed to quantify the impact of optimised sensor layout. Having said this, special attention may be given to the type of flooding sensors. The framework presented herein does not require pneumatic flooding sensors, which enable inflow-rate estimates. Hence, the flooding sensors may be of a simpler (and less expensive) type, such as limit switches.

On the other hand, the time-variant characteristics, such as time-to-capsize may require the estimate of flooding rates and the flooding sensors providing estimates of inflow-rate. The configuration (i.e. types) and layout of flooding sensors, offering the best trade-offs between accuracy of flooding prediction and complexity, could be a part of the optimisation. It is important to stress that the present framework, does not provide a means for estimating the time-to-capsize. It does provide, however, the foundations for decision support which could be extended to accommodate for assesment of the likely outcome of the flooding accident. Needless to say that the accurate prediction of flooding extent, such as presented herein, is a fundamental prerequisite and it could be of great assistance in decision making in emergencies. Nevertheless, additional research should be performed to include a fully probabilistic measure for the TtC, linking the identified damage extents (initial- and progressive) to their respective (possible) breach sizes, for a complete assessment of the time available for evacuation.

Further consideration needs to be given to sensor availabillity, as two of the test-cases indicated sensors located critically close to the damage breach boundary. Sensor availability, as such, has not been considered at this point although the reliability has been partly considered by accounting for frequency of *Error*- and *Working* states. There are many alternatives to incorporate the availability which, for example, may be assessed in a similar manner to the Monte Carlo (MC) sampling performed in Chapter 6 while checking for overlap with the sensors position (and cabling). Sufficient sample size could also account for the appropriate conditionality, i.e. probability of a sensor to be damaged, given specific initial damage extent. The same method could be applied to a range of systems availability (active barriers) and even to pipe-routing (damaged pipes could be considered a source of progressive flooding). A simpler (and more conservative) approach may involve an assumption that all the system components within the initial breach are unavailable, a logic consistent with the underlying assumptions behind Safe Return to Port. Technology, and in particular connectivity may provide wireless solutions for the sensors, reducing the need for cabling, which will increase sensor reliability in terms of availability in a damaged condition, simply because sensor cables will increase the probability of them being located in the breach boundary. A final note to be made regarding sensor positions is regarding the MSC.1/Circ.1291, "*Guidelines for flooding detection systems on passenger ships*" (IMO, 2008). The guidelines recommended to position sensors on both sides of the ship, without

providing any recommendations or limits to how close to the side shell the sensor should be positioned. This (as indicated by the sensor layout of the sample vessel) might lead to low sensor availability as a large amount of shallow penetration damages could possibly lead to sensor damage. A simple transverse limit could provide the appropriate solution. e.g. B/5 or similar.

In order to demonstrate how the environmental variables can be accounted for, a method utilising motion sensors for inferring the significant wave height has been presented. This method significantly reduces uncertainty in comparison to the available a priori wave height statistics but it has several limitations that should be investigated further. Firstly, the method has been developed for the case without forward speed and, therefore, cannot be used for inference in normal operational conditions. Secondly, the recursive implementation of the method should incorporate a state transition model for better accuracy and performance (eliminate insensitiveness to rapid increase in wave height as observed in the results). Finally, alternative methods for uncertainty reduction as was discussed in Chapter 5 could be investigated, and how they could be combined with the presented methodology for further refinement and improved prediction accuracy (with emphasis on damaged condition). Wind-induced forces and their impact on both the floating position as well as dynamic responses were not considered at this stage of development. The developed model incorporating AIS data indicates that evidence on striking vessel length provides a global shift in probabilities. This is particularly evident in case of smaller striking vessels. For larger vessels, the data suggest that the full range of damage extent is still possible with both minor as well as major damage extents. It can be argued however, that additional variables, such as relative speed and heading, would provide further evidence and result in a similar shift in probabilities for larger striking vessel lengths. The challenges relate to the availability of data. The GOALDS database utilised in this development does not contain sufficient datapoints for such implementation and improved alternatives are necessary.

It should also be noted that the developed likelihood functions are derived based on 30 minutes long simulations. As progressive flooding scenarios may take several hours before reaching a stationary state or loss, the likelihood models could be made time-dependent. Considering for example several of the negative data-points (floodwater levels failing to reach the external waterplane within the duration of simulations) observed in the

floodwater exceedance probability, developed in Chapter 6, would shift towards the positive side with longer duration of the simulations. Including the time aspect, allows for providing additional supportive evidence in a way similar to that of the evidence of larger wave height, where compartments showing no flooding were assigned increasingly less probability as the floodwater levels failing to reach the external waterplane would be less likely with time. One of the objectives discussed in the introductory chapters was to examine the feasibility of use of the framework for life-cycle flooding risk management. It is evident that such development would entail extensive time-domain simulations and in-depth analysis of all the variables relevant to a flooding scenario. Undoubtedly, such undertaking would require detailed ship-specific knowledge far in excess of that linked to the regulatory framework of SOLAS (2009). Furthermore, it would be well aligned with the risk-based ship design philosophy mentioned in the introduction. In the design stage, the process described in the foregoing could be used to examine in detail the critical flooding scenarios to identify and address local vulnerabilities. Such an approach would allow comprehensive testing of the watertight subdivision, internal openings and flooding sensor layout. In addition, it would offer a platform for systematic verification and validation of the design assumptions. Furthermore, the sensor data collected during the operation of existing ships could be used as a priori beliefs.

In operation, the probabilistic models could provide a measure of vulnerability to flooding in a way similar to the developments presented in Chapter 3 (Jasionowski: 2010, 2011). In principle, the vulnerability can be expressed as an average product of probability of damage occurrence (e.g. p-factor) and probability of capsizing or sinking (e.g. complement to s-factor). Unlike the static A-index approach the operational vulnerability measure would be a dynamic quantity calculated with the use of evidence from onboard sensors such as door, draught and motion sensors. It should also be noted that the likelihood functions are vessel specific and, therefore, additional investigations would be required to examine the possibility of parameterising the models. In the short term, this would require considerably more simulations. However, if successfully identified, the parametric models would significantly reduce the need for simulations resulting in long-term benefits.

The above discussion allows to formulate the main suggestions for future research as in the following:

- Perform comprehensive testing of the methodology for risk-optimised positioning of sensors (or any other optimisation parameters).
- Incorporate within the framework probabilistic measure for the Time-to-Capsize (TtC).
- Incorporate sensor availability assessment and combine it with sensor reliability.
- Develop a procedure for positioning of flooding sensors considering post-casualty sensor availability.
- Develop a procedure for incorporating pipe routing in progressive flooding stages prediction (e.g. with use of graph model).
- Add forward speed in the wave-height prediction model.
- Implement a transition model in the wave-height prediction to improve performance of the model.
- Perform a more comprehensive assessment of the effects of wind.
- Investigate source of data sufficient for incorporating speed and heading into the AIS inference model.
- Parameterise (generalise) the developed likelihood functions.
- Adapt the developed methodology for use within a life-cycle flooding risk management framework.

The above discussion further allows to summarise what significant novelties the presented development contributes to the field of Naval Architecture:

- Bayesian Inference is widely used in various applications and in different fields. The presented development, however, is the first attempt to implement this approach for a more comprehensive life-cycle risk framework, with application on the prediction of damaged compartments in emergency situations, by considering information coming from a range of available (existing) sensors.
- Utilising *Copula Theory* to model statistical dependencies between damage characteristics in the analysis of the GOALDS accident database of ship casualties.
- Development of a fully probabilistic methodology for accounting progressive flooding through openings, by considering both opening status and leak/collapse heads, by utilising uncertain (probabilistic) graphs.
- Development of a risk-based methodology for determine the position of flooding sensors.

11.2 Concluding remarks

The foregoing details a fully probabilistic methodology developed with the aim to improve real-time information, providing risk-informed situational awareness in flooding emergencies. The methodology utilises probabilistic inference in the form of multi-sensor data fusion techniques for manipulating conditional probability distributions. Implementation and testing of the framework on a range of realistic test scenarios demonstrates that the method accurately identifies the extent of the actual flooding casualty even with a sparse flooding sensor array. The correct prediction of the flooding extent is essential in survival assessment and in managing timely, targeted and efficient emergency response. The successful test-cases indicate that the methodology may be implemented on a large cruise vessel without any changes to the existing sensor layout (i.e. with as-built sensor arrays) although use of the optimised layout could improve both the accuracy and convergence rates of the prediction model. The framework, based on Bayesian inference, relies on multi-sensor data fusion with sequential updates, which is a memory efficient way of utilising the previous posterior as the current a priori belief.

The range of probabilistic models (likelihood functions) has been developed for the specific sample vessel using the state-of-the-art time-domain simulation code PROTEUS3, enabling the simulation of a damaged ship in a dynamic operational climate capturing dynamic variables in greater detail than the traditional static calculation tools. The variables governing a flooding scenario have been identified and reviewed for the purpose of implementation in the respective probabilistic models, categorised as: environmental-, damage-, and ship-specific. The challenges in emergency response to a flooding scenario on large cruise vessels have been discussed and highlighted. Traditional emergency response is shown to be a highly time consuming and manual process, prone to human error or misjudgement that might lead to severe consequences. This is highly paradoxical, given that the most important variable is time, specifically, Time-to-Capsize (TtC) and Time-to-Evacuate (TtE) are the two drivers of risk in any flooding emergency. The developed framework provides the main foundations needed for assessing vessel survivability and TtC, as the latter requires detailed knowledge about the actual damage extent.

The traditional tools supporting the emergency response focus mainly on controlling and containing the flooding process. Inadequate situational assessment entails that the process under control is rather hypothetical and may be significantly different from the actual one. This may result in implementing suboptimal (in the best case) or even utterly wrong mitigation measures. In the latter case the action intended to improve the situation may in fact worsen it. Hence, providing a tool for risk-informed and time-optimised emergency response and damage control is of high value to the vessel operators. The advantages provided would further be a valuable addition to the third-party emergency response services. The drawbacks to the current approach in terms of minimum response time and reliance on second-hand information would clearly benefit from having direct access to real-time information from such a probabilistic framework rather than relying singlehandedly on the operators (biased) perception.

An important part of the development relates to the a priori statistical data for collision damages and it is necessary to discuss the shortcomings of the available damage distributions tailored to use within SOLAS. The data, simplified to enable harmonisation for all ship types, lacks important ship-type dependent properties as well as conditional dependencies between variables. For that reason, a priori distributions from available damage statistics have been derived with the use of advanced methods capturing conditional dependencies between variables. Monte Carlo sampling enabled discrete a priori probability to identify initial breach (i.e. the compartments open to sea). Furthermore, use of time-domain simulations has allowed developing a probabilistic model capturing the probability of initial flooding based on the vertical elevation of the damage breach with respect to the waterplane and conditional on vessel's draught and significant wave height. One of the main challenges in flooding prediction has always been associated with the modelling of progressive flooding in waves. The process, while intrinsically stochastic due to the nature of ship motions, is also combinatorially complex due to the presence of multiple internal openings. For these reasons it has been proposed to utilise Uncertain Graphs for modelling compartment connectivity. Such an approach has two main advantages. Firstly, it allows for random sampling of the graphs based on the probability of particular door status. Secondly, it allows state-of-the-art search algorithms for maintaining the probabilistic conditionality of connection to source (initial extent). This simplifies the problem significantly as non-existing connections to the source are disregarded and the search space contracts rapidly.

The realistic case studies presented demonstrate that the method identifies a manageable number of possible progressive flooding extents. The choice of detail, and number of resulting cases are governed by the confidence interval and number of samples used. Apart from survivability assessment, the method may also be employed in emergencies to avoid compartments imposed by floodwater, smoke, or fire in a range of emergency situations and may, therefore, provide a tool in identifying optimal evacuation routes. An important aspect considered while modelling progressive flooding is the status of the internal openings. This entails not only the open/close status but also leaking and collapse under the build-up of floodwater. Hence, the likelihood model developed for the framework takes into account not only the status of the opening (e.g. open/close) but also its position with respect to the external calm waterplane and the probability of leaking or collapse, both given as distributions around the nominal leak/collapse hydrostatic pressure heads. Representing the waterplane as a mathematical (dynamically changing) plane, enables a continuous reference point from the observed waterplane from any arbitrary point in the vessel coordinate system and has been crucial in the development of a dynamically changing progressive flooding probability. Combined with the Uncertain Graph Sampling (UGS) method, this blend into a robust probabilistic model for progressive flooding stages.

It is also noteworthy that the framework addresses both aleatory and epistemic uncertainties and although the former category has been the main focus within this thesis the latter has also been accounted for within the door- and flooding sensor models in the form of false-positives and -negatives. A discrete version of Bayes formula for application on binary values has been utilised for the developed door sensor model enabling correct normalisation. The likelihood function for updating the posterior probability for the initial damage extent, based on actual operating draft, has been developed and presented, including a likelihood function for modelling the energy availability from AIS data. Due to few samples for speed and heading the model only considers the vessel size particulars in the form of striking vessel length, but from the implemented test-cases, it provide a large reduction in uncertainty by updating the posterior belief based on actual knowledge on the size of the vessel involved in a collision incident with, especially so for smaller striking vessels.

A fully exhaustive sensor array is not feasible, hence the available sensor resources need to be managed properly. One should make sure that high risk loss scenarios are covered with optimised uncertainty reduction, which is catered for by the methodology for risk-based positioning of flooding sensors. It can be accepted that low risk scenarios (survival) are provided with less prediction accuracy, simply because we have much more time available and may deploy traditional emergency response teams for support. The study confirms that the extent of a damage case or geometrical properties of the compartments alone are insufficient criteria for the positioning of the flooding sensors for the accurate estimate of survivability during flooding casualties. The regulatory requirements should also be complemented by the systematic, risk-based rating to determine critical spaces and flooding pathways. This should lead to targeted and efficient sensor positioning. In addition, the results reveal that the same compartment may have different criticality rating in the initial and progressive stages of flooding. For this reason, these stages should be ranked separately, as smaller compartments may form critical flooding paths to larger rooms (through up- and cross-flooding) and should also be fitted with sensors for early warning of capsizing. Separating initial stage and progressive stage may also help identifying sensor type and position.

Finally, a range of findings have been discussed in the previous section, where several limitations and alternative implementation approaches have been discussed. These have been summarised and listed as suggestions for future research and development. In summary, the work presented herein lays the foundations for a fully probabilistic methodology for predicting the outcome of flooding casualties and lays the foundations for a comprehensive framework for life-cycle flooding risk management. This allows for reliable estimation of real-time flooding risk in passenger ships through its life-cycles and most importantly, when it really matters, namely in emergencies. This is an innovation offering unique tangible benefits.

Appendix I - Wave prediction method – Complete test-case results

Table I-1: Sensor readings and statistical prediction data for all test-cases.

	Case	Roll	Pitch	Heave	Actual	Exp.	Diff.	Priori	Posterior	Diff.
	[#]	$\varphi_s [^\circ]$	$\theta_s [^\circ]$	$Z_s [m]$	$H_s [m]$	$\overline{H}_s [m]$	$\Delta H_s [m]$	$\sigma [-]$	$\sigma [-]$	$\Delta\sigma [-]$
World-wide	1	0.733	0.118	0.294	2.893	3.429	-0.536	2.189	0.849	-1.339
	2	0.307	0.052	0.047	1.298	2.015	-0.717	2.189	0.601	-1.588
	3	0.044	0.014	0.012	1.418	1.205	0.213	2.189	0.281	-1.908
	4	1.085	0.283	0.145	4.323	4.291	0.032	2.189	0.970	-1.219
	5	0.215	0.033	0.020	1.538	1.602	-0.064	2.189	0.460	-1.729
North-Atlantic	1	0.094	0.038	0.093	1.692	1.815	-0.123	3.333	0.579	-2.754
	2	6.699	0.792	1.695	8.688	8.939	-0.251	3.333	1.631	-1.702
	3	0.873	0.176	0.357	3.295	4.269	-0.974	3.333	0.970	-2.363
	4	0.311	0.136	0.107	4.391	3.122	1.268	3.333	0.839	-2.494
	5	0.319	0.050	0.108	2.282	2.348	-0.065	3.333	0.671	-2.662
Caribbean	1	0.580	0.072	0.054	1.781	2.458	-0.677	2.366	0.669	-1.697
	2	0.221	0.043	0.032	1.939	1.737	0.202	2.366	0.581	-1.785
	3	0.045	0.022	0.007	0.763	0.906	-0.143	2.366	0.430	-1.936
	4	1.666	0.319	0.192	3.274	4.428	-1.154	2.366	0.879	-1.487
	5	0.038	0.013	0.006	0.555	0.725	-0.170	2.366	0.371	-1.995
Extreme wave	1	10.933	0.818	2.564	10.312	9.762	0.549	3.333	1.761	-1.572
	2	13.882	0.660	2.585	10.081	9.638	0.443	3.333	1.771	-1.562
	3	16.073	0.619	4.451	12.211	9.890	2.320	3.333	1.812	-1.521
	4	11.307	0.721	3.153	10.027	9.677	0.349	3.333	1.761	-1.572
	5	21.420	1.117	4.022	13.984	11.090	2.894	3.333	1.868	-1.465

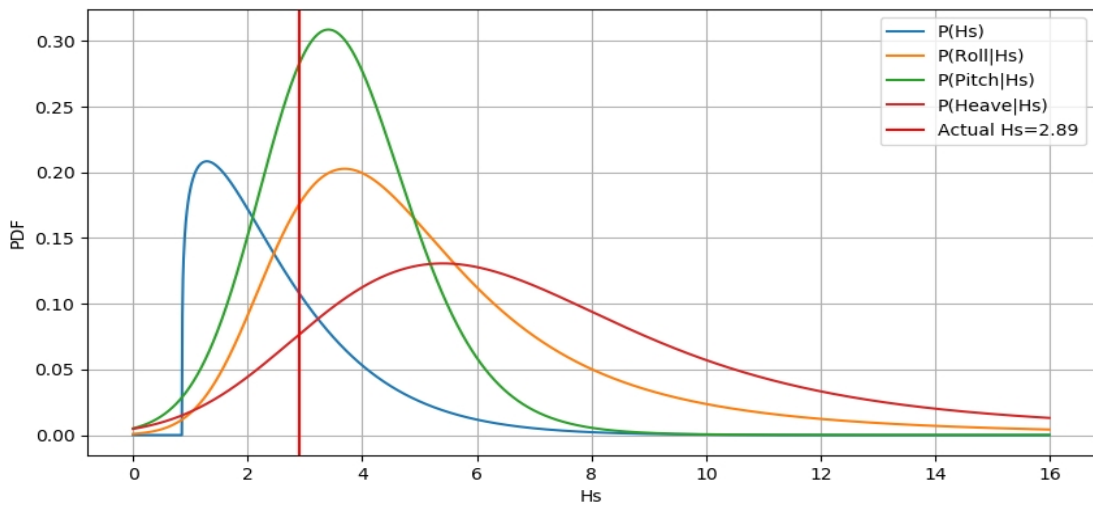


Figure I-1: A priori, and likelihood functions (C1-World-wide).

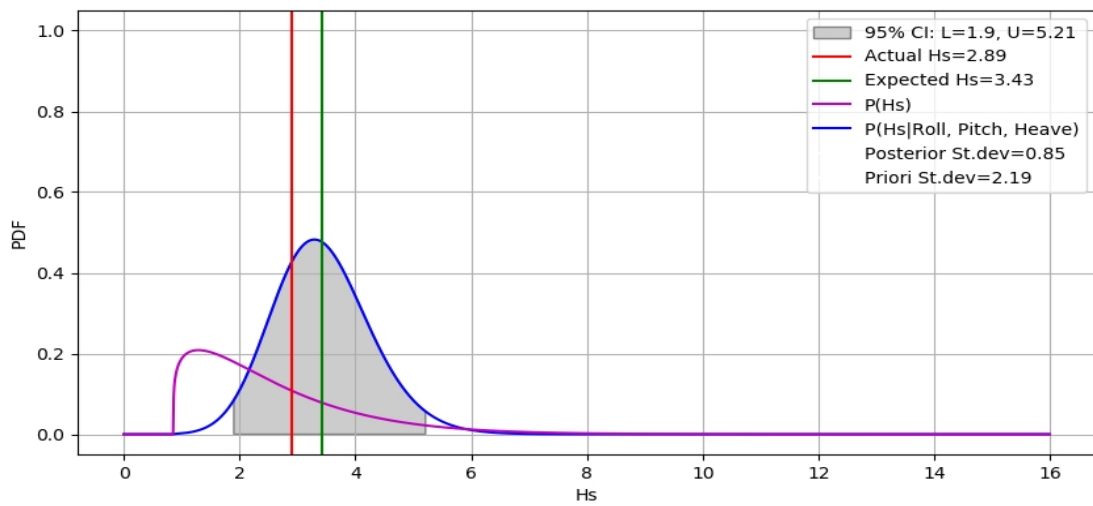


Figure I-2: A priori and posterior including actual and expected value (C1-World-wide).

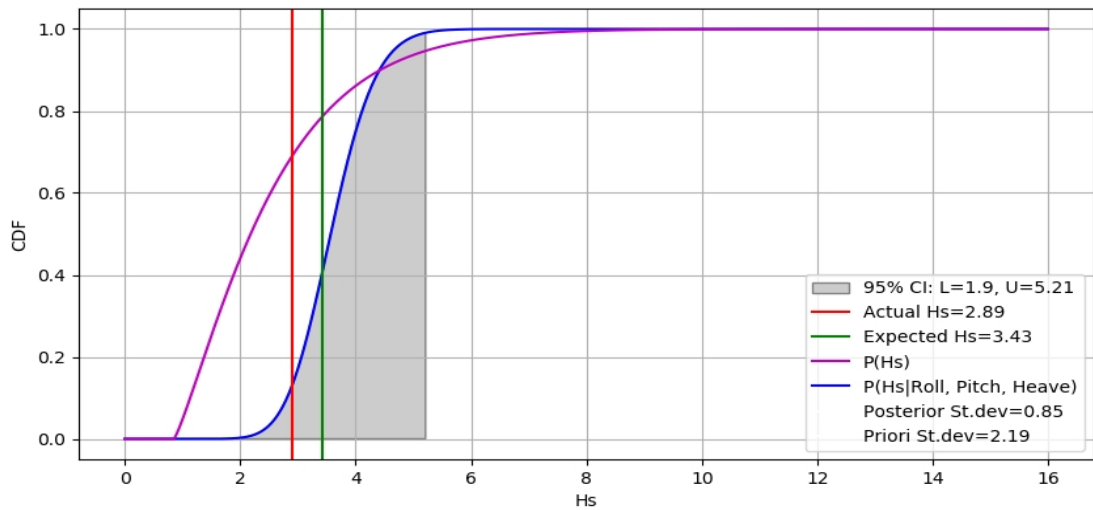


Figure I-3: Cumulative a priori and posterior including actual and expected value (C1-World-wide).

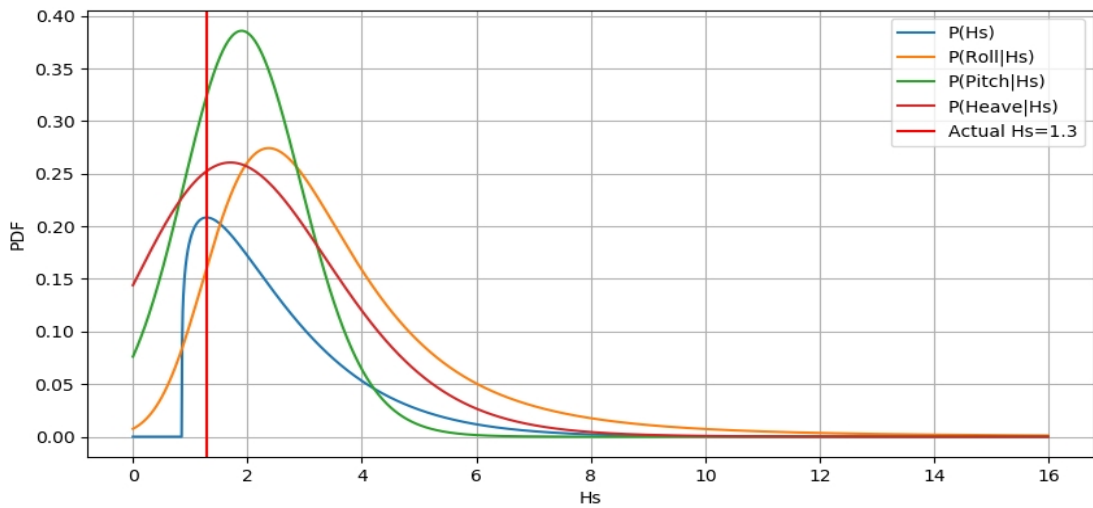


Figure I-4: A priori, and likelihood functions (C2-World-wide).

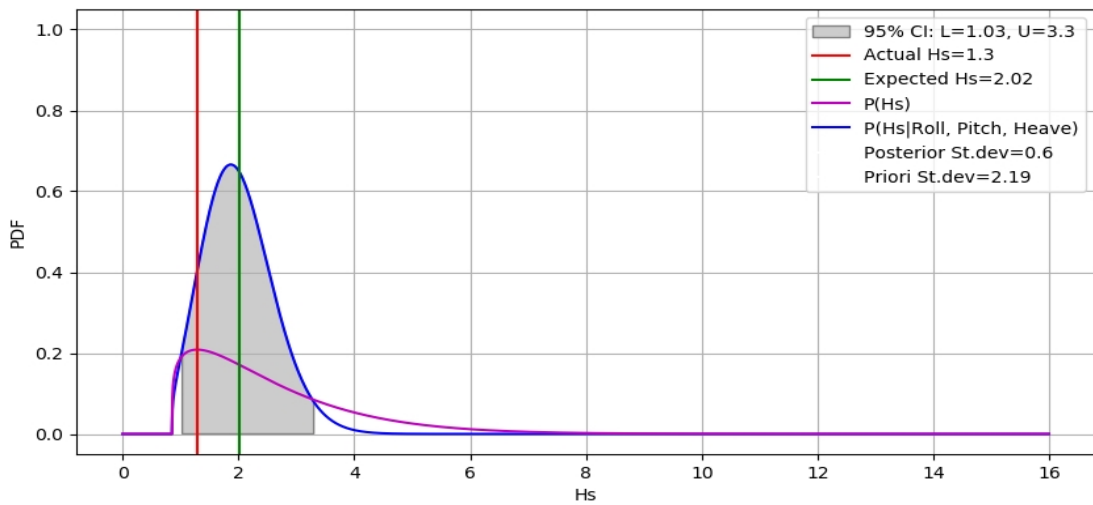


Figure I-5: A priori and posterior including actual and expected value (C2-World-wide).

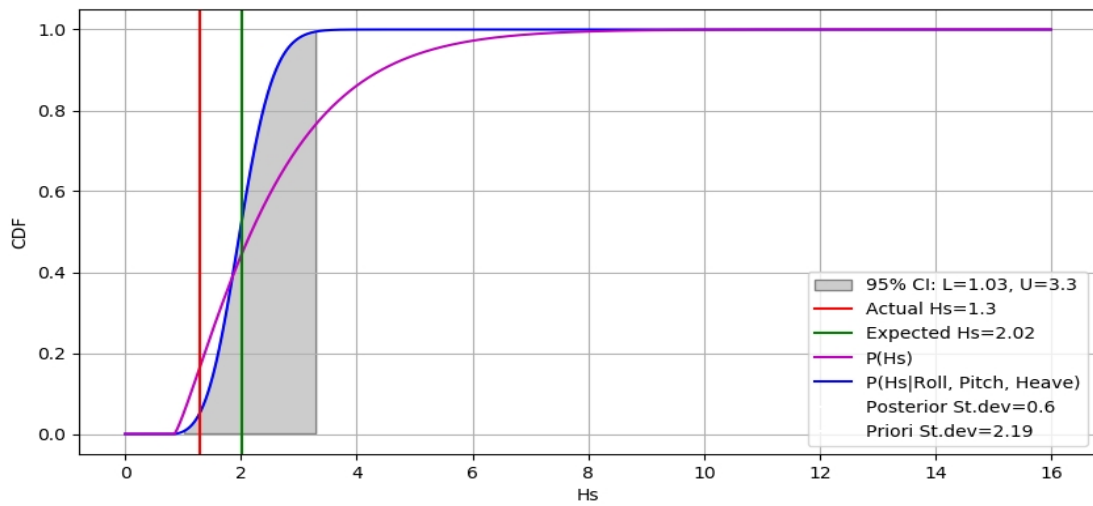


Figure I-6: Cumulative a priori and posterior including actual and expected value (C2-World-wide).

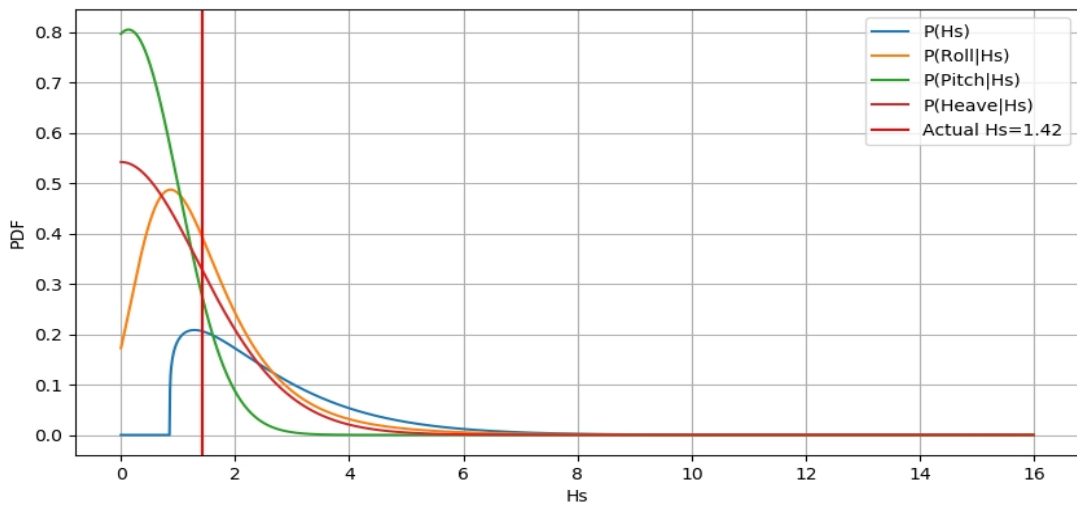


Figure I-7: A priori, and likelihood functions (C3-World-wide).

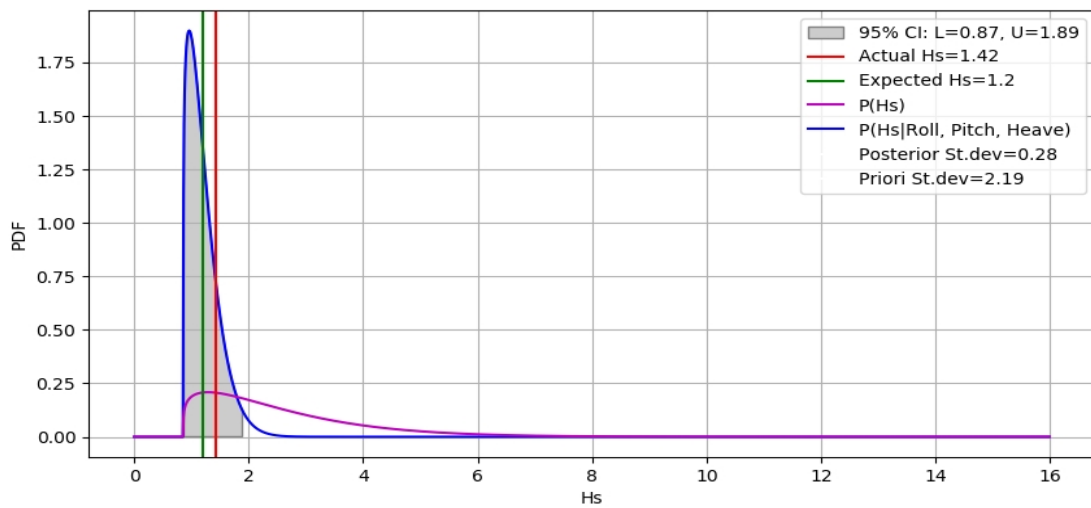


Figure I-8: A priori and posterior including actual and expected value (C3-World-wide).

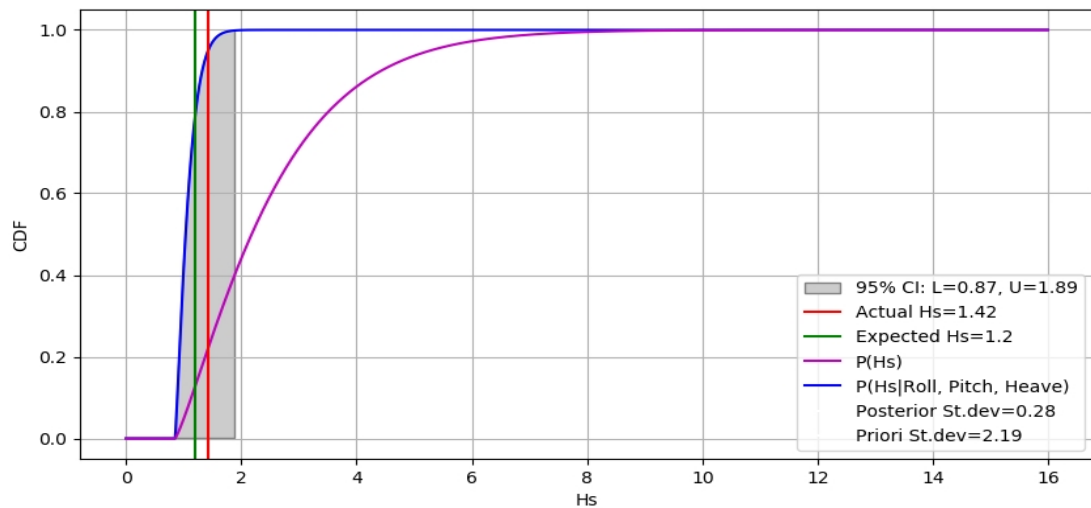


Figure I-9: Cumulative a priori and posterior including actual and expected value (C3-World-wide).

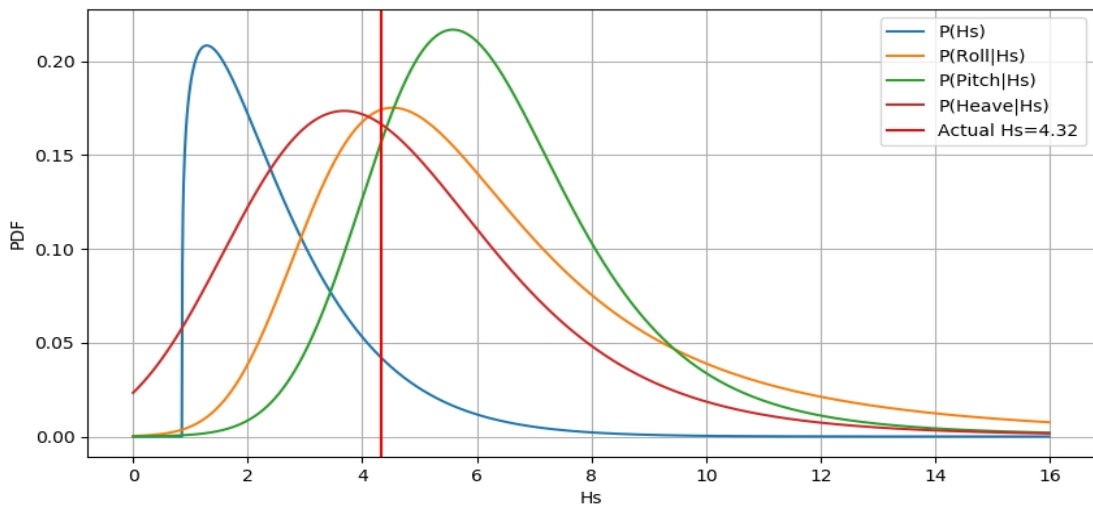


Figure I-10: A priori, and likelihood functions (C4-World-wide).

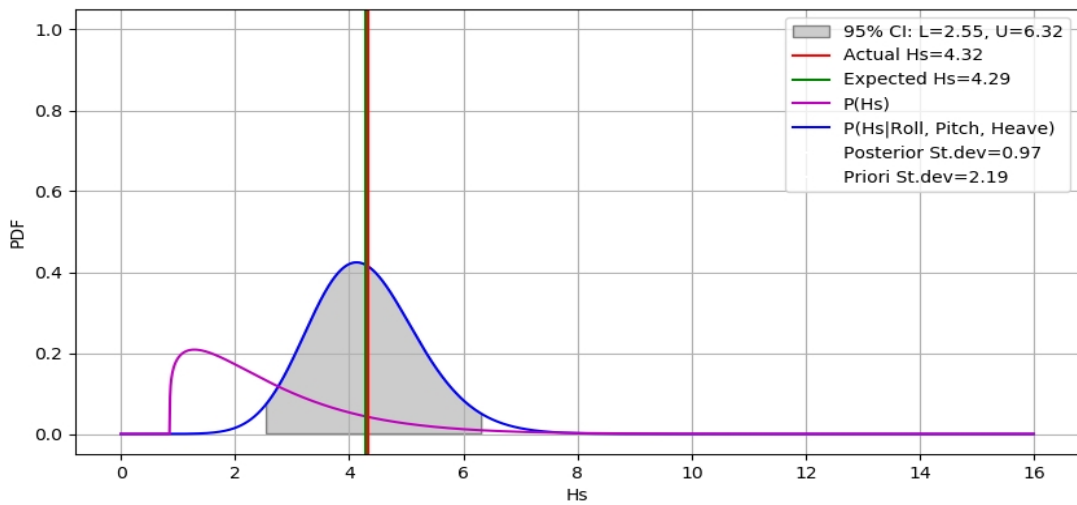


Figure I-11: A priori and posterior including actual and expected value (C4-World-wide).

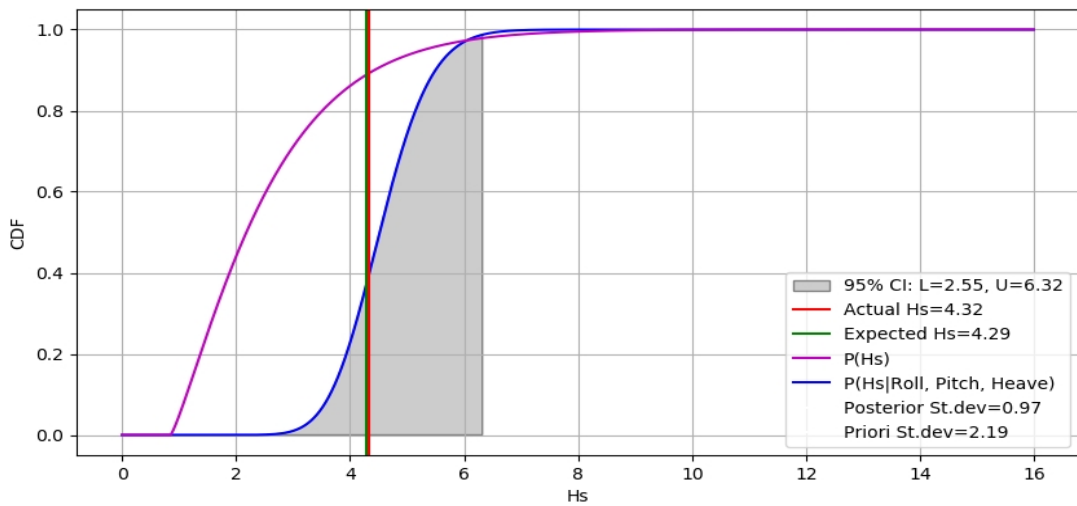


Figure I-12: Cumulative a priori and posterior including actual and expected value (C4-World-wide).

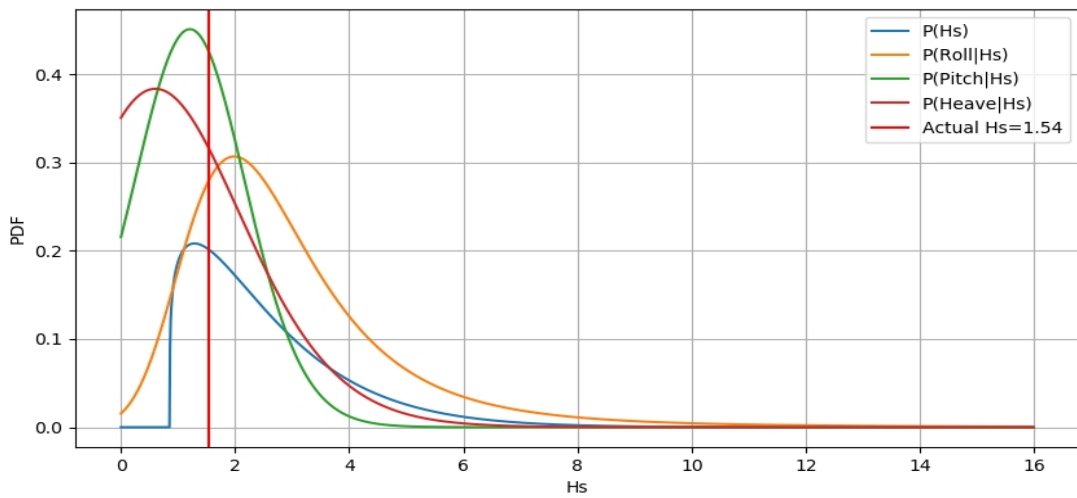


Figure I-13: A priori, and likelihood functions (C5-World-wide).

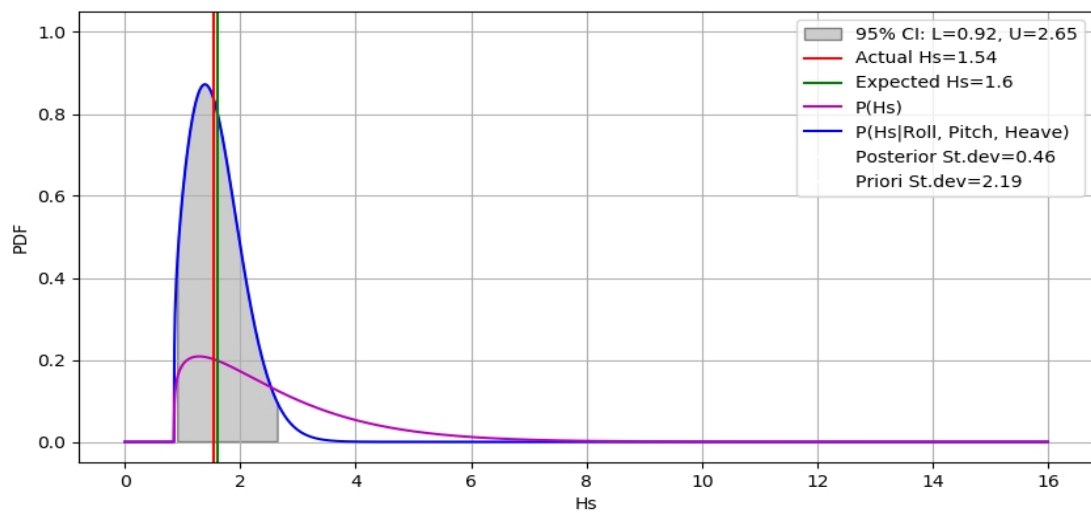


Figure I-14: A priori and posterior including actual and expected value (C5-World-wide).

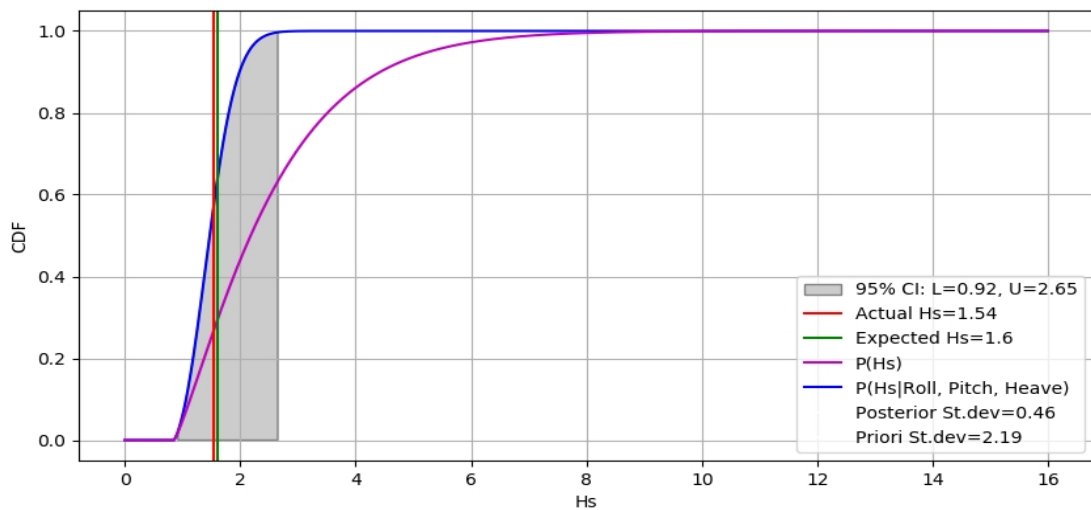


Figure I-15: Cumulative a priori and posterior including actual and expected value (C5-World-wide).

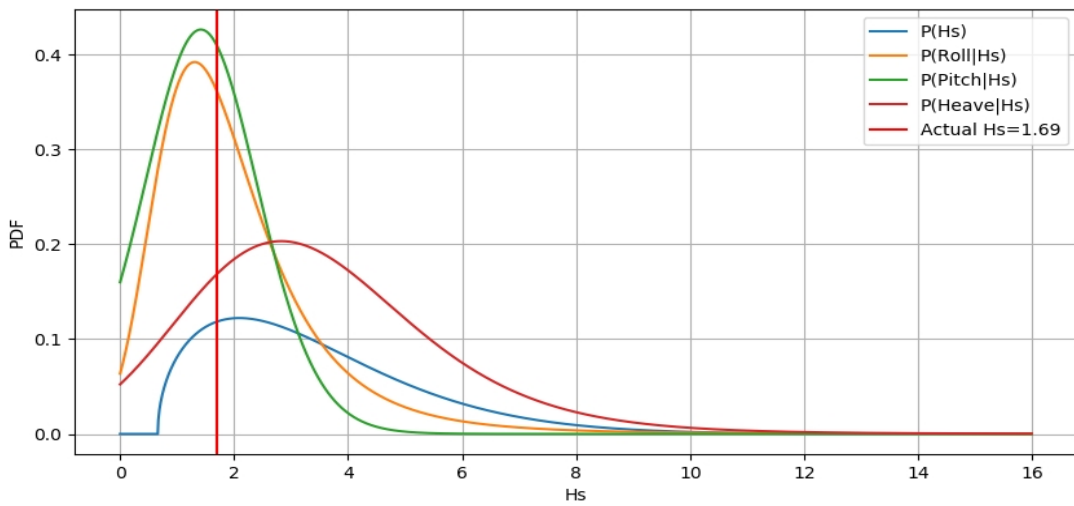


Figure I-16: A priori, and likelihood functions (C1- North-Atlantic).

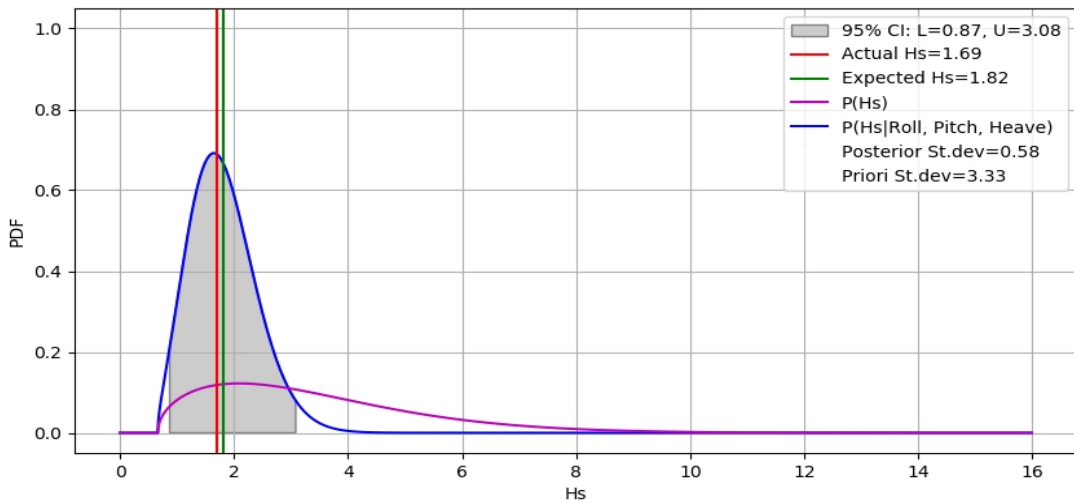


Figure I-17: A priori and posterior including actual and expected value (C1- North-Atlantic).

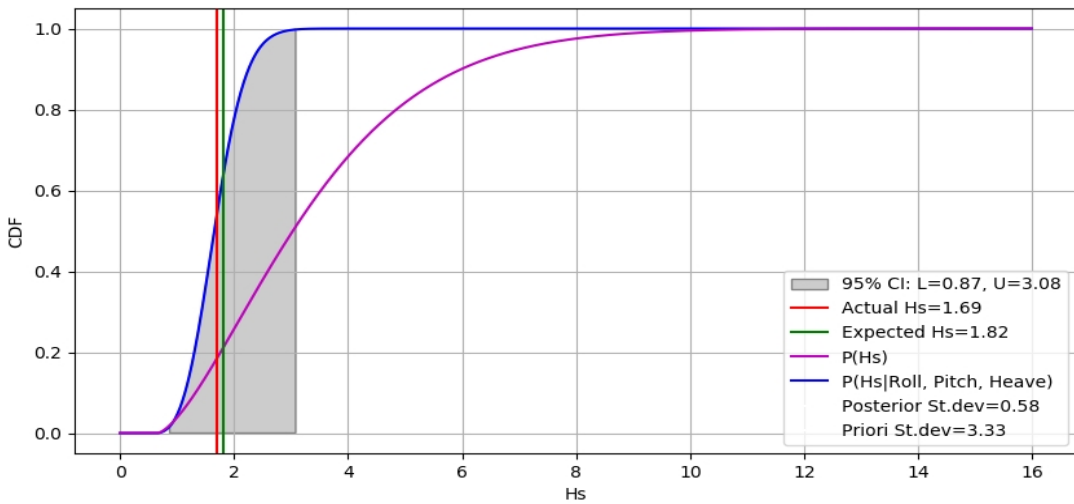


Figure I-18: Cum. a priori and posterior including actual and expected value (C1-North-Atlantic).

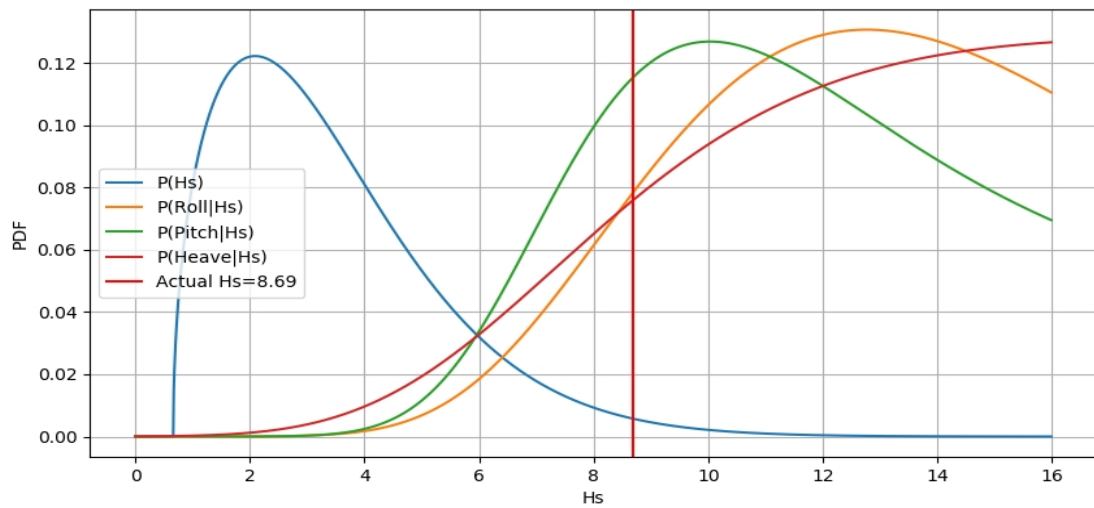


Figure I-19: A priori, and likelihood functions (C2-North-Atlantic).

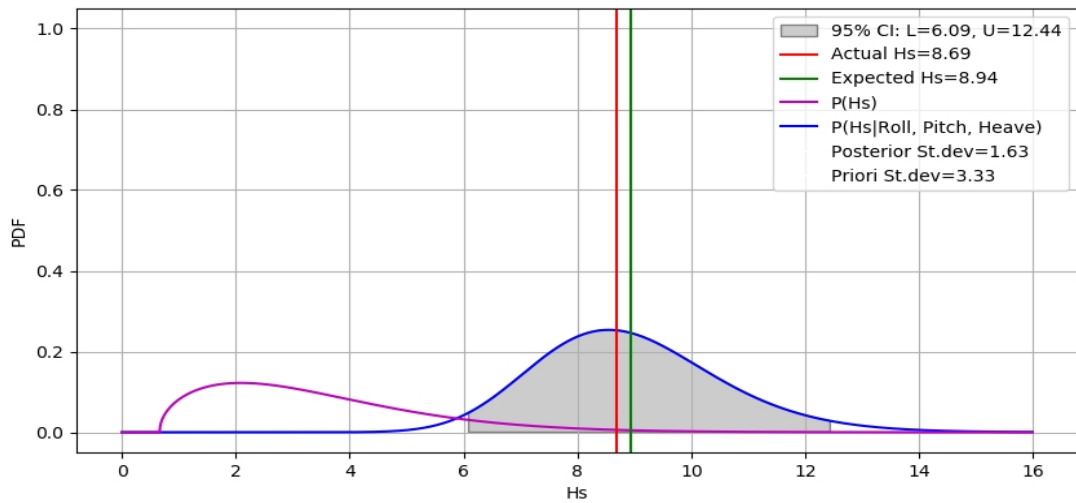


Figure I-20: A priori and posterior including actual and expected value (C2-North-Atlantic).

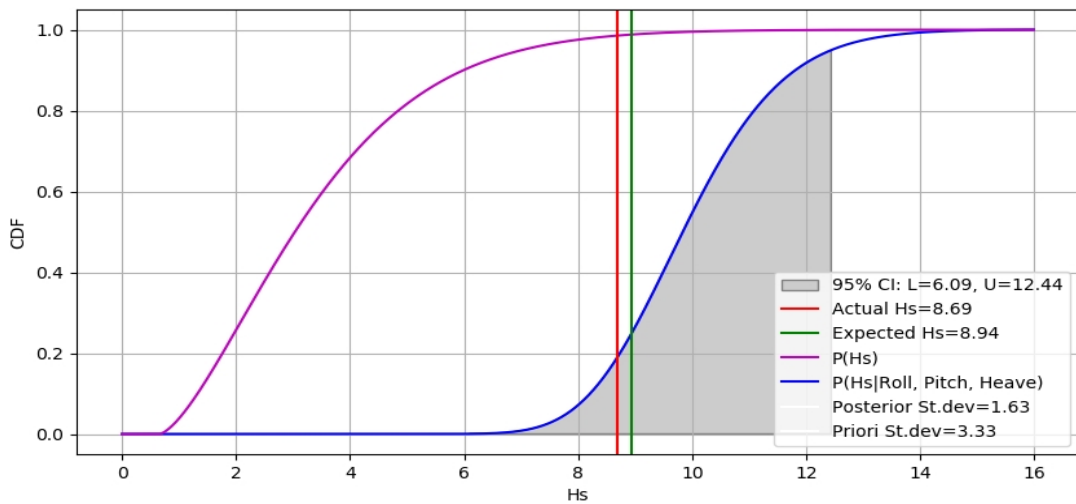


Figure I-21: Cum. a priori and posterior including actual and expected value (C2-North-Atlantic).

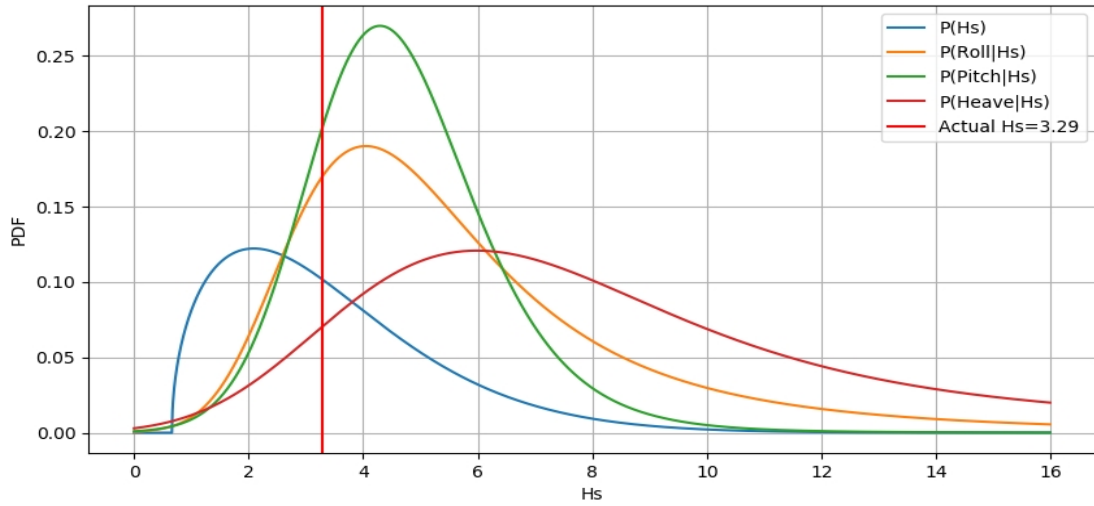


Figure I-22: A priori, and likelihood functions (C3-North-Atlantic).

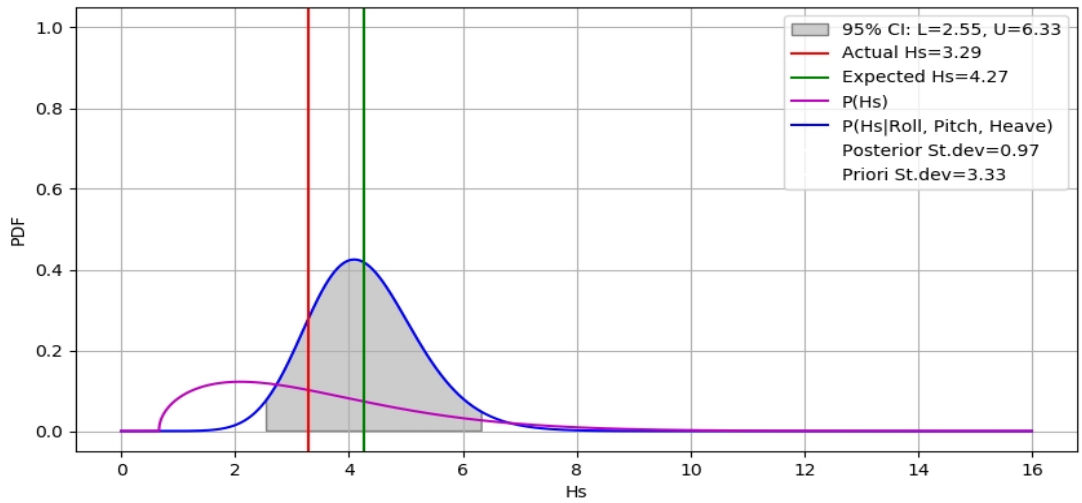


Figure I-23: A priori and posterior including actual and expected value (C3-North-Atlantic).

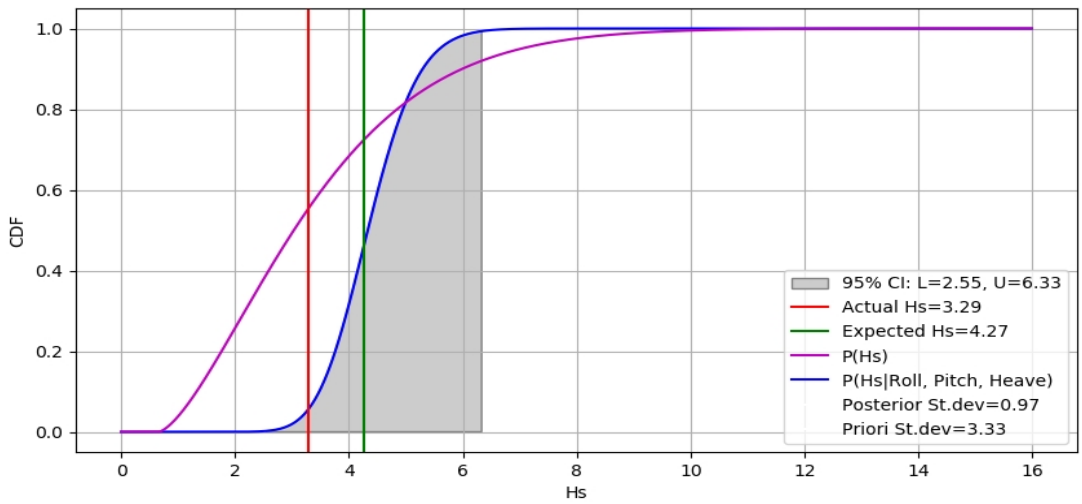


Figure I-24: Cum. a priori and posterior including actual and expected value (C3-North-Atlantic).

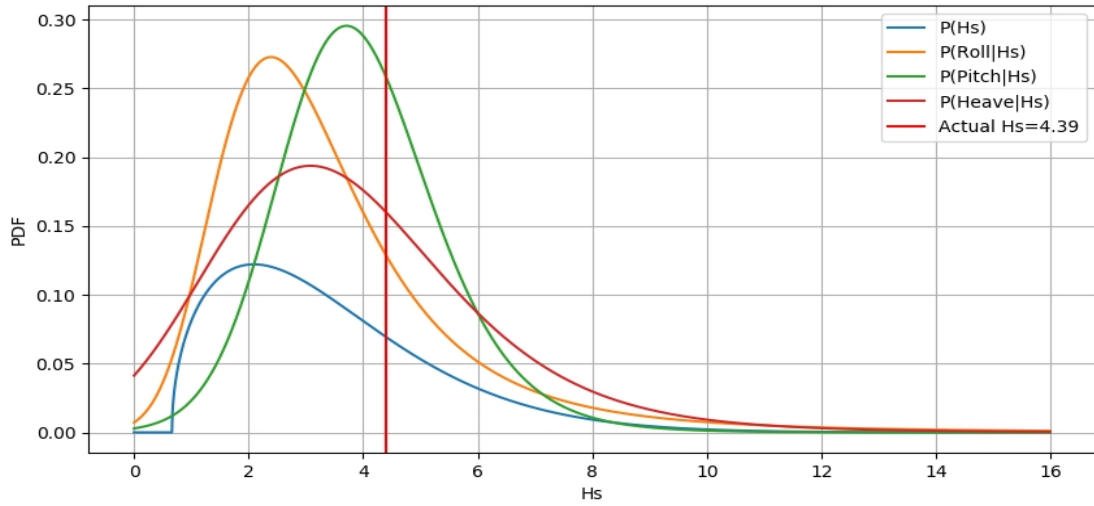


Figure I-25: A priori, and likelihood functions (C4-North-Atlantic).

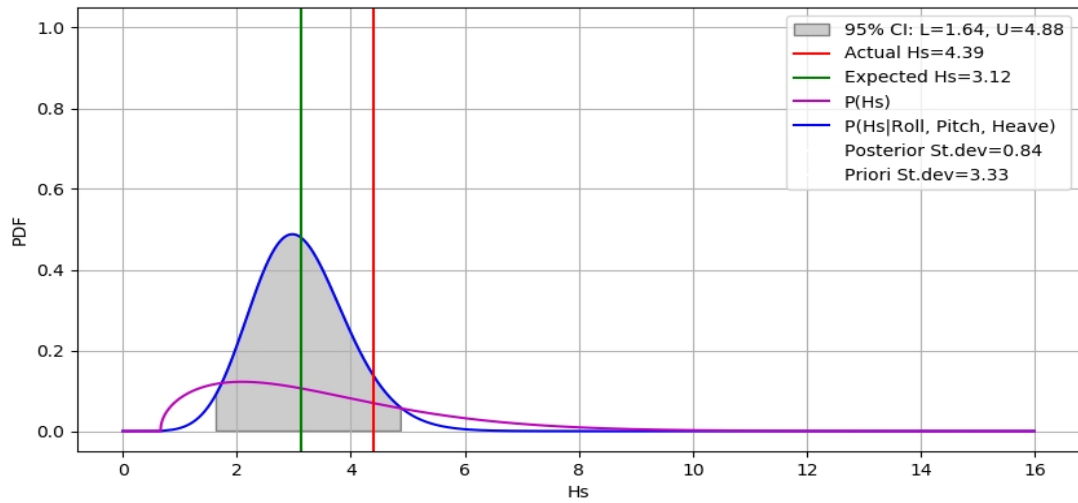


Figure I-26: A priori and posterior including actual and expected value (C4-North-Atlantic).

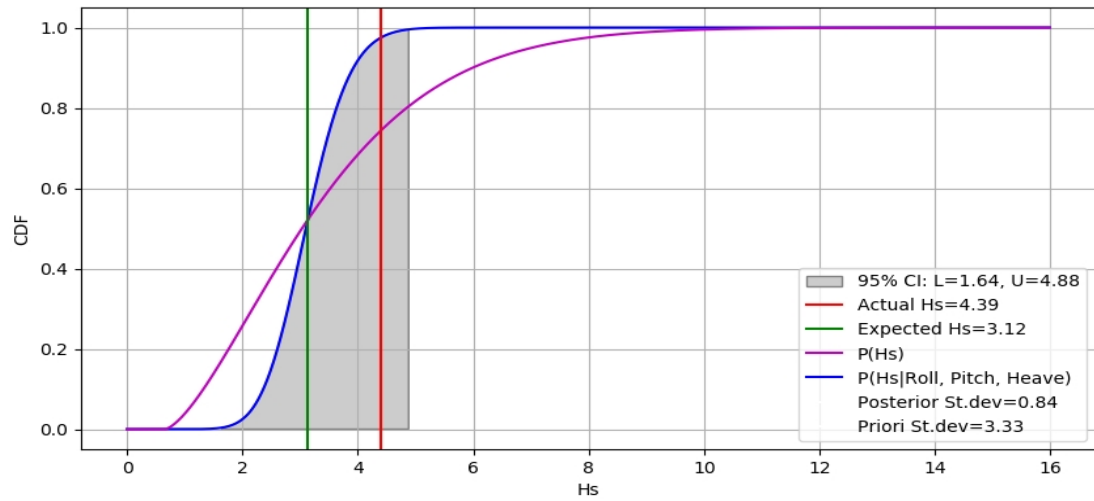


Figure I-27: Cum. a priori and posterior including actual and expected value (C4-North-Atlantic).

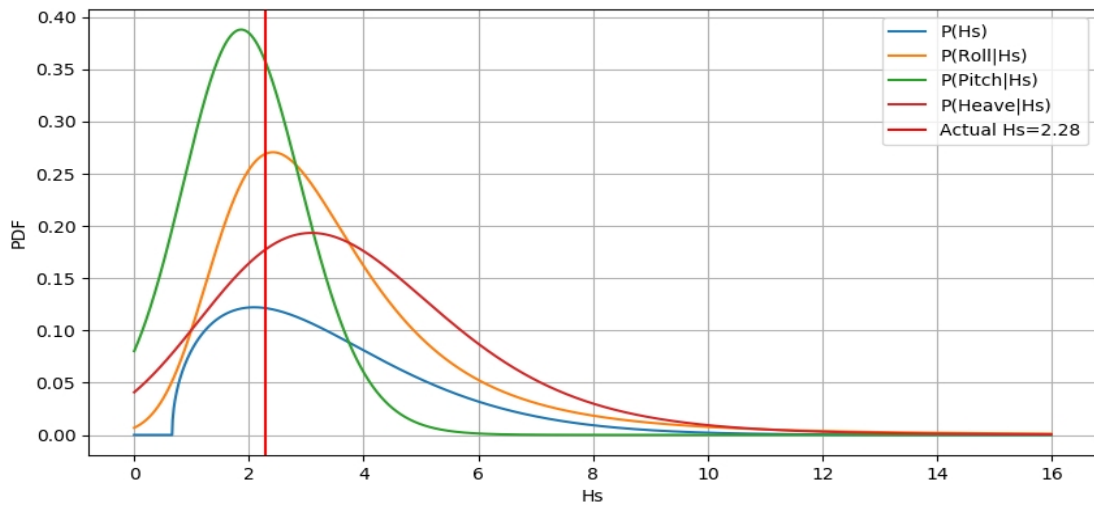


Figure I-28: A priori, and likelihood functions (C5-North-Atlantic).

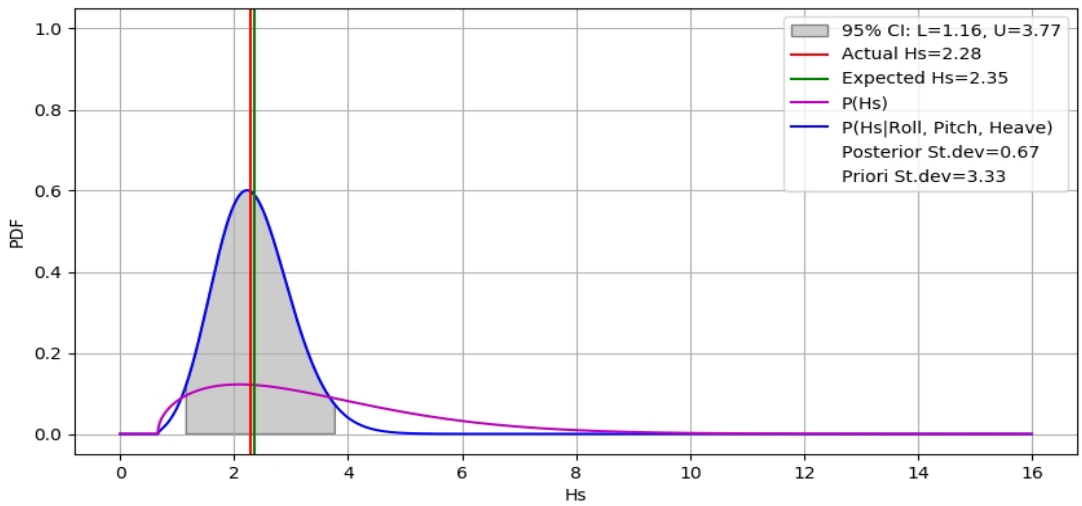


Figure I-29: A priori and posterior including actual and expected value (C5-North-Atlantic).

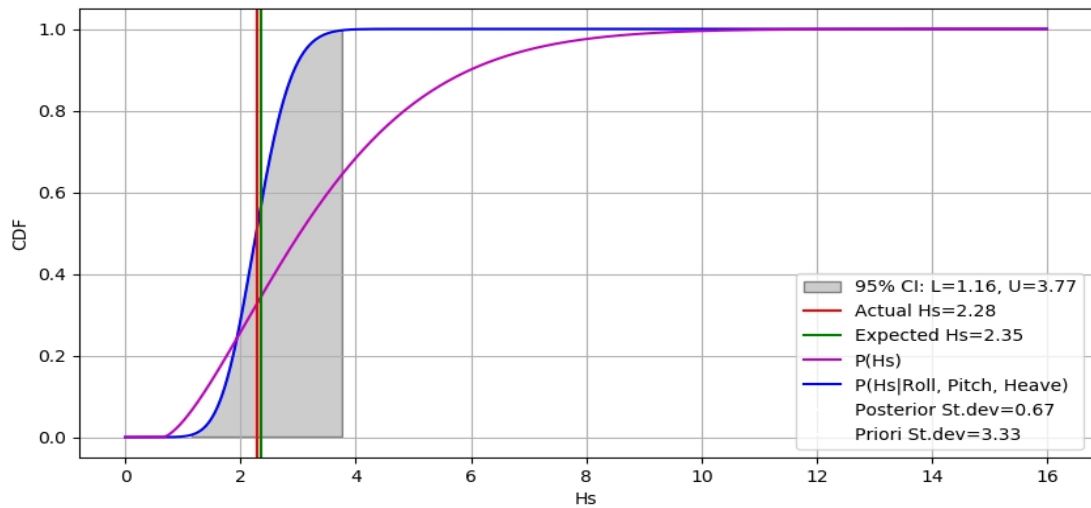


Figure I-30: Cum. a priori and posterior including actual and expected value (C5-North-Atlantic).

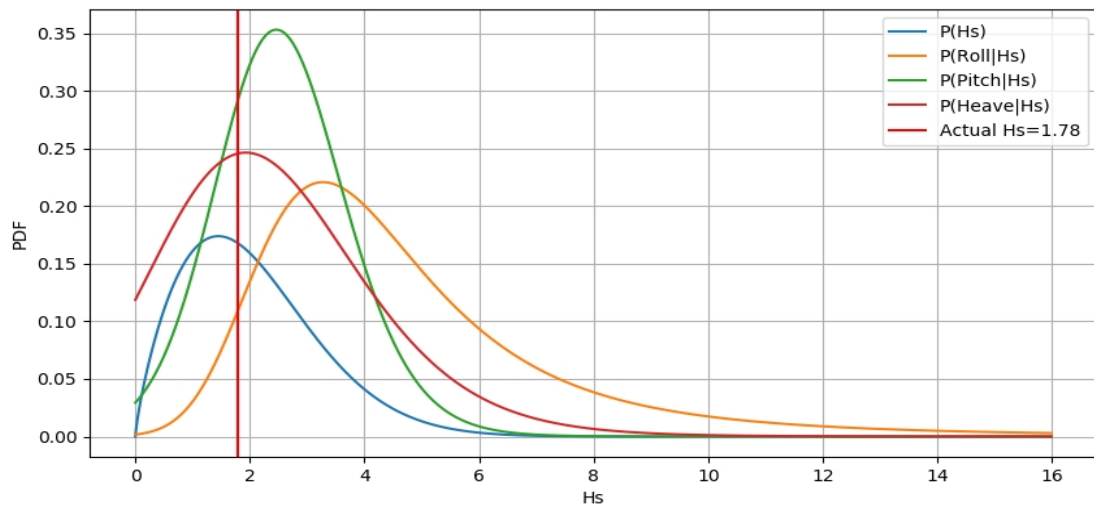


Figure I-31: A priori, and likelihood functions (C1-Caribbean).

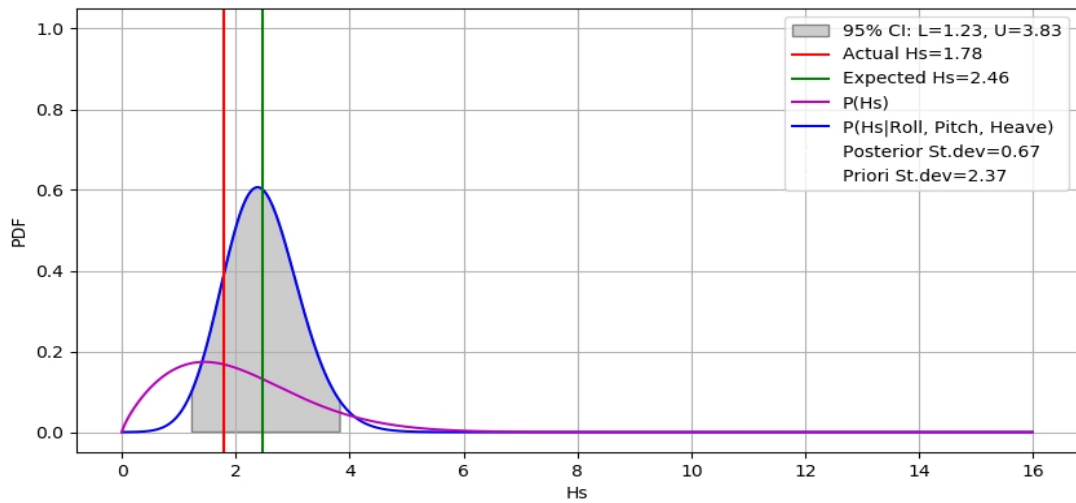


Figure I-32: A priori and posterior including actual and expected value (C1-Caribbean).

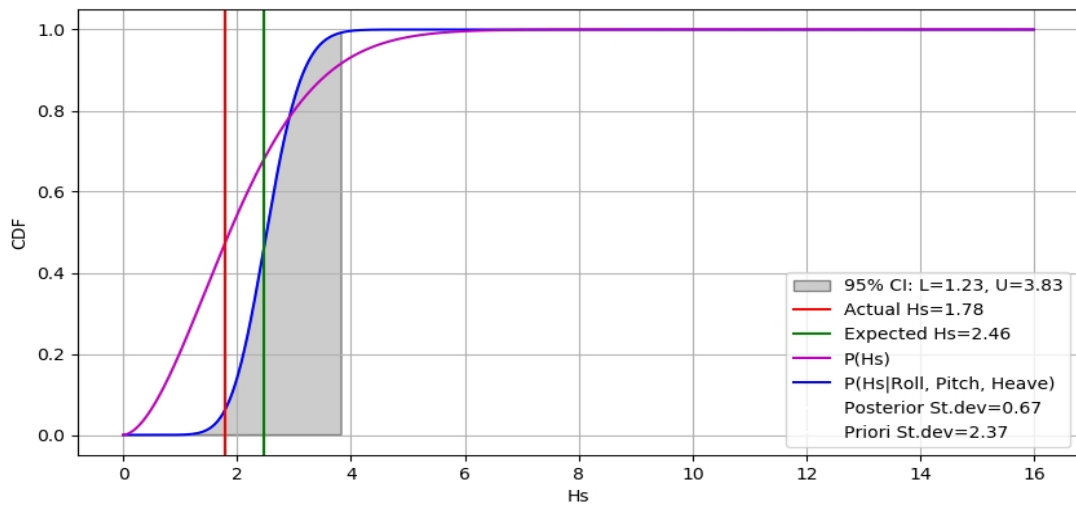


Figure I-33: Cum. a priori and posterior including actual and expected value (C1-Caribbean).

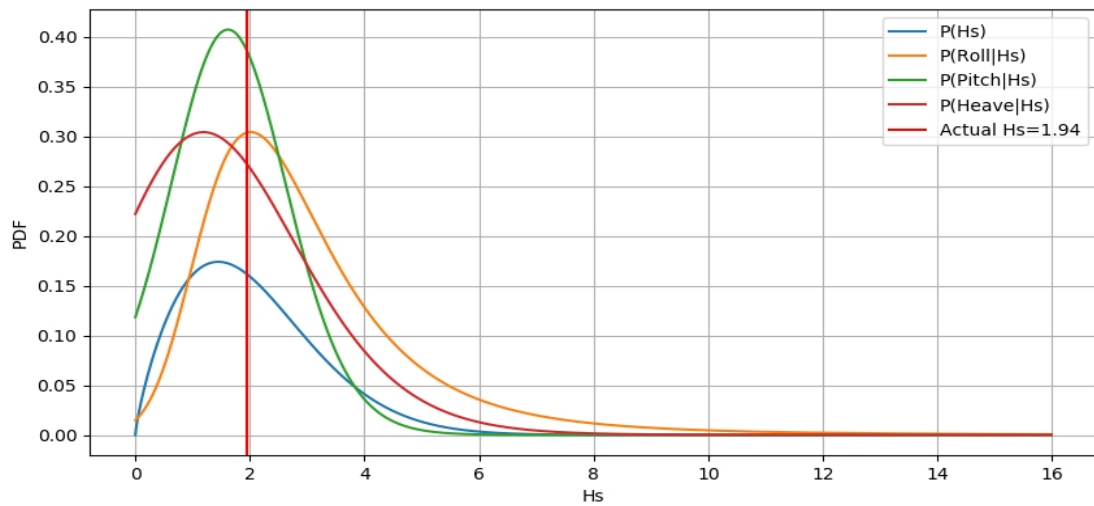


Figure I-34: A priori, and likelihood functions (C2-Caribbean).

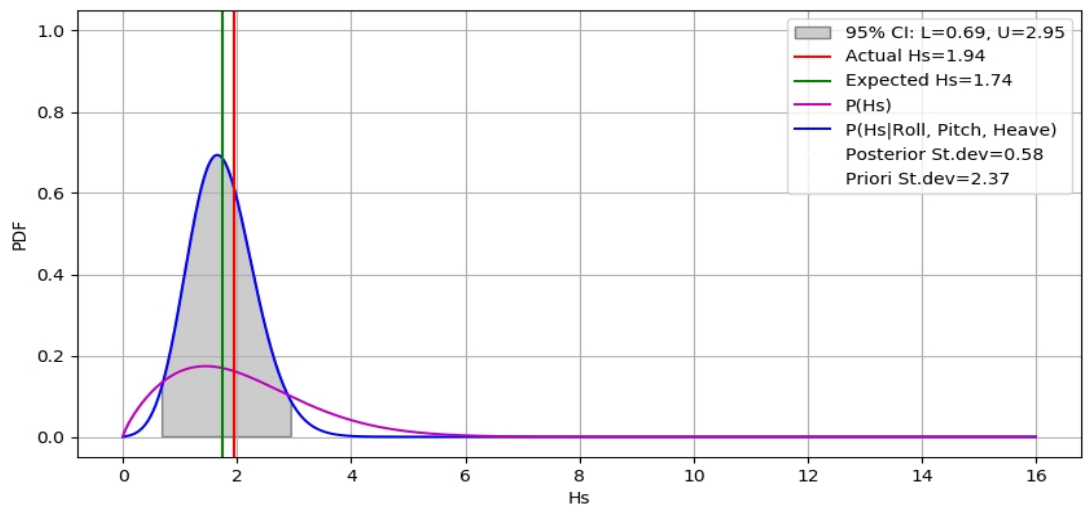


Figure I-35: A priori and posterior including actual and expected value (C2-Caribbean).

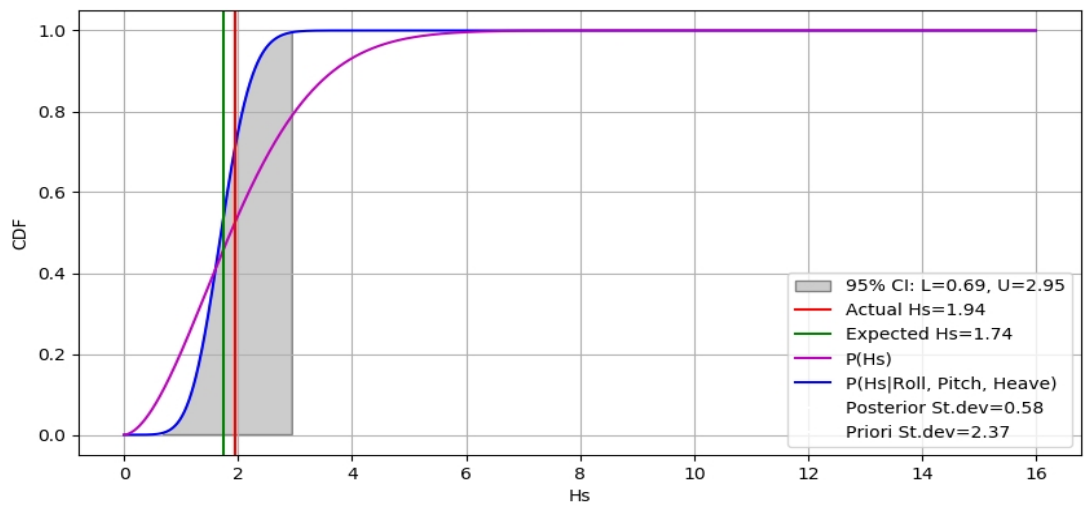


Figure I-36: Cum. a priori and posterior including actual and expected value (C2-Caribbean).

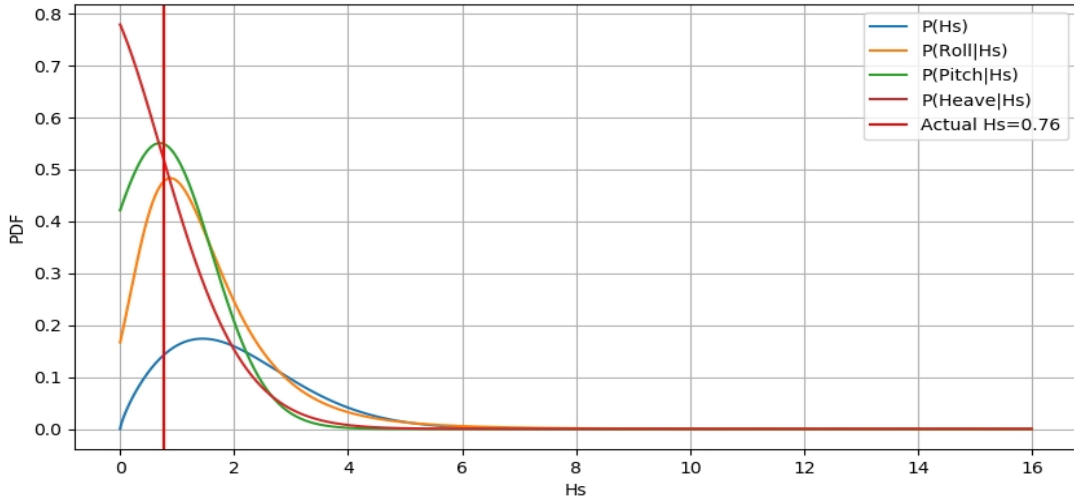


Figure I-37: A priori, and likelihood functions (C3-Caribbean).

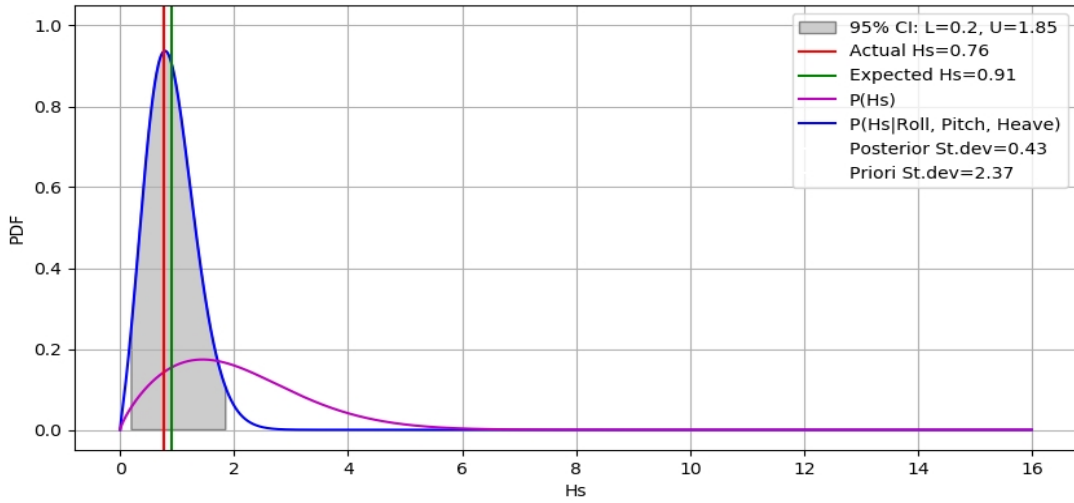


Figure I-38: A priori and posterior including actual and expected value (C3-Caribbean).

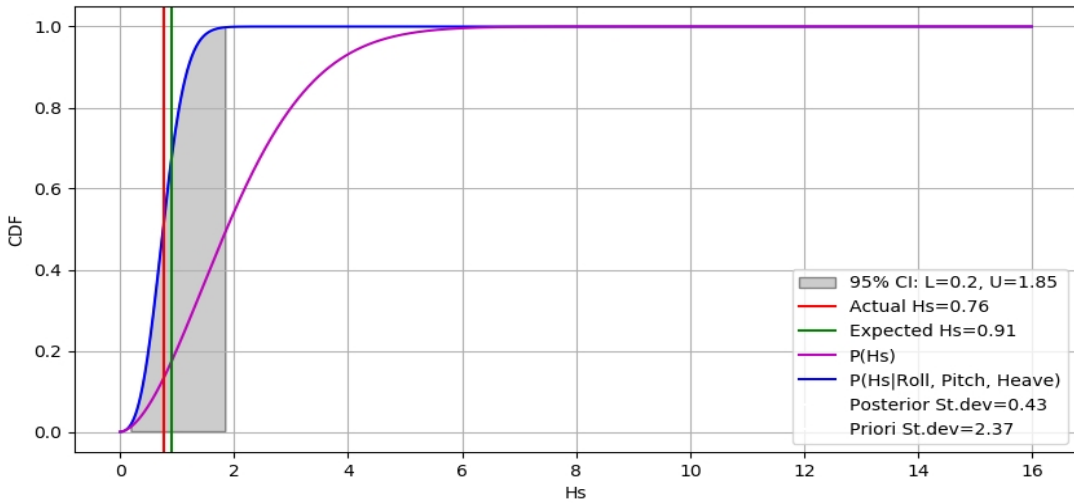


Figure I-39: Cum. a priori and posterior including actual and expected value (C3-Caribbean).

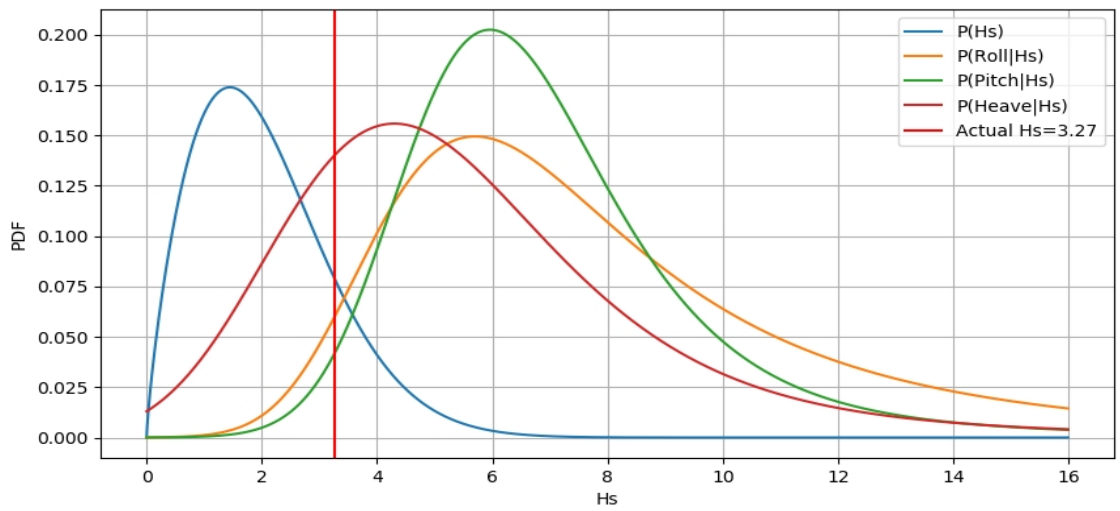


Figure I-40: A priori, and likelihood functions (C4-Caribbean).

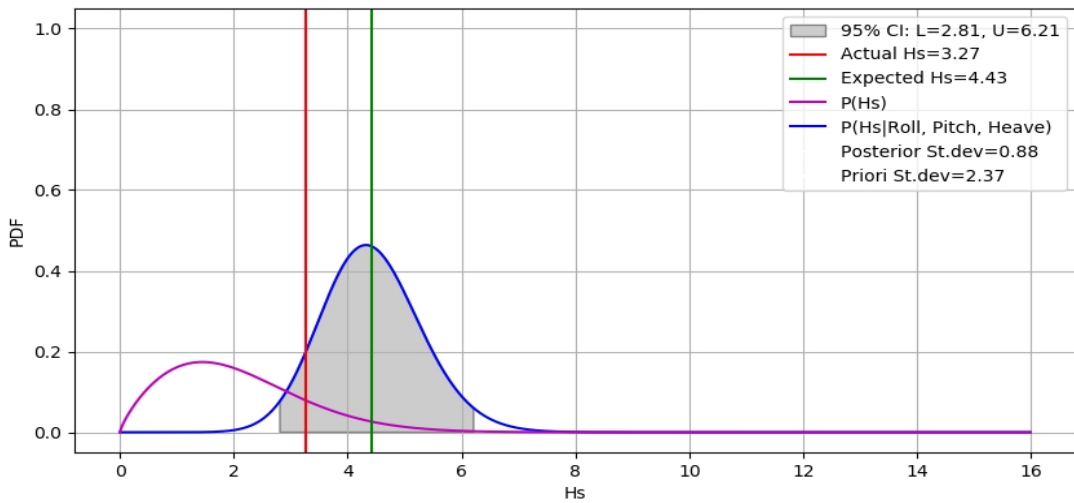


Figure I-41: A priori and posterior including actual and expected value (C4-Caribbean).

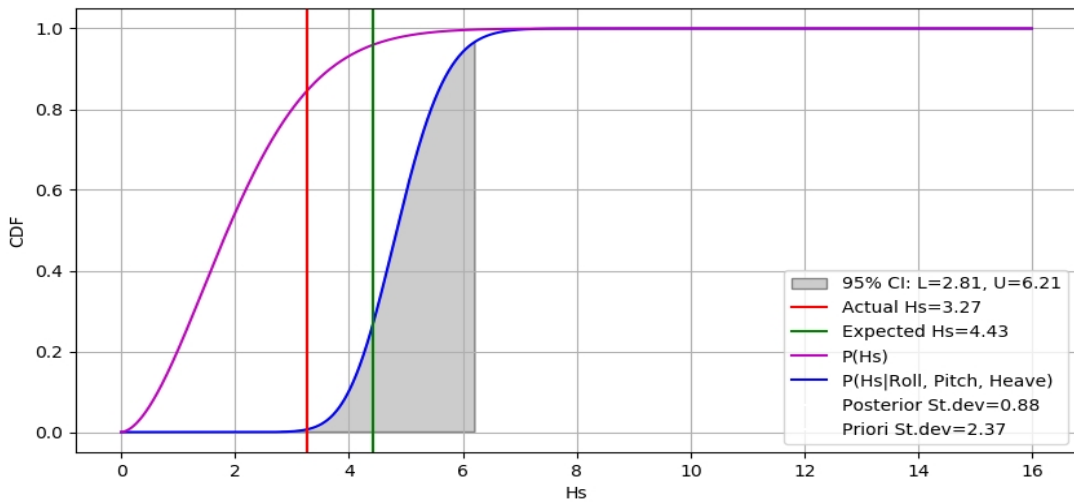


Figure I-42: Cum. a priori and posterior including actual and expected value (C4-Caribbean).

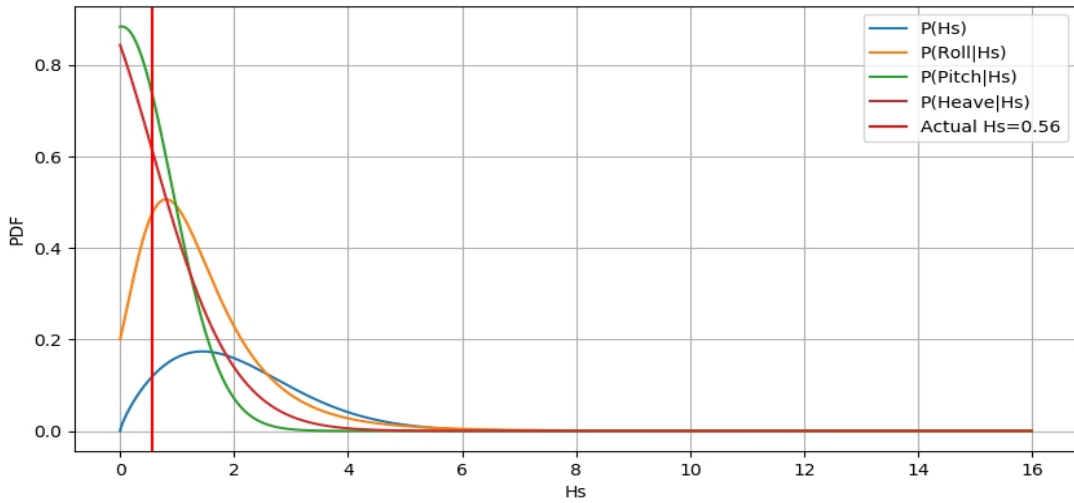


Figure I-43: A priori, and likelihood functions (C5-Caribbean).

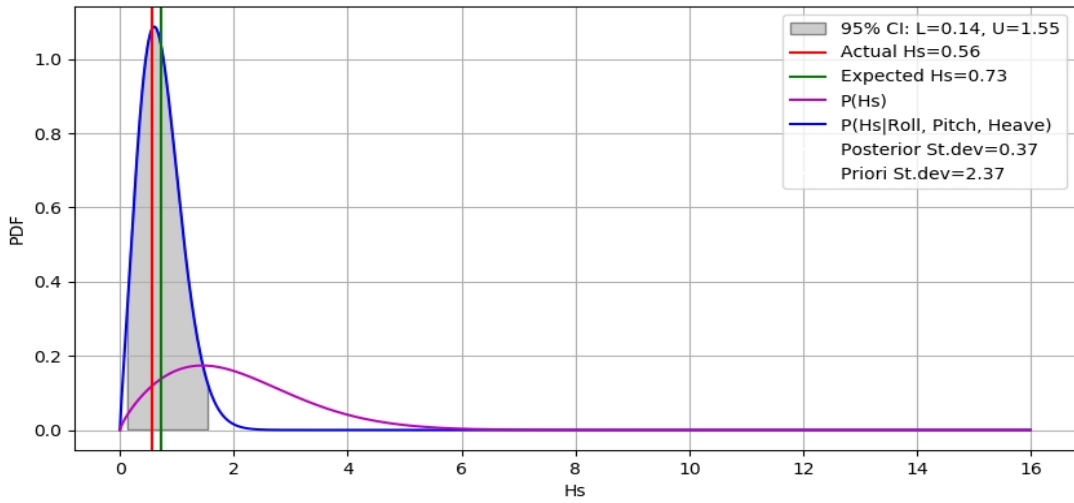


Figure I-44: A priori and posterior including actual and expected value (C5-Caribbean).

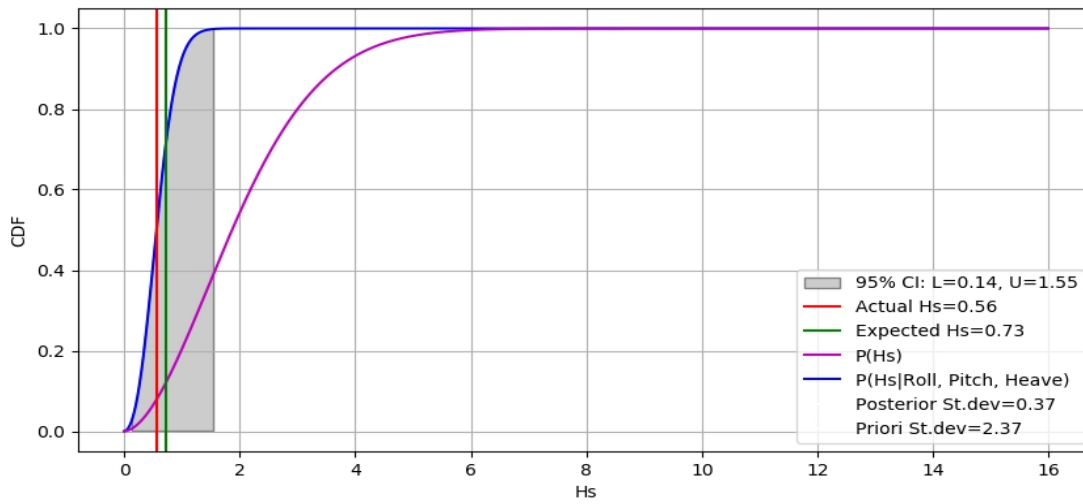


Figure I-45: Cum. a priori and posterior including actual and expected value (C5-Caribbean).

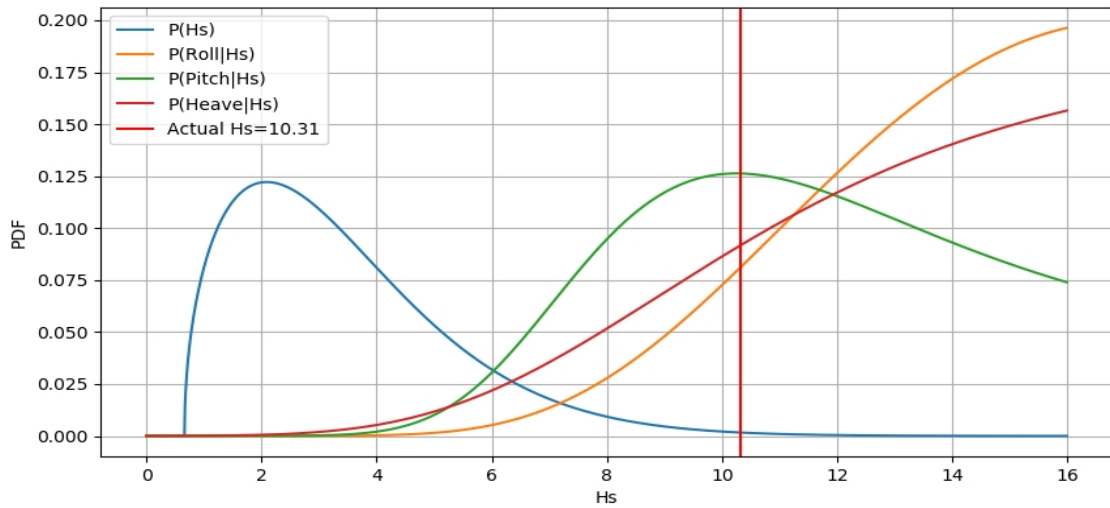


Figure I-46: A priori, and likelihood functions (C1-Extreme wave).

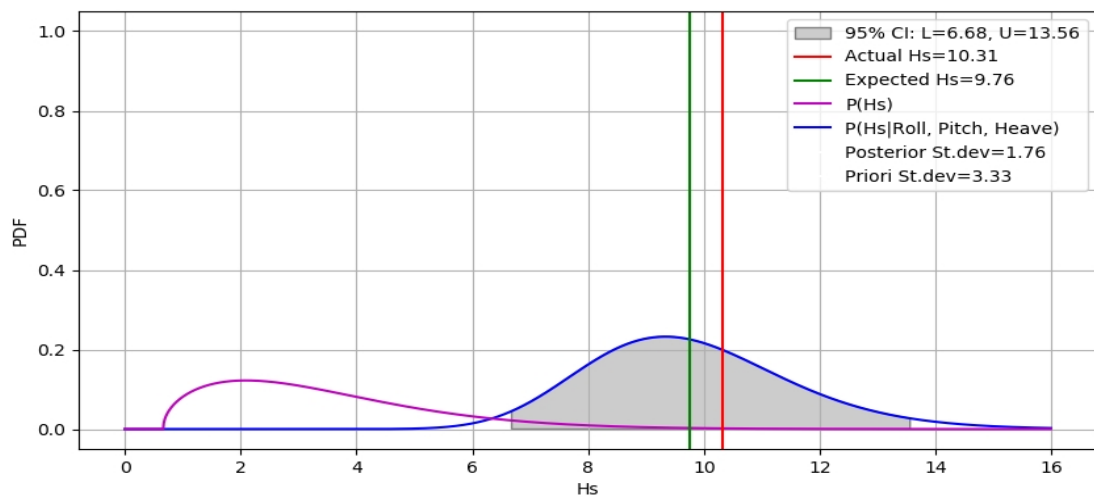


Figure I-47: A priori and posterior including actual and expected value (C1-Extreme wave).

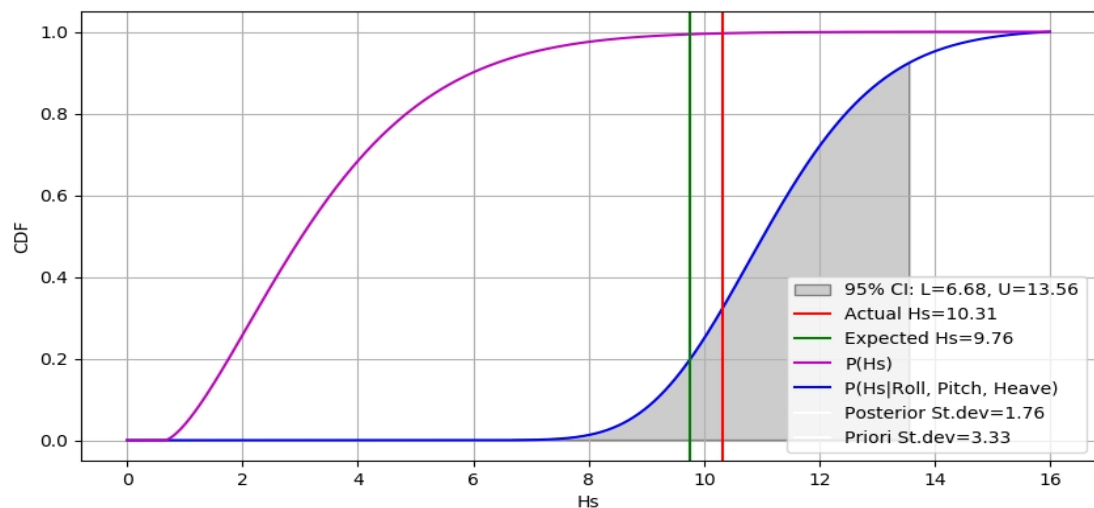


Figure I-48: Cum. a priori and posterior including actual and expected value (C1-Extreme wave).

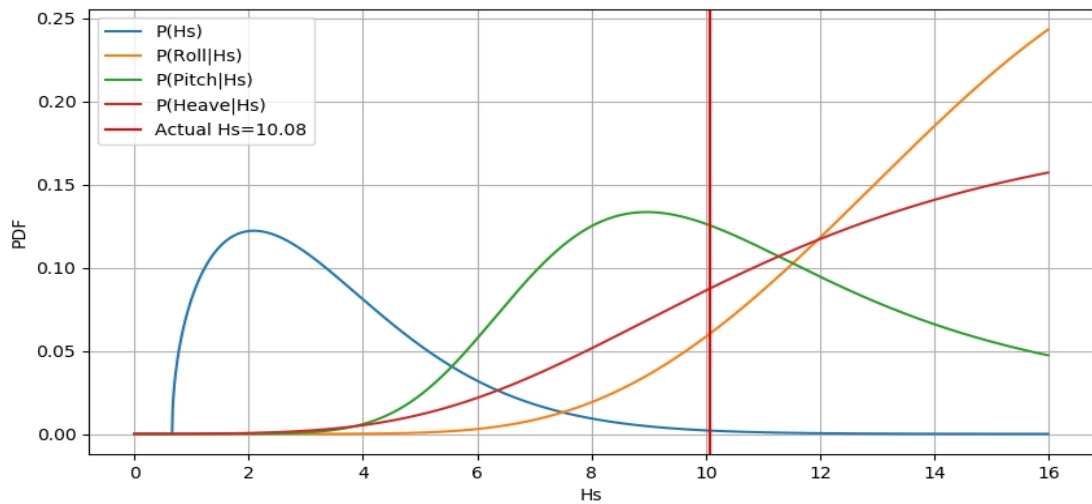


Figure I-49: A priori, and likelihood functions (C2-Extreme wave).

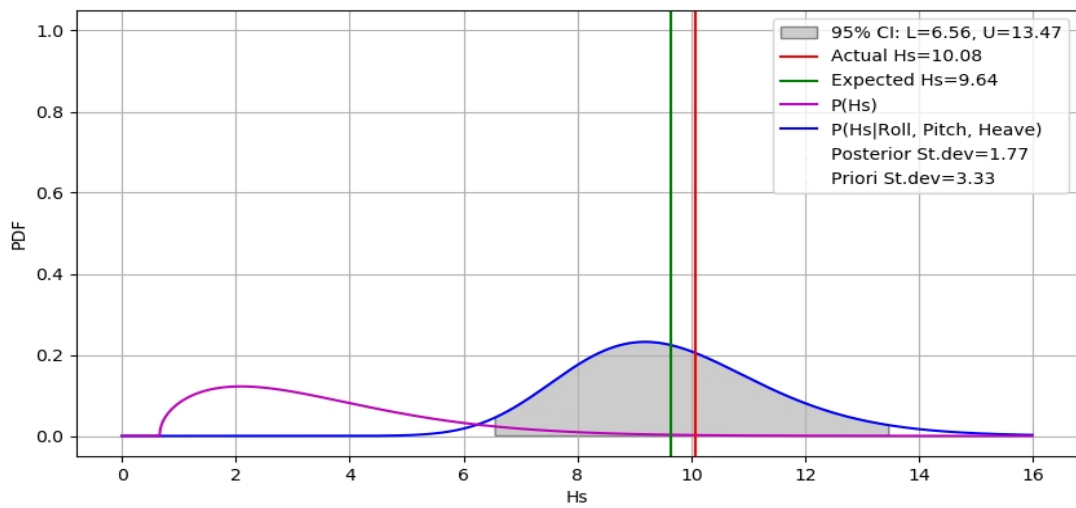


Figure I-50: A priori and posterior including actual and expected value (C2-Extreme wave).

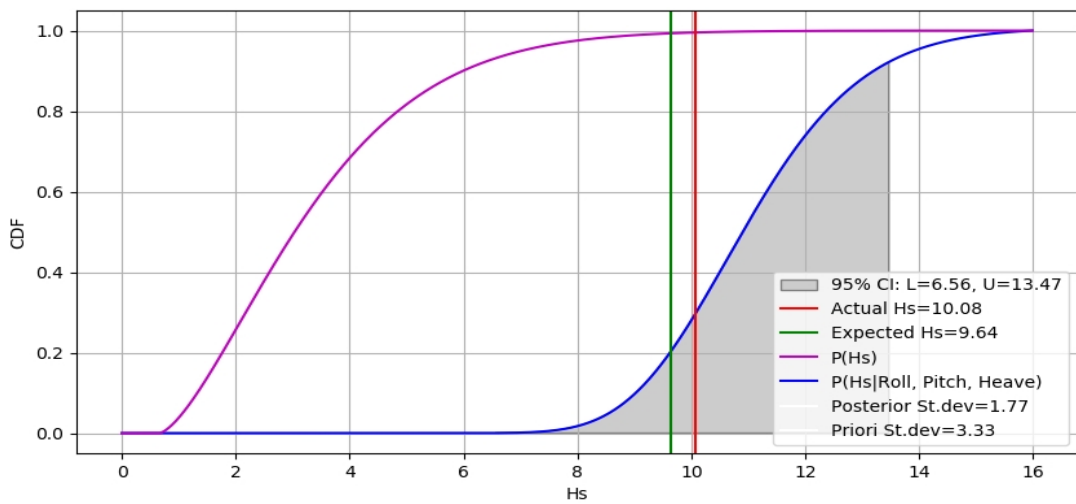


Figure I-51: Cum. a priori and posterior including actual and expected value (C2-Extreme wave).

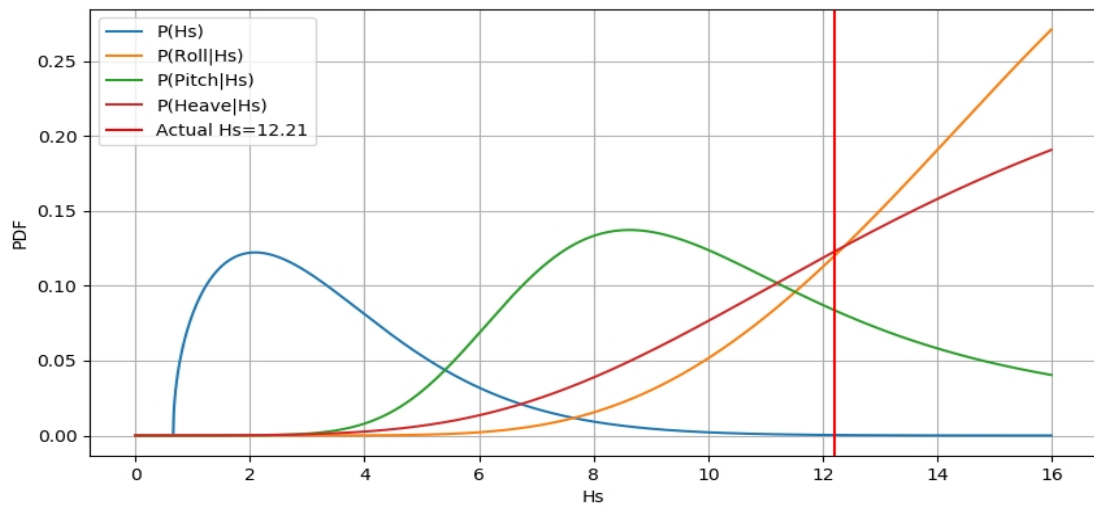


Figure I-52: A priori, and likelihood functions (C3-Extreme wave).

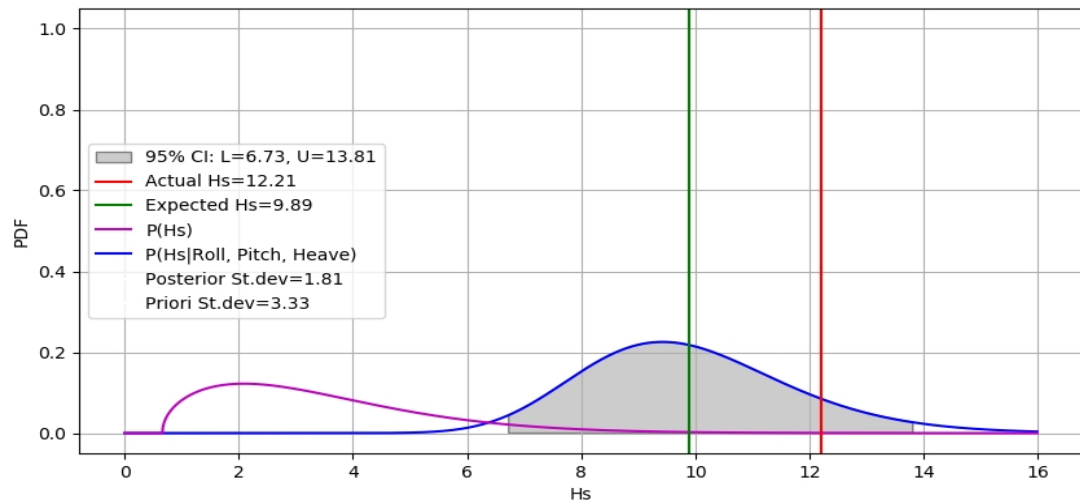


Figure I-53: A priori and posterior including actual and expected value (C3-Extreme wave).

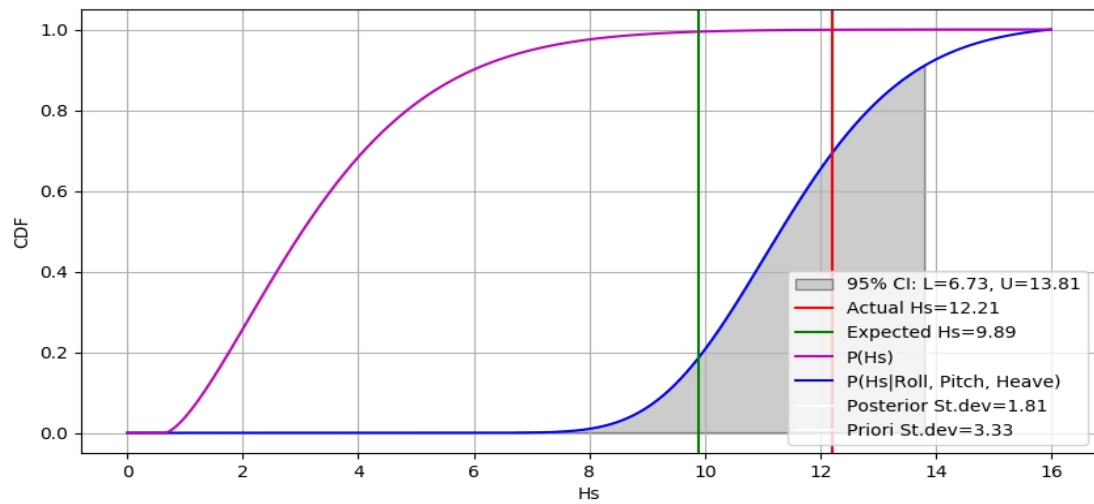


Figure I-54: Cum. a priori and posterior including actual and expected value (C3-Extreme wave).

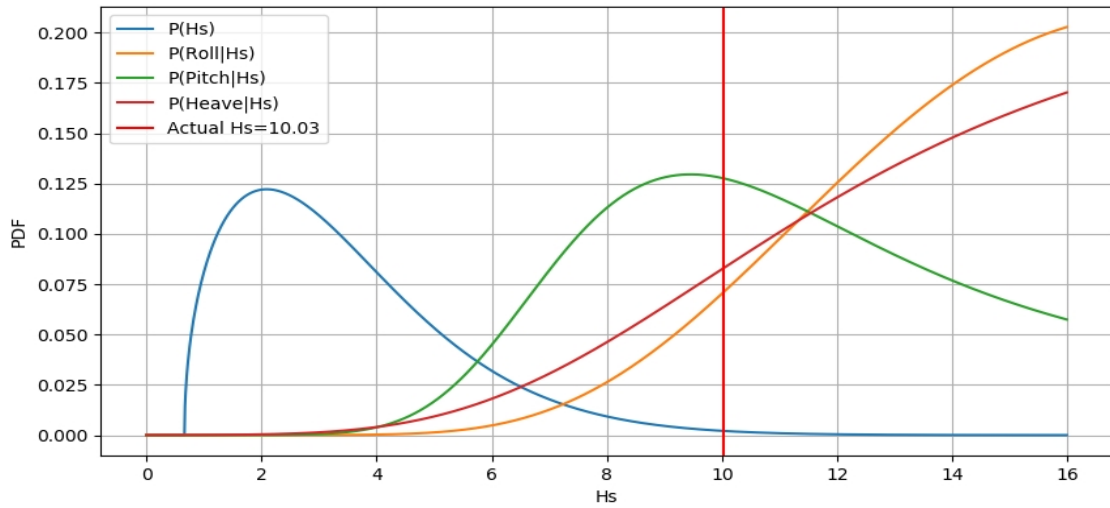


Figure I-55: A priori, and likelihood functions (C4-Extreme wave).

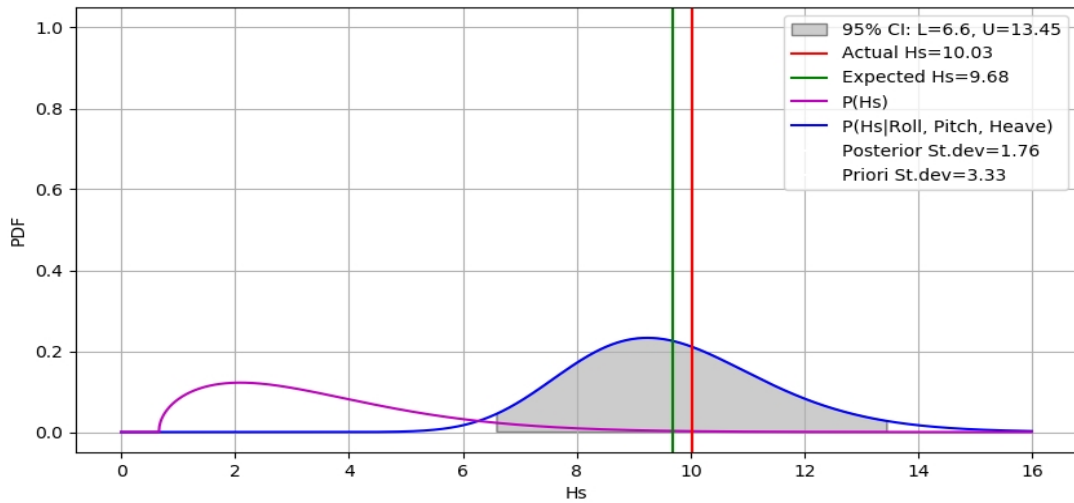


Figure I-56: A priori and posterior including actual and expected value (C4-Extreme wave).

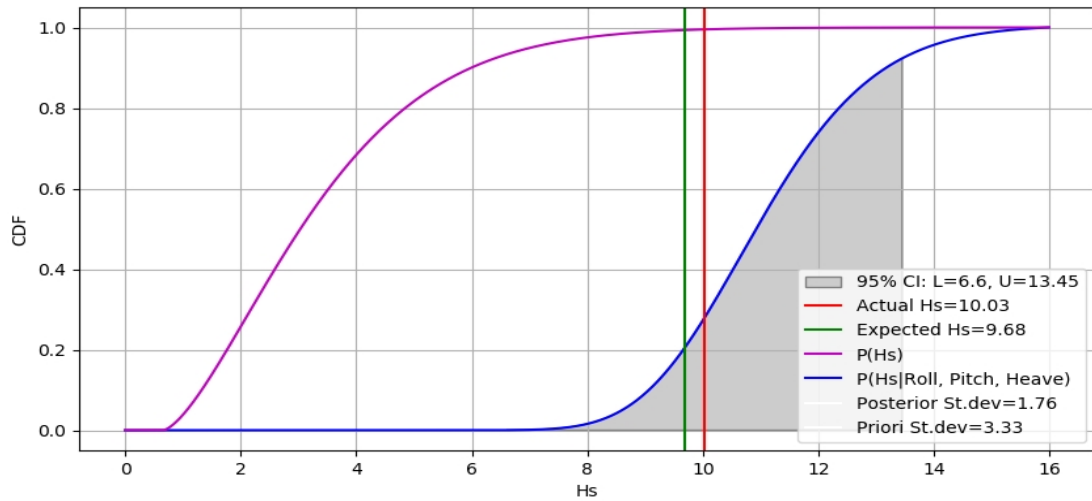


Figure I-57: Cum. a priori and posterior including actual and expected value (C4-Extreme wave).

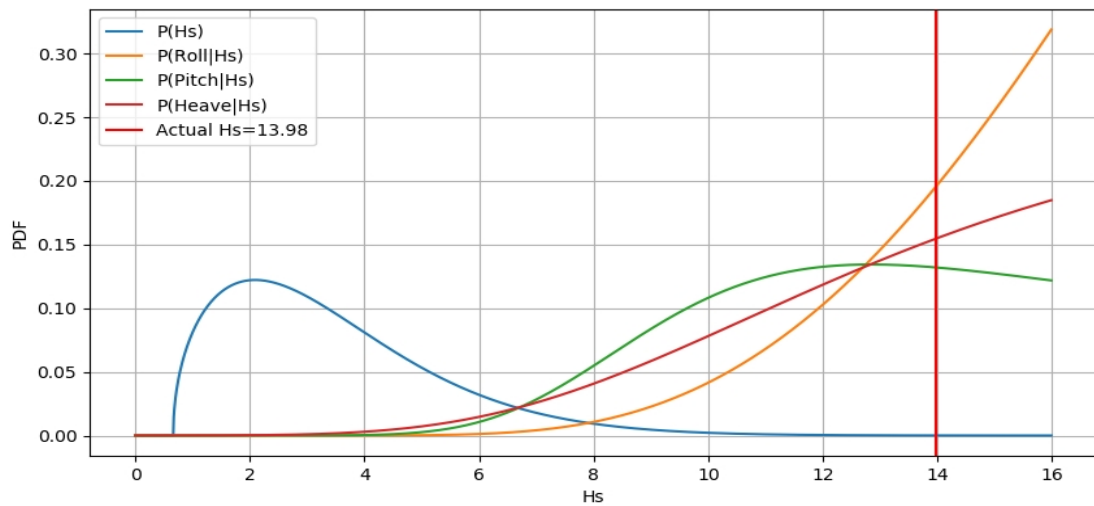


Figure I-58: A priori, and likelihood functions (C5- Extreme wave).

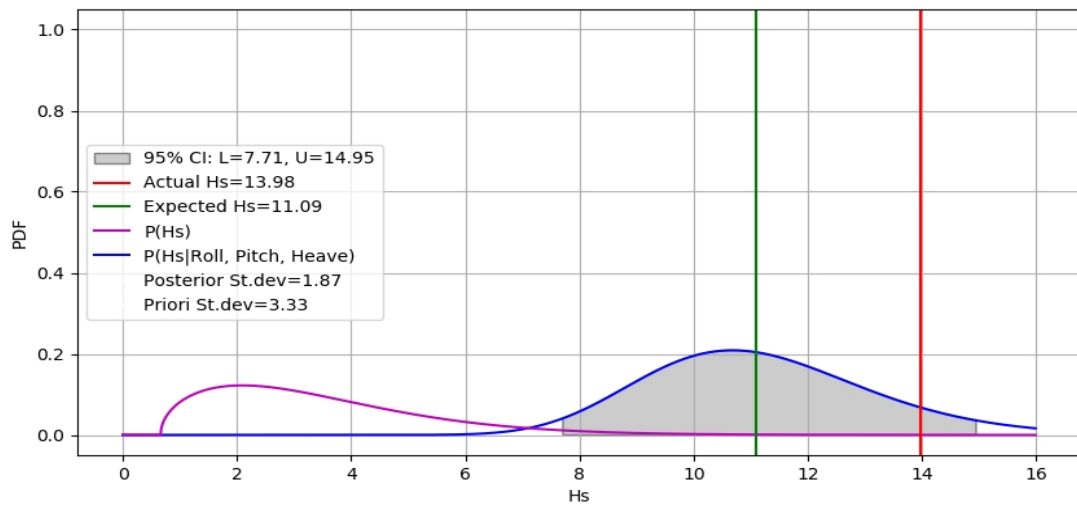


Figure I-59: A priori and posterior including actual and expected value (C5-Extreme wave).

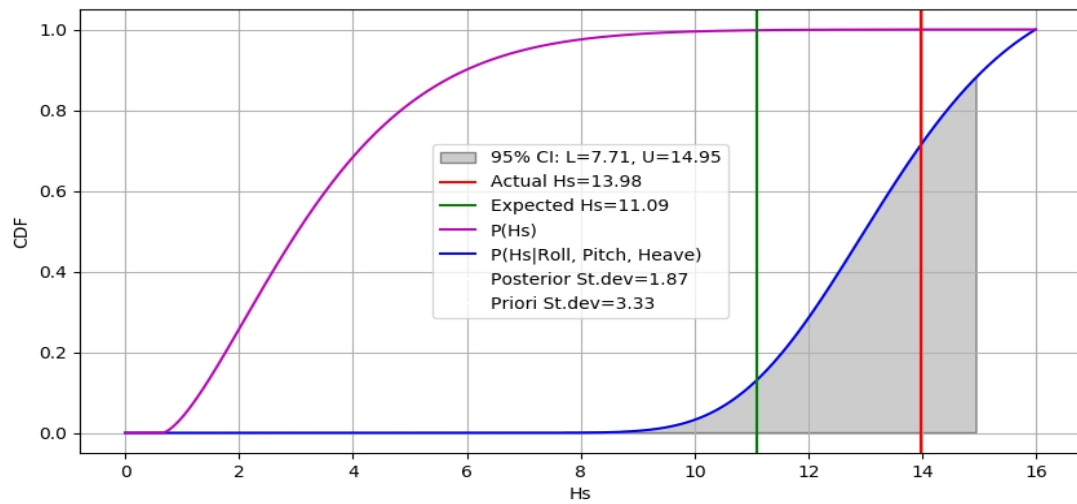


Figure I-60: Cum. a priori and posterior including actual and expected value (C5-Extreme wave).

Appendix II - GoF statistics for damage breach distributions with multiple distribution candidates

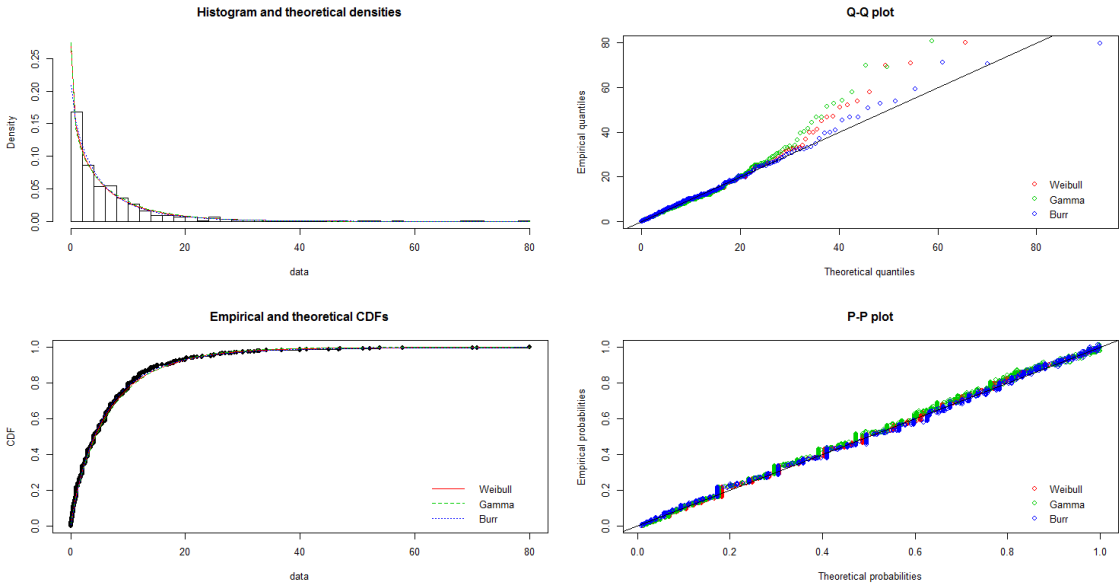


Figure II-1: GoF statistics for damage length L .

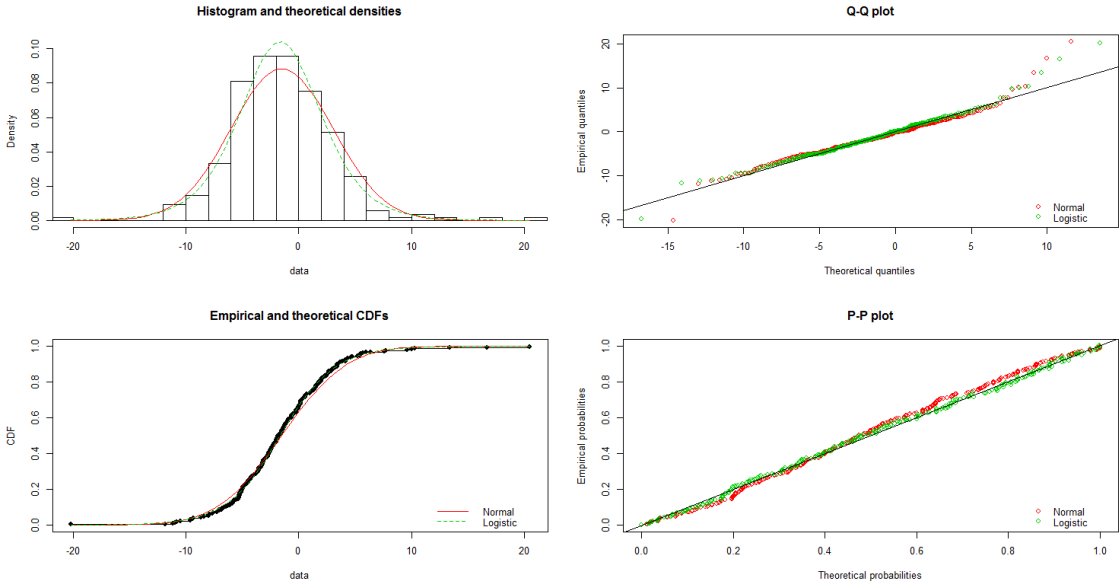


Figure II-2: GoF statistics for vertical damage location Z .

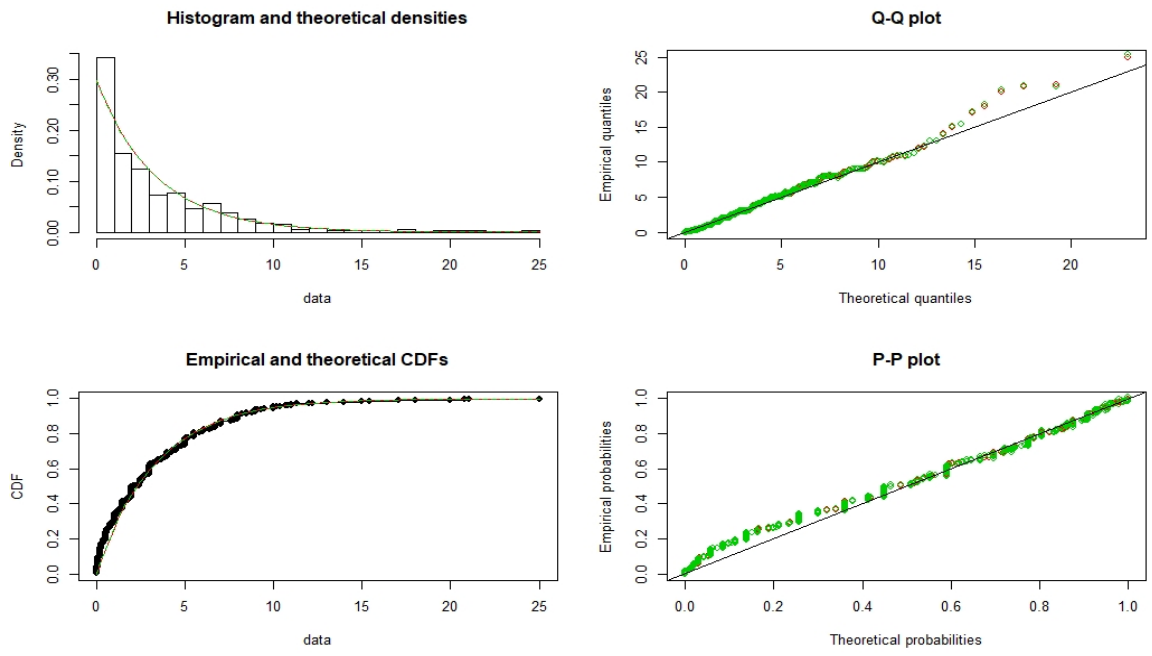


Figure II-3: GoF statistics for damage penetration Y .

Appendix III - Excerpt of (500) MC samples for initial damage extent

Table III-1: Excerpt of 500 samples from the Monte Carlo sampling for initial damage extent.

B. No.	X	Z	L	H	Y	B. No.	X	Z	L	H	Y
B1	270.908	6.737	11.473	3.488	0.317	B34	142.926	6.479	0.032	10.621	0.852
B2	257.282	0.000	8.178	4.201	0.865	B35	255.693	2.147	1.354	0.247	1.501
B3	178.174	6.482	3.794	3.113	0.475	B36	236.800	4.762	18.141	6.496	0.525
B4	243.536	4.168	12.225	2.429	2.185	B37	128.940	0.568	3.796	4.283	1.006
B5	-12.819	0.540	1.927	3.905	1.697	B38	199.539	6.099	4.538	0.759	2.845
B6	260.035	9.728	23.396	1.711	0.175	B39	258.903	6.771	1.801	1.724	4.034
B7	268.789	3.925	1.042	2.757	0.846	B40	78.265	6.743	2.147	4.221	5.745
B8	275.748	5.311	1.277	0.156	0.507	B41	257.131	4.584	2.622	4.377	2.012
B9	-0.229	4.898	3.811	9.439	0.575	B42	-2.703	2.860	4.438	3.383	0.526
B10	273.038	0.811	1.757	2.756	1.651	B43	242.604	4.291	5.696	3.552	1.715
B11	166.964	12.765	1.423	3.078	0.789	B44	8.085	9.025	15.356	8.075	1.125
B12	257.393	7.229	1.807	4.394	3.696	B45	159.661	10.062	23.072	7.038	1.068
B13	56.391	7.058	4.304	10.042	2.664	B46	49.405	4.421	21.118	3.818	0.667
B14	189.176	0.000	6.210	0.219	5.191	B47	253.404	8.607	3.721	2.041	7.877
B15	129.281	3.852	1.057	0.533	3.115	B48	6.327	9.788	10.272	0.912	2.076
B16	249.619	1.551	1.257	6.699	2.306	B49	245.491	10.033	0.877	1.546	1.932
B17	262.090	6.000	1.039	11.100	0.858	B50	36.150	6.588	7.127	0.028	0.055
B18	151.393	4.752	6.283	1.845	2.894	B51	172.408	8.652	0.699	6.631	0.760
B19	264.497	10.926	1.547	0.485	1.547	B52	-8.476	0.000	11.039	1.952	0.237
B20	228.345	0.061	29.777	6.231	1.556	B53	227.399	9.669	18.871	7.431	0.849
B21	165.228	6.671	0.278	0.061	1.369	B54	31.357	2.108	31.635	3.695	0.868
B22	254.509	5.520	5.129	5.627	1.673	B55	126.248	0.252	3.703	5.376	4.402
B23	234.554	5.297	5.500	2.927	0.016	B56	260.894	0.000	1.842	7.541	0.914
B24	-10.513	13.088	2.204	2.429	0.286	B57	265.030	5.344	5.715	3.975	0.859
B25	204.881	8.228	8.076	4.663	0.611	B58	225.369	15.377	17.684	1.723	0.338
B26	271.530	14.432	0.315	2.668	0.840	B59	270.000	0.000	10.663	3.230	0.497
B27	108.556	16.858	2.981	0.242	2.294	B60	102.674	7.821	1.734	1.576	2.113
B28	215.662	4.902	0.381	1.595	0.550	B61	43.462	3.261	2.911	12.665	5.261
B29	236.943	0.243	1.712	0.706	0.844	B62	225.701	9.478	3.702	2.390	1.526
B30	263.360	7.460	0.033	9.640	0.178	B63	268.418	1.598	5.487	9.584	1.987
B31	211.419	2.074	24.967	0.138	1.390	B64	241.219	2.104	8.527	2.086	0.906
B32	251.338	6.819	0.588	9.580	2.436	B65	244.284	10.235	7.238	0.330	1.957
B33	265.688	6.384	3.115	6.161	2.870	B66	88.859	0.000	0.394	0.400	2.121

B. No.	X	Z	L	H	Y	B. No.	X	Z	L	H	Y
B67	251.471	1.962	4.675	7.778	0.130	B109	267.014	5.680	21.904	7.969	3.084
B68	265.118	3.312	4.546	3.395	0.743	B110	194.685	4.329	0.220	8.989	0.967
B69	96.737	4.417	3.099	7.267	1.761	B111	129.598	2.241	0.715	4.295	0.573
B70	76.753	8.157	3.825	1.165	0.642	B112	192.627	5.341	1.616	6.756	3.250
B71	52.222	5.340	7.081	4.790	2.261	B113	11.216	9.600	28.019	6.077	1.666
B72	218.639	9.308	19.350	2.356	0.217	B114	-10.951	10.616	2.632	3.884	0.458
B73	74.146	6.716	10.503	10.384	0.030	B115	16.332	7.694	2.226	0.268	0.074
B74	210.457	4.159	18.981	7.771	0.910	B116	263.713	6.431	7.230	10.669	0.853
B75	239.190	4.651	3.991	4.296	2.049	B117	237.262	13.588	14.284	0.797	3.800
B76	146.950	8.016	1.496	9.084	1.167	B118	20.623	1.934	4.372	1.798	0.028
B77	268.227	8.376	0.151	8.724	2.398	B119	216.837	4.857	1.800	6.243	4.119
B78	-12.708	5.884	2.584	0.333	0.094	B120	262.326	0.626	4.893	4.573	0.718
B79	78.146	8.323	0.564	0.185	1.527	B121	58.327	3.871	4.485	6.460	0.238
B80	259.476	7.829	2.384	9.271	0.498	B122	250.360	4.705	28.757	1.140	5.091
B81	265.346	5.644	20.995	9.547	5.552	B123	130.474	12.677	9.841	2.706	0.189
B82	270.518	11.795	14.939	5.305	3.592	B124	274.852	0.846	5.862	0.018	0.668
B83	222.681	3.617	6.978	5.637	7.225	B125	201.538	4.109	8.268	12.991	1.702
B84	256.952	3.177	8.627	2.680	1.631	B126	219.165	11.819	6.787	0.267	0.113
B85	41.634	6.242	6.103	2.347	0.152	B127	79.541	4.377	3.657	6.295	7.902
B86	152.082	2.946	1.136	8.599	1.122	B128	84.737	0.000	22.129	3.890	1.536
B87	200.854	6.992	7.962	10.108	2.165	B129	150.692	3.629	0.857	5.470	1.046
B88	188.563	3.789	10.775	8.193	1.734	B130	84.663	14.514	0.808	2.586	1.183
B89	207.485	9.937	1.973	1.387	1.107	B131	70.741	0.000	1.801	6.898	6.011
B90	275.172	7.551	0.260	0.196	5.899	B132	254.597	4.115	11.809	10.305	0.962
B91	62.295	3.268	11.112	0.530	1.040	B133	241.047	2.685	15.373	3.317	1.396
B92	270.290	9.442	3.602	0.763	0.791	B134	258.972	6.589	3.590	10.511	2.879
B93	266.041	0.000	6.831	4.761	1.201	B135	273.963	1.198	2.457	5.383	1.202
B94	240.013	10.452	3.243	3.541	2.029	B136	256.082	13.293	4.819	3.807	0.168
B95	239.716	0.000	1.486	4.263	0.377	B137	47.225	7.362	10.716	0.709	2.214
B96	193.364	4.717	6.897	5.714	2.320	B138	179.298	7.027	12.222	0.212	1.272
B97	57.637	1.654	5.132	6.532	2.732	B139	265.841	5.901	24.230	0.068	3.612
B98	84.419	7.197	8.528	1.783	0.151	B140	236.791	9.251	0.406	3.100	0.057
B99	257.143	7.659	2.052	5.074	1.877	B141	246.789	5.453	5.593	3.055	0.799
B100	39.353	5.820	23.947	1.087	2.863	B142	109.967	11.263	1.348	5.837	0.520
B101	266.476	6.543	9.105	8.981	4.289	B143	55.881	0.000	3.146	4.120	8.007
B102	226.362	7.474	3.245	0.314	3.206	B144	101.802	6.686	7.909	4.090	0.786
B103	77.927	7.301	7.202	3.669	2.392	B145	155.878	6.370	4.455	0.758	2.650
B104	88.123	0.000	5.177	17.047	3.511	B146	172.733	6.076	13.257	7.150	0.975
B105	276.998	2.048	1.998	15.052	2.689	B147	104.111	9.876	8.452	7.224	0.377
B106	97.026	7.072	2.071	1.690	2.431	B148	36.485	0.000	0.700	2.438	2.660
B107	257.649	4.602	1.885	3.434	0.361	B149	276.117	0.000	3.760	7.506	1.226
B108	81.170	10.904	4.307	1.356	2.305	B150	93.843	3.296	0.717	10.311	1.152

B. No.	X	Z	L	H	Y	B. No.	X	Z	L	H	Y
B151	247.343	11.452	2.591	0.034	0.523	B193	256.620	10.234	11.542	0.027	2.208
B152	261.313	6.893	1.697	4.069	3.836	B194	214.278	3.956	6.748	6.547	0.112
B153	264.611	4.772	1.839	4.056	0.593	B195	63.533	1.109	0.039	5.584	0.154
B154	260.915	1.011	31.345	4.335	0.407	B196	157.461	8.436	3.625	4.035	8.016
B155	255.860	3.909	7.953	4.420	0.668	B197	263.809	4.667	3.232	2.134	1.523
B156	99.363	2.104	9.457	3.366	2.971	B198	53.859	16.100	1.462	1.000	7.990
B157	265.473	4.564	18.307	12.536	0.055	B199	263.360	3.453	0.173	11.698	0.281
B158	93.617	6.260	8.479	4.509	0.325	B200	113.582	16.959	4.809	0.141	0.818
B159	78.650	6.856	35.217	5.478	2.528	B201	242.051	5.603	17.950	6.393	0.352
B160	152.013	8.653	0.849	8.447	3.341	B202	252.949	4.383	3.233	4.473	1.092
B161	131.586	13.662	0.942	0.542	1.596	B203	262.466	5.922	0.662	0.525	2.327
B162	38.038	4.335	7.836	11.226	2.236	B204	190.657	1.847	7.181	3.103	0.633
B163	96.109	13.911	3.436	3.189	1.449	B205	126.414	4.139	2.896	0.601	5.039
B164	135.092	10.564	1.656	1.421	2.495	B206	185.436	6.663	2.329	2.566	4.136
B165	103.696	6.580	8.557	10.139	1.666	B207	262.745	11.119	3.795	5.625	0.718
B166	218.363	8.923	3.164	1.400	0.166	B208	234.452	12.942	1.266	1.944	0.510
B167	220.376	7.593	5.766	7.470	1.446	B209	191.791	4.003	2.471	13.097	2.585
B168	264.822	0.044	1.650	5.052	0.933	B210	262.269	8.332	1.972	1.734	0.237
B169	197.874	14.088	2.062	3.012	1.483	B211	161.683	3.035	5.866	14.065	1.382
B170	166.943	0.306	3.798	4.330	6.416	B212	228.728	4.679	7.441	5.974	0.560
B171	215.251	10.069	3.994	4.761	0.131	B213	40.039	0.313	0.272	5.396	1.566
B172	248.454	3.874	3.482	6.610	0.452	B214	269.009	1.272	2.918	5.438	0.727
B173	42.609	11.262	4.008	5.838	9.469	B215	271.452	5.956	10.516	1.633	5.854
B174	112.855	4.608	2.411	12.324	1.576	B216	50.370	9.366	0.078	2.544	0.718
B175	240.871	6.768	7.696	1.159	1.706	B217	253.040	9.416	1.830	7.198	0.920
B176	238.965	8.866	12.213	5.516	0.089	B218	128.690	5.360	68.380	7.512	0.975
B177	265.240	15.344	1.913	0.737	1.922	B219	262.703	2.283	1.766	4.305	0.730
B178	81.596	5.825	13.199	11.275	1.152	B220	257.150	0.885	13.174	3.761	0.397
B179	247.957	6.694	6.203	2.774	2.118	B221	107.698	7.721	3.936	3.415	0.741
B180	205.674	8.903	3.349	1.368	0.161	B222	239.501	8.945	2.646	5.317	0.955
B181	220.128	8.214	18.670	4.423	0.075	B223	183.368	6.836	4.598	1.739	6.817
B182	77.763	7.236	0.821	2.134	1.760	B224	113.350	16.555	0.810	0.545	0.054
B183	155.538	2.484	4.768	4.281	0.989	B225	187.963	15.454	1.784	1.646	0.772
B184	241.275	3.365	0.165	8.866	0.623	B226	229.516	12.498	2.828	4.602	1.861
B185	138.738	13.386	23.547	2.660	1.264	B227	257.551	0.000	15.425	9.718	0.972
B186	165.446	0.000	0.467	0.610	3.735	B228	242.265	7.744	6.162	4.094	1.079
B187	140.439	7.282	2.722	9.818	4.726	B229	266.261	12.254	0.810	1.323	3.199
B188	217.851	3.584	1.182	6.704	1.086	B230	146.234	4.133	4.258	0.489	0.570
B189	232.410	0.000	9.222	0.698	0.598	B231	266.883	4.057	4.909	3.860	0.490
B190	-11.432	6.076	5.135	6.198	1.670	B232	93.957	9.380	1.653	7.720	0.928
B191	260.780	9.767	2.833	1.231	1.468	B233	156.313	2.722	2.322	5.181	0.331
B192	257.979	5.968	6.577	11.132	0.376	B234	263.275	8.367	15.048	5.872	1.920

B. No.	X	Z	L	H	Y	B. No.	X	Z	L	H	Y
B235	173.268	6.146	0.240	3.039	3.462	B277	153.655	8.404	6.915	4.734	2.889
B236	224.173	0.000	10.986	2.491	1.777	B278	176.014	10.059	42.627	6.108	11.860
B237	181.842	16.897	4.014	0.203	2.371	B279	192.893	10.675	17.771	0.345	0.469
B238	9.288	0.000	3.020	0.267	1.227	B280	253.460	5.459	19.908	4.943	2.037
B239	136.079	4.755	7.067	1.333	1.719	B281	150.396	5.416	5.017	11.684	3.917
B240	254.602	6.900	3.656	10.200	0.419	B282	34.785	10.055	1.586	7.045	1.610
B241	71.033	7.449	7.189	9.497	1.728	B283	240.115	4.096	5.318	3.760	0.196
B242	256.032	4.810	7.606	0.856	0.133	B284	111.270	7.342	0.105	4.978	3.939
B243	91.759	0.000	0.426	8.886	3.900	B285	240.985	5.090	0.560	6.402	1.143
B244	192.197	7.459	0.918	2.444	1.410	B286	267.462	4.499	0.641	9.221	0.659
B245	238.788	9.110	0.557	0.338	0.206	B287	128.595	11.213	26.080	0.236	0.918
B246	86.323	9.097	13.864	4.522	3.432	B288	273.670	15.248	8.650	1.852	0.248
B247	-2.803	7.876	21.117	1.357	0.077	B289	215.120	11.030	0.877	2.361	1.440
B248	277.437	11.030	1.121	4.204	4.314	B290	156.390	6.715	0.006	8.987	1.036
B249	252.396	8.006	15.923	0.286	1.143	B291	14.809	4.993	3.614	12.107	6.291
B250	75.106	5.466	2.015	0.242	0.076	B292	122.943	5.664	1.961	2.746	1.947
B251	81.968	4.669	1.793	0.807	1.553	B293	263.267	2.481	2.204	10.806	3.723
B252	190.674	12.035	0.038	5.065	0.375	B294	202.020	5.066	0.450	1.991	0.881
B253	128.869	5.872	3.160	6.315	2.142	B295	255.821	5.608	11.083	3.569	0.156
B254	45.951	9.294	7.990	7.806	1.906	B296	248.414	3.847	29.153	6.045	0.966
B255	56.572	9.153	2.051	0.042	0.331	B297	249.775	15.157	7.158	1.943	3.062
B256	-5.444	5.505	3.937	2.602	2.009	B298	162.818	4.611	13.981	1.718	1.238
B257	74.502	15.669	1.836	1.431	1.046	B299	198.419	9.830	4.491	7.270	0.030
B258	249.520	4.880	1.623	12.220	0.259	B300	261.508	4.566	0.778	10.722	0.132
B259	195.518	10.034	0.798	7.066	0.149	B301	47.424	0.000	0.216	1.557	3.902
B260	265.943	8.368	1.163	0.026	7.901	B302	239.491	4.272	4.683	0.151	0.597
B261	249.341	4.960	1.878	12.140	3.274	B303	227.582	5.116	3.779	11.984	2.325
B262	267.000	5.646	1.055	2.163	3.606	B304	66.853	0.000	15.575	1.370	0.168
B263	257.829	6.408	5.103	4.619	0.395	B305	257.445	11.737	3.686	5.363	0.258
B264	257.350	10.082	6.053	4.076	1.427	B306	259.032	3.499	4.449	3.538	1.622
B265	262.178	4.014	9.373	2.219	1.240	B307	265.839	10.665	7.963	6.435	0.724
B266	242.175	1.169	4.598	0.833	4.578	B308	151.739	7.349	4.998	7.624	1.997
B267	28.399	8.184	0.442	0.415	0.862	B309	14.152	6.374	2.544	1.430	0.070
B268	102.289	9.527	26.010	4.524	5.557	B310	239.027	5.287	1.104	11.813	0.758
B269	264.233	4.006	1.552	13.094	0.817	B311	269.965	10.276	5.196	4.103	1.170
B270	266.048	11.759	1.548	3.124	3.304	B312	23.741	6.367	3.162	2.605	0.298
B271	230.078	2.988	1.470	1.942	3.163	B313	248.905	11.374	1.644	0.107	1.848
B272	245.356	0.000	2.383	3.505	5.622	B314	62.649	13.678	4.568	3.318	3.284
B273	200.728	7.380	1.367	7.544	0.093	B315	59.943	0.000	6.156	4.504	0.074
B274	181.751	4.254	19.367	10.629	3.233	B316	261.430	5.079	2.393	2.840	0.096
B275	80.424	11.052	5.445	1.050	0.942	B317	37.167	15.538	2.492	1.562	1.374
B276	262.835	5.736	3.774	3.527	0.359	B318	50.844	8.712	18.443	5.563	2.210

B. No.	X	Z	L	H	Y	B. No.	X	Z	L	H	Y
B319	264.254	10.219	4.174	0.475	2.357	B361	273.752	3.414	2.622	8.808	0.331
B320	90.865	1.574	1.714	5.181	1.666	B362	5.299	5.824	2.901	3.834	0.985
B321	223.120	8.005	1.410	9.095	5.258	B363	250.705	0.000	2.644	4.058	0.355
B322	188.378	0.000	11.404	4.105	0.190	B364	244.454	10.201	6.112	0.698	0.145
B323	69.993	11.792	0.715	5.308	0.167	B365	268.897	8.822	6.034	7.428	0.604
B324	97.551	4.765	13.190	0.375	2.311	B366	261.037	8.920	3.921	3.806	0.233
B325	264.510	9.564	1.892	6.898	5.973	B367	173.830	5.559	3.012	5.389	0.923
B326	18.371	15.412	5.214	1.688	0.688	B368	266.924	0.000	1.384	0.295	4.607
B327	91.501	7.430	3.223	3.884	4.074	B369	253.835	16.230	1.621	0.870	0.801
B328	159.265	0.000	6.365	9.679	1.181	B370	194.013	4.516	2.923	12.584	1.028
B329	124.708	6.839	17.097	0.193	3.783	B371	257.254	3.851	0.069	1.310	9.417
B330	266.101	5.074	8.825	12.026	7.474	B372	251.774	13.659	17.325	0.346	0.812
B331	247.838	7.699	6.146	3.226	1.780	B373	10.255	8.807	0.553	7.280	0.237
B332	124.957	5.266	16.644	2.348	2.548	B374	228.731	9.934	3.323	4.717	0.854
B333	260.672	2.770	4.816	6.122	17.114	B375	172.244	12.263	11.618	0.942	0.509
B334	169.215	8.415	8.385	3.164	0.563	B376	189.575	4.447	4.371	3.158	1.378
B335	196.687	16.365	9.538	0.735	1.110	B377	262.153	1.822	3.998	3.122	1.927
B336	38.490	0.000	6.628	3.279	2.727	B378	249.545	1.348	2.808	15.752	0.787
B337	252.967	8.354	18.332	5.014	2.782	B379	163.540	5.423	12.785	4.836	2.869
B338	129.657	2.399	1.854	3.538	0.444	B380	276.542	4.256	2.909	5.233	6.598
B339	251.344	0.000	7.830	8.536	3.005	B381	264.645	0.000	5.814	5.298	4.701
B340	164.541	7.529	3.812	1.089	1.075	B382	122.175	11.942	7.285	0.224	0.227
B341	191.586	3.796	0.655	13.183	1.216	B383	174.084	6.984	32.501	2.218	1.590
B342	248.303	3.570	1.789	5.259	1.723	B384	269.631	5.005	1.444	4.406	0.028
B343	239.568	12.102	2.399	4.998	1.534	B385	124.242	6.119	2.287	0.702	1.978
B344	2.649	8.147	0.044	5.810	4.584	B386	117.890	8.987	7.366	4.302	3.076
B345	-10.943	7.567	6.112	0.488	0.756	B387	179.815	3.071	24.301	4.835	11.779
B346	187.697	4.259	0.118	4.322	0.463	B388	28.597	7.481	2.103	8.232	2.661
B347	266.816	13.836	14.217	0.893	2.416	B389	224.618	6.847	0.308	1.529	6.378
B348	259.344	11.119	0.200	0.077	4.797	B390	189.176	8.749	15.851	8.351	0.767
B349	84.775	5.034	0.718	4.021	1.276	B391	205.561	5.134	4.274	4.279	1.946
B350	246.106	7.986	29.074	0.442	4.103	B392	276.066	4.661	3.861	11.731	6.094
B351	77.687	0.000	12.830	2.197	2.598	B393	3.125	10.641	8.073	6.459	0.317
B352	9.305	7.361	9.505	2.148	4.123	B394	-7.976	8.497	1.890	8.603	2.249
B353	269.358	2.922	0.231	2.904	1.859	B395	252.289	7.671	8.475	5.363	1.005
B354	218.923	3.962	1.025	11.970	0.196	B396	260.694	5.257	2.581	0.028	0.254
B355	177.764	6.401	24.164	0.000	1.185	B397	209.448	5.744	0.888	0.194	0.643
B356	122.041	4.219	21.847	0.578	4.064	B398	157.588	7.190	0.839	1.777	2.047
B357	269.880	4.383	7.964	2.007	0.032	B399	267.043	8.609	7.479	8.491	0.328
B358	76.214	7.628	11.707	3.110	1.991	B400	147.214	6.009	11.760	3.499	0.501
B359	222.696	0.000	0.410	0.865	6.176	B401	60.319	5.483	6.006	6.067	1.176
B360	267.448	14.509	10.084	1.020	2.043	B402	241.469	4.186	0.578	3.408	3.236

B. No.	X	Z	L	H	Y	B. No.	X	Z	L	H	Y
B403	212.697	8.411	2.355	0.363	0.546	B445	112.511	12.515	0.904	4.585	0.286
B404	240.786	1.310	2.324	14.124	7.593	B446	249.353	0.000	12.808	3.395	3.493
B405	264.693	0.529	3.623	12.122	0.284	B447	85.747	11.462	6.627	5.638	0.235
B406	55.846	0.376	2.829	6.313	7.232	B448	265.588	3.615	8.243	1.688	3.915
B407	216.845	4.012	0.290	4.616	2.002	B449	84.275	4.918	1.431	0.899	3.117
B408	117.090	6.582	16.386	2.280	0.392	B450	61.295	7.357	2.472	9.437	0.566
B409	110.859	10.818	2.516	2.236	0.724	B451	272.601	6.974	2.808	7.317	1.965
B410	248.301	6.904	0.835	0.553	0.402	B452	261.564	3.963	22.301	7.812	0.013
B411	231.132	11.511	4.237	5.589	2.195	B453	274.463	4.736	7.065	0.198	0.852
B412	254.557	4.163	29.608	2.766	0.961	B454	262.652	1.216	3.316	0.774	1.196
B413	58.748	0.634	3.199	1.778	3.859	B455	257.797	14.017	7.527	3.083	9.883
B414	159.015	0.000	5.405	1.192	0.185	B456	63.507	4.471	1.099	3.588	0.345
B415	44.390	7.009	9.986	2.776	3.191	B457	246.395	15.447	1.799	1.653	2.170
B416	2.814	10.508	1.347	1.090	0.208	B458	238.720	5.400	14.782	2.218	0.652
B417	216.101	9.054	4.829	3.148	1.090	B459	256.072	12.422	0.430	4.678	0.735
B418	101.847	0.000	8.025	0.980	0.341	B460	39.205	4.026	18.590	1.986	0.054
B419	264.748	6.581	0.237	0.399	0.647	B461	49.147	0.000	2.457	14.174	2.276
B420	-8.159	8.716	7.053	4.072	1.461	B462	28.379	4.856	10.132	0.543	0.163
B421	271.499	8.982	0.445	1.775	1.954	B463	206.783	0.282	1.600	0.006	1.174
B422	64.165	3.611	0.467	13.489	1.417	B464	243.224	2.548	26.264	4.653	0.337
B423	256.459	3.030	8.785	4.289	2.383	B465	235.013	10.005	3.788	0.788	1.079
B424	130.261	12.800	3.273	0.098	0.873	B466	194.096	1.563	7.328	0.851	4.639
B425	145.517	6.395	1.143	2.645	1.964	B467	260.751	5.698	4.092	2.064	0.545
B426	144.922	2.995	5.951	9.118	0.088	B468	260.975	8.700	0.684	2.322	0.321
B427	0.628	5.794	10.511	5.170	1.567	B469	180.255	7.480	0.588	0.053	0.613
B428	25.872	0.000	1.615	1.240	0.134	B470	-0.161	6.546	0.401	6.372	4.184
B429	56.786	2.493	5.145	0.354	2.482	B471	131.416	8.465	24.963	8.635	3.796
B430	4.376	4.762	12.714	1.798	1.320	B472	131.483	5.914	0.262	4.163	3.974
B431	256.475	2.918	1.470	9.268	1.961	B473	264.652	3.143	6.286	0.272	1.553
B432	129.940	0.000	3.419	2.227	0.041	B474	-0.700	14.618	0.706	1.559	0.411
B433	42.746	9.754	8.156	4.123	4.836	B475	205.913	2.997	13.983	4.704	0.827
B434	269.760	7.566	11.605	4.006	0.587	B476	270.983	2.809	2.297	3.278	0.073
B435	271.628	8.135	12.124	0.013	0.621	B477	260.381	9.349	5.126	6.559	2.338
B436	248.945	9.884	1.281	1.001	0.523	B478	211.977	6.040	3.380	11.060	3.725
B437	50.681	5.613	4.509	10.428	2.381	B479	140.081	4.887	6.657	1.306	0.659
B438	13.516	0.000	19.908	10.565	0.993	B480	16.777	4.001	15.671	3.755	4.009
B439	259.220	6.710	2.067	4.040	0.198	B481	52.354	6.509	8.290	2.434	0.168
B440	167.911	12.427	5.047	4.673	0.288	B482	266.533	1.961	0.261	11.834	5.153
B441	162.259	4.795	0.123	1.661	4.323	B483	82.337	6.065	20.704	0.094	2.682
B442	7.995	6.334	25.939	7.874	0.084	B484	54.013	6.722	2.008	2.303	1.097
B443	264.661	0.000	2.607	0.241	3.332	B485	99.660	2.555	2.006	12.011	0.794
B444	249.246	7.039	10.480	8.820	1.347	B486	76.136	13.307	5.383	3.793	0.048

B. No.	X	Z	L	H	Y	B. No.	X	Z	L	H	Y
B487	135.043	9.971	4.185	7.129	2.247	B494	16.630	5.783	0.230	10.462	1.909
B488	264.629	8.768	1.035	8.332	0.764	B495	247.168	5.360	11.240	11.740	2.001
B489	274.811	7.808	2.659	0.452	1.292	B496	166.680	3.069	6.229	9.079	1.802
B490	96.083	1.865	11.974	0.021	1.743	B497	245.776	4.661	1.076	8.113	1.180
B491	268.803	8.412	1.035	4.495	3.960	B498	244.402	5.334	1.698	2.190	1.189
B492	145.120	0.000	8.070	3.655	3.148	B499	254.529	2.462	12.165	12.936	0.626
B493	267.281	3.587	4.846	6.176	3.178	B500	67.274	10.908	1.650	0.482	0.209

Appendix IV - A priori and posterior opening data

Table IV-1: A priori and posterior opening data.

Type	Priori	Test-case 1				Test-case 2				Test-case 3			
		Stat.	Col	Leak	Post.	Stat.	Col	Leak	Post.	Stat.	Col	Leak	Post.
Slid. WT	0.000	0	19.96	0.00	0.000	0	19.97	0.00	0.000	0	19.88	0.00	0.000
Hng. Esc.	0.438	1	0.00	0.00	0.438	1	0.00	0.00	0.438	1	0.00	0.00	0.438
Slid. WT	0.019	0	19.88	0.00	0.000	0	19.96	0.00	0.000	0	20.12	0.00	0.000
Slid. WT	0.006	0	20.02	0.00	0.000	0	19.99	0.00	0.000	0	19.87	0.00	0.000
Slid. WT	0.000	0	19.81	0.00	0.000	0	20.16	0.00	0.000	0	20.08	0.00	0.000
Hng. Fire	0.398	0	2.44	0.00	0.398	0	2.50	0.04	0.398	0	2.50	0.02	0.398
Hng. Fire	0.601	1	0.00	0.00	0.601	1	0.00	0.00	0.601	0	2.52	0.04	0.601
Hng. Esc.	0.649	1	0.00	0.00	0.649	1	0.00	0.00	0.649	1	0.00	0.00	0.649
Hng. Esc.	0.997	1	0.00	0.00	0.997	1	0.00	0.00	0.997	1	0.00	0.00	0.997
Hng. Esc.	0.613	0	2.32	0.01	0.613	1	0.00	0.00	0.613	1	0.00	0.00	0.613
Hng. Esc.	0.365	0	2.61	0.07	0.365	0	2.34	0.03	0.365	0	2.52	0.04	0.365
Slid. WT	0.021	0	19.99	0.00	0.000	0	20.00	0.00	0.000	0	20.00	0.00	0.000
Hng. Esc.	0.492	1	0.00	0.00	0.492	1	0.00	0.00	0.492	0	2.38	0.04	0.492
Slid. WT	0.006	0	19.87	0.00	0.000	0	19.89	0.00	0.000	0	19.93	0.00	0.000
Hng. Esc.	0.662	0	2.37	0.05	0.662	1	0.00	0.00	0.662	1	0.00	0.00	0.662
Hng. Fire	0.893	1	0.00	0.00	0.893	1	0.00	0.00	0.893	1	0.00	0.00	0.893
Hng. Esc.	0.910	1	0.00	0.00	0.910	1	0.00	0.00	0.910	1	0.00	0.00	0.910
Slid. WT	0.021	0	19.99	0.00	0.000	0	19.97	0.00	0.000	0	19.97	0.00	0.000
Hng. Esc.	0.819	1	0.00	0.00	0.819	1	0.00	0.00	0.819	1	0.00	0.00	0.819
Slid. WT	0.003	0	19.95	0.00	0.000	0	19.91	0.00	0.000	0	19.89	0.00	0.000
Hng. Fire	0.566	1	0.00	0.00	0.566	1	0.00	0.00	0.566	1	0.00	0.00	0.566
Hng. Fire	0.963	1	0.00	0.00	0.963	1	0.00	0.00	0.963	1	0.00	0.00	0.963
Hng. Fire	0.185	0	2.45	0.06	0.185	0	2.39	0.01	0.185	1	0.00	0.00	0.185
Hng. Fire	0.610	0	2.55	0.00	0.610	1	0.00	0.00	0.610	0	2.45	0.01	0.610
Hng. Fire	0.559	1	0.00	0.00	0.559	1	0.00	0.00	0.559	0	2.43	0.01	0.559
Hng. Fire	0.546	1	0.00	0.00	0.546	0	2.38	0.20	0.546	1	0.00	0.00	0.546
Hng. Fire	0.833	1	0.00	0.00	0.833	0	2.56	0.00	0.833	1	0.00	0.00	0.833
Hng. Fire	0.921	1	0.00	0.00	0.921	0	2.64	0.01	0.921	1	0.00	0.00	0.921
Hng. Fire	0.912	1	0.00	0.00	0.912	1	0.00	0.00	0.912	1	0.00	0.00	0.912
Hng. Esc.	0.181	0	2.53	0.01	0.181	1	0.00	0.00	0.181	1	0.00	0.00	0.181
Slid. WT	0.000	0	20.11	0.00	0.000	0	20.03	0.00	0.000	0	20.04	0.00	0.000
Hng. Esc.	0.792	0	2.54	0.01	0.792	0	2.55	0.02	0.792	1	0.00	0.00	0.792
Hng. Fire	0.884	1	0.00	0.00	0.884	1	0.00	0.00	0.884	1	0.00	0.00	0.884

Slid. WT	0.000	0	20.16	0.00	0.000	0	20.05	0.00	0.000	0	19.97	0.00	0.000
Hng. Esc.	0.435	1	0.00	0.00	0.435	0	2.55	0.01	0.435	1	0.00	0.00	0.435
Hng. Esc.	0.436	0	2.46	0.02	0.436	0	2.39	0.07	0.436	1	0.00	0.00	0.436
Hng. Esc.	0.817	1	0.00	0.00	0.817	1	0.00	0.00	0.817	0	2.50	0.06	0.817
Hole	1.000	1	0.00	0.00	1.000	1	0.00	0.00	1.000	1	0.00	0.00	1.000
Hng. Esc.	0.935	1	0.00	0.00	0.935	1	0.00	0.00	0.935	1	0.00	0.00	0.935
Hole	1.000	1	0.00	0.00	1.000	1	0.00	0.00	1.000	1	0.00	0.00	1.000
Hole	1.000	1	0.00	0.00	1.000	1	0.00	0.00	1.000	1	0.00	0.00	1.000
Hng. Non-WT	0.902	1	0.00	0.00	0.902	1	0.00	0.00	0.902	1	0.00	0.00	0.902
Slid. Lift	0.091	0	1.61	0.01	0.091	0	1.38	0.00	0.091	0	1.50	0.02	0.091
Slid. Lift	0.007	0	1.60	0.00	0.007	0	1.52	0.04	0.007	0	1.50	0.02	0.007
Hng. Fire	0.694	1	0.00	0.00	0.694	1	0.00	0.00	0.694	1	0.00	0.00	0.694
Hng. Fire	0.714	1	0.00	0.00	0.714	0	2.66	0.01	0.714	0	2.52	0.00	0.714
Hng. Fire	0.508	0	2.50	0.05	0.508	1	0.00	0.00	0.508	0	2.42	0.02	0.508
Hole	1.000	1	0.00	0.00	1.000	1	0.00	0.00	1.000	1	0.00	0.00	1.000
Hng. Dbl. Fire	0.888	1	0.00	0.00	0.888	1	0.00	0.00	0.888	1	0.00	0.00	0.888
Hng. Esc.	0.996	1	0.00	0.00	0.996	1	0.00	0.00	0.996	1	0.00	0.00	0.996
Hng. Non-WT	0.335	1	0.00	0.00	0.335	1	0.00	0.00	0.335	0	1.40	0.02	0.335
Hng. Esc.	0.430	1	0.00	0.00	0.430	1	0.00	0.00	0.430	0	2.50	0.03	0.430
Hng. Esc.	0.251	1	0.00	0.00	0.251	1	0.00	0.00	0.251	0	2.24	0.01	0.251
Hng. Dbl. Fire	0.821	1	0.00	0.00	0.821	1	0.00	0.00	0.821	1	0.00	0.00	0.821
Hng. Esc.	0.917	1	0.00	0.00	0.917	1	0.00	0.00	0.917	1	0.00	0.00	0.917
Hng. Esc.	0.980	1	0.00	0.00	0.980	1	0.00	0.00	0.980	1	0.00	0.00	0.980
Slid. Lift	0.028	0	1.71	0.01	0.028	1	0.00	0.00	0.028	0	1.63	0.00	0.028
Hng. Fire	0.725	1	0.00	0.00	0.725	1	0.00	0.00	0.725	1	0.00	0.00	0.725
Hng. Fire	0.017	0	2.62	0.02	0.017	0	2.43	0.02	0.017	0	2.52	0.01	0.017
Hng. Fire	0.448	0	2.51	0.00	0.448	0	2.70	0.00	0.448	0	2.71	0.04	0.448
Hng. Fire	0.659	1	0.00	0.00	0.659	1	0.00	0.00	0.659	0	2.61	0.05	0.659
Hng. Fire	0.630	1	0.00	0.00	0.630	1	0.00	0.00	0.630	1	0.00	0.00	0.630
Hng. Fire	0.208	1	0.00	0.00	0.208	0	2.53	0.01	0.208	0	2.34	0.01	0.208
Hng. Fire	0.545	1	0.00	0.00	0.545	1	0.00	0.00	0.545	1	0.00	0.00	0.545
Slid. Lift	0.325	0	1.62	0.07	0.325	0	1.41	0.01	0.325	0	1.31	0.06	0.325
Slid. Lift	0.274	0	1.53	0.04	0.274	1	0.00	0.00	0.274	0	1.57	0.03	0.274
Hng. Fire	0.162	0	2.37	0.02	0.162	0	2.45	0.02	0.162	0	2.59	0.05	0.162
Hng. Fire	0.986	1	0.00	0.00	0.986	1	0.00	0.00	0.986	1	0.00	0.00	0.986
Hng. Fire	0.388	1	0.00	0.00	0.388	1	0.00	0.00	0.388	0	2.50	0.00	0.388
Hng. Fire	0.259	0	2.43	0.07	0.259	0	2.39	0.00	0.259	0	2.47	0.03	0.259
Hng. Fire	0.876	1	0.00	0.00	0.876	0	2.57	0.04	0.876	1	0.00	0.00	0.876
Hng. Esc.	0.843	0	2.58	0.06	0.843	1	0.00	0.00	0.843	1	0.00	0.00	0.843
Hng. Esc.	0.961	1	0.00	0.00	0.961	1	0.00	0.00	0.961	1	0.00	0.00	0.961
Hole	1.000	1	0.00	0.00	1.000	1	0.00	0.00	1.000	1	0.00	0.00	1.000
Hng. Esc.	0.550	0	2.67	0.05	0.550	1	0.00	0.00	0.550	1	0.00	0.00	0.550
Hng. Fire	0.418	0	2.24	0.12	0.418	1	0.00	0.00	0.418	0	2.65	0.01	0.418

Slid. Prov. Room	0.040	0	2.34	0.01	0.040	1	0.00	0.00	0.040	0	2.55	0.01	0.040
Hole	1.000	1	0.00	0.00	1.000	1	0.00	0.00	1.000	1	0.00	0.00	1.000
Hng. Dbl. Fire	0.459	1	0.00	0.00	0.459	0	2.01	0.00	0.459	0	2.05	0.04	0.459
Hole	1.000	1	0.00	0.00	1.000	1	0.00	0.00	1.000	1	0.00	0.00	1.000
Hng. Fire	0.796	1	0.00	0.00	0.796	1	0.00	0.00	0.796	1	0.00	0.00	0.796
Hng. Dbl. Fire	0.752	1	0.00	0.00	0.752	1	0.00	0.00	0.752	1	0.00	0.00	0.752
Hng. Fire	0.649	1	0.00	0.00	0.649	1	0.00	0.00	0.649	1	0.00	0.00	0.649
Hng. Dbl. Fire	0.841	1	0.00	0.00	0.841	1	0.00	0.00	0.841	1	0.00	0.00	0.841
Hng. Esc.	0.955	1	0.00	0.00	0.955	1	0.00	0.00	0.955	1	0.00	0.00	0.955
Hng. Fire	0.471	1	0.00	0.00	0.471	0	2.73	0.03	0.471	1	0.00	0.00	0.471
Hole	1.000	1	0.00	0.00	1.000	1	0.00	0.00	1.000	1	0.00	0.00	1.000
Hng. Dbl. Fire	0.800	1	0.00	0.00	0.800	1	0.00	0.00	0.800	1	0.00	0.00	0.800
Hng. Cold Room	0.166	0	3.70	0.00	0.166	0	3.35	0.06	0.166	0	3.47	0.00	0.166
Hng. Non-WT	0.706	0	1.57	0.00	0.706	0	1.33	0.10	0.706	0	1.33	0.01	0.706
Hng. Fire	0.987	1	0.00	0.00	0.987	1	0.00	0.00	0.987	1	0.00	0.00	0.987
Hng. Fire	0.803	1	0.00	0.00	0.803	1	0.00	0.00	0.803	0	2.56	0.01	0.803
Hng. Non-WT	0.168	0	1.47	0.16	0.168	1	0.00	0.00	0.168	0	1.61	0.02	0.168
Slid. Lift	0.082	0	1.49	0.01	0.082	0	1.37	0.00	0.082	0	1.62	0.02	0.082
Slid. Lift	0.221	0	1.59	0.03	0.221	0	1.50	0.02	0.221	1	0.00	0.00	0.221
Slid. Lift	0.006	0	1.49	0.02	0.006	0	1.52	0.02	0.006	0	1.35	0.10	0.006
Hng. Fire	0.888	1	0.00	0.00	0.888	1	0.00	0.00	0.888	1	0.00	0.00	0.888
Hng. Non-WT	0.323	1	0.00	0.00	0.323	1	0.00	0.00	0.323	0	1.60	0.01	0.323
Hng. Fire	0.586	1	0.00	0.00	0.586	0	2.60	0.00	0.586	1	0.00	0.00	0.586
Hng. Non-WT	0.638	1	0.00	0.00	0.638	1	0.00	0.00	0.638	1	0.00	0.00	0.638
Hng. Esc.	0.913	0	2.43	0.03	0.913	1	0.00	0.00	0.913	1	0.00	0.00	0.913
Hng. Fire	0.985	1	0.00	0.00	0.985	1	0.00	0.00	0.985	1	0.00	0.00	0.985
Hng. Esc.	0.459	1	0.00	0.00	0.459	0	2.56	0.07	0.459	1	0.00	0.00	0.459
Hng. Fire	0.389	1	0.00	0.00	0.389	0	2.77	0.09	0.389	0	2.48	0.04	0.389
Hng. Fire	0.795	1	0.00	0.00	0.795	0	2.54	0.08	0.795	1	0.00	0.00	0.795
Hole	1.000	1	0.00	0.00	1.000	1	0.00	0.00	1.000	1	0.00	0.00	1.000
Hole	1.000	1	0.00	0.00	1.000	1	0.00	0.00	1.000	1	0.00	0.00	1.000
Hole	1.000	1	0.00	0.00	1.000	1	0.00	0.00	1.000	1	0.00	0.00	1.000
Hole	1.000	1	0.00	0.00	1.000	1	0.00	0.00	1.000	1	0.00	0.00	1.000
Hng. Fire	0.827	1	0.00	0.00	0.827	1	0.00	0.00	0.827	1	0.00	0.00	0.827
Hng. Esc.	0.727	0	2.54	0.03	0.727	1	0.00	0.00	0.727	0	2.47	0.01	0.727
Hng. Esc.	0.838	1	0.00	0.00	0.838	1	0.00	0.00	0.838	1	0.00	0.00	0.838
Hng. Esc.	0.621	1	0.00	0.00	0.621	1	0.00	0.00	0.621	1	0.00	0.00	0.621
Hng. Esc.	0.860	1	0.00	0.00	0.860	1	0.00	0.00	0.860	1	0.00	0.00	0.860
Hng. Fire	0.661	1	0.00	0.00	0.661	0	2.40	0.01	0.661	1	0.00	0.00	0.661
Hng. Fire	0.758	1	0.00	0.00	0.758	0	2.57	0.01	0.758	1	0.00	0.00	0.758
Hng. Esc.	0.179	0	2.51	0.03	0.179	0	2.43	0.08	0.179	0	2.36	0.07	0.179
Hole	1.000	1	0.00	0.00	1.000	1	0.00	0.00	1.000	1	0.00	0.00	1.000
Hole	1.000	1	0.00	0.00	1.000	1	0.00	0.00	1.000	1	0.00	0.00	1.000

Hng. Esc.	0.382	0	2.41	0.02	0.382	0	2.44	0.02	0.382	1	0.00	0.00	0.382
Hng. Fire	0.967	0	2.49	0.00	0.967	1	0.00	0.00	0.967	1	0.00	0.00	0.967
Hng. Fire	0.675	1	0.00	0.00	0.675	1	0.00	0.00	0.675	1	0.00	0.00	0.675
Hng. Fire	0.672	1	0.00	0.00	0.672	1	0.00	0.00	0.672	1	0.00	0.00	0.672
Hng. Fire	0.871	0	2.41	0.03	0.871	1	0.00	0.00	0.871	1	0.00	0.00	0.871
Hng. Dbl. Fire	0.889	1	0.00	0.00	0.889	1	0.00	0.00	0.889	1	0.00	0.00	0.889
Hole	1.000	1	0.00	0.00	1.000	1	0.00	0.00	1.000	1	0.00	0.00	1.000
Hng. Fire	0.487	0	2.42	0.01	0.487	1	0.00	0.00	0.487	1	0.00	0.00	0.487
Hng. Fire	0.527	0	2.74	0.05	0.527	1	0.00	0.00	0.527	1	0.00	0.00	0.527
Hng. Fire	0.642	0	2.44	0.01	0.642	1	0.00	0.00	0.642	1	0.00	0.00	0.642
Hole	1.000	1	0.00	0.00	1.000	1	0.00	0.00	1.000	1	0.00	0.00	1.000
Hng. Esc.	0.879	1	0.00	0.00	0.879	1	0.00	0.00	0.879	1	0.00	0.00	0.879
Hng. Esc.	0.624	0	2.52	0.03	0.624	1	0.00	0.00	0.624	0	2.56	0.03	0.624
Hng. Dbl. Fire	0.856	1	0.00	0.00	0.856	1	0.00	0.00	0.856	1	0.00	0.00	0.856
Hng. Fire	0.954	1	0.00	0.00	0.954	1	0.00	0.00	0.954	1	0.00	0.00	0.954
Hng. Fire	0.506	0	2.56	0.01	0.506	1	0.00	0.00	0.506	1	0.00	0.00	0.506
Esc. Hatch	0.722	1	0.00	0.00	0.722	1	0.00	0.00	0.722	1	0.00	0.00	0.722
Hng. Fire	0.471	1	0.00	0.00	0.471	1	0.00	0.00	0.471	0	2.42	0.07	0.471
Hng. Non-WT	0.762	1	0.00	0.00	0.762	1	0.00	0.00	0.762	1	0.00	0.00	0.762
Slid. WT	0.133	0	20.06	0.00	0.002	0	20.03	0.00	0.002	0	19.88	0.00	0.002
Esc. Hatch	0.542	1	0.00	0.00	0.542	1	0.00	0.00	0.542	1	0.00	0.00	0.542
Hng. Fire	0.683	1	0.00	0.00	0.683	1	0.00	0.00	0.683	1	0.00	0.00	0.683
Hng. Fire	0.602	1	0.00	0.00	0.602	1	0.00	0.00	0.602	1	0.00	0.00	0.602
Slid. Lift	0.133	1	0.00	0.00	0.133	0	1.39	0.00	0.133	1	0.00	0.00	0.133
Slid. Lift	0.112	0	1.41	0.00	0.112	0	1.29	0.01	0.112	0	1.41	0.03	0.112
Hng. Fire	0.882	1	0.00	0.00	0.882	1	0.00	0.00	0.882	1	0.00	0.00	0.882
Hng. Fire	0.747	1	0.00	0.00	0.747	1	0.00	0.00	0.747	1	0.00	0.00	0.747
Hole	1.000	1	0.00	0.00	1.000	1	0.00	0.00	1.000	1	0.00	0.00	1.000
Esc. Hatch	0.573	0	2.35	0.00	0.573	0	2.40	0.06	0.573	1	0.00	0.00	0.573
Esc. Hatch	0.213	0	2.45	0.01	0.213	0	2.55	0.01	0.213	1	0.00	0.00	0.213
Esc. Hatch	0.547	0	2.52	0.07	0.547	1	0.00	0.00	0.547	1	0.00	0.00	0.547
Slid. WT	0.121	0	20.07	0.00	0.001	0	19.94	0.00	0.001	0	20.15	0.00	0.001
Esc. Hatch	0.389	1	0.00	0.00	0.389	1	0.00	0.00	0.389	0	2.63	0.06	0.389
Hng. Fire	0.637	1	0.00	0.00	0.637	1	0.00	0.00	0.637	1	0.00	0.00	0.637
Hng. Fire	0.953	1	0.00	0.00	0.953	1	0.00	0.00	0.953	1	0.00	0.00	0.953
Hng. Fire	0.517	1	0.00	0.00	0.517	1	0.00	0.00	0.517	1	0.00	0.00	0.517
Esc. Hatch	0.661	0	2.57	0.02	0.661	1	0.00	0.00	0.661	1	0.00	0.00	0.661
Hng. Non-WT	0.439	0	1.49	0.02	0.439	0	1.50	0.04	0.439	1	0.00	0.00	0.439
Slid. WT	0.054	0	20.08	0.00	0.001	0	19.95	0.00	0.001	0	20.01	0.00	0.001
Hng. Fire	0.988	1	0.00	0.00	0.988	1	0.00	0.00	0.988	1	0.00	0.00	0.988
Hng. Fire	0.967	1	0.00	0.00	0.967	1	0.00	0.00	0.967	1	0.00	0.00	0.967
Slid. WT	0.387	1	0.00	0.00	0.006	0	20.13	0.00	0.006	0	20.21	0.00	0.006
Hng. Non-WT	0.277	1	0.00	0.00	0.277	0	1.42	0.01	0.277	0	1.54	0.03	0.277

Hng. Non-WT	0.495	0	1.57	0.01	0.495	1	0.00	0.00	0.495	1	0.00	0.00	0.495
Hng. Non-WT	0.663	0	1.53	0.06	0.663	1	0.00	0.00	0.663	1	0.00	0.00	0.663
Hng. Fire	0.999	1	0.00	0.00	0.999	1	0.00	0.00	0.999	1	0.00	0.00	0.999
Hng. Non-WT	0.558	1	0.00	0.00	0.558	0	1.56	0.00	0.558	0	1.45	0.03	0.558
Hng. Fire	0.499	0	2.58	0.03	0.499	0	2.48	0.01	0.499	1	0.00	0.00	0.499
Hng. Non-WT	0.785	1	0.00	0.00	0.785	1	0.00	0.00	0.785	1	0.00	0.00	0.785
Slid. Lift	0.220	0	1.42	0.02	0.220	0	1.53	0.10	0.220	0	1.46	0.01	0.220
Hole	1.000	1	0.00	0.00	1.000	1	0.00	0.00	1.000	1	0.00	0.00	1.000
Hng. Non-WT	0.967	1	0.00	0.00	0.967	1	0.00	0.00	0.967	1	0.00	0.00	0.967
Hng. Non-WT	0.500	1	0.00	0.00	0.500	1	0.00	0.00	0.500	0	1.39	0.05	0.500
Hng. Fire	0.844	0	2.55	0.04	0.844	1	0.00	0.00	0.844	1	0.00	0.00	0.844
Hng. Fire	0.947	1	0.00	0.00	0.947	1	0.00	0.00	0.947	1	0.00	0.00	0.947
Slid. Fire	0.390	0	0.98	0.01	0.390	1	0.00	0.00	0.390	1	0.00	0.00	0.390
Slid. Lift	0.001	0	1.56	0.11	0.001	0	1.36	0.01	0.001	0	1.49	0.01	0.001
Slid. Lift	0.088	0	1.39	0.07	0.088	0	1.52	0.01	0.088	0	1.49	0.03	0.088
Hng. Dbl. Fire	0.634	0	1.91	0.02	0.634	1	0.00	0.00	0.634	1	0.00	0.00	0.634
Hng. Fire	0.601	1	0.00	0.00	0.601	1	0.00	0.00	0.601	0	2.51	0.05	0.601
Hole	1.000	1	0.00	0.00	1.000	1	0.00	0.00	1.000	1	0.00	0.00	1.000
Hole	1.000	1	0.00	0.00	1.000	1	0.00	0.00	1.000	1	0.00	0.00	1.000
Hng. Esc.	0.746	1	0.00	0.00	0.746	0	2.48	0.00	0.746	1	0.00	0.00	0.746
Hng. Esc.	0.392	1	0.00	0.00	0.392	0	2.65	0.02	0.392	1	0.00	0.00	0.392
Hng. Fire	0.909	1	0.00	0.00	0.909	1	0.00	0.00	0.909	1	0.00	0.00	0.909
Hng. Fire	0.533	0	1.55	0.01	0.533	1	0.00	0.00	0.533	1	0.00	0.00	0.533
Hng. Non-WT	0.252	0	1.43	0.02	0.252	0	1.38	0.01	0.252	0	1.53	0.04	0.252
Hng. Fire	0.809	1	0.00	0.00	0.809	1	0.00	0.00	0.809	1	0.00	0.00	0.809
Hng. Fire	0.593	1	0.00	0.00	0.593	1	0.00	0.00	0.593	0	2.37	0.08	0.593
Hng. Esc.	0.867	1	0.00	0.00	0.867	1	0.00	0.00	0.867	1	0.00	0.00	0.867
Hole	1.000	1	0.00	0.00	1.000	1	0.00	0.00	1.000	1	0.00	0.00	1.000
Hng. Fire	0.698	0	2.45	0.02	0.698	1	0.00	0.00	0.698	1	0.00	0.00	0.698
Hng. Fire	0.893	1	0.00	0.00	0.893	1	0.00	0.00	0.893	0	2.43	0.02	0.893
Slid. WT	0.000	0	19.98	0.00	0.000	0	20.20	0.00	0.000	0	20.00	0.00	0.000
Hng. Esc.	0.780	1	0.00	0.00	0.780	1	0.00	0.00	0.780	0	2.60	0.12	0.780
Hng. Esc.	0.314	0	2.42	0.02	0.314	0	2.41	0.01	0.314	0	2.45	0.10	0.314
Hng. Esc.	0.307	0	2.52	0.01	0.307	0	2.43	0.01	0.307	0	2.48	0.03	0.307
Hng. Fire	0.791	0	2.42	0.11	0.791	1	0.00	0.00	0.791	1	0.00	0.00	0.791
Hng. Fire	0.741	1	0.00	0.00	0.741	0	2.57	0.02	0.741	1	0.00	0.00	0.741
Hng. Esc.	0.124	0	2.55	0.02	0.124	0	2.60	0.02	0.124	0	2.59	0.00	0.124
Hng. Esc.	0.906	1	0.00	0.00	0.906	1	0.00	0.00	0.906	1	0.00	0.00	0.906
Hole	1.000	1	0.00	0.00	1.000	1	0.00	0.00	1.000	1	0.00	0.00	1.000
Hng. Prov. Room	0.013	0	3.38	0.00	0.013	0	3.42	0.04	0.013	0	3.48	0.02	0.013
Hng. Fire	0.790	1	0.00	0.00	0.790	1	0.00	0.00	0.790	0	2.38	0.04	0.790
Hng. Prov. Room	0.031	0	3.46	0.06	0.031	0	3.25	0.02	0.031	0	3.54	0.01	0.031
Hng. Esc.	0.670	1	0.00	0.00	0.670	0	2.48	0.10	0.670	0	2.37	0.16	0.670

Slid. Prov. Room	0.020	0	2.56	0.03	0.020	0	2.33	0.10	0.020	0	2.35	0.00	0.020
Slid. Prov. Room	0.030	0	2.59	0.02	0.030	0	2.44	0.01	0.030	0	2.63	0.03	0.030
Hng. Prov. Room	0.031	0	3.46	0.01	0.031	0	3.49	0.01	0.031	0	3.52	0.00	0.031
Hng. Prov. Room	0.100	0	3.53	0.01	0.100	0	3.51	0.00	0.100	0	3.53	0.04	0.100
Hng. Fire	0.449	0	2.52	0.00	0.449	1	0.00	0.00	0.449	1	0.00	0.00	0.449
Slid. Prov. Room	0.004	0	2.47	0.02	0.004	0	2.40	0.00	0.004	0	2.68	0.02	0.004
Slid. Prov. Room	0.047	0	2.51	0.01	0.047	0	2.34	0.01	0.047	0	2.53	0.02	0.047
Slid. Semi-WT	0.930	1	0.00	0.00	0.118	1	0.00	0.00	0.118	1	0.00	0.00	0.118
Hng. Esc.	0.358	0	2.48	0.09	0.358	1	0.00	0.00	0.358	0	2.41	0.02	0.358
Slid. Cold Room	0.106	0	3.45	0.00	0.106	0	3.55	0.01	0.106	0	3.59	0.02	0.106
Slid. Cold Room	0.015	0	3.56	0.08	0.015	0	3.41	0.02	0.015	0	3.39	0.07	0.015
Hng. Fire	0.635	0	2.39	0.02	0.635	0	2.39	0.06	0.635	0	2.42	0.11	0.635
Hole	1.000	1	0.00	0.00	1.000	1	0.00	0.00	1.000	1	0.00	0.00	1.000
Hole	1.000	1	0.00	0.00	1.000	1	0.00	0.00	1.000	1	0.00	0.00	1.000
Slid. Cold Room	0.049	0	3.52	0.02	0.049	0	3.43	0.09	0.049	0	3.37	0.08	0.049
Slid. Prov. Room	0.093	0	2.41	0.04	0.093	1	0.00	0.00	0.093	1	0.00	0.00	0.093
Slid. Prov. Room	0.142	0	2.54	0.03	0.142	0	2.44	0.01	0.142	0	2.58	0.02	0.142
Slid. Prov. Room	0.040	0	2.38	0.02	0.040	0	2.53	0.02	0.040	0	2.58	0.05	0.040
Slid. Prov. Room	0.061	0	2.40	0.06	0.061	0	2.54	0.04	0.061	0	2.36	0.01	0.061
Hng. Non-WT	0.613	1	0.00	0.00	0.613	1	0.00	0.00	0.613	0	1.55	0.05	0.613
Hole	1.000	1	0.00	0.00	1.000	1	0.00	0.00	1.000	1	0.00	0.00	1.000
Hole	1.000	1	0.00	0.00	1.000	1	0.00	0.00	1.000	1	0.00	0.00	1.000
Shell	0.000	1	1.00	0.00	0.000	1	1.00	0.00	0.000	1	1.00	0.00	0.000
Shell	0.000	1	1.00	0.00	0.000	1	1.00	0.00	0.000	1	1.00	0.00	0.000
Hng. Prov. Room	0.056	0	3.47	0.01	0.056	0	3.45	0.01	0.056	0	3.40	0.01	0.056
Hng. Prov. Room	0.045	0	3.46	0.01	0.045	0	3.40	0.01	0.045	0	3.53	0.01	0.045
Hng. Prov. Room	0.086	0	3.29	0.01	0.086	1	0.00	0.00	0.086	0	3.49	0.00	0.086
Hng. Non-WT	0.235	0	1.49	0.01	0.235	0	1.47	0.00	0.235	0	1.27	0.01	0.235
Hng. Prov. Room	0.101	0	3.42	0.00	0.101	0	3.60	0.04	0.101	0	3.33	0.03	0.101
Hng. Fire	0.912	1	0.00	0.00	0.912	1	0.00	0.00	0.912	0	2.49	0.01	0.912
Hng. Prov. Room	0.029	0	3.57	0.00	0.029	0	3.48	0.04	0.029	0	3.61	0.02	0.029
Hng. Prov. Room	0.011	0	3.64	0.00	0.011	0	3.54	0.03	0.011	0	3.50	0.08	0.011
Hng. Dbl. Fire	0.859	1	0.00	0.00	0.859	1	0.00	0.00	0.859	1	0.00	0.00	0.859
Hng. Fire	0.979	1	0.00	0.00	0.979	1	0.00	0.00	0.979	1	0.00	0.00	0.979
Hng. Fire	0.347	1	0.00	0.00	0.347	0	2.25	0.01	0.347	0	2.51	0.02	0.347
Hng. Prov. Room	0.020	0	3.49	0.05	0.020	0	3.57	0.01	0.020	0	3.43	0.05	0.020
Hng. Prov. Room	0.016	0	3.29	0.02	0.016	0	3.45	0.06	0.016	0	3.55	0.01	0.016
Slid. Lift	0.094	0	1.45	0.01	0.094	0	1.46	0.01	0.094	0	1.57	0.00	0.094
Slid. Lift	0.349	1	0.00	0.00	0.349	0	1.56	0.00	0.349	0	1.57	0.02	0.349
Slid. Lift	0.142	0	1.51	0.04	0.142	0	1.54	0.01	0.142	0	1.46	0.05	0.142
Hng. Prov. Room	0.021	0	3.60	0.03	0.021	0	3.50	0.05	0.021	0	3.44	0.01	0.021
Hng. Cold Room	0.003	0	3.48	0.01	0.003	0	3.36	0.00	0.003	0	3.53	0.00	0.003
Hng. Fire	0.880	1	0.00	0.00	0.880	1	0.00	0.00	0.880	1	0.00	0.00	0.880

Hng. Cold Room	0.004	0	3.55	0.11	0.004	0	3.57	0.01	0.004	0	3.47	0.12	0.004
Hng. Prov. Room	0.179	0	3.55	0.06	0.179	0	3.67	0.13	0.179	0	3.63	0.12	0.179
Hng. Fire	0.615	0	2.30	0.08	0.615	1	0.00	0.00	0.615	1	0.00	0.00	0.615
Hng. Fire	0.944	1	0.00	0.00	0.944	1	0.00	0.00	0.944	1	0.00	0.00	0.944
Hole	1.000	1	0.00	0.00	1.000	1	0.00	0.00	1.000	1	0.00	0.00	1.000
Slid. Light-WT	0.000	0	8.02	0.14	0.000	0	7.97	0.04	0.000	0	8.19	0.04	0.000
Slid. Semi-WT	0.635	1	0.00	0.00	0.017	0	7.96	0.00	0.017	1	0.00	0.00	0.017
Hole	1.000	1	0.00	0.00	1.000	1	0.00	0.00	1.000	1	0.00	0.00	1.000
Hng. Esc.	0.631	1	0.00	0.00	0.631	0	2.52	0.03	0.631	1	0.00	0.00	0.631
Hng. Fire	0.977	1	0.00	0.00	0.977	1	0.00	0.00	0.977	0	2.28	0.04	0.977
Hng. Fire	0.983	1	0.00	0.00	0.983	1	0.00	0.00	0.983	1	0.00	0.00	0.983
Hng. Fire	0.330	0	2.34	0.07	0.330	0	2.41	0.03	0.330	0	2.59	0.01	0.330
Esc. Hatch	0.960	1	0.00	0.00	0.960	1	0.00	0.00	0.960	1	0.00	0.00	0.960
Esc. Hatch	0.312	1	0.00	0.00	0.312	0	2.45	0.06	0.312	0	2.43	0.03	0.312
Hng. Fire	0.912	1	0.00	0.00	0.912	1	0.00	0.00	0.912	1	0.00	0.00	0.912
Hng. Fire	0.965	1	0.00	0.00	0.965	1	0.00	0.00	0.965	1	0.00	0.00	0.965
Hng. Fire	0.692	0	2.44	0.02	0.692	1	0.00	0.00	0.692	1	0.00	0.00	0.692
Hng. Fire	0.799	1	0.00	0.00	0.799	1	0.00	0.00	0.799	1	0.00	0.00	0.799
Esc. Hatch	0.205	0	2.48	0.00	0.205	0	2.55	0.03	0.205	0	2.37	0.03	0.205
Hng. Dbl. Fire	0.506	1	0.00	0.00	0.506	1	0.00	0.00	0.506	0	2.02	0.01	0.506
Hng. Fire	0.535	1	0.00	0.00	0.535	1	0.00	0.00	0.535	1	0.00	0.00	0.535
Hng. Fire	0.511	0	2.64	0.05	0.511	0	2.49	0.01	0.511	1	0.00	0.00	0.511
Hng. Fire	0.649	0	2.31	0.00	0.649	1	0.00	0.00	0.649	1	0.00	0.00	0.649
Hng. Fire	0.647	1	0.00	0.00	0.647	1	0.00	0.00	0.647	1	0.00	0.00	0.647
Hole	1.000	1	0.00	0.00	1.000	1	0.00	0.00	1.000	1	0.00	0.00	1.000
Shell	0.000	1	1.00	0.00	0.000	1	1.00	0.00	0.000	1	1.00	0.00	0.000
Hng. Dbl. Fire	0.699	1	0.00	0.00	0.699	0	2.13	0.05	0.699	1	0.00	0.00	0.699
Hng. Dbl. Fire	0.150	1	0.00	0.00	0.150	0	1.96	0.02	0.150	0	2.06	0.04	0.150
Hole	1.000	1	0.00	0.00	1.000	1	0.00	0.00	1.000	1	0.00	0.00	1.000
Hng. Esc.	0.512	0	2.33	0.05	0.512	1	0.00	0.00	0.512	0	2.46	0.02	0.512
Esc. Hatch	0.987	1	0.00	0.00	0.987	1	0.00	0.00	0.987	1	0.00	0.00	0.987
Hng. Fire	0.998	1	0.00	0.00	0.998	1	0.00	0.00	0.998	1	0.00	0.00	0.998
Hng. Non-WT	0.326	1	0.00	0.00	0.326	0	1.45	0.03	0.326	1	0.00	0.00	0.326
Hng. Fire	0.551	1	0.00	0.00	0.551	1	0.00	0.00	0.551	0	2.59	0.02	0.551
Hng. Non-WT	0.833	1	0.00	0.00	0.833	1	0.00	0.00	0.833	1	0.00	0.00	0.833
Hng. Non-WT	0.939	1	0.00	0.00	0.939	1	0.00	0.00	0.939	1	0.00	0.00	0.939
Hng. Fire	0.947	1	0.00	0.00	0.947	1	0.00	0.00	0.947	1	0.00	0.00	0.947
Shell	0.000	1	1.00	0.00	0.000	1	1.00	0.00	0.000	1	1.00	0.00	0.000
Hng. Fire	0.828	1	0.00	0.00	0.828	1	0.00	0.00	0.828	0	2.48	0.01	0.828
Hng. Fire	0.931	0	2.64	0.01	0.931	1	0.00	0.00	0.931	1	0.00	0.00	0.931
Hole	1.000	1	0.00	0.00	1.000	1	0.00	0.00	1.000	1	0.00	0.00	1.000
Slid. Semi-WT	0.472	0	8.12	0.07	0.009	0	8.01	0.00	0.009	1	0.00	0.00	0.009
Hng. Fire	0.894	1	0.00	0.00	0.894	1	0.00	0.00	0.894	1	0.00	0.00	0.894

Slid. Light-WT	0.097	0	8.03	0.02	0.001	0	7.97	0.05	0.001	0	7.99	0.10	0.001
Hole	1.000	1	0.00	0.00	1.000	1	0.00	0.00	1.000	1	0.00	0.00	1.000
Hole	1.000	1	0.00	0.00	1.000	1	0.00	0.00	1.000	1	0.00	0.00	1.000
Shell	0.000	1	1.00	0.00	0.000	1	1.00	0.00	0.000	1	1.00	0.00	0.000
Hole	1.000	1	0.00	0.00	1.000	1	0.00	0.00	1.000	1	0.00	0.00	1.000
Hng. Fire	0.930	1	0.00	0.00	0.930	1	0.00	0.00	0.930	1	0.00	0.00	0.930
Hng. Fire	0.923	1	0.00	0.00	0.923	1	0.00	0.00	0.923	1	0.00	0.00	0.923
Hng. Fire	0.592	1	0.00	0.00	0.592	1	0.00	0.00	0.592	1	0.00	0.00	0.592
Hng. Dbl. Fire	0.406	1	0.00	0.00	0.406	0	2.10	0.02	0.406	0	1.94	0.01	0.406
Shell	0.000	1	1.00	0.00	0.000	1	1.00	0.00	0.000	1	1.00	0.00	0.000
Hng. Fire	0.961	1	0.00	0.00	0.961	1	0.00	0.00	0.961	1	0.00	0.00	0.961
Hng. Fire	0.978	1	0.00	0.00	0.978	1	0.00	0.00	0.978	1	0.00	0.00	0.978
Hng. Fire	0.924	1	0.00	0.00	0.924	1	0.00	0.00	0.924	1	0.00	0.00	0.924
Hng. Non-WT	0.961	1	0.00	0.00	0.961	1	0.00	0.00	0.961	1	0.00	0.00	0.961
Hng. Fire	0.935	1	0.00	0.00	0.935	1	0.00	0.00	0.935	1	0.00	0.00	0.935
Hng. Fire	0.568	1	0.00	0.00	0.568	1	0.00	0.00	0.568	0	2.64	0.10	0.568
Hng. Fire	0.353	1	0.00	0.00	0.353	0	2.52	0.03	0.353	0	2.57	0.06	0.353
Hng. Esc.	0.093	0	2.55	0.04	0.093	0	2.67	0.02	0.093	1	0.00	0.00	0.093
Hng. Dbl. Fire	0.840	1	0.00	0.00	0.840	1	0.00	0.00	0.840	0	1.90	0.09	0.840
Shell	0.000	1	1.00	0.00	0.000	1	1.00	0.00	0.000	1	1.00	0.00	0.000
Hng. Dbl. Fire	0.849	1	0.00	0.00	0.849	1	0.00	0.00	0.849	1	0.00	0.00	0.849
Hng. Dbl. Fire	0.724	0	1.96	0.02	0.724	1	0.00	0.00	0.724	0	1.96	0.04	0.724
Hng. Dbl. Fire	0.330	0	1.92	0.04	0.330	0	2.12	0.04	0.330	0	2.04	0.01	0.330
Shell	0.000	1	1.00	0.00	0.000	1	1.00	0.00	0.000	1	1.00	0.00	0.000
Slid. Lift	0.154	0	1.60	0.02	0.154	0	1.44	0.01	0.154	0	1.41	0.02	0.154
Slid. Lift	0.175	0	1.61	0.01	0.175	0	1.43	0.00	0.175	0	1.49	0.10	0.175
Hole	1.000	1	0.00	0.00	1.000	1	0.00	0.00	1.000	1	0.00	0.00	1.000
Hole	1.000	1	0.00	0.00	1.000	1	0.00	0.00	1.000	1	0.00	0.00	1.000
Slid. Lift	0.057	0	1.39	0.03	0.057	0	1.50	0.03	0.057	0	1.33	0.00	0.057
Slid. Lift	0.139	0	1.46	0.00	0.139	0	1.46	0.00	0.139	0	1.55	0.08	0.139
Hole	1.000	1	0.00	0.00	1.000	1	0.00	0.00	1.000	1	0.00	0.00	1.000
Hole	1.000	1	0.00	0.00	1.000	1	0.00	0.00	1.000	1	0.00	0.00	1.000
Slid. Fire	0.496	1	0.00	0.00	0.496	0	1.06	0.04	0.496	0	1.01	0.03	0.496
Hole	1.000	1	0.00	0.00	1.000	1	0.00	0.00	1.000	1	0.00	0.00	1.000
Slid. Lift	0.029	0	1.54	0.02	0.029	0	1.44	0.02	0.029	0	1.58	0.01	0.029
Slid. Lift	0.116	0	1.37	0.02	0.116	0	1.45	0.00	0.116	0	1.44	0.02	0.116
Hole	1.000	1	0.00	0.00	1.000	1	0.00	0.00	1.000	1	0.00	0.00	1.000
Hole	1.000	1	0.00	0.00	1.000	1	0.00	0.00	1.000	1	0.00	0.00	1.000
Hng. Fire	0.504	1	0.00	0.00	0.504	1	0.00	0.00	0.504	0	2.56	0.03	0.504
Hng. Dbl. Fire	0.991	1	0.00	0.00	0.991	1	0.00	0.00	0.991	1	0.00	0.00	0.991
Hng. Dbl. Fire	0.867	1	0.00	0.00	0.867	0	2.10	0.00	0.867	1	0.00	0.00	0.867
Hng. Dbl. Fire	0.563	1	0.00	0.00	0.563	0	2.04	0.02	0.563	1	0.00	0.00	0.563
Shell	0.000	1	1.00	0.00	0.000	1	1.00	0.00	0.000	1	1.00	0.00	0.000

Hng. Fire	0.804	1	0.00	0.00	0.804	1	0.00	0.00	0.804	1	0.00	0.00	0.804
Slid. Semi-WT	0.696	1	0.00	0.00	0.023	0	8.00	0.03	0.023	1	0.00	0.00	0.023
Hng. Fire	0.658	1	0.00	0.00	0.658	1	0.00	0.00	0.658	1	0.00	0.00	0.658
Hole	1.000	1	0.00	0.00	1.000	1	0.00	0.00	1.000	1	0.00	0.00	1.000
Hng. Fire	0.274	0	2.46	0.06	0.274	1	0.00	0.00	0.274	1	0.00	0.00	0.274
Hng. Fire	0.727	0	2.53	0.02	0.727	1	0.00	0.00	0.727	1	0.00	0.00	0.727
Hng. Fire	0.251	0	2.41	0.04	0.251	0	2.47	0.01	0.251	0	2.41	0.11	0.251
Hng. Dbl. Fire	0.502	1	0.00	0.00	0.502	0	1.80	0.01	0.502	0	2.00	0.04	0.502
Hng. Fire	0.885	1	0.00	0.00	0.885	1	0.00	0.00	0.885	1	0.00	0.00	0.885
Hole	1.000	1	0.00	0.00	1.000	1	0.00	0.00	1.000	1	0.00	0.00	1.000
Hole	1.000	1	0.00	0.00	1.000	1	0.00	0.00	1.000	1	0.00	0.00	1.000
Hng. Fire	0.680	1	0.00	0.00	0.680	1	0.00	0.00	0.680	1	0.00	0.00	0.680
Slid. Semi-WT	0.517	1	0.00	0.00	0.011	0	8.05	0.05	0.011	1	0.00	0.00	0.011
Hng. Fire	0.738	1	0.00	0.00	0.738	1	0.00	0.00	0.738	0	2.45	0.03	0.738
Slid. Lift	0.017	1	0.00	0.00	0.017	0	1.57	0.05	0.017	0	1.39	0.00	0.017
Slid. Lift	0.187	0	1.56	0.05	0.187	0	1.63	0.00	0.187	0	1.39	0.01	0.187
Shell	0.000	1	1.00	0.00	0.000	1	1.00	0.00	0.000	1	1.00	0.00	0.000
Shell	0.000	1	1.00	0.00	0.000	1	1.00	0.00	0.000	1	1.00	0.00	0.000
Hng. Fire	0.798	1	0.00	0.00	0.798	0	2.61	0.01	0.798	1	0.00	0.00	0.798
Hng. Fire	0.922	1	0.00	0.00	0.922	0	2.41	0.00	0.922	1	0.00	0.00	0.922
Hole	1.000	1	0.00	0.00	1.000	1	0.00	0.00	1.000	1	0.00	0.00	1.000
Hng. Fire	0.840	0	2.63	0.01	0.840	1	0.00	0.00	0.840	1	0.00	0.00	0.840
Hng. Fire	0.921	1	0.00	0.00	0.921	1	0.00	0.00	0.921	1	0.00	0.00	0.921
Hole	1.000	1	0.00	0.00	1.000	1	0.00	0.00	1.000	1	0.00	0.00	1.000
Hng. Fire	0.821	0	2.21	0.04	0.821	1	0.00	0.00	0.821	1	0.00	0.00	0.821
Hng. Fire	0.969	1	0.00	0.00	0.969	1	0.00	0.00	0.969	1	0.00	0.00	0.969
Hng. Fire	0.943	0	2.35	0.01	0.943	1	0.00	0.00	0.943	1	0.00	0.00	0.943
Hng. Fire	0.881	1	0.00	0.00	0.881	0	2.44	0.05	0.881	1	0.00	0.00	0.881
Hole	1.000	1	0.00	0.00	1.000	1	0.00	0.00	1.000	1	0.00	0.00	1.000
Slid. Light-WT	0.080	0	8.03	0.03	0.001	0	8.07	0.03	0.001	0	7.92	0.07	0.001
Hng. Fire	0.946	1	0.00	0.00	0.946	0	2.50	0.03	0.946	1	0.00	0.00	0.946
Hng. Fire	0.997	1	0.00	0.00	0.997	1	0.00	0.00	0.997	1	0.00	0.00	0.997
Hng. Fire	0.418	0	2.48	0.02	0.418	0	2.49	0.01	0.418	0	2.51	0.00	0.418
Hole	1.000	1	0.00	0.00	1.000	1	0.00	0.00	1.000	1	0.00	0.00	1.000
Hng. Fire	0.892	1	0.00	0.00	0.892	1	0.00	0.00	0.892	1	0.00	0.00	0.892
Hole	1.000	1	0.00	0.00	1.000	1	0.00	0.00	1.000	1	0.00	0.00	1.000
Hng. Fire	0.741	1	0.00	0.00	0.741	1	0.00	0.00	0.741	1	0.00	0.00	0.741
Slid. Semi-WT	0.492	1	0.00	0.00	0.010	1	0.00	0.00	0.010	1	0.00	0.00	0.010
Hole	1.000	1	0.00	0.00	1.000	1	0.00	0.00	1.000	1	0.00	0.00	1.000
Hng. Fire	0.489	0	2.49	0.01	0.489	0	2.51	0.02	0.489	1	0.00	0.00	0.489
Hole	1.000	1	0.00	0.00	1.000	1	0.00	0.00	1.000	1	0.00	0.00	1.000
Hng. Fire	0.566	1	0.00	0.00	0.566	0	2.47	0.02	0.566	1	0.00	0.00	0.566
Hng. Dbl. Fire	0.945	1	0.00	0.00	0.945	1	0.00	0.00	0.945	1	0.00	0.00	0.945

Hng. Fire	0.580	0	2.55	0.22	0.580	1	0.00	0.00	0.580	1	0.00	0.00	0.580
Hng. Fire	0.403	1	0.00	0.00	0.403	0	2.52	0.09	0.403	0	2.50	0.05	0.403
Hng. Fire	0.774	1	0.00	0.00	0.774	1	0.00	0.00	0.774	1	0.00	0.00	0.774
Hole	1.000	1	0.00	0.00	1.000	1	0.00	0.00	1.000	1	0.00	0.00	1.000
Hole	1.000	1	0.00	0.00	1.000	1	0.00	0.00	1.000	1	0.00	0.00	1.000
Hng. Fire	0.825	0	2.51	0.05	0.825	1	0.00	0.00	0.825	1	0.00	0.00	0.825
Hng. Fire	0.924	1	0.00	0.00	0.924	1	0.00	0.00	0.924	1	0.00	0.00	0.924
Hole	1.000	1	0.00	0.00	1.000	1	0.00	0.00	1.000	1	0.00	0.00	1.000
Slid. Semi-WT	0.477	1	0.00	0.00	0.009	0	7.99	0.11	0.009	0	7.95	0.05	0.009
Slid. Semi-WT	0.514	1	0.00	0.00	0.011	0	8.10	0.01	0.011	1	0.00	0.00	0.011
Hng. Fire	0.337	1	0.00	0.00	0.337	0	2.54	0.07	0.337	0	2.52	0.00	0.337
Hng. Fire	0.670	1	0.00	0.00	0.670	1	0.00	0.00	0.670	1	0.00	0.00	0.670
Slid. Lift	0.109	0	1.45	0.05	0.109	0	1.36	0.11	0.109	1	0.00	0.00	0.109
Slid. Lift	0.095	0	1.43	0.05	0.095	0	1.48	0.04	0.095	0	1.49	0.00	0.095
Hole	1.000	1	0.00	0.00	1.000	1	0.00	0.00	1.000	1	0.00	0.00	1.000
Hole	1.000	1	0.00	0.00	1.000	1	0.00	0.00	1.000	1	0.00	0.00	1.000
Hng. Non-WT	0.798	1	0.00	0.00	0.798	1	0.00	0.00	0.798	1	0.00	0.00	0.798
Hng. Non-WT	0.746	0	1.64	0.00	0.746	1	0.00	0.00	0.746	1	0.00	0.00	0.746
Hole	1.000	1	0.00	0.00	1.000	1	0.00	0.00	1.000	1	0.00	0.00	1.000
Hole	1.000	1	0.00	0.00	1.000	1	0.00	0.00	1.000	1	0.00	0.00	1.000
Slid. Lift	0.371	0	1.53	0.03	0.371	0	1.61	0.12	0.371	0	1.49	0.01	0.371
Slid. Lift	0.017	0	1.34	0.01	0.017	0	1.55	0.01	0.017	0	1.41	0.02	0.017
Hng. Non-WT	0.410	0	1.66	0.00	0.410	0	1.59	0.02	0.410	1	0.00	0.00	0.410
Hng. Dbl. Fire	0.397	1	0.00	0.00	0.397	0	1.84	0.01	0.397	0	1.95	0.05	0.397
Hng. Dbl. Fire	0.288	0	1.80	0.01	0.288	1	0.00	0.00	0.288	1	0.00	0.00	0.288
Hng. Dbl. Fire	0.757	1	0.00	0.00	0.757	1	0.00	0.00	0.757	1	0.00	0.00	0.757
Hng. Dbl. Fire	0.789	0	2.07	0.11	0.789	0	2.00	-0.19	0.789	1	0.00	0.00	0.789
Shell	0.000	1	1.00	0.00	0.000	1	1.00	0.00	0.000	1	1.00	0.00	0.000
Shell	0.000	1	1.00	0.00	0.000	1	1.00	0.00	0.000	1	1.00	0.00	0.000
Hng. Fire	0.656	0	2.52	0.02	0.656	1	0.00	0.00	0.656	1	0.00	0.00	0.656
Hole	1.000	1	0.00	0.00	1.000	1	0.00	0.00	1.000	1	0.00	0.00	1.000
Slid. Semi-WT	0.518	0	7.88	0.00	0.011	1	0.00	0.00	0.011	1	0.00	0.00	0.011
Hole	1.000	1	0.00	0.00	1.000	1	0.00	0.00	1.000	1	0.00	0.00	1.000
Hng. Fire	0.937	1	0.00	0.00	0.937	1	0.00	0.00	0.937	1	0.00	0.00	0.937
Hng. Fire	0.955	1	0.00	0.00	0.955	1	0.00	0.00	0.955	0	2.47	0.03	0.955
Hng. Non-WT	0.893	1	0.00	0.00	0.893	1	0.00	0.00	0.893	1	0.00	0.00	0.893
Hng. Fire	0.122	0	2.30	0.04	0.122	0	2.58	0.04	0.122	0	2.61	0.02	0.122
Hng. Fire	0.861	0	2.31	0.11	0.861	0	2.63	0.09	0.861	1	0.00	0.00	0.861
Slid. Lift	0.286	0	1.36	0.00	0.286	0	1.38	0.03	0.286	1	0.00	0.00	0.286
Slid. Lift	0.246	0	1.32	0.05	0.246	0	1.55	0.03	0.246	0	1.50	0.01	0.246
Esc. Hatch	0.346	0	2.47	0.02	0.346	0	2.44	0.03	0.346	1	0.00	0.00	0.346
Esc. Hatch	0.367	0	2.58	0.01	0.367	0	2.43	0.06	0.367	0	2.45	0.05	0.367
Hng. Non-WT	0.724	0	1.45	0.07	0.724	1	0.00	0.00	0.724	1	0.00	0.00	0.724

Hng. Non-WT	0.782	1	0.00	0.00	0.782	1	0.00	0.00	0.782	0	1.53	0.02	0.782
Hng. Fire	0.997	1	0.00	0.00	0.997	1	0.00	0.00	0.997	1	0.00	0.00	0.997
Hole	1.000	1	0.00	0.00	1.000	1	0.00	0.00	1.000	1	0.00	0.00	1.000
Hng. Non-WT	0.952	0	1.34	0.07	0.952	0	1.47	0.02	0.952	1	0.00	0.00	0.952
Hng. Non-WT	0.867	0	1.54	0.02	0.867	1	0.00	0.00	0.867	1	0.00	0.00	0.867
Hng. Fire	0.939	1	0.00	0.00	0.939	1	0.00	0.00	0.939	1	0.00	0.00	0.939
Hng. Dbl. Fire	0.888	1	0.00	0.00	0.888	1	0.00	0.00	0.888	1	0.00	0.00	0.888
Hng. Non-WT	0.980	1	0.00	0.00	0.980	1	0.00	0.00	0.980	1	0.00	0.00	0.980
Hole	1.000	1	0.00	0.00	1.000	1	0.00	0.00	1.000	1	0.00	0.00	1.000
Hng. Non-WT	0.899	1	0.00	0.00	0.899	1	0.00	0.00	0.899	1	0.00	0.00	0.899
Hng. Fire	0.171	0	2.41	0.00	0.171	0	2.33	0.01	0.171	0	2.63	0.08	0.171
Hng. Fire	0.229	0	2.48	0.00	0.229	0	2.61	0.05	0.229	0	2.61	0.07	0.229
Hng. Esc.	0.124	0	2.46	0.02	0.124	1	0.00	0.00	0.124	0	2.58	0.02	0.124
Hng. Non-WT	0.920	1	0.00	0.00	0.920	1	0.00	0.00	0.920	0	1.48	0.09	0.920
Hole	1.000	1	0.00	0.00	1.000	1	0.00	0.00	1.000	1	0.00	0.00	1.000
Slid. Lift	0.061	0	1.64	0.03	0.061	0	1.62	0.11	0.061	0	1.47	0.02	0.061
Hole	1.000	1	0.00	0.00	1.000	1	0.00	0.00	1.000	1	0.00	0.00	1.000
Slid. Light-WT	0.121	0	8.16	0.08	0.001	0	8.17	0.03	0.001	1	0.00	0.00	0.001
Hng. Fire	0.458	0	2.39	0.01	0.458	0	2.59	0.07	0.458	0	2.56	0.06	0.458
Hng. Fire	0.420	0	2.49	0.05	0.420	0	2.47	0.00	0.420	1	0.00	0.00	0.420
Hng. Esc.	0.618	0	2.44	0.00	0.618	1	0.00	0.00	0.618	1	0.00	0.00	0.618
Esc. Hatch	0.658	1	0.00	0.00	0.658	0	2.74	0.04	0.658	1	0.00	0.00	0.658
Esc. Hatch	0.341	1	0.00	0.00	0.341	0	2.48	0.01	0.341	1	0.00	0.00	0.341
Hng. Esc.	0.481	1	0.00	0.00	0.481	0	2.60	0.01	0.481	0	2.41	0.03	0.481
Hng. Weat.	0.229	0	3.47	0.01	0.229	0	3.48	0.00	0.229	0	3.47	0.03	0.229
Hng. Weat.	0.011	0	3.54	0.01	0.011	0	3.45	0.02	0.011	0	3.33	0.01	0.011
Hng. Weat.	0.019	0	3.29	0.02	0.019	0	3.48	0.06	0.019	0	3.58	0.06	0.019
Hng. Weat.	0.000	0	3.23	0.01	0.000	0	3.44	0.02	0.000	0	3.51	0.14	0.000
Hng. Weat.	0.047	0	3.37	0.01	0.047	0	3.34	0.00	0.047	0	3.53	0.01	0.047
Hng. Weat.	0.023	0	3.58	0.08	0.023	0	3.44	0.06	0.023	0	3.39	0.04	0.023
Hng. Weat.	0.000	0	3.56	0.01	0.000	0	3.39	0.02	0.000	0	3.53	0.03	0.000
Hole	1.000	1	0.00	0.00	1.000	1	0.00	0.00	1.000	1	0.00	0.00	1.000
Hole	1.000	1	0.00	0.00	1.000	1	0.00	0.00	1.000	1	0.00	0.00	1.000
Hole	1.000	1	0.00	0.00	1.000	1	0.00	0.00	1.000	1	0.00	0.00	1.000
Hng. Cold Room	0.026	1	0.00	0.00	0.026	0	3.44	0.02	0.026	0	3.66	0.02	0.026
Hng. Fire	0.922	1	0.00	0.00	0.922	1	0.00	0.00	0.922	0	2.55	0.01	0.922
Hng. Non-WT	0.668	0	1.56	0.05	0.668	1	0.00	0.00	0.668	0	1.41	0.00	0.668
Hng. Non-WT	0.686	1	0.00	0.00	0.686	1	0.00	0.00	0.686	1	0.00	0.00	0.686
Hole	1.000	1	0.00	0.00	1.000	1	0.00	0.00	1.000	1	0.00	0.00	1.000
Hng. Prov. Room	0.164	0	3.62	0.00	0.164	0	3.29	0.01	0.164	0	3.56	0.00	0.164
Hng. Fire	0.761	1	0.00	0.00	0.761	1	0.00	0.00	0.761	1	0.00	0.00	0.761
Hng. Fire	0.570	0	2.61	0.05	0.570	1	0.00	0.00	0.570	1	0.00	0.00	0.570
Hng. Cold Room	0.063	0	3.41	0.01	0.063	0	3.40	0.04	0.063	0	3.34	0.08	0.063

Hng. Fire	0.935	1	0.00	0.00	0.935	1	0.00	0.00	0.935	1	0.00	0.00	0.935
Hng. Non-WT	0.863	1	0.00	0.00	0.863	0	1.42	0.01	0.863	1	0.00	0.00	0.863
Hng. Fire	0.554	1	0.00	0.00	0.554	1	0.00	0.00	0.554	1	0.00	0.00	0.554
Hng. Fire	0.088	0	2.35	0.00	0.088	0	2.51	0.04	0.088	0	2.57	0.11	0.088
Hng. Fire	0.631	1	0.00	0.00	0.631	0	2.45	0.03	0.631	0	2.59	0.00	0.631
Hng. Fire	0.641	1	0.00	0.00	0.641	0	2.49	0.01	0.641	1	0.00	0.00	0.641
Hng. Fire	0.990	1	0.00	0.00	0.990	1	0.00	0.00	0.990	1	0.00	0.00	0.990
Hng. Fire	0.722	1	0.00	0.00	0.722	0	2.46	0.01	0.722	0	2.45	0.04	0.722
Hng. Fire	0.871	1	0.00	0.00	0.871	1	0.00	0.00	0.871	1	0.00	0.00	0.871
Hng. Esc.	0.874	1	0.00	0.00	0.874	1	0.00	0.00	0.874	1	0.00	0.00	0.874
Hng. Dbl. Fire	0.362	0	2.03	0.03	0.362	0	1.98	0.03	0.362	1	0.00	0.00	0.362
Hng. Fire	0.796	1	0.00	0.00	0.796	1	0.00	0.00	0.796	1	0.00	0.00	0.796
Slid. Lift	0.151	0	1.46	0.14	0.151	0	1.74	0.01	0.151	0	1.54	0.01	0.151
Slid. Lift	0.167	0	1.41	0.01	0.167	0	1.43	0.11	0.167	0	1.68	0.03	0.167
Slid. Lift	0.114	0	1.60	0.03	0.114	0	1.27	0.02	0.114	0	1.50	0.03	0.114
Hng. Fire	0.989	1	0.00	0.00	0.989	1	0.00	0.00	0.989	1	0.00	0.00	0.989
Hng. Fire	0.503	1	0.00	0.00	0.503	0	2.46	0.03	0.503	1	0.00	0.00	0.503
Hole	1.000	1	0.00	0.00	1.000	1	0.00	0.00	1.000	1	0.00	0.00	1.000
Hole	1.000	1	0.00	0.00	1.000	1	0.00	0.00	1.000	1	0.00	0.00	1.000
Hole	1.000	1	0.00	0.00	1.000	1	0.00	0.00	1.000	1	0.00	0.00	1.000
Hng. Fire	0.936	1	0.00	0.00	0.936	1	0.00	0.00	0.936	1	0.00	0.00	0.936
Hng. Fire	0.045	0	2.50	0.02	0.045	0	2.54	0.00	0.045	0	2.46	0.01	0.045
Hng. Fire	0.507	0	2.60	0.01	0.507	1	0.00	0.00	0.507	0	2.41	0.01	0.507
Hng. Fire	0.713	1	0.00	0.00	0.713	1	0.00	0.00	0.713	1	0.00	0.00	0.713
Hng. Dbl. Fire	0.393	0	1.82	0.04	0.393	0	2.12	0.01	0.393	0	2.00	0.05	0.393
Hng. Non-WT	0.766	1	0.00	0.00	0.766	1	0.00	0.00	0.766	1	0.00	0.00	0.766
Hng. Non-WT	0.598	0	1.59	0.07	0.598	1	0.00	0.00	0.598	1	0.00	0.00	0.598
Hng. Dbl. Fire	0.427	1	0.00	0.00	0.427	0	1.83	0.00	0.427	0	2.02	0.02	0.427
Hng. Dbl. Fire	0.462	0	2.01	0.00	0.462	0	1.81	0.01	0.462	0	1.95	0.00	0.462
Hng. Fire	0.172	0	2.62	0.01	0.172	0	2.53	0.00	0.172	0	2.48	0.03	0.172
Hng. Non-WT	0.671	1	0.00	0.00	0.671	0	1.65	0.00	0.671	1	0.00	0.00	0.671
Hng. Non-WT	0.660	1	0.00	0.00	0.660	0	1.59	0.04	0.660	1	0.00	0.00	0.660
Hng. Fire	0.113	0	2.39	0.07	0.113	0	2.56	0.04	0.113	0	2.35	0.02	0.113
Slid. Fire	0.399	0	1.09	0.02	0.399	1	0.00	0.00	0.399	1	0.00	0.00	0.399
Slid. Fire	0.479	0	1.08	0.13	0.479	1	0.00	0.00	0.479	1	0.00	0.00	0.479
Hng. Fire	0.527	0	2.50	0.03	0.527	1	0.00	0.00	0.527	1	0.00	0.00	0.527
Hng. Fire	0.808	0	2.45	0.02	0.808	1	0.00	0.00	0.808	1	0.00	0.00	0.808
Hng. Non-WT	0.618	1	0.00	0.00	0.618	1	0.00	0.00	0.618	0	1.53	0.05	0.618
Hng. Non-WT	0.883	0	1.46	0.02	0.883	1	0.00	0.00	0.883	1	0.00	0.00	0.883
Hole	1.000	1	0.00	0.00	1.000	1	0.00	0.00	1.000	1	0.00	0.00	1.000
Hole	1.000	1	0.00	0.00	1.000	1	0.00	0.00	1.000	1	0.00	0.00	1.000
Hng. Fire	0.310	0	2.70	0.04	0.310	0	2.71	0.00	0.310	0	2.53	0.04	0.310
Hole	1.000	1	0.00	0.00	1.000	1	0.00	0.00	1.000	1	0.00	0.00	1.000

Hng. Fire	0.715	1	0.00	0.00	0.715	0	2.56	0.03	0.715	0	2.38	0.01	0.715
Slid. Lift	0.035	0	1.51	0.03	0.035	0	1.32	0.06	0.035	1	0.00	0.00	0.035
Slid. Lift	0.036	0	1.49	0.00	0.036	0	1.60	0.03	0.036	0	1.54	0.00	0.036
Shell	0.000	1	1.00	0.00	0.000	1	1.00	0.00	0.000	1	1.00	0.00	0.000
Slid. Weat.	0.516	1	0.00	0.00	0.516	1	0.00	0.00	0.516	0	1.16	0.00	0.516
Hole	1.000	1	0.00	0.00	1.000	1	0.00	0.00	1.000	1	0.00	0.00	1.000
Slid. Lift	0.238	1	0.00	0.00	0.238	0	1.38	0.02	0.238	0	1.51	0.03	0.238
Slid. Lift	0.109	1	0.00	0.00	0.109	0	1.50	0.04	0.109	0	1.51	0.08	0.109
Slid. Lift	0.064	0	1.46	0.02	0.064	0	1.41	0.02	0.064	0	1.51	0.04	0.064
Slid. Lift	0.042	0	1.48	0.01	0.042	0	1.39	0.01	0.042	0	1.70	0.04	0.042
Slid. Weat.	0.318	0	1.03	0.05	0.318	1	0.00	0.00	0.318	0	1.04	0.01	0.318
Shell	0.000	1	1.00	0.00	0.000	1	1.00	0.00	0.000	1	1.00	0.00	0.000
Slid. Fire	0.836	1	0.00	0.00	0.836	1	0.00	0.00	0.836	1	0.00	0.00	0.836
Hng. Fire	0.941	1	0.00	0.00	0.941	1	0.00	0.00	0.941	1	0.00	0.00	0.941
Slid. Fire	0.968	1	0.00	0.00	0.968	1	0.00	0.00	0.968	1	0.00	0.00	0.968
Hng. Fire	0.409	0	2.51	0.02	0.409	1	0.00	0.00	0.409	0	2.53	0.10	0.409
Hng. Fire	0.863	0	2.58	0.05	0.863	1	0.00	0.00	0.863	0	2.40	0.00	0.863
Hng. Fire	0.919	1	0.00	0.00	0.919	1	0.00	0.00	0.919	1	0.00	0.00	0.919
Hng. Fire	0.924	1	0.00	0.00	0.924	1	0.00	0.00	0.924	1	0.00	0.00	0.924
Hng. Fire	0.937	1	0.00	0.00	0.937	1	0.00	0.00	0.937	1	0.00	0.00	0.937
Slid. Semi-WT	0.580	1	0.00	0.00	0.014	1	0.00	0.00	0.014	0	8.01	0.06	0.014
Hng. Fire	0.872	1	0.00	0.00	0.872	1	0.00	0.00	0.872	1	0.00	0.00	0.872
Hng. Fire	0.954	1	0.00	0.00	0.954	1	0.00	0.00	0.954	1	0.00	0.00	0.954
Slid. Lift	0.343	0	1.55	0.03	0.343	0	1.53	0.05	0.343	0	1.46	0.00	0.343
Slid. Lift	0.106	0	1.54	0.01	0.106	0	1.56	0.04	0.106	0	1.47	0.09	0.106
Hng. Fire	0.925	1	0.00	0.00	0.925	1	0.00	0.00	0.925	1	0.00	0.00	0.925
Hng. Fire	0.881	1	0.00	0.00	0.881	1	0.00	0.00	0.881	1	0.00	0.00	0.881
Hole	1.000	1	0.00	0.00	1.000	1	0.00	0.00	1.000	1	0.00	0.00	1.000
Hole	1.000	1	0.00	0.00	1.000	1	0.00	0.00	1.000	1	0.00	0.00	1.000
Hole	1.000	1	0.00	0.00	1.000	1	0.00	0.00	1.000	1	0.00	0.00	1.000
Hng. Esc.	0.837	1	0.00	0.00	0.837	0	2.42	-0.05	0.837	1	0.00	0.00	0.837
B-Class Struct.	1.000	1	0.00	0.00	1.000	1	0.00	0.00	1.000	1	0.00	0.00	1.000
B-Class Struct.	1.000	1	0.00	0.00	1.000	1	0.00	0.00	1.000	1	0.00	0.00	1.000
Hng. Fire	0.818	0	2.65	0.00	0.818	1	0.00	0.00	0.818	1	0.00	0.00	0.818
Hng. Fire	0.585	0	2.56	0.01	0.585	0	2.37	0.03	0.585	1	0.00	0.00	0.585
Hng. Fire	0.753	1	0.00	0.00	0.753	1	0.00	0.00	0.753	1	0.00	0.00	0.753
Slid. Semi-WT	0.946	1	0.00	0.00	0.150	1	0.00	0.00	0.150	1	0.00	0.00	0.150
Hole	1.000	1	0.00	0.00	1.000	1	0.00	0.00	1.000	1	0.00	0.00	1.000
Hng. Fire	0.660	0	2.38	0.01	0.660	1	0.00	0.00	0.660	1	0.00	0.00	0.660
Hng. Non-WT	0.278	0	1.43	0.01	0.278	0	1.64	0.02	0.278	0	1.60	0.00	0.278
Hng. Fire	0.422	1	0.00	0.00	0.422	0	2.53	0.02	0.422	0	2.44	0.01	0.422
B-Class Struct.	1.000	1	0.00	0.00	1.000	1	0.00	0.00	1.000	1	0.00	0.00	1.000
B-Class Struct.	1.000	1	0.00	0.00	1.000	1	0.00	0.00	1.000	1	0.00	0.00	1.000

Hng. Fire	0.220	0	2.52	0.01	0.220	1	0.00	0.00	0.220	0	2.45	0.01	0.220
Hng. Non-WT	0.952	1	0.00	0.00	0.952	1	0.00	0.00	0.952	1	0.00	0.00	0.952
Hng. Fire	0.596	0	2.51	0.10	0.596	0	2.42	0.02	0.596	1	0.00	0.00	0.596
Slid. Lift	0.031	0	1.38	0.10	0.031	0	1.49	0.01	0.031	0	1.44	0.02	0.031
Slid. Lift	0.128	0	1.43	0.01	0.128	0	1.41	0.01	0.128	0	1.50	0.04	0.128
Slid. Lift	0.127	0	1.37	0.01	0.127	1	0.00	0.00	0.127	0	1.55	0.08	0.127
Slid. Lift	0.327	0	1.42	0.01	0.327	0	1.56	0.00	0.327	0	1.48	0.02	0.327
Hole	1.000	1	0.00	0.00	1.000	1	0.00	0.00	1.000	1	0.00	0.00	1.000
Hng. Fire	0.559	0	2.52	0.02	0.559	1	0.00	0.00	0.559	0	2.58	-0.03	0.559
Hng. Fire	0.710	1	0.00	0.00	0.710	1	0.00	0.00	0.710	1	0.00	0.00	0.710
Hole	1.000	1	0.00	0.00	1.000	1	0.00	0.00	1.000	1	0.00	0.00	1.000
Hng. Fire	0.900	1	0.00	0.00	0.900	1	0.00	0.00	0.900	1	0.00	0.00	0.900
Slid. Semi-WT	0.479	1	0.00	0.00	0.009	0	8.06	0.11	0.009	0	7.99	0.11	0.009
Hng. Fire	0.295	1	0.00	0.00	0.295	0	2.58	0.05	0.295	0	2.44	0.05	0.295
Slid. Semi-WT	0.541	1	0.00	0.00	0.012	1	0.00	0.00	0.012	1	0.00	0.00	0.012
Hole	1.000	1	0.00	0.00	1.000	1	0.00	0.00	1.000	1	0.00	0.00	1.000
Hng. Non-WT	0.891	0	1.56	0.07	0.891	1	0.00	0.00	0.891	0	1.59	0.06	0.891
B-Class Struct.	1.000	1	0.00	0.00	1.000	1	0.00	0.00	1.000	1	0.00	0.00	1.000
Hng. Fire	0.444	1	0.00	0.00	0.444	0	2.42	0.04	0.444	0	2.42	0.04	0.444
Hng. Fire	0.145	0	2.62	0.02	0.145	0	2.43	0.03	0.145	0	2.51	0.04	0.145
Hng. Fire	0.462	0	2.71	0.02	0.462	0	2.51	0.03	0.462	1	0.00	0.00	0.462
Hng. Non-WT	0.931	1	0.00	0.00	0.931	1	0.00	0.00	0.931	1	0.00	0.00	0.931
Hng. Non-WT	0.575	1	0.00	0.00	0.575	1	0.00	0.00	0.575	1	0.00	0.00	0.575
Hng. Non-WT	0.678	0	1.59	0.00	0.678	0	1.37	0.02	0.678	0	1.50	0.03	0.678
Hng. Non-WT	0.560	0	1.53	0.01	0.560	1	0.00	0.00	0.560	0	1.49	0.01	0.560
Slid. Lift	0.087	0	1.39	0.01	0.087	0	1.60	0.03	0.087	0	1.42	0.01	0.087
Slid. Lift	0.187	1	0.00	0.00	0.187	0	1.46	0.01	0.187	0	1.23	0.06	0.187
Hng. Fire	0.400	0	2.64	0.06	0.400	0	2.49	0.03	0.400	1	0.00	0.00	0.400
Hng. Fire	0.947	1	0.00	0.00	0.947	1	0.00	0.00	0.947	1	0.00	0.00	0.947
Hng. Fire	0.609	1	0.00	0.00	0.609	1	0.00	0.00	0.609	0	2.59	0.05	0.609
Hole	1.000	1	0.00	0.00	1.000	1	0.00	0.00	1.000	1	0.00	0.00	1.000
Hng. Non-WT	0.157	0	1.54	0.02	0.157	0	1.53	0.00	0.157	0	1.42	0.00	0.157
Hole	1.000	1	0.00	0.00	1.000	1	0.00	0.00	1.000	1	0.00	0.00	1.000
Hole	1.000	1	0.00	0.00	1.000	1	0.00	0.00	1.000	1	0.00	0.00	1.000
Hng. Non-WT	0.792	0	1.46	0.02	0.792	1	0.00	0.00	0.792	1	0.00	0.00	0.792
Hng. Non-WT	0.573	1	0.00	0.00	0.573	1	0.00	0.00	0.573	1	0.00	0.00	0.573
Hole	1.000	1	0.00	0.00	1.000	1	0.00	0.00	1.000	1	0.00	0.00	1.000
Hng. Non-WT	0.375	0	1.44	0.02	0.375	0	1.43	0.00	0.375	0	1.49	0.05	0.375
Hng. Non-WT	0.935	1	0.00	0.00	0.935	1	0.00	0.00	0.935	1	0.00	0.00	0.935
Hng. Fire	0.957	1	0.00	0.00	0.957	1	0.00	0.00	0.957	1	0.00	0.00	0.957
Hng. Fire	0.383	0	2.69	0.01	0.383	0	2.41	0.07	0.383	0	2.54	0.01	0.383
Hng. Dbl. Fire	0.963	1	0.00	0.00	0.963	1	0.00	0.00	0.963	1	0.00	0.00	0.963
Hng. Fire	0.752	1	0.00	0.00	0.752	1	0.00	0.00	0.752	1	0.00	0.00	0.752

Hng. Fire	0.588	1	0.00	0.00	0.588	1	0.00	0.00	0.588	1	0.00	0.00	0.588
Hng. Fire	0.781	1	0.00	0.00	0.781	1	0.00	0.00	0.781	0	2.50	0.02	0.781
Hng. Fire	0.448	0	2.39	0.01	0.448	0	2.51	0.00	0.448	1	0.00	0.00	0.448
Slid. Lift	0.057	0	1.45	0.11	0.057	0	1.85	0.05	0.057	0	1.65	0.02	0.057
Hole	1.000	1	0.00	0.00	1.000	1	0.00	0.00	1.000	1	0.00	0.00	1.000
Slid. Semi-WT	0.460	0	7.86	0.00	0.009	0	8.22	0.05	0.009	1	0.00	0.00	0.009
Slid. Semi-WT	0.506	1	0.00	0.00	0.010	0	8.04	0.02	0.010	1	0.00	0.00	0.010
Hng. Fire	0.580	1	0.00	0.00	0.580	1	0.00	0.00	0.580	1	0.00	0.00	0.580
Hng. Non-WT	0.328	1	0.00	0.00	0.328	0	1.54	0.00	0.328	0	1.50	0.02	0.328
Hole	1.000	1	0.00	0.00	1.000	1	0.00	0.00	1.000	1	0.00	0.00	1.000
Hole	1.000	1	0.00	0.00	1.000	1	0.00	0.00	1.000	1	0.00	0.00	1.000
Hng. Fire	0.566	0	2.55	0.01	0.566	1	0.00	0.00	0.566	0	2.66	0.00	0.566
Hng. Esc.	0.694	1	0.00	0.00	0.694	1	0.00	0.00	0.694	1	0.00	0.00	0.694
Hng. Fire	0.798	1	0.00	0.00	0.798	1	0.00	0.00	0.798	1	0.00	0.00	0.798
Hng. Esc.	0.785	1	0.00	0.00	0.785	1	0.00	0.00	0.785	1	0.00	0.00	0.785
Hng. Non-WT	0.987	1	0.00	0.00	0.987	1	0.00	0.00	0.987	1	0.00	0.00	0.987
Hng. Fire	0.749	1	0.00	0.00	0.749	0	2.59	0.01	0.749	1	0.00	0.00	0.749
Hng. Non-WT	0.936	1	0.00	0.00	0.936	1	0.00	0.00	0.936	1	0.00	0.00	0.936
Hng. Dbl. Fire	0.745	1	0.00	0.00	0.745	1	0.00	0.00	0.745	0	1.86	0.01	0.745
Hng. Fire	0.387	1	0.00	0.00	0.387	1	0.00	0.00	0.387	0	2.57	0.00	0.387
Hng. Fire	0.952	1	0.00	0.00	0.952	1	0.00	0.00	0.952	1	0.00	0.00	0.952
Hng. Fire	0.349	0	2.39	0.01	0.349	0	2.70	0.03	0.349	0	2.40	0.00	0.349
Hng. Fire	0.697	1	0.00	0.00	0.697	1	0.00	0.00	0.697	0	2.51	0.00	0.697
Hng. Fire	0.980	1	0.00	0.00	0.980	1	0.00	0.00	0.980	1	0.00	0.00	0.980
Hng. Fire	0.431	0	2.35	0.02	0.431	1	0.00	0.00	0.431	1	0.00	0.00	0.431
Hole	1.000	1	0.00	0.00	1.000	1	0.00	0.00	1.000	1	0.00	0.00	1.000
Hng. Fire	0.861	1	0.00	0.00	0.861	1	0.00	0.00	0.861	1	0.00	0.00	0.861
Hng. Fire	0.660	1	0.00	0.00	0.660	1	0.00	0.00	0.660	1	0.00	0.00	0.660
Hole	1.000	1	0.00	0.00	1.000	1	0.00	0.00	1.000	1	0.00	0.00	1.000
Hng. Fire	0.733	0	2.37	0.01	0.733	0	2.35	0.01	0.733	1	0.00	0.00	0.733
Hng. Non-WT	0.900	0	1.47	0.03	0.900	1	0.00	0.00	0.900	1	0.00	0.00	0.900
Hng. Non-WT	0.674	1	0.00	0.00	0.674	0	1.53	0.01	0.674	0	1.64	0.00	0.674
Hng. Lift	0.095	0	1.55	0.07	0.095	0	1.55	0.06	0.095	0	1.66	0.05	0.095
Hng. Non-WT	0.357	0	1.36	0.00	0.357	0	1.50	0.03	0.357	0	1.50	0.02	0.357
Hng. Fire	0.182	0	2.66	0.11	0.182	0	2.59	0.00	0.182	0	2.62	0.04	0.182
Hng. Fire	0.821	0	2.58	0.01	0.821	0	2.47	0.03	0.821	1	0.00	0.00	0.821
Hng. Non-WT	0.894	1	0.00	0.00	0.894	1	0.00	0.00	0.894	1	0.00	0.00	0.894
Hng. Cold Room	0.020	0	3.40	0.03	0.020	0	3.71	0.02	0.020	0	3.40	0.02	0.020
Hng. Non-WT	0.881	0	1.56	0.00	0.881	1	0.00	0.00	0.881	1	0.00	0.00	0.881
Hng. Non-WT	0.271	1	0.00	0.00	0.271	1	0.00	0.00	0.271	0	1.50	0.04	0.271
Hng. Non-WT	0.546	1	0.00	0.00	0.546	1	0.00	0.00	0.546	0	1.55	0.04	0.546
Hng. Cold Room	0.025	0	3.50	0.01	0.025	0	3.50	0.03	0.025	0	3.39	0.02	0.025
Hng. Prov. Room	0.009	0	3.53	0.02	0.009	0	3.47	0.00	0.009	0	3.36	0.00	0.009

Hng. Fire	0.851	1	0.00	0.00	0.851	1	0.00	0.00	0.851	1	0.00	0.00	0.851
Hng. Cold Room	0.069	0	3.41	0.01	0.069	0	3.36	0.01	0.069	0	3.57	0.06	0.069
Hole	1.000	1	0.00	0.00	1.000	1	0.00	0.00	1.000	1	0.00	0.00	1.000
Hng. Fire	0.509	1	0.00	0.00	0.509	0	2.54	0.02	0.509	1	0.00	0.00	0.509
Hng. Cold Room	0.141	0	3.39	0.04	0.141	0	3.46	0.00	0.141	0	3.58	0.01	0.141
Hng. Fire	0.663	1	0.00	0.00	0.663	0	2.50	0.03	0.663	1	0.00	0.00	0.663
Hng. Fire	0.986	1	0.00	0.00	0.986	1	0.00	0.00	0.986	1	0.00	0.00	0.986
Hng. Fire	0.979	1	0.00	0.00	0.979	1	0.00	0.00	0.979	1	0.00	0.00	0.979
Slid. Lift	0.036	0	1.41	0.00	0.036	0	1.43	0.09	0.036	0	1.61	0.00	0.036
Slid. Lift	0.181	1	0.00	0.00	0.181	0	1.53	0.00	0.181	0	1.62	0.01	0.181
Slid. Lift	0.241	0	1.48	0.00	0.241	1	0.00	0.00	0.241	0	1.64	0.07	0.241
Slid. Fire	0.438	0	1.11	0.11	0.438	0	0.76	0.03	0.438	1	0.00	0.00	0.438
Slid. Fire	0.430	0	0.97	0.04	0.430	1	0.00	0.00	0.430	0	1.14	0.02	0.430
Hng. Prov. Room	0.029	0	3.56	0.05	0.029	0	3.58	0.04	0.029	0	3.38	0.04	0.029
Slid. Fire	0.553	0	1.20	0.01	0.553	1	0.00	0.00	0.553	1	0.00	0.00	0.553
Hole	1.000	1	0.00	0.00	1.000	1	0.00	0.00	1.000	1	0.00	0.00	1.000
Hole	1.000	1	0.00	0.00	1.000	1	0.00	0.00	1.000	1	0.00	0.00	1.000
Hng. Prov. Room	0.080	0	3.62	0.00	0.080	0	3.26	0.03	0.080	0	3.48	0.01	0.080
Slid. Fire	0.751	1	0.00	0.00	0.751	1	0.00	0.00	0.751	0	1.22	0.03	0.751
Hole	1.000	1	0.00	0.00	1.000	1	0.00	0.00	1.000	1	0.00	0.00	1.000
Hng. Dbl. Fire	0.676	1	0.00	0.00	0.676	0	2.13	0.02	0.676	1	0.00	0.00	0.676
Hng. Fire	0.629	0	2.67	0.00	0.629	0	2.45	0.00	0.629	1	0.00	0.00	0.629
Hole	1.000	1	0.00	0.00	1.000	1	0.00	0.00	1.000	1	0.00	0.00	1.000
Hng. Non-WT	0.694	0	1.44	0.01	0.694	0	1.56	0.01	0.694	1	0.00	0.00	0.694
Hng. Non-WT	0.707	1	0.00	0.00	0.707	0	1.54	0.08	0.707	0	1.38	0.09	0.707
Hng. Fire	0.754	1	0.00	0.00	0.754	0	2.35	0.01	0.754	1	0.00	0.00	0.754
Slid. Fire	0.849	1	0.00	0.00	0.849	0	0.99	0.01	0.849	1	0.00	0.00	0.849
Slid. Fire	0.419	1	0.00	0.00	0.419	1	0.00	0.00	0.419	0	0.87	0.01	0.419
Hng. Fire	0.943	1	0.00	0.00	0.943	1	0.00	0.00	0.943	1	0.00	0.00	0.943
Hng. Dbl. Fire	0.925	1	0.00	0.00	0.925	1	0.00	0.00	0.925	1	0.00	0.00	0.925
Hng. Dbl. Fire	0.833	1	0.00	0.00	0.833	1	0.00	0.00	0.833	1	0.00	0.00	0.833
Hole	1.000	1	0.00	0.00	1.000	1	0.00	0.00	1.000	1	0.00	0.00	1.000
Hole	1.000	1	0.00	0.00	1.000	1	0.00	0.00	1.000	1	0.00	0.00	1.000
Hole	1.000	1	0.00	0.00	1.000	1	0.00	0.00	1.000	1	0.00	0.00	1.000
Hole	1.000	1	0.00	0.00	1.000	1	0.00	0.00	1.000	1	0.00	0.00	1.000
Hole	1.000	1	0.00	0.00	1.000	1	0.00	0.00	1.000	1	0.00	0.00	1.000
Hole	1.000	1	0.00	0.00	1.000	1	0.00	0.00	1.000	1	0.00	0.00	1.000
Hole	1.000	1	0.00	0.00	1.000	1	0.00	0.00	1.000	1	0.00	0.00	1.000
Hng. Fire	0.979	1	0.00	0.00	0.979	1	0.00	0.00	0.979	1	0.00	0.00	0.979
Slid. Fire	0.724	1	0.00	0.00	0.724	0	1.08	0.19	0.724	1	0.00	0.00	0.724
Slid. Fire	0.873	1	0.00	0.00	0.873	0	0.84	0.03	0.873	1	0.00	0.00	0.873
Hng. Dbl. Fire	0.569	0	2.05	0.01	0.569	1	0.00	0.00	0.569	0	1.96	0.02	0.569
Hng. Fire	0.356	0	2.60	0.00	0.356	0	2.57	0.03	0.356	0	2.52	0.05	0.356

Hng. Fire	0.893	1	0.00	0.00	0.893	1	0.00	0.00	0.893	1	0.00	0.00	0.893
Hng. Fire	0.697	1	0.00	0.00	0.697	1	0.00	0.00	0.697	1	0.00	0.00	0.697
Hng. Fire	0.962	1	0.00	0.00	0.962	1	0.00	0.00	0.962	1	0.00	0.00	0.962
Hng. Fire	0.992	1	0.00	0.00	0.992	1	0.00	0.00	0.992	1	0.00	0.00	0.992
Hng. Fire	0.560	1	0.00	0.00	0.560	1	0.00	0.00	0.560	1	0.00	0.00	0.560
Hng. Fire	0.863	0	2.40	0.05	0.863	1	0.00	0.00	0.863	1	0.00	0.00	0.863
Hng. Dbl. Fire	0.923	1	0.00	0.00	0.923	1	0.00	0.00	0.923	1	0.00	0.00	0.923
Hng. Dbl. Fire	0.737	1	0.00	0.00	0.737	1	0.00	0.00	0.737	1	0.00	0.00	0.737
Hole	1.000	1	0.00	0.00	1.000	1	0.00	0.00	1.000	1	0.00	0.00	1.000
Hole	1.000	1	0.00	0.00	1.000	1	0.00	0.00	1.000	1	0.00	0.00	1.000
Hng. Fire	0.851	0	2.47	0.01	0.851	1	0.00	0.00	0.851	1	0.00	0.00	0.851
Hng. Fire	0.995	1	0.00	0.00	0.995	1	0.00	0.00	0.995	1	0.00	0.00	0.995
Shell	0.000	1	1.00	0.00	0.000	1	1.00	0.00	0.000	1	1.00	0.00	0.000
Hng. Non-WT	0.842	1	0.00	0.00	0.842	1	0.00	0.00	0.842	1	0.00	0.00	0.842
Hng. Dbl. Fire	0.860	1	0.00	0.00	0.860	1	0.00	0.00	0.860	1	0.00	0.00	0.860
Slid. Fire	0.709	0	1.00	0.00	0.709	1	0.00	0.00	0.709	0	0.99	0.01	0.709
Slid. Fire	0.534	1	0.00	0.00	0.534	0	1.14	0.03	0.534	0	1.11	0.03	0.534
Hng. Fire	0.872	1	0.00	0.00	0.872	1	0.00	0.00	0.872	1	0.00	0.00	0.872
Slid. Lift	0.245	0	1.36	0.02	0.245	0	1.32	0.00	0.245	1	0.00	0.00	0.245
Slid. Lift	0.082	0	1.51	0.02	0.082	0	1.42	0.01	0.082	0	1.65	0.00	0.082
Hng. Non-WT	0.395	1	0.00	0.00	0.395	0	1.57	0.00	0.395	1	0.00	0.00	0.395
Hng. Non-WT	0.809	1	0.00	0.00	0.809	1	0.00	0.00	0.809	1	0.00	0.00	0.809
Slid. Lift	0.178	1	0.00	0.00	0.178	0	1.48	0.01	0.178	0	1.66	0.01	0.178
Slid. Lift	0.071	0	1.65	0.01	0.071	0	1.43	0.02	0.071	0	1.24	0.02	0.071
Hng. Non-WT	0.463	0	1.50	0.03	0.463	1	0.00	0.00	0.463	1	0.00	0.00	0.463
Slid. Lift	0.204	0	1.50	0.06	0.204	0	1.61	0.01	0.204	0	1.59	0.08	0.204
Slid. Lift	0.093	0	1.55	0.04	0.093	0	1.60	0.02	0.093	0	1.50	0.00	0.093
Slid. Fire	0.531	1	0.00	0.00	0.531	0	0.88	0.02	0.531	0	0.86	0.02	0.531
Hole	1.000	1	0.00	0.00	1.000	1	0.00	0.00	1.000	1	0.00	0.00	1.000
Shell	0.000	1	1.00	0.00	0.000	1	1.00	0.00	0.000	1	1.00	0.00	0.000
Hng. Fire	0.643	1	0.00	0.00	0.643	0	2.58	0.02	0.643	1	0.00	0.00	0.643
Slid. Fire	0.735	0	0.90	0.02	0.735	1	0.00	0.00	0.735	1	0.00	0.00	0.735
Hng. Fire	0.682	1	0.00	0.00	0.682	1	0.00	0.00	0.682	0	2.45	0.08	0.682
Hng. Fire	0.717	1	0.00	0.00	0.717	1	0.00	0.00	0.717	1	0.00	0.00	0.717
Hng. Fire	0.924	0	2.51	0.06	0.924	1	0.00	0.00	0.924	0	2.74	0.00	0.924
Hng. Fire	0.769	0	2.48	0.15	0.769	1	0.00	0.00	0.769	1	0.00	0.00	0.769
Hng. Fire	0.995	1	0.00	0.00	0.995	1	0.00	0.00	0.995	1	0.00	0.00	0.995
Slid. Lift	0.150	1	0.00	0.00	0.150	0	1.40	0.00	0.150	0	1.53	0.05	0.150
Slid. Lift	0.351	1	0.00	0.00	0.351	0	1.34	0.02	0.351	0	1.43	0.02	0.351
Hng. Fire	0.548	0	2.37	0.07	0.548	0	2.55	0.01	0.548	0	2.61	0.05	0.548
Hng. Fire	0.802	1	0.00	0.00	0.802	0	2.47	0.01	0.802	1	0.00	0.00	0.802
Slid. Fire	0.657	0	1.07	0.00	0.657	0	0.96	0.00	0.657	0	1.06	0.06	0.657
Hole	1.000	1	0.00	0.00	1.000	1	0.00	0.00	1.000	1	0.00	0.00	1.000

Hole	1.000	1	0.00	0.00	1.000	1	0.00	0.00	1.000	1	0.00	0.00	1.000
Hng. Fire	0.709	1	0.00	0.00	0.709	1	0.00	0.00	0.709	1	0.00	0.00	0.709
Hng. Non-WT	0.323	0	1.53	0.06	0.323	1	0.00	0.00	0.323	0	1.49	0.03	0.323
Hng. Non-WT	0.860	1	0.00	0.00	0.860	1	0.00	0.00	0.860	1	0.00	0.00	0.860
Hng. Dbl. Fire	0.703	1	0.00	0.00	0.703	1	0.00	0.00	0.703	1	0.00	0.00	0.703
Hng. Fire	0.714	0	2.66	0.02	0.714	0	2.60	0.07	0.714	1	0.00	0.00	0.714
Hng. Non-WT	0.836	1	0.00	0.00	0.836	0	1.60	0.02	0.836	0	1.49	0.01	0.836
Hng. Dbl. Fire	0.524	1	0.00	0.00	0.524	0	2.18	0.05	0.524	0	2.09	0.05	0.524
Hng. Dbl. Fire	0.691	0	1.96	0.01	0.691	1	0.00	0.00	0.691	1	0.00	0.00	0.691
Hng. Dbl. Fire	0.668	0	2.08	0.03	0.668	1	0.00	0.00	0.668	0	1.99	0.06	0.668
Hng. Fire	0.425	0	2.28	0.01	0.425	0	2.56	0.00	0.425	0	2.64	0.04	0.425
Hng. Fire	0.697	1	0.00	0.00	0.697	1	0.00	0.00	0.697	1	0.00	0.00	0.697
Hole	1.000	1	0.00	0.00	1.000	1	0.00	0.00	1.000	1	0.00	0.00	1.000
Hng. Non-WT	0.834	1	0.00	0.00	0.834	1	0.00	0.00	0.834	1	0.00	0.00	0.834
Hole	1.000	1	0.00	0.00	1.000	1	0.00	0.00	1.000	1	0.00	0.00	1.000
Hng. Fire	0.406	0	2.37	0.01	0.406	1	0.00	0.00	0.406	0	2.52	0.01	0.406
Hole	1.000	1	0.00	0.00	1.000	1	0.00	0.00	1.000	1	0.00	0.00	1.000
Hng. Non-WT	0.230	0	1.42	0.03	0.230	0	1.47	0.02	0.230	1	0.00	0.00	0.230
Hng. Non-WT	0.923	1	0.00	0.00	0.923	1	0.00	0.00	0.923	1	0.00	0.00	0.923
Hole	1.000	1	0.00	0.00	1.000	1	0.00	0.00	1.000	1	0.00	0.00	1.000
Hole	1.000	1	0.00	0.00	1.000	1	0.00	0.00	1.000	1	0.00	0.00	1.000
Hng. Non-WT	0.260	0	1.60	0.04	0.260	0	1.53	0.02	0.260	0	1.59	0.05	0.260
Hng. Non-WT	0.509	1	0.00	0.00	0.509	0	1.54	0.06	0.509	1	0.00	0.00	0.509
Hng. Fire	0.617	1	0.00	0.00	0.617	0	2.47	0.02	0.617	1	0.00	0.00	0.617
Hng. Fire	0.879	1	0.00	0.00	0.879	1	0.00	0.00	0.879	1	0.00	0.00	0.879
Hng. Fire	0.865	1	0.00	0.00	0.865	1	0.00	0.00	0.865	0	2.46	0.02	0.865
Hng. Dbl. Fire	0.815	1	0.00	0.00	0.815	1	0.00	0.00	0.815	1	0.00	0.00	0.815
Slid. Fire	0.962	1	0.00	0.00	0.962	0	1.06	0.01	0.962	1	0.00	0.00	0.962
Hng. Fire	0.643	0	2.36	0.08	0.643	1	0.00	0.00	0.643	1	0.00	0.00	0.643
Hole	1.000	1	0.00	0.00	1.000	1	0.00	0.00	1.000	1	0.00	0.00	1.000
Hole	1.000	1	0.00	0.00	1.000	1	0.00	0.00	1.000	1	0.00	0.00	1.000
Hole	1.000	1	0.00	0.00	1.000	1	0.00	0.00	1.000	1	0.00	0.00	1.000
Hng. Fire	0.461	1	0.00	0.00	0.461	1	0.00	0.00	0.461	1	0.00	0.00	0.461
Hng. Non-WT	0.439	0	1.47	0.12	0.439	0	1.55	0.11	0.439	1	0.00	0.00	0.439
Hole	1.000	1	0.00	0.00	1.000	1	0.00	0.00	1.000	1	0.00	0.00	1.000
Hole	1.000	1	0.00	0.00	1.000	1	0.00	0.00	1.000	1	0.00	0.00	1.000
Hole	1.000	1	0.00	0.00	1.000	1	0.00	0.00	1.000	1	0.00	0.00	1.000
Slid. Lift	0.025	0	1.50	0.02	0.025	0	1.54	0.01	0.025	0	1.58	0.06	0.025
Slid. Lift	0.027	0	1.41	0.01	0.027	0	1.45	0.00	0.027	0	1.49	0.05	0.027
Hng. Dbl. Fire	0.471	0	2.01	0.03	0.471	1	0.00	0.00	0.471	0	2.10	0.01	0.471
Slid. Lift	0.050	0	1.52	0.03	0.050	0	1.39	0.04	0.050	0	1.56	0.06	0.050
Slid. Lift	0.044	0	1.72	0.01	0.044	0	1.57	0.03	0.044	0	1.70	0.02	0.044
Hng. Fire	0.590	1	0.00	0.00	0.590	1	0.00	0.00	0.590	0	2.40	0.02	0.590

Hng. Fire	0.462	0	2.56	0.00	0.462	1	0.00	0.00	0.462	0	2.37	0.04	0.462
Slid. Fire	0.922	1	0.00	0.00	0.922	1	0.00	0.00	0.922	1	0.00	0.00	0.922
Hole	1.000	1	0.00	0.00	1.000	1	0.00	0.00	1.000	1	0.00	0.00	1.000
Hole	1.000	1	0.00	0.00	1.000	1	0.00	0.00	1.000	1	0.00	0.00	1.000
Hng. Non-WT	0.802	0	1.41	0.04	0.802	1	0.00	0.00	0.802	1	0.00	0.00	0.802
Hng. Non-WT	0.910	1	0.00	0.00	0.910	1	0.00	0.00	0.910	1	0.00	0.00	0.910
Hole	1.000	1	0.00	0.00	1.000	1	0.00	0.00	1.000	1	0.00	0.00	1.000
Hng. Non-WT	0.400	0	1.45	0.04	0.400	1	0.00	0.00	0.400	0	1.51	0.02	0.400
Hng. Fire	0.924	0	2.64	0.09	0.924	1	0.00	0.00	0.924	1	0.00	0.00	0.924
Hng. Fire	0.784	1	0.00	0.00	0.784	0	2.49	0.08	0.784	1	0.00	0.00	0.784
Hng. Fire	0.679	1	0.00	0.00	0.679	1	0.00	0.00	0.679	0	2.69	0.01	0.679
Hng. Fire	0.925	1	0.00	0.00	0.925	1	0.00	0.00	0.925	1	0.00	0.00	0.925
Slid. Fire	0.329	1	0.00	0.00	0.329	0	1.16	0.02	0.329	0	0.89	0.02	0.329
Slid. Fire	0.969	1	0.00	0.00	0.969	1	0.00	0.00	0.969	1	0.00	0.00	0.969
Hng. Fire	0.676	1	0.00	0.00	0.676	1	0.00	0.00	0.676	1	0.00	0.00	0.676
Hng. Fire	0.166	0	2.55	0.03	0.166	0	2.50	0.02	0.166	0	2.51	0.01	0.166
Hng. Fire	0.953	1	0.00	0.00	0.953	1	0.00	0.00	0.953	1	0.00	0.00	0.953
Hng. Fire	0.875	1	0.00	0.00	0.875	1	0.00	0.00	0.875	1	0.00	0.00	0.875
Hng. Non-WT	0.929	1	0.00	0.00	0.929	1	0.00	0.00	0.929	1	0.00	0.00	0.929
Hng. Fire	0.636	0	2.48	0.00	0.636	0	2.47	0.00	0.636	1	0.00	0.00	0.636
Hng. Fire	0.707	1	0.00	0.00	0.707	0	2.47	0.01	0.707	1	0.00	0.00	0.707
Hng. Fire	0.255	0	2.59	0.01	0.255	0	2.57	0.00	0.255	0	2.45	0.00	0.255
Slid. Lift	0.017	0	1.53	0.01	0.017	0	1.31	0.00	0.017	0	1.50	0.04	0.017
Slid. Lift	0.356	1	0.00	0.00	0.356	0	1.58	0.03	0.356	0	1.64	0.00	0.356
Hng. Dbl. Fire	0.918	1	0.00	0.00	0.918	1	0.00	0.00	0.918	1	0.00	0.00	0.918
Hng. Dbl. Fire	0.682	1	0.00	0.00	0.682	1	0.00	0.00	0.682	1	0.00	0.00	0.682
Hng. Fire	0.805	1	0.00	0.00	0.805	1	0.00	0.00	0.805	0	2.53	0.04	0.805
Hng. Fire	0.595	1	0.00	0.00	0.595	1	0.00	0.00	0.595	1	0.00	0.00	0.595
Hng. Non-WT	0.430	1	0.00	0.00	0.430	0	1.44	0.02	0.430	0	1.55	0.01	0.430
Hng. Fire	0.659	0	2.63	0.00	0.659	0	2.47	0.01	0.659	1	0.00	0.00	0.659
Hng. Fire	0.718	1	0.00	0.00	0.718	0	2.43	0.04	0.718	1	0.00	0.00	0.718
Hole	1.000	1	0.00	0.00	1.000	1	0.00	0.00	1.000	1	0.00	0.00	1.000
Hole	1.000	1	0.00	0.00	1.000	1	0.00	0.00	1.000	1	0.00	0.00	1.000
Hng. Fire	0.847	1	0.00	0.00	0.847	1	0.00	0.00	0.847	1	0.00	0.00	0.847
Hng. Fire	0.816	1	0.00	0.00	0.816	0	2.16	0.00	0.816	1	0.00	0.00	0.816
Hng. Fire	0.721	1	0.00	0.00	0.721	1	0.00	0.00	0.721	1	0.00	0.00	0.721
Hng. Fire	0.541	0	2.51	0.00	0.541	0	2.68	0.07	0.541	0	2.51	0.04	0.541
Hng. Fire	0.590	1	0.00	0.00	0.590	0	2.68	0.01	0.590	1	0.00	0.00	0.590
Hole	1.000	1	0.00	0.00	1.000	1	0.00	0.00	1.000	1	0.00	0.00	1.000
Hng. Fire	0.619	1	0.00	0.00	0.619	1	0.00	0.00	0.619	1	0.00	0.00	0.619
Hng. Fire	0.625	0	2.40	0.00	0.625	1	0.00	0.00	0.625	1	0.00	0.00	0.625
Hng. Fire	0.205	0	2.51	0.01	0.205	0	2.42	0.01	0.205	0	2.68	0.08	0.205
Hng. Fire	0.294	0	2.36	0.01	0.294	1	0.00	0.00	0.294	0	2.71	0.04	0.294

Connection	1.000	1	0.00	0.00	1.000	1	0.00	0.00	1.000	1	0.00	0.00	1.000
Connection	1.000	1	0.00	0.00	1.000	1	0.00	0.00	1.000	1	0.00	0.00	1.000
Connection	1.000	1	0.00	0.00	1.000	1	0.00	0.00	1.000	1	0.00	0.00	1.000
Connection	1.000	1	0.00	0.00	1.000	1	0.00	0.00	1.000	1	0.00	0.00	1.000
Connection	1.000	1	0.00	0.00	1.000	1	0.00	0.00	1.000	1	0.00	0.00	1.000
Connection	1.000	1	0.00	0.00	1.000	1	0.00	0.00	1.000	1	0.00	0.00	1.000
Connection	1.000	1	0.00	0.00	1.000	1	0.00	0.00	1.000	1	0.00	0.00	1.000
Connection	1.000	1	0.00	0.00	1.000	1	0.00	0.00	1.000	1	0.00	0.00	1.000
Connection	1.000	1	0.00	0.00	1.000	1	0.00	0.00	1.000	1	0.00	0.00	1.000
Connection	1.000	1	0.00	0.00	1.000	1	0.00	0.00	1.000	1	0.00	0.00	1.000
Connection	1.000	1	0.00	0.00	1.000	1	0.00	0.00	1.000	1	0.00	0.00	1.000
Connection	1.000	1	0.00	0.00	1.000	1	0.00	0.00	1.000	1	0.00	0.00	1.000
Connection	1.000	1	0.00	0.00	1.000	1	0.00	0.00	1.000	1	0.00	0.00	1.000
Connection	1.000	1	0.00	0.00	1.000	1	0.00	0.00	1.000	1	0.00	0.00	1.000
Connection	1.000	1	0.00	0.00	1.000	1	0.00	0.00	1.000	1	0.00	0.00	1.000
Connection	1.000	1	0.00	0.00	1.000	1	0.00	0.00	1.000	1	0.00	0.00	1.000
Connection	1.000	1	0.00	0.00	1.000	1	0.00	0.00	1.000	1	0.00	0.00	1.000
Connection	1.000	1	0.00	0.00	1.000	1	0.00	0.00	1.000	1	0.00	0.00	1.000
Connection	1.000	1	0.00	0.00	1.000	1	0.00	0.00	1.000	1	0.00	0.00	1.000

Table IV-2: A priori and posterior opening data.

Type	Priori	Test-case 4				Test-case 5			
		Stat.	Col	Leak	Post.	Stat.	Col	Leak	Post.
Slid. WT	0.000	0	20.04	0.00	0.000	0	19.99	0.00	0.000
Hng. Esc.	0.438	0	2.55	0.02	0.438	0	2.40	0.03	0.438
Slid. WT	0.019	0	20.13	0.00	0.000	0	19.92	0.00	0.000
Slid. WT	0.006	0	19.98	0.00	0.000	0	19.93	0.00	0.000
Slid. WT	0.000	0	20.17	0.00	0.000	0	19.87	0.00	0.000
Hng. Fire	0.398	1	0.00	0.00	0.398	1	0.00	0.00	0.398
Hng. Fire	0.601	1	0.00	0.00	0.601	1	0.00	0.00	0.601
Hng. Esc.	0.649	0	2.49	0.03	0.649	1	0.00	0.00	0.649
Hng. Esc.	0.997	1	0.00	0.00	0.997	1	0.00	0.00	0.997
Hng. Esc.	0.613	1	0.00	0.00	0.613	1	0.00	0.00	0.613
Hng. Esc.	0.365	1	0.00	0.00	0.365	0	2.45	0.10	0.365
Slid. WT	0.021	0	19.99	0.00	0.000	0	19.91	0.00	0.000
Hng. Esc.	0.492	0	2.48	0.00	0.492	0	2.50	0.01	0.492
Slid. WT	0.006	0	20.13	0.00	0.000	0	20.06	0.00	0.000
Hng. Esc.	0.662	0	2.37	0.01	0.662	0	2.28	0.01	0.662
Hng. Fire	0.893	1	0.00	0.00	0.893	1	0.00	0.00	0.893
Hng. Esc.	0.910	1	0.00	0.00	0.910	1	0.00	0.00	0.910
Slid. WT	0.021	0	19.93	0.00	0.000	0	19.93	0.00	0.000
Hng. Esc.	0.819	1	0.00	0.00	0.819	1	0.00	0.00	0.819
Slid. WT	0.003	0	19.97	0.00	0.000	0	20.10	0.00	0.000
Hng. Fire	0.566	1	0.00	0.00	0.566	0	2.43	0.01	0.566

Hng. Fire	0.963	1	0.00	0.00	0.963	1	0.00	0.00	0.963
Hng. Fire	0.185	1	0.00	0.00	0.185	0	2.51	0.07	0.185
Hng. Fire	0.610	1	0.00	0.00	0.610	1	0.00	0.00	0.610
Hng. Fire	0.559	1	0.00	0.00	0.559	0	2.52	0.02	0.559
Hng. Fire	0.546	1	0.00	0.00	0.546	1	0.00	0.00	0.546
Hng. Fire	0.833	1	0.00	0.00	0.833	1	0.00	0.00	0.833
Hng. Fire	0.921	1	0.00	0.00	0.921	1	0.00	0.00	0.921
Hng. Fire	0.912	1	0.00	0.00	0.912	1	0.00	0.00	0.912
Hng. Esc.	0.181	0	2.51	0.02	0.181	0	2.53	0.04	0.181
Slid. WT	0.000	0	20.22	0.00	0.000	0	20.27	0.00	0.000
Hng. Esc.	0.792	1	0.00	0.00	0.792	1	0.00	0.00	0.792
Hng. Fire	0.884	1	0.00	0.00	0.884	1	0.00	0.00	0.884
Slid. WT	0.000	0	20.06	0.00	0.000	0	19.94	0.00	0.000
Hng. Esc.	0.435	0	2.51	0.04	0.435	0	2.76	0.03	0.435
Hng. Esc.	0.436	0	2.42	0.01	0.436	0	2.51	0.02	0.436
Hng. Esc.	0.817	1	0.00	0.00	0.817	1	0.00	0.00	0.817
Hole	1.000	1	0.00	0.00	1.000	1	0.00	0.00	1.000
Hng. Esc.	0.935	1	0.00	0.00	0.935	1	0.00	0.00	0.935
Hole	1.000	1	0.00	0.00	1.000	1	0.00	0.00	1.000
Hole	1.000	1	0.00	0.00	1.000	1	0.00	0.00	1.000
Hng. Non-WT	0.902	1	0.00	0.00	0.902	1	0.00	0.00	0.902
Slid. Lift	0.091	0	1.50	0.01	0.091	0	1.68	0.05	0.091
Slid. Lift	0.007	0	1.58	0.03	0.007	0	1.37	0.01	0.007
Hng. Fire	0.694	1	0.00	0.00	0.694	0	2.45	0.01	0.694
Hng. Fire	0.714	1	0.00	0.00	0.714	1	0.00	0.00	0.714
Hng. Fire	0.508	0	2.41	0.02	0.508	1	0.00	0.00	0.508
Hole	1.000	1	0.00	0.00	1.000	1	0.00	0.00	1.000
Hng. Dbl. Fire	0.888	1	0.00	0.00	0.888	1	0.00	0.00	0.888
Hng. Esc.	0.996	1	0.00	0.00	0.996	1	0.00	0.00	0.996
Hng. Non-WT	0.335	0	1.59	0.02	0.335	0	1.44	0.01	0.335
Hng. Esc.	0.430	0	2.47	0.01	0.430	1	0.00	0.00	0.430
Hng. Esc.	0.251	1	0.00	0.00	0.251	0	2.50	0.08	0.251
Hng. Dbl. Fire	0.821	1	0.00	0.00	0.821	1	0.00	0.00	0.821
Hng. Esc.	0.917	1	0.00	0.00	0.917	1	0.00	0.00	0.917
Hng. Esc.	0.980	1	0.00	0.00	0.980	1	0.00	0.00	0.980
Slid. Lift	0.028	0	1.63	0.01	0.028	0	1.64	0.01	0.028
Hng. Fire	0.725	1	0.00	0.00	0.725	1	0.00	0.00	0.725
Hng. Fire	0.017	0	2.46	0.05	0.017	0	2.51	0.01	0.017
Hng. Fire	0.448	0	2.41	0.03	0.448	0	2.64	0.03	0.448
Hng. Fire	0.659	1	0.00	0.00	0.659	1	0.00	0.00	0.659
Hng. Fire	0.630	0	2.47	0.02	0.630	0	2.51	0.00	0.630
Hng. Fire	0.208	0	2.64	0.03	0.208	0	2.31	0.02	0.208
Hng. Fire	0.545	1	0.00	0.00	0.545	0	2.41	0.02	0.545

Slid. Lift	0.325	0	1.48	0.07	0.325	0	1.46	0.06	0.325
Slid. Lift	0.274	0	1.54	0.04	0.274	0	1.43	0.00	0.274
Hng. Fire	0.162	0	2.32	0.00	0.162	0	2.50	0.06	0.162
Hng. Fire	0.986	1	0.00	0.00	0.986	1	0.00	0.00	0.986
Hng. Fire	0.388	0	2.41	0.01	0.388	1	0.00	0.00	0.388
Hng. Fire	0.259	1	0.00	0.00	0.259	0	2.39	0.01	0.259
Hng. Fire	0.876	1	0.00	0.00	0.876	1	0.00	0.00	0.876
Hng. Esc.	0.843	0	2.63	0.02	0.843	1	0.00	0.00	0.843
Hng. Esc.	0.961	1	0.00	0.00	0.961	0	2.72	0.08	0.961
Hole	1.000	1	0.00	0.00	1.000	1	0.00	0.00	1.000
Hng. Esc.	0.550	0	2.55	0.02	0.550	1	0.00	0.00	0.550
Hng. Fire	0.418	0	2.50	0.01	0.418	1	0.00	0.00	0.418
Slid. Prov. Room	0.040	0	2.39	0.14	0.040	0	2.50	0.02	0.040
Hole	1.000	1	0.00	0.00	1.000	1	0.00	0.00	1.000
Hng. Dbl. Fire	0.459	1	0.00	0.00	0.459	0	2.02	0.08	0.459
Hole	1.000	1	0.00	0.00	1.000	1	0.00	0.00	1.000
Hng. Fire	0.796	0	2.52	0.01	0.796	1	0.00	0.00	0.796
Hng. Dbl. Fire	0.752	0	2.02	0.00	0.752	1	0.00	0.00	0.752
Hng. Fire	0.649	1	0.00	0.00	0.649	1	0.00	0.00	0.649
Hng. Dbl. Fire	0.841	1	0.00	0.00	0.841	0	1.77	0.02	0.841
Hng. Esc.	0.955	1	0.00	0.00	0.955	1	0.00	0.00	0.955
Hng. Fire	0.471	0	2.40	0.18	0.471	1	0.00	0.00	0.471
Hole	1.000	1	0.00	0.00	1.000	1	0.00	0.00	1.000
Hng. Dbl. Fire	0.800	1	0.00	0.00	0.800	1	0.00	0.00	0.800
Hng. Cold Room	0.166	0	3.49	0.00	0.166	0	3.43	0.04	0.166
Hng. Non-WT	0.706	1	0.00	0.00	0.706	1	0.00	0.00	0.706
Hng. Fire	0.987	1	0.00	0.00	0.987	1	0.00	0.00	0.987
Hng. Fire	0.803	1	0.00	0.00	0.803	1	0.00	0.00	0.803
Hng. Non-WT	0.168	0	1.58	0.02	0.168	0	1.52	0.06	0.168
Slid. Lift	0.082	0	1.60	0.02	0.082	0	1.43	0.03	0.082
Slid. Lift	0.221	0	1.53	0.04	0.221	1	0.00	0.00	0.221
Slid. Lift	0.006	0	1.48	0.03	0.006	0	1.55	0.05	0.006
Hng. Fire	0.888	1	0.00	0.00	0.888	1	0.00	0.00	0.888
Hng. Non-WT	0.323	1	0.00	0.00	0.323	0	1.61	0.00	0.323
Hng. Fire	0.586	1	0.00	0.00	0.586	1	0.00	0.00	0.586
Hng. Non-WT	0.638	1	0.00	0.00	0.638	0	1.48	0.01	0.638
Hng. Esc.	0.913	1	0.00	0.00	0.913	1	0.00	0.00	0.913
Hng. Fire	0.985	1	0.00	0.00	0.985	1	0.00	0.00	0.985
Hng. Esc.	0.459	1	0.00	0.00	0.459	1	0.00	0.00	0.459
Hng. Fire	0.389	1	0.00	0.00	0.389	1	0.00	0.00	0.389
Hng. Fire	0.795	0	2.38	0.00	0.795	0	2.53	0.01	0.795
Hole	1.000	1	0.00	0.00	1.000	1	0.00	0.00	1.000
Hole	1.000	1	0.00	0.00	1.000	1	0.00	0.00	1.000

Hole	1.000	1	0.00	0.00	1.000	1	0.00	0.00	1.000
Hole	1.000	1	0.00	0.00	1.000	1	0.00	0.00	1.000
Hng. Fire	0.827	1	0.00	0.00	0.827	1	0.00	0.00	0.827
Hng. Esc.	0.727	1	0.00	0.00	0.727	1	0.00	0.00	0.727
Hng. Esc.	0.838	1	0.00	0.00	0.838	1	0.00	0.00	0.838
Hng. Esc.	0.621	0	2.50	0.07	0.621	1	0.00	0.00	0.621
Hng. Esc.	0.860	1	0.00	0.00	0.860	1	0.00	0.00	0.860
Hng. Fire	0.661	0	2.54	0.00	0.661	0	2.40	0.01	0.661
Hng. Fire	0.758	1	0.00	0.00	0.758	1	0.00	0.00	0.758
Hng. Esc.	0.179	1	0.00	0.00	0.179	1	0.00	0.00	0.179
Hole	1.000	1	0.00	0.00	1.000	1	0.00	0.00	1.000
Hole	1.000	1	0.00	0.00	1.000	1	0.00	0.00	1.000
Hng. Esc.	0.382	0	2.41	0.03	0.382	1	0.00	0.00	0.382
Hng. Fire	0.967	1	0.00	0.00	0.967	1	0.00	0.00	0.967
Hng. Fire	0.675	1	0.00	0.00	0.675	1	0.00	0.00	0.675
Hng. Fire	0.672	0	2.56	0.02	0.672	0	2.67	0.01	0.672
Hng. Fire	0.871	1	0.00	0.00	0.871	1	0.00	0.00	0.871
Hng. Dbl. Fire	0.889	1	0.00	0.00	0.889	1	0.00	0.00	0.889
Hole	1.000	1	0.00	0.00	1.000	1	0.00	0.00	1.000
Hng. Fire	0.487	1	0.00	0.00	0.487	0	2.39	0.07	0.487
Hng. Fire	0.527	1	0.00	0.00	0.527	1	0.00	0.00	0.527
Hng. Fire	0.642	1	0.00	0.00	0.642	1	0.00	0.00	0.642
Hole	1.000	1	0.00	0.00	1.000	1	0.00	0.00	1.000
Hng. Esc.	0.879	1	0.00	0.00	0.879	1	0.00	0.00	0.879
Hng. Esc.	0.624	0	2.50	0.16	0.624	0	2.48	0.03	0.624
Hng. Dbl. Fire	0.856	0	1.97	0.01	0.856	1	0.00	0.00	0.856
Hng. Fire	0.954	1	0.00	0.00	0.954	1	0.00	0.00	0.954
Hng. Fire	0.506	0	2.59	0.11	0.506	1	0.00	0.00	0.506
Esc. Hatch	0.722	0	2.29	0.00	0.722	1	0.00	0.00	0.722
Hng. Fire	0.471	0	2.41	0.02	0.471	0	2.36	0.02	0.471
Hng. Non-WT	0.762	1	0.00	0.00	0.762	1	0.00	0.00	0.762
Slid. WT	0.133	0	19.92	0.00	0.002	0	20.12	0.00	0.002
Esc. Hatch	0.542	1	0.00	0.00	0.542	1	0.00	0.00	0.542
Hng. Fire	0.683	0	2.37	0.05	0.683	1	0.00	0.00	0.683
Hng. Fire	0.602	1	0.00	0.00	0.602	1	0.00	0.00	0.602
Slid. Lift	0.133	0	1.44	0.09	0.133	0	1.51	0.04	0.133
Slid. Lift	0.112	0	1.47	0.01	0.112	1	0.00	0.00	0.112
Hng. Fire	0.882	1	0.00	0.00	0.882	1	0.00	0.00	0.882
Hng. Fire	0.747	1	0.00	0.00	0.747	1	0.00	0.00	0.747
Hole	1.000	1	0.00	0.00	1.000	1	0.00	0.00	1.000
Esc. Hatch	0.573	0	2.42	0.03	0.573	0	2.63	0.04	0.573
Esc. Hatch	0.213	0	2.41	0.05	0.213	0	2.48	0.04	0.213
Esc. Hatch	0.547	0	2.42	0.02	0.547	1	0.00	0.00	0.547

Slid. WT	0.121	0	20.12	0.00	0.001	0	19.99	0.00	0.001
Esc. Hatch	0.389	0	2.54	0.01	0.389	0	2.40	0.02	0.389
Hng. Fire	0.637	1	0.00	0.00	0.637	1	0.00	0.00	0.637
Hng. Fire	0.953	1	0.00	0.00	0.953	1	0.00	0.00	0.953
Hng. Fire	0.517	0	2.53	0.02	0.517	1	0.00	0.00	0.517
Esc. Hatch	0.661	0	2.47	0.06	0.661	1	0.00	0.00	0.661
Hng. Non-WT	0.439	0	1.28	0.01	0.439	0	1.56	0.03	0.439
Slid. WT	0.054	0	20.11	0.00	0.001	0	20.05	0.00	0.001
Hng. Fire	0.988	1	0.00	0.00	0.988	1	0.00	0.00	0.988
Hng. Fire	0.967	1	0.00	0.00	0.967	1	0.00	0.00	0.967
Slid. WT	0.387	1	0.00	0.00	0.006	0	20.04	0.00	0.006
Hng. Non-WT	0.277	0	1.39	0.00	0.277	0	1.68	0.04	0.277
Hng. Non-WT	0.495	0	1.63	0.00	0.495	0	1.53	0.03	0.495
Hng. Non-WT	0.663	1	0.00	0.00	0.663	0	1.33	0.01	0.663
Hng. Fire	0.999	1	0.00	0.00	0.999	1	0.00	0.00	0.999
Hng. Non-WT	0.558	1	0.00	0.00	0.558	1	0.00	0.00	0.558
Hng. Fire	0.499	0	2.44	0.02	0.499	1	0.00	0.00	0.499
Hng. Non-WT	0.785	1	0.00	0.00	0.785	1	0.00	0.00	0.785
Slid. Lift	0.220	0	1.55	0.02	0.220	0	1.70	0.02	0.220
Hole	1.000	1	0.00	0.00	1.000	1	0.00	0.00	1.000
Hng. Non-WT	0.967	1	0.00	0.00	0.967	1	0.00	0.00	0.967
Hng. Non-WT	0.500	1	0.00	0.00	0.500	0	1.66	0.00	0.500
Hng. Fire	0.844	1	0.00	0.00	0.844	1	0.00	0.00	0.844
Hng. Fire	0.947	1	0.00	0.00	0.947	0	2.46	0.05	0.947
Slid. Fire	0.390	1	0.00	0.00	0.390	0	1.04	0.04	0.390
Slid. Lift	0.001	0	1.38	0.03	0.001	0	1.65	0.04	0.001
Slid. Lift	0.088	1	0.00	0.00	0.088	0	1.58	0.02	0.088
Hng. Dbl. Fire	0.634	0	1.91	0.04	0.634	1	0.00	0.00	0.634
Hng. Fire	0.601	1	0.00	0.00	0.601	1	0.00	0.00	0.601
Hole	1.000	1	0.00	0.00	1.000	1	0.00	0.00	1.000
Hole	1.000	1	0.00	0.00	1.000	1	0.00	0.00	1.000
Hng. Esc.	0.746	1	0.00	0.00	0.746	1	0.00	0.00	0.746
Hng. Esc.	0.392	0	2.45	0.02	0.392	1	0.00	0.00	0.392
Hng. Fire	0.909	1	0.00	0.00	0.909	1	0.00	0.00	0.909
Hng. Fire	0.533	1	0.00	0.00	0.533	1	0.00	0.00	0.533
Hng. Non-WT	0.252	0	1.51	0.00	0.252	0	1.38	0.24	0.252
Hng. Fire	0.809	1	0.00	0.00	0.809	1	0.00	0.00	0.809
Hng. Fire	0.593	0	2.44	0.08	0.593	0	2.55	0.01	0.593
Hng. Esc.	0.867	1	0.00	0.00	0.867	1	0.00	0.00	0.867
Hole	1.000	1	0.00	0.00	1.000	1	0.00	0.00	1.000
Hng. Fire	0.698	0	2.55	0.16	0.698	1	0.00	0.00	0.698
Hng. Fire	0.893	1	0.00	0.00	0.893	1	0.00	0.00	0.893
Slid. WT	0.000	0	20.07	0.00	0.000	0	19.99	0.00	0.000

Hng. Esc.	0.780	0	2.57	0.05	0.780	1	0.00	0.00	0.780
Hng. Esc.	0.314	1	0.00	0.00	0.314	1	0.00	0.00	0.314
Hng. Esc.	0.307	1	0.00	0.00	0.307	0	2.37	0.00	0.307
Hng. Fire	0.791	1	0.00	0.00	0.791	1	0.00	0.00	0.791
Hng. Fire	0.741	1	0.00	0.00	0.741	1	0.00	0.00	0.741
Hng. Esc.	0.124	0	2.55	0.05	0.124	1	0.00	0.00	0.124
Hng. Esc.	0.906	1	0.00	0.00	0.906	1	0.00	0.00	0.906
Hole	1.000	1	0.00	0.00	1.000	1	0.00	0.00	1.000
Hng. Prov. Room	0.013	0	3.45	0.01	0.013	0	3.44	0.07	0.013
Hng. Fire	0.790	1	0.00	0.00	0.790	0	2.38	0.04	0.790
Hng. Prov. Room	0.031	0	3.37	0.04	0.031	0	3.53	0.01	0.031
Hng. Esc.	0.670	0	2.57	0.02	0.670	1	0.00	0.00	0.670
Slid. Prov. Room	0.020	0	2.45	0.03	0.020	0	2.42	0.08	0.020
Slid. Prov. Room	0.030	0	2.44	0.04	0.030	0	2.42	0.07	0.030
Hng. Prov. Room	0.031	0	3.49	0.02	0.031	0	3.64	0.01	0.031
Hng. Prov. Room	0.100	1	0.00	0.00	0.100	0	3.66	0.11	0.100
Hng. Fire	0.449	1	0.00	0.00	0.449	0	2.47	0.01	0.449
Slid. Prov. Room	0.004	0	2.54	0.02	0.004	0	2.45	0.05	0.004
Slid. Prov. Room	0.047	0	2.42	0.00	0.047	0	2.47	0.09	0.047
Slid. Semi-WT	0.930	1	0.00	0.00	0.118	1	0.00	0.00	0.118
Hng. Esc.	0.358	1	0.00	0.00	0.358	0	2.41	0.01	0.358
Slid. Cold Room	0.106	0	3.50	0.01	0.106	0	3.40	0.02	0.106
Slid. Cold Room	0.015	0	3.45	0.04	0.015	0	3.48	0.05	0.015
Hng. Fire	0.635	0	2.40	0.04	0.635	1	0.00	0.00	0.635
Hole	1.000	1	0.00	0.00	1.000	1	0.00	0.00	1.000
Hole	1.000	1	0.00	0.00	1.000	1	0.00	0.00	1.000
Slid. Cold Room	0.049	0	3.41	0.08	0.049	0	3.53	0.00	0.049
Slid. Prov. Room	0.093	0	2.40	0.19	0.093	0	2.56	0.01	0.093
Slid. Prov. Room	0.142	1	0.00	0.00	0.142	0	2.40	0.11	0.142
Slid. Prov. Room	0.040	0	2.57	0.04	0.040	0	2.62	0.04	0.040
Slid. Prov. Room	0.061	0	2.57	0.05	0.061	0	2.44	0.06	0.061
Hng. Non-WT	0.613	1	0.00	0.00	0.613	1	0.00	0.00	0.613
Hole	1.000	1	0.00	0.00	1.000	1	0.00	0.00	1.000
Hole	1.000	1	0.00	0.00	1.000	1	0.00	0.00	1.000
Shell	0.000	1	1.00	0.00	0.000	1	1.00	0.00	0.000
Shell	0.000	1	1.00	0.00	0.000	1	1.00	0.00	0.000
Hng. Prov. Room	0.056	0	3.34	0.09	0.056	0	3.41	0.02	0.056
Hng. Prov. Room	0.045	0	3.53	0.06	0.045	0	3.54	0.01	0.045
Hng. Prov. Room	0.086	0	3.51	0.01	0.086	0	3.40	0.06	0.086
Hng. Non-WT	0.235	0	1.47	0.08	0.235	0	1.38	0.00	0.235
Hng. Prov. Room	0.101	0	3.48	0.03	0.101	0	3.36	0.04	0.101
Hng. Fire	0.912	1	0.00	0.00	0.912	1	0.00	0.00	0.912
Hng. Prov. Room	0.029	0	3.55	0.02	0.029	0	3.39	0.06	0.029

Hng. Prov. Room	0.011	0	3.49	0.02	0.011	0	3.49	0.01	0.011
Hng. Dbl. Fire	0.859	1	0.00	0.00	0.859	1	0.00	0.00	0.859
Hng. Fire	0.979	1	0.00	0.00	0.979	1	0.00	0.00	0.979
Hng. Fire	0.347	0	2.34	0.00	0.347	1	0.00	0.00	0.347
Hng. Prov. Room	0.020	0	3.35	0.04	0.020	0	3.50	0.10	0.020
Hng. Prov. Room	0.016	0	3.65	0.03	0.016	0	3.51	0.02	0.016
Slid. Lift	0.094	0	1.52	0.00	0.094	0	1.51	0.02	0.094
Slid. Lift	0.349	0	1.54	0.01	0.349	0	1.62	0.03	0.349
Slid. Lift	0.142	0	1.45	0.01	0.142	0	1.46	0.00	0.142
Hng. Prov. Room	0.021	0	3.43	0.00	0.021	0	3.40	0.08	0.021
Hng. Cold Room	0.003	0	3.63	0.00	0.003	0	3.46	0.09	0.003
Hng. Fire	0.880	1	0.00	0.00	0.880	1	0.00	0.00	0.880
Hng. Cold Room	0.004	0	3.33	-0.07	0.004	0	3.53	0.10	0.004
Hng. Prov. Room	0.179	1	0.00	0.00	0.179	0	3.47	-0.08	0.179
Hng. Fire	0.615	1	0.00	0.00	0.615	1	0.00	0.00	0.615
Hng. Fire	0.944	1	0.00	0.00	0.944	1	0.00	0.00	0.944
Hole	1.000	1	0.00	0.00	1.000	1	0.00	0.00	1.000
Slid. Light-WT	0.000	0	7.88	0.01	0.000	0	8.12	0.01	0.000
Slid. Semi-WT	0.635	1	0.00	0.00	0.017	0	7.84	0.05	0.017
Hole	1.000	1	0.00	0.00	1.000	1	0.00	0.00	1.000
Hng. Esc.	0.631	0	2.33	0.07	0.631	0	2.47	0.01	0.631
Hng. Fire	0.977	1	0.00	0.00	0.977	1	0.00	0.00	0.977
Hng. Fire	0.983	1	0.00	0.00	0.983	1	0.00	0.00	0.983
Hng. Fire	0.330	1	0.00	0.00	0.330	1	0.00	0.00	0.330
Esc. Hatch	0.960	1	0.00	0.00	0.960	1	0.00	0.00	0.960
Esc. Hatch	0.312	1	0.00	0.00	0.312	0	2.44	0.00	0.312
Hng. Fire	0.912	1	0.00	0.00	0.912	1	0.00	0.00	0.912
Hng. Fire	0.965	1	0.00	0.00	0.965	1	0.00	0.00	0.965
Hng. Fire	0.692	0	2.47	0.00	0.692	0	2.57	0.03	0.692
Hng. Fire	0.799	1	0.00	0.00	0.799	1	0.00	0.00	0.799
Esc. Hatch	0.205	0	2.50	0.10	0.205	1	0.00	0.00	0.205
Hng. Dbl. Fire	0.506	1	0.00	0.00	0.506	0	2.11	0.02	0.506
Hng. Fire	0.535	1	0.00	0.00	0.535	1	0.00	0.00	0.535
Hng. Fire	0.511	0	2.40	0.01	0.511	0	2.55	0.03	0.511
Hng. Fire	0.649	1	0.00	0.00	0.649	0	2.47	0.05	0.649
Hng. Fire	0.647	1	0.00	0.00	0.647	1	0.00	0.00	0.647
Hole	1.000	1	0.00	0.00	1.000	1	0.00	0.00	1.000
Shell	0.000	1	1.00	0.00	0.000	1	1.00	0.00	0.000
Hng. Dbl. Fire	0.699	1	0.00	0.00	0.699	1	0.00	0.00	0.699
Hng. Dbl. Fire	0.150	0	1.95	0.01	0.150	0	1.99	0.01	0.150
Hole	1.000	1	0.00	0.00	1.000	1	0.00	0.00	1.000
Hng. Esc.	0.512	1	0.00	0.00	0.512	1	0.00	0.00	0.512
Esc. Hatch	0.987	1	0.00	0.00	0.987	1	0.00	0.00	0.987

Hng. Fire	0.998	1	0.00	0.00	0.998	1	0.00	0.00	0.998
Hng. Non-WT	0.326	1	0.00	0.00	0.326	0	1.49	0.12	0.326
Hng. Fire	0.551	0	2.53	0.04	0.551	1	0.00	0.00	0.551
Hng. Non-WT	0.833	1	0.00	0.00	0.833	1	0.00	0.00	0.833
Hng. Non-WT	0.939	1	0.00	0.00	0.939	1	0.00	0.00	0.939
Hng. Fire	0.947	1	0.00	0.00	0.947	1	0.00	0.00	0.947
Shell	0.000	1	1.00	0.00	0.000	1	1.00	0.00	0.000
Hng. Fire	0.828	1	0.00	0.00	0.828	1	0.00	0.00	0.828
Hng. Fire	0.931	1	0.00	0.00	0.931	1	0.00	0.00	0.931
Hole	1.000	1	0.00	0.00	1.000	1	0.00	0.00	1.000
Slid. Semi-WT	0.472	1	0.00	0.00	0.009	0	8.13	0.03	0.009
Hng. Fire	0.894	1	0.00	0.00	0.894	0	2.61	0.07	0.894
Slid. Light-WT	0.097	0	8.05	0.10	0.001	0	8.13	0.01	0.001
Hole	1.000	1	0.00	0.00	1.000	1	0.00	0.00	1.000
Hole	1.000	1	0.00	0.00	1.000	1	0.00	0.00	1.000
Shell	0.000	1	1.00	0.00	0.000	1	1.00	0.00	0.000
Hole	1.000	1	0.00	0.00	1.000	1	0.00	0.00	1.000
Hng. Fire	0.930	1	0.00	0.00	0.930	1	0.00	0.00	0.930
Hng. Fire	0.923	1	0.00	0.00	0.923	1	0.00	0.00	0.923
Hng. Fire	0.592	0	2.47	0.00	0.592	0	2.40	0.02	0.592
Hng. Dbl. Fire	0.406	1	0.00	0.00	0.406	0	1.92	0.03	0.406
Shell	0.000	1	1.00	0.00	0.000	1	1.00	0.00	0.000
Hng. Fire	0.961	1	0.00	0.00	0.961	1	0.00	0.00	0.961
Hng. Fire	0.978	1	0.00	0.00	0.978	1	0.00	0.00	0.978
Hng. Fire	0.924	1	0.00	0.00	0.924	1	0.00	0.00	0.924
Hng. Non-WT	0.961	1	0.00	0.00	0.961	1	0.00	0.00	0.961
Hng. Fire	0.935	1	0.00	0.00	0.935	1	0.00	0.00	0.935
Hng. Fire	0.568	1	0.00	0.00	0.568	1	0.00	0.00	0.568
Hng. Fire	0.353	0	2.36	0.02	0.353	0	2.52	0.02	0.353
Hng. Esc.	0.093	0	2.57	0.05	0.093	0	2.62	0.00	0.093
Hng. Dbl. Fire	0.840	1	0.00	0.00	0.840	1	0.00	0.00	0.840
Shell	0.000	1	1.00	0.00	0.000	1	1.00	0.00	0.000
Hng. Dbl. Fire	0.849	1	0.00	0.00	0.849	1	0.00	0.00	0.849
Hng. Dbl. Fire	0.724	0	2.13	0.00	0.724	1	0.00	0.00	0.724
Hng. Dbl. Fire	0.330	0	1.99	0.04	0.330	0	2.11	0.01	0.330
Shell	0.000	1	1.00	0.00	0.000	1	1.00	0.00	0.000
Slid. Lift	0.154	0	1.48	0.02	0.154	0	1.42	0.00	0.154
Slid. Lift	0.175	1	0.00	0.00	0.175	0	1.57	0.01	0.175
Hole	1.000	1	0.00	0.00	1.000	1	0.00	0.00	1.000
Hole	1.000	1	0.00	0.00	1.000	1	0.00	0.00	1.000
Slid. Lift	0.057	0	1.58	0.05	0.057	0	1.68	0.03	0.057
Slid. Lift	0.139	0	1.51	0.01	0.139	0	1.46	0.03	0.139
Hole	1.000	1	0.00	0.00	1.000	1	0.00	0.00	1.000

Hole	1.000	1	0.00	0.00	1.000	1	0.00	0.00	1.000
Slid. Fire	0.496	1	0.00	0.00	0.496	1	0.00	0.00	0.496
Hole	1.000	1	0.00	0.00	1.000	1	0.00	0.00	1.000
Slid. Lift	0.029	0	1.32	0.02	0.029	0	1.53	0.07	0.029
Slid. Lift	0.116	0	1.22	0.08	0.116	1	0.00	0.00	0.116
Hole	1.000	1	0.00	0.00	1.000	1	0.00	0.00	1.000
Hole	1.000	1	0.00	0.00	1.000	1	0.00	0.00	1.000
Hng. Fire	0.504	1	0.00	0.00	0.504	0	2.54	0.00	0.504
Hng. Dbl. Fire	0.991	1	0.00	0.00	0.991	1	0.00	0.00	0.991
Hng. Dbl. Fire	0.867	1	0.00	0.00	0.867	1	0.00	0.00	0.867
Hng. Dbl. Fire	0.563	0	2.17	0.01	0.563	0	1.95	0.02	0.563
Shell	0.000	1	1.00	0.00	0.000	1	1.00	0.00	0.000
Hng. Fire	0.804	1	0.00	0.00	0.804	1	0.00	0.00	0.804
Slid. Semi-WT	0.696	1	0.00	0.00	0.023	1	0.00	0.00	0.023
Hng. Fire	0.658	0	2.33	0.04	0.658	1	0.00	0.00	0.658
Hole	1.000	1	0.00	0.00	1.000	1	0.00	0.00	1.000
Hng. Fire	0.274	0	2.53	0.03	0.274	1	0.00	0.00	0.274
Hng. Fire	0.727	1	0.00	0.00	0.727	1	0.00	0.00	0.727
Hng. Fire	0.251	1	0.00	0.00	0.251	0	2.54	0.05	0.251
Hng. Dbl. Fire	0.502	1	0.00	0.00	0.502	0	1.96	0.00	0.502
Hng. Fire	0.885	1	0.00	0.00	0.885	1	0.00	0.00	0.885
Hole	1.000	1	0.00	0.00	1.000	1	0.00	0.00	1.000
Hole	1.000	1	0.00	0.00	1.000	1	0.00	0.00	1.000
Hng. Fire	0.680	0	2.42	0.04	0.680	1	0.00	0.00	0.680
Slid. Semi-WT	0.517	0	7.93	0.01	0.011	0	8.14	0.01	0.011
Hng. Fire	0.738	1	0.00	0.00	0.738	0	2.34	0.03	0.738
Slid. Lift	0.017	0	1.50	0.02	0.017	0	1.41	0.01	0.017
Slid. Lift	0.187	1	0.00	0.00	0.187	0	1.53	0.05	0.187
Shell	0.000	1	1.00	0.00	0.000	1	1.00	0.00	0.000
Shell	0.000	1	1.00	0.00	0.000	1	1.00	0.00	0.000
Hng. Fire	0.798	1	0.00	0.00	0.798	1	0.00	0.00	0.798
Hng. Fire	0.922	1	0.00	0.00	0.922	1	0.00	0.00	0.922
Hole	1.000	1	0.00	0.00	1.000	1	0.00	0.00	1.000
Hng. Fire	0.840	0	2.47	0.01	0.840	1	0.00	0.00	0.840
Hng. Fire	0.921	1	0.00	0.00	0.921	1	0.00	0.00	0.921
Hole	1.000	1	0.00	0.00	1.000	1	0.00	0.00	1.000
Hng. Fire	0.821	0	2.37	0.03	0.821	1	0.00	0.00	0.821
Hng. Fire	0.969	1	0.00	0.00	0.969	1	0.00	0.00	0.969
Hng. Fire	0.943	1	0.00	0.00	0.943	1	0.00	0.00	0.943
Hng. Fire	0.881	1	0.00	0.00	0.881	1	0.00	0.00	0.881
Hole	1.000	1	0.00	0.00	1.000	1	0.00	0.00	1.000
Slid. Light-WT	0.080	1	0.00	0.00	0.001	1	0.00	0.00	0.001
Hng. Fire	0.946	1	0.00	0.00	0.946	1	0.00	0.00	0.946

Hng. Fire	0.997	1	0.00	0.00	0.997	1	0.00	0.00	0.997
Hng. Fire	0.418	0	2.48	0.07	0.418	0	2.44	0.10	0.418
Hole	1.000	1	0.00	0.00	1.000	1	0.00	0.00	1.000
Hng. Fire	0.892	1	0.00	0.00	0.892	0	2.75	0.02	0.892
Hole	1.000	1	0.00	0.00	1.000	1	0.00	0.00	1.000
Hng. Fire	0.741	1	0.00	0.00	0.741	1	0.00	0.00	0.741
Slid. Semi-WT	0.492	1	0.00	0.00	0.010	0	7.87	0.02	0.010
Hole	1.000	1	0.00	0.00	1.000	1	0.00	0.00	1.000
Hng. Fire	0.489	0	2.42	0.03	0.489	1	0.00	0.00	0.489
Hole	1.000	1	0.00	0.00	1.000	1	0.00	0.00	1.000
Hng. Fire	0.566	0	2.31	0.00	0.566	0	2.40	0.02	0.566
Hng. Dbl. Fire	0.945	1	0.00	0.00	0.945	1	0.00	0.00	0.945
Hng. Fire	0.580	1	0.00	0.00	0.580	1	0.00	0.00	0.580
Hng. Fire	0.403	0	2.69	0.01	0.403	1	0.00	0.00	0.403
Hng. Fire	0.774	0	2.51	0.04	0.774	1	0.00	0.00	0.774
Hole	1.000	1	0.00	0.00	1.000	1	0.00	0.00	1.000
Hole	1.000	1	0.00	0.00	1.000	1	0.00	0.00	1.000
Hng. Fire	0.825	1	0.00	0.00	0.825	1	0.00	0.00	0.825
Hng. Fire	0.924	1	0.00	0.00	0.924	1	0.00	0.00	0.924
Hole	1.000	1	0.00	0.00	1.000	1	0.00	0.00	1.000
Slid. Semi-WT	0.477	1	0.00	0.00	0.009	0	7.99	0.01	0.009
Slid. Semi-WT	0.514	1	0.00	0.00	0.011	1	0.00	0.00	0.011
Hng. Fire	0.337	1	0.00	0.00	0.337	0	2.67	0.04	0.337
Hng. Fire	0.670	1	0.00	0.00	0.670	0	2.53	0.01	0.670
Slid. Lift	0.109	0	1.47	0.00	0.109	0	1.48	0.06	0.109
Slid. Lift	0.095	0	1.48	0.01	0.095	0	1.43	0.03	0.095
Hole	1.000	1	0.00	0.00	1.000	1	0.00	0.00	1.000
Hole	1.000	1	0.00	0.00	1.000	1	0.00	0.00	1.000
Hng. Non-WT	0.798	1	0.00	0.00	0.798	1	0.00	0.00	0.798
Hng. Non-WT	0.746	0	1.41	0.04	0.746	1	0.00	0.00	0.746
Hole	1.000	1	0.00	0.00	1.000	1	0.00	0.00	1.000
Hole	1.000	1	0.00	0.00	1.000	1	0.00	0.00	1.000
Slid. Lift	0.371	0	1.52	0.01	0.371	0	1.57	0.00	0.371
Slid. Lift	0.017	0	1.62	0.01	0.017	0	1.53	0.07	0.017
Hng. Non-WT	0.410	0	1.73	0.04	0.410	0	1.48	0.02	0.410
Hng. Dbl. Fire	0.397	1	0.00	0.00	0.397	1	0.00	0.00	0.397
Hng. Dbl. Fire	0.288	1	0.00	0.00	0.288	0	2.03	0.00	0.288
Hng. Dbl. Fire	0.757	1	0.00	0.00	0.757	1	0.00	0.00	0.757
Hng. Dbl. Fire	0.789	1	0.00	0.00	0.789	0	1.95	0.13	0.789
Shell	0.000	1	1.00	0.00	0.000	1	1.00	0.00	0.000
Shell	0.000	1	1.00	0.00	0.000	1	1.00	0.00	0.000
Hng. Fire	0.656	1	0.00	0.00	0.656	1	0.00	0.00	0.656
Hole	1.000	1	0.00	0.00	1.000	1	0.00	0.00	1.000

Slid. Semi-WT	0.518	0	7.98	0.01	0.011	1	0.00	0.00	0.011
Hole	1.000	1	0.00	0.00	1.000	1	0.00	0.00	1.000
Hng. Fire	0.937	1	0.00	0.00	0.937	1	0.00	0.00	0.937
Hng. Fire	0.955	1	0.00	0.00	0.955	1	0.00	0.00	0.955
Hng. Non-WT	0.893	1	0.00	0.00	0.893	1	0.00	0.00	0.893
Hng. Fire	0.122	0	2.30	0.03	0.122	0	2.65	0.01	0.122
Hng. Fire	0.861	1	0.00	0.00	0.861	1	0.00	0.00	0.861
Slid. Lift	0.286	0	1.58	0.03	0.286	0	1.50	0.00	0.286
Slid. Lift	0.246	1	0.00	0.00	0.246	1	0.00	0.00	0.246
Esc. Hatch	0.346	0	2.56	0.01	0.346	0	2.28	0.02	0.346
Esc. Hatch	0.367	0	2.48	0.00	0.367	0	2.58	0.01	0.367
Hng. Non-WT	0.724	1	0.00	0.00	0.724	0	1.57	0.07	0.724
Hng. Non-WT	0.782	1	0.00	0.00	0.782	0	1.58	0.06	0.782
Hng. Fire	0.997	1	0.00	0.00	0.997	1	0.00	0.00	0.997
Hole	1.000	1	0.00	0.00	1.000	1	0.00	0.00	1.000
Hng. Non-WT	0.952	1	0.00	0.00	0.952	1	0.00	0.00	0.952
Hng. Non-WT	0.867	1	0.00	0.00	0.867	0	1.29	0.03	0.867
Hng. Fire	0.939	1	0.00	0.00	0.939	1	0.00	0.00	0.939
Hng. Dbl. Fire	0.888	1	0.00	0.00	0.888	1	0.00	0.00	0.888
Hng. Non-WT	0.980	1	0.00	0.00	0.980	1	0.00	0.00	0.980
Hole	1.000	1	0.00	0.00	1.000	1	0.00	0.00	1.000
Hng. Non-WT	0.899	1	0.00	0.00	0.899	0	1.54	0.04	0.899
Hng. Fire	0.171	0	2.55	0.03	0.171	1	0.00	0.00	0.171
Hng. Fire	0.229	0	2.54	0.02	0.229	1	0.00	0.00	0.229
Hng. Esc.	0.124	0	2.50	0.06	0.124	0	2.57	0.05	0.124
Hng. Non-WT	0.920	1	0.00	0.00	0.920	0	1.46	0.00	0.920
Hole	1.000	1	0.00	0.00	1.000	1	0.00	0.00	1.000
Slid. Lift	0.061	0	1.40	0.01	0.061	0	1.47	0.07	0.061
Hole	1.000	1	0.00	0.00	1.000	1	0.00	0.00	1.000
Slid. Light-WT	0.121	0	8.09	0.02	0.001	0	7.91	0.02	0.001
Hng. Fire	0.458	1	0.00	0.00	0.458	1	0.00	0.00	0.458
Hng. Fire	0.420	0	2.65	0.00	0.420	0	2.71	0.01	0.420
Hng. Esc.	0.618	1	0.00	0.00	0.618	1	0.00	0.00	0.618
Esc. Hatch	0.658	0	2.66	0.03	0.658	0	2.55	0.00	0.658
Esc. Hatch	0.341	0	2.36	0.02	0.341	1	0.00	0.00	0.341
Hng. Esc.	0.481	0	2.46	0.02	0.481	1	0.00	0.00	0.481
Hng. Weat.	0.229	1	0.00	0.00	0.229	0	3.47	0.10	0.229
Hng. Weat.	0.011	0	3.55	0.03	0.011	0	3.66	0.01	0.011
Hng. Weat.	0.019	0	3.59	0.02	0.019	0	3.66	0.01	0.019
Hng. Weat.	0.000	0	3.51	0.02	0.000	0	3.58	0.02	0.000
Hng. Weat.	0.047	0	3.48	0.12	0.047	0	3.65	0.04	0.047
Hng. Weat.	0.023	0	3.67	0.02	0.023	0	3.53	0.06	0.023
Hng. Weat.	0.000	0	3.45	0.04	0.000	0	3.44	0.02	0.000

Hole	1.000	1	0.00	0.00	1.000	1	0.00	0.00	1.000
Hole	1.000	1	0.00	0.00	1.000	1	0.00	0.00	1.000
Hole	1.000	1	0.00	0.00	1.000	1	0.00	0.00	1.000
Hng. Cold Room	0.026	0	3.38	0.02	0.026	0	3.42	0.00	0.026
Hng. Fire	0.922	1	0.00	0.00	0.922	0	2.67	0.04	0.922
Hng. Non-WT	0.668	1	0.00	0.00	0.668	0	1.48	0.02	0.668
Hng. Non-WT	0.686	1	0.00	0.00	0.686	1	0.00	0.00	0.686
Hole	1.000	1	0.00	0.00	1.000	1	0.00	0.00	1.000
Hng. Prov. Room	0.164	0	3.79	0.00	0.164	0	3.54	0.02	0.164
Hng. Fire	0.761	1	0.00	0.00	0.761	1	0.00	0.00	0.761
Hng. Fire	0.570	0	2.44	0.02	0.570	1	0.00	0.00	0.570
Hng. Cold Room	0.063	0	3.58	0.05	0.063	0	3.55	0.00	0.063
Hng. Fire	0.935	1	0.00	0.00	0.935	1	0.00	0.00	0.935
Hng. Non-WT	0.863	1	0.00	0.00	0.863	0	1.59	0.00	0.863
Hng. Fire	0.554	1	0.00	0.00	0.554	1	0.00	0.00	0.554
Hng. Fire	0.088	0	2.70	0.00	0.088	0	2.51	0.00	0.088
Hng. Fire	0.631	1	0.00	0.00	0.631	1	0.00	0.00	0.631
Hng. Fire	0.641	1	0.00	0.00	0.641	0	2.40	0.00	0.641
Hng. Fire	0.990	1	0.00	0.00	0.990	1	0.00	0.00	0.990
Hng. Fire	0.722	1	0.00	0.00	0.722	1	0.00	0.00	0.722
Hng. Fire	0.871	1	0.00	0.00	0.871	1	0.00	0.00	0.871
Hng. Esc.	0.874	1	0.00	0.00	0.874	1	0.00	0.00	0.874
Hng. Dbl. Fire	0.362	0	1.91	0.05	0.362	1	0.00	0.00	0.362
Hng. Fire	0.796	1	0.00	0.00	0.796	1	0.00	0.00	0.796
Slid. Lift	0.151	1	0.00	0.00	0.151	1	0.00	0.00	0.151
Slid. Lift	0.167	0	1.63	0.02	0.167	0	1.60	0.04	0.167
Slid. Lift	0.114	0	1.55	0.02	0.114	1	0.00	0.00	0.114
Hng. Fire	0.989	1	0.00	0.00	0.989	1	0.00	0.00	0.989
Hng. Fire	0.503	1	0.00	0.00	0.503	0	2.55	0.11	0.503
Hole	1.000	1	0.00	0.00	1.000	1	0.00	0.00	1.000
Hole	1.000	1	0.00	0.00	1.000	1	0.00	0.00	1.000
Hole	1.000	1	0.00	0.00	1.000	1	0.00	0.00	1.000
Hng. Fire	0.936	1	0.00	0.00	0.936	1	0.00	0.00	0.936
Hng. Fire	0.045	0	2.46	0.01	0.045	0	2.53	0.00	0.045
Hng. Fire	0.507	0	2.64	0.07	0.507	0	2.61	0.01	0.507
Hng. Fire	0.713	0	2.35	0.02	0.713	1	0.00	0.00	0.713
Hng. Dbl. Fire	0.393	1	0.00	0.00	0.393	1	0.00	0.00	0.393
Hng. Non-WT	0.766	1	0.00	0.00	0.766	1	0.00	0.00	0.766
Hng. Non-WT	0.598	0	1.53	0.03	0.598	1	0.00	0.00	0.598
Hng. Dbl. Fire	0.427	0	2.03	0.01	0.427	1	0.00	0.00	0.427
Hng. Dbl. Fire	0.462	1	0.00	0.00	0.462	0	2.04	0.03	0.462
Hng. Fire	0.172	0	2.25	0.03	0.172	0	2.61	0.04	0.172
Hng. Non-WT	0.671	0	1.46	0.01	0.671	0	1.47	0.01	0.671

Hng. Non-WT	0.660	1	0.00	0.00	0.660	0	1.53	0.01	0.660
Hng. Fire	0.113	1	0.00	0.00	0.113	0	2.47	0.03	0.113
Slid. Fire	0.399	1	0.00	0.00	0.399	1	0.00	0.00	0.399
Slid. Fire	0.479	1	0.00	0.00	0.479	0	1.11	0.01	0.479
Hng. Fire	0.527	0	2.52	0.00	0.527	0	2.61	0.06	0.527
Hng. Fire	0.808	0	2.64	0.05	0.808	1	0.00	0.00	0.808
Hng. Non-WT	0.618	1	0.00	0.00	0.618	1	0.00	0.00	0.618
Hng. Non-WT	0.883	1	0.00	0.00	0.883	1	0.00	0.00	0.883
Hole	1.000	1	0.00	0.00	1.000	1	0.00	0.00	1.000
Hole	1.000	1	0.00	0.00	1.000	1	0.00	0.00	1.000
Hng. Fire	0.310	0	2.41	0.01	0.310	0	2.52	0.02	0.310
Hole	1.000	1	0.00	0.00	1.000	1	0.00	0.00	1.000
Hng. Fire	0.715	1	0.00	0.00	0.715	1	0.00	0.00	0.715
Slid. Lift	0.035	0	1.53	0.01	0.035	0	1.37	0.01	0.035
Slid. Lift	0.036	1	0.00	0.00	0.036	0	1.34	0.00	0.036
Shell	0.000	1	1.00	0.00	0.000	1	1.00	0.00	0.000
Slid. Weat.	0.516	0	0.98	0.00	0.516	1	0.00	0.00	0.516
Hole	1.000	1	0.00	0.00	1.000	1	0.00	0.00	1.000
Slid. Lift	0.238	0	1.41	0.02	0.238	0	1.64	0.03	0.238
Slid. Lift	0.109	0	1.67	0.04	0.109	0	1.43	0.02	0.109
Slid. Lift	0.064	0	1.41	0.02	0.064	0	1.58	0.01	0.064
Slid. Lift	0.042	0	1.65	0.01	0.042	0	1.53	0.07	0.042
Slid. Weat.	0.318	0	0.95	0.00	0.318	0	0.91	0.01	0.318
Shell	0.000	1	1.00	0.00	0.000	1	1.00	0.00	0.000
Slid. Fire	0.836	1	0.00	0.00	0.836	1	0.00	0.00	0.836
Hng. Fire	0.941	1	0.00	0.00	0.941	1	0.00	0.00	0.941
Slid. Fire	0.968	1	0.00	0.00	0.968	1	0.00	0.00	0.968
Hng. Fire	0.409	0	2.57	0.04	0.409	0	2.66	-0.14	0.409
Hng. Fire	0.863	1	0.00	0.00	0.863	1	0.00	0.00	0.863
Hng. Fire	0.919	1	0.00	0.00	0.919	1	0.00	0.00	0.919
Hng. Fire	0.924	1	0.00	0.00	0.924	1	0.00	0.00	0.924
Hng. Fire	0.937	1	0.00	0.00	0.937	1	0.00	0.00	0.937
Slid. Semi-WT	0.580	1	0.00	0.00	0.014	1	0.00	0.00	0.014
Hng. Fire	0.872	1	0.00	0.00	0.872	1	0.00	0.00	0.872
Hng. Fire	0.954	1	0.00	0.00	0.954	1	0.00	0.00	0.954
Slid. Lift	0.343	0	1.52	0.04	0.343	0	1.32	0.02	0.343
Slid. Lift	0.106	0	1.55	0.01	0.106	0	1.45	0.00	0.106
Hng. Fire	0.925	1	0.00	0.00	0.925	1	0.00	0.00	0.925
Hng. Fire	0.881	1	0.00	0.00	0.881	1	0.00	0.00	0.881
Hole	1.000	1	0.00	0.00	1.000	1	0.00	0.00	1.000
Hole	1.000	1	0.00	0.00	1.000	1	0.00	0.00	1.000
Hole	1.000	1	0.00	0.00	1.000	1	0.00	0.00	1.000
Hng. Esc.	0.837	1	0.00	0.00	0.837	1	0.00	0.00	0.837

B-Class Struct.	1.000	1	0.00	0.00	1.000	1	0.00	0.00	1.000
B-Class Struct.	1.000	1	0.00	0.00	1.000	1	0.00	0.00	1.000
Hng. Fire	0.818	0	2.60	0.00	0.818	1	0.00	0.00	0.818
Hng. Fire	0.585	0	2.34	0.01	0.585	0	2.52	0.07	0.585
Hng. Fire	0.753	0	2.42	0.02	0.753	1	0.00	0.00	0.753
Slid. Semi-WT	0.946	1	0.00	0.00	0.150	1	0.00	0.00	0.150
Hole	1.000	1	0.00	0.00	1.000	1	0.00	0.00	1.000
Hng. Fire	0.660	0	2.40	0.07	0.660	0	2.65	0.04	0.660
Hng. Non-WT	0.278	0	1.52	0.01	0.278	0	1.44	0.01	0.278
Hng. Fire	0.422	0	2.65	0.01	0.422	0	2.54	0.04	0.422
B-Class Struct.	1.000	1	0.00	0.00	1.000	1	0.00	0.00	1.000
B-Class Struct.	1.000	1	0.00	0.00	1.000	1	0.00	0.00	1.000
Hng. Fire	0.220	0	2.44	0.03	0.220	1	0.00	0.00	0.220
Hng. Non-WT	0.952	1	0.00	0.00	0.952	1	0.00	0.00	0.952
Hng. Fire	0.596	1	0.00	0.00	0.596	1	0.00	0.00	0.596
Slid. Lift	0.031	0	1.46	0.06	0.031	0	1.62	0.04	0.031
Slid. Lift	0.128	0	1.69	0.00	0.128	1	0.00	0.00	0.128
Slid. Lift	0.127	0	1.53	0.02	0.127	1	0.00	0.00	0.127
Slid. Lift	0.327	0	1.55	0.00	0.327	0	1.31	0.02	0.327
Hole	1.000	1	0.00	0.00	1.000	1	0.00	0.00	1.000
Hng. Fire	0.559	0	2.59	0.00	0.559	1	0.00	0.00	0.559
Hng. Fire	0.710	0	2.46	0.02	0.710	0	2.56	0.05	0.710
Hole	1.000	1	0.00	0.00	1.000	1	0.00	0.00	1.000
Hng. Fire	0.900	1	0.00	0.00	0.900	1	0.00	0.00	0.900
Slid. Semi-WT	0.479	0	7.80	0.03	0.009	0	8.13	0.02	0.009
Hng. Fire	0.295	0	2.29	0.02	0.295	1	0.00	0.00	0.295
Slid. Semi-WT	0.541	1	0.00	0.00	0.012	1	0.00	0.00	0.012
Hole	1.000	1	0.00	0.00	1.000	1	0.00	0.00	1.000
Hng. Non-WT	0.891	1	0.00	0.00	0.891	1	0.00	0.00	0.891
B-Class Struct.	1.000	1	0.00	0.00	1.000	1	0.00	0.00	1.000
Hng. Fire	0.444	1	0.00	0.00	0.444	0	2.39	0.01	0.444
Hng. Fire	0.145	0	2.48	0.01	0.145	0	2.34	0.00	0.145
Hng. Fire	0.462	0	2.46	0.02	0.462	0	2.66	0.01	0.462
Hng. Non-WT	0.931	1	0.00	0.00	0.931	1	0.00	0.00	0.931
Hng. Non-WT	0.575	1	0.00	0.00	0.575	1	0.00	0.00	0.575
Hng. Non-WT	0.678	1	0.00	0.00	0.678	1	0.00	0.00	0.678
Hng. Non-WT	0.560	1	0.00	0.00	0.560	1	0.00	0.00	0.560
Slid. Lift	0.087	0	1.38	0.04	0.087	0	1.45	0.01	0.087
Slid. Lift	0.187	0	1.57	0.00	0.187	1	0.00	0.00	0.187
Hng. Fire	0.400	1	0.00	0.00	0.400	0	2.53	0.02	0.400
Hng. Fire	0.947	1	0.00	0.00	0.947	1	0.00	0.00	0.947
Hng. Fire	0.609	0	2.41	0.02	0.609	1	0.00	0.00	0.609
Hole	1.000	1	0.00	0.00	1.000	1	0.00	0.00	1.000

Hng. Non-WT	0.157	0	1.54	0.01	0.157	0	1.50	0.01	0.157
Hole	1.000	1	0.00	0.00	1.000	1	0.00	0.00	1.000
Hole	1.000	1	0.00	0.00	1.000	1	0.00	0.00	1.000
Hng. Non-WT	0.792	1	0.00	0.00	0.792	1	0.00	0.00	0.792
Hng. Non-WT	0.573	0	1.45	0.05	0.573	1	0.00	0.00	0.573
Hole	1.000	1	0.00	0.00	1.000	1	0.00	0.00	1.000
Hng. Non-WT	0.375	0	1.65	0.02	0.375	0	1.48	0.02	0.375
Hng. Non-WT	0.935	1	0.00	0.00	0.935	1	0.00	0.00	0.935
Hng. Fire	0.957	1	0.00	0.00	0.957	1	0.00	0.00	0.957
Hng. Fire	0.383	0	2.45	0.02	0.383	1	0.00	0.00	0.383
Hng. Dbl. Fire	0.963	1	0.00	0.00	0.963	1	0.00	0.00	0.963
Hng. Fire	0.752	1	0.00	0.00	0.752	1	0.00	0.00	0.752
Hng. Fire	0.588	1	0.00	0.00	0.588	0	2.74	0.01	0.588
Hng. Fire	0.781	1	0.00	0.00	0.781	1	0.00	0.00	0.781
Hng. Fire	0.448	0	2.45	0.00	0.448	1	0.00	0.00	0.448
Slid. Lift	0.057	0	1.62	0.03	0.057	0	1.54	0.05	0.057
Hole	1.000	1	0.00	0.00	1.000	1	0.00	0.00	1.000
Slid. Semi-WT	0.460	0	7.95	0.06	0.009	1	0.00	0.00	0.009
Slid. Semi-WT	0.506	1	0.00	0.00	0.010	1	0.00	0.00	0.010
Hng. Fire	0.580	0	2.61	0.01	0.580	1	0.00	0.00	0.580
Hng. Non-WT	0.328	1	0.00	0.00	0.328	1	0.00	0.00	0.328
Hole	1.000	1	0.00	0.00	1.000	1	0.00	0.00	1.000
Hole	1.000	1	0.00	0.00	1.000	1	0.00	0.00	1.000
Hng. Fire	0.566	0	2.48	0.00	0.566	0	2.47	0.07	0.566
Hng. Esc.	0.694	0	2.54	0.02	0.694	0	2.57	0.08	0.694
Hng. Fire	0.798	1	0.00	0.00	0.798	1	0.00	0.00	0.798
Hng. Esc.	0.785	1	0.00	0.00	0.785	1	0.00	0.00	0.785
Hng. Non-WT	0.987	1	0.00	0.00	0.987	1	0.00	0.00	0.987
Hng. Fire	0.749	1	0.00	0.00	0.749	0	2.56	0.09	0.749
Hng. Non-WT	0.936	1	0.00	0.00	0.936	1	0.00	0.00	0.936
Hng. Dbl. Fire	0.745	0	1.82	0.01	0.745	1	0.00	0.00	0.745
Hng. Fire	0.387	0	2.53	0.00	0.387	0	2.39	0.01	0.387
Hng. Fire	0.952	1	0.00	0.00	0.952	1	0.00	0.00	0.952
Hng. Fire	0.349	0	2.50	0.04	0.349	0	2.52	0.05	0.349
Hng. Fire	0.697	1	0.00	0.00	0.697	0	2.40	0.02	0.697
Hng. Fire	0.980	1	0.00	0.00	0.980	1	0.00	0.00	0.980
Hng. Fire	0.431	1	0.00	0.00	0.431	1	0.00	0.00	0.431
Hole	1.000	1	0.00	0.00	1.000	1	0.00	0.00	1.000
Hng. Fire	0.861	1	0.00	0.00	0.861	1	0.00	0.00	0.861
Hng. Fire	0.660	1	0.00	0.00	0.660	1	0.00	0.00	0.660
Hole	1.000	1	0.00	0.00	1.000	1	0.00	0.00	1.000
Hng. Fire	0.733	0	2.54	0.07	0.733	1	0.00	0.00	0.733
Hng. Non-WT	0.900	1	0.00	0.00	0.900	1	0.00	0.00	0.900

Hng. Non-WT	0.674	1	0.00	0.00	0.674	1	0.00	0.00	0.674
Hng. Lift	0.095	0	1.55	0.02	0.095	0	1.53	0.03	0.095
Hng. Non-WT	0.357	1	0.00	0.00	0.357	0	1.42	0.06	0.357
Hng. Fire	0.182	0	2.46	0.01	0.182	0	2.50	0.02	0.182
Hng. Fire	0.821	1	0.00	0.00	0.821	1	0.00	0.00	0.821
Hng. Non-WT	0.894	1	0.00	0.00	0.894	1	0.00	0.00	0.894
Hng. Cold Room	0.020	0	3.44	0.06	0.020	0	3.62	0.03	0.020
Hng. Non-WT	0.881	1	0.00	0.00	0.881	1	0.00	0.00	0.881
Hng. Non-WT	0.271	0	1.43	0.07	0.271	1	0.00	0.00	0.271
Hng. Non-WT	0.546	0	1.63	0.02	0.546	0	1.46	0.01	0.546
Hng. Cold Room	0.025	0	3.51	0.05	0.025	0	3.48	0.04	0.025
Hng. Prov. Room	0.009	0	3.43	0.01	0.009	0	3.63	0.01	0.009
Hng. Fire	0.851	1	0.00	0.00	0.851	1	0.00	0.00	0.851
Hng. Cold Room	0.069	0	3.47	0.05	0.069	0	3.46	0.12	0.069
Hole	1.000	1	0.00	0.00	1.000	1	0.00	0.00	1.000
Hng. Fire	0.509	1	0.00	0.00	0.509	0	2.57	0.02	0.509
Hng. Cold Room	0.141	0	3.38	0.01	0.141	0	3.35	0.06	0.141
Hng. Fire	0.663	0	2.41	0.01	0.663	1	0.00	0.00	0.663
Hng. Fire	0.986	1	0.00	0.00	0.986	1	0.00	0.00	0.986
Hng. Fire	0.979	1	0.00	0.00	0.979	1	0.00	0.00	0.979
Slid. Lift	0.036	0	1.44	0.01	0.036	0	1.54	0.03	0.036
Slid. Lift	0.181	0	1.71	0.01	0.181	0	1.48	0.00	0.181
Slid. Lift	0.241	0	1.58	0.01	0.241	0	1.39	0.01	0.241
Slid. Fire	0.438	0	0.92	0.02	0.438	0	0.96	0.01	0.438
Slid. Fire	0.430	0	1.02	0.06	0.430	0	1.08	0.01	0.430
Hng. Prov. Room	0.029	0	3.52	0.01	0.029	1	0.00	0.00	0.029
Slid. Fire	0.553	0	1.03	0.05	0.553	1	0.00	0.00	0.553
Hole	1.000	1	0.00	0.00	1.000	1	0.00	0.00	1.000
Hole	1.000	1	0.00	0.00	1.000	1	0.00	0.00	1.000
Hng. Prov. Room	0.080	0	3.56	0.07	0.080	0	3.45	0.04	0.080
Slid. Fire	0.751	0	0.92	0.03	0.751	1	0.00	0.00	0.751
Hole	1.000	1	0.00	0.00	1.000	1	0.00	0.00	1.000
Hng. Dbl. Fire	0.676	1	0.00	0.00	0.676	0	1.99	0.02	0.676
Hng. Fire	0.629	1	0.00	0.00	0.629	0	2.41	0.06	0.629
Hole	1.000	1	0.00	0.00	1.000	1	0.00	0.00	1.000
Hng. Non-WT	0.694	0	1.66	0.01	0.694	1	0.00	0.00	0.694
Hng. Non-WT	0.707	1	0.00	0.00	0.707	1	0.00	0.00	0.707
Hng. Fire	0.754	1	0.00	0.00	0.754	1	0.00	0.00	0.754
Slid. Fire	0.849	1	0.00	0.00	0.849	0	1.05	0.01	0.849
Slid. Fire	0.419	0	0.92	0.00	0.419	0	0.99	0.13	0.419
Hng. Fire	0.943	1	0.00	0.00	0.943	1	0.00	0.00	0.943
Hng. Dbl. Fire	0.925	1	0.00	0.00	0.925	1	0.00	0.00	0.925
Hng. Dbl. Fire	0.833	0	2.16	0.02	0.833	1	0.00	0.00	0.833

Hole	1.000	1	0.00	0.00	1.000	1	0.00	0.00	1.000
Hole	1.000	1	0.00	0.00	1.000	1	0.00	0.00	1.000
Hole	1.000	1	0.00	0.00	1.000	1	0.00	0.00	1.000
Hole	1.000	1	0.00	0.00	1.000	1	0.00	0.00	1.000
Hole	1.000	1	0.00	0.00	1.000	1	0.00	0.00	1.000
Hole	1.000	1	0.00	0.00	1.000	1	0.00	0.00	1.000
Hole	1.000	1	0.00	0.00	1.000	1	0.00	0.00	1.000
Hng. Fire	0.979	1	0.00	0.00	0.979	1	0.00	0.00	0.979
Slid. Fire	0.724	1	0.00	0.00	0.724	0	1.03	0.02	0.724
Slid. Fire	0.873	1	0.00	0.00	0.873	1	0.00	0.00	0.873
Hng. Dbl. Fire	0.569	1	0.00	0.00	0.569	0	1.93	0.03	0.569
Hng. Fire	0.356	0	2.48	0.03	0.356	0	2.37	0.01	0.356
Hng. Fire	0.893	1	0.00	0.00	0.893	1	0.00	0.00	0.893
Hng. Fire	0.697	1	0.00	0.00	0.697	1	0.00	0.00	0.697
Hng. Fire	0.962	1	0.00	0.00	0.962	1	0.00	0.00	0.962
Hng. Fire	0.992	1	0.00	0.00	0.992	1	0.00	0.00	0.992
Hng. Fire	0.560	0	2.64	0.01	0.560	1	0.00	0.00	0.560
Hng. Fire	0.863	1	0.00	0.00	0.863	1	0.00	0.00	0.863
Hng. Dbl. Fire	0.923	0	1.93	0.12	0.923	1	0.00	0.00	0.923
Hng. Dbl. Fire	0.737	1	0.00	0.00	0.737	0	1.95	0.01	0.737
Hole	1.000	1	0.00	0.00	1.000	1	0.00	0.00	1.000
Hole	1.000	1	0.00	0.00	1.000	1	0.00	0.00	1.000
Hng. Fire	0.851	0	2.52	0.04	0.851	1	0.00	0.00	0.851
Hng. Fire	0.995	1	0.00	0.00	0.995	1	0.00	0.00	0.995
Shell	0.000	1	1.00	0.00	0.000	1	1.00	0.00	0.000
Hng. Non-WT	0.842	1	0.00	0.00	0.842	1	0.00	0.00	0.842
Hng. Dbl. Fire	0.860	1	0.00	0.00	0.860	1	0.00	0.00	0.860
Slid. Fire	0.709	1	0.00	0.00	0.709	0	0.80	0.01	0.709
Slid. Fire	0.534	1	0.00	0.00	0.534	1	0.00	0.00	0.534
Hng. Fire	0.872	1	0.00	0.00	0.872	1	0.00	0.00	0.872
Slid. Lift	0.245	0	1.66	0.02	0.245	0	1.48	0.02	0.245
Slid. Lift	0.082	0	1.57	0.02	0.082	0	1.44	0.05	0.082
Hng. Non-WT	0.395	1	0.00	0.00	0.395	0	1.52	0.03	0.395
Hng. Non-WT	0.809	0	1.58	0.06	0.809	1	0.00	0.00	0.809
Slid. Lift	0.178	0	1.45	0.00	0.178	0	1.42	0.02	0.178
Slid. Lift	0.071	0	1.50	0.00	0.071	0	1.59	0.03	0.071
Hng. Non-WT	0.463	1	0.00	0.00	0.463	1	0.00	0.00	0.463
Slid. Lift	0.204	0	1.42	0.02	0.204	0	1.50	0.03	0.204
Slid. Lift	0.093	0	1.61	0.01	0.093	0	1.42	0.01	0.093
Slid. Fire	0.531	1	0.00	0.00	0.531	1	0.00	0.00	0.531
Hole	1.000	1	0.00	0.00	1.000	1	0.00	0.00	1.000
Shell	0.000	1	1.00	0.00	0.000	1	1.00	0.00	0.000
Hng. Fire	0.643	1	0.00	0.00	0.643	1	0.00	0.00	0.643

Slid. Fire	0.735	1	0.00	0.00	0.735	1	0.00	0.00	0.735
Hng. Fire	0.682	1	0.00	0.00	0.682	1	0.00	0.00	0.682
Hng. Fire	0.717	1	0.00	0.00	0.717	0	2.44	0.00	0.717
Hng. Fire	0.924	1	0.00	0.00	0.924	1	0.00	0.00	0.924
Hng. Fire	0.769	0	2.51	0.04	0.769	1	0.00	0.00	0.769
Hng. Fire	0.995	1	0.00	0.00	0.995	1	0.00	0.00	0.995
Slid. Lift	0.150	0	1.58	0.01	0.150	0	1.50	0.00	0.150
Slid. Lift	0.351	0	1.39	0.00	0.351	0	1.48	0.02	0.351
Hng. Fire	0.548	1	0.00	0.00	0.548	1	0.00	0.00	0.548
Hng. Fire	0.802	1	0.00	0.00	0.802	1	0.00	0.00	0.802
Slid. Fire	0.657	0	1.23	0.09	0.657	1	0.00	0.00	0.657
Hole	1.000	1	0.00	0.00	1.000	1	0.00	0.00	1.000
Hole	1.000	1	0.00	0.00	1.000	1	0.00	0.00	1.000
Hng. Fire	0.709	0	2.53	0.05	0.709	1	0.00	0.00	0.709
Hng. Non-WT	0.323	1	0.00	0.00	0.323	1	0.00	0.00	0.323
Hng. Non-WT	0.860	1	0.00	0.00	0.860	1	0.00	0.00	0.860
Hng. Dbl. Fire	0.703	1	0.00	0.00	0.703	0	1.92	0.03	0.703
Hng. Fire	0.714	1	0.00	0.00	0.714	0	2.44	0.04	0.714
Hng. Non-WT	0.836	1	0.00	0.00	0.836	1	0.00	0.00	0.836
Hng. Dbl. Fire	0.524	1	0.00	0.00	0.524	0	1.93	0.00	0.524
Hng. Dbl. Fire	0.691	0	2.15	0.01	0.691	1	0.00	0.00	0.691
Hng. Dbl. Fire	0.668	1	0.00	0.00	0.668	1	0.00	0.00	0.668
Hng. Fire	0.425	0	2.55	0.05	0.425	1	0.00	0.00	0.425
Hng. Fire	0.697	1	0.00	0.00	0.697	1	0.00	0.00	0.697
Hole	1.000	1	0.00	0.00	1.000	1	0.00	0.00	1.000
Hng. Non-WT	0.834	1	0.00	0.00	0.834	1	0.00	0.00	0.834
Hole	1.000	1	0.00	0.00	1.000	1	0.00	0.00	1.000
Hng. Fire	0.406	1	0.00	0.00	0.406	1	0.00	0.00	0.406
Hole	1.000	1	0.00	0.00	1.000	1	0.00	0.00	1.000
Hng. Non-WT	0.230	1	0.00	0.00	0.230	0	1.48	0.01	0.230
Hng. Non-WT	0.923	1	0.00	0.00	0.923	1	0.00	0.00	0.923
Hole	1.000	1	0.00	0.00	1.000	1	0.00	0.00	1.000
Hole	1.000	1	0.00	0.00	1.000	1	0.00	0.00	1.000
Hng. Non-WT	0.260	1	0.00	0.00	0.260	1	0.00	0.00	0.260
Hng. Non-WT	0.509	0	1.30	0.05	0.509	0	1.68	0.00	0.509
Hng. Fire	0.617	0	2.54	0.02	0.617	0	2.44	0.09	0.617
Hng. Fire	0.879	1	0.00	0.00	0.879	1	0.00	0.00	0.879
Hng. Fire	0.865	1	0.00	0.00	0.865	0	2.36	0.00	0.865
Hng. Dbl. Fire	0.815	1	0.00	0.00	0.815	1	0.00	0.00	0.815
Slid. Fire	0.962	1	0.00	0.00	0.962	1	0.00	0.00	0.962
Hng. Fire	0.643	1	0.00	0.00	0.643	1	0.00	0.00	0.643
Hole	1.000	1	0.00	0.00	1.000	1	0.00	0.00	1.000
Hole	1.000	1	0.00	0.00	1.000	1	0.00	0.00	1.000

Hole	1.000	1	0.00	0.00	1.000	1	0.00	0.00	1.000
Hng. Fire	0.461	1	0.00	0.00	0.461	1	0.00	0.00	0.461
Hng. Non-WT	0.439	1	0.00	0.00	0.439	1	0.00	0.00	0.439
Hole	1.000	1	0.00	0.00	1.000	1	0.00	0.00	1.000
Hole	1.000	1	0.00	0.00	1.000	1	0.00	0.00	1.000
Hole	1.000	1	0.00	0.00	1.000	1	0.00	0.00	1.000
Slid. Lift	0.025	0	1.51	0.00	0.025	0	1.43	0.00	0.025
Slid. Lift	0.027	0	1.50	0.05	0.027	0	1.58	0.02	0.027
Hng. Dbl. Fire	0.471	0	1.93	0.01	0.471	0	2.01	0.02	0.471
Slid. Lift	0.050	0	1.45	0.03	0.050	0	1.64	0.05	0.050
Slid. Lift	0.044	0	1.25	0.04	0.044	0	1.54	0.00	0.044
Hng. Fire	0.590	1	0.00	0.00	0.590	1	0.00	0.00	0.590
Hng. Fire	0.462	1	0.00	0.00	0.462	0	2.64	0.01	0.462
Slid. Fire	0.922	1	0.00	0.00	0.922	1	0.00	0.00	0.922
Hole	1.000	1	0.00	0.00	1.000	1	0.00	0.00	1.000
Hole	1.000	1	0.00	0.00	1.000	1	0.00	0.00	1.000
Hng. Non-WT	0.802	1	0.00	0.00	0.802	1	0.00	0.00	0.802
Hng. Non-WT	0.910	1	0.00	0.00	0.910	1	0.00	0.00	0.910
Hole	1.000	1	0.00	0.00	1.000	1	0.00	0.00	1.000
Hng. Non-WT	0.400	0	1.40	0.00	0.400	1	0.00	0.00	0.400
Hng. Fire	0.924	1	0.00	0.00	0.924	0	2.47	0.07	0.924
Hng. Fire	0.784	1	0.00	0.00	0.784	1	0.00	0.00	0.784
Hng. Fire	0.679	1	0.00	0.00	0.679	1	0.00	0.00	0.679
Hng. Fire	0.925	1	0.00	0.00	0.925	1	0.00	0.00	0.925
Slid. Fire	0.329	1	0.00	0.00	0.329	1	0.00	0.00	0.329
Slid. Fire	0.969	1	0.00	0.00	0.969	1	0.00	0.00	0.969
Hng. Fire	0.676	0	2.42	0.04	0.676	1	0.00	0.00	0.676
Hng. Fire	0.166	0	2.39	0.08	0.166	0	2.46	0.02	0.166
Hng. Fire	0.953	1	0.00	0.00	0.953	1	0.00	0.00	0.953
Hng. Fire	0.875	1	0.00	0.00	0.875	1	0.00	0.00	0.875
Hng. Non-WT	0.929	1	0.00	0.00	0.929	1	0.00	0.00	0.929
Hng. Fire	0.636	1	0.00	0.00	0.636	1	0.00	0.00	0.636
Hng. Fire	0.707	1	0.00	0.00	0.707	1	0.00	0.00	0.707
Hng. Fire	0.255	0	2.45	0.02	0.255	1	0.00	0.00	0.255
Slid. Lift	0.017	0	1.38	0.03	0.017	0	1.40	0.00	0.017
Slid. Lift	0.356	1	0.00	0.00	0.356	1	0.00	0.00	0.356
Hng. Dbl. Fire	0.918	1	0.00	0.00	0.918	1	0.00	0.00	0.918
Hng. Dbl. Fire	0.682	0	1.98	0.09	0.682	0	2.13	0.02	0.682
Hng. Fire	0.805	0	2.42	0.01	0.805	1	0.00	0.00	0.805
Hng. Fire	0.595	1	0.00	0.00	0.595	0	2.50	0.01	0.595
Hng. Non-WT	0.430	1	0.00	0.00	0.430	0	1.54	0.02	0.430
Hng. Fire	0.659	1	0.00	0.00	0.659	0	2.50	0.03	0.659
Hng. Fire	0.718	1	0.00	0.00	0.718	1	0.00	0.00	0.718

Hole	1.000	1	0.00	0.00	1.000	1	0.00	0.00	1.000
Hole	1.000	1	0.00	0.00	1.000	1	0.00	0.00	1.000
Hng. Fire	0.847	1	0.00	0.00	0.847	1	0.00	0.00	0.847
Hng. Fire	0.816	1	0.00	0.00	0.816	0	2.48	0.00	0.816
Hng. Fire	0.721	1	0.00	0.00	0.721	0	2.53	0.11	0.721
Hng. Fire	0.541	1	0.00	0.00	0.541	1	0.00	0.00	0.541
Hng. Fire	0.590	1	0.00	0.00	0.590	0	2.52	0.04	0.590
Hole	1.000	1	0.00	0.00	1.000	1	0.00	0.00	1.000
Hng. Fire	0.619	1	0.00	0.00	0.619	1	0.00	0.00	0.619
Hng. Fire	0.625	1	0.00	0.00	0.625	0	2.40	0.01	0.625
Hng. Fire	0.205	0	2.41	0.02	0.205	1	0.00	0.00	0.205
Hng. Fire	0.294	0	2.64	0.00	0.294	0	2.50	0.05	0.294
Hng. Fire	0.597	0	2.55	0.05	0.597	0	2.67	0.01	0.597
Slid. Lift	0.103	0	1.35	0.01	0.103	0	1.69	0.06	0.103
Hng. Weat.	0.013	0	3.52	0.01	0.013	0	3.38	0.01	0.013
Hng. Weat.	0.006	0	3.51	0.06	0.006	0	3.57	0.00	0.006
Hng. Weat.	0.013	0	3.40	0.01	0.013	0	3.50	0.01	0.013
Hng. Weat.	0.000	0	3.50	0.01	0.000	0	3.70	0.01	0.000
Hng. Weat.	0.027	0	3.71	0.02	0.027	0	3.40	0.02	0.027
WT Hatch	0.169	0	14.82	0.00	0.169	0	15.05	0.00	0.169
Hole	1.000	1	0.00	0.00	1.000	1	0.00	0.00	1.000
Hole	1.000	1	0.00	0.00	1.000	1	0.00	0.00	1.000
Hole	1.000	1	0.00	0.00	1.000	1	0.00	0.00	1.000
Hole	1.000	1	0.00	0.00	1.000	1	0.00	0.00	1.000
Hole	1.000	1	0.00	0.00	1.000	1	0.00	0.00	1.000
Hole	1.000	1	0.00	0.00	1.000	1	0.00	0.00	1.000
Hole	1.000	1	0.00	0.00	1.000	1	0.00	0.00	1.000
Hole	1.000	1	0.00	0.00	1.000	1	0.00	0.00	1.000
Hole	1.000	1	0.00	0.00	1.000	1	0.00	0.00	1.000
Hole	1.000	1	0.00	0.00	1.000	1	0.00	0.00	1.000
Hole	1.000	1	0.00	0.00	1.000	1	0.00	0.00	1.000
Connection	1.000	1	0.00	0.00	1.000	1	0.00	0.00	1.000
Connection	1.000	1	0.00	0.00	1.000	1	0.00	0.00	1.000
Connection	1.000	1	0.00	0.00	1.000	1	0.00	0.00	1.000
Connection	1.000	1	0.00	0.00	1.000	1	0.00	0.00	1.000
Connection	1.000	1	0.00	0.00	1.000	1	0.00	0.00	1.000
Connection	1.000	1	0.00	0.00	1.000	1	0.00	0.00	1.000
Connection	1.000	1	0.00	0.00	1.000	1	0.00	0.00	1.000
Connection	1.000	1	0.00	0.00	1.000	1	0.00	0.00	1.000
Connection	1.000	1	0.00	0.00	1.000	1	0.00	0.00	1.000
Connection	1.000	1	0.00	0.00	1.000	1	0.00	0.00	1.000
Connection	1.000	1	0.00	0.00	1.000	1	0.00	0.00	1.000
Connection	1.000	1	0.00	0.00	1.000	1	0.00	0.00	1.000
Connection	1.000	1	0.00	0.00	1.000	1	0.00	0.00	1.000
Connection	1.000	1	0.00	0.00	1.000	1	0.00	0.00	1.000
Hole	1.000	1	0.00	0.00	1.000	1	0.00	0.00	1.000
Connection	1.000	1	0.00	0.00	1.000	1	0.00	0.00	1.000
Connection	1.000	1	0.00	0.00	1.000	1	0.00	0.00	1.000

Appendix V - Posterior update of damage extent from sensors

V.1 A priori belief – No sensor evidence

Table V-1: A priori belief - Ten most likely cases based on no sensor evidence.

Predicted initial extent			
Damage:	Probability:	Compartments:	
DAM6	0.0842	R180001	
DAM1	0.0305	R180001, R180002	
DAM13	0.0247	R180001, R180401	
DAM17	0.0234	R170101	
DAM65	0.0139	R180001, R180002, R180401	
DAM29	0.0137	R180001, R170101	
DAM46	0.0105	R040112	
DAM2	0.0090	R180001, R170001, R170101	
DAM14	0.0085	R100108	
DAM147	0.0084	R090113	
100% CI	99% CI	95% CI	90% CI
19225	10915	3057	1499

V.2 Test-case 1

V.2.1 Draft and AIS sensor evidence

Table V-2: Test-case 1 - Ten most likely cases inferred from draft and AIS sensor.

Predicted initial extent				
Damage:	Probability:	Compartments:		
DAM13	0.0424	R180001, R180401		
DAM17	0.0194	R170101		
DAM107	0.0187	R090113, R090305		
DAM345	0.0185	R170101, R170307		
DAM519	0.0173	R170101, R170302, R170308		
DAM162	0.0165	R180002		
DAM421	0.0155	R070101		
DAM523	0.0148	R050019, R050301		
DAM195	0.0139	R080116, R090113		
DAM199	0.0128	R100009, R110201		
100% CI:	99% CI:	95% CI:	90% CI:	Case rank.:
19225	1106	536	356	188
Actual initial extent:				
Damage:		Compartments:		
DAM16		R100009		

V.2.2 Flooding sensor evidence - $H_s = 0.00$ m

Table V-3: Test-case 1 - Ten most likely cases inferred from flooding sensors, $H_s = 0.0$ m, time = 5 min.

Predicted (complete damage) extent					
Dam:	Prob.:	Compartments:			
		Initial:	Progressive:		
DAM199	0.2223	R100009, R110201	R110203, R110202		
DAM199	0.1494	R100009, R110201	R110202		
DAM16	0.1414	R100009	NA		
DAM1062	0.0946	R100009, R110201, R110301	R110203, R110202		
DAM199	0.0776	R100009, R110201	R110203		
DAM199	0.0733	R100009, R110201	NA		
DAM1062	0.0631	R100009, R110201, R110301	R110202		
DAM1062	0.0330	R100009, R110201, R110301	R110203		
DAM1062	0.0312	R100009, R110201, R110301	NA		
DAM307	0.0233	R100009, R110201, R110301, R110401	R110203, R110202		
100% CI:	99% CI:	95% CI:	90% CI:	Case rank.:	
158889	23	14	10	3	
Positive sensor reading in:		R100009			
Actual (complete damage) extent:					
Name:	Initial:	Progressive:			
DAM16	R100009	None			

Table V-4: Test-case 1 - Ten most likely cases inferred from flooding sensors, $H_S = 0.0$ m, time = 10 min.

Predicted (complete damage) extent					
Dam:	Prob.:	Compartments:			
		Initial:	Progressive:		
DAM16	0.3218	R100009	None		
DAM199	0.1777	R100009, R110201	R110203, R110202		
DAM199	0.1402	R100009, R110201	R110202		
DAM1062	0.0759	R100009, R110201, R110301	R110203, R110202		
DAM1062	0.0594	R100009, R110201, R110301	R110202		
DAM199	0.0542	R100009, R110201	R110203		
DAM199	0.0400	R100009, R110201	None		
DAM1062	0.0231	R100009, R110201, R110301	R110203		
DAM307	0.0186	R100009, R110201, R110301, R110401	R110203, R110202		
DAM1062	0.0171	R100009, R110201, R110301	None		
100% CI:		99% CI:	95% CI:	90% CI:	Case rank.:
43372		19	12	9	1
Positive sensor reading in:		R100009			
Actual (complete damage) extent:					
Name:	Initial:	Progressive:			
DAM16	R100009	None			

Table V-5: Test-case 1 - Ten most likely cases inferred from flooding sensors, $H_S = 0.0$ m, time = 15 min.

Predicted (complete damage) extent					
Dam:	Prob.:	Compartments:			
		Initial:	Progressive:		
DAM16	0.5764	R100009	None		
DAM199	0.1002	R100009, R110201	R110203, R110202		
DAM199	0.0930	R100009, R110201	R110202		
DAM1062	0.0424	R100009, R110201, R110301	R110203, R110202		
DAM1062	0.0399	R100009, R110201, R110301	R110202		
DAM199	0.0359	R100009, R110201	R110203		
DAM199	0.0273	R100009, R110201	None		
DAM1062	0.0152	R100009, R110201, R110301	R110203		
DAM1062	0.0117	R100009, R110201, R110301	None		
DAM307	0.0104	R100009, R110201, R110301, R110401	R110203, R110202		
100% CI:		99% CI:	95% CI:	90% CI:	Case rank.:
47924		18	10	7	1
Positive sensor reading in:		R100009			
Actual (complete damage) extent:					
Name:	Initial:	Progressive:			
DAM16	R100009	None			

Table V-6: Test-case 1 - Ten most likely cases inferred from flooding sensors, $H_S = 0.0$ m, time = 20 min.

Predicted (complete damage) extent					
Dam:	Prob.:	Compartments:			
		Initial:	Progressive:		
DAM16	0.7884	R100009	None		
DAM199	0.0600	R100009, R110201	R110203, R110202		
DAM199	0.0399	R100009, R110201	R110202		
DAM1062	0.0257	R100009, R110201, R110301	R110203, R110202		
DAM1062	0.0171	R100009, R110201, R110301	R110202		
DAM199	0.0153	R100009, R110201	None		
DAM199	0.0145	R100009, R110201	R110203		
DAM1062	0.0064	R100009, R110201, R110301	None		
DAM307	0.0063	R100009, R110201, R110301, R110401	R110203, R110202		
DAM1062	0.0061	R100009, R110201, R110301	R110203		
100% CI:		99% CI:	95% CI:	90% CI:	Case rank.:
48121		14	7	4	1
Positive sensor reading in:		R100009			
Actual (complete damage) extent:					
Name:	Initial:		Progressive:		
DAM16	R100009		None		

Table V-7: Test-case 1 - Ten most likely cases inferred from flooding sensors, $H_S = 0.0$ m, time = 25 min.

Predicted (complete damage) extent					
Dam:	Prob.:	Compartments:			
		Initial:	Progressive:		
DAM16	0.9133	R100009	None		
DAM199	0.0214	R100009, R110201	R110203, R110202		
DAM199	0.0181	R100009, R110201	R110202		
DAM1062	0.0091	R100009, R110201, R110301	R110203, R110202		
DAM1062	0.0078	R100009, R110201, R110301	R110202		
DAM199	0.0076	R100009, R110201	R110203		
DAM199	0.0055	R100009, R110201	None		
DAM1062	0.0033	R100009, R110201, R110301	R110203		
DAM1062	0.0024	R100009, R110201, R110301	None		
DAM307	0.0022	R100009, R110201, R110301, R110401	R110203, R110202		
100% CI:		99% CI:	95% CI:	90% CI:	Case rank.:
47256		10	3	1	1
Positive sensor reading in:		R100009			
Actual (complete damage) extent:					
Name:	Initial:		Progressive:		
DAM16	R100009		None		

Table V-8: Test-case 1 - Ten most likely cases inferred from flooding sensors, $H_s = 0.0$ m, time = 30 min.

Predicted (complete damage) extent					
Dam:	Prob.:	Compartments:			
		Initial:	Progressive:		
DAM16	0.9697	R100009	None		
DAM199	0.0081	R100009, R110201	R110203, R110202		
DAM199	0.0061	R100009, R110201	R110202		
DAM1062	0.0035	R100009, R110201, R110301	R110203, R110202		
DAM1062	0.0026	R100009, R110201, R110301	R110202		
DAM199	0.0024	R100009, R110201	R110203		
DAM199	0.0015	R100009, R110201	None		
DAM1062	0.0010	R100009, R110201, R110301	R110203		
DAM1062	0.0008	R100009, R110201, R110301	None		
DAM307	0.0006	R100009, R110201, R110301, R110401	R110203, R110202		
100% CI:		99% CI:	95% CI:	90% CI:	Case rank.:
49241		6	1	1	1
Positive sensor reading in:		R100009			
Actual (complete damage) extent:					
Name:	Initial:		Progressive:		
DAM16	R100009		None		

V.2.3 Flooding sensor evidence - $H_s = 5.00$ m

Table V-9: Test-case 1 - Ten most likely cases inferred from flooding sensors, $H_s = 5.0$ m, time = 5 min.

Predicted (complete damage) extent					
Dam:	Prob.:	Compartments:			
		Initial:	Progressive:		
DAM16	0.4123	R100009	None		
DAM199	0.2220	R100009, R110201	R110203, R110202		
DAM1062	0.0448	R100009, R110201, R110301	R110203, R110202		
DAM199	0.0415	R100009, R110201	R110203, R110202, R110303		
DAM199	0.0260	R100009, R110201	R110202		
DAM199	0.0126	R100009, R110201	R110101, R110203, R110202, EX110101		
DAM199	0.0119	R100009, R110201	R110303, R110203, R110202, R110302		
DAM199	0.0107	R100009, R110201	R110203		
DAM307	0.0102	R100009, R110201, R110301, R110401	R110203, R110202		
DAM199	0.0087	R100009, R110201	R110202, R110303		
100% CI:		99% CI:	95% CI:	90% CI:	Case rank.:
382749		276	110	40	1
Positive sensor reading in:		R100009			
Actual (complete damage) extent:					
Name:	Initial:		Progressive:		
DAM16	R100009		None		

Table V-10: Test-case 1 - Ten most likely cases inferred from flooding sensors, $H_S = 5.0$ m, time = 10 min.

Predicted (complete damage) extent					
Dam:	Prob.:	Compartments:			
		Initial:	Progressive:		
DAM16	0.8815	R100009	None		
DAM199	0.0407	R100009, R110201	R110203, R110202		
DAM199	0.0092	R100009, R110201	R110202		
DAM199	0.0082	R100009, R110201	R110203, R110202, R110303		
DAM1062	0.0067	R100009, R110201, R110301	R110203, R110202		
DAM199	0.0029	R100009, R110201	R110203		
DAM199	0.0025	R100009, R110201	R110202, R110303		
DAM199	0.0022	R100009, R110201	R110101, R110203, R110202, EX110101		
DAM199	0.0018	R100009, R110201	R110203, R110202, EX110101		
DAM199	0.0017	R100009, R110201	None		
100% CI:		99% CI:	95% CI:	90% CI:	Case rank.:
68492		144	7	2	1
Positive sensor reading in:		R100009			
Actual (complete damage) extent:					
Name:	Initial:		Progressive:		
DAM16	R100009		None		

Table V-11: Test-case 1 - Ten most likely cases inferred from flooding sensors, $H_S = 5.0$ m, time = 15 min.

Predicted (complete damage) extent					
Dam:	Prob.:	Compartments:			
		Initial:	Progressive:		
DAM16	0.9882	R100009	None		
DAM199	0.0038	R100009, R110201	R110203, R110202		
DAM199	0.0012	R100009, R110201	R110202		
DAM199	7.9E-04	R100009, R110201	R110203, R110202, R110303		
DAM1062	6.1E-04	R100009, R110201, R110301	R110203, R110202		
DAM199	3.3E-04	R100009, R110201	R110203		
DAM199	3.3E-04	R100009, R110201	R110203, R110202, EX110101		
DAM199	2.5E-04	R100009, R110201	R110101, R110203, R110202, EX110101		
DAM1062	2.4E-04	R100009, R110201, R110301	R110202		
DAM199	1.8E-04	R100009, R110201	None		
100% CI:		99% CI:	95% CI:	90% CI:	Case rank.:
72008		2	1	1	1
Positive sensor reading in:		R100009			
Actual (complete damage) extent:					
Name:	Initial:		Progressive:		
DAM16	R100009		None		

Table V-12: Test-case 1 - Ten most likely cases inferred from flooding sensors, $H_s = 5.0$ m, time = 20 min.

Predicted (complete damage) extent					
Dam:	Prob.:	Compartments:			
		Initial:	Progressive:		
DAM16	0.9991	R100009	None		
DAM199	3.3E-04	R100009, R110201	R110203, R110202		
DAM199	6.5E-05	R100009, R110201	R110203, R110202, R110303		
DAM1062	5.0E-05	R100009, R110201, R110301	R110203, R110202		
DAM199	4.9E-05	R100009, R110201	R110202		
DAM199	4.1E-05	R100009, R110201	R110202, R110303		
DAM199	3.2E-05	R100009, R110201	R110203		
DAM199	2.3E-05	R100009, R110201	R110101, R110203, R110202, EX110101		
DAM1062	1.5E-05	R100009, R110201, R110301	R110202		
DAM199	1.3E-05	R100009, R110201	R110203, R110202, EX110101		
100% CI:		99% CI:	95% CI:	90% CI:	Case rank.:
71665		1	1	1	1
Positive sensor reading in:		R100009			
Actual (complete damage) extent:					
Name:	Initial:		Progressive:		
DAM16	R100009		None		

Table V-13: Test-case 1 - Ten most likely cases inferred from flooding sensors, $H_s = 5.0$ m, time = 25 min.

Predicted (complete damage) extent					
Dam:	Prob.:	Compartments:			
		Initial:	Progressive:		
DAM16	0.9999	R100009	None		
DAM199	3.2E-05	R100009, R110201	R110203, R110202		
DAM199	7.7E-06	R100009, R110201	R110202		
DAM199	5.6E-06	R100009, R110201	R110203, R110202, R110303		
DAM1062	5.3E-06	R100009, R110201, R110301	R110203, R110202		
DAM199	2.9E-06	R100009, R110201	R110203		
DAM199	2.1E-06	R100009, R110201	R110203, R110202, EX110101		
DAM199	1.9E-06	R100009, R110201	R110202, EX110101		
DAM199	1.8E-06	R100009, R110201	R110101, R110203, R110202, EX110101		
DAM1062	1.3E-06	R100009, R110201, R110301	R110202		
100% CI:		99% CI:	95% CI:	90% CI:	Case rank.:
69364		1	1	1	1
Positive sensor reading in:		R100009			
Actual (complete damage) extent:					
Name:	Initial:		Progressive:		
DAM16	R100009		None		

Table V-14: Test-case 1 - Ten most likely cases inferred from flooding sensors, $H_s = 5.0$ m, time = 30 min.

Predicted (complete damage) extent					
Dam:	Prob.:	Compartments:			
		Initial:	Progressive:		
DAM16	0.9999	R100009	None		
DAM199	3.0E-06	R100009, R110201	R110203, R110202		
DAM199	1.1E-06	R100009, R110201	R110202		
DAM199	4.9E-07	R100009, R110201	R110203, R110202, R110303		
DAM1062	3.5E-07	R100009, R110201, R110301	R110203, R110202		
DAM199	3.5E-07	R100009, R110201	R110203		
DAM199	3.1E-07	R100009, R110201	R110202, R110303		
DAM199	1.8E-07	R100009, R110201	R110203, R110202, EX110101		
DAM199	1.7E-07	R100009, R110201	R110101, R110203, R110202, EX110101		
DAM1062	1.5E-07	R100009, R110201, R110301	R110202		
100% CI:		99% CI:	95% CI:	90% CI:	Case rank.:
69804		1	1	1	1
Positive sensor reading in: R100009					
Actual (complete damage) extent:					
Name:	Initial:		Progressive:		
DAM16	R100009		None		

V.2.4 Flooding sensor evidence - $H_s = 10.00$ m

Table V-15: Test-case 1 - Ten most likely cases inferred from flooding sensors, $H_s = 10.0$ m, time = 5 min.

Predicted (complete damage) extent					
Dam:	Prob.:	Compartments:			
		Initial:	Progressive:		
DAM16	0.9097	R100009	None		
DAM199	0.0371	R100009,	R110203, R110202		
DAM199	0.0093	R100009,	R110203, R110202, R110303		
DAM199	0.0069	R100009,	R110303, R110203, R110202, R110302, R110305		
DAM199	0.0065	R100009,	R110101, R110203, R110202, EX110101		
DAM199	0.0035	R100009,	R110303, R110203, R110202, R110302		
DAM199	0.0035	R100009,	R110203, R110202, EX110101		
DAM199	0.0012	R100009,	R110203		
DAM199	0.0012	R100009, R110201	R130503, R110203, R130309, PL02, PL03, PL04, R130310, R130312, R110301, R130311, R120301, R130301, R110304, R130203, R130308, R110202, R110306, R130302, R130303, R110302, R110303, R130306, R130307, R130304, R130305		
DAM199	0.0012	R100009, R110201	R120304, R130401, R130303, R130203, R110203, R130309, PL02, PL03, R130311, R130310, R130313, R130312, R120303, R110301, R110302, R130301, R110304, R130307, R130202, R130308, R110202, R110306, R130302, R120302, R120301, R110303, R130306, R110305, R130304, R130305		
100% CI:		99% CI:	95% CI:	90% CI:	Case rank.:
620278		24	3	1	1
Positive sensor reading in: R100009					
Actual (complete damage) extent:					
Name:	Initial:		Progressive:		
DAM16	R100009		None		

Table V-16: Test-case 1 - Ten most likely cases inferred from flooding sensors, $H_S = 10.0$ m, time = 10 min.

Predicted (complete damage) extent					
Dam:	Prob.:	Compartments:			
		Initial:	Progressive:		
DAM16	0.9992	R100009	None		
DAM199	3.3E-04	R100009, R110201	R110203, R110202		
DAM199	9.3E-05	R100009, R110201	R110203, R110202, R110303		
DAM199	8.8E-05	R100009, R110201	R110202, R110303		
DAM199	5.3E-05	R100009, R110201	R110101, R110203, R110202, EX110101		
DAM199	4.1E-05	R100009, R110201	R110203, R110202, EX110101		
DAM199	3.1E-05	R100009, R110201	R110303, R110203, R110202, R110302, R110305		
DAM199	1.0E-05	R100009, R110201	R110203, R110202, R110303, EX110101, R110306		
DAM199	1.0E-05	R100009, R110201	R130401, R130309, PL01, PL02, PL03, PL04, R130412, R130411, R130303, R110301, R130203, R110203, R110202, R110306, R130204, R120303, R120302, R110302, R110303, R110304, R110305, R130304, R120304		
DAM199	1.0E-05	R100009, R110201	R130401, R110203, R130309, PL01, PL02, PL04, R130312, R120303, R110301, R130311, R110302, R130301, R110304, R130307, R130203, R130308, R110202, R110306, R130204, R130302, R120302, R120301, R110303, R130306, R110305, R130304		
100% CI:		99% CI:	95% CI:	90% CI:	Case rank.:
93533		1	1	1	1
Positive sensor reading in:		R100009			
Actual (complete damage) extent:					
Name:	Initial:		Progressive:		
DAM16	R100009		None		

Table V-17: Test-case 1 - Ten most likely cases inferred from flooding sensors, $H_S = 10.0$ m, time = 15 min.

Predicted (complete damage) extent					
Dam:	Prob.:	Compartments:			
		Initial:	Progressive:		
DAM16	0.9990	R100009	None		
DAM199	2.6E-06	R100009, R110201	R110203, R110202		
DAM199	7.7E-07	R100009, R110201	R110202, EX110101		
DAM199	7.3E-07	R100009, R110201	R110203, R110202, R110303		
DAM199	5.1E-07	R100009, R110201	R110101, R110203, R110202, EX110101		
DAM199	1.8E-07	R100009, R110201	R110203, R110202, EX110101		
DAM199	1.1E-07	R100009, R110201	R110101, R110203, R110202, R110303, EX110101		
DAM199	9.1E-08	R100009, R110201	R110303, R120301, R130301, R110203, R110202, R130313, R130303, R110301, R110302, R110304, R110305, R110306, R130309		
DAM199	9.1E-08	R100009, R110201	R110303, R110203, R110202, R110302, R110305		
DAM199	9.1E-08	R100009, R110201	R110305, R110203, R110202, R110302, R110303, EX110101		
100% CI:		99% CI:	95% CI:	90% CI:	Case rank.:
99728		1	1	1	1
Positive sensor reading in:		R100009			
Actual (complete damage) extent:					
Name:	Initial:		Progressive:		
DAM16	R100009		None		

Table V-18: Test-case 1 - Ten most likely cases inferred from flooding sensors, $H_S = 10.0$ m, time = 20 min.

Predicted (complete damage) extent					
Dam:	Prob.:	Compartments:			
		Initial:	Progressive:		
DAM16	0.9990	R100009	None		
DAM199	3.0E-08	R100009, R110201	R110203, R110202		
DAM199	8.7E-09	R100009, R110201	R110203, R110202, R110303		
DAM199	4.0E-09	R100009, R110201	R110101, R110203, R110202, EX110101		
DAM199	2.2E-09	R100009, R110201	R110303, R110203, R110202, R110302, R110305		
DAM199	1.4E-09	R100009, R110201	R110203		
DAM199	9.4E-10	R100009, R110201	R110101, R110203, R110202, R110303, EX110101		
DAM199	7.2E-10	R100009, R110201	R130405, R090306, R090305, R130401, R090302, R130404, R130503, R100301, R100303, R100302, R100304, R130203, PL03, PL04, R090310, R110302, R110203, R110202, R110306, R110301, R120301, R110303, R110304, R110305, R130304		
DAM199	7.2E-10	R100009, R110201	R110203, R110202, R110303, EX110101		
DAM199	7.2E-10	R100009, R110201	R130405, R130404, R130401, R130402, R110402, R130203, R110203, R130210, R140403, R130309, R140407, PL01, PL02, PL03, PL04, R130412, R130209, R140408, R140402, R110302, R130301, R130202, R130201, R110202, R110306, R130205, R130204, R120303, R110301, R120301, R110303, R110304, R110305, R130304		
100% CI:		99% CI:	95% CI:	90% CI:	Case rank.:
97841		1	1	1	1
Positive sensor reading in:		R100009			
Actual (complete damage) extent:					
Name:	Initial:		Progressive:		
DAM16	R100009		None		

Table V-19: Test-case 1 - Ten most likely cases inferred from flooding sensors, $H_S = 10.0$ m, time = 25 min.

Predicted (complete damage) extent					
Dam:	Prob.:	Compartments:			
		Initial:	Progressive:		
DAM16	0.9990	R100009	None		
DAM199	2.4E-10	R100009, R110201	R110203, R110202		
DAM199	5.7E-11	R100009, R110201	R110202		
DAM199	4.7E-11	R100009, R110201	R110303, R110203, R110202, R110302, R110305		
DAM199	3.8E-11	R100009, R110201	R110101, R110203, R110202, EX110101		
DAM199	3.3E-11	R100009, R110201	R110203, R110202, R110303		
DAM199	3.3E-11	R100009, R110201	R110203, R110202, EX110101		
DAM199	1.3E-11	R100009, R110201	R110203		
DAM199	9.3E-12	R100009, R110201	R110101, R110203, R110202, R110303, EX110101		
DAM199	6.7E-12	R100009, R110201	R110203, R110202, R110303, EX110101		
100% CI:		99% CI:	95% CI:	90% CI:	Case rank.:
96134		1	1	1	1
Positive sensor reading in:		R100009			
Actual (complete damage) extent:					
Name:	Initial:		Progressive:		
DAM16	R100009		None		

Table V-20: Test-case 1 - Ten most likely cases inferred from flooding sensors, $H_S = 10.0$ m, time = 30 min.

Predicted (complete damage) extent					
Dam:	Prob.:	Compartments:			
		Initial:	Progressive:		
DAM16	0.9990	R100009	None		
DAM199	2.5E-12	R100009, R110201	R110203, R110202		
DAM199	6.3E-13	R100009, R110201	R110203, R110202, R110303		
DAM199	3.2E-13	R100009, R110201	R110101, R110203, R110202, EX110101		
DAM199	2.5E-13	R100009, R110201	R110203, R110202, EX110101		
DAM199	6.3E-14	R100009, R110201	R110303, R110203, R110202, R110302, R110306		
DAM199	6.3E-14	R100009, R110201	R110303, R110203, R110202, R110306		
DAM199	6.3E-14	R100009, R110201	R110303, R110203, R110202, R110302		
DAM199	6.3E-14	R100009, R110201	R110303, R110203, R110202, R110302, R110305		
DAM199	6.3E-14	R100009, R110201	R090307, R090306, R090305, R090303, R090302, R090309, R090308, R100301, R100302, R130309, PL03, R090310, R110301, R120301, R130301, R110203, R110202, R110306, R120303, R120302, R110302, R110303, R110304, R110305, R130304, R120304		
100% CI:		99% CI:	95% CI:	90% CI:	Case rank.:
97208		1	1	1	1
Positive sensor reading in:		R100009			
Actual (complete damage) extent:					
Name:	Initial:	Progressive:			
DAM16	R100009	None			

V.3 Test-case 2

V.3.1 Draft and AIS sensor evidence

Table V-21: Test-case 2- Ten most likely cases inferred from draft and AIS sensor.

Predicted initial extent				
Damage:	Probability:	Compartments:		
DAM13	0.0328	R180001, R180401		
DAM6	0.0232	R180001		
DAM1	0.0220	R180001, R180002		
DAM17	0.0217	R170101		
DAM65	0.0129	R180001, R180002, R180401		
DAM345	0.0121	R170101, R170307		
DAM107	0.0097	R090113, R090305		
DAM421	0.0094	R070101		
DAM24	0.0088	R090113, R090305, R090401		
DAM519	0.0081	R170101, R170302, R170308		
100% CI:	99% CI:	95% CI:	90% CI:	Case rank.:
19225	3062	1223	763	8
Actual initial extent:				
Damage:	Compartments:			
DAM421	R070101			

V.3.2 Flooding sensor evidence - $H_s = 0.00$ m

Table V-22: Test-case 2- Ten most likely cases inferred from flooding sensors, $H_s = 0.0$ m, time = 5 min.

Predicted (complete damage) extent					
Dam:	Prob.:	Compartments:			
		Initial:	Progressive:		
DAM421	0.4041	R070101	EX070101, R070102		
DAM1506	0.0670	R070101, R070204	EX070101, R070102		
DAM421	0.0588	R070101	EX070101, R070102, R070203, R070201		
DAM421	0.0540	R070101	EX070101, R070102, R070201		
DAM421	0.0309	R070101	R070201, R070202, R070203, R070205, R070102, EX070101		
DAM421	0.0270	R070101	R070201, R070202, R070205, R070102, EX070101		
DAM421	0.0266	R070101	EX070101, R070102, R070205, R070201		
DAM421	0.0266	R070101	R070201, R070203, R070205, R070102, EX070101		
DAM40	0.0193	R070101, R070201	EX070101, R070203, R070102		
DAM40	0.0172	R070101, R070201	EX070101, R070102		
100% CI:		99% CI:	95% CI:	90% CI:	Case rank.:
421153		81	49	33	4
Positive sensor reading in:		R070101	Sensor, but no reading:		R070201
Actual (complete damage) extent:					
Name:	Initial:		Progressive:		
DAM421	R070101		R070201, EX070101, R070102		

Table V-23: Test-case 2- Ten most likely cases inferred from flooding sensors, $H_s = 0.0$ m, time = 10 min.

Predicted (complete damage) extent					
Dam:	Prob.:	Compartments:			
		Initial:	Progressive:		
DAM421	0.4932	R070101	EX070101, R070102		
DAM1506	0.0766	R070101, R070204	EX070101, R070102		
DAM421	0.0667	R070101	EX070101, R070102, R070203, R070201		
DAM421	0.0517	R070101	EX070101, R070102, R070201		
DAM421	0.0357	R070101	R070201, R070203, R070205, R070102, EX070101		
DAM421	0.0351	R070101	R070201, R070202, R070203, R070205, R070102, EX070101		
DAM421	0.0351	R070101	EX070101, R070102, R070205, R070201		
DAM421	0.0346	R070101	R070201, R070202, R070205, R070102, EX070101		
DAM2394	0.0137	R070101, R070204, R080402	EX070101, R070102		
DAM1506	0.0107	R070101, R070204	R070201, R070203, R070102, EX070101		
100% CI:		99% CI:	95% CI:	90% CI:	Case rank.:
19381		66	33	18	4
Positive sensor reading in:		R070101	Sensor in, but no reading:		R070201
Actual (complete damage) extent:					
Name:	Initial:		Progressive:		
DAM421	R070101		R070201, EX070101, R070102		

Table V-24: Test-case 2- Ten most likely cases inferred from flooding sensors, $H_S = 0.0$ m, time = 15 min.

Predicted (complete damage) extent					
Dam:	Prob.:	Compartments:			
		Initial:	Progressive:		
DAM421	0.5599	R070101	EX070101, R070102		
DAM1506	0.0811	R070101, R070204	EX070101, R070102		
DAM421	0.0606	R070101	EX070101, R070102, R070203, R070201		
DAM421	0.0573	R070101	EX070101, R070102, R070201		
DAM421	0.0399	R070101	R070201, R070202, R070203, R070205, R070102, EX070101		
DAM421	0.0328	R070101	EX070101, R070102, R070205, R070201		
DAM421	0.0317	R070101	R070201, R070203, R070205, R070102, EX070101		
DAM421	0.0306	R070101	R070201, R070202, R070205, R070102, EX070101		
DAM2394	0.0155	R070101, R070204, R080402	EX070101, R070102		
DAM1506	0.0091	R070101, R070204	R070201, R070203, R070102, EX070101		
100% CI:		99% CI:	95% CI:	90% CI:	Case rank.:
19357		50	16	9	4
Positive sensor reading in:		R070101	Sensor, but no reading:		R070201
Actual (complete damage) extent:					
Name:	Initial:		Progressive:		
DAM421	R070101		R070201, EX070101, R070102		

Table V-25: Test-case 2- Ten most likely cases inferred from flooding sensors, $H_S = 0.0$ m, time = 20 min.

Predicted (complete damage) extent					
Dam:	Prob.:	Compartments:			
		Initial:	Progressive:		
DAM421	0.5416	R070101	EX070101, R070102		
DAM1506	0.0733	R070101, R070204	EX070101, R070102		
DAM421	0.0670	R070101	EX070101, R070102, R070201		
DAM421	0.0670	R070101	EX070101, R070102, R070203, R070201		
DAM421	0.0489	R070101	R070201, R070202, R070203, R070205, R070102, EX070101		
DAM421	0.0390	R070101	EX070101, R070102, R070205, R070201		
DAM421	0.0385	R070101	R070201, R070202, R070205, R070102, EX070101		
DAM421	0.0373	R070101	R070201, R070203, R070205, R070102, EX070101		
DAM2394	0.0150	R070101, R070204, R080402	EX070101, R070102		
DAM1506	0.0094	R070101, R070204	EX070101, R070102, R070201		
100% CI:		99% CI:	95% CI:	90% CI:	Case rank.:
22662		37	12	8	3
Positive sensor reading in:		R070101	Sensor in, but no reading:		R070201
Actual (complete damage) extent:					
Name:	Initial:		Progressive:		
DAM421	R070101		R070201, EX070101, R070102		

Table V-26: Test-case 2- Ten most likely cases inferred from flooding sensors, $H_S = 0.0$ m, time = 25 min.

Predicted (complete damage) extent					
Dam:	Prob.:	Compartments:			
		Initial:	Progressive:		
DAM421	0.5438	R070101	EX070101, R070102		
DAM421	0.0715	R070101	EX070101, R070102, R070201		
DAM1506	0.0688	R070101, R070204	EX070101, R070102		
DAM421	0.0674	R070101	EX070101, R070102, R070203, R070201		
DAM421	0.0483	R070101	R070201, R070202, R070205, R070102, EX070101		
DAM421	0.0435	R070101	R070201, R070202, R070203, R070205, R070102, EX070101		
DAM421	0.0423	R070101	R070201, R070203, R070205, R070102, EX070101		
DAM421	0.0381	R070101	EX070101, R070102, R070205, R070201		
DAM2394	0.0151	R070101, R070204, R080402	EX070101, R070102		
DAM1506	0.0094	R070101, R070204	EX070101, R070102, R070201		
100% CI:		99% CI:	95% CI:	90% CI:	Case rank.:
22551		22	11	8	2
Positive sensor reading in:		R070101	Sensor, but no reading:		R070201
Actual (complete damage) extent:					
Name:	Initial:		Progressive:		
DAM421	R070101		R070201, EX070101, R070102		

Table V-27: Test-case 2- Ten most likely cases inferred from flooding sensors, $H_S = 0.0$ m, time = 30 min.

Predicted (complete damage) extent					
Dam:	Prob.:	Compartments:			
		Initial:	Progressive:		
DAM421	0.5609	R070101	EX070101, R070102		
DAM421	0.0711	R070101	EX070101, R070102, R070203, R070201		
DAM1506	0.0662	R070101, R070204	EX070101, R070102		
DAM421	0.0657	R070101	EX070101, R070102, R070201		
DAM421	0.0442	R070101	R070201, R070203, R070205, R070102, EX070101		
DAM421	0.0424	R070101	R070201, R070202, R070205, R070102, EX070101		
DAM421	0.0400	R070101	R070201, R070202, R070203, R070205, R070102, EX070101		
DAM421	0.0394	R070101	EX070101, R070102, R070205, R070201		
DAM2394	0.0155	R070101, R070204, R080402	EX070101, R070102		
DAM1506	0.0087	R070101, R070204	R070201, R070203, R070102, EX070101		
100% CI:		99% CI:	95% CI:	90% CI:	Case rank.:
224525		19	10	8	4
Positive sensor reading in:		R070101	Sensor in, but no reading:		R070201
Actual (complete damage) extent:					
Name:	Initial:		Progressive:		
DAM421	R070101		R070201, EX070101, R070102		

Flooding sensor evidence - $H_s = 5.00$ m

Table V-28: Test-case 2- Ten most likely cases inferred from flooding sensors, $H_s = 5.0$ m, time = 5 min.

Predicted (complete damage) extent					
Dam:	Prob.:	Compartments:			
		Initial:	Progressive:		
DAM421	0.4108	R070101	EX070101, R070102		
DAM421	0.0641	R070101	R070201, R070202, R070203, R070205, R070102, EX070101		
DAM1506	0.0537	R070101, R070204	EX070101, R070102		
DAM421	0.0315	R070101	EX070101, R070102, R070203, R070201		
DAM421	0.0272	R070101	R070201, R070202, R070205, R070102, EX070101		
DAM421	0.0210	R070101	R070201, R070203, R070205, R070102, EX070101		
DAM421	0.0194	R070101	R070201, R070202, R070203, R070205, R070102, AC070302, EX070101		
DAM421	0.0179	R070101	R070201, R070202, R070203, R070205, R070102, EX070101, R070303		
DAM421	0.0155	R070101	R070201, R070202, R070205, R070102, AC070302, EX070101		
DAM421	0.0101	R070101	EX070101, R070102, R070201		
	100% CI:	99% CI:	95% CI:	90% CI:	Case rank.:
	842418	6643	1856	330	10
Positive sensor reading in:		R070101	Sensor, but no reading:		R070201
Actual (complete damage) extent:					
Name:	Initial:	Progressive:			
DAM421	R070101	R070201, EX070101, R070102			

Table V-29: Test-case 2- Ten most likely cases inferred from flooding sensors, $H_s = 5.0$ m, time = 10 min.

Predicted (complete damage) extent					
Dam:	Prob.:	Compartments:			
		Initial:	Progressive:		
DAM421	0.4618	R070101	EX070101, R070102		
DAM421	0.0700	R070101	R070201, R070202, R070203, R070205, R070102, EX070101		
DAM1506	0.0561	R070101, R070204	EX070101, R070102		
DAM421	0.0369	R070101	EX070101, R070102, R070203, R070201		
DAM421	0.0327	R070101	R070201, R070202, R070205, R070102, EX070101		
DAM421	0.0323	R070101	R070201, R070202, R070203, R070205, R070102, AC070302, EX070101		
DAM421	0.0263	R070101	R070201, R070202, R070203, R070205, R070102, EX070101, R070303		
DAM421	0.0235	R070101	R070201, R070203, R070205, R070102, EX070101		
DAM421	0.0161	R070101	EX070101, R070102, R070201		
DAM421	0.0157	R070101	R070201, R070203, R070102, AC070302, EX070101		
	100% CI:	99% CI:	95% CI:	90% CI:	Case rank.:
	29479	1545	132	34	4
Positive sensor reading in:		R070101	Sensor, but no reading:		R070201
Actual (complete damage) extent:					
Name:	Initial:	Progressive:			
DAM421	R070101	R070201, R070203, EX070101, R070102			

Table V-30: Test-case 2- Ten most likely cases inferred from flooding sensors, $H_S = 5.0$ m, time = 15 min.

Predicted (complete damage) extent					
Dam:	Prob.:	Compartments:			
		Initial:	Progressive:		
DAM421	0.1935	R070101	R070201, R070202, R070203, R070205, R070102, EX070101		
DAM421	0.0890	R070101	EX070101, R070102, R070203, R070201		
DAM421	0.0712	R070101	R070201, R070202, R070203, R070102, EX070101		
DAM421	0.0623	R070101	R070201, R070203, R070205, R070102, EX070101		
DAM421	0.0500	R070101	R070201, R070202, R070203, R070205, R070102, AC070302, EX070101		
DAM421	0.0467	R070101	R070201, R070202, R070203, R070205, R070102, EX070101, R070303		
DAM421	0.0445	R070101	EX070101, R070102, R070201		
DAM421	0.0378	R070101	EX070101, R070102, R070205, R070201		
DAM421	0.0278	R070101	R070201, R070203, R070102, AC070302, EX070101		
DAM421	0.0278	R070101	R070201, R070203, R070205, R070102, AC070302, EX070101		
100% CI:		99% CI:	95% CI:	90% CI:	Case rank.:
23971		583	117	53	3
Positive sensor reading in:		R070101, R070201			
Actual (complete damage) extent:					
Name:	Initial:	Progressive:			
DAM421	R070101	R070201, R070203, EX070101, R070102, R070202			

Table V-31: Test-case 2- Ten most likely cases inferred from flooding sensors, $H_S = 5.0$ m, time = 20 min.

Predicted (complete damage) extent					
Dam:	Prob.:	Compartments:			
		Initial:	Progressive:		
DAM421	0.1658	R070101	R070201, R070202, R070203, R070205, R070102, EX070101		
DAM421	0.0829	R070101	EX070101, R070102, R070203, R070201		
DAM421	0.0730	R070101	R070201, R070202, R070203, R070205, R070102, AC070302, EX070101		
DAM421	0.0685	R070101	R070201, R070202, R070205, R070102, EX070101		
DAM421	0.0652	R070101	R070201, R070203, R070205, R070102, EX070101		
DAM421	0.0508	R070101	R070201, R070202, R070203, R070205, R070102, EX070101, R070303		
DAM421	0.0431	R070101	R070201, R070203, R070102, AC070302, EX070101		
DAM421	0.0298	R070101	EX070101, R070102, R070205, R070201		
DAM421	0.0298	R070101	R070201, R070202, R070205, R070102, AC070302, EX070101		
DAM421	0.0287	R070101	EX070101, R070102, R070201		
100% CI:		99% CI:	95% CI:	90% CI:	Case rank.:
79902		984	146	57	1
Positive sensor reading in:		R070101, R070201			
Actual (complete damage) extent:					
Name:	Initial:	Progressive:			
DAM421	R070101	R070201, R070205, R070203, EX070101, R070102, R070202			

Table V-32: Test-case 2- Ten most likely cases inferred from flooding sensors, $H_S = 5.0$ m, time = 25 min.

Predicted (complete damage) extent					
Dam:	Prob.:	Compartments:			
		Initial:	Progressive:		
DAM421	0.1794	R070101	R070201, R070202, R070203, R070205, R070102, EX070101		
DAM421	0.0880	R070101	R070201, R070202, R070205, R070102, EX070101		
DAM421	0.0812	R070101	R070201, R070202, R070203, R070205, R070102, AC070302, EX070101		
DAM421	0.0711	R070101	EX070101, R070102, R070203, R070201		
DAM421	0.0508	R070101	R070201, R070202, R070203, R070205, R070102, EX070101, R070303		
DAM421	0.0485	R070101	R070201, R070203, R070205, R070102, EX070101		
DAM421	0.0327	R070101	R070201, R070203, R070205, R070102, AC070302, EX070101		
DAM421	0.0316	R070101	EX070101, R070102, R070201		
DAM421	0.0305	R070101	R070201, R070202, R070205, R070102, AC070302, EX070101		
DAM421	0.0260	R070101	R070201, R070203, R070102, AC070302, EX070101		
100% CI:		99% CI:	95% CI:	90% CI:	Case rank.:
83522		1081	135	49	1
Positive sensor reading in:			R070101, R070201		
Actual (complete damage) extent:					
Name:	Initial:		Progressive:		
DAM421	R070101		R070201, R070205, R070203, EX070101, R070102, R070202		

Table V-33: Test-case 2- Ten most likely cases inferred from flooding sensors, $H_S = 5.0$ m, time = 30 min.

Predicted (complete damage) extent					
Dam:	Prob.:	Compartments:			
		Initial:	Progressive:		
DAM421	0.1663	R070101	R070201, R070202, R070203, R070205, R070102, EX070101		
DAM421	0.0963	R070101	EX070101, R070102, R070203, R070201		
DAM421	0.0941	R070101	R070201, R070202, R070205, R070102, EX070101		
DAM421	0.0755	R070101	R070201, R070203, R070205, R070102, EX070101		
DAM421	0.0613	R070101	R070201, R070202, R070203, R070205, R070102, EX070101, R070303		
DAM421	0.0460	R070101	R070201, R070202, R070203, R070205, R070102, AC070302, EX070101		
DAM421	0.0416	R070101	EX070101, R070102, R070201		
DAM421	0.0350	R070101	R070201, R070202, R070205, R070102, AC070302, EX070101		
DAM421	0.0339	R070101	EX070101, R070102, R070205, R070201		
DAM421	0.0252	R070101	R070201, R070203, R070102, EX070101, R070303		
100% CI:		99% CI:	95% CI:	90% CI:	Case rank.:
77450		733	117	45	1
Positive sensor reading in:			R070101, R070201		
Actual (complete damage) extent:					
Name:	Initial:		Progressive:		
DAM421	R070101		R070201, R070205, R070203, EX070101, R070102, R070202		

V.3.3 Flooding sensor evidence - $H_s = 10.00$ m

Table V-34: Test-case 2- Ten most likely cases inferred from flooding sensors, $H_s = 10.0$ m, time = 5 min.

Predicted (complete damage) extent					
Dam:	Prob.:	Compartments:			
		Initial:	Progressive:		
DAM421	0.4142	R070101	EX070101, R070102		
DAM421	0.0791	R070101	R070201, R070202, R070203, R070205, R070102, AC070302, EX070101		
DAM421	0.0581	R070101	R070201, R070202, R070203, R070205, R070102, AC070302, EX070101, R070303		
DAM1506	0.0434	R070101, R070204	EX070101, R070102		
DAM421	0.0343	R070101	R070201, R070202, R070203, R070205, R070102, EX070101		
DAM421	0.0271	R070101	R070201, R070202, R070203, R070205, R070102, EX070101, R070303		
DAM421	0.0227	R070101	R070201, R070202, R070205, R070102, AC070302, EX070101		
DAM421	0.0188	R070101	R070201, R070202, R070205, R070102, EX070101		
DAM421	0.0166	R070101	R070201, R070203, R070205, R070102, AC070302, EX070101		
DAM421	0.0133	R070101	R070201, R070203, R070102, AC070302, EX070101		
	100% CI:	99% CI:	95% CI:	90% CI:	Case rank.:
	1348567	6144	1183	192	29
Positive sensor reading in:		R070101	Sensor, but no reading:		R070201
Actual (complete damage) extent:					
Name:	Initial:	Progressive:			
DAM421	R070101	R070201, EX070101, R070102			

Table V-35: Test-case 2- Ten most likely cases inferred from flooding sensors, $H_s = 10.0$ m, time = 10 min.

Predicted (complete damage) extent					
Dam:	Prob.:	Compartments:			
		Initial:	Progressive:		
DAM421	0.6208	R070101	EX070101, R070102		
DAM421	0.0783	R070101	R070201, R070202, R070203, R070205, R070102, AC070302, EX070101		
DAM421	0.0545	R070101	R070201, R070202, R070203, R070205, R070102, AC070302, EX070101, R070303		
DAM421	0.0336	R070101	R070201, R070202, R070203, R070205, R070102, EX070101		
DAM421	0.0278	R070101	R070201, R070202, R070205, R070102, AC070302, EX070101		
DAM421	0.0215	R070101	R070201, R070202, R070203, R070205, R070102, EX070101, R070303		
DAM1506	0.0194	R070101, R070204	EX070101, R070102		
DAM421	0.0122	R070101	R070201, R070203, R070102, AC070302, EX070101		
DAM421	0.0110	R070101	R070201, R070202, R070205, R070102, EX070101		
DAM421	0.0104	R070101	R070201, R070203, R070102, AC070302, EX070101, R070303		
	100% CI:	99% CI:	95% CI:	90% CI:	Case rank.:
	73399	203	54	12	4
Positive sensor reading in:		R070101	Sensor, but no reading:		R070201
Actual (complete damage) extent:					
Name:	Initial:	Progressive:			
DAM421	R070101	R070201, R070205, R070203, EX070101, R070102, R070202			

Table V-36: Test-case 2- Ten most likely cases inferred from flooding sensors, $H_S = 10.0$ m, time = 15 min.

Predicted (complete damage) extent					
Dam:	Prob.:	Compartments:			
		Initial:	Progressive:		
DAM421	0.1801	R070101	R070201, R070202, R070203, R070205, R070102, AC070302, EX070101		
DAM421	0.1315	R070101	R070201, R070202, R070203, R070205, R070102, AC070302, EX070101, R070303		
DAM421	0.1287	R070101	R070201, R070202, R070203, R070205, R070102, EX070101		
DAM421	0.0901	R070101	R070201, R070202, R070205, R070102, AC070302, EX070101		
DAM421	0.0600	R070101	R070201, R070202, R070203, R070205, R070102, EX070101, R070303		
DAM421	0.0486	R070101	R070201, R070202, R070205, R070102, EX070101		
DAM421	0.0372	R070101	R070201, R070203, R070102, AC070302, EX070101		
DAM421	0.0272	R070101	R070201, R070203, R070205, R070102, AC070302, EX070101		
DAM421	0.0214	R070101	R070201, R070203, R070102, EX070101, R070303		
DAM421	0.0200	R070101	R070201, R070203, R070102, AC070302, EX070101, R070303		
100% CI:		99% CI:	95% CI:	90% CI:	Case rank.:
100954		275	99	64	3
Positive sensor reading in:			R070101, R070201		
Actual (complete damage) extent:					
Name:	Initial:	Progressive:			
DAM421	R070101	R070201, R070205, R070203, EX070101, R070102, R070202			

Table V-37: Test-case 2- Ten most likely cases inferred from flooding sensors, $H_S = 10.0$ m, time = 20 min.

Predicted (complete damage) extent					
Dam:	Prob.:	Compartments:			
		Initial:	Progressive:		
DAM421	0.1547	R070101	R070201, R070202, R070203, R070205, R070102, AC070302, EX070101		
DAM421	0.1044	R070101	R070201, R070202, R070203, R070205, R070102, EX070101		
DAM421	0.0792	R070101	R070201, R070202, R070203, R070205, R070102, AC070302, EX070101, R070303		
DAM421	0.0692	R070101	R070201, R070202, R070203, R070205, R070102, EX070101, R070303		
DAM421	0.0629	R070101	R070201, R070202, R070205, R070102, AC070302, EX070101		
DAM421	0.0553	R070101	R070201, R070202, R070205, R070102, EX070101		
DAM421	0.0428	R070101	R070201, R070203, R070102, AC070302, EX070101		
DAM421	0.0340	R070101	R070201, R070203, R070205, R070102, AC070302, EX070101		
DAM421	0.0327	R070101	R070201, R070203, R070102, EX070101, R070303		
DAM421	0.0314	R070101	EX070101, R070102, R070203, R070201		
100% CI:		99% CI:	95% CI:	90% CI:	Case rank.:
89442		345	139	99	2
Positive sensor reading in:			R070101, R070201		
Actual (complete damage) extent:					
Name:	Initial:	Progressive:			
DAM421	R070101	R070201, R070205, R070203, EX070101, R070102, R070202			

Table V-38: Test-case 2- Ten most likely cases inferred from flooding sensors, $H_S = 10.0$ m, time = 25 min.

Predicted (complete damage) extent					
Dam:	Prob.:	Compartments:			
		Initial:	Progressive:		
DAM421	0.1462	R070101	R070201, R070202, R070203, R070205, R070102, EX070101		
DAM421	0.1111	R070101	R070201, R070202, R070205, R070102, EX070101		
DAM421	0.0892	R070101	EX070101, R070102, R070203, R070201		
DAM421	0.0746	R070101	R070201, R070202, R070203, R070205, R070102, AC070302, EX070101		
DAM421	0.0687	R070101	EX070101, R070102, R070201		
DAM421	0.0526	R070101	R070201, R070203, R070102, AC070302, EX070101		
DAM421	0.0512	R070101	R070201, R070202, R070203, R070205, R070102, EX070101, R070303		
DAM421	0.0512	R070101	R070201, R070202, R070205, R070102, AC070302, EX070101		
DAM421	0.0483	R070101	R070201, R070203, R070205, R070102, EX070101		
DAM421	0.0336	R070101	R070201, R070203, R070205, R070102, AC070302, EX070101		
100% CI:		99% CI:	95% CI:	90% CI:	Case rank.:
76759		204	55	21	1
Positive sensor reading in:			R070101, R070201		
Actual (complete damage) extent:					
Name:	Initial:	Progressive:			
DAM421	R070101	R070201, R070205, R070203, EX070101, R070102, R070202			

Table V-39: Test-case 2- Ten most likely cases inferred from flooding sensors, $H_S = 10.0$ m, time = 30 min.

Predicted (complete damage) extent					
Dam:	Prob.:	Compartments:			
		Initial:	Progressive:		
DAM421	0.3836	R070101	R070201, R070202, R070203, R070205, R070102, AC070302, EX070101		
DAM421	0.2757	R070101	R070201, R070202, R070203, R070205, R070102, AC070302, EX070101, R070303		
DAM421	0.1049	R070101	R070201, R070202, R070205, R070102, AC070302, EX070101		
DAM421	0.0540	R070101	R070201, R070202, R070203, R070205, R070102, EX070101		
DAM421	0.0420	R070101	R070201, R070202, R070203, R070205, R070102, EX070101, R070303		
DAM421	0.0210	R070101	R070201, R070203, R070102, AC070302, EX070101		
DAM421	0.0210	R070101	R070201, R070203, R070102, AC070302, EX070101, R070303		
DAM421	0.0150	R070101	R070201, R070202, R070205, R070102, EX070101		
DAM421	0.0120	R070101	R070201, R070203, R070205, R070102, AC070302, EX070101, R070303		
DAM421	0.0090	R070101	R070201, R070203, R070205, R070102, AC070302, EX070101		
100% CI:		99% CI:	95% CI:	90% CI:	Case rank.:
113458		25	12	7	4
Positive sensor reading in:			R070101, R070201		
Actual (complete damage) extent:					
Name:	Initial:	Progressive:			
DAM421	R070101	R070201, R070205, R070203, EX070101, R070102, R070202			

V.4 Test-case 3

V.4.1 Draft and AIS sensor evidence

Table V-40: Test-case 3- Ten most likely cases inferred from draft and AIS sensor.

Predicted initial extent				
Damage:	Probability:	Compartments:		
DAM13	0.0357	R180001, R180401		
DAM6	0.0260	R180001		
DAM1	0.0212	R180001, R180002		
DAM17	0.0196	R170101		
DAM65	0.0150	R180001, R180002, R180401		
DAM345	0.0109	R170101, R170307		
DAM107	0.0078	R090113, R090305		
DAM24	0.0077	R090113, R090305, R090401		
DAM421	0.0076	R070101		
DAM11	0.0074	R090009, R090113		
100% CI:	99% CI:	95% CI:	90% CI:	Case rank.:
19225	3416	1346	850	280
Actual initial extent:				
Damage:		Compartments:		
DAM49		R160111, R160201, R160204		

V.4.2 Flooding sensor evidence - $H_s = 0.00$ m

Table V-41: Test-case 3 - Ten most likely cases inferred from flooding sensors, $H_s = 0.0$ m, time = 5 min.

Predicted (complete damage) extent				
Dam:	Prob.:	Compartments:		
		Initial:	Progressive:	
DAM359	0.0649	R160111, R160204	R160206, R160207, R160205, R160202, R160201, R160103, EX160101	
DAM359	0.0421	R160111, R160204	R160206, R160205, R160202, R160201, R160103, EX160101	
DAM120	0.0341	R160111, R160204, R160301, R160306	R160206, R160207, R160205, R160202, R160201, R160103, EX160101	
DAM120	0.0221	R160111, R160204, R160301, R160306	R160206, R160205, R160202, R160201, R160103, EX160101	
DAM395	0.0216	R160111, R160204, R160301, R160306, R160404	R160206, R160207, R160205, R160202, R160201, R160103, EX160101	
DAM18	0.0193	R160111	R160206, R160207, R160204, R160205, R160202, R160201, R160103, EX160101	
DAM575	0.0143	R160111, R160201, R160301	R160206, R160207, R160204, R160205, R160202, R160103, EX160101	
DAM395	0.0140	R160111, R160204, R160301, R160306, R160404	R160206, R160205, R160202, R160201, R160103, EX160101	
DAM18	0.0132	R160111	R160206, R160204, R160205, R160202, R160201, R160103, EX160101	
DAM134	0.0132	R160111, R160201	R160206, R160207, R160204, R160205, R160202, R160103, EX160101	
100% CI:	99% CI:	95% CI:	90% CI:	Case rank.:
309602	2741	1116	618	46
Positive sensor reading in:		R160103, R160201		
Actual (complete damage) extent:				
Name:	Initial:		Progressive:	
DAM49	R160111, R160201, R160204		R160202, R160205, EX160101, R160103, R160206	

Table V-42: Test-case 3 - Ten most likely cases inferred from flooding sensors, $H_S = 0.0$ m, time = 10 min.

Predicted (complete damage) extent					
Dam:	Prob.:	Compartments:			
		Initial:	Progressive:		
DAM359	0.0772	R160111, R160204	R160206, R160207, R160205, R160202, R160201, R160103, EX160101		
DAM359	0.0519	R160111, R160204	R160206, R160205, R160202, R160201, R160103, EX160101		
DAM120	0.0409	R160111, R160204, R160301, R160306	R160206, R160207, R160205, R160202, R160201, R160103, EX160101		
DAM120	0.0275	R160111, R160204, R160301, R160306	R160206, R160205, R160202, R160201, R160103, EX160101		
DAM395	0.0259	R160111, R160204, R160301, R160306,	R160206, R160207, R160205, R160202, R160201, R160103, EX160101		
DAM18	0.0196	R160111	R160206, R160207, R160204, R160205, R160202, R160201, R160103, EX160101		
DAM395	0.0174	R160111, R160204, R160301, R160306,	R160206, R160205, R160202, R160201, R160103, EX160101		
DAM381	0.0158	R160111, R160204, R160301	R160206, R160207, R160205, R160202, R160201, R160103, EX160101		
DAM1992	0.0152	R160111, R160204, R160301, R160404	R160206, R160207, R160205, R160202, R160201, R160103, EX160101		
DAM18	0.0121	R160111	R160206, R160204, R160205, R160202, R160201, R160103, EX160101		
	100% CI:	99% CI:	95% CI:	90% CI:	Case rank.:
	25584	2216	940	523	56
Positive sensor reading in:		R160103, R160201			
Actual (complete damage) extent:					
Name:	Initial:	Progressive:			
DAM49	R160111, R160201, R160204	R160202, R160205, EX160101, R160103, R160206			

Table V-43: Test-case 3 - Ten most likely cases inferred from flooding sensors, $H_S = 0.0$ m, time = 15 min.

Predicted (complete damage) extent					
Dam:	Prob.:	Compartments:			
		Initial:	Progressive:		
DAM359	0.0842	R160111, R160204	R160206, R160207, R160205, R160202, R160201, R160103, EX160101		
DAM359	0.0564	R160111, R160204	R160206, R160205, R160202, R160201, R160103, EX160101		
DAM120	0.0445	R160111, R160204, R160301, R160306	R160206, R160207, R160205, R160202, R160201, R160103, EX160101		
DAM120	0.0298	R160111, R160204, R160301, R160306	R160206, R160205, R160202, R160201, R160103, EX160101		
DAM395	0.0282	R160111, R160204, R160301, R160306,	R160206, R160207, R160205, R160202, R160201, R160103, EX160101		
DAM395	0.0189	R160111, R160204, R160301, R160306,	R160206, R160205, R160202, R160201, R160103, EX160101		
DAM381	0.0174	R160111, R160204, R160301	R160206, R160207, R160205, R160202, R160201, R160103, EX160101		
DAM1992	0.0166	R160111, R160204, R160301, R160404	R160206, R160207, R160205, R160202, R160201, R160103, EX160101		
DAM18	0.0150	R160111	R160206, R160207, R160204, R160205, R160202, R160201, R160103, EX160101		
DAM359	0.0142	R160111, R160204	R160207, R160202, R160201, R160103, EX160101		
	100% CI:	99% CI:	95% CI:	90% CI:	Case rank.:
	23998	1939	840	472	72
Positive sensor reading in:		R160103, R160201			
Actual (complete damage) extent:					
Name:	Initial:	Progressive:			
DAM49	R160111, R160201, R160204	R160202, R160205, EX160101, R160103, R160206			

Table V-44: Test-case 3 - Ten most likely cases inferred from flooding sensors, $H_s = 0.0$ m, time = 20 min.

Predicted (complete damage) extent					
Dam:	Prob.:	Compartments:			
		Initial:	Progressive:		
DAM359	0.0863	R160111, R160204	R160206, R160207, R160205, R160202, R160201, R160103, EX160101		
DAM359	0.0690	R160111, R160204	R160206, R160205, R160202, R160201, R160103, EX160101		
DAM120	0.0455	R160111, R160204, R160301, R160306	R160206, R160207, R160205, R160202, R160201, R160103, EX160101		
DAM120	0.0364	R160111, R160204, R160301, R160306	R160206, R160205, R160202, R160201, R160103, EX160101		
DAM395	0.0289	R160111, R160204, R160301, R160306, R160404	R160206, R160207, R160205, R160202, R160201, R160103, EX160101		
DAM395	0.0230	R160111, R160204, R160301, R160306, R160404	R160206, R160205, R160202, R160201, R160103, EX160101		
DAM381	0.0181	R160111, R160204, R160301	R160206, R160207, R160205, R160202, R160201, R160103, EX160101		
DAM1992	0.0172	R160111, R160204, R160301, R160404	R160206, R160207, R160205, R160202, R160201, R160103, EX160101		
DAM359	0.0146	R160111, R160204	R160207, R160202, R160201, R160103, EX160101		
DAM381	0.0144	R160111, R160204, R160301	R160206, R160205, R160202, R160201, R160103, EX160101		
100% CI:		99% CI:	95% CI:	90% CI:	Case rank.:
23564		1813	761	420	81
Positive sensor reading in:		R160103, R160201			
Actual (complete damage) extent:					
Name:	Initial:	Progressive:			
DAM49	R160111, R160201, R160204	R160202, R160205, EX160101, R160103, R160206			

Table V-45: Test-case 3 - Ten most likely cases inferred from flooding sensors, $H_s = 0.0$ m, time = 25 min.

Predicted (complete damage) extent					
Dam:	Prob.:	Compartments:			
		Initial:	Progressive:		
DAM359	0.0999	R160111, R160204	R160206, R160207, R160205, R160202, R160201, R160103, EX160101		
DAM359	0.0707	R160111, R160204	R160206, R160205, R160202, R160201, R160103, EX160101		
DAM120	0.0525	R160111, R160204, R160301, R160306	R160206, R160207, R160205, R160202, R160201, R160103, EX160101		
DAM120	0.0374	R160111, R160204, R160301, R160306	R160206, R160205, R160202, R160201, R160103, EX160101		
DAM395	0.0332	R160111, R160204, R160301, R160306, R160404	R160206, R160207, R160205, R160202, R160201, R160103, EX160101		
DAM395	0.0237	R160111, R160204, R160301, R160306, R160404	R160206, R160205, R160202, R160201, R160103, EX160101		
DAM381	0.0208	R160111, R160204, R160301	R160206, R160207, R160205, R160202, R160201, R160103, EX160101		
DAM1992	0.0196	R160111, R160204, R160301, R160404	R160206, R160207, R160205, R160202, R160201, R160103, EX160101		
DAM381	0.0148	R160111, R160204, R160301	R160206, R160205, R160202, R160201, R160103, EX160101		
DAM1992	0.0140	R160111, R160204, R160301, R160404	R160206, R160205, R160202, R160201, R160103, EX160101		
100% CI:		99% CI:	95% CI:	90% CI:	Case rank.:
23460		1700	672	361	109
Positive sensor reading in:		R160103, R160201			
Actual (complete damage) extent:					
Name:	Initial:	Progressive:			
DAM49	R160111, R160201, R160204	R160202, R160205, EX160101, R160103, R160206			

Table V-46: Test-case 3 - Ten most likely cases inferred from flooding sensors, $H_s = 0.0$ m, time = 30 min.

Predicted (complete damage) extent					
Dam:	Prob.:	Compartments:			
		Initial:	Progressive:		
DAM359	0.1072	R160111, R160204	R160206, R160207, R160205, R160202, R160201, R160103, EX160101		
DAM359	0.0708	R160111, R160204	R160206, R160205, R160202, R160201, R160103, EX160101		
DAM120	0.0561	R160111, R160204, R160301, R160306	R160206, R160207, R160205, R160202, R160201, R160103, EX160101		
DAM120	0.0368	R160111, R160204, R160301, R160306	R160206, R160205, R160202, R160201, R160103, EX160101		
DAM395	0.0356	R160111, R160204, R160301, R160306, R160404	R160206, R160207, R160205, R160202, R160201, R160103, EX160101		
DAM395	0.0233	R160111, R160204, R160301, R160306, R160404	R160206, R160205, R160202, R160201, R160103, EX160101		
DAM381	0.0226	R160111, R160204, R160301	R160206, R160207, R160205, R160202, R160201, R160103, EX160101		
DAM1992	0.0212	R160111, R160204, R160301, R160404	R160206, R160207, R160205, R160202, R160201, R160103, EX160101		
DAM381	0.0149	R160111, R160204, R160301	R160206, R160205, R160202, R160201, R160103, EX160101		
DAM1773	0.0148	R160111, R160204, R160301, R160306, R140401, R160404, R160405, R160412	R160206, R160207, R160205, R160202, R160201, R160103, EX160101		
	100% CI:	99% CI:	95% CI:	90% CI:	Case rank.:
	22951	1510	590	309	138
Positive sensor reading in:		R160103, R160201			
Actual (complete damage) extent:					
Name:	Initial:	Progressive:			
DAM49	R160111, R160201, R160204	R160202, R160205, EX160101, R160103, R160206			

V.4.3 Flooding sensor evidence - $H_s = 5.00$ m

Table V-47: Test-case 3 - Ten most likely cases inferred from flooding sensors, $H_s = 5.0$ m, time = 5 min.

Predicted (complete damage) extent					
Dam:	Prob.:	Compartments:			
		Initial:	Progressive:		
DAM359	0.0404	R160111, R160204	R160206, R160207, R160205, R160202, R160201, R160103, EX160101		
DAM18	0.0180	R160111	R160206, R160207, R160204, R160205, R160202, R160201, R160103, EX160101		
DAM18	0.0121	R160111	EX160101, R160103		
DAM359	0.0115	R160111, R160204	R160206, R160205, R160202, R160201, R160103, EX160101		
DAM151	0.0105	R160204	R160206, R160207, R160205, R160202, R160201, R160111, R160103, EX160101		
DAM120	0.0087	R160111, R160204, R160301, R160306	R160206, R160207, R160205, R160202, R160201, R160103, EX160101		
DAM18	0.0084	R160111	R160205, EX160101, R160103		
DAM18	0.0077	R160111	R160206, R160205, EX160101, R160103		
DAM359	0.0066	R160111, R160204	R160206, R160207, R160205, R160202, R160201, R160103, EX160101, R160303		
DAM359	0.0062	R160111, R160204	EX160101, R160103		
	100% CI:	99% CI:	95% CI:	90% CI:	Case rank.:
	982264	114376	42664	23021	228
Positive sensor reading in:		R160103		Sensor, but no reading:	R160201
Actual (complete damage) extent:					
Name:	Initial:	Progressive:			
DAM49	R160111, R160201, R160204	R160202, R160205, EX160101, R160103, R160206			

Table V-48: Test-case 3 - Ten most likely cases inferred from flooding sensors, $H_s = 5.0$ m, time = 10 min.

Predicted (complete damage) extent					
Dam:	Prob.:	Compartments:			
		Initial:	Progressive:		
DAM359	0.0519	R160111, R160204	R160206, R160207, R160205, R160202, R160201, R160103, EX160101		
DAM18	0.0274	R160111	R160206, R160207, R160204, R160205, R160202, R160201, R160103, EX160101		
DAM359	0.0192	R160111, R160204	R160206, R160205, R160202, R160201, R160103, EX160101		
DAM18	0.0189	R160111	EX160101, R160103		
DAM18	0.0170	R160111	R160206, R160205, EX160101, R160103		
DAM18	0.0138	R160111	R160205, EX160101, R160103		
DAM120	0.0133	R160111, R160204, R160301, R160306	R160206, R160207, R160205, R160202, R160201, R160103, EX160101		
DAM18	0.0111	R160111	R160206, R160204, R160205, R160202, R160201, R160103, EX160101		
DAM151	0.0080	R160204	R160206, R160207, R160205, R160202, R160201, R160111, R160103, EX160101		
DAM395	0.0080	R160111, R160204, R160301, R160306, R160404	R160206, R160207, R160205, R160202, R160201, R160103, EX160101		
100% CI:		99% CI:	95% CI:	90% CI:	Case rank.:
278724		72570	20787	8979	1161
Positive sensor reading in:			R160103	Sensor, but no reading:	R160201
Actual (complete damage) extent:					
Name:	Initial:		Progressive:		
DAM49	R160111, R160201, R160204		R160202, R160205, EX160101, R160103, R160206		

Table V-49: Test-case 3 - Ten most likely cases inferred from flooding sensors, $H_s = 5.0$ m, time = 15 min.

Predicted (complete damage) extent					
Dam:	Prob.:	Compartments:			
		Initial:	Progressive:		
DAM359	0.0703	R160111, R160204	R160206, R160207, R160205, R160202, R160201, R160103, EX160101		
DAM18	0.0474	R160111	R160206, R160207, R160204, R160205, R160202, R160201, R160103, EX160101		
DAM359	0.0242	R160111, R160204	R160206, R160205, R160202, R160201, R160103, EX160101		
DAM18	0.0176	R160111	R160206, R160204, R160205, R160202, R160201, R160103, EX160101		
DAM18	0.0160	R160111	R160206, R160207, R160205, R160202, R160201, R160103, EX160101		
DAM120	0.0145	R160111, R160204, R160301, R160306	R160206, R160207, R160205, R160202, R160201, R160103, EX160101		
DAM359	0.0115	R160111, R160204	R160206, R160207, R160205, R160202, R160201, R160103, EX160101, R160303		
DAM18	0.0091	R160111	R160206, R160207, R160204, R160205, R160202, R160201, R160103, EX160101, R160303		
DAM395	0.0084	R160111, R160204, R160301, R160306, R160404	R160206, R160207, R160205, R160202, R160201, R160103, EX160101		
DAM151	0.0067	R160204	R160206, R160207, R160205, R160202, R160201, R160111, R160103, EX160101		
100% CI:		99% CI:	95% CI:	90% CI:	Case rank.:
184114		35962	10616	5377	1162
Positive sensor reading in:			R160103, R160201		
Actual (complete damage) extent:					
Name:	Initial:		Progressive:		
DAM49	R160111, R160201, R160204		R160202, R160205, EX160101, R160103, R160206		

Table V-50: Test-case 3 - Ten most likely cases inferred from flooding sensors, $H_5 = 5.0$ m, time = 20 min.

Predicted (complete damage) extent					
Dam:	Prob.:	Compartments:			
		Initial:	Progressive:		
DAM359	0.0764	R160111, R160204	R160206, R160207, R160205, R160202, R160201, R160103, EX160101		
DAM18	0.0473	R160111	R160206, R160207, R160204, R160205, R160202, R160201, R160103, EX160101		
DAM359	0.0215	R160111, R160204	R160206, R160205, R160202, R160201, R160103, EX160101		
DAM120	0.0160	R160111, R160204, R160301, R160306	R160206, R160207, R160205, R160202, R160201, R160103, EX160101		
DAM18	0.0158	R160111	R160206, R160207, R160205, R160202, R160201, R160103, EX160101		
DAM18	0.0148	R160111	R160206, R160204, R160205, R160202, R160201, R160103, EX160101		
DAM359	0.0128	R160111, R160204	R160206, R160207, R160205, R160202, R160201, R160103, EX160101, R160303		
DAM395	0.0094	R160111, R160204, R160301, R160306, R160404	R160206, R160207, R160205, R160202, R160201, R160103, EX160101		
DAM18	0.0073	R160111	R160206, R160207, R160204, R160205, R160202, R160201, R160103, EX160101, R160303		
DAM120	0.0061	R160111, R160204, R160301, R160306	R160206, R160207, R160205, R160202, R160201, R160103, R160302, EX160101, R160304, R160303, R160305		
	100% CI:	99% CI:	95% CI:	90% CI:	Case rank.:
	113904	29742	9515	4893	1527
	Positive sensor reading in:		R160103, R160201		
Actual (complete damage) extent:					
Name:	Initial:		Progressive:		
DAM49	R160111, R160201, R160204		R160202, R160205, EX160101, R160103, R160206		

Table V-51: Test-case 3 - Ten most likely cases inferred from flooding sensors, $H_S = 5.0$ m, time = 25 min.

Predicted (complete damage) extent					
Dam:	Prob.:	Compartments:			
		Initial:		Progressive:	
DAM359	0.0815	R160111, R160204		R160206, R160207, R160205, R160202, R160201, R160103, EX160101	
DAM18	0.0506	R160111		R160206, R160207, R160204, R160205, R160202, R160201, R160103, EX160101	
DAM359	0.0270	R160111, R160204		R160206, R160205, R160202, R160201, R160103, EX160101	
DAM120	0.0160	R160111, R160204, R160301, R160306		R160206, R160207, R160205, R160202, R160201, R160103, EX160101	
DAM18	0.0156	R160111		R160206, R160204, R160205, R160202, R160201, R160103, EX160101	
DAM18	0.0128	R160111		R160206, R160207, R160205, R160202, R160201, R160103, EX160101	
DAM359	0.0125	R160111, R160204		R160206, R160207, R160205, R160202, R160201, R160103, EX160101, R160303	
DAM395	0.0093	R160111, R160204, R160301, R160306, R160404		R160206, R160207, R160205, R160202, R160201, R160103, EX160101	
DAM18	0.0073	R160111		R160206, R160207, R160204, R160205, R160202, R160201, R160103, EX160101, R160303	
DAM359	0.0062	R160111, R160204		R160206, R160205, R160202, R160201, R160103, EX160101, R160303	
100% CI:		99% CI:		95% CI:	
88739		23692		7846	
90% CI:		Case rank.:			
4052		1470			
Positive sensor reading in:		R160103, R160201			
Actual (complete damage) extent:					
Name:	Initial:		Progressive:		
DAM49	R160111, R160201, R160204		R160202, R160205, EX160101, R160103, R160206		

Table V-52: Test-case 3 - Ten most likely cases inferred from flooding sensors, $H_5 = 5.0$ m, time = 30 min.

Predicted (complete damage) extent					
Dam:	Prob.:	Compartments:			
		Initial:		Progressive:	
DAM359	0.0852	R160111, R160204		R160206, R160207, R160205, R160202, R160201, R160103, EX160101	
DAM18	0.0461	R160111		R160206, R160207, R160204, R160205, R160202, R160201, R160103, EX160101	
DAM359	0.0240	R160111, R160204		R160206, R160205, R160202, R160201, R160103, EX160101	
DAM120	0.0161	R160111, R160204, R160301, R160306		R160206, R160207, R160205, R160202, R160201, R160103, EX160101	
DAM359	0.0144	R160111, R160204		R160206, R160207, R160205, R160202, R160201, R160103, EX160101, R160303	
DAM18	0.0128	R160111		R160206, R160207, R160205, R160202, R160201, R160103, EX160101	
DAM18	0.0121	R160111		R160206, R160204, R160205, R160202, R160201, R160103, EX160101	
DAM395	0.0099	R160111, R160204, R160301, R160306, R160404		R160206, R160207, R160205, R160202, R160201, R160103, EX160101	
DAM18	0.0070	R160111		R160206, R160207, R160204, R160205, R160202, R160201, R160103, EX160101, R160303	
DAM120	0.0057	R160111, R160204, R160301, R160306		R160206, R160207, R160205, R160202, R160201, R160103, R160302, EX160101, R160304, R160303, R160305	
100% CI:		99% CI:		95% CI:	90% CI:
77399		19832		6907	3538
Positive sensor reading in:			R160103, R160201		
Actual (complete damage) extent:					
Name:	Initial:		Progressive:		
DAM49	R160111, R160201, R160204		R160202, R160205, EX160101, R160103, R160206		

V.4.4 Flooding sensor evidence - $H_s = 10.00$ m

Table V-53: Test-case 3 - Ten most likely cases inferred from flooding sensors, $H_s = 10.0$ m, time = 5 min.

Predicted (complete damage) extent					
Dam:	Prob.:	Compartments:			
		Initial:	Progressive:		
DAM359	0.0223	R160111, R160204	R160206, R160207, R160205, R160202, R160201, R160103, EX160101		
DAM18	0.0113	R160111	R160206, R160207, R160204, R160205, R160202, R160201, R160103, EX160101		
DAM134	0.0087	R160111, R160201	R160206, R160207, R160204, R160205, R160202, R160103, EX160101		
DAM151	0.0064	R160204	R160206, R160207, R160205, R160202, R160201, R160111, R160103, EX160101		
DAM251	0.0050	R160201	R160206, R160207, R160204, R160205, R160202, R160111, R160103, EX160101		
DAM49	0.0029	R160111, R160201, R160204	R160206, R160207, R160205, R160202, R160103, EX160101		
DAM120	0.0027	R160111, R160204, R160301, R160306	R160206, R160207, R160205, R160202, R160201, R160103, R160302, EX160101, R160304, R160303, R160305		
DAM602	0.0023	R160201, R160204	R160206, R160207, R160205, R160202, R160111, R160103, EX160101		
DAM359	0.0022	R160111, R160204	R160206, R160205, R160202, R160201, R160103, EX160101		
DAM359	0.0022	R160111, R160204	R160206, R160207, R160205, R160202, R160201, R160103, R160302, R160307, R160306, EX160101, R160304, R160303, R160305, R160301		
	100% CI:	99% CI:	95% CI:	90% CI:	Case rank.:
	1749360	132784	53282	31212	211
	Positive sensor reading in:		R160103, R160201		
Actual (complete damage) extent:					
Name:	Initial:	Progressive:			
DAM49	R160111, R160201, R160204	R160202, R160205, EX160101, R160103, R160206			

Table V-54: Test-case 3 - Ten most likely cases inferred from flooding sensors, $H_S = 10.0$ m, time = 10 min.

Predicted (complete damage) extent					
Dam:	Prob.:	Compartments:			
		Initial:	Progressive:		
DAM359	0.0314	R160111, R160204	R160206, R160207, R160205, R160202, R160201, R160103, EX160101		
DAM18	0.0158	R160111	R160206, R160207, R160204, R160205, R160202, R160201, R160103, EX160101		
DAM134	0.0115	R160111, R160201	R160206, R160207, R160204, R160205, R160202, R160103, EX160101		
DAM151	0.0079	R160204	R160206, R160207, R160205, R160202, R160201, R160111, R160103, EX160101		
DAM251	0.0063	R160201	R160206, R160207, R160204, R160205, R160202, R160111, R160103, EX160101		
DAM359	0.0038	R160111, R160204	R160206, R160205, R160202, R160201, R160103, EX160101		
DAM359	0.0038	R160111, R160204	R160206, R160207, R160205, R160202, R160203, R160201, R160103, R160302, SL01, R160306, EX160101, R160304, R160303, R160305, R160301		
DAM49	0.0037	R160111, R160201, R160204	R160206, R160207, R160205, R160202, R160103, EX160101		
DAM359	0.0034	R160111, R160204	R160206, R160207, R160205, R160202, R160203, R160201, R160103, R160302, R160307, R160308, SL01, R160306, EX160101, R160304, R160303, R160305,		
DAM359	0.0031	R160111, R160204	R160206, R160207, R160205, R160202, R160203, R160201, R160103, SL01, EX160101, R160303		
	100% CI:	99% CI:	95% CI:	90% CI:	Case rank.:
	657104	77584	32089	18666	155
Positive sensor reading in:		R160103, R160201			
Actual (complete damage) extent:					
Name:	Initial:		Progressive:		
DAM49	R160111, R160201, R160204		R160202, R160205, EX160101, R160103, R160206		

Table V-55: Test-case 3 - Ten most likely cases inferred from flooding sensors, $H_S = 10.0$ m, time = 15 min.

Predicted (complete damage) extent				
Dam:	Prob.:	Compartments:		
		Initial:	Progressive:	
DAM359	0.0329	R160111, R160204	R160206, R160207, R160205, R160202, R160201, R160103, EX160101	
DAM18	0.0158	R160111	R160206, R160207, R160204, R160205, R160202, R160201, R160103, EX160101	
DAM134	0.0103	R160111, R160201	R160206, R160207, R160204, R160205, R160202, R160103, EX160101	
DAM151	0.0073	R160204	R160206, R160207, R160205, R160202, R160201, R160111, R160103, EX160101	
DAM251	0.0056	R160201	R160206, R160207, R160204, R160205, R160202, R160111, R160103, EX160101	
DAM359	0.0043	R160111, R160204	R160206, R160207, R160205, R160202, R160203, R160201, R160103, R160302, R160307, R160308, SL01, R160306, EX160101, R160304, R160303, R160305, R160301	
DAM359	0.0043	R160111, R160204	R160206, R160207, R160205, R160202, R160201, R160103, R160302, R160308, R160307, R160306, EX160101, R160304, R160303, R160305, R160301	
DAM359	0.0038	R160111, R160204	R160206, R160207, R160205, R160202, R160201, R160103, R160302, R160306, EX160101, R160304, R160303, R160305, R160301	
DAM49	0.0034	R160111, R160201, R160204	R160206, R160207, R160205, R160202, R160103, EX160101	
DAM359	0.0033	R160111, R160204	R160206, R160205, R160202, R160201, R160103, EX160101	
	100% CI:	99% CI:	95% CI:	90% CI:
	484196	72933	30051	17062
	Positive sensor reading in:	R160103, R160201		
Actual (complete damage) extent:				
Name:	Initial:	Progressive:		
DAM49	R160111, R160201, R160204	R160202, R160205, EX160101, R160103, R160206		

Table V-56: Test-case 3 - Ten most likely cases inferred from flooding sensors, $H_S = 10.0$ m, time = 20 min.

Predicted (complete damage) extent					
Dam:	Prob.:	Compartments:			
		Initial:	Progressive:		
DAM359	0.0405	R160111, R160204	R160206, R160207, R160205, R160202, R160201, R160103, EX160101		
DAM18	0.0195	R160111	R160206, R160207, R160204, R160205, R160202, R160201, R160103, EX160101		
DAM134	0.0114	R160111, R160201	R160206, R160207, R160204, R160205, R160202, R160103, EX160101		
DAM151	0.0080	R160204	R160206, R160207, R160205, R160202, R160201, R160111, R160103, EX160101		
DAM359	0.0077	R160111, R160204	R160206, R160205, R160202, R160201, R160103, EX160101		
DAM251	0.0063	R160201	R160206, R160207, R160204, R160205, R160202, R160111, R160103, EX160101		
DAM359	0.0049	R160111, R160204	R160206, R160207, R160205, R160202, R160201, R160103, R160302, R160306, EX160101, R160304, R160303, R160305, R160301		
DAM359	0.0049	R160111, R160204	R160206, R160207, R160205, R160202, R160203, R160201, R160103, R160403, SL01, EX160101, R160303		
DAM359	0.0049	R160111, R160204	R160206, R160207, R160205, R160202, R160203, R160201, R160103, R160302, R160403, SL01, R160306, EX160101, R160304, R160303, R160305, R160301		
DAM18	0.0042	R160111	R160206, R160204, R160205, R160202, R160201, R160103,		
	100% CI:	99% CI:	95% CI:	90% CI:	Case rank.:
	415303	51438	20602	11227	96
Positive sensor reading in:		R160103, R160201			
Actual (complete damage) extent:					
Name:	Initial:		Progressive:		
DAM49	R160111, R160201, R160204		R160202, R160205, EX160101, R160103, R160206		

Table V-57: Test-case 3 - Ten most likely cases inferred from flooding sensors, $H_S = 10.0$ m, time = 25 min.

Predicted (complete damage) extent					
Dam:	Prob.:	Compartments:			
		Initial:	Progressive:		
DAM359	0.0412	R160111, R160204	R160206, R160207, R160205, R160202, R160201, R160103, EX160101		
DAM18	0.0221	R160111	R160206, R160207, R160204, R160205, R160202, R160201, R160103, EX160101		
DAM134	0.0117	R160111, R160201	R160206, R160207, R160204, R160205, R160202, R160103, EX160101		
DAM359	0.0105	R160111, R160204	R160206, R160207, R160205, R160202, R160201, R160103, R160302, R160308, R160307, R160306, EX160101, R160304, R160303, R160305, R160301		
DAM151	0.0081	R160204	R160206, R160207, R160205, R160202, R160201, R160111, R160103, EX160101		
DAM359	0.0075	R160111, R160204	R160206, R160207, R160205, R160202, R160203, R160201, R160103, R160302, SL01, R160306, EX160101, R160304, R160303, R160305, R160301		
DAM251	0.0064	R160201	R160206, R160207, R160204, R160205, R160202, R160111, R160103, EX160101		
DAM359	0.0052	R160111, R160204	R160206, R160207, R160205, R160202, R160201, R160103, R160302, R160306, EX160101, R160304, R160303, R160305, R160301		
DAM359	0.0052	R160111, R160204	R160206, R160207, R160205, R160202, R160203, R160201, R160103, R160302, R160307, R160308, SL01, R160306, EX160101, R160304, R160303, R160305, R160301		
DAM18	0.0045	R160111	R160206, R160207, R160204, R160205, R160202, R160201, R160103, R160302, R160308, R160307, R160306, EX160101, R160304, R160303, R160305, R160301		
100% CI:		99% CI:	95% CI:	90% CI:	Case rank.:
361710		53007	20513	10536	578
Positive sensor reading in:		R160103, R160201			
Actual (complete damage) extent:					
Name:	Initial:		Progressive:		
DAM49	R160111, R160201, R160204		R160202, R160205, EX160101, R160103, R160206		

Table V-58: Test-case 3 - Ten most likely cases inferred from flooding sensors, $H_S = 10.0$ m, time = 30 min.

Predicted (complete damage) extent					
Dam:	Prob.:	Compartments:			
		Initial:	Progressive:		
DAM359	0.0603	R160111, R160204	R160206, R160207, R160205, R160202, R160201, R160103, EX160101		
DAM18	0.0295	R160111	R160206, R160207, R160204, R160205, R160202, R160201, R160103, EX160101		
DAM134	0.0145	R160111, R160201	R160206, R160207, R160204, R160205, R160202, R160103, EX160101		
DAM151	0.0098	R160204	R160206, R160207, R160205, R160202, R160201, R160111, R160103, EX160101		
DAM359	0.0091	R160111, R160204	R160206, R160207, R160205, R160202, R160201, R160103, R160302, R160308, R160307, R160306, EX160101, R160304, R160303, R160305, R160301		
DAM359	0.0080	R160111, R160204	R160206, R160205, R160202, R160201, R160103, EX160101		
DAM251	0.0078	R160201	R160206, R160207, R160204, R160205, R160202, R160111, R160103, EX160101		
DAM359	0.0070	R160111, R160204	R160206, R160207, R160205, R160202, R160203, R160201, R160103, R160302, SL01, R160306, EX160101, R160304, R160303, R160305, R160301		
DAM359	0.0070	R160111, R160204	R160206, R160207, R160205, R160202, R160203, R160201, R160103, R160302, R160307, R160308, SL01, R160306, EX160101, R160304, R160303, R160305, R160301		
DAM359	0.0050	R160111, R160204	R160206, R160207, R160205, R160202, R160201, R160103, R160302, R160306, EX160101, R160304, R160303, R160305, R160301		
100% CI:		99% CI:	95% CI:	90% CI:	Case rank.:
339270		40941	13908	6555	233
Positive sensor reading in:		R160103, R160201			
Actual (complete damage) extent:					
Name:	Initial:		Progressive:		
DAM49	R160111, R160201, R160204		R160202, R160205, EX160101, R160103, R160206		

V.5 Test-case 4

V.5.1 Draft and AIS sensor evidence

Table V-59: Test-case 4 - Ten most likely cases inferred from draft and AIS sensor.

Predicted initial extent				
Damage:	Probability:	Compartments:		
DAM13	0.0364	R180001, R180401		
DAM6	0.0265	R180001		
DAM1	0.0202	R180001, R180002		
DAM17	0.0187	R170101		
DAM65	0.0148	R180001, R180002, R180401		
DAM345	0.0103	R170101, R170307		
DAM11	0.0075	R090009, R090113		
DAM107	0.0072	R090113, R090305		
DAM24	0.0071	R090113, R090305, R090401		
DAM136	0.0071	R040112, R040301		
100% CI:	99% CI:	95% CI:	90% CI:	Case rank.:
19225	3459	1370	871	267
Actual initial extent:				
Damage:		Compartments:		
DAM342		R180001, R170101, R180002		

V.5.2 Flooding sensor evidence - $H_s = 0.00$ m

Table V-60: Test-case 4 - Ten most likely cases inferred from flooding sensors, $H_s = 0.0$ m, time = 5 min.

Predicted (complete damage) extent				
Dam:	Prob.:	Compartments:		
		Initial:	Progressive:	
DAM29	0.2932	R180001, R170101	EX170201	
DAM29	0.1890	R180001, R170101	None	
DAM9	0.0932	R180001, R170101, R170307	EX170201	
DAM88	0.0628	R180001, R170101, R170307, R170406, R170407, R180401	EX170201	
DAM9	0.0597	R180001, R170101, R170307	None	
DAM88	0.0402	R180001, R170101, R170307, R170406, R170407, R180401	None	
DAM70	0.0216	R180001, R170101, R180002, R170307	EX170201	
DAM342	0.0214	R180001, R170101, R180002	EX170201	
DAM352	0.0202	R180001, R170101, R170302, R170308, R170307	EX170201	
DAM70	0.0139	R180001, R170101, R180002, R170307	None	
100% CI:	99% CI:	95% CI:	90% CI:	Case rank.:
316107	120	31	19	8
Positive sensor reading in:		R180001, R170101		
Actual (complete damage) extent:				
Name:	Initial:	Progressive:		
DAM342	R180001, R170101, R180002	EX170201		

Table V-61: Test-case 4 - Ten most likely cases inferred from flooding sensors, $H_s = 0.0$ m, time = 10 min.

Predicted (complete damage) extent					
Dam:	Prob.:	Compartments:			
		Initial:			Progressive:
DAM29	0.3795	R180001, R170101			EX170201
DAM29	0.2586	R180001, R170101			None
DAM9	0.0482	R180001, R170101, R170307			EX170201
DAM9	0.0325	R180001, R170101, R170307			None
DAM88	0.0290	R180001, R170101, R170307, R170406, R170407, R180401			EX170201
DAM352	0.0262	R180001, R170101, R170302, R170308, R170307			EX170201
DAM88	0.0196	R180001, R170101, R170307, R170406, R170407, R180401			None
DAM352	0.0177	R180001, R170101, R170302, R170308, R170307			None
DAM70	0.0153	R180001, R170101, R180002, R170307			EX170201
DAM342	0.0152	R180001, R170101, R180002			EX170201
	100% CI:	99% CI:	95% CI:	90% CI:	Case rank.:
	22864	87	23	16	10
Positive sensor reading in:		R180001, R170101			
Actual (complete damage) extent:					
Name:	Initial:			Progressive:	
DAM342	R180001, R170101, R180002			EX170201	

Table V-62: Test-case 4 - Ten most likely cases inferred from flooding sensors, $H_s = 0.0$ m, time = 15 min.

Predicted (complete damage) extent					
Dam:	Prob.:	Compartments:			
		Initial:			Progressive:
DAM29	0.4142	R180001, R170101			EX170201
DAM29	0.3143	R180001, R170101			None
DAM352	0.0285	R180001, R170101, R170302, R170308, R170307			EX170201
DAM352	0.0214	R180001, R170101, R170302, R170308, R170307			None
DAM9	0.0210	R180001, R170101, R170307			EX170201
DAM9	0.0158	R180001, R170101, R170307			None
DAM1197	0.0158	R180001, R170101, R170302, R170308, R170307, R170406, R170407, R180401			EX170201
DAM699	0.0139	R180001, R170101, R170302, R170308, R170307, R170406, R170407, R170408, R180401			EX170201
DAM1197	0.0118	R180001, R170101, R170302, R170308, R170307, R170406, R170407, R180401			None
DAM88	0.0113	R180001, R170101, R170307, R170406, R170407, R180401			EX170201
	100% CI:	99% CI:	95% CI:	90% CI:	Case rank.:
	20678	65	21	14	13
Positive sensor reading in:		R180001, R170101			
Actual (complete damage) extent:					
Name:	Initial:			Progressive:	
DAM342	R180001, R170101, R180002			EX170201	

Table V-63: Test-case 4 - Ten most likely cases inferred from flooding sensors, $H_S = 0.0$ m, time = 20 min.

Predicted (complete damage) extent				
Dam:	Prob.:	Compartments:		
		Initial:	Progressive:	
DAM29	0.4292	R180001, R170101		EX170201
DAM29	0.3158	R180001, R170101		None
DAM352	0.0296	R180001, R170101, R170302, R170308, R170307		EX170201
DAM352	0.0216	R180001, R170101, R170302, R170308, R170307		None
DAM7528	0.0211	R180001, R170101, R170302, R170308, R170307, R170407		EX170201
DAM1197	0.0164	R180001, R170101, R170302, R170308, R170307, R170406, R170407, R180401		EX170201
DAM7528	0.0154	R180001, R170101, R170302, R170308, R170307, R170407,		None
DAM699	0.0144	R180001, R170101, R170302, R170308, R170307, R170406, R170407, R170408, R180401		EX170201
DAM1197	0.0120	R180001, R170101, R170302, R170308, R170307, R170406, R170407, R180401		None
DAM699	0.0105	R180001, R170101, R170302, R170308, R170307, R170406, R170407, R170408, R180401		None
100% CI:		99% CI:	95% CI:	90% CI:
20123		52	20	12
Positive sensor reading in:		R180001, R170101		
Actual (complete damage) extent:				
Name:	Initial:	Progressive:		
DAM342	R180001, R170101, R180002	EX170201		

Table V-64: Test-case 4 - Ten most likely cases inferred from flooding sensors, $H_S = 0.0$ m, time = 25 min.

Predicted (complete damage) extent				
Dam:	Prob.:	Compartments:		
		Initial:	Progressive:	
DAM29	0.3909	R180001, R170101		EX170201
DAM29	0.2782	R180001, R170101		None
DAM7528	0.0656	R180001, R170101, R170302, R170308, R170307, R170407		EX170201
DAM7528	0.0462	R180001, R170101, R170302, R170308, R170307, R170407		None
DAM352	0.0270	R180001, R170101, R170302, R170308, R170307		EX170201
DAM352	0.0190	R180001, R170101, R170302, R170308, R170307		None
DAM8809	0.0172	R180001, R170101, R180002, EX170201, R170302, R170306, R170308, R170307, R170404, R170406, R170407, R170408, R170409, R180401		None
DAM1197	0.0150	R180001, R170101, R170302, R170308, R170307, R170406, R170407, R180401		EX170201
DAM6771	0.0143	R180001, R170101, R180002, EX170201, R170302, R170306, R170308, R170307, R170404, R170406, R170407, R170409, R180401		None
DAM699	0.0130	R180001, R170101, R170302, R170308, R170307, R170406, R170407, R170408, R180401		EX170201
100% CI:		99% CI:	95% CI:	90% CI:
20794		47	21	12
Positive sensor reading in:		R180001, R170101		
Actual (complete damage) extent:				
Name:	Initial:	Progressive:		
DAM342	R180001, R170101, R180002	EX170201		

Table V-65: Test-case 4 - Ten most likely cases inferred from flooding sensors, $H_s = 0.0$ m, time = 30 min.

Predicted (complete damage) extent					
Dam:	Prob.:	Compartments:			Progressive:
		Initial:			
DAM29	0.2794	R180001, R170101,			EX170201
DAM29	0.1905	R180001, R170101,			None
DAM7528	0.1600	R180001, R170101, R170302, R170308, R170307, R170407			EX170201
DAM7528	0.1077	R180001, R170101, R170302, R170308, R170307, R170407			None
DAM8809	0.0412	R180001, R170101, R180002, EX170201, R170302, R170306, R170308, R170307, R170404, R170406, R170407, R170408, R170409, R180401			None
DAM6771	0.0341	R180001, R170101, R180002, EX170201, R170302, R170306, R170308, R170307, R170404, R170406, R170407, R170409, R180401			None
DAM352	0.0193	R180001, R170101, R170302, R170308, R170307			EX170201
DAM16495	0.0130	R180001, R170101, R180002, EX170201, R170302, R170303, R170306, R170308, R170307, R170401, R170403, R170404, R170405, R170406, R170407, R170409, R180401			None
DAM352	0.0130	R180001, R170101, R170302, R170308, R170307			None
DAM12803	0.0125	R180001, R170101, R170302, R170304, R170305, R170306, SL01, R170308, R170307, EC170401, R160403, R170402, R170404, R170406, R170407, R170408, R170409, R180401			EX170201
100% CI:		99% CI:	95% CI:	90% CI:	Case rank.:
20590		44	20	13	27
Positive sensor reading in:			R180001, R170101		
Actual (complete damage) extent:					
Name:	Initial:		Progressive:		
DAM342	R180001, R170101, R180002		EX170201		

V.5.3 Flooding sensor evidence - $H_s = 5.00$ m

Table V-66: Test-case 4 - Ten most likely cases inferred from flooding sensors, $H_s = 5.0$ m, time = 5 min.

Predicted (complete damage) extent					
Dam:	Prob.:	Compartments:			Progressive:
		Initial:			
DAM29	0.1633	R180001, R170101			EX170201
DAM9	0.1386	R180001, R170101, R170307			EX170201
DAM88	0.0924	R180001, R170101, R170307, R170406, R170407, R180401			EX170201
DAM29	0.0696	R180001, R170101			None
DAM29	0.0504	R180001, R170101			EX170201, R170307
DAM9	0.0295	R180001, R170101, R170307			R170306, EX170201
DAM88	0.0286	R180001, R170101, R170307, R170406, R170407, R180401			EX170201, R170306
DAM9	0.0263	R180001, R170101, R170307			None
DAM70	0.0238	R180001, R170101, R180002, R170307			EX170201
DAM342	0.0219	R180001, R170101, R180002			EX170201
100% CI:		99% CI:	95% CI:	90% CI:	Case rank.:
967952		586	148	67	10
Positive sensor reading in:			R180001, R170101		
Actual (complete damage) extent:					
Name:	Initial:		Progressive:		
DAM342	R180001, R170101, R180002		EX170201		

Table V-67: Test-case 4 - Ten most likely cases inferred from flooding sensors, $H_S = 5.0$ m, time = 10 min.

Predicted (complete damage) extent					
Dam:	Prob.:	Compartments:			
		Initial:			Progressive:
DAM29	0.1714	R180001, R170101			EX170201
DAM9	0.1375	R180001, R170101, R170307			EX170201
DAM88	0.0914	R180001, R170101, R170307, R170406, R170407, R180401			EX170201
DAM29	0.0695	R180001, R170101			
DAM29	0.0406	R180001, R170101			EX170201, R170307
DAM88	0.0299	R180001, R170101, R170307, R170406, R170407, R180401			EX170201, R170306
DAM9	0.0278	R180001, R170101, R170307			R170306, EX170201
DAM9	0.0254	R180001, R170101, R170307			None
DAM70	0.0238	R180001, R170101, R180002, R170307			EX170201
DAM342	0.0231	R180001, R170101, R180002			EX170201
	100% CI:	99% CI:	95% CI:	90% CI:	Case rank.:
	42155	563	145	67	10
Positive sensor reading in:		R180001, R170101			
Actual (complete damage) extent:					
Name:	Initial:			Progressive:	
DAM342	R180001, R170101, R180002			EX170201	

Table V-68: Test-case 4 - Ten most likely cases inferred from flooding sensors, $H_S = 5.0$ m, time = 15 min.

Predicted (complete damage) extent					
Dam:	Prob.:	Compartments:			
		Initial:			Progressive:
DAM29	0.1567	R180001, R170101			EX170201
DAM9	0.1355	R180001, R170101, R170307			EX170201
DAM88	0.0899	R180001, R170101, R170307, R170406, R170407, R180401			EX170201
DAM29	0.0766	R180001, R170101			None
DAM29	0.0510	R180001, R170101			EX170201, R170307
DAM88	0.0304	R180001, R170101, R170307, R170406, R170407, R180401			EX170201, R170306
DAM9	0.0280	R180001, R170101, R170307			None
DAM9	0.0266	R180001, R170101, R170307			R170306, EX170201
DAM70	0.0237	R180001, R170101, R180002, R170307			EX170201
DAM342	0.0212	R180001, R170101, R180002			EX170201
	100% CI:	99% CI:	95% CI:	90% CI:	Case rank.:
	22304	479	129	61	10
Positive sensor reading in:		R180001, R170101			
Actual (complete damage) extent:					
Name:	Initial:			Progressive:	
DAM342	R180001, R170101, R180002			EX170201	

Table V-69: Test-case 4 - Ten most likely cases inferred from flooding sensors, $H_S = 5.0$ m, time = 20 min.

Predicted (complete damage) extent					
Dam:	Prob.:	Compartments:			
		Initial:		Progressive:	
DAM29	0.1611	R180001, R170101		EX170201	
DAM9	0.1357	R180001, R170101, R170307		EX170201	
DAM88	0.0890	R180001, R170101, R170307, R170406, R170407, R180401		EX170201	
DAM29	0.0784	R180001, R170101		None	
DAM29	0.0483	R180001, R170101		EX170201, R170307	
DAM9	0.0291	R180001, R170101, R170307		None	
DAM9	0.0248	R180001, R170101, R170307		R170306, EX170201	
DAM88	0.0241	R180001, R170101, R170307, R170406, R170407, R180401,		EX170201, R170306	
DAM70	0.0240	R180001, R170101, R180002, R170307		EX170201	
DAM342	0.0220	R180001, R170101, R180002		EX170201	
	100% CI:	99% CI:	95% CI:	90% CI:	Case rank.:
	22674	545	146	69	10
Positive sensor reading in:		R180001, R170101			
Actual (complete damage) extent:					
Name:	Initial:		Progressive:		
DAM342	R180001, R170101, R180002		EX170201		

Table V-70: Test-case 4 - Ten most likely cases inferred from flooding sensors, $H_S = 5.0$ m, time = 25 min.

Predicted (complete damage) extent					
Dam:	Prob.:	Compartments:			
		Initial:		Progressive:	
DAM29	0.1551	R180001, R170101		EX170201	
DAM9	0.1407	R180001, R170101, R170307		EX170201	
DAM88	0.0964	R180001, R170101, R170307, R170406, R170407, R180401		EX170201	
DAM29	0.0749	R180001, R170101		None	
DAM29	0.0507	R180001, R170101		EX170201, R170307	
DAM9	0.0271	R180001, R170101, R170307		None	
DAM88	0.0255	R180001, R170101, R170307, R170406, R170407, R180401		EX170201, R170306	
DAM70	0.0251	R180001, R170101, R180002, R170307,		EX170201	
DAM342	0.0213	R180001, R170101, R180002		EX170201	
DAM9	0.0206	R180001, R170101, R170307		R170306, EX170201	
	100% CI:	99% CI:	95% CI:	90% CI:	Case rank.:
	23518	547	143	66	9
Positive sensor reading in:		R180001, R170101			
Actual (complete damage) extent:					
Name:	Initial:		Progressive:		
DAM342	R180001, R170101, R180002		EX170201		

Table V-71: Test-case 4 - Ten most likely cases inferred from flooding sensors, $H_s = 5.0$ m, time = 30 min.

Predicted (complete damage) extent					
Dam:	Prob.:	Compartments:			
		Initial:		Progressive:	
DAM29	0.1779	R180001, R170101		EX170201	
DAM9	0.1419	R180001, R170101, R170307		EX170201	
DAM88	0.0971	R180001, R170101, R170307, R170406, R170407, R180401		EX170201	
DAM29	0.0742	R180001, R170101		None	
DAM29	0.0424	R180001, R170101		EX170201, R170307	
DAM9	0.0315	R180001, R170101, R170307		None	
DAM9	0.0294	R180001, R170101, R170307		R170306, EX170201	
DAM88	0.0281	R180001, R170101, R170307, R170406, R170407, R180401		EX170201, R170306	
DAM70	0.0256	R180001, R170101, R180002, R170307		EX170201	
DAM342	0.0245	R180001, R170101, R180002		EX170201	
	100% CI:	99% CI:	95% CI:	90% CI:	Case rank.:
	22150	472	119	55	10
Positive sensor reading in:		R180001, R170101			
Actual (complete damage) extent:					
Name:	Initial:		Progressive:		
DAM342	R180001, R170101, R180002		EX170201		

V.5.4 Flooding sensor evidence - $H_s = 10.00$ m

Table V-72: Test-case 4 - Ten most likely cases inferred from flooding sensors, $H_s = 10.0$ m, time = 5 min.

Predicted (complete damage) extent					
Dam:	Prob.:	Compartments:			
		Initial:		Progressive:	
DAM29	0.0491	R180001, R170101		EX170201	
DAM9	0.0405	R180001, R170101, R170307		EX170201	
DAM29	0.0332	R180001, R170101		EX170201, R170307	
DAM29	0.0273	R180001, R170101		None	
DAM29	0.0273	R180001, R170101		EX170201, R170307, R170306	
DAM9	0.0224	R180001, R170101, R170307		EX170201, R170305, R170306, R170304	
DAM9	0.0224	R180001, R170101, R170307		EX170201, R170306	
DAM29	0.0188	R180001, R170101		EX170201, R170305, R170306, R170307, R170304	
DAM9	0.0145	R180001, R170101, R170307		EX170201, R170305, R170306	
DAM29	0.0123	R180001, R170101		EX170201, R170305, R170306, R170307	
	100% CI:	99% CI:	95% CI:	90% CI:	Case rank.:
	1717438	9928	3411	1665	14
Positive sensor reading in:		R180001, R170101			
Actual (complete damage) extent:					
Name:	Initial:		Progressive:		
DAM342	R180001, R170101, R180002		EX170201		

Table V-73: Test-case 4 - Ten most likely cases inferred from flooding sensors, $H_S = 10.0$ m, time = 10 min.

Predicted (complete damage) extent					
Dam:	Prob.:	Compartments:			
		Initial:	Progressive:		
DAM2	0.0693	R180001, R170101	EX170201		
\hat{D} AM9	0.0558	R180001, R170101, R170307	EX170201		
DAM2	0.0498	R180001, R170101	EX170201, R170307		
\hat{D} AM2	0.0354	R180001, R170101	None		
\hat{D} AM2	0.0300	R180001, R170101	EX170201, R170307, R170306		
\hat{D} AM9	0.0296	R180001, R170101, R170307	EX170201, R170305, R170306, R170304		
DAM2	0.0256	R180001, R170101	EX170201, R170305, R170306, R170307, R170304		
\hat{D} AM9	0.0244	R180001, R170101, R170307	EX170201, R170306		
DAM9	0.0187	R180001, R170101, R170307	EX170201, R170305, R170306		
DAM2	0.0170	R180001, R170101	EX170201, R170305, R170306, R170307		
100% CI:		99% CI:	95% CI:	90% CI:	Case rank.:
90940		9603	3421	1789	13
Positive sensor reading in:		R180001, R170101			
Actual (complete damage) extent:					
Name:	Initial:		Progressive:		
DAM342	R180001, R170101, R180002		EX170201		

Table V-74: Test-case 4 - Ten most likely cases inferred from flooding sensors, $H_S = 10.0$ m, time = 15 min.

Predicted (complete damage) extent					
Dam:	Prob.:	Compartments:			
		Initial:	Progressive:		
DAM29	0.1251	R180001, R170101	EX170201		
DAM9	0.0939	R180001, R170101, R170307	EX170201		
DAM29	0.0737	R180001, R170101	None		
DAM29	0.0551	R180001, R170101	EX170201, R170307		
DAM29	0.0296	R180001, R170101	EX170201, R170307, R170306		
DAM88	0.0292	R180001, R170101, R170307, R170406, R170407	EX170201		
DAM9	0.0254	R180001, R170101, R170307	EX170201, R170306		
DAM9	0.0215	R180001, R170101, R170307	R170306, EX170201		
DAM9	0.0173	R180001, R170101, R170307	EX170201, R170305, R170306		
DAM342	0.0167	R180001, R170101, R180002	EX170201		
100% CI:		99% CI:	95% CI:	90% CI:	Case rank.:
62294		3270	904	400	10
Positive sensor reading in:		R180001, R170101			
Actual (complete damage) extent:					
Name:	Initial:		Progressive:		
DAM342	R180001, R170101, R180002		EX170201		

Table V-75: Test-case 4 - Ten most likely cases inferred from flooding sensors, $H_S = 10.0$ m, time = 20 min.

Predicted (complete damage) extent					
Dam:	Prob.:	Compartments:			
		Initial:	Progressive:		
DAM29	0.0828	R180001, R170101	EX170201		
DAM29	0.0535	R180001, R170101	EX170201, R170307		
DAM9	0.0531	R180001, R170101, R170307	EX170201		
DAM29	0.0375	R180001, R170101	EX170201, R170307, R170306		
DAM29	0.0352	R180001, R170101	None		
DAM29	0.0307	R180001, R170101	EX170201, R170305, R170306, R170307, R170304		
DAM9	0.0287	R180001, R170101, R170307	EX170201, R170305, R170306, R170304		
DAM9	0.0284	R180001, R170101, R170307	EX170201, R170306		
DAM29	0.0156	R180001, R170101	EX170201, R170305, R170306, R170307		
DAM9	0.0148	R180001, R170101, R170307	EX170201, R170305, R170306		
100% CI:		99% CI:	95% CI:	90% CI:	Case rank.:
95121		9380	3171	1527	12
Positive sensor reading in:		R180001, R170101			
Actual (complete damage) extent:					
Name:	Initial:		Progressive:		
DAM342	R180001, R170101, R180002		EX170201		

Table V-76: Test-case 4 - Ten most likely cases inferred from flooding sensors, $H_S = 10.0$ m, time = 25 min.

Predicted (complete damage) extent					
Dam:	Prob.:	Compartments:			
		Initial:	Progressive:		
DAM29	0.1130	R180001, R170101	EX170201		
DAM9	0.0747	R180001, R170101, R170307	EX170201		
DAM29	0.0661	R180001, R170101	EX170201, R170307		
DAM29	0.0649	R180001, R170101	None		
DAM29	0.0419	R180001, R170101	EX170201, R170307, R170306		
DAM9	0.0295	R180001, R170101, R170307	EX170201, R170306		
DAM9	0.0215	R180001, R170101, R170307	EX170201, R170305, R170306, R170304		
DAM29	0.0197	R180001, R170101	EX170201, R170305, R170306, R170307, R170304		
DAM9	0.0193	R180001, R170101, R170307	EX170201, R170305, R170306		
DAM29	0.0160	R180001, R170101	EX170201, R170305, R170306, R170307		
100% CI:		99% CI:	95% CI:	90% CI:	Case rank.:
79130		4777	1379	644	12
Positive sensor reading in:		R180001, R170101			
Actual (complete damage) extent:					
Name:	Initial:		Progressive:		
DAM342	R180001, R170101, R180002		EX170201		

Table V-77: Test-case 4 - Ten most likely cases inferred from flooding sensors, $H_S = 10.0$ m, time = 30 min.

Predicted (complete damage) extent					
Dam:	Prob.:	Compartments:			
		Initial:	Progressive:		
DAM29	0.0983	R180001, R170101	EX170201		
DAM29	0.0708	R180001, R170101	EX170201, R170307		
DAM9	0.0629	R180001, R170101, R170307	EX170201		
DAM29	0.0475	R180001, R170101	None		
DAM29	0.0457	R180001, R170101	EX170201, R170307, R170306		
DAM29	0.0298	R180001, R170101	EX170201, R170305, R170306, R170307, R170304		
DAM9	0.0283	R180001, R170101, R170307	EX170201, R170306		
DAM9	0.0270	R180001, R170101, R170307	EX170201, R170305, R170306, R170304		
DAM29	0.0233	R180001, R170101	EX170201, R170305, R170306, R170307		
DAM9	0.0187	R180001, R170101, R170307	EX170201, R170305, R170306		
	100% CI:	99% CI:	95% CI:	90% CI:	Case rank.:
	75569	6039	1915	884	11
Positive sensor reading in:		R180001, R170101			
Actual (complete damage) extent:					
Name:	Initial:		Progressive:		
DAM342	R180001, R170101, R180002		EX170201		

V.6 Test-case 5

V.6.1 Draft and AIS sensor evidence

Table V-78: Test-case 5 - Ten most likely cases inferred from draft and AIS sensor.

Predicted initial extent					
Damage:	Probability:	Compartments:			
DAM13	0.0366	R180001, R180401			
DAM6	0.0266	R180001			
DAM1	0.0198	R180001, R180002			
DAM17	0.0183	R170101			
DAM65	0.0146	R180001, R180002, R180401			
DAM345	0.0101	R170101, R170307			
DAM11	0.0078	R090009, R090113			
DAM136	0.0070	R040112, R040301			
DAM10	0.0070	R040112, R040301, R040401			
DAM421	0.0070	R070101			
	100% CI:	99% CI:	95% CI:	90% CI:	Case rank.:
	19225	3461	1374	876	4064
Actual initial extent:					
Damage:	Compartments:				
DAM7043	R100009, R090009, R080116, R100108, R090113				

V.6.2 Flooding sensor evidence - $H_s = 0.00$ m

Table V-79: Test-case 5 - Ten most likely cases inferred from flooding sensors, $H_s = 0.0$ m, time = 5 min.

Predicted (complete damage) extent				
Dam:	Prob.:	Compartments:		
		Initial:	Progressive:	
DAM7043	0.8178	R100009, R090009, R080116, R100108, R090113	EX080101, R100107, EX100101	
DAM7043	0.0912	R100009, R090009, R080116, R100108, R090113	EX080101, R100107, EX100101, R080202, R080201	
DAM7043	0.0483	R100009, R090009, R080116, R100108, R090113	R100201, R100202, EX080101, R100107, EX100101	
DAM7043	0.0122	R100009, R090009, R080116, R100108, R090113	R100201, EX080101, R100107, EX100101	
DAM7043	0.0062	R100009, R090009, R080116, R100108, R090113	R100201, R100202, EX080101, R100107, EX100101, R080202, R080201	
DAM7043	0.0053	R100009, R090009, R080116, R100108, R090113	EX080101, R100107	
DAM7043	0.0053	R100009, R090009, R080116, R100108, R090113	R100107, EX100101	
DAM7043	0.0050	R100009, R090009, R080116, R100108, R090113	EX080101, R100107, EX100101, R080201	
DAM7043	0.0026	R100009, R090009, R080116, R100108, R090113	R100201, R100202, EX080101, R100107, AC100302, EX100101	
DAM7043	0.0015	R100009, R090009, R080116, R100108, R090113	R100201, EX080101, R100107, EX100101, R080202, R080201	
	100% CI:	99% CI:	95% CI:	90% CI:
	357757	8	3	2
	Case rank.:			8
Positive sensor reading in:		R090009, R100009, R080116, R080116, R090113, R100107, R100108		
Sensor, but no reading:		R080201		
Actual (complete damage) extent:				
Name:	Initial:	Progressive:		
DAM7043	R100009, R090009, R080116, R100108, R090113	R080201, EX080101, EX100101, R100107		

Table V-80: Test-case 5 - Ten most likely cases inferred from flooding sensors, $H_s = 0.0$ m, time = 10 min.

Predicted (complete damage) extent				
Dam:	Prob.:	Compartments:		
		Initial:	Progressive:	
DAM7043	0.8089	R100009, R090009, R080116, R100108, R090113	EX080101, R100107, EX100101	
DAM7043	0.0966	R100009, R090009, R080116, R100108, R090113	EX080101, R100107, EX100101, R080202, R080201	
DAM7043	0.0510	R100009, R090009, R080116, R100108, R090113	R100201, R100202, EX080101, R100107, EX100101	
DAM7043	0.0155	R100009, R090009, R080116, R100108, R090113	R100201, EX080101, R100107, EX100101	
DAM7043	0.0087	R100009, R090009, R080116, R100108, R090113	EX080101, R100107, EX100101, R080201	
DAM7043	0.0059	R100009, R090009, R080116, R100108, R090113	R100201, R100202, EX080101, R100107, EX100101, R080202, R080201	
DAM7043	0.0056	R100009, R090009, R080116, R100108, R090113	R100107, EX100101	
DAM7043	0.0021	R100009, R090009, R080116, R100108, R090113	R100201, R100202, EX080101, R100107, AC100302, EX100101	
DAM7043	0.0019	R100009, R090009, R080116, R100108, R090113	R100201, EX080101, R100107, EX100101, R080202, R080201	
DAM7043	0.0013	R100009, R090009, R080116, R100108, R090113	R080304, EX080101, R100107, EX100101, R080202, R080201	
	100% CI:	99% CI:	95% CI:	90% CI:
	26672	7	3	2
				Case rank.:
				5
Positive sensor reading in:		R090009, R100009, R080116, R080116, R090113, R100107, R100108		
Sensor, but no reading:		R080201		
Actual (complete damage) extent:				
Name:	Initial:	Progressive:		
DAM7043	R100009, R090009, R080116, R100108, R090113	R080201, EX080101, EX100101, R100107		

Table V-81: Test-case 5 - Ten most likely cases inferred from flooding sensors, $H_s = 0.0$ m, time = 15 min.

Predicted (complete damage) extent				
Dam:	Prob.:	Compartments:		
		Initial:	Progressive:	
DAM7043	0.8141	R100009,R090009, R080116, R100108, R090113	EX080101, R100107, EX100101	
DAM7043	0.088	R100009,R090009, R080116, R100108, R090113	EX080101, R100107, EX100101, R080202, R080201	
DAM7043	0.0512	R100009,R090009, R080116, R100108, R090113	R100201, R100202, EX080101, R100107, EX100101	
DAM7043	0.0148	R100009,R090009, R080116, R100108, R090113	R100201, EX080101, R100107, EX100101	
DAM7043	0.0091	R100009,R090009, R080116, R100108, R090113	EX080101, R100107, EX100101, R080201	
DAM7043	0.0062	R100009,R090009, R080116, R100108, R090113	R100201, R100202, EX080101, R100107, EX100101, R080202, R080201	
DAM7043	0.0055	R100009,R090009, R080116, R100108, R090113	R100107, EX100101	
DAM7043	0.0055	R100009,R090009, R080116, R100108, R090113	EX080101, R100107	
DAM7043	0.0018	R100009,R090009, R080116, R100108, R090113	R100201, EX080101, R100107, EX100101, R080202, R080201	
DAM7043	0.0015	R100009,R090009, R080116, R100108, R090113	R100201, R100202, EX080101, R100107, AC100302, EX100101	
	100% CI:	99% CI:	95% CI:	90% CI:
	26977	8	3	2
Positive sensor reading in:		R090009, R100009, R080116, R080116, R090113, R100107, R100108		
Sensor, but no reading:		R080201		
Actual (complete damage) extent:				
Name:	Initial:	Progressive:		
DAM7043	R100009, R090009, R080116, R100108, R090113	R080201, EX080101, EX100101, R100107		

Table V-82: Test-case 5 - Ten most likely cases inferred from flooding sensors, $H_S = 0.0$ m, time = 20 min.

Predicted (complete damage) extent				
Dam:	Prob.:	Compartments:		
		Initial:	Progressive:	
DAM7043	0.8407	R100009,R090009, R080116, R100108, R090113	EX080101, R100107, EX100101	
DAM7043	0.0810	R100009,R090009, R080116, R100108, R090113	EX080101, R100107, EX100101, R080202, R080201	
DAM7043	0.0478	R100009,R090009, R080116, R100108, R090113	R100201, R100202, EX080101, R100107, EX100101	
DAM7043	0.0140	R100009,R090009, R080116, R100108, R090113	R100201, EX080101, R100107, EX100101	
DAM7043	0.0061	R100009,R090009, R080116, R100108, R090113	EX080101, R100107, EX100101, R080201	
DAM7043	0.0052	R100009,R090009, R080116, R100108, R090113	R100201, R100202, EX080101, R100107, EX100101, R080202, R080201	
DAM7043	0.0015	R100009,R090009, R080116, R100108, R090113	R080304, EX080101, R100107, EX100101, R080202, R080201	
DAM7043	0.0013	R100009,R090009, R080116, R100108, R090113	R100201, EX080101, R100107, EX100101, R080202, R080201	
DAM7043	0.0008	R100009,R090009, R080116, R100108, R090113	EX080101, R100107, R080202, R080201	
DAM7043	0.0005	R100009,R090009, R080116, R100108, R090113	R100201, R100202, EX080101, R100107, AC100302, EX100101	
	100% CI:	99% CI:	95% CI:	90% CI:
	27029	6	3	2
Positive sensor reading in:		R090009, R100009, R080116, R080116, R090113, R100107, R100108		
Sensor, but no reading:		R080201		
Actual (complete damage) extent:				
Name:	Initial:	Progressive:		
DAM7043	R100009, R090009, R080116, R100108, R090113	R080201, EX080101, EX100101, R100107		

Table V-83: Test-case 5 - Ten most likely cases inferred from flooding sensors, $H_s = 0.0$ m, time = 25 min.

Predicted (complete damage) extent				
Dam:	Prob.:	Compartments:		
		Initial:	Progressive:	
DAM7043	0.8139	R100009, R090009, R080116, R100108, R090113	EX080101, R100107, EX100101	
DAM7043	0.0935	R100009, R090009, R080116, R100108, R090113	EX080101, R100107, EX100101, R080202, R080201	
DAM7043	0.0514	R100009, R090009, R080116, R100108, R090113	R100201, R100202, EX080101, R100107, EX100101	
DAM7043	0.0131	R100009, R090009, R080116, R100108, R090113	R100201, EX080101, R100107, EX100101	
DAM7043	0.0075	R100009, R090009, R080116, R100108, R090113	EX080101, R100107, EX100101, R080201	
DAM7043	0.0055	R100009, R090009, R080116, R100108, R090113	R100201, R100202, EX080101, R100107, EX100101, R080202, R080201	
DAM7043	0.0053	R100009, R090009, R080116, R100108, R090113	R100107, EX100101	
DAM7043	0.0053	R100009, R090009, R080116, R100108, R090113	EX080101, R100107	
DAM7043	0.0016	R100009, R090009, R080116, R100108, R090113	R100201, EX080101, R100107, EX100101, R080202, R080201	
DAM7043	0.0012	R100009, R090009, R080116, R100108, R090113	EX080101, R100107, R080202, R080201	
	100% CI:	99% CI:	95% CI:	90% CI:
	27331	7	3	2
Positive sensor reading in:		R090009, R100009, R080116, R080116, R090113, R100107, R100108		
Sensor, but no reading:		R080201		
Actual (complete damage) extent:				
Name:	Initial:	Progressive:		
DAM7043	R100009, R090009, R080116, R100108, R090113	R080201, EX080101, EX100101, R100107		

Table V-84: Test-case 5 - Ten most likely cases inferred from flooding sensors, $H_s = 0.0$ m, time = 30 min.

Predicted (complete damage) extent				
Dam:	Prob.:	Compartments:		
		Initial:	Progressive:	
DAM7043	0.8502	R100009, R090009, R080116, R100108, R090113	EX080101, R100107, EX100101, R080202, R080201	
DAM7043	0.0596	R100009, R090009, R080116, R100108, R090113	R100201, R100202, EX080101, R100107, EX100101, R080202, R080201	
DAM7043	0.0516	R100009, R090009, R080116, R100108, R090113	EX080101, R100107, EX100101, R080201	
DAM7043	0.0159	R100009, R090009, R080116, R100108, R090113	R080304, EX080101, R100107, EX100101, R080202, R080201	
DAM7043	0.0140	R100009, R090009, R080116, R100108, R090113	R100201, EX080101, R100107, EX100101, R080202, R080201	
DAM7043	0.0042	R100009, R090009, R080116, R100108, R090113	R100201, R100202, EX080101, R100107, EX100101, R080201	
DAM7043	0.0013	R100009, R090009, R080116, R100108, R090113	R100201, R100202, EX080101, R100107, R100304, EX100101, R080202, R080201	
DAM7043	0.0011	R100009, R090009, R080116, R100108, R090113	R100201, EX080101, R100107, EX100101, R080201	
DAM7043	0.0011	R100009, R090009, R080116, R100108, R090113	R100201, R100202, EX080101, R100107, AC100302, EX100101, R080202, R080201	
DAM7043	0.0004	R100009, R090009, R080116, R100108, R090113	R100201, EX080101, R100107, AC100302, EX100101, R080202, R080201	
	100% CI:	99% CI:	95% CI:	90% CI:
	27790	5	3	2
Positive sensor reading in:		R090009, R100009, R080116, R080116, R090113, R100107, R100108, R080201		
Actual (complete damage) extent:				
Name:	Initial:	Progressive:		
DAM7043	R100009, R090009, R080116, R100108, R090113	R080201, EX080101, EX100101, R100107		

V.6.3 Flooding sensor evidence - $H_s = 5.00$ m

Table V-85: Test-case 5 - Ten most likely cases inferred from flooding sensors, $H_s = 5.0$ m, time = 5 min.

Predicted (complete damage) extent					
Dam:	Prob.:	Compartments:			
		Initial:	Progressive:		
DAM7043	0.7330	R100009, R090009, R080116, R100108, R090113	EX080101, R100107, EX100101		
DAM7043	0.0666	R100009, R090009, R080116, R100108, R090113	EX080101, R100107		
DAM7043	0.0548	R100009, R090009, R080116, R100108, R090113	EX080101, R100107, EX100101, R080202, R080201		
DAM7043	0.0238	R100009, R090009, R080116, R100108, R090113	R100201, R100202, EX080101, R100107, EX100101		
DAM7043	0.0151	R100009, R090009, R080116, R100108, R090113	R100201, R100202, EX080101, R100107, AC100302, EX100101		
DAM7043	0.0133	R100009, R090009, R080116, R100108, R090113	R100107, EX100101		
DAM7043	0.0132	R100009, R090009, R080116, R100108, R090113	R080304, EX080101, R100107, EX100101, R080202, R080201		
DAM7043	0.0082	R100009, R090009, R080116, R100108, R090113	R100201, EX080101, R100107, AC100302, EX100101		
DAM7043	0.0078	R100009, R090009, R080116, R100108, R090113	R100201, EX080101, R100107, EX100101		
DAM7043	0.0073	R100009, R090009, R080116, R100108, R090113	R100201, R100202, EX080101, R100107, EX100101, R100304		
100% CI:		99% CI:	95% CI:	90% CI:	Case rank.:
1123010		64	12	6	14
Positive sensor reading in:		R090009, R100009, R080116, R080116, R090113, R100107, R100108			
Sensor, but no reading:		R080201			
Actual (complete damage) extent:					
Name:	Initial:	Progressive:			
DAM7043	R100009, R090009, R080116, R100108, R090113	R080201, EX080101, EX100101, R100107			

Table V-86: Test-case 5 - Ten most likely cases inferred from flooding sensors, $H_S = 5.0$ m, time = 10 min.

Predicted (complete damage) extent					
Dam:	Prob.:	Compartments:			
		Initial:	Progressive:		
DAM7043	0.7167	R100009, R090009, R080116, R100108, R090113	EX080101, R100107, EX100101		
DAM7043	0.0768	R100009, R090009, R080116, R100108, R090113	EX080101, R100107		
DAM7043	0.0489	R100009, R090009, R080116, R100108, R090113	EX080101, R100107, EX100101, R080202, R080201		
DAM7043	0.0256	R100009, R090009, R080116, R100108, R090113	R100107, EX100101		
DAM7043	0.0171	R100009, R090009, R080116, R100108, R090113	R100201, R100202, EX080101, R100107, EX100101		
DAM7043	0.0163	R100009, R090009, R080116, R100108, R090113	R100201, R100202, EX080101, R100107, AC100302, EX100101		
DAM7043	0.0100	R100009, R090009, R080116, R100108, R090113	R080304, EX080101, R100107, EX100101, R080202, R080201		
DAM7043	0.0097	R100009, R090009, R080116, R100108, R090113	R100201, EX080101, R100107, EX100101		
DAM7043	0.0068	R100009, R090009, R080116, R100108, R090113	EX080101, R100107, R080202, R080201		
DAM7043	0.0066	R100009, R090009, R080116, R100108, R090113	R100201, R100202, EX080101, R100107, AC100302, EX100101, R100304		
	100% CI:	99% CI:	95% CI:	90% CI:	Case rank.:
	80079	64	14	6	12
Positive sensor reading in:		R090009, R100009, R080116, R080116, R090113, R100107, R100108			
Sensor, but no reading:		R080201			
Actual (complete damage) extent:					
Name:	Initial:	Progressive:			
DAM7043	R100009, R090009, R080116, R100108, R090113	R080201, EX080101, EX100101, R100107			

Table V-87: Test-case 5 - Ten most likely cases inferred from flooding sensors, HS = 5.0 m, time = 15 min.

Predicted (complete damage) extent				
Dam:	Prob.:	Compartments:		
		Initial:	Progressive:	
DAM7043	0.6587	R100009, R090009, R080116, R100108, R090113	EX080101, R100107, EX100101	
DAM7043	0.1208	R100009, R090009, R080116, R100108, R090113	EX080101, R100107	
DAM7043	0.0553	R100009, R090009, R080116, R100108, R090113	EX080101, R100107, EX100101, R080202, R080201	
DAM7043	0.0549	R100009, R090009, R080116, R100108, R090113	R100107, EX100101	
DAM7043	0.0174	R100009, R090009, R080116, R100108, R090113	R100201, R100202, EX080101, R100107, EX100101	
DAM7043	0.0132	R100009, R090009, R080116, R100108, R090113	R100201, R100202, EX080101, R100107, AC100302, EX100101	
DAM7043	0.0129	R100009, R090009, R080116, R100108, R090113	R080304, EX080101, R100107, EX100101, R080202, R080201	
DAM7043	0.0062	R100009, R090009, R080116, R100108, R090113	R100201, EX080101, R100107, EX100101	
DAM7043	0.0050	R100009, R090009, R080116, R100108, R090113	R100201, EX080101, R100107, AC100302, EX100101	
DAM7043	0.0046	R100009, R090009, R080116, R100108, R090113	R080304, R080302, AC080401, EX080101, R100107, EX100101, R080202, R080201	
	100% CI:	99% CI:	95% CI:	90% CI:
	87716	62	11	5
Positive sensor reading in:		R090009, R100009, R080116, R080116, R090113, R100107, R100108		
Sensor, but no reading:		R080201		
Actual (complete damage) extent:				
Name:	Initial:	Progressive:		
DAM7043	R100009, R090009, R080116, R100108, R090113	R080201, EX080101, EX100101, R100107		

Table V-88: Test-case 5 - Ten most likely cases inferred from flooding sensors, $H_S = 5.0$ m, time = 20 min.

Predicted (complete damage) extent				
Dam:	Prob.:	Compartments:		
		Initial:	Progressive:	
DAM7043	0.6882	R100009, R090009, R080116, R100108, R090113	EX080101, R100107, EX100101	
DAM7043	0.0732	R100009, R090009, R080116, R100108, R090113	EX080101, R100107	
DAM7043	0.0651	R100009, R090009, R080116, R100108, R090113	EX080101, R100107, EX100101, R080202, R080201	
DAM7043	0.0209	R100009, R090009, R080116, R100108, R090113	R100201, R100202, EX080101, R100107, EX100101	
DAM7043	0.0203	R100009, R090009, R080116, R100108, R090113	R080304, EX080101, R100107, EX100101, R080202, R080201	
DAM7043	0.0199	R100009, R090009, R080116, R100108, R090113	R100201, R100202, EX080101, R100107, AC100302, EX100101	
DAM7043	0.0146	R100009, R090009, R080116, R100108, R090113	R100107, EX100101	
DAM7043	0.0146	R100009, R090009, R080116, R100108, R090113	R100107	
DAM7043	0.0085	R100009, R090009, R080116, R100108, R090113	R100201, EX080101, R100107, EX100101	
DAM7043	0.0065	R100009, R090009, R080116, R100108, R090113	R100201, R100202, EX080101, R100107, EX100101, R100304	
	100% CI:	99% CI:	95% CI:	90% CI:
	86052	61	14	7
Positive sensor reading in:		R090009, R100009, R080116, R080116, R090113, R100107, R100108		
Sensor, but no reading:		R080201		
Actual (complete damage) extent:				
Name:	Initial:	Progressive:		
DAM7043	R100009, R090009, R080116, R100108, R090113	R080201, EX080101, EX100101, R100107		

Table V-89: Test-case 5 - Ten most likely cases inferred from flooding sensors, $H_S = 5.0$ m, time = 25 min.

Predicted (complete damage) extent					
Dam:	Prob.:	Compartments:			
		Initial:		Progressive:	
DAM7043	0.4531	R100009, R090009, R080116, R100108, R090113		EX080101, R100107, EX100101, R080202, R080201	
DAM7043	0.1757	R100009, R090009, R080116, R100108, R090113		R080304, EX080101, R100107, EX100101, R080202, R080201	
DAM7043	0.0647	R100009, R090009, R080116, R100108, R090113		EX080101, R100107, EX100101, R080201	
DAM7043	0.0416	R100009, R090009, R080116, R100108, R090113		R080304, EX080101, R100107, R080305, EX100101, R080202, R080201	
DAM7043	0.0370	R100009, R090009, R080116, R100108, R090113		EX080101, R100107, R080202, R080201	
DAM7043	0.0231	R100009, R090009, R080116, R100108, R090113		R080304, R080302, EX080101, R100107, EX100101, R080202, R080201	
DAM7043	0.0185	R100009, R090009, R080116, R100108, R090113		R080306, R080304, R080302, EX080101, R100107, EX100101, R080202, R080201	
DAM7043	0.0138	R100009, R090009, R080116, R100108, R090113		R100201, R100202, EX080101, R100107, EX100101, R080202, R080201	
DAM7043	0.0092	R100009, R090009, R080116, R100108, R090113		R080304, EX080101, R100107, R080202, R080201	
DAM7043	0.0092	R100009, R090009, R080116, R100108, R090113		R080307, R080304, R080301, EX080101, R100107, R080305, EX100101, R080202, R080201	
100% CI:		99% CI:		95% CI:	
89462		134		32	
90% CI:		Case rank.:			
21		3			
Positive sensor reading in:		R090009, R100009, R080116, R080116, R090113, R100107, R100108, R080201, R080201			
Actual (complete damage) extent:					
Name:	Initial:			Progressive:	
DAM7043	R100009, R090009, R080116, R100108, R090113			R080201, EX080101, EX100101, R100107	

Table V-90: Test-case 5 - Ten most likely cases inferred from flooding sensors, $H_S = 5.0$ m, time = 30 min.

Predicted (complete damage) extent					
Dam:	Prob.:	Compartments:			
		Initial:	Progressive:		
DAM7043	0.4746	R100009, R090009, R080116, R100108, R090113	EX080101, R100107, EX100101, R080202, R080201		
DAM7043	0.1477	R100009, R090009, R080116, R100108, R090113	R080304, EX080101, R100107, EX100101, R080202, R080201		
DAM7043	0.0527	R100009, R090009, R080116, R100108, R090113	EX080101, R100107, EX100101, R080201		
DAM7043	0.0369	R100009, R090009, R080116, R100108, R090113	EX080101, R100107, R080202, R080201		
DAM7043	0.0264	R100009, R090009, R080116, R100108, R090113	R080304, EX080101, R100107, R080305, EX100101, R080202, R080201		
DAM7043	0.0158	R100009, R090009, R080116, R100108, R090113	R080307, R080304, EX080101, R100107, R080305, EX100101, R080202, R080201		
DAM7043	0.0153	R100009, R090009, R080116, R100108, R090113	R100201, R100202, EX080101, R100107, EX100101, R080202, R080201		
DAM7043	0.0108	R100009, R090009, R080116, R100108, R090113	R100201, R100202, EX080101, R100107, AC100302, EX100101, R080202, R080201		
DAM7043	0.0105	R100009, R090009, R080116, R100108, R090113	R080304, R080302, EX080101, R100107, EX100101, R080202, R080201		
DAM7043	0.0105	R100009, R090009, R080116, R100108, R090113	EX080101, R100107, R080201		
100% CI:		99% CI:	95% CI:	90% CI:	Case rank.:
88372		148	35	25	3
Positive sensor reading in:		R090009, R100009, R080116, R080116, R090113, R100107, R100108, R080201			
Actual (complete damage) extent:					
Name:	Initial:	Progressive:			
DAM7043	R100009, R090009, R080116, R100108, R090113	R080201, EX080101, EX100101, R100107			

V.6.4 Flooding sensor evidence - $H_s = 10.00$ m

Table V-91: Test-case 5 - Ten most likely cases inferred from flooding sensors, $H_s = 10.0$ m, time = 5 min.

Predicted (complete damage) extent				
Dam:	Prob.:	Compartments:		
		Initial:	Progressive:	
DAM7043	0.8055	R100009, R090009, R080116, R100108, R090113	EX080101, R100107, EX100101	
DAM7043	0.0671	R100009, R090009, R080116, R100108, R090113	R100107, EX100101	
DAM7043	0.0671	R100009, R090009, R080116, R100108, R090113	EX080101, R100107	
DAM7043	0.0165	R100009, R090009, R080116, R100108, R090113	EX080101, R100107, EX100101, R080202, R080201	
DAM7043	0.0105	R100009, R090009, R080116, R100108, R090113	R100201, R100202, EX080101, R100107, AC100302, EX100101	
DAM7043	0.0039	R100009, R090009, R080116, R100108, R090113	R100201, R100202, EX080101, R100107, EX100101	
DAM7043	0.0033	R100009, R090009, R080116, R100108, R090113	R100201, EX080101, R100107, AC100302, EX100101	
DAM7043	0.0019	R100009, R090009, R080116, R100108, R090113	R080304, EX080101, R100107, EX100101, R080202, R080201	
DAM7043	0.0017	R100009, R090009, R080116, R100108, R090113	R100201, R100202, EX080101, R100107, AC100302, EX100101, R100304	
DAM7043	0.0017	R100009, R090009, R080116, R100108, R090113	R100201, EX080101, R100107, EX100101	
	100% CI:	99% CI:	95% CI:	90% CI:
	1573709	23	4	3
				Case rank.:
				11
	Positive sensor reading in:	R090009, R100009, R080116, R080116, R090113, R100107, R100108		
	Sensor, but no reading:	R080201		
Actual (complete damage) extent:				
Name:	Initial:	Progressive:		
DAM7043	R100009, R090009, R080116, R100108, R090113	R080201, EX080101, EX100101, R100107		

Table V-92: Test-case 5 - Ten most likely cases inferred from flooding sensors, $H_S = 10.0$ m, time = 10 min.

Predicted (complete damage) extent				
Dam:	Prob.:	Compartments:		
		Initial:	Progressive:	
DAM7043	0.7522	R100009, R090009, R080116, R100108, R090113	EX080101, R100107, EX100101	
DAM7043	0.1254	R100009, R090009, R080116, R100108, R090113	EX080101, R100107	
DAM7043	0.0627	R100009, R090009, R080116, R100108, R090113	R100107, EX100101	
DAM7043	0.0182	R100009, R090009, R080116, R100108, R090113	EX080101, R100107, EX100101, R080202, R080201	
DAM7043	0.0106	R100009, R090009, R080116, R100108, R090113	R100201, R100202, EX080101, R100107, AC100302, EX100101	
DAM7043	0.0049	R100009, R090009, R080116, R100108, R090113	R080304, EX080101, R100107, EX100101, R080202, R080201	
DAM7043	0.0027	R100009, R090009, R080116, R100108, R090113	R100201, R100202, EX080101, R100107, EX100101	
DAM7043	0.0027	R100009, R090009, R080116, R100108, R090113	R100201, R100202, EX080101, R100107, AC100302, EX100101, R100304	
DAM7043	0.0021	R100009, R090009, R080116, R100108, R090113	R100201, EX080101, R100107, EX100101	
DAM7043	0.0018	R100009, R090009, R080116, R100108, R090113	EX080101, R100107, R080202, R080201	
	100% CI:	99% CI:	95% CI:	90% CI:
	111121	17	4	3
	Case rank.:			11
Positive sensor reading in:		R090009, R100009, R080116, R080116, R090113, R100107, R100108		
Sensor, but no reading:		R080201		
Actual (complete damage) extent:				
Name:	Initial:	Progressive:		
DAM7043	R100009, R090009, R080116, R100108, R090113	R080201, EX080101, EX100101, R100107		

Table V-93: Test-case 5 - Ten most likely cases inferred from flooding sensors, $H_S = 10.0$ m, time = 15 min.

Predicted (complete damage) extent			
Dam:	Prob.:	Compartments:	
		Initial:	Progressive:
DAM7043	0.5316	R100009, R090009, R080116, R100108, R090113	EX080101, R100107, EX100101, R080202, R080201
DAM7043	0.0857	R100009, R090009, R080116, R100108, R090113	R080304, EX080101, R100107, EX100101, R080202, R080201
DAM7043	0.0686	R100009, R090009, R080116, R100108, R090113	EX080101, R100107, EX100101, R080201
DAM7043	0.0343	R100009, R090009, R080116, R100108, R090113	R080304, R080302, AC080401, EX080101, R100107, EX100101, R080202, R080201
DAM7043	0.0343	R100009, R090009, R080116, R100108, R090113	R080306, R080307, R080304, R080302, AC080401, EX080101, R100107, R080305, R080301, EX100101, R080202, R080201, R080303
DAM7043	0.0171	R100009, R090009, R080116, R100108, R090113	R060403, R070503, R080402, R060503, R060409, R060408, R070403, R070204, AC080401, PL09, R070207, R100107, R070304, PL08, R090502, R060205, AC070301, R060302, R060303, R060305, PL06, PL07, R080306, R080307, R080304, R080305, R080302, R080303, R070206, R080301, R060410, R070302, EX100101, R080202, R080201, EX080101, PL05, R060317
DAM7043	0.0171	R100009, R090009, R080116, R100108, R090113	R080304, EX080101, R100107, R080202, R080201
DAM7043	0.0171	R100009, R090009, R080116, R100108, R090113	R060403, R070406, R070407, R070402, R070403, R070401, R070204, R070408, AC080401, R060309, R070207, R100107, PL08, R060203, R060205, AC070301, R060207, R060301, R060302, R060303, R060305, PL06, PL07, R080306, R080307, R080304, R080305, R080302, R080303, R070206, R080301, R060410, R070301, R070303, EX100101, R080202, R080201, EX080101, PL09, PL05, R060311, PL10
DAM7043	0.0171	R100009, R090009, R080116, R100108, R090113	R060403, R060401, R060307, R060503, R070406, R070403, R070401, R070204, R060308, AC080401, R060309, R070207, R100107, R070304, PL08, R060318, R060205, AC070301, R060301, R060302, R060303, R060304, R060305, PL06, PL07, R080306, R080307, R080304, R080305, R080302, R080303, R070206, R080301, R060410, R070301, R070302, EX100101, R080202, R080201, R050313, EX080101, PL05, R060306, R060311, R060310, R060317, R060316, R060314

DAM7043	0.0171	R100009, R090009, R080116, R100108, R090113	R060407, R060406, R060405, PL10, R060403, R060402, R060401, R060503, R060408, R070406, R070405, R070401, R040401, R040403, AC080401, PL09, R070207, R100107, EC030401, R040402, PL08, R060203, R050308, R060205, R060207, R060309, R060302, R060303, R060304, PL05, PL06, PL07, R080306, R080307, R080304, R080305, R080302, R080303, R070206, R080301, R060301, EX100101, R080202, R080201, R050313, EX080101, R060305, R060306, R060310, R060316, R060315, R060314		
	100% CI:	99% CI:	95% CI:	90% CI:	Case rank.:
	112191	32	17	14	3
Positive sensor reading in:		R090009, R100009, R080116, R080116, R090113, R100107, R100108, R080201			
Actual (complete damage) extent:					
Name:	Initial:			Progressive:	
DAM7043	R100009, R090009, R080116, R100108, R090113			R080201, EX080101, EX100101, R100107	

Table V-94: Test-case 5 - Ten most likely cases inferred from flooding sensors, $H_5 = 10.0$ m, time = 20 min.

Predicted (complete damage) extent					
Dam:	Prob.:	Compartments:			
		Initial:	Progressive:		
DAM7043	0.5291	R100009, R090009, R080116, R100108, R090113	EX080101, R100107, EX100101, R080202, R080201		
DAM7043	0.1150	R100009, R090009, R080116, R100108, R090113	R080304, EX080101, R100107, EX100101, R080202, R080201		
DAM7043	0.0230	R100009, R090009, R080116, R100108, R090113	R070204, AC080401, R060309, R100107, R060308, R060203, AC070301, R060301, R060302, R060305, R060306, R060307, R080306, R080307, R080304, R080305, R080302, R080303, R080301, EX100101, R080202, R080201, EX080101, R060310, R060317, R060315, R060314		
DAM7043	0.0230	R100009, R090009, R080116, R100108, R090113	R080306, R080307, R080304, R080301, EX080101, R100107, R080305, R080302, EX100101, R080202, R080201		
DAM7043	0.0230	R100009, R090009, R080116, R100108, R090113	R060407, R060405, R060403, R070503, R080402, R070406, R070407, R070403, R070401, R070204, AC080401, R060309, R070207, R100107, PL08, R060203, R060205, R060207, R060301, R060302, R060303, R060304, R060305, PL06, PL07, R080306, R080307, R080304, R080305, R080302, R080303, R070206, R080301, R060410, R080202, R080201, EX080101, EC080401, PL09, PL05, R060306, R060311, PL10, R060316, R060314		

DAM7043	0.0230	R100009, R090009, R080116, R100108, R090113	R060406, R060403, R060402, R070406, R070401, R070204, PL08, AC080401, R060309, R070207, R100107, R070304, R060308, R060205, R060209, R060301, R060302, R060303, R060305, PL06, PL07, R080306, R080307, R080304, R080305, R080302, R080303, R070206, R080301, R060410, R070301, R070302, R080202, R080201, EX080101, PL09, PL05, R060318, R060311, R060317		
DAM7043	0.0230	R100009, R090009, R080116, R100108, R090113	R060407, R060405, R060403, R060402, R060401, R060307, R060503, R070204, R060308, AC080401, R060309, R070207, R100107, R080202, PL08, R060318, R060205, AC070301, R060207, R060301, R060302, R060303, PL05, PL06, PL07, R080306, R080307, R080304, R080305, R080302, PL09, R070206, R080301, R070301, R070302, EX100101, R070304, R080201, EX080101, R060305, R060306, PL10, R060317, R060314		
DAM7043	0.0230	R100009, R090009, R080116, R100108, R090113	R060407, R060406, R060403, R060402, R060401, R060307, R060503, R070406, R070204, R060308, AC080401, PL09, R070207, R100107, R080202, PL08, R060205, AC070301, R060309, R060302, R060303, R060304, PL05, PL06, PL07, R080306, R080307, R080304, R080305, R080302, R080303, R070206, R080301, R060301, EX100101, R070304, R080201, R060310, EX080101, R060305, R060306, R060311, PL10, R060317, R060316, R060315, R060314		
DAM7043	0.0230	R100009, R090009, R080116, R100108, R090113	R080306, R080307, R080304, R080302, AC080401, EX080101, R100107, R080305, R080301, EX100101, R080202, R080201, R080303		
DAM7043	0.0230	R100009, R090009, R080116, R100108, R090113	R080304, EX080101, R100107, R080202, R080201		
	100% CI:	99% CI:	95% CI:	90% CI:	Case rank.:
	112619	45	16	14	1
Positive sensor reading in:		R090009, R100009, R080116, R080116, R090113, R100107, R100108, R080201, R080202			
Actual (complete damage) extent:					
Name:	Initial:			Progressive:	
DAM7043	R100009, R090009, R080116, R100108, R090113			EX080101, R100107, EX100101, R080202, R080201	

Table V-95: Test-case 5 - Ten most likely cases inferred from flooding sensors, $H_S = 10.0$ m, time = 25 min.

Predicted (complete damage) extent			
Dam:	Prob.:	Compartments:	
		Initial:	Progressive:
DAM7043	0.4149	R100009, R090009, R080116, R100108, R090113	EX080101, R100107, EX100101, R080202, R080201
DAM7043	0.1383	R100009, R090009, R080116, R100108, R090113	EX080101, R100107, R080202, R080201
DAM7043	0.1152	R100009, R090009, R080116, R100108, R090113	R080304, EX080101, R100107, EX100101, R080202, R080201
DAM7043	0.0461	R100009, R090009, R080116, R100108, R090113	R080304, R080302, AC080401, EX080101, R100107, EX100101, R080202, R080201
DAM7043	0.0230	R100009, R090009, R080116, R100108, R090113	R060407, R060404, R060403, R060401, R060307, R070406, R070401, R060308, AC080401, R060309, R070207, R100107, R070304, PL08, R060203, AC070301, R060207, R060301, R060302, R060303, R060304, R060305, PL06, R060306, R080306, R080307, R080304, R080305, R080302, R080303, R080301, R070301, R070303, R070302, EX100101, R080202, R080201, EX080101, PL05, R060318, R060311, PL10, R060317, R060315, R060314
DAM7043	0.0230	R100009, R090009, R080116, R100108, R090113	R060405, R060404, R060403, R060401, R060503, R060409, R060408, R070406, R070407, R070403, R070401, AC080401, PL09, R100107, R070304, PL08, R060205, R060207, R060303, PL05, PL06, PL07, R080306, R080304, R080302, R070206, R070207, R070301, R070302, EX100101, R080202, R080201, EX080101, R060318, R060311, PL10
DAM7043	0.0230	R100009, R090009, R080116, R100108, R090113	R060407, R060403, R060401, R060307, R060503, R070406, R070407, R070401, R070204, R040403, R060308, AC080401, PL09, R070207, R100107, R080202, PL08, R060203, AC070301, R060207, R060309, R060302, R060303, PL05, PL06, PL07, R080306, R080307, R080304, R080305, R080302, R080303, R070206, R080301, R060301, R070301, R070303, R070302, EX100101, R070304, R080201, R040401, EX080101, R060305, R060318, EC050401, R060311, PL10, R060317
DAM7043	0.0230	R100009, R090009, R080116, R100108, R090113	R080301, R080304, R080303, EX080101, R100107, R080305, EX100101, R080202, R080201
DAM7043	0.0230	R100009, R090009, R080116, R100108, R090113	R080301, R080304, R080303, EX080101, R100107, R080305, R080202, R080201

DAM7043	0.0230	R100009, R090009, R080116, R100108, R090113	R060405, R060403, R060307, R080402, R060503, R070406, R070407, R070403, R070401, R060410, R060309, R070207, R100107, R080202, R060308, R060205, AC070301, R060207, R060301, R060302, R060303, PL05, PL06, PL07, R080306, R080307, R080304, R080305, R080302, R080301, R090401, R070303, R070302, EX100101, R070304, R080201, R060310, EX080101, EC080401, R090405, R060311, PL10, R060316, R060314		
	100% CI: 113589	99% CI: 43	95% CI: 15	90% CI: 13	Case rank.: 1
Positive sensor reading in:		R090009, R100009, R080116, R080116, R090113, R100107, R100108, R080201			
Actual (complete damage) extent:					
Name:	Initial:			Progressive:	
DAM7043	R100009, R090009, R080116, R100108, R090113			EX080101, R100107, EX100101, R080202, R080201	

Table V-96: Test-case 5 - Ten most likely cases inferred from flooding sensors, $H_S = 10.0$ m, time = 30 min.

Predicted (complete damage) extent					
Dam:	Prob.:	Compartments:			
		Initial:		Progressive:	
DAM7043	0.5525	R100009, R090009, R080116, R100108, R090113		EX080101, R100107, EX100101, R080202, R080201	
DAM7043	0.1151	R100009, R090009, R080116, R100108, R090113		R080304, EX080101, R100107, EX100101, R080202, R080201	
DAM7043	0.0460	R100009, R090009, R080116, R100108, R090113		EX080101, R100107, R080202, R080201	
DAM7043	0.0460	R100009, R090009, R080116, R100108, R090113		EX080101, R100107, EX100101, R080201	
DAM7043	0.0230	R100009, R090009, R080116, R100108, R090113		R090505, R060403, R060506, R070503, R060503, R070406, R070401, R060410, R070408, AC080401, PL09, R100107, R080202, PL08, R060203, R060205, AC070301, R060207, R060507, R060309, R060302, R060303, R060305, PL06, PL07, R080306, R080307, R080304, R080302, R090507, R070206, R070207, R090506, R090508, R070301, R070302, EX100101, R070304, R080201, R100509, EX080101, R070204, PL05, R100507, R060318, R060311, PL10, R090510	
DAM7043	0.0230	R100009, R090009, R080116, R100108, R090113		R080306, R080307, R080304, R080302, EX080101, R100107, R080305, R080301, EX100101, R080202, R080201	

DAM7043	0.0230	R100009, R090009, R080116, R100108, R090113	R060407, R060405, R060403, R060402, R060401, R060503, R060410, R060308, R040403, PL09, R070207, R100107, PL08, R060203, R060205, R060301, R060302, R060303, R060304, PL05, PL06, PL07, R080306, R080307, R080304, R080305, R080302, R080303, R070206, R080301, R060309, R080202, R080201, R060310, R040401, EX080101, R070204, R060305, R060306, R060311, PL10, R060317, R060316, R060315, R060314			
DAM7043	0.0230	R100009, R090009, R080116, R100108, R090113	R060404, R060403, R080401, R060307, R080403, R070407, R070402, R070401, R070204, R070409, R060308, AC080401, R060309, R070207, R100107, R080202, PL08, R060318, R060205, R060207, R060209, R060301, R060302, R060303, R060304, R060305, PL06, PL07, R080306, R080307, R080304, R080305, R080302, R080303, R070206, R080301, R060410, R070301, R070302, EX100101, R070304, R080201, EX080101, EC080401, PL09, PL05, R060306, R060311, PL10, R060317, R060316, R060315, R060314			
DAM7043	0.0230	R100009, R090009, R080116, R100108, R090113	R060403, R060402, R080402, R060409, R070406, R070407, R070403, R070401, R070204, R070408, R070409, AC080401, R060309, R070207, R100107, R070304, PL08, R060203, R060205, R060207, R060301, R060302, R060303, R060305, PL06, PL07, R080306, R080307, R080304, R080305, R080302, R080303, R070206, R080301, EX100101, R080202, R080201, EX080101, EC080401, PL09, PL05, PL10, R060317, R060314			
DAM7043	0.0230	R100009, R090009, R080116, R100108, R090113	R060407, R060406, R060403, R060401, R060307, R080402, R060408, R070407, R070403, R070401, AC050401, R070204, R040403, R060308, AC080401, R060309, R070207, R100107, PL08, R060203, R060205, R060207, R060301, R060302, R060303, R060305, PL06, PL07, R080306, R080307, R080304, R080305, R080302, R080303, R070206, R080301, EX100101, R080202, R080201, R080201, R060310, R040401, EX080101, PL09, PL05, EC050401, R060311, PL10, R060317, R060316, R060314			
100% CI:			99% CI:	95% CI:	90% CI:	Case rank.:
112781			46	13	11	1
Positive sensor reading in:			R090009, R100009, R080116, R080116, R090113, R100107, R100108, R080201			
Actual (complete damage) extent:						
Name:	Initial:		Progressive:			
DAM7043	R100009, R090009, R080116, R100108, R090113		EX080101, R100107, EX100101, R080202, R080201			

Appendix VI - Heat-maps for compartment flooding probability

VI.1 Test-case 1, $H_s = 0.00$ m

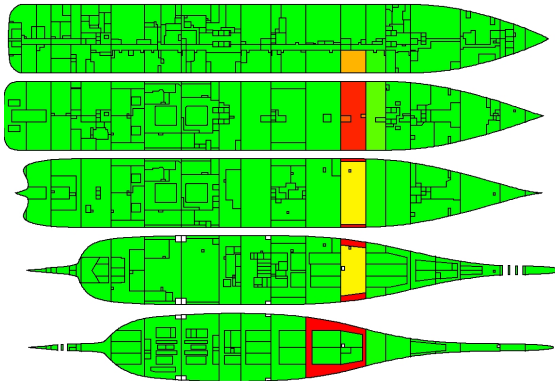


Figure VI-1: TC-1, $H_s = 0$ m, Time-step, $t = 5$ min

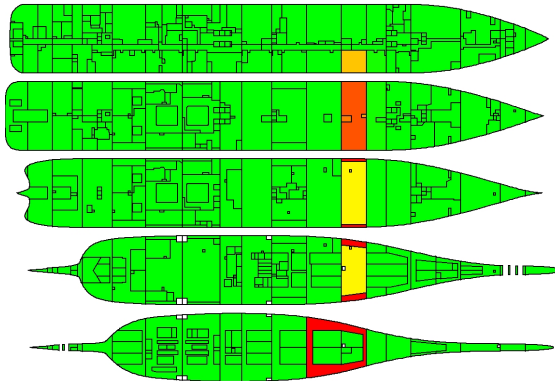


Figure VI-2: TC-1, $H_s = 0$ m, Time-step, $t = 10$ min

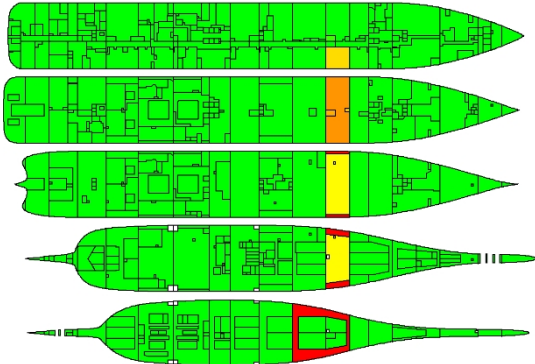


Figure VI-3: TC-1, $H_s = 0$ m, Time-step, $t = 15$ min

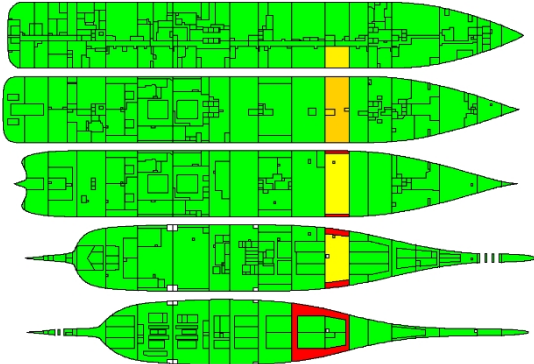


Figure VI-4: TC-1, $H_s = 0$ m, Time-step, $t = 20$ min

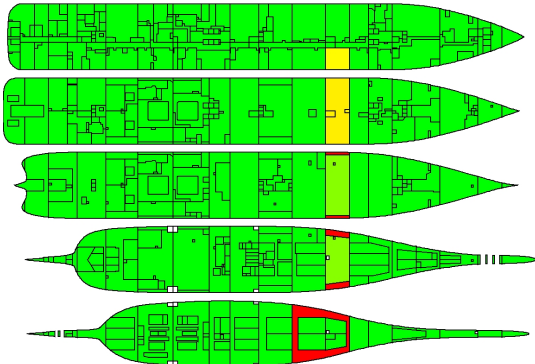


Figure VI-5: TC-1, $H_s = 0$ m, Time-step, $t = 25$ min

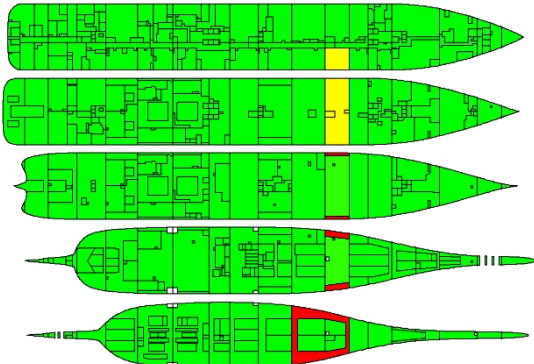


Figure VI-6: TC-1, $H_s = 0$ m, Time-step, $t = 30$ min

VI.2 Test-case 1, $H_s = 10.00$ m

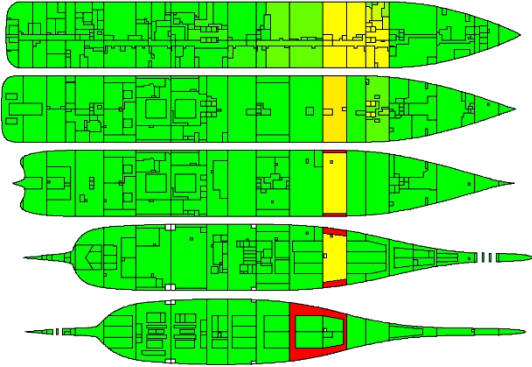


Figure VI-7: TC-1, $H_s = 10$ m, Time-step, $t = 5$ min

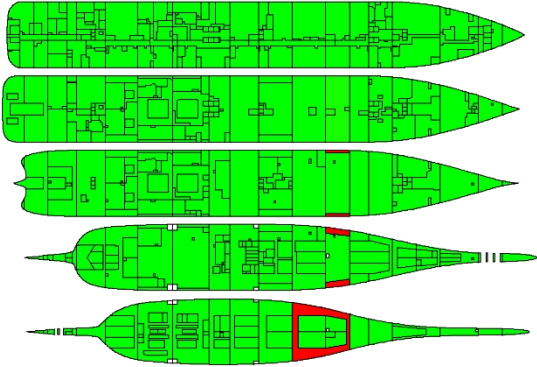


Figure VI-8: TC-1, $H_s = 10$ m, Time-step, $t = 10$ min

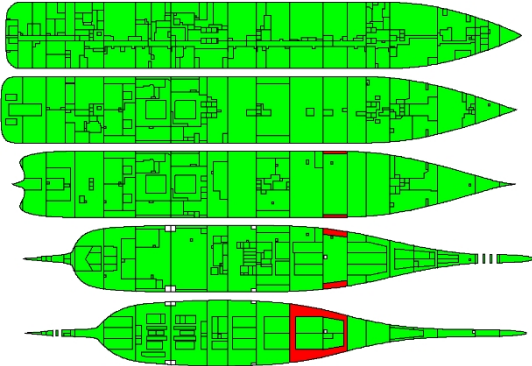


Figure VI-9: TC-1, $H_s = 10$ m, Time-step, $t = 15$ min

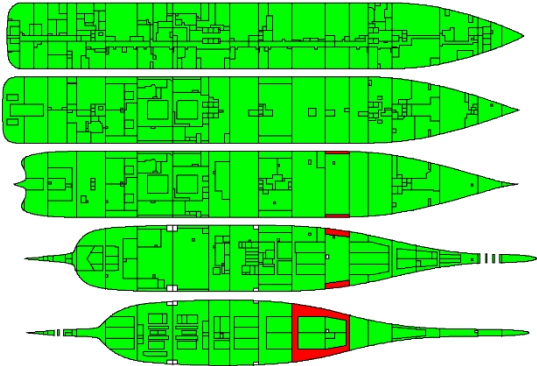


Figure VI-10: TC-1, $H_s = 10$ m, Time-step, $t = 20$ min

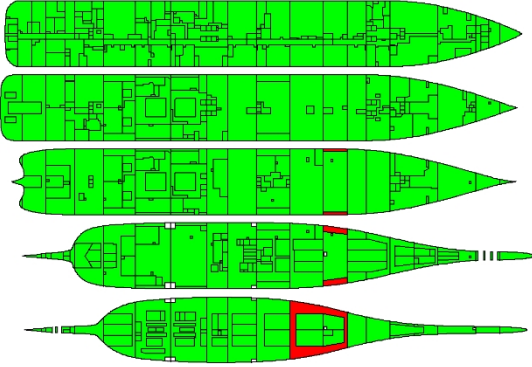


Figure VI-11: TC-1, $H_s = 10$ m, Time-step, $t = 25$ min

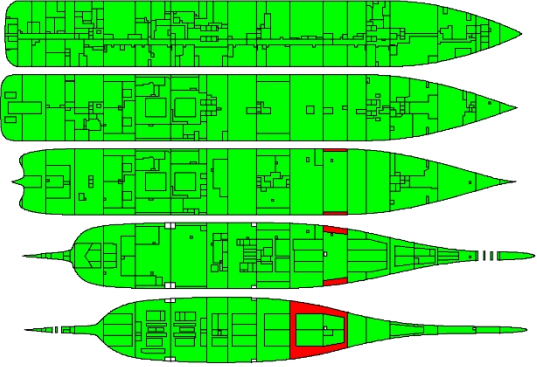


Figure VI-12: TC-1, $H_s = 10$ m, Time-step, $t = 30$ min

VI.3 Test-case 2, $H_s = 0.00$ m

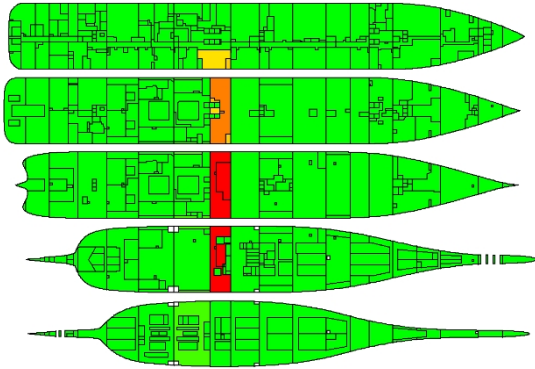


Figure VI-13: TC-2, $H_s = 0$ m, Time-step, $t = 5$ min

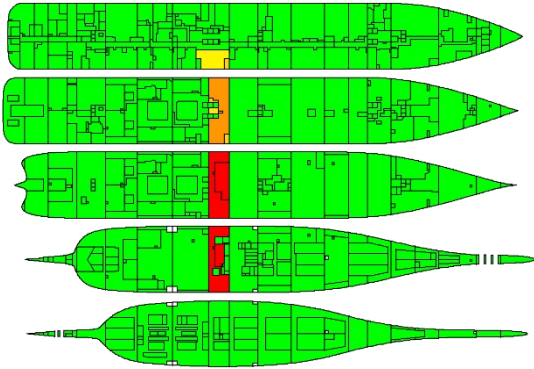


Figure VI-14: TC-2, $H_s = 0$ m, Time-step, $t = 10$ min

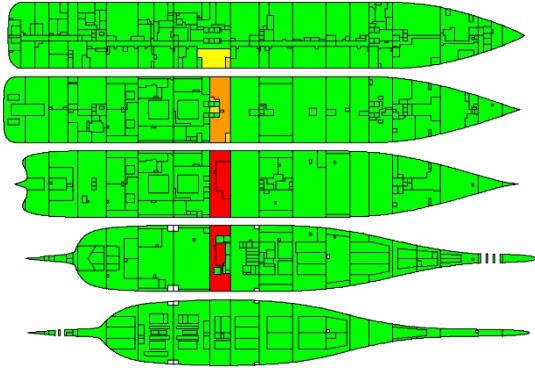


Figure VI-15: TC-2, $H_s = 0$ m, Time-step, $t = 15$ min

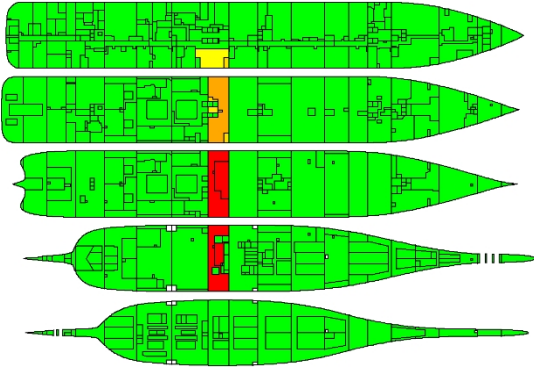


Figure VI-16: TC-2, $H_s = 0$ m, Time-step, $t = 20$ min

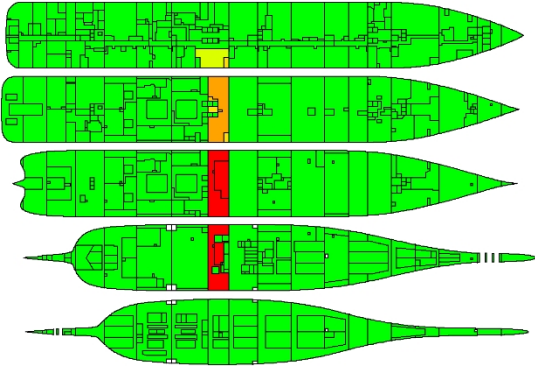


Figure VI-17: TC-2, $H_s = 0$ m, Time-step, $t = 25$ min

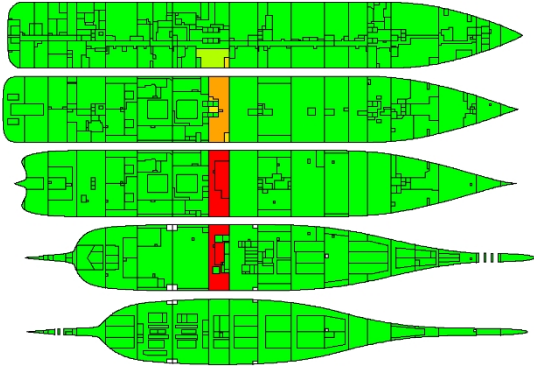


Figure VI-18: TC-2, $H_s = 0$ m, Time-step, $t = 30$ min

VI.4 Test-case 2, $H_s = 10.00$ m

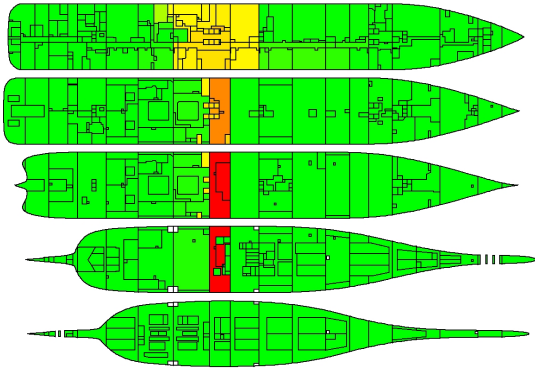


Figure VI-19: TC-2, $H_s = 10$ m, Time-step, $t = 5$ min

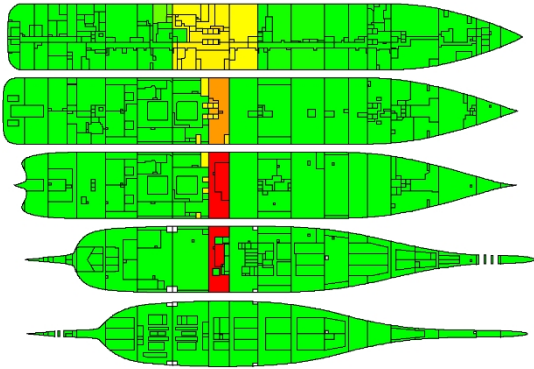


Figure VI-20: TC-2, $H_s = 10$ m, Time-step, $t = 10$ min

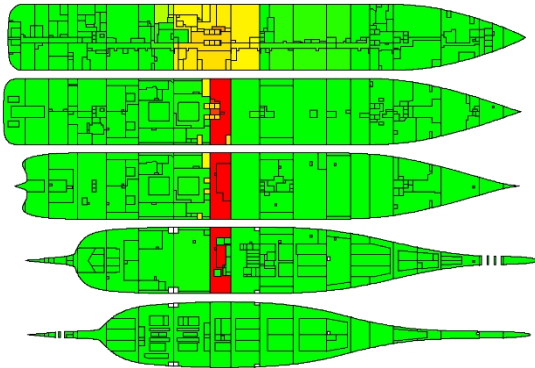


Figure VI-21: TC-2, $H_s = 10$ m, Time-step, $t = 15$ min

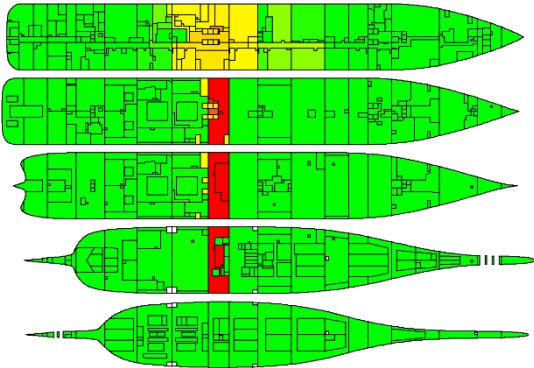


Figure VI-22: TC-2, $H_s = 10$ m, Time-step, $t = 20$ min

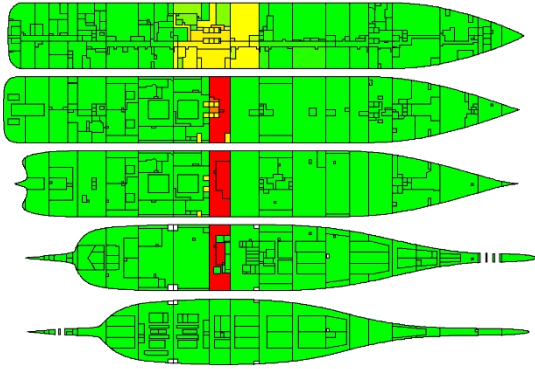


Figure VI-23: TC-2, $H_s = 10$ m, Time-step, $t = 25$ min

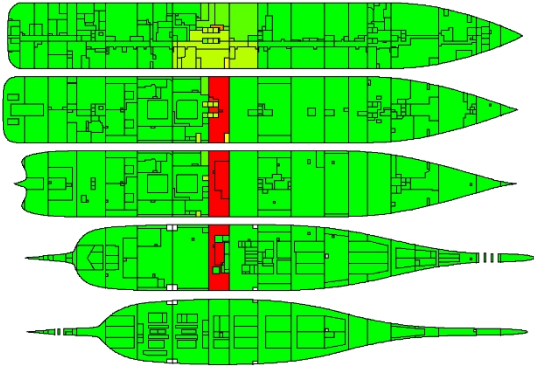


Figure VI-24: TC-2, $H_s = 10$ m, Time-step, $t = 30$ min

VI.5 Test-case 3, $H_s = 0.00$ m

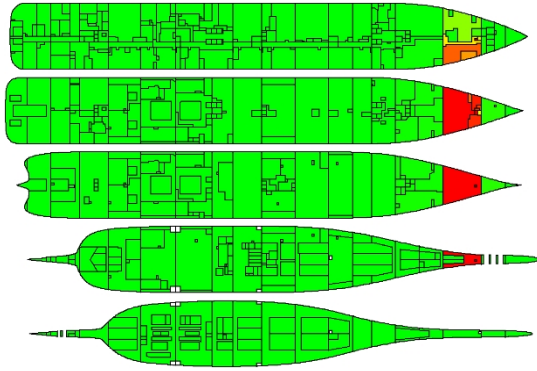


Figure VI-25: TC-3, $H_s = 0$ m, Time-step, $t = 5$ min

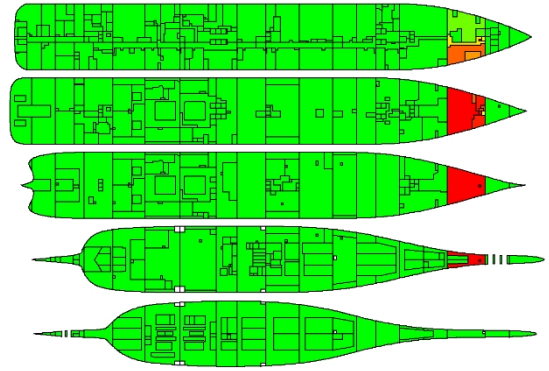


Figure VI-26: TC-3, $H_s = 0$ m, Time-step, $t = 10$ min

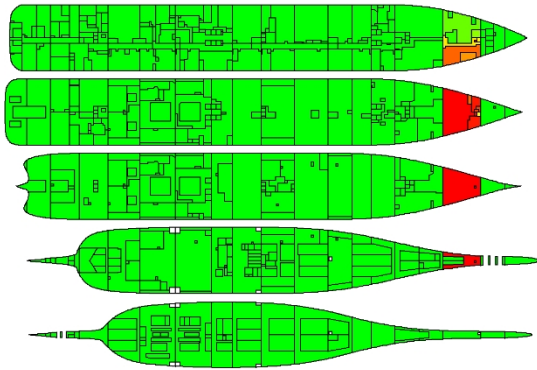


Figure VI-27: TC-3, $H_s = 0$ m, Time-step, $t = 15$ min

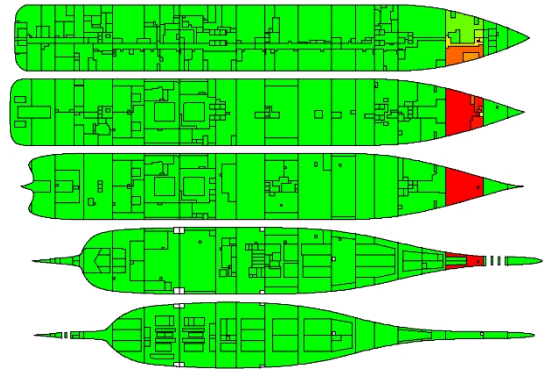


Figure VI-28: TC-3, $H_s = 0$ m, Time-step, $t = 20$ min

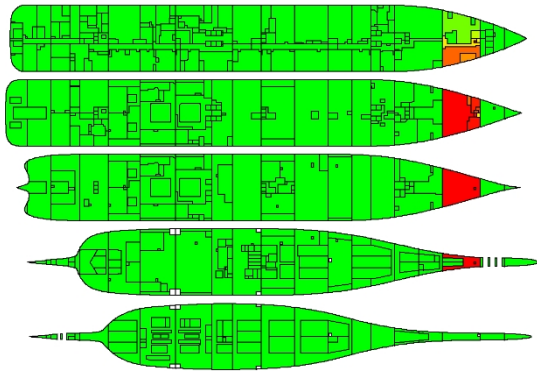


Figure VI-29: TC-3, $H_s = 0$ m, Time-step, $t = 25$ min

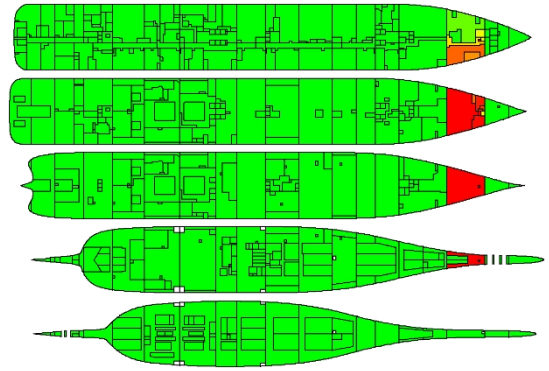


Figure VI-30: TC-3, $H_s = 0$ m, Time-step, $t = 30$ min

VI.6 Test-case 3, $H_s = 10.00$ m

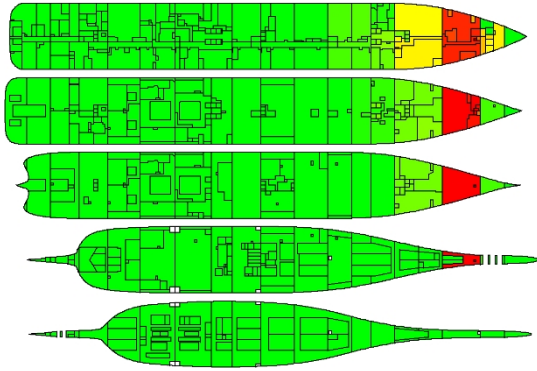


Figure VI-31: TC-3, $H_s = 10$ m, Time-step, $t = 5$ min

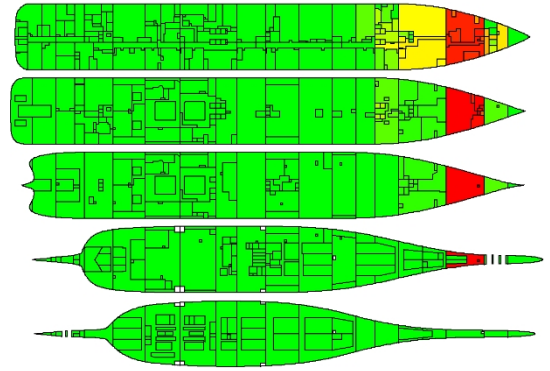


Figure VI-32: TC-3, $H_s = 10$ m, Time-step, $t = 10$ min

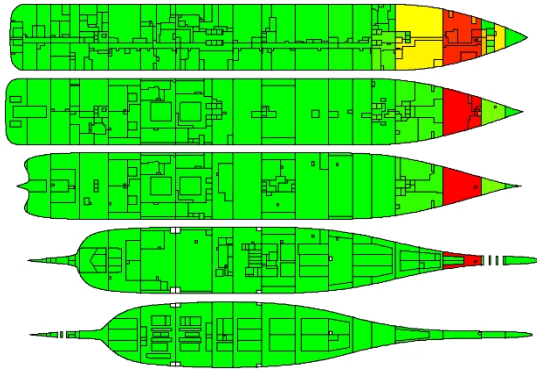


Figure VI-33: TC-3, $H_s = 10$ m, Time-step, $t = 15$ min

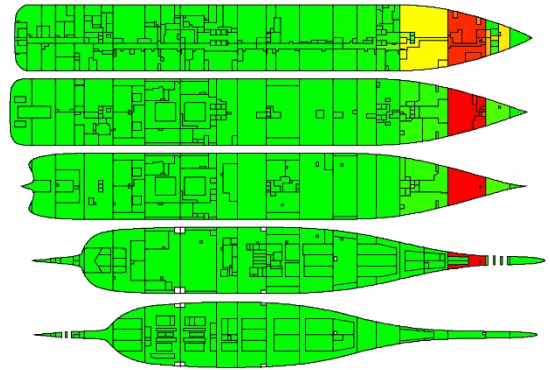


Figure VI-34: TC-3, $H_s = 10$ m, Time-step, $t = 20$ min

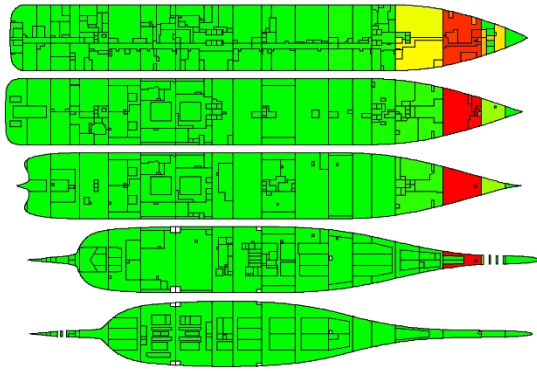


Figure VI-35: TC-3, $H_s = 10$ m, Time-step, $t = 25$ min

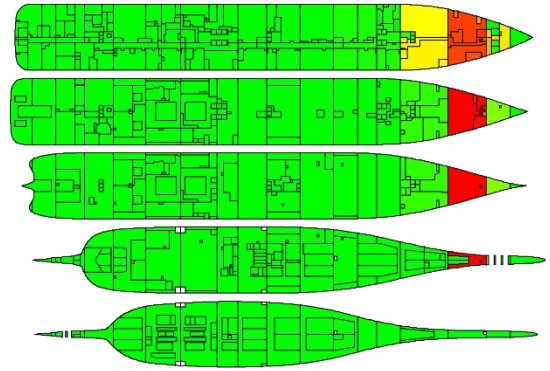


Figure VI-36: TC-3, $H_s = 10$ m, Time-step, $t = 30$ min

VI.7 Test-case 4, $H_s = 0.00$ m

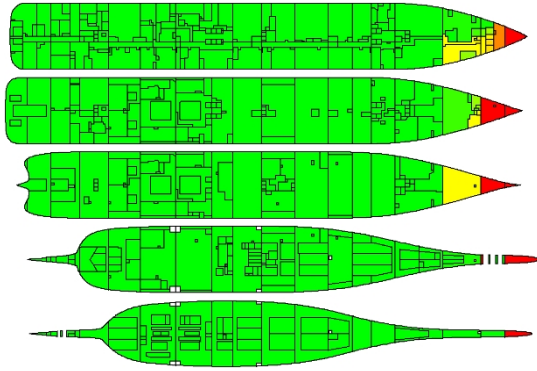


Figure VI-37: TC-4, $H_s = 0$ m, Time-step, $t = 5$ min

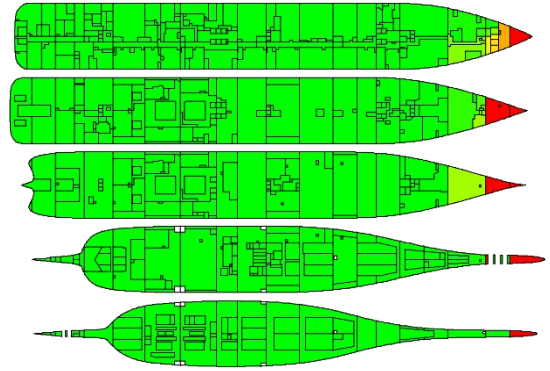


Figure VI-38: TC-4, $H_s = 0$ m, Time-step, $t = 10$ min

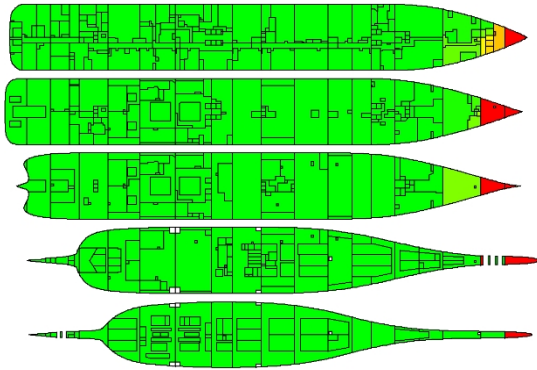


Figure VI-39: TC-4, $H_s = 0$ m, Time-step, $t = 15$ min

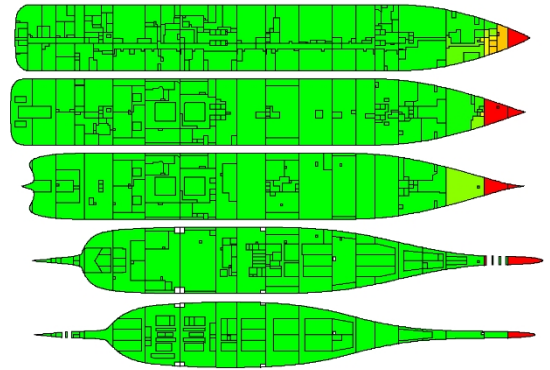


Figure VI-40: TC-4, $H_s = 0$ m, Time-step, $t = 20$ min

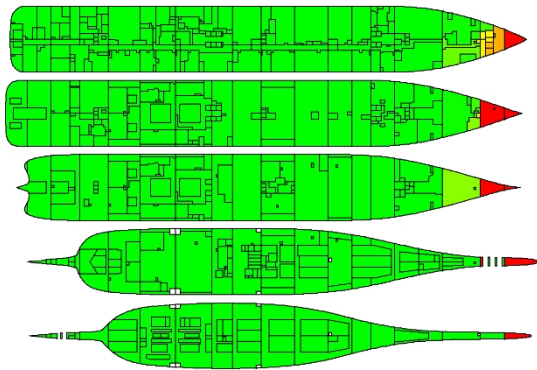


Figure VI-41: TC-4, $H_s = 0$ m, Time-step, $t = 25$ min

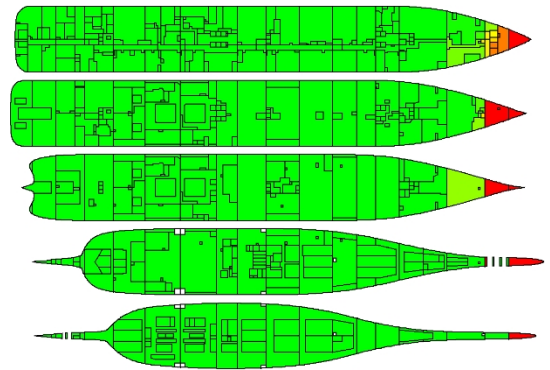


Figure VI-42: TC-4, $H_s = 0$ m, Time-step, $t = 30$ min

VI.8 Test-case 4, $H_s = 10.00$ m

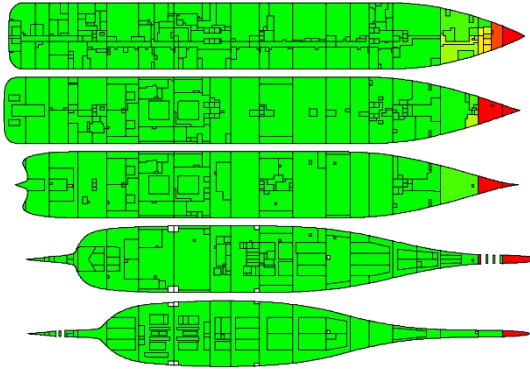


Figure VI-43: TC-4, $H_s = 10$ m, Time-step, $t = 5$ min

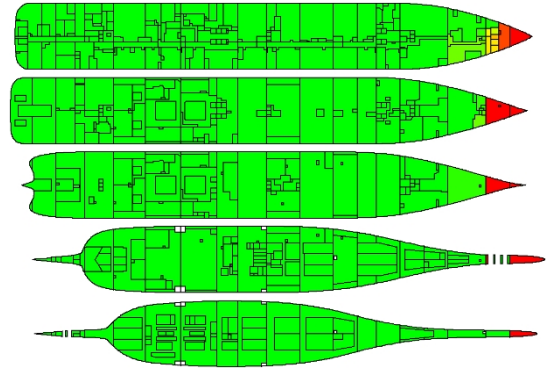


Figure VI-44: TC-4, $H_s = 10$ m, Time-step, $t = 10$ min

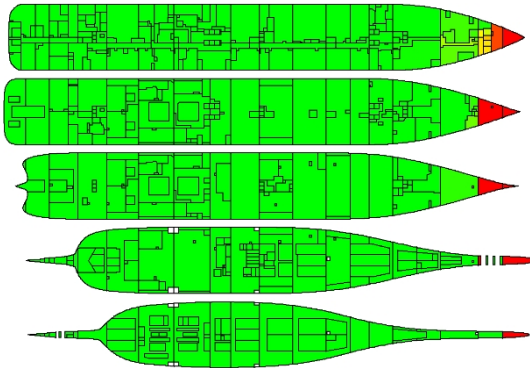


Figure VI-45: TC-4, $H_s = 10$ m, Time-step, $t = 15$ min

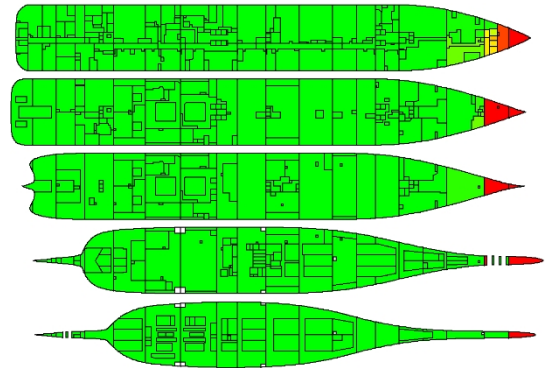


Figure VI-46: TC-4, $H_s = 10$ m, Time-step, $t = 20$ min

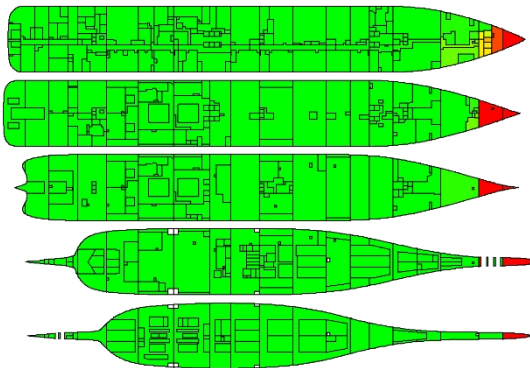


Figure VI-47: TC-4, $H_s = 10$ m, Time-step, $t = 25$ min

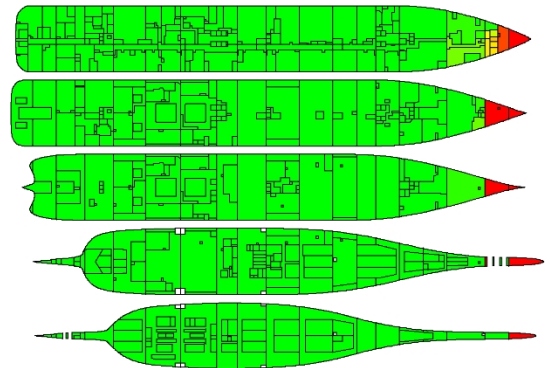


Figure VI-48: TC-4, $H_s = 10$ m, Time-step, $t = 30$ min

VI.9 Test-case 5, $H_s = 0.00$ m

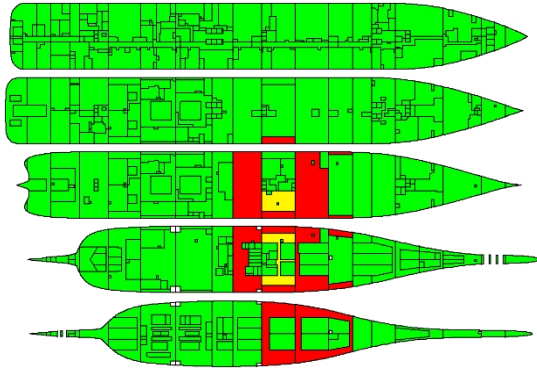


Figure VI-49: TC-5, $H_s = 0$ m, Time-step, $t = 5$ min

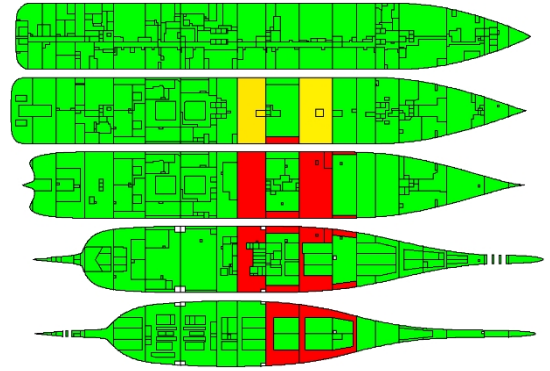


Figure VI-50: TC-5, $H_s = 0$ m, Time-step, $t = 10$ min

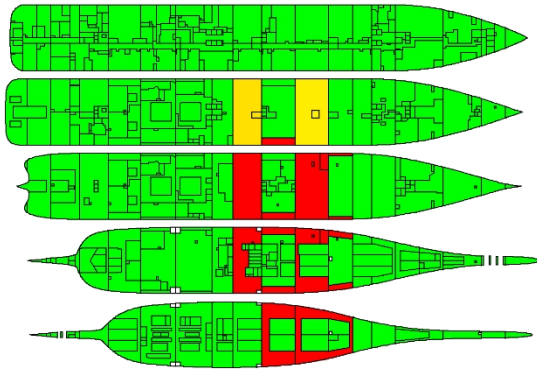


Figure VI-51: TC-5, $H_s = 0$ m, Time-step, $t = 15$ min

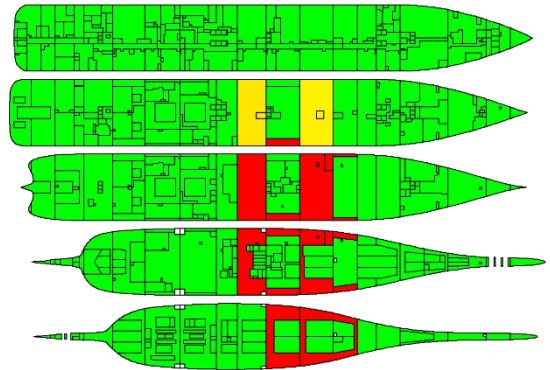


Figure VI-52: TC-5, $H_s = 0$ m, Time-step, $t = 20$ min

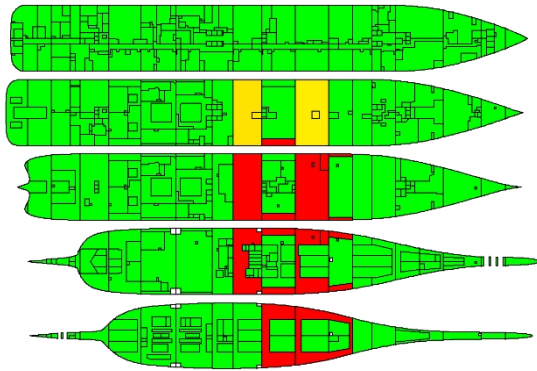


Figure VI-53: TC-5, $H_s = 0$ m, Time-step, $t = 25$ min

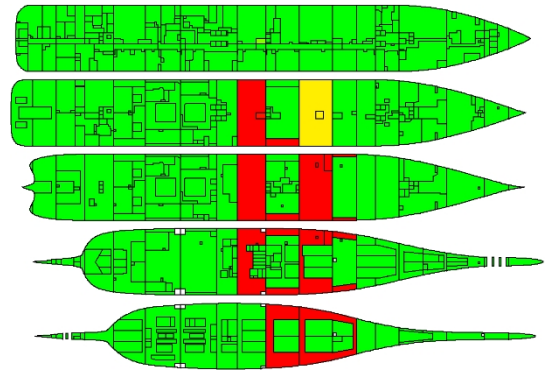


Figure VI-54: TC-5, $H_s = 0$ m, Time-step, $t = 30$ min

VI.10 Test-case 5, $H_s = 10.00$ m

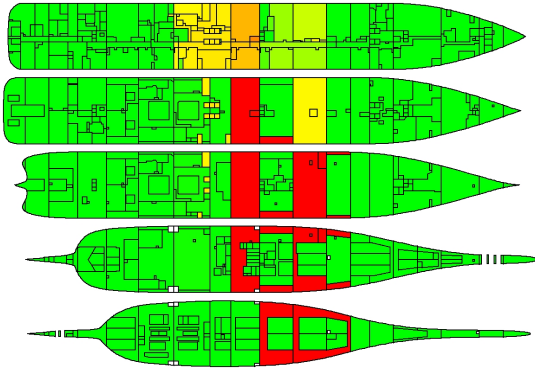


Figure VI-55: TC-5, $H_s = 10$ m, Time-step, $t = 5$ min

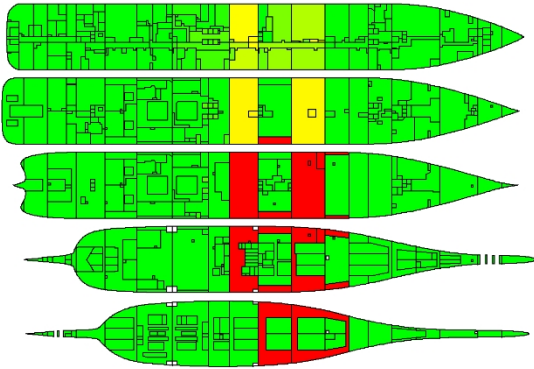


Figure VI-56: TC-5, $H_s = 10$ m, Time-step, $t = 10$ min

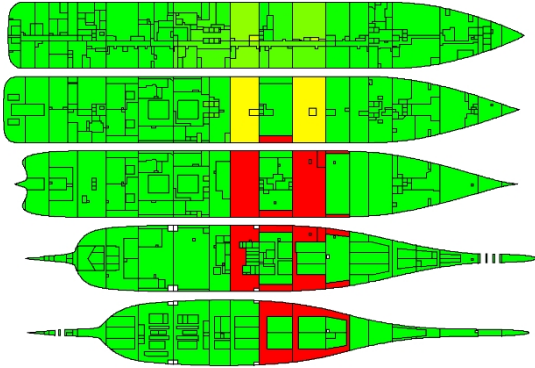


Figure VI-57: TC-5, $H_s = 10$ m, Time-step, $t = 15$ min

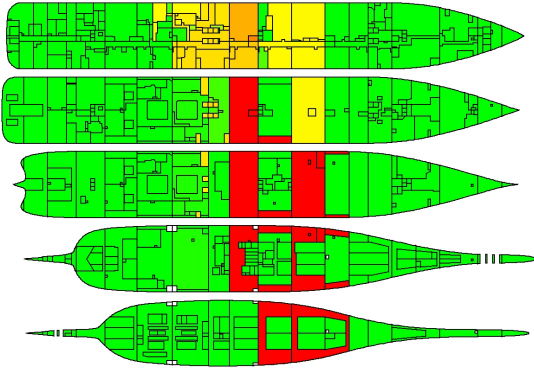


Figure VI-58: TC-5, $H_s = 10$ m, Time-step, $t = 20$ min

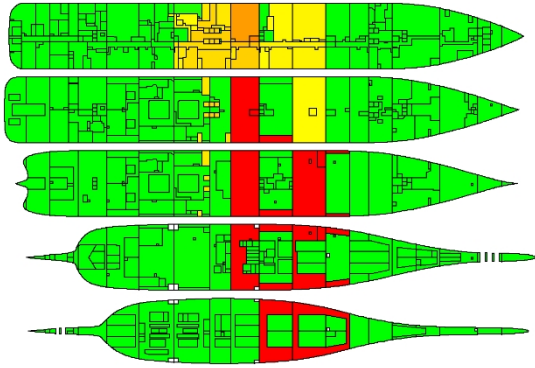


Figure VI-59: TC-5, $H_s = 10$ m, Time-step, $t = 25$ min

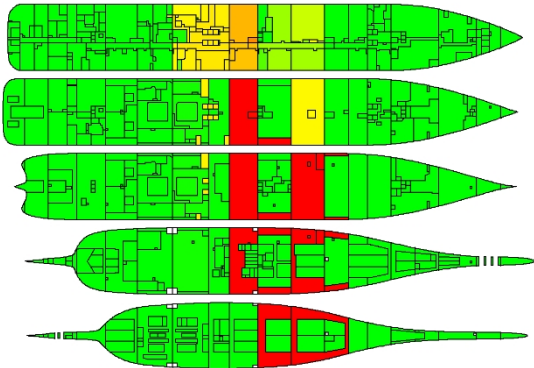


Figure VI-60: TC-5, $H_s = 10$ m, Time-step, $t = 30$ min